

AD/A-006 232

**COMPARISON OF ORTHOGONAL TRANSFORMS
FOR TELESEISMIC DATA**

C. H. Chen

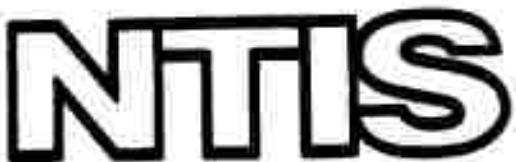
Southeastern Massachusetts University

Prepared for:

Air Force Office of Scientific Research

31 October 1974

DISTRIBUTED BY:



**National Technical Information Service
U. S. DEPARTMENT OF COMMERCE
5285 Port Royal Road, Springfield Va. 22151**

UNCLASSIFIED

SECURITY CLASSIFICATION OF THIS PAGE (When Data Entered)

REPORT DOCUMENTATION PAGE

READ INSTRUCTIONS
BEFORE COMPLETING FORM

1. REPORT NUMBER AFOSR - IR - 75 - 272	2. GOVT ACCESSION NO. AD/A-006232	3. RECIPIENT'S CATALOG NUMBER
4. TITLE (and Subtitle) COMPARISON OF ORTHOGONAL TRANSFORMS FOR TELESEISMIC DATA		5. TYPE OF REPORT & PERIOD COVERED Interim
7. AUTHOR(s) C.H. Chen		6. PERFORMING ORG. REPORT NUMBER TN N. EE-74-5
9. PERFORMING ORGANIZATION NAME AND ADDRESS Southeastern Massachusetts University Department of Electrical Engineering North Dartmouth, Massachusetts 02747		10. PROGRAM ELEMENT, PROJECT, TASK AREA & WORK UNIT NUMBERS 61102F 9769-02
11. CONTROLLING OFFICE NAME AND ADDRESS Air Force Office of Scientific Research (NM) 1400 Wilson Blvd Arlington, Virginia 22209		12. REPORT DATE October 31, 1974
14. MONITORING AGENCY NAME & ADDRESS (if different from Controlling Office)		13. NUMBER OF PAGES 392
		15. SECURITY CLASS. (of this report) UNCLASSIFIED
		16a. DECLASSIFICATION/DOWNGRADING SCHEDULE
16. DISTRIBUTION STATEMENT (of this Report) Approved for public release; distribution unlimited.		
17. DISTRIBUTION STATEMENT (of the abstract entered in Block 20, if different from Report)		
18. SUPPLEMENTARY NOTES		
19. KEY WORDS (Continue on reverse side if necessary and identify by block number)		

Reproduced by
**NATIONAL TECHNICAL
INFORMATION SERVICE**
 US Department of Commerce
 Springfield, VA. 22151

20. ABSTRACT (Continue on reverse side if necessary and identify by block number)
 The availability of fast algorithms for computing the orthogonal transforms such as the fast Fourier transform (FFT), Walsh-Hadamard transform (WHT), discrete Chebyshev transform (DCT), and related transforms has made such transforms increasingly popular in data processing. This paper is concerned with the comparative evaluation of these transforms as applied to the ACDA teleseismic data. Computer results and program listings are provided. The paper is concluded with the recommendation that better orthogonal transforms are needed for both signal processing and seismic discrimination.

Technical Note
TN No. EE-74-5
Grant AFOSR 71-2119
October 31, 1974

COMPARISON OF ORTHOGONAL
TRANSFORMS FOR TELESEISMIC DATA

by

C. H. Chen
Southeastern Massachusetts University
North Dartmouth, Massachusetts 02747



Abstract

The availability of fast algorithms for computing the orthogonal transforms such as the fast Fourier transform (FFT), Walsh-Hadamard transform (WHT), discrete Chebyshev transform (DCT), and related transforms has made such transforms increasingly popular in data processing. This paper is concerned with the comparative evaluation of these transforms as applied to the ACDA teleseismic data. Computer results and program listings are provided. The paper is concluded with the recommendation that better orthogonal transforms are needed for both signal processing and seismic discrimination.

Approved for public release;
Approved for unlimited.
Distribution unlimited.

Comparison of Orthogonal Transforms for Teleseismic Data

C. H. Chen

I. Introduction

In recent years there has been an increasing interest with respect to using a class of orthogonal transforms in the areas of pattern recognition and digital signal processing. In pattern recognition, orthogonal transforms enable a noninvertible transformation from the pattern space to a reduced dimensionality feature space. This allows a classification scheme to be implemented with substantially less features, with only a small increase in classification error. In digital processing, orthogonal transforms implemented by fast algorithms are basic operations for digital filtering, spectral estimation, etc. In discrete (Wiener) filtering for signal parameter estimation, orthogonal transforms "compress" the useful data to a substantially small number of elements and thus simplifies the filter structure and reduces the computation load. Orthogonal transforms are also useful in designing multiplexing communication systems.

The Walsh-Hadamard transform, discrete Fourier transform, the Haar transform, the slant transform, and discrete Chebyshev transform (also called discrete cosine transform) have been considered for various applications, since these are orthogonal transforms that can be computed using fast algorithms. The Karhunen-Loeve transform (KLT) is an orthogonal transform which is optimal in the minimum mean squared error sense; but is computationally difficult. In this paper we are concerned with the comparative evaluation of these orthogonal transforms for teleseismic data study including signal processing and seismic discrimination (pattern recognition).

II. The Orthogonal Transforms

Of all the orthogonal transforms presently available, the discrete Fourier transform is probably the most conveniently available and provides the most familiar frequency domain informations on the seismic data. The fast Fourier transform also serves as

the groundwork for all transforms with sinusoidal basis functions such as the discrete Chebyshev transform and nonrecursive digital filtering. The phase spectrum which is often ignored contains much useful information. To utilize both amplitude and phase spectra in the Fourier domain is not a simple task. The homomorphic deconvolution or the complex cepstrum accomplishes this objective by taking the logarithm of the complex Fourier spectrum. The problem with the cepstral approach is that it is difficult to obtain accurate long pass and short pass system outputs especially with the noisy data. The teleseismic data is highly sinusoidal in nature and thus the Fourier domain transforms appear to be most appropriate. Once digitized for computer compatibility, the amount of data needed to analyze the seismic waveforms can be reduced by the orthogonal transforms. A fast Fourier transform reduces the data needed to analyze the waveform by a factor of 10 (it would be a factor of 5 if both amplitude and phase spectra are used) with a very small percentage of the reconstructed root-mean-squared error. The fast Fourier transform accomplishes the data compression by changing the usual time domain representation of the seismic signal to one of frequency representation. A representation of the seismic wave requires less data points in the frequency domain than in the original time domain. A Walsh-Hadamard transform may also be used in a similar manner to yield a data compression factor of four. (The factor is reduced if the plus and minus signs are included.)

Haar transform and slant transform are more suitable for image processing than for seismic study. The discrete Chebyshev transform has the important advantage in that it is closest to KLT in mean square error while computable by fast algorithms. It does require much more computation time than Fourier or Walsh transforms. The Walsh transform is computationally the best. The data compression factor for DCT is nearly the same as for FFT. The DCT should be considered as a member of Fourier domain transforms with good promise for wide range of applications.

For seismic data study, the minimum mean squared error criterion, however, is of questionable value. Such criterion depends only up to the second order statistics (the mean and covariance functions) which may be not enough to characterize the seismic waves. Furthermore, reconstruction of the seismic wave is not an important objective. To estimate some parameters such as to determine the P-wave amplitude, and to discriminate explosion from earthquake, are among the important objectives of the seismic study. Both DCT and WHT spread the signal energy to higher spectral components than the FFT and thus may not be as effective in dimensionality reduction for pattern recognition as compared with FFT. Note that DCT is better than WHT in this sense. Unfortunately, the reduced feature space provided by all orthogonal transforms is still too large in dimension and the subsequent classifier is too complex in structure or computation. For two-dimensional display, the transformed data has to be considerably compressed further to make the display possible.

Therefore we conclude that the presently available orthogonal transforms have to be considerably improved for seismic study in processing, display, and discrimination. At the present time, the Fourier domain transforms are still most useful for seismic study. New transforms must be computable in fast algorithms while drastically compress the data so that the dimension of the reduced feature space falls below 10, which is a factor of 100 in reduction of 1024 data points typically used in digital seismic data study.

III. Computer Results

The seismic data considered is the ACDA Seismic Signature Data Base provided by Lt. Colonel Russell B. Ives. A complete spectral plot of all 269 records was submitted to him with report, "Fourier Spectral Plot of ACDA Seismic Signature Data Base", dated September 12, 1974. Some conclusions of the spectral analysis are:

- 1) With a few exceptions, all explosions have a pronounced spectral peak at 0.5 - 0.7 Hz.
- 2) The earthquakes have many discrete frequency components, i.e. they are rich in subharmonics.
- 3) The explosion spectra spread to higher frequencies than the earthquake spectra.
- 4) Most records have strong DC components which could be removed to provide better discrimination results.

An important reason for providing spectral plot of all records is to enable us to get an accurate interpretation of the results. In the attachments of this report we have included the following:

1. Computer program to plot the original seismic waveform with 1024 data points (samples) at 10 samples per second, and to plot the amplitude of FFT up to 5 Hz.
2. Application note on DCT.
3. Computer program to plot WHT and DCT.
4. A complete plot of DCT and WHT for each record. On each page there are two graphs, the upper one is for DCT up to 512 data points and the lower one is for WHT up to 1024 data points.

The following are conclusions which can be drawn from the plot of DCT and WHT:

- 1) DCT appears as a low-passed filtered WHT. Theoretical explanation of this phenomenon is not available. There might be some theoretical relationship between the two which is not yet discovered.
- 2) The DCT for explosion is a more smooth function of the number of data points than the earthquake.
- 3) The WHT is nearly periodic (except in amplitude) with a period of approximately 256 data points.

Attachment #1 Computer Program to Plot Seismic Wave and its
Amplitude Spectrum for PDP 11-45 Computer

FORTRAN V004A

00:00:00

21-SEP-74

PAGE

1

```
0001      DIMENSION C(257)
0002      COMPLEX E(2000)
0003      REAL X(2,2000), B(2000)
0004      BYTE IA(70), IX(9), IQ(10), TEST
0005      EQUIVALENCE (E,X)
0006      DATA TEST, IX, IQ/ 'X', 'E', 'X', 'P', 'L', 'O', 'S', 'I', 'O', 'N',
+                  'E', 'A', 'R', 'T', 'H', 'Q', 'U', 'A', 'K', 'E'/
0007      CALL XYINIT(B, 2000)
0008      CALL SIZE(C, 1024)
0009      CALL CHSIZE(0, 4, 90, 0)
0010      6      FORMAT(I3)
0011      7      IC=0
0012      1      READ(6,6) IF
0013      DO 9 I=1,2000
0014      X(2,I)=0.0
0015      9      X(1,I)=0.0
0016      11     IC=IC+1
0017      READ(1,END=10) IA
0018      READ(1)NPT, (X(1,I), I=1,NPT)
0019      IF(IF.GE. IC) GO TO 8
0020      REWIND 1
0021      GO TO 7
0022      8      IF(IF.NE. IC) GO TO 11
0023      CALL IXYPT(230,0,0)
0024      CALL XYCHAR(IA,20)
0025      CALL IXYPT(486,0,0)
0026      IF(IA(70).EQ. TEST) GO TO 2
0027      CALL XYCHAR(IQ,10)
0028      GO TO 3
0029      2      CALL XYCHAR(IX,9)
0030      3      CALL IXYPT(500,0,0)
0031      CALL IXYPT(2190,0,1)
0032      XMAX=X(1,1)
0033      XMIN=XMAX
0034      DO 4 I=1,NPT
0035      IF(XMIN.GT. X(1,I)) XMIN=X(1,I)
0036      4      IF(XMAX.LT. X(1,I)) XMAX=X(1,I)
0037      XS=1690.0/(XMAX-XMIN)
0038      N=2190.0+XMIN*XS
0039      CALL IXYPT(N,0,0)
0040      CALL IXYPT(N,4000,1)
0041      IXX=0
0042      IY=2190.0+(XMIN-X(1,1))*XS
0043      CALL IXYPT(IY,IXX,0)
0044      DO 5 I=2,NPT
0045      IXX=IXX+1
0046      IY=2190.0+(XMIN-X(1,I))*XS
0047      5      CALL IXYPT(IY,IXX,1)
0048      CALL IXYPT(2390,0,0)
0049      CALL IXYPT(4090,0,1)
0050      CALL IXYPT(4090,4095,1)
0051      NP=NPT-1024
0052      IF(NP.GT.0) CALL SHIFTL(X,2000,NP)
0053      CALL FFOUT(X,1024,C,-1.0)
0054      XMAX=CABS(E(1))
```

FORTRAN V004A

00:00:00

21-SEP-74

PAGE

2

```

0055      DO 12 I=1,512
0056      X(1,I)=CABS(E(I))
0057 12      IF(XMAX.LT.X(1,I)) XMAX=X(1,I)
0058      XS=1690.0/XMAX
0059      N=4090.0-X(1,1)*XS
0060      CALL IXYPT(N,0,0)
0061      DO 13 I=1,512
0062      IXX=8*I-4
0063      IY=4090.0-X(1,I)*XS
0064 13      CALL IXYPT(IY,IXX,1)
0065      CALL IXYPT(0,4095,0)
0066      CALL IXYPT(0,0,0)
0067      CALL IXYPT(4095,0,0)
0068      CALL IXYPT(4095,4095,0)
0069      GO TO 1
0070 10      CALL XYEND
0071      CALL EXIT
0072      END

```

ROUTINES CALLED:

XYINIT, SIZE, CHSIZE, IXYPT, XYCHAR, SHIFTL, FFOUR
CABS, XYEND, EXIT

SWITCHES = /ON

BLOCK	LENGTH
MAIN.	13422 (064334)*

```

**COMPILER ----- CORE**
    PHASE      USED   FREE
DECLARATIVES 00366 05535
EXECUTABLES  00937 04964
ASSEMBLY     01478 07340

```

Attachment #2 Application Note on DCT
DCT - Discrete Chebyshev Transform

A. Implementation:

The Discrete Chebyshev Transform of a data set $y(m)$ is defined by [1]

$$Y(k) = \frac{A}{N} \operatorname{Re} \left\{ e^{-kwi/2N} \sum_{m=0}^{N-1} y(m) e^{-2mkwi/2N} \right\}$$

$$\text{and } A = \begin{cases} \sqrt{2} & k = 0 \\ 2 & k = 1, 2, \dots, N-1 \end{cases}$$

$$k = 0, 1, \dots, N-1$$

The DCT program evaluates this expression utilizing an in-place, $4N$ -point Fast Fourier Transform; the various parameters employed are as follows:

$$\begin{aligned} N &= \text{number of data pts } y(m) \\ &= 2^p \text{ where } p \text{ is integral} \\ N_2 &= 2N \\ N_4 &= 4N \\ NM &= \text{number of sub-matrices employed in the FFT} \\ &= p + 2 \\ \text{Sign} &= -1.0 \text{ for forward transform} \\ &= +1.0 \text{ for inverse transform} \end{aligned}$$

Because the computations are done in-place, Y is both input and output arrays; X is a complex buffer array.

The program generates $2N$ output coefficients, of which the first N contain the correctly-ordered, desired output. Although this program utilizes an FFT, unlike the FFT only the $2N$ real output points from the forward transform are required to generate the inverse.

B. Program Notes

The FFT employed is Robinson's decimation-in-frequency algorithm[2]. The 'phase-shift' operates on the complex X array only when its components represent functions of k ; i.e., for the forward transform the FFT is done first, then the array is phase-shifted; for the inverse transform the reverse procedure is followed.

Each time the FFT is performed, the bit-reversed outputs are unscrambled within the subroutine to produce a sequentially-ordered array; the output consists of the real component of the complex array.

C. References

1. N. Ahmed, T. Natarajan, and K. R. Rao, IEEE Trans. Computers, C-23, 90(1974).
2. E. A. Robinson, Multichannel Time Series Analysis, Holden-Day, San Francisco, 1967.

Attachment #3 Computer Program to Plot DCT and WHT

FORTRAN V004A

00:00:00

21-SEP-74

PAGE

1

```

DIMENSION Z(1024)
DIMENSION Y(1024), MM(12)
REAL X(2,2048), B(100)
BYTE IA(70), IX(9), IQ(10), TEST
EQUIVALENCE (E,X)
DATA TEST, IX, IQ/'X','E','X','P','L','O','S','I','Q','N',
+                               'E','A','R','T','H','Q','U','A','K','E'
CALL XYINIT(B, 100)
CALL CHSIZE(0.4, 90.0)
6   FORMAT(I3)
7   IC=0
1   READ(6,6) IF
      DO 20 I=1, 1024
20   Y(I)=0.0
11   IC=IC+1
      READ(1,END=10) IA
      READ(1) NPT, (Y(I), I=1, NPT)
      IF(IF.GE. IC) GO TO 8
      REWIND 1
      GO TO 7
8   IF(IF.NE. IC) GO TO 11
      CALL IXYPT(230, 0, 0)
      CALL XYCHAR(IA, 20)
      CALL IXYPT(486, 0, 0)
      IF(IA(70).EQ. TEST) GO TO 2
      CALL XYCHAR(IQ, 10)
      GO TO 3
2   CALL XYCHAR(IX, 9)
3   CALL IXYPT(500, 0, 0)
      CALL IXYPT(2190, 0, 1)
      DO 15 I=1, 1024
15   Z(I)=Y(I)
      CALL DCT(512, 1024, 2048, 11, MM, X, Y, -1, 0)
      XMAX=Y(1)
      XMIN=XMAX
      DO 4 I=2, 512
      IF(XMIN.GT. Y(I)) XMIN=Y(I)
4     IF(XMAX.LT. Y(I)) XMAX=Y(I)
      XS=1690.0/(XMAX-XMIN)
      N=2190.0+XMIN*XS
      CALL IXYPT(N, 0, 0)
      CALL IXYPT(N, 4000, 1)
      IXX=0
      IY=2190.0+(XMIN-Y(1))*XS
      CALL IXYPT(IY, IXX, 0)
      DO 5 I=2, NPT
      IXX=4*I-4
      IY=2190.0+(XMIN-Y(I))*XS
5     CALL IXYPT(IY, IXX, 1)
      CALL IXYPT(2390, 0, 0)
      CALL IXYPT(4090, 0, 1)
      DO 9 I=1, 1024
      X(1,I)=Z(I)
9     X(2,I)=0.0
      DO 14 I=1025, 2048

```

FORTRAN V004A

00:00:00

21-SEP-74

PAGE

2

```

        X(1, I)=0. 0
14      X(2, I)=0. 0
        CALL FWT(X, 1024)
        XMAX=X(1, I)
        XMIN=XMAX
        DO 12 I=1, 1024
        IF(XMIN. GT. X(1, I)) XMIN=X(1, I)
12      IF(XMAX. LT. X(1, I)) XMAX=X(1, I)
        XS=1690. 0/(XMAX-XMIN)
        N=4090. 0+XMIN*XS
        CALL IXYPT(N, 0, 0)
        CALL IXYPT(N, 4095, 1)
        N=4090. 0+(XMIN-X(1, I))*XS
        CALL IXYPT(N, 0, 0)
        DO 13 I=2, 1024
        IXX=4*I-4
        IY=4090. 0+(XMIN-X(1, I))*XS
13      CALL IXYPT(IY, IXX, 1)
        CALL IXYPT(0, 4095, 0)
        CALL IXYPT(0, 0, 0)
        CALL IXYPT(4095, 0, 0)
        CALL IXYPT(4095, 4095, 0)
        GO TO 1
10      CALL XYEND
        CALL EXIT
        END

```

ROUTINES CALLED:

XYINIT, CHSIZE, IXYPT, XYCHAR, DCT, FWT, XYEND
EXIT

SWITCHES = /ON, /SU

BLOCK	LENGTH
MAIN.	13316 (064010)*

##COMPILER ---- CORE##		
PHASE	USED	FREE
DECLARATIVES	00366	05529
EXECUTABLES	00937	04958
ASSEMBLY	01472	07340

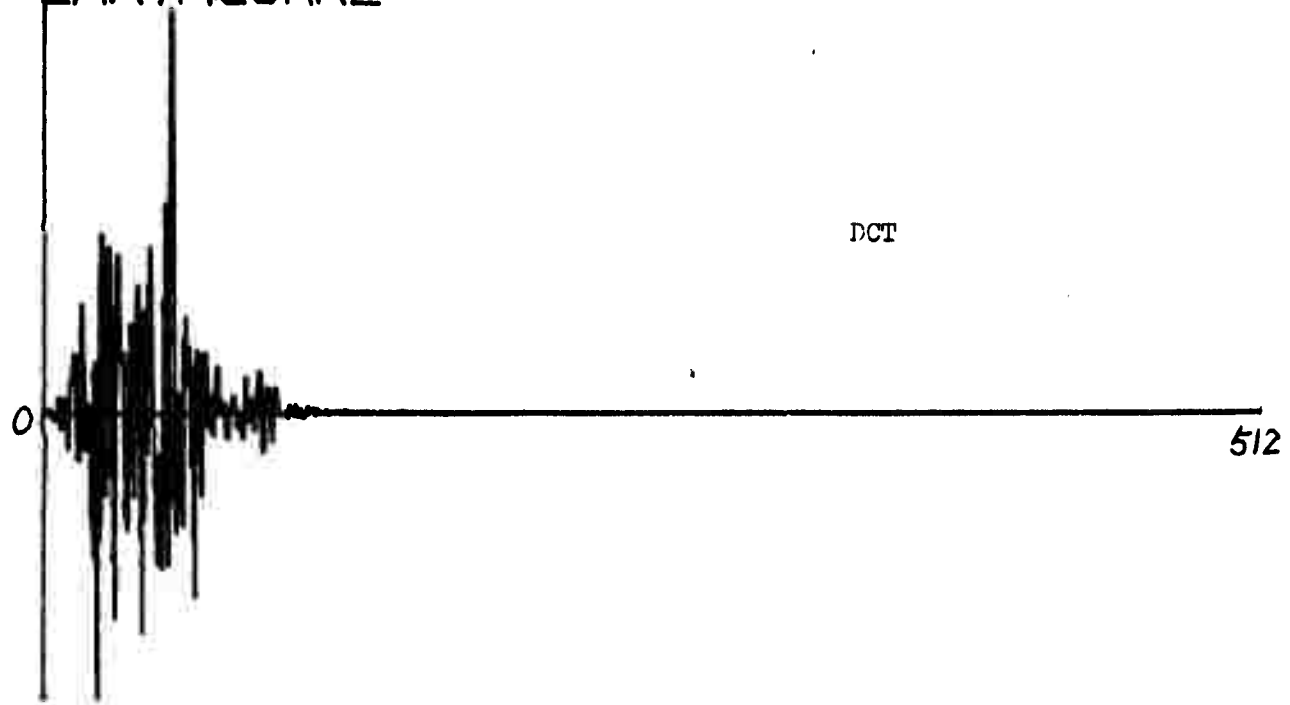
Attachment #4

**Plot of DCT and WHT for
ACDA Seismic Signature Data Base**

Q002

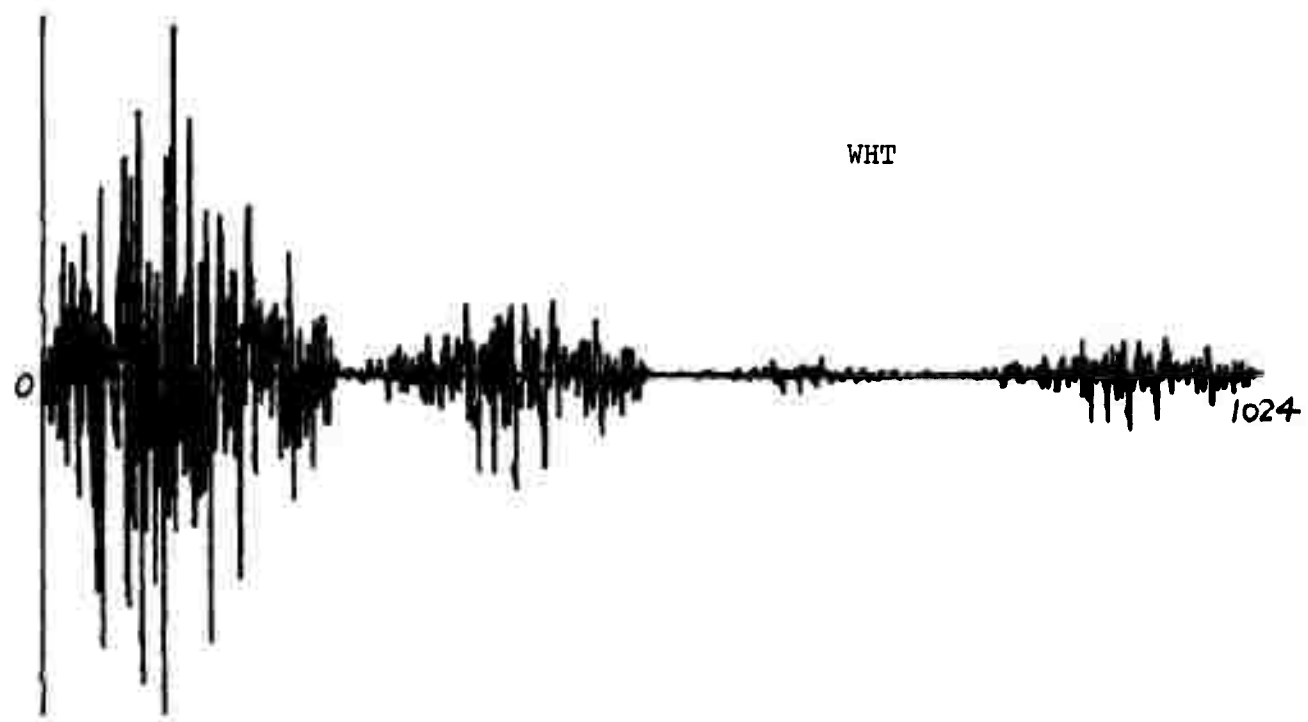
EVENT NUMBER 2019

EARTHQUAKE



DCT

512



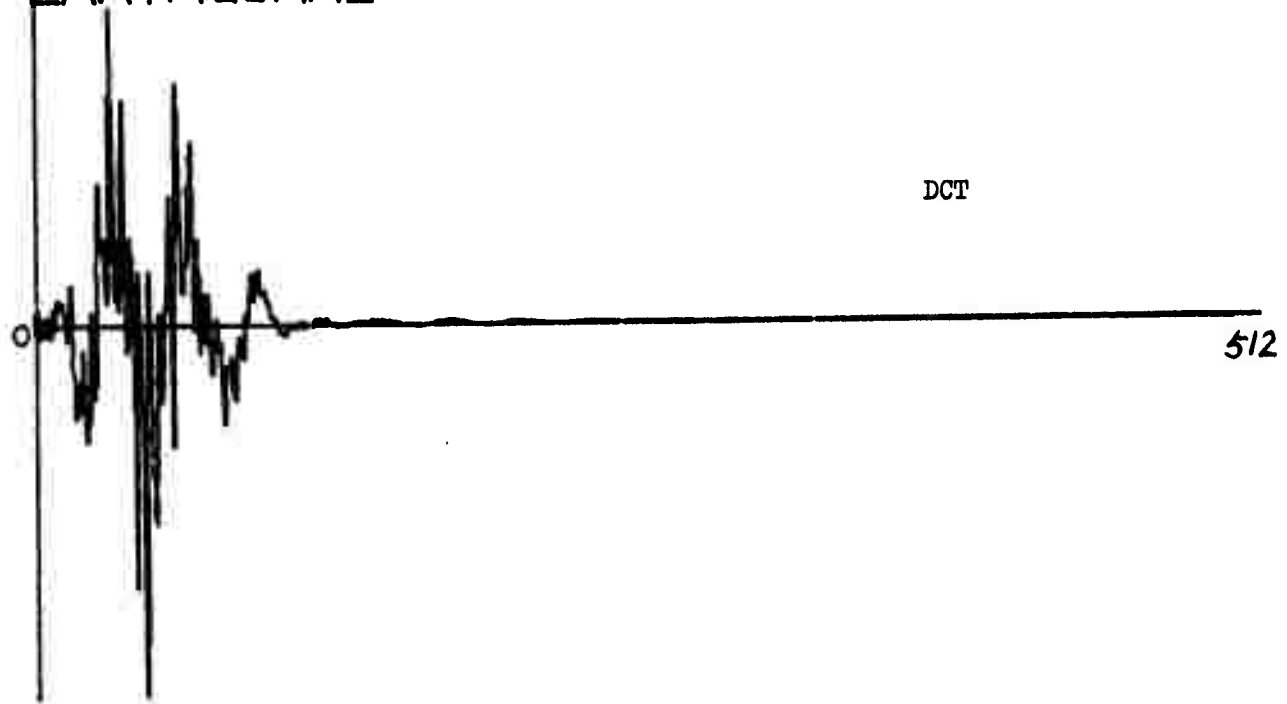
WHT

1024

Q004

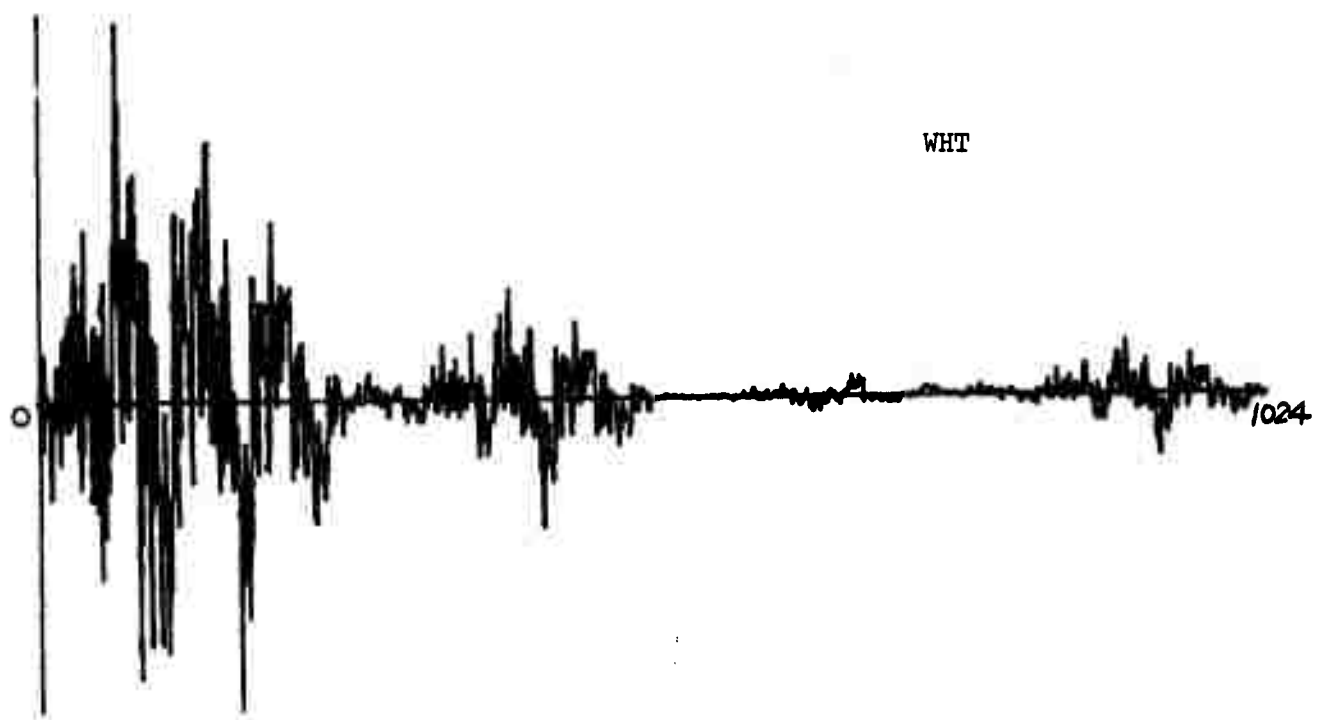
EVENT NUMBER 2010

EARTHQUAKE



DCT

512

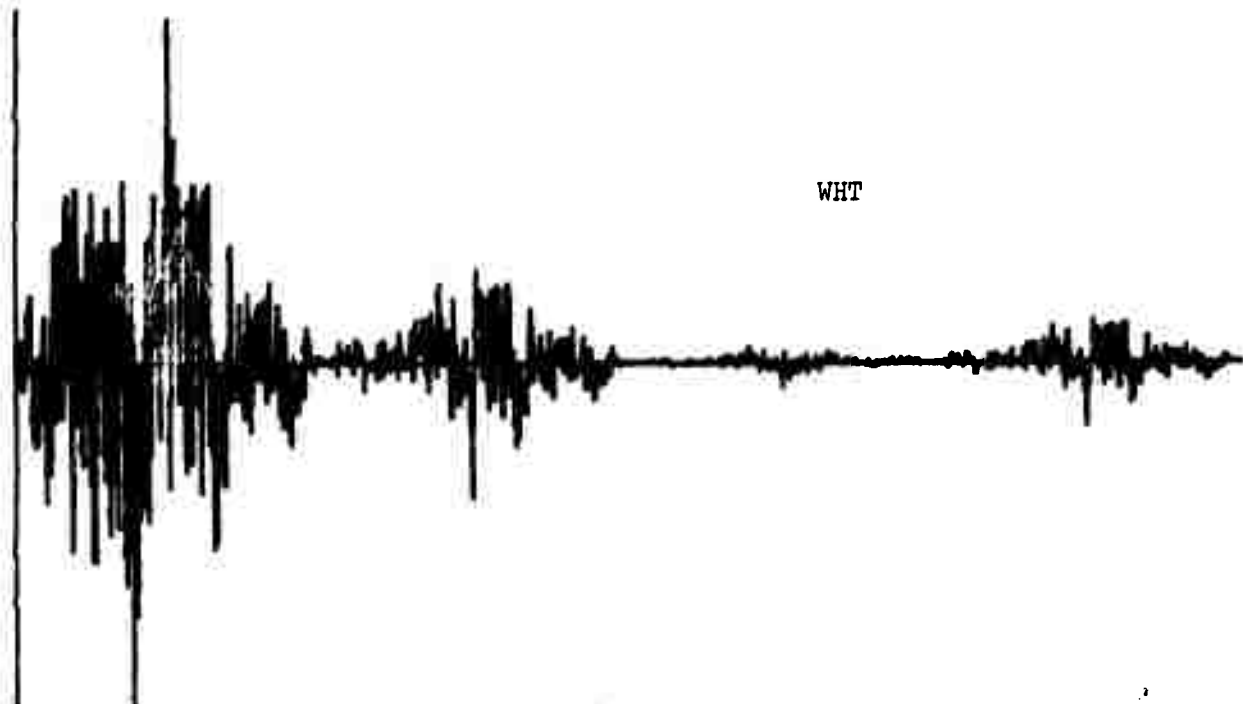
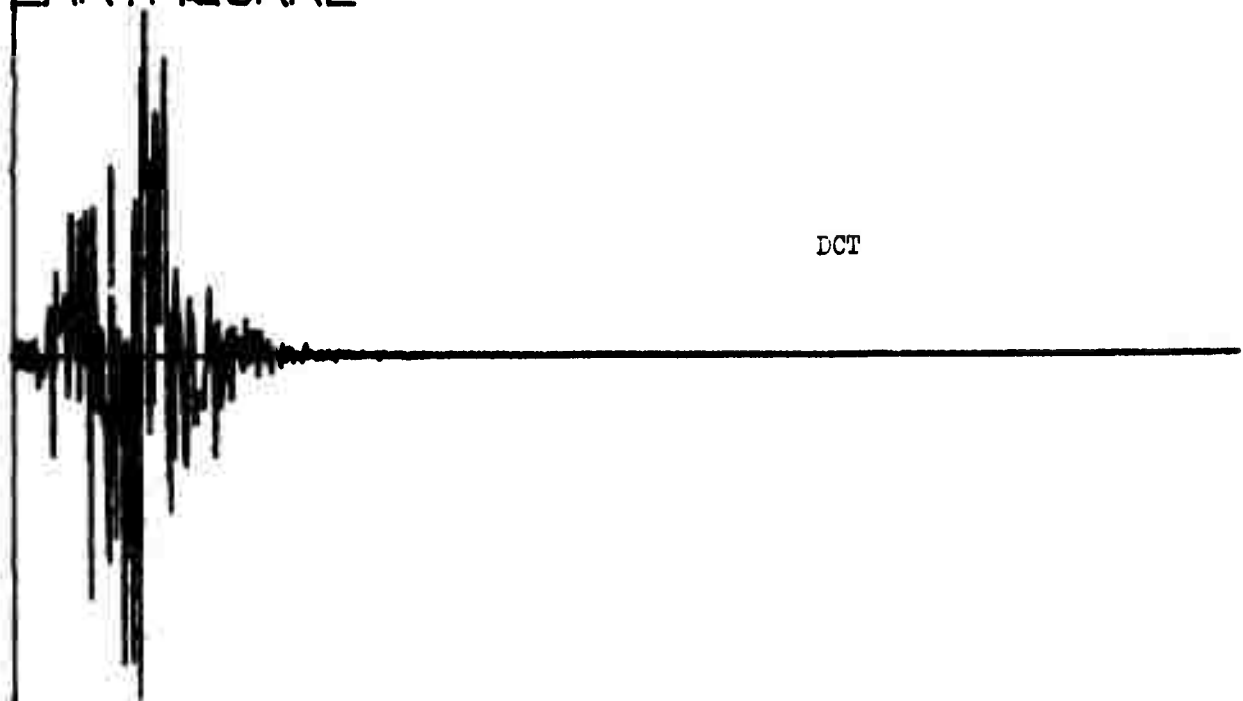


WHT

1024

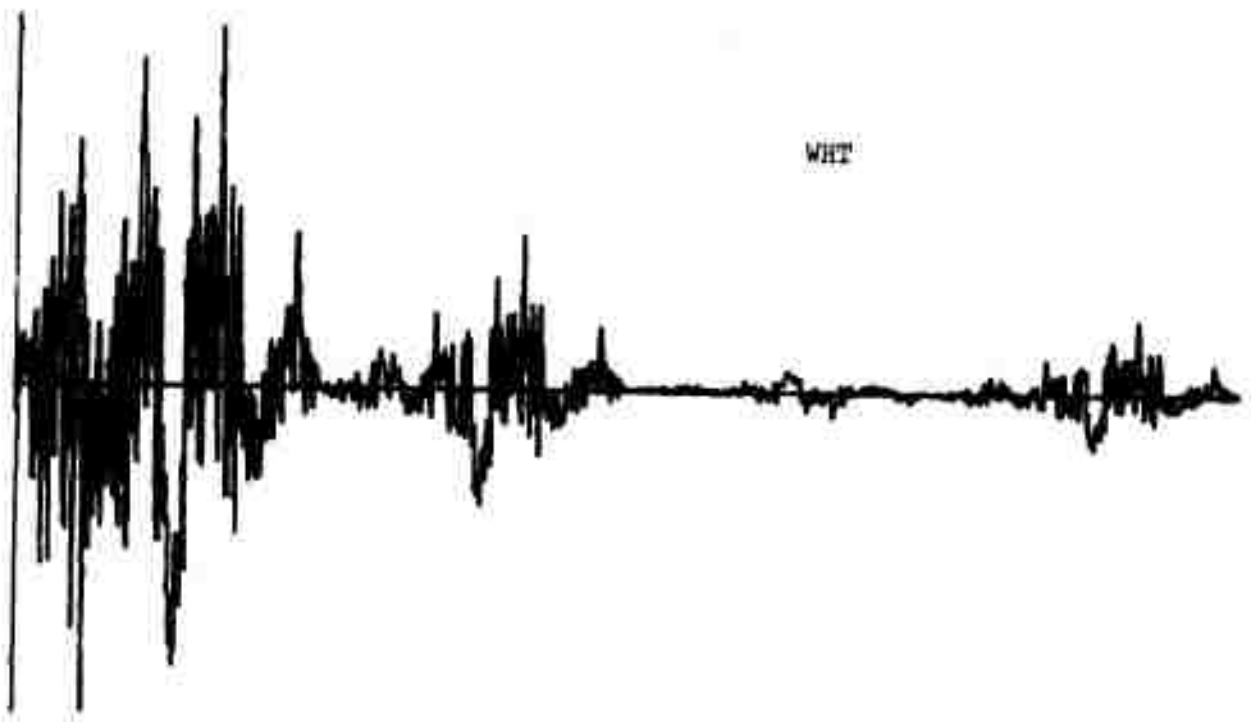
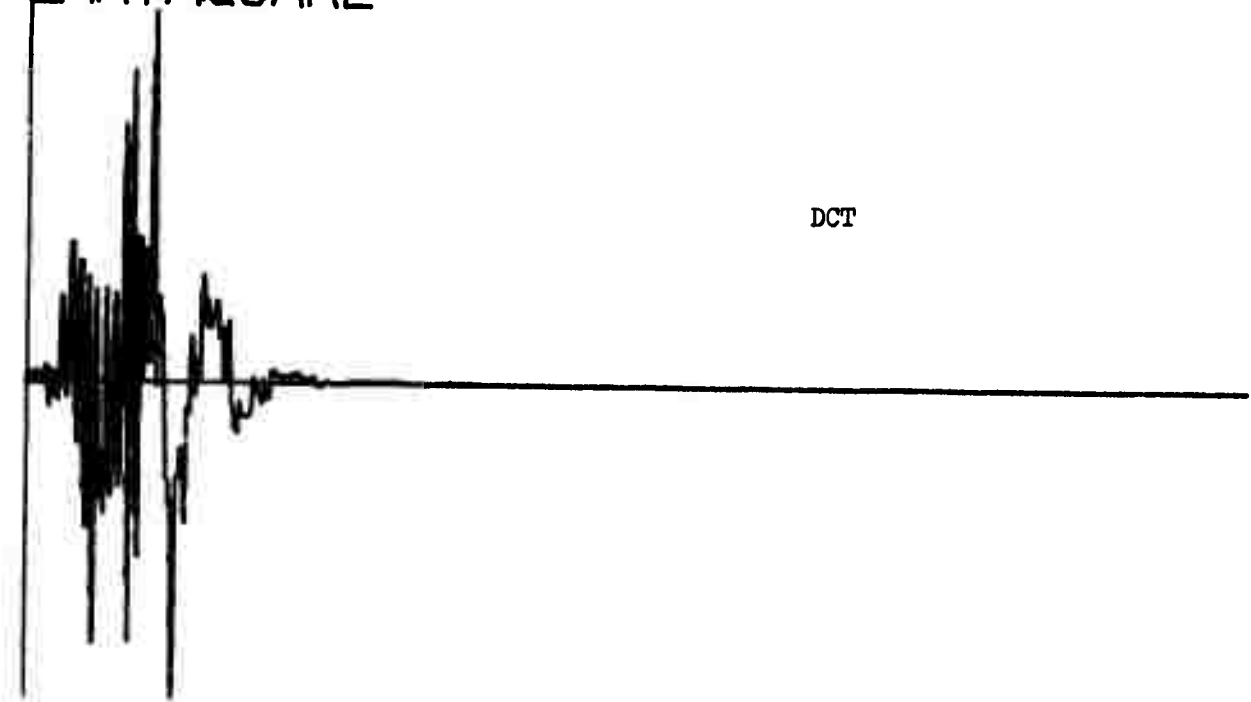
Q006

EVENT NUMBER 2029
EARTHQUAKE



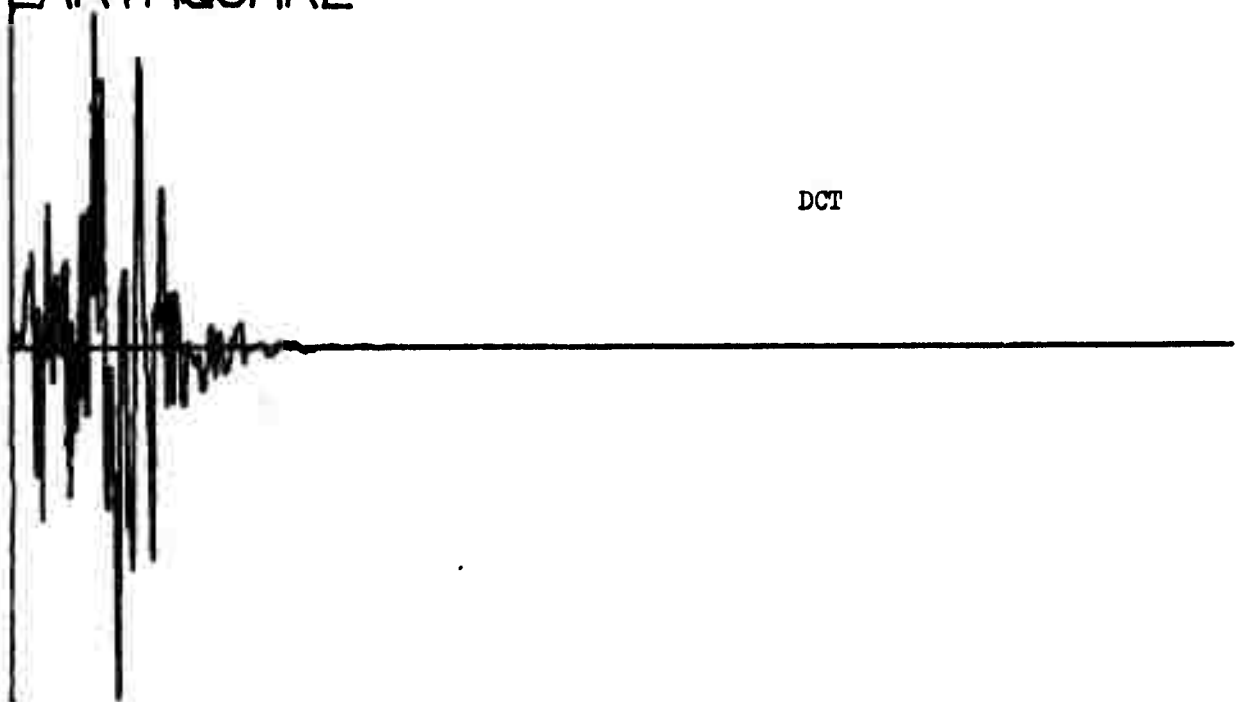
Q008

EVENT NUMBER 2030
EARTHQUAKE

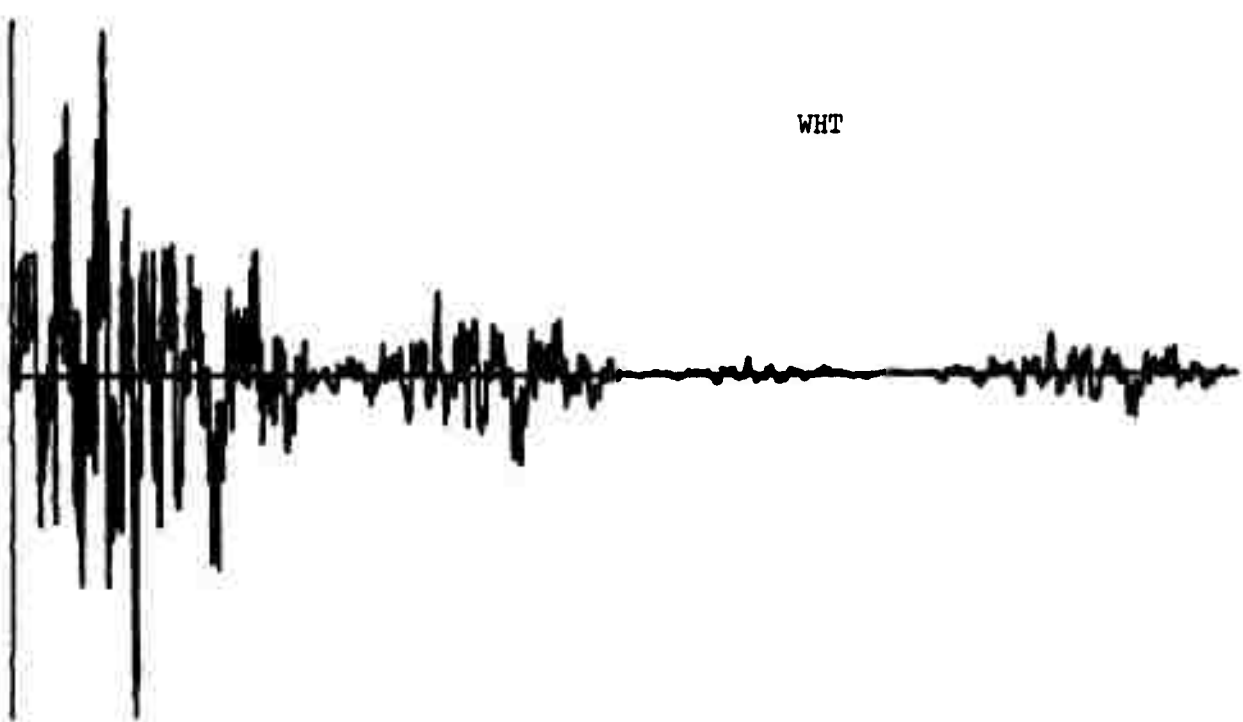


Q010

EVENT NUMBER 2031
EARTHQUAKE



DCT

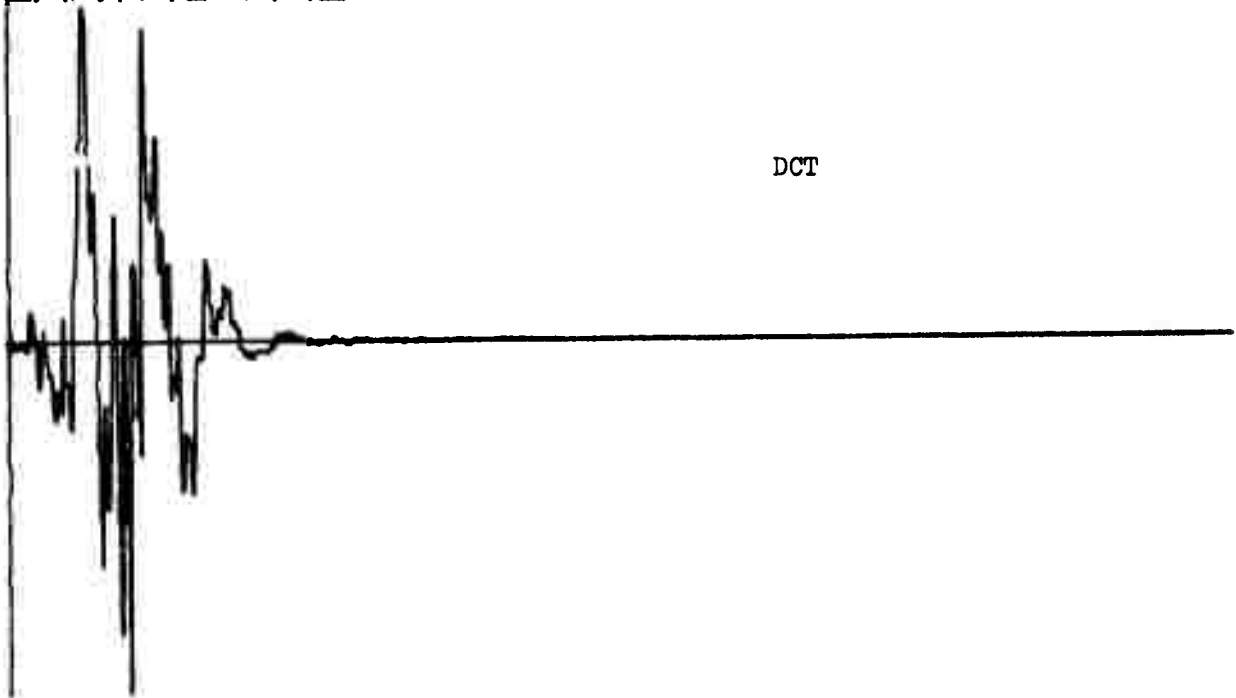


WHT

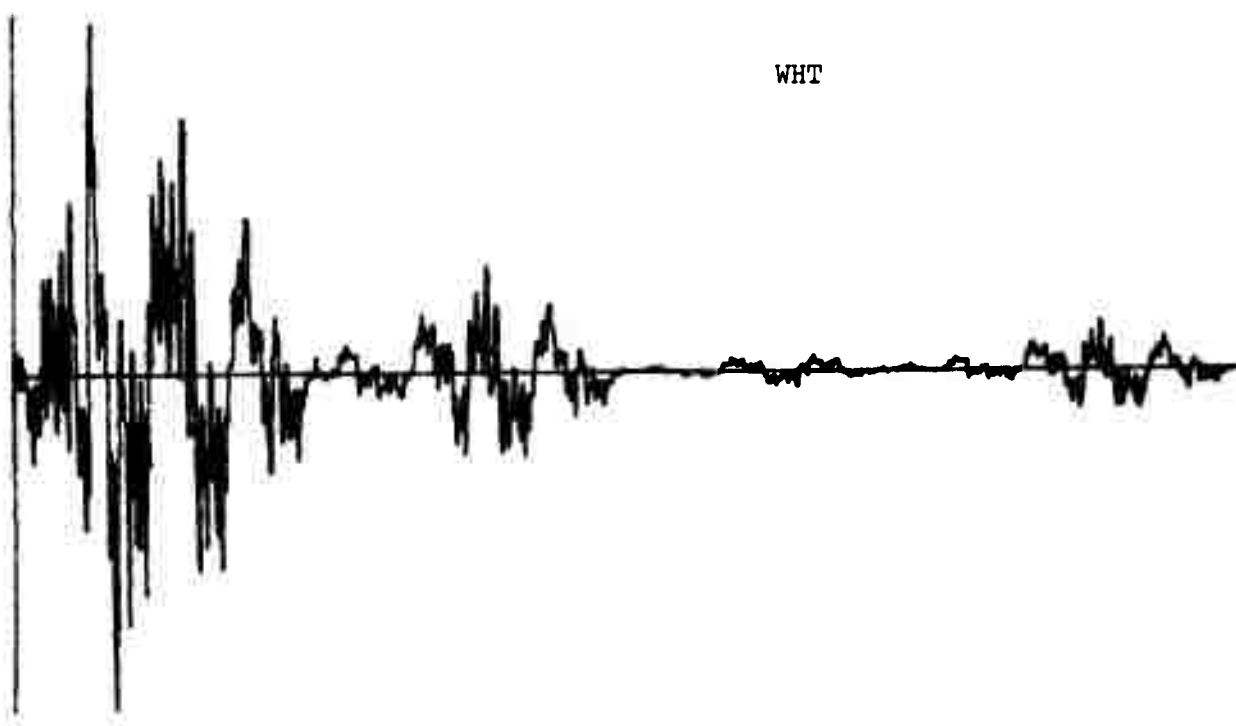
Q012

EVENT NUMBER 2035

EARTHQUAKE



DCT



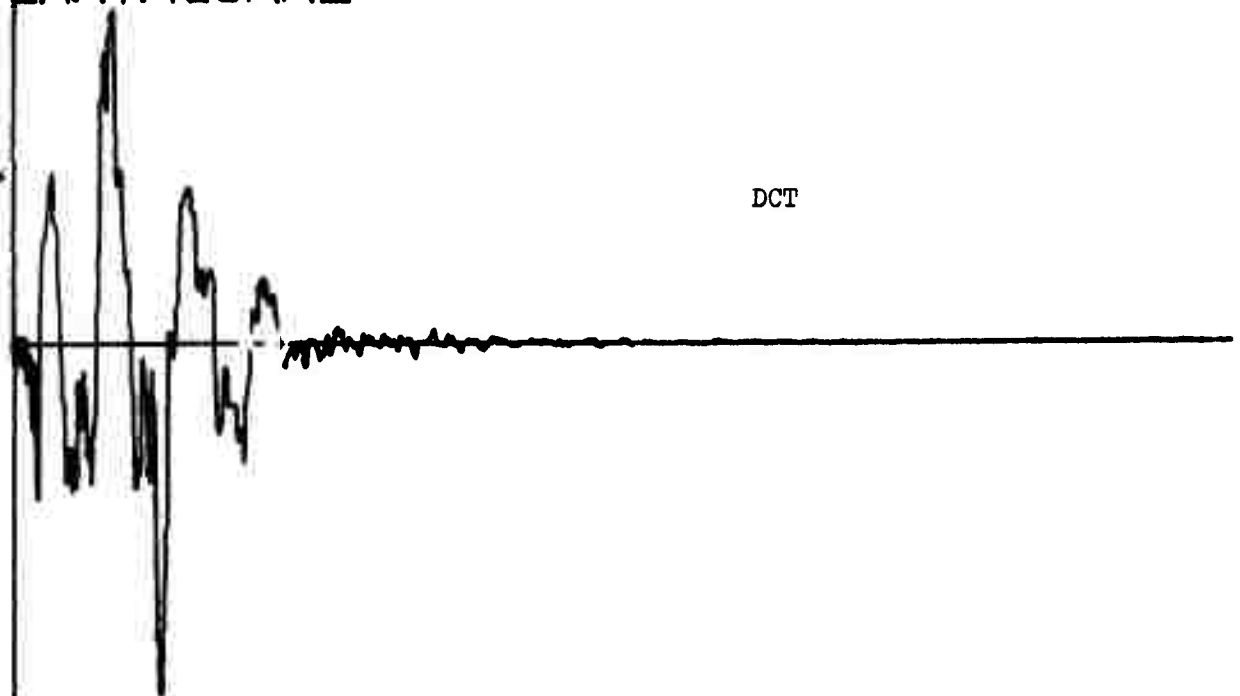
WHT

Q014

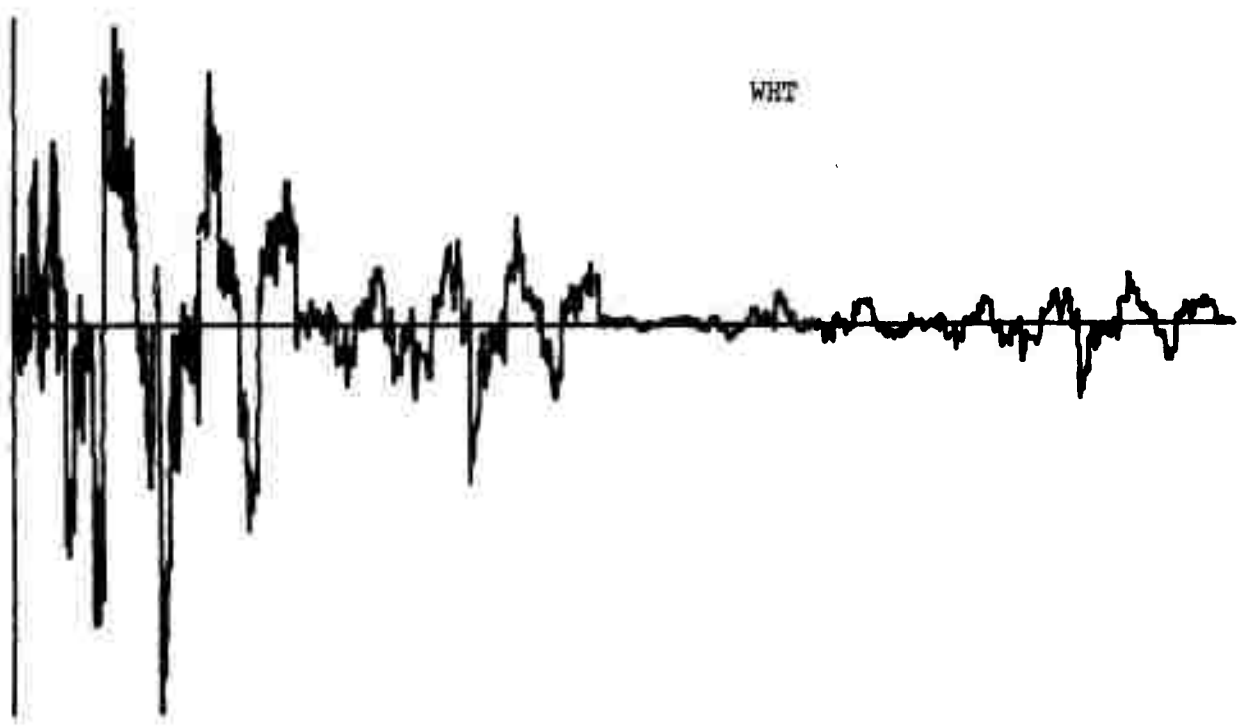
EVENT NUMBER 2024

EARTHQUAKE

DCT

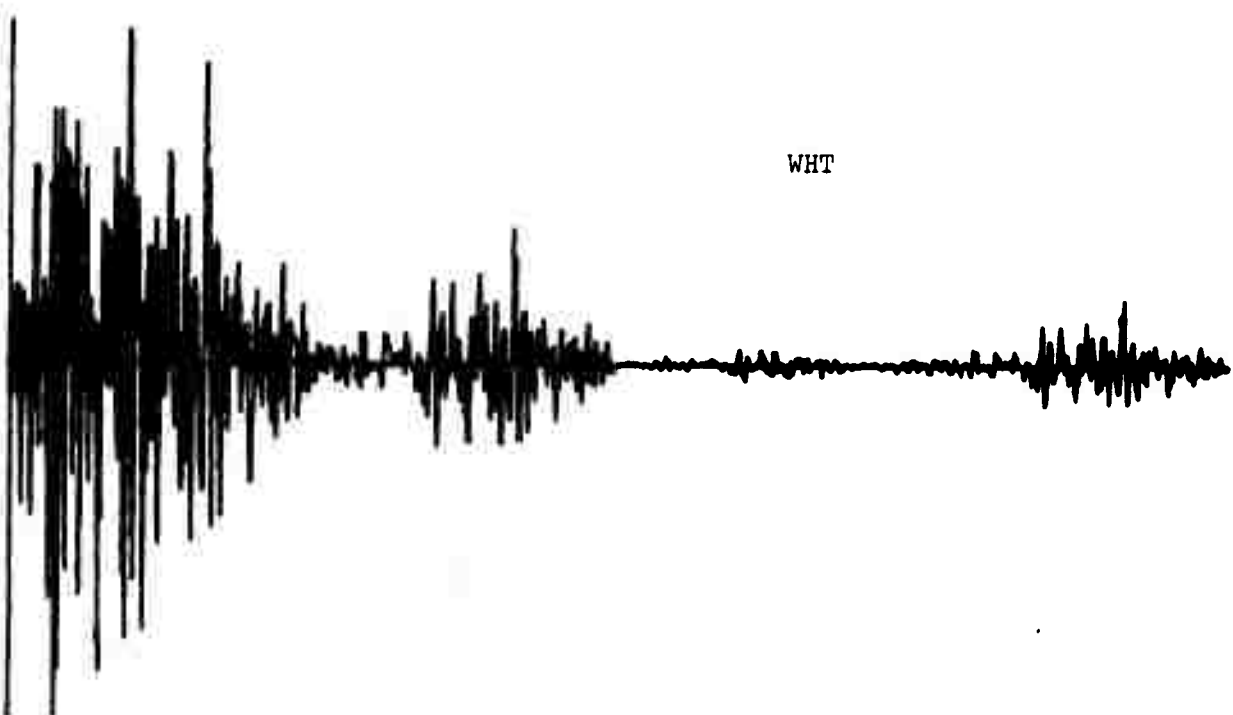
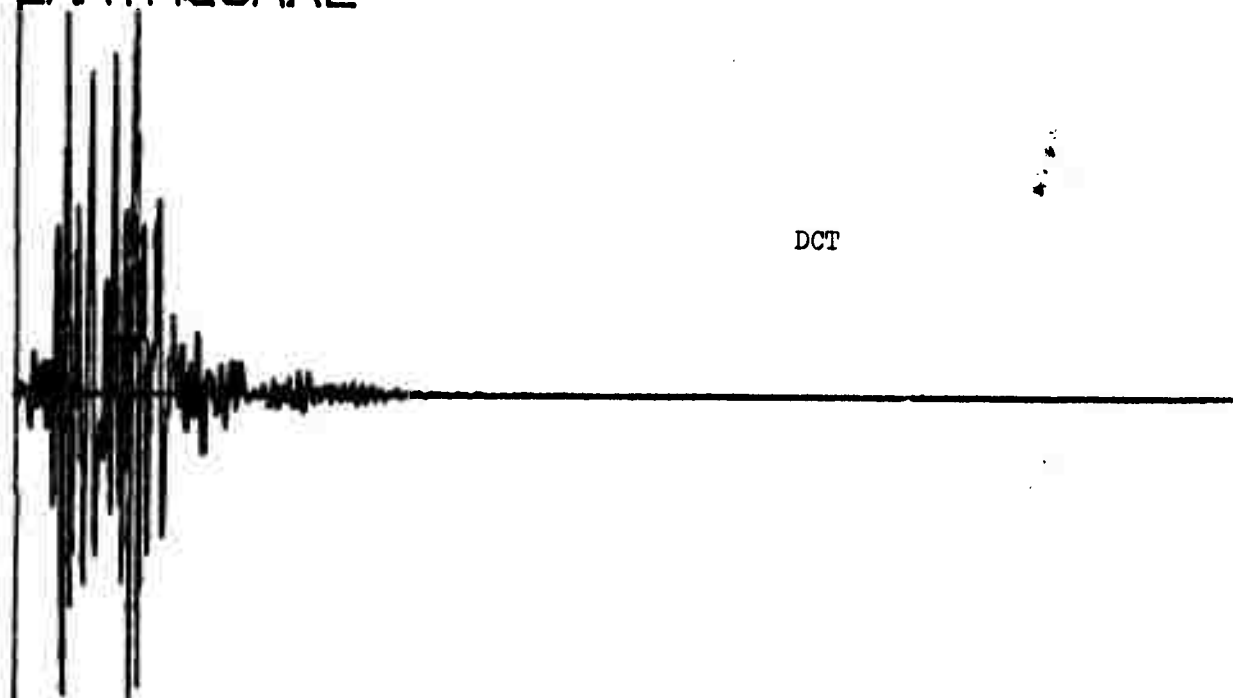


WHT



Q016

EVENT NUMBER 2006
EARTHQUAKE

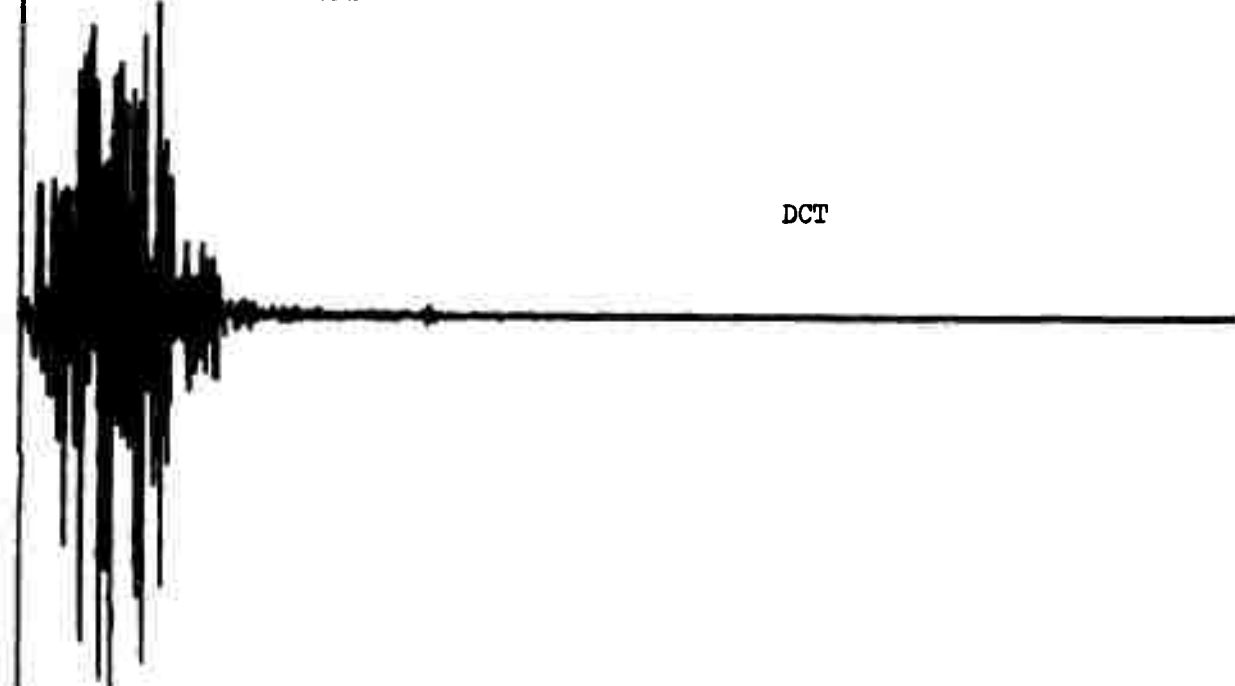


Q018

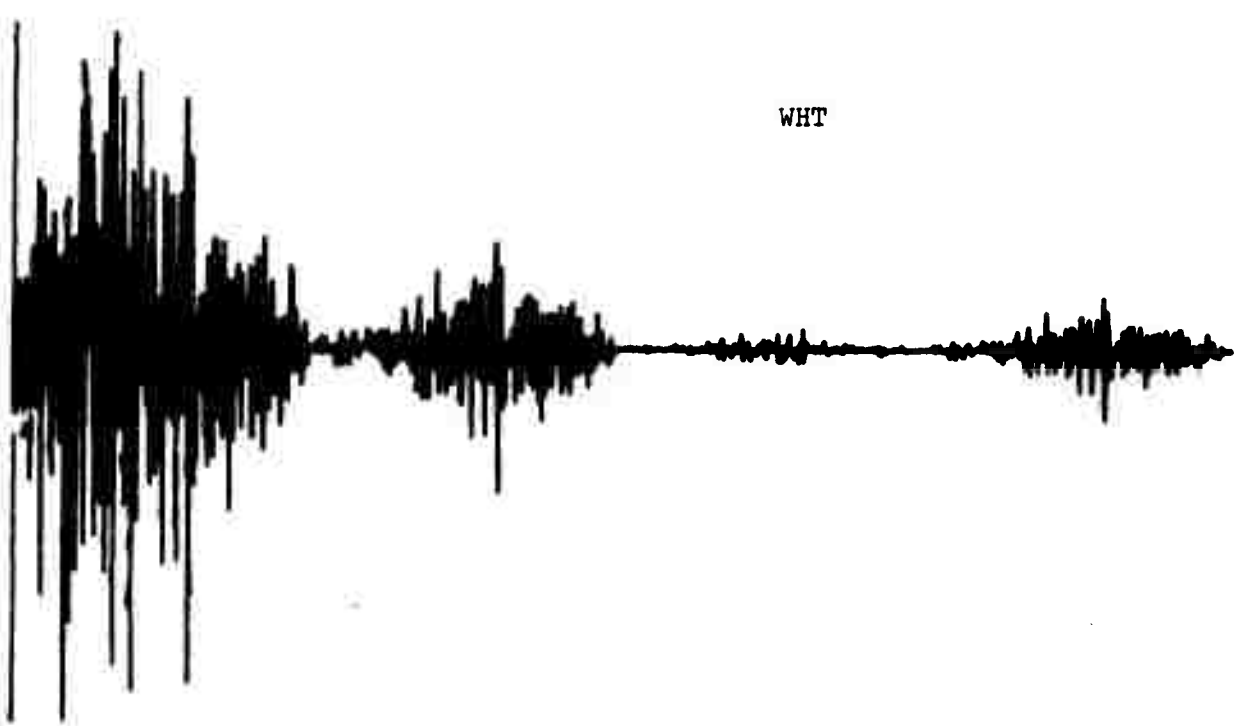
EVENT NUMBER 2017

EARTHQUAKE

DCT



WHT



EVENT NUMBER 2003
EARTHQUAKE

Q020

DCT

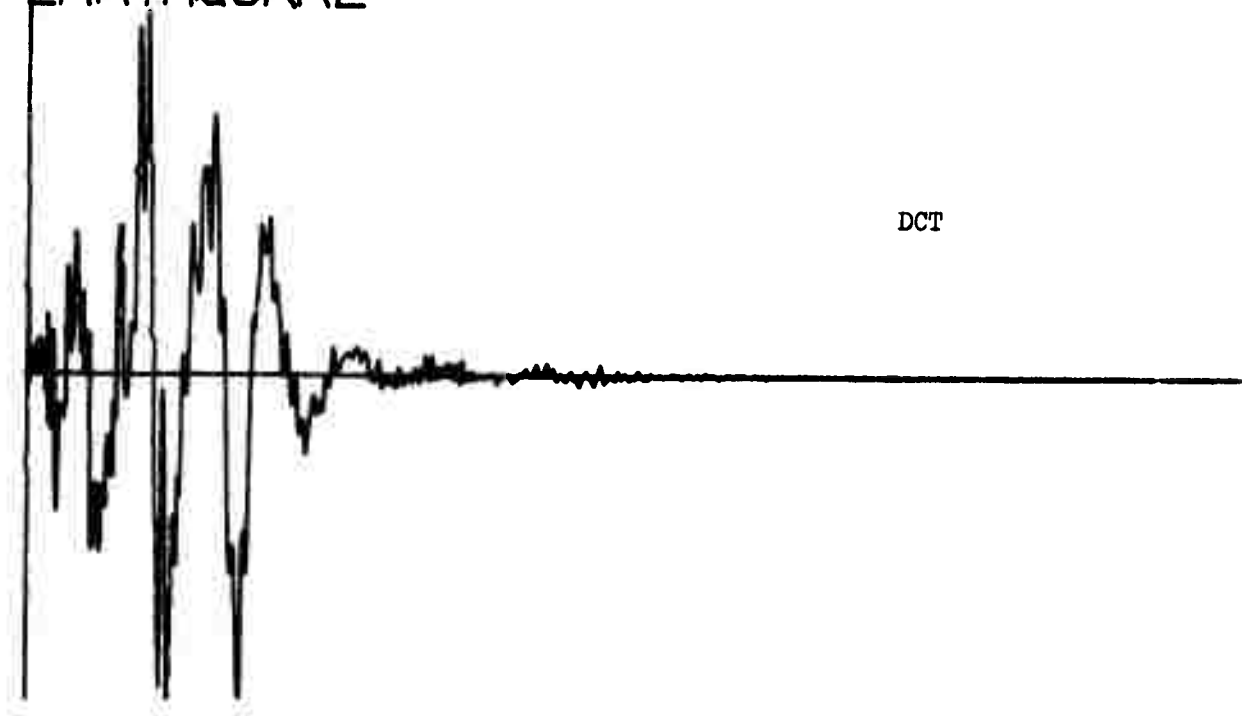
WHT

Q022

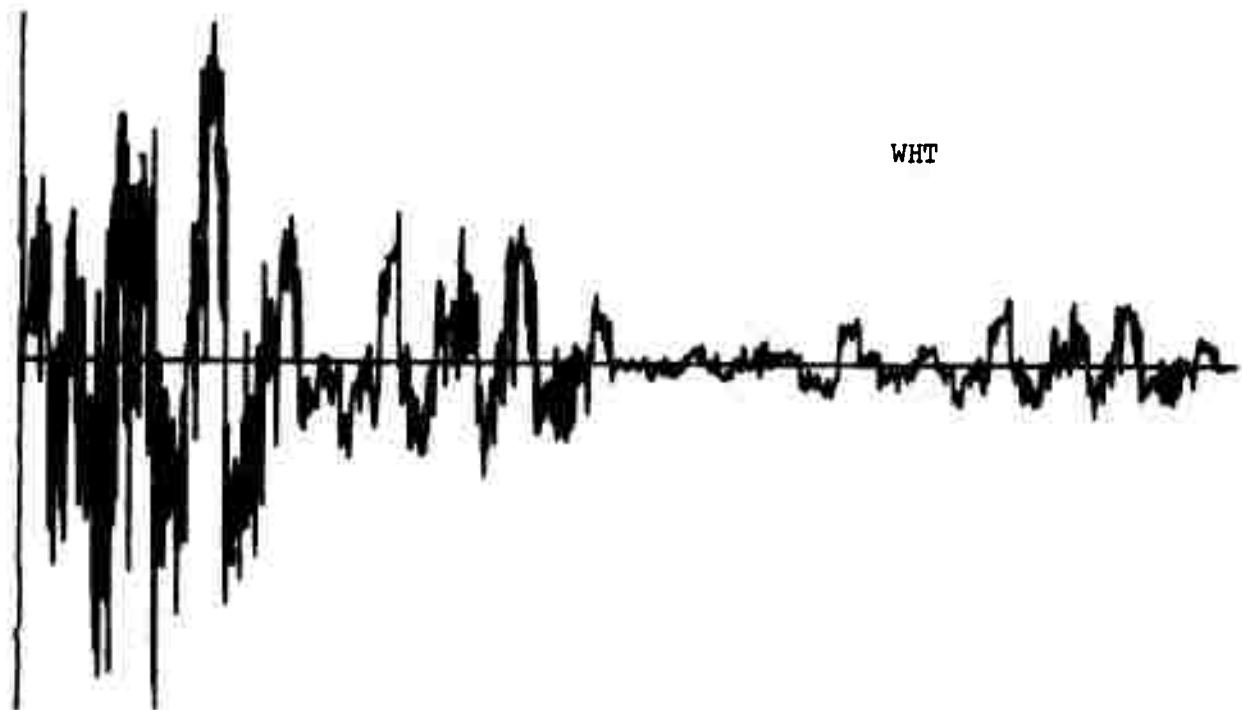
EVENT NUMBER 2011

EARTHQUAKE

DCT



WHT

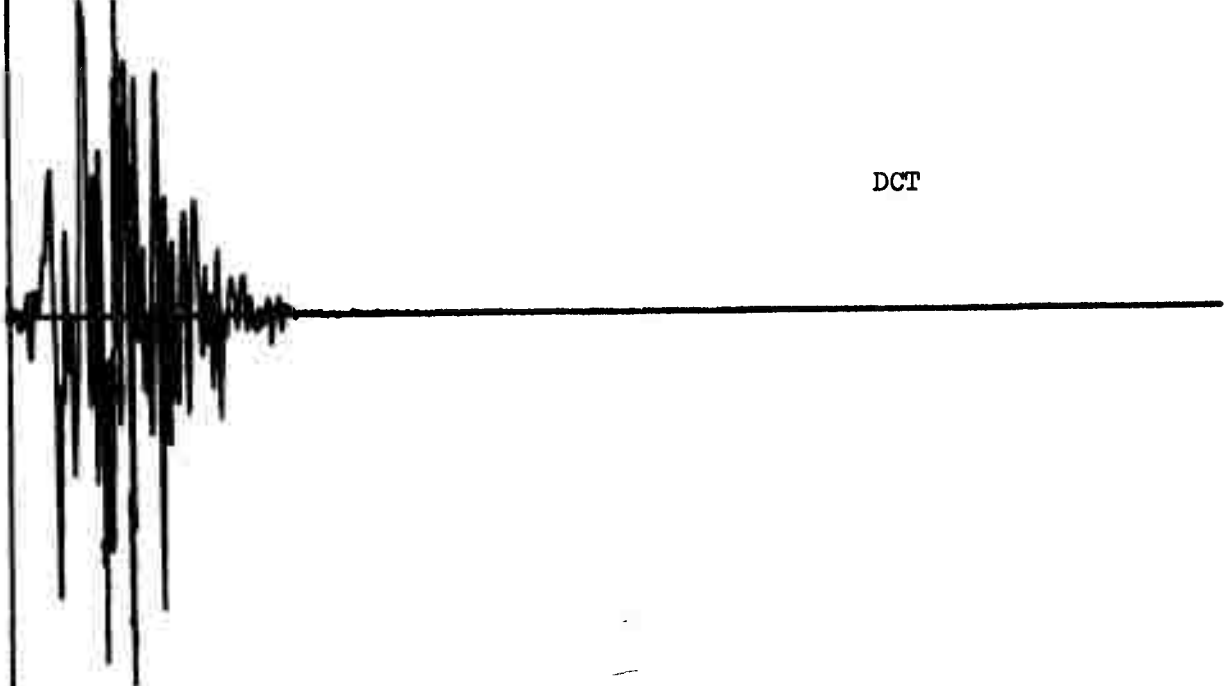


Q024

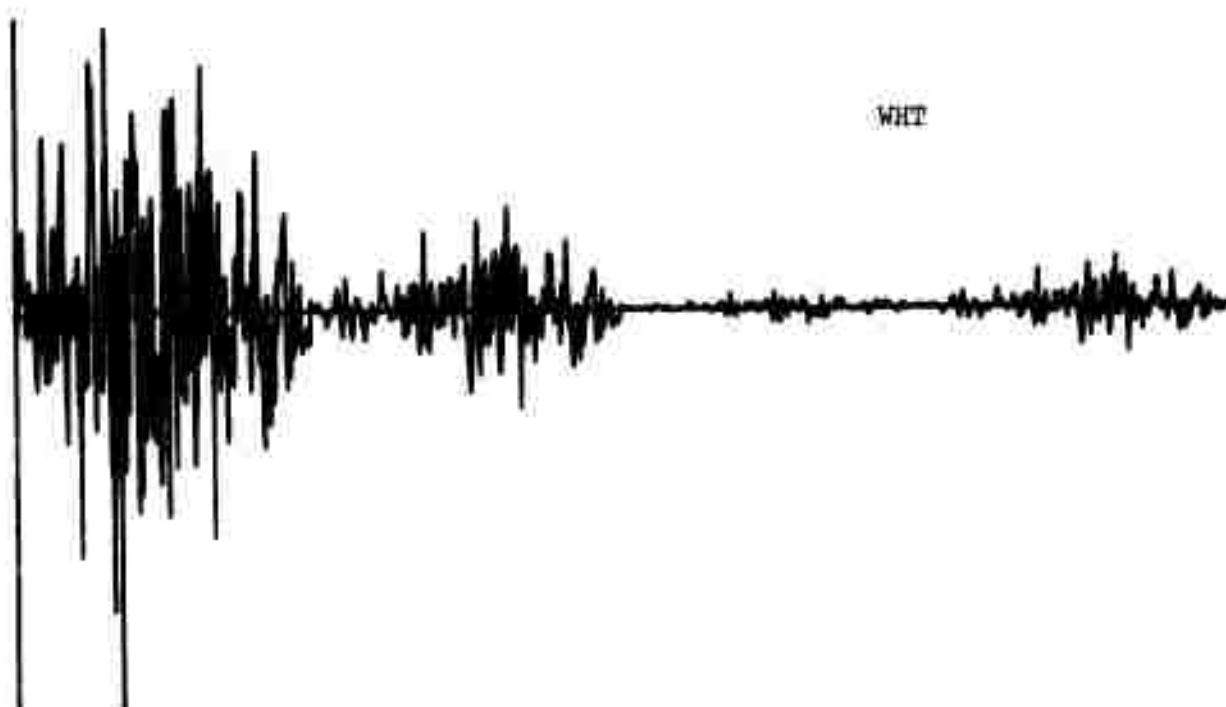
EVENT NUMBER 2012

EARTHQUAKE

DCT



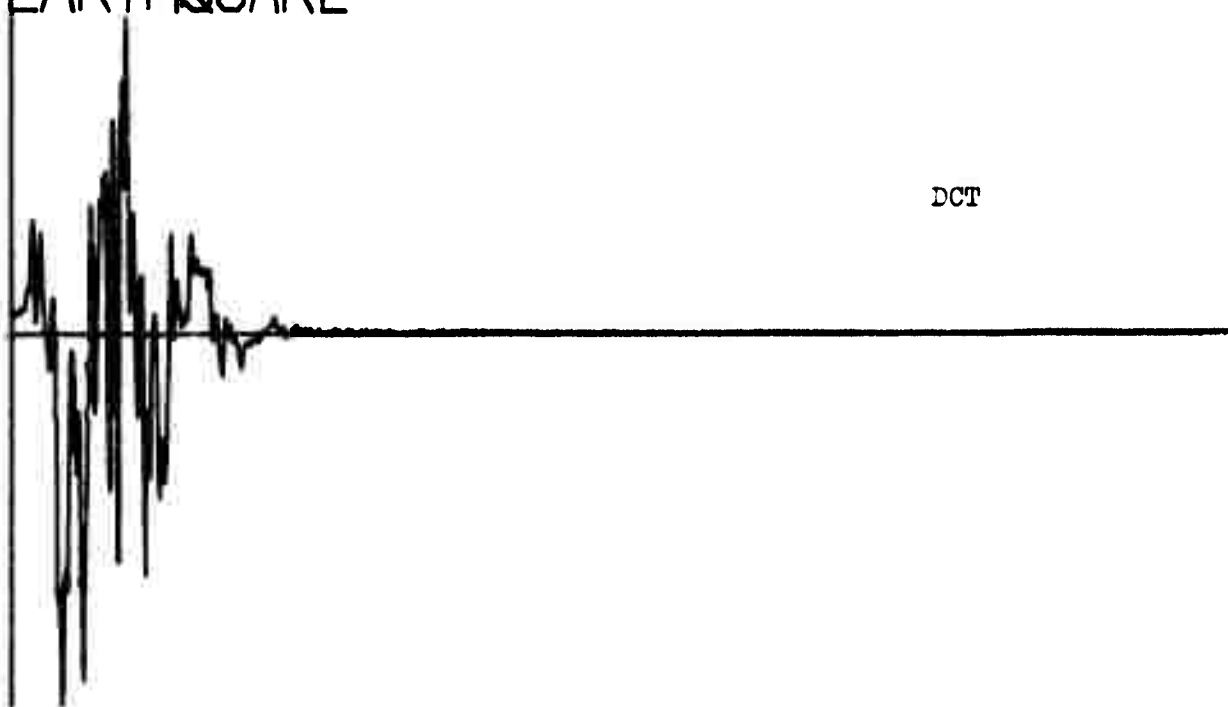
WHT



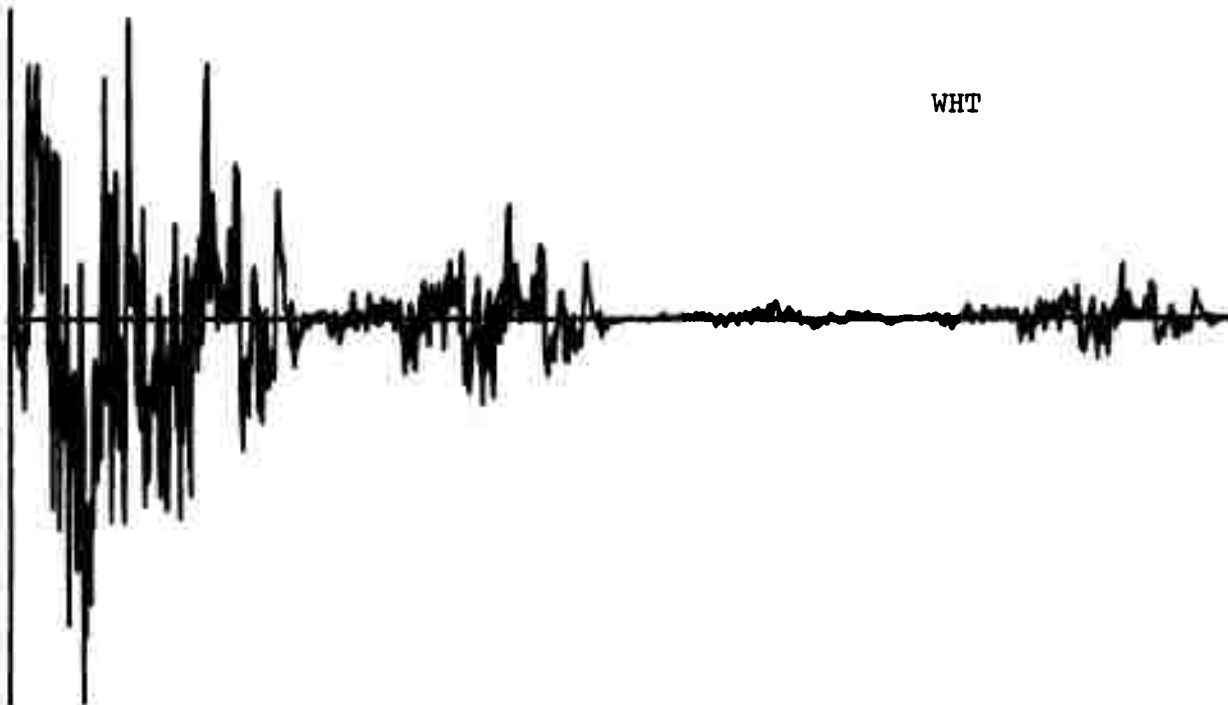
Q026

EVENT NUMBER 2014

EARTHQUAKE



DCT

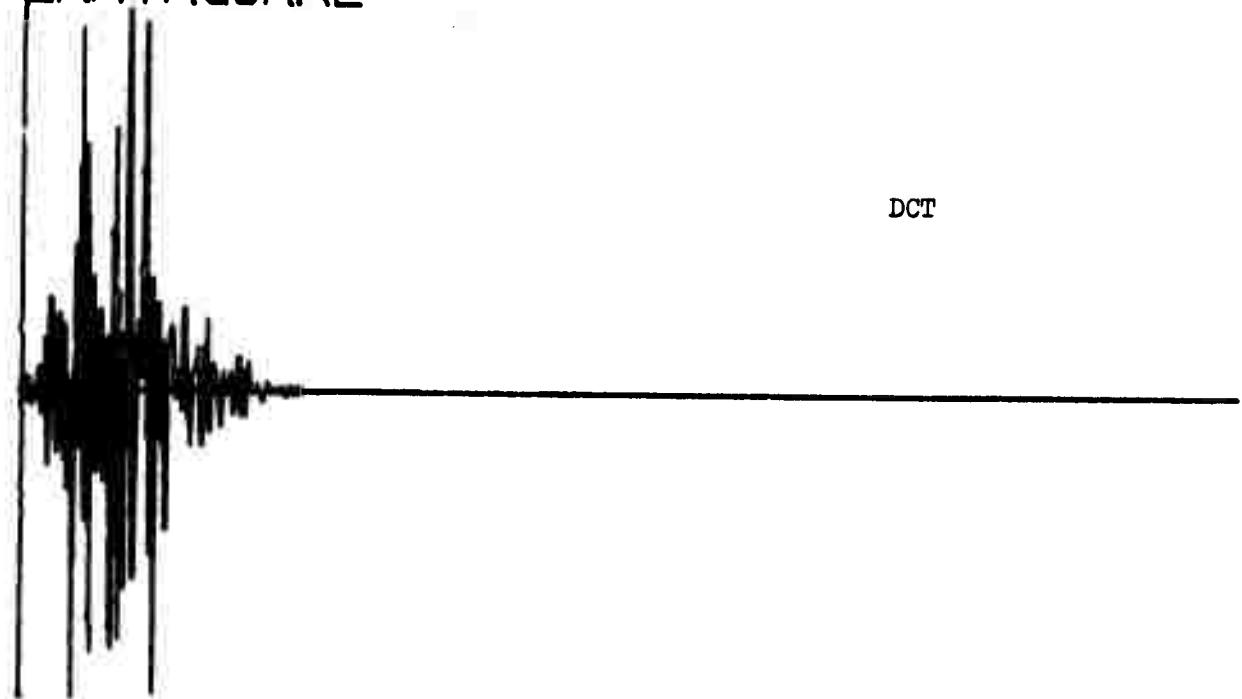


WHT

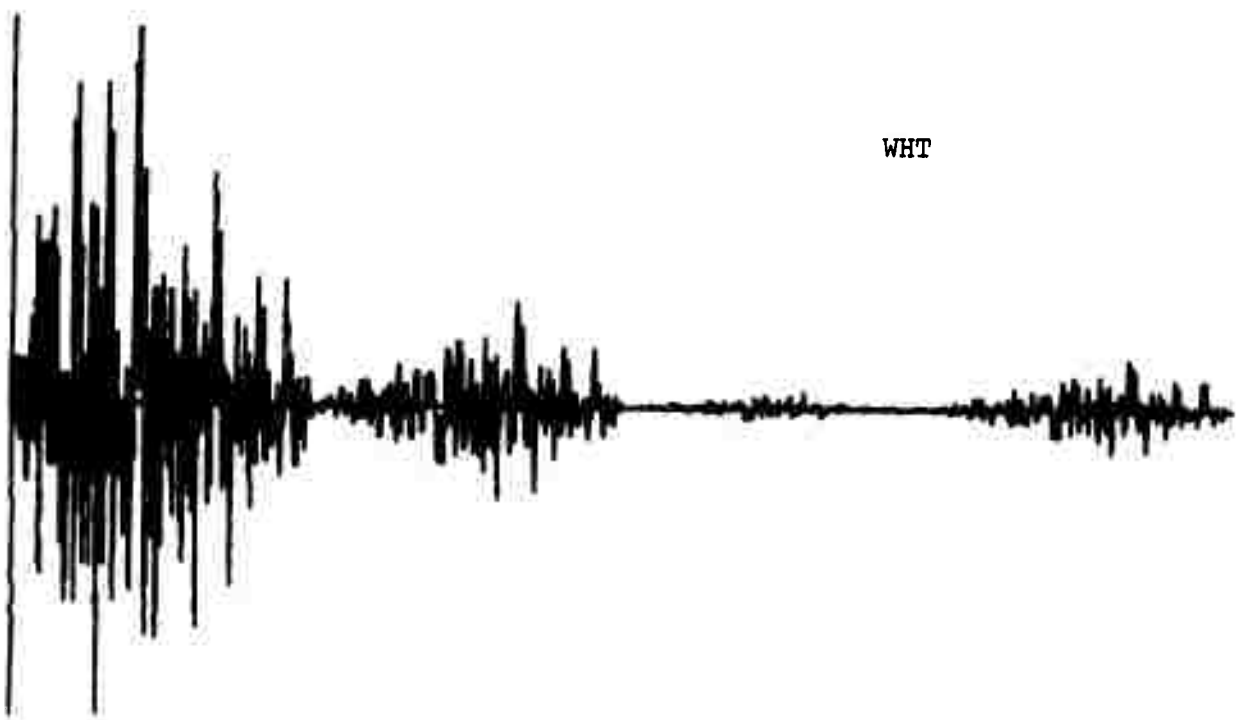
Q028

EVENT NUMBER 2018

EARTHQUAKE



DCT

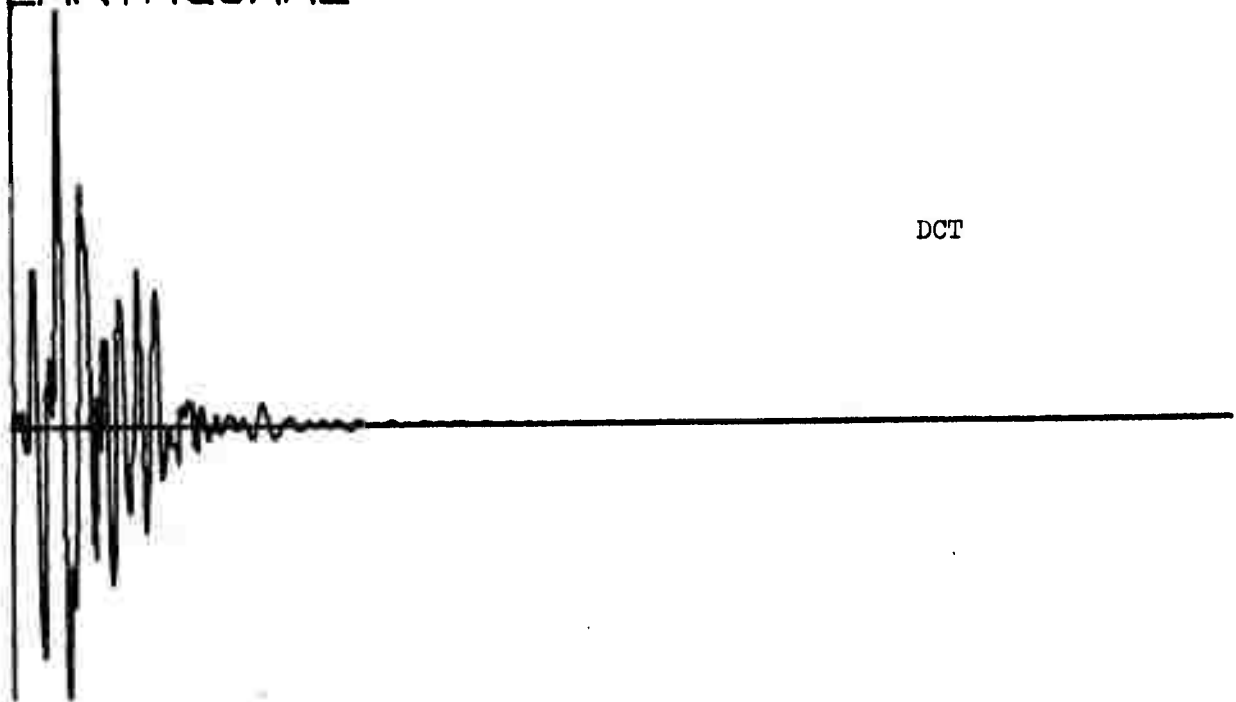


WHT

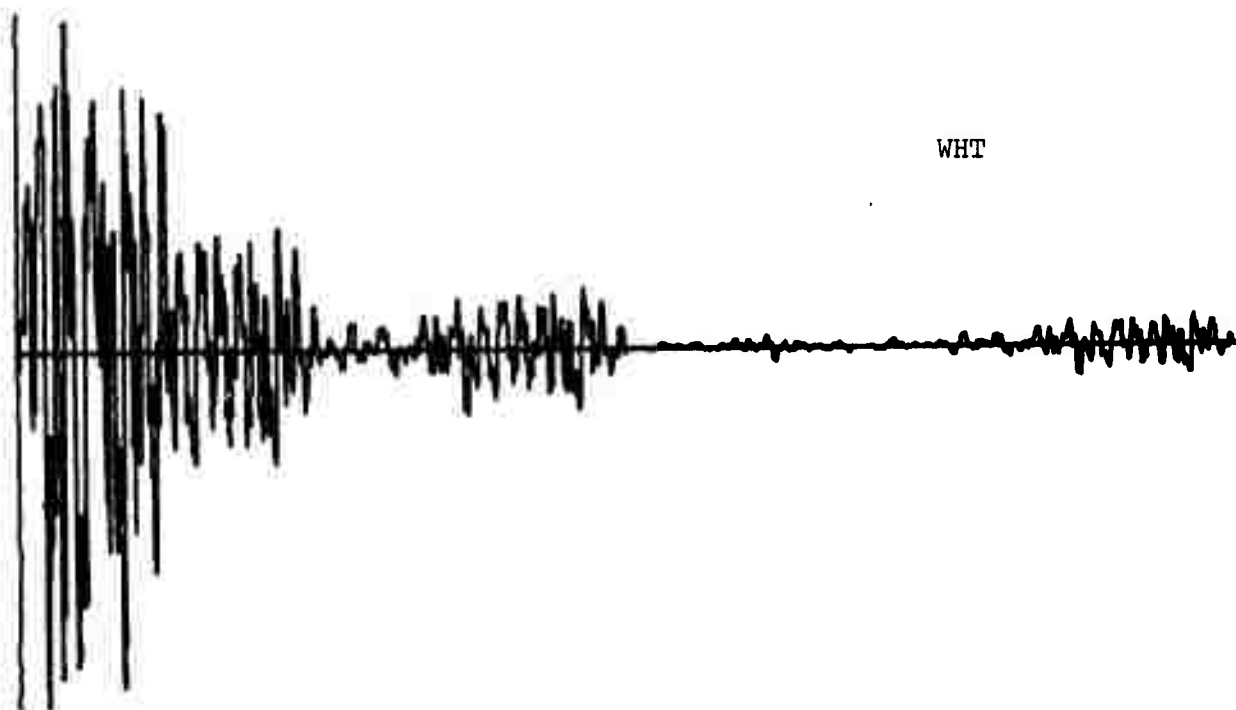
Q030

EVENT NUMBER 2016

EARTHQUAKE



DCT

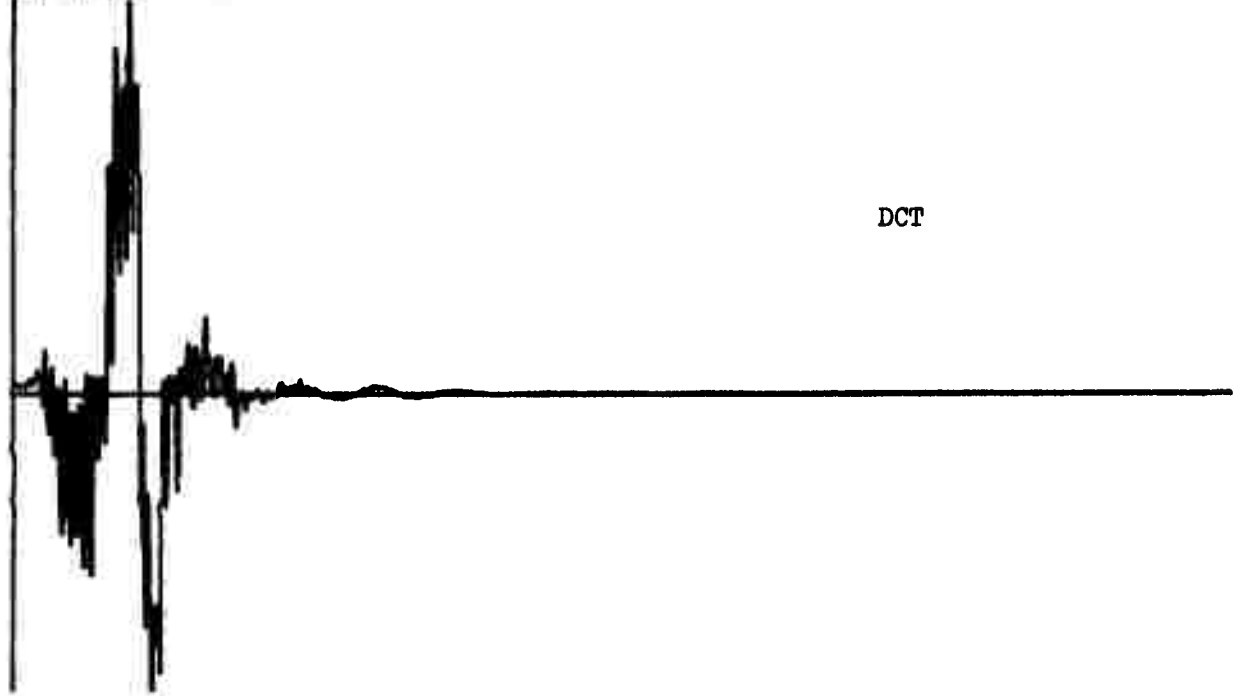


WHT

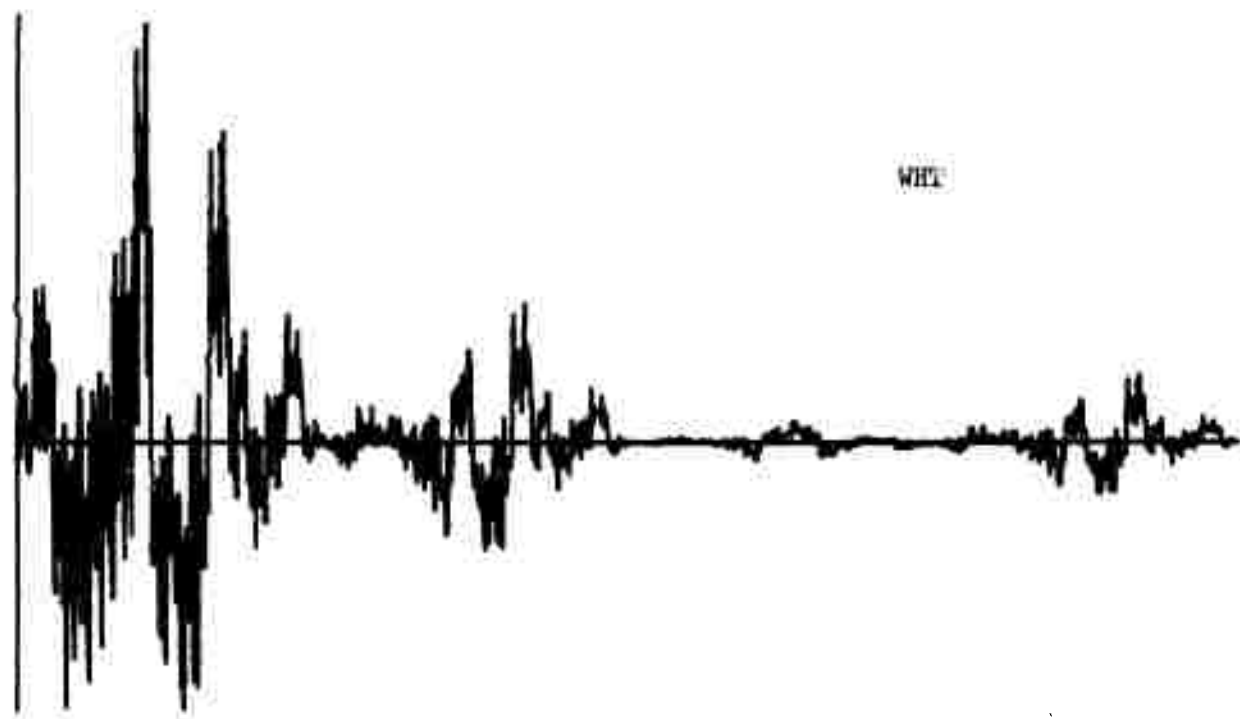
Q032

EVENT NUMBER 2008

EARTHQUAKE



DCT

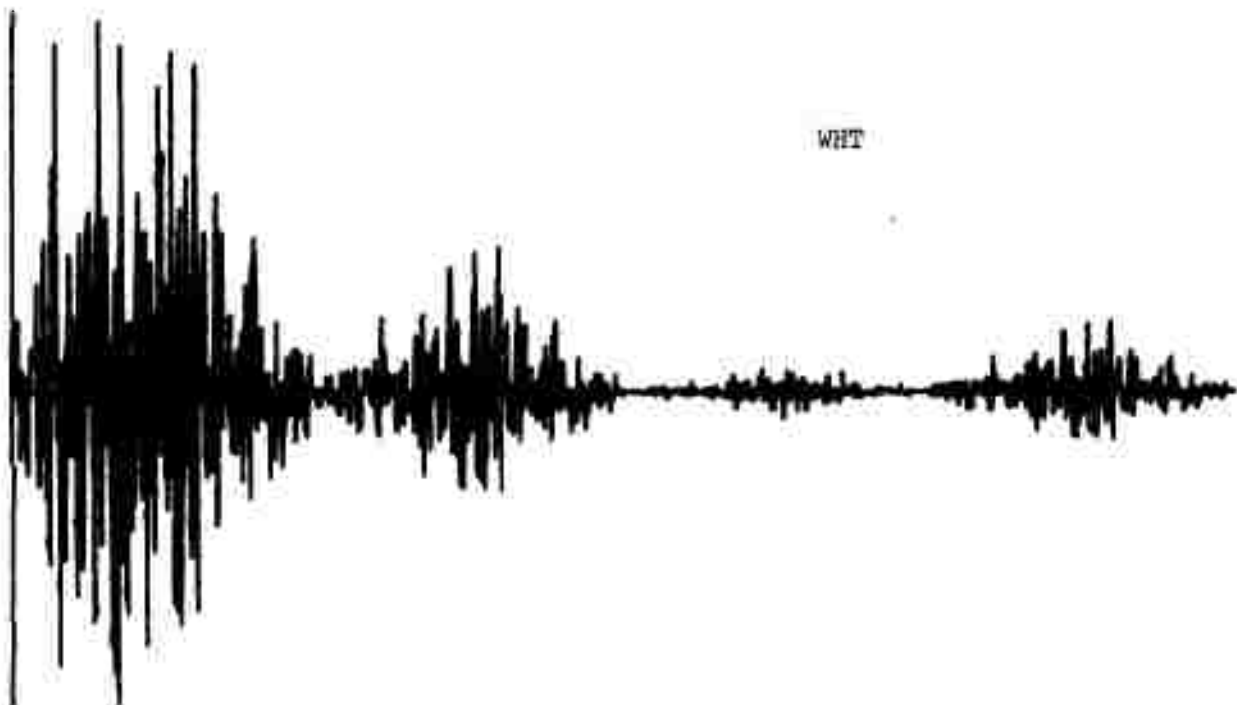
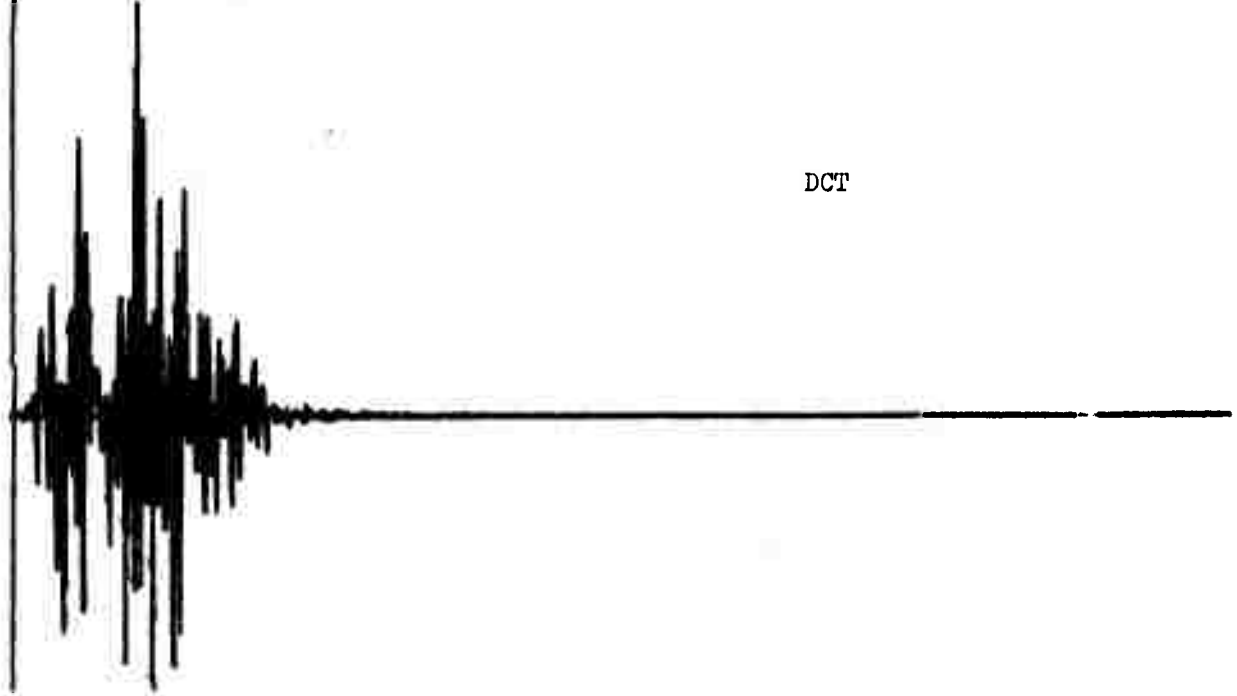


WHT

Q034

EVENT NUMBER 2020

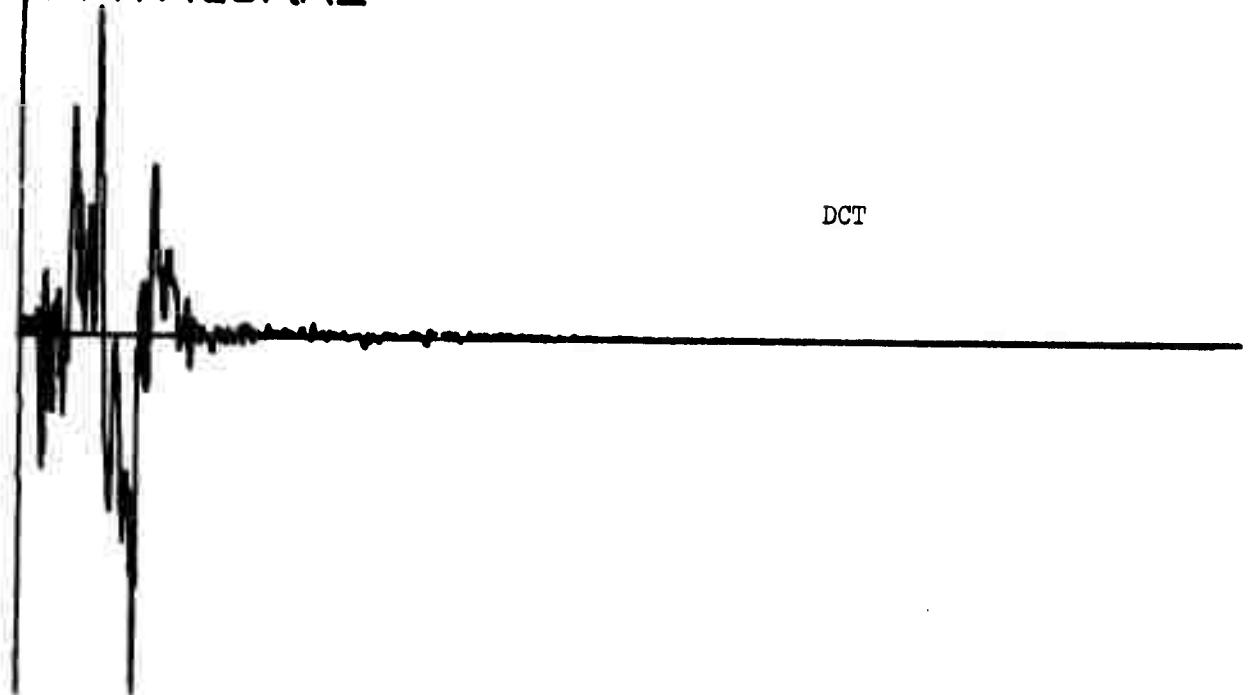
EARTHQUAKE



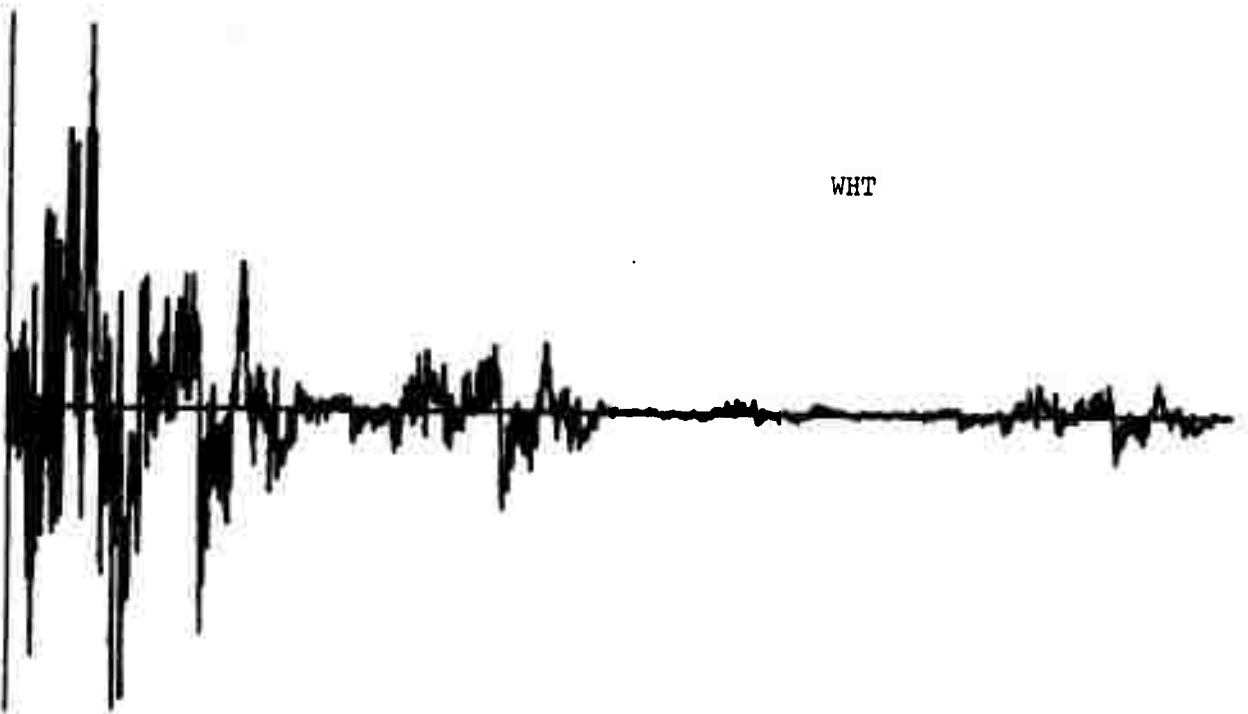
Q036

EVENT NUMBER 2023

EARTHQUAKE



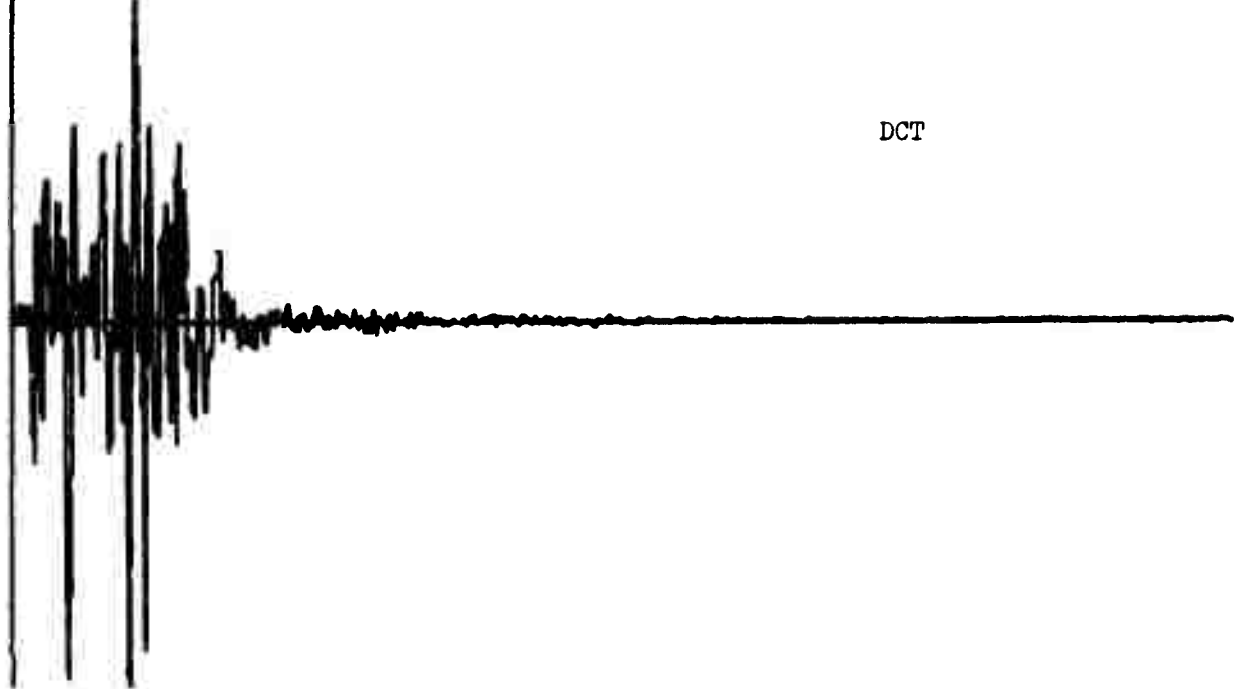
DCT



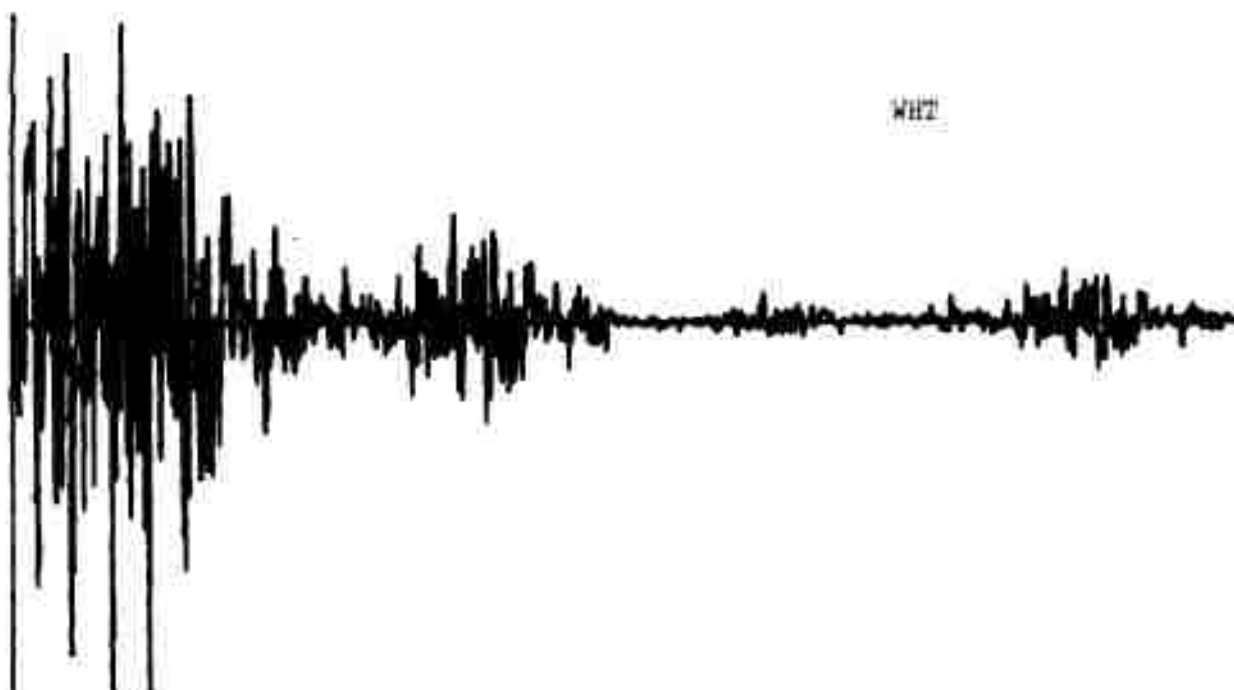
WHT

Q038

EVENT NUMBER 2025
EARTHQUAKE



DCT

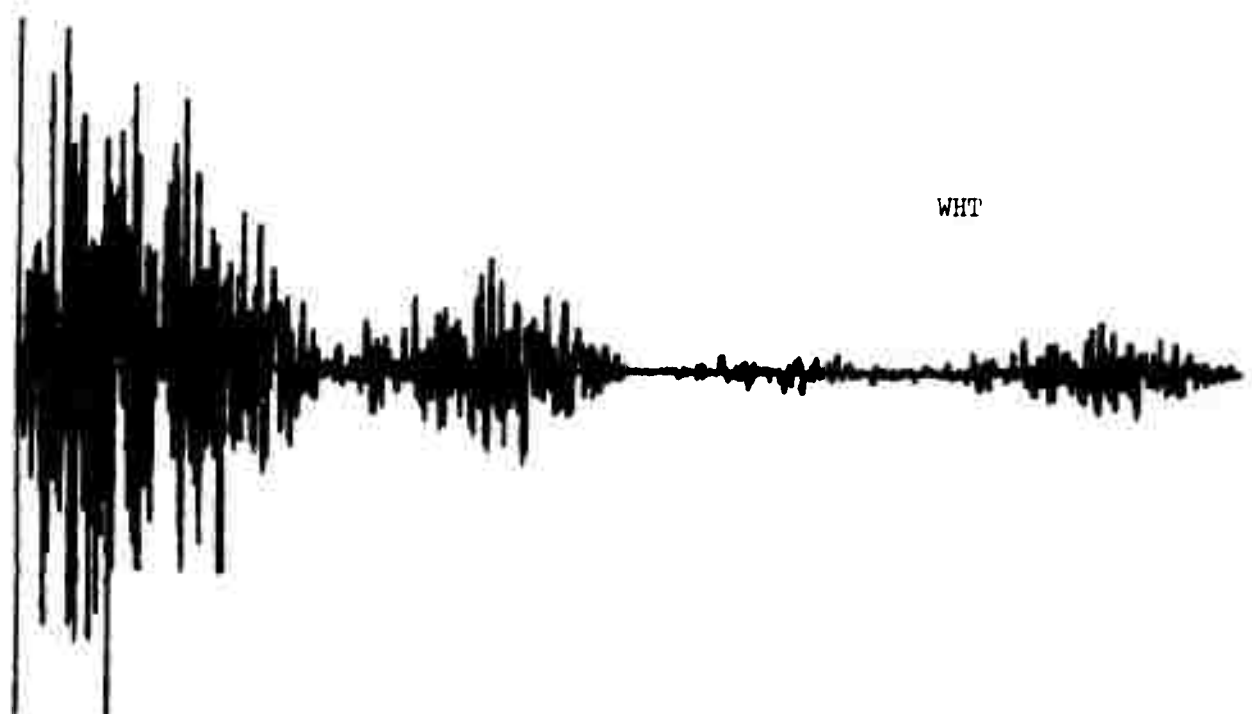
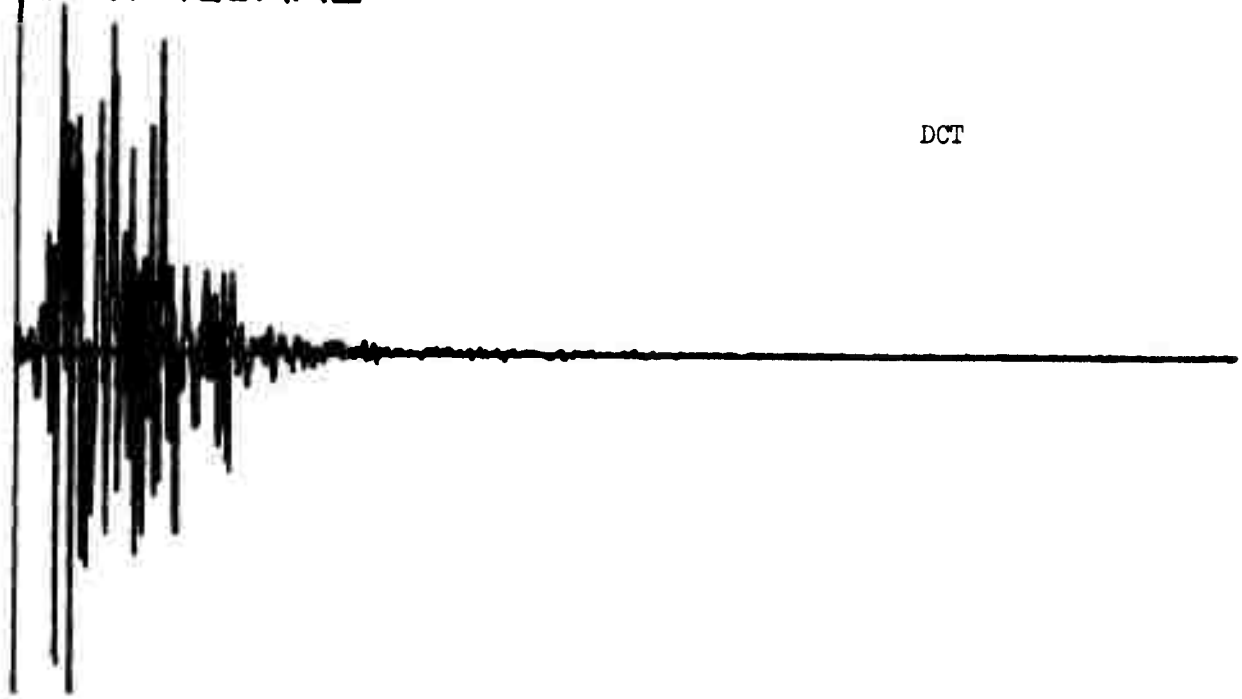
A seismogram showing a sharp, vertical initial pulse followed by a period of low-frequency ground motion. The signal then returns to baseline.

NHT

A seismogram showing a complex, multi-phased seismic wave, starting with a large initial pulse and continuing with several smaller, higher-frequency oscillations.

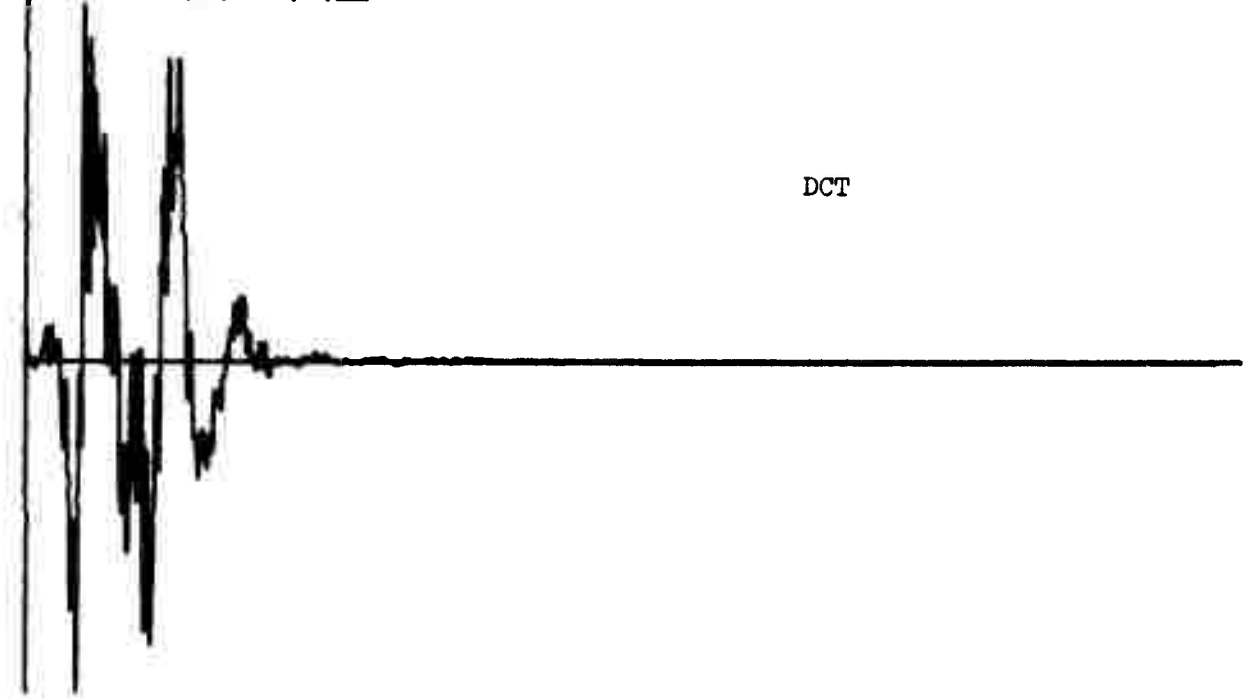
Q040

EVENT NUMBER 2026
EARTHQUAKE

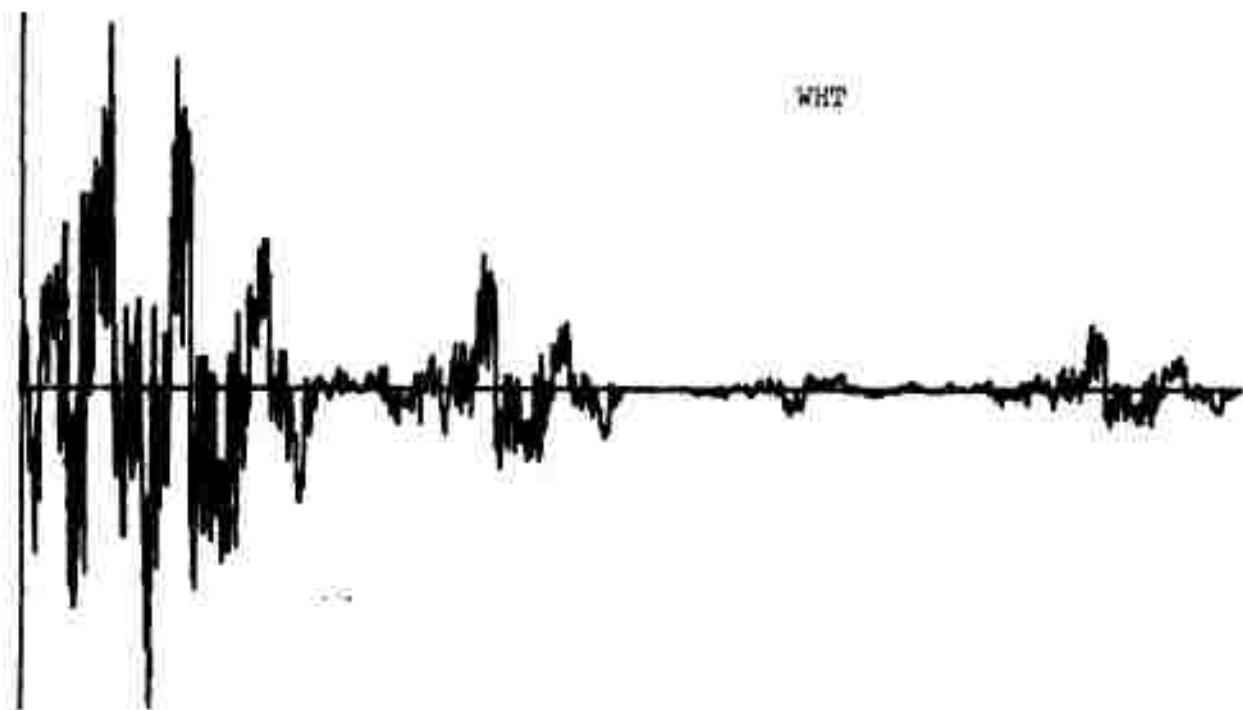


Q042

EVENT NUMBER 2027
EARTHQUAKE



DCT



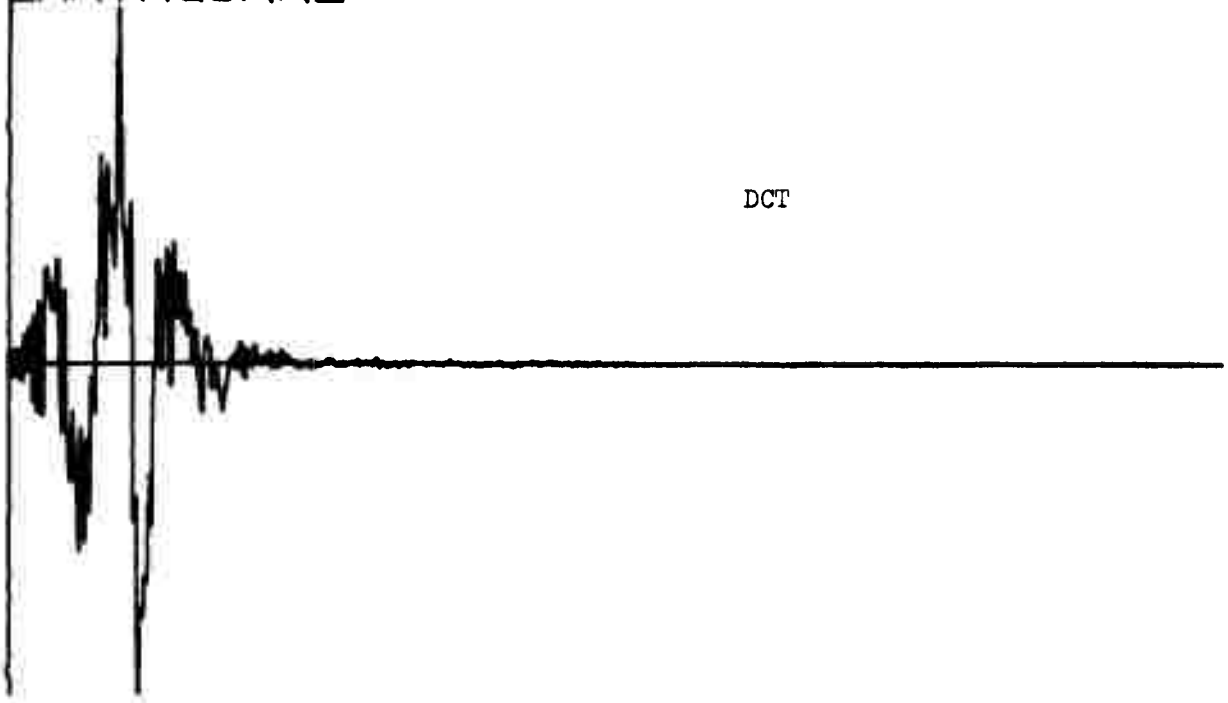
WHT

QC44

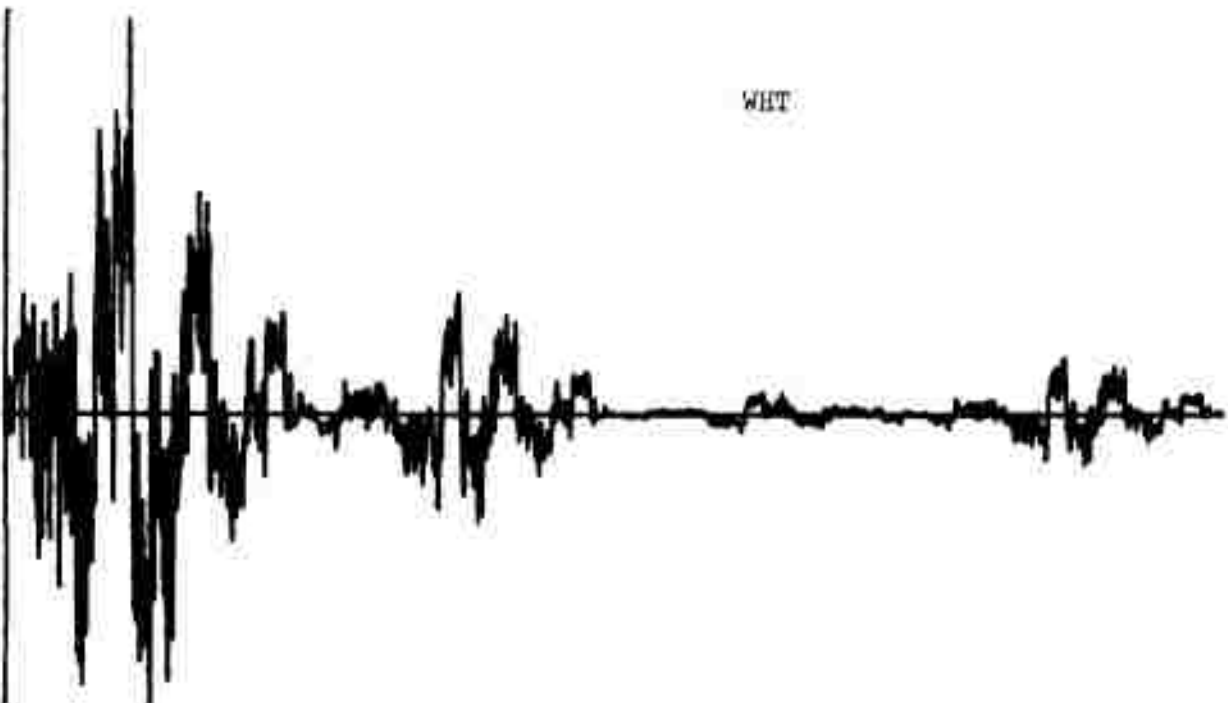
EVENT NUMBER 2028

EARTHQUAKE

DCT

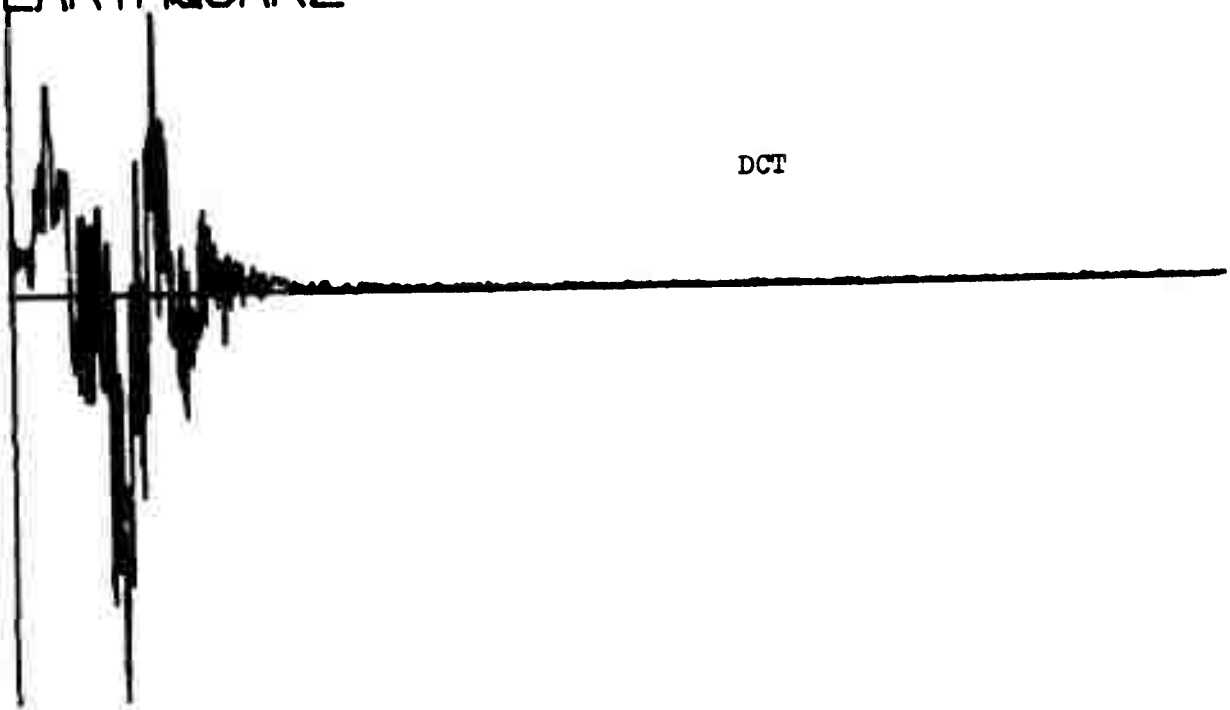


WHT

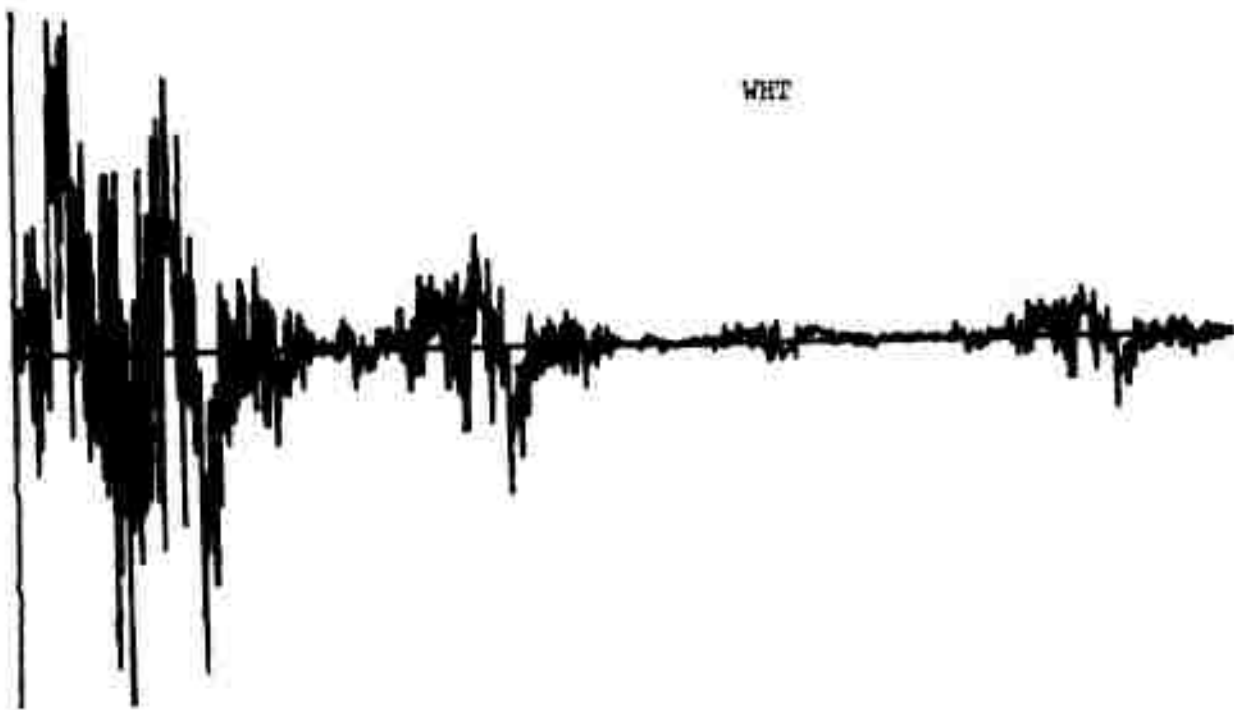


Q046

EVENT NUMBER 2032
EARTHQUAKE



DCT

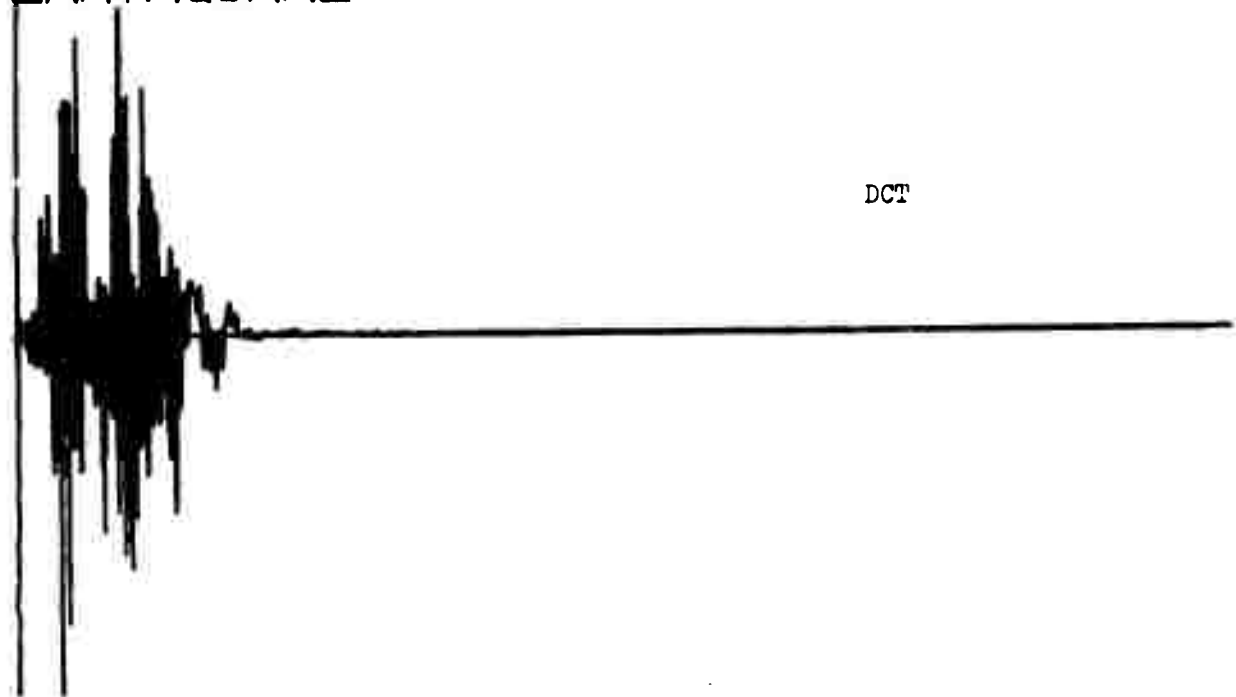
A seismogram showing ground motion over time. The signal starts with a large, sharp negative deflection followed by a series of smaller positive and negative pulses. After approximately 10 seconds, the signal becomes relatively flat, indicating a period of low seismic activity.

WHT

A seismogram showing ground motion over time. The signal exhibits a continuous series of high-frequency, low-amplitude oscillations, characteristic of noise or a distant event. There is no distinct primary wave or aftershock.

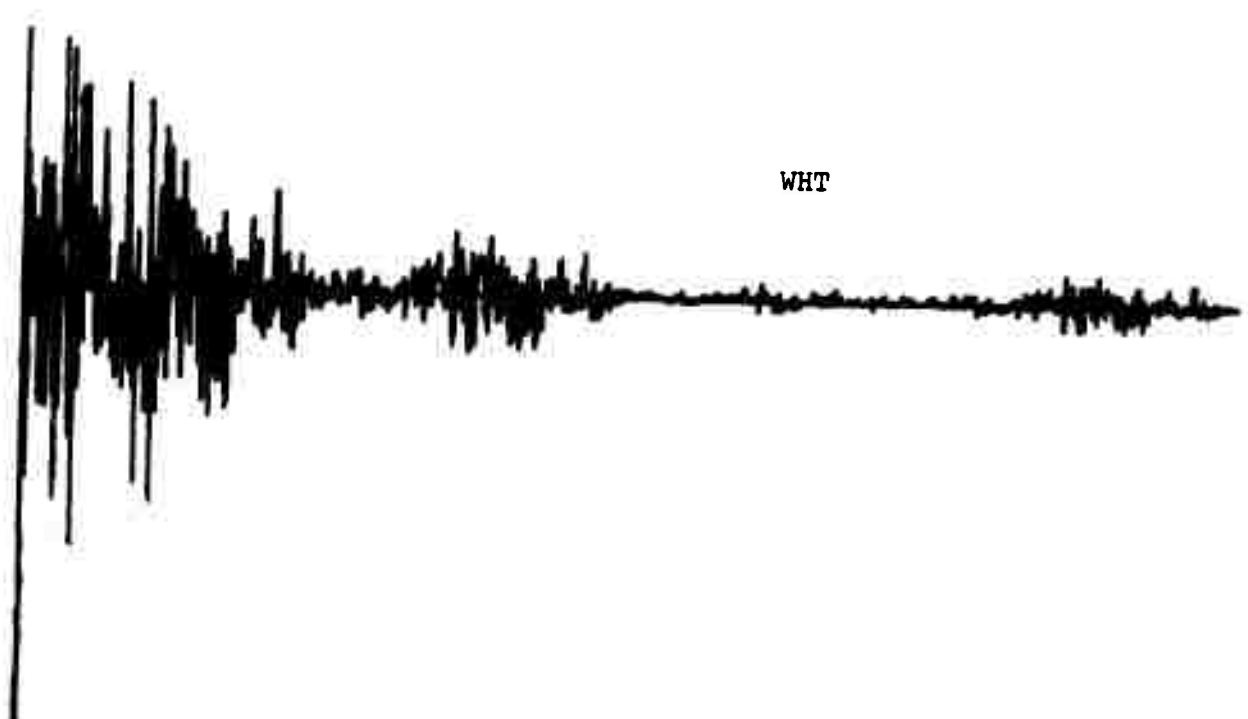
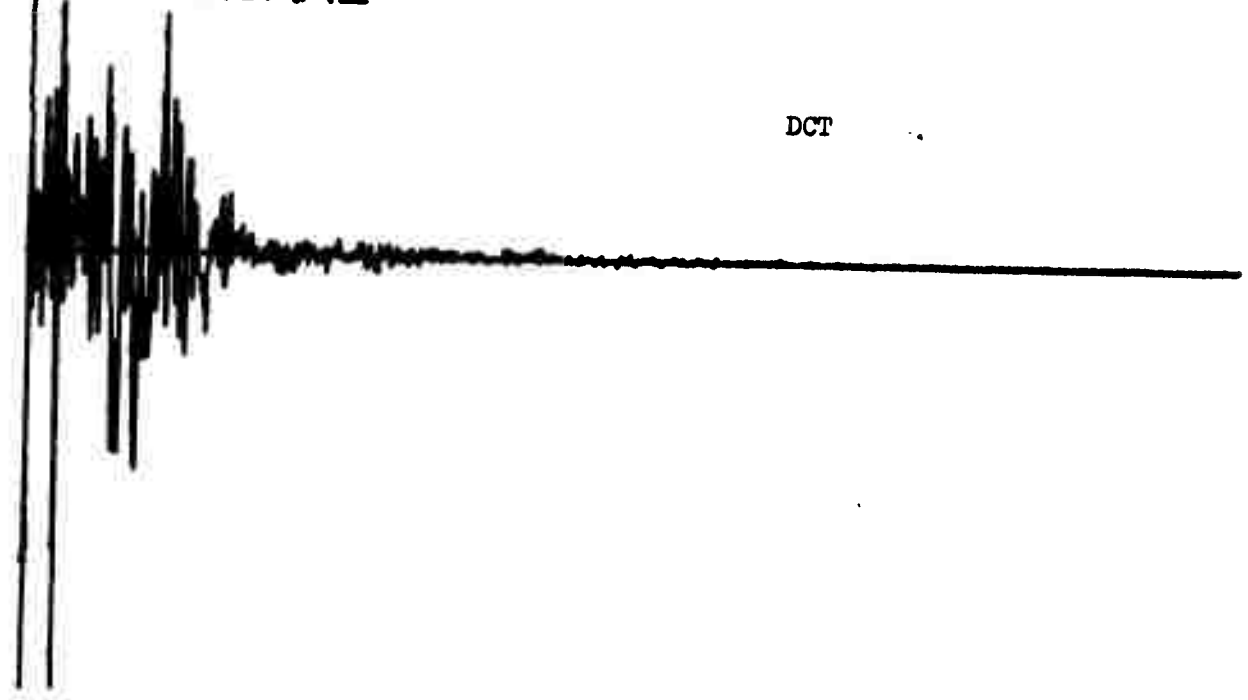
Q048

EVENT NUMBER 2033
EARTHQUAKE



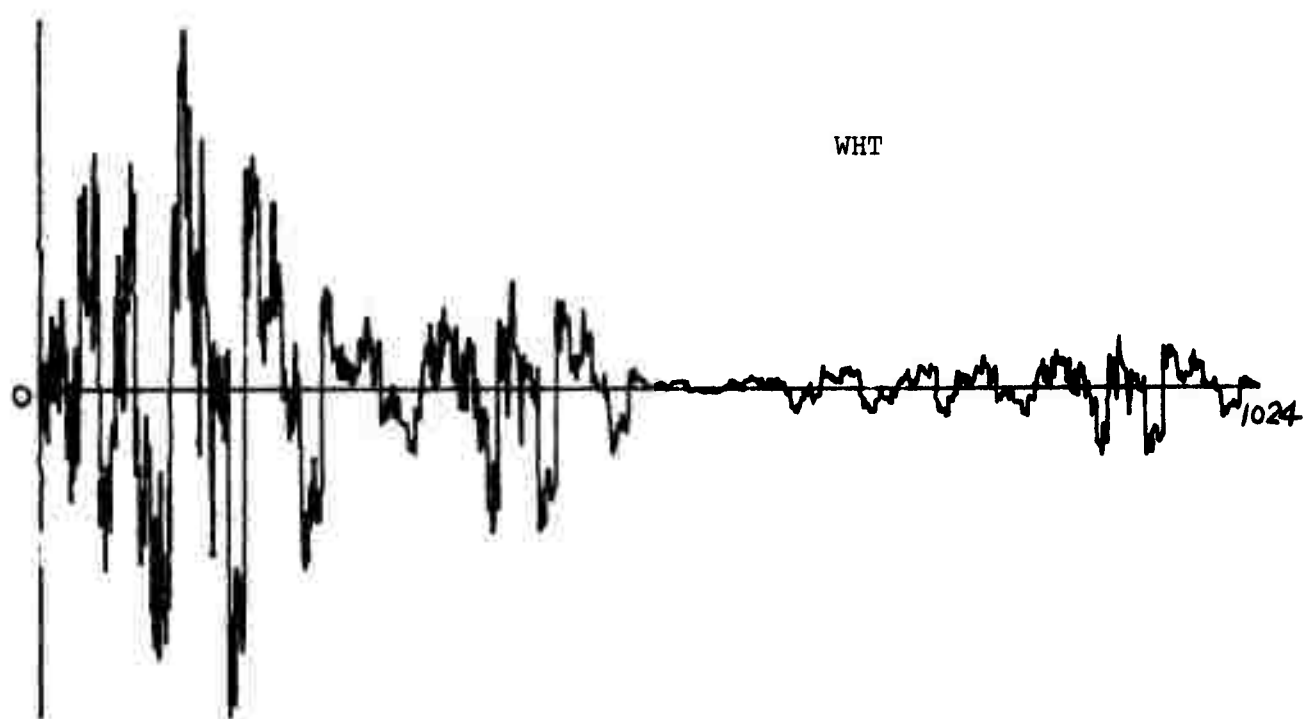
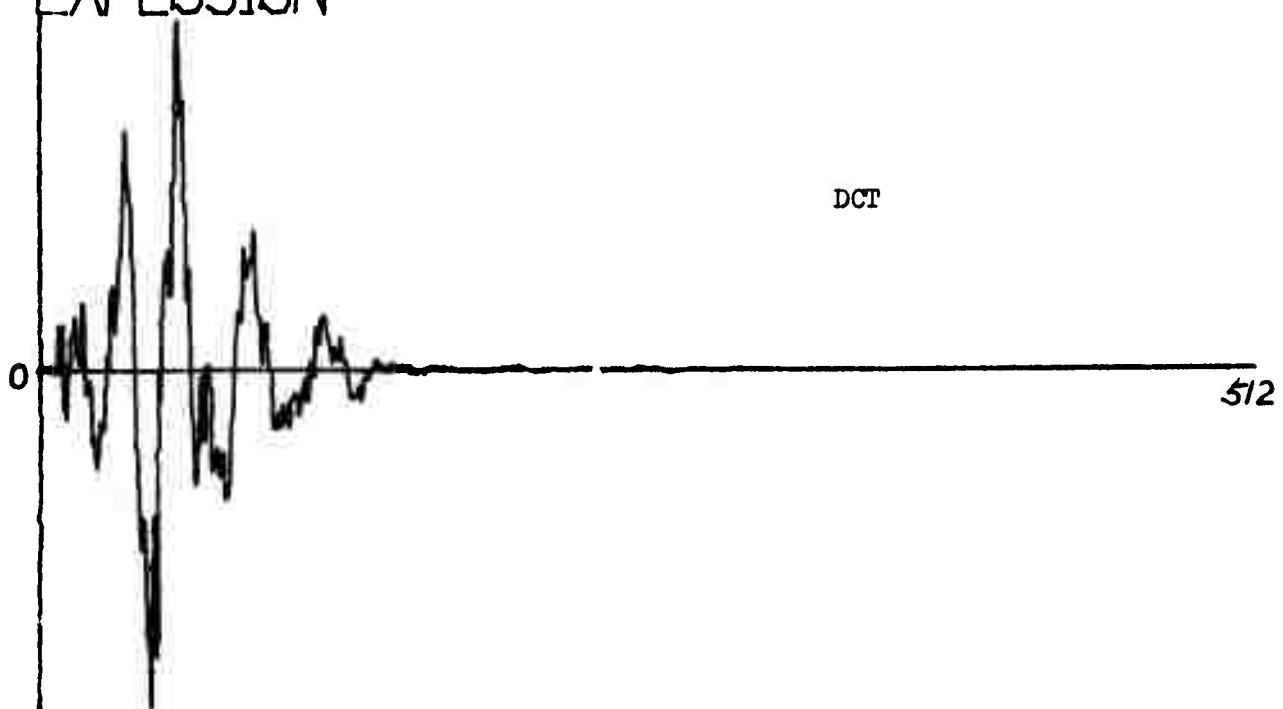
Q050

EVENT NUMBER 2034
EARTHQUAKE



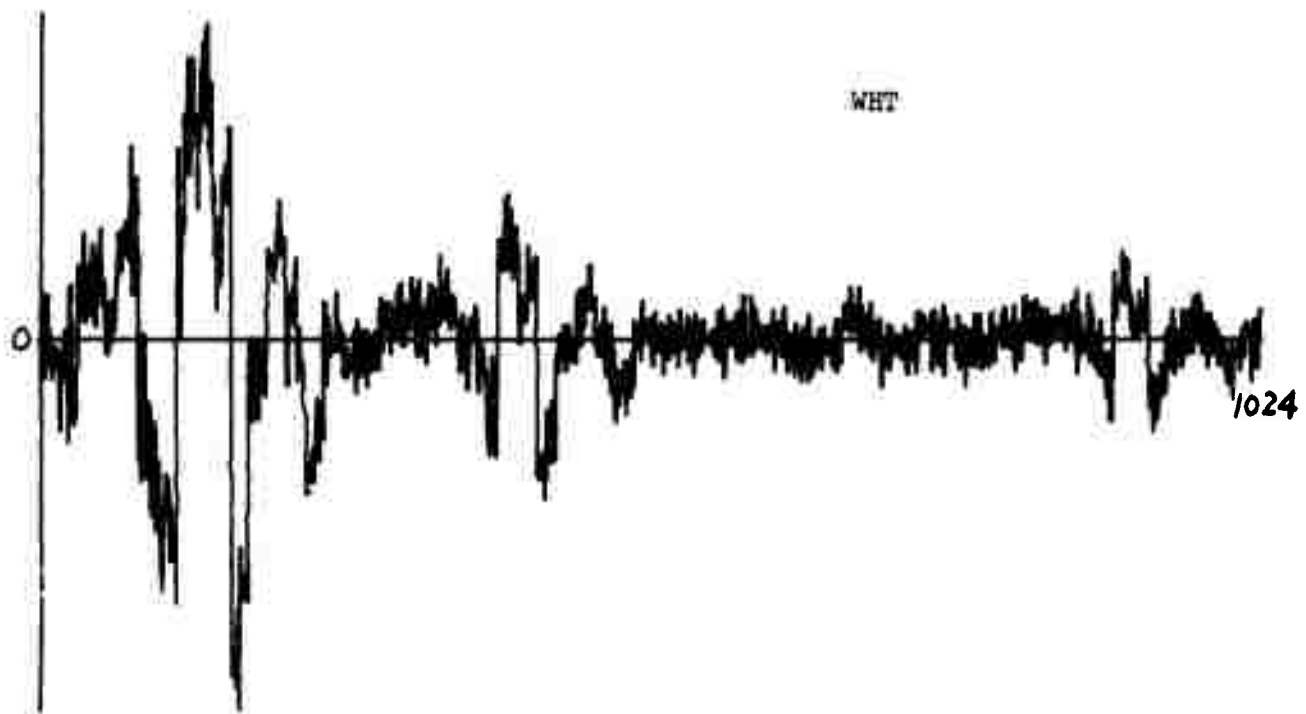
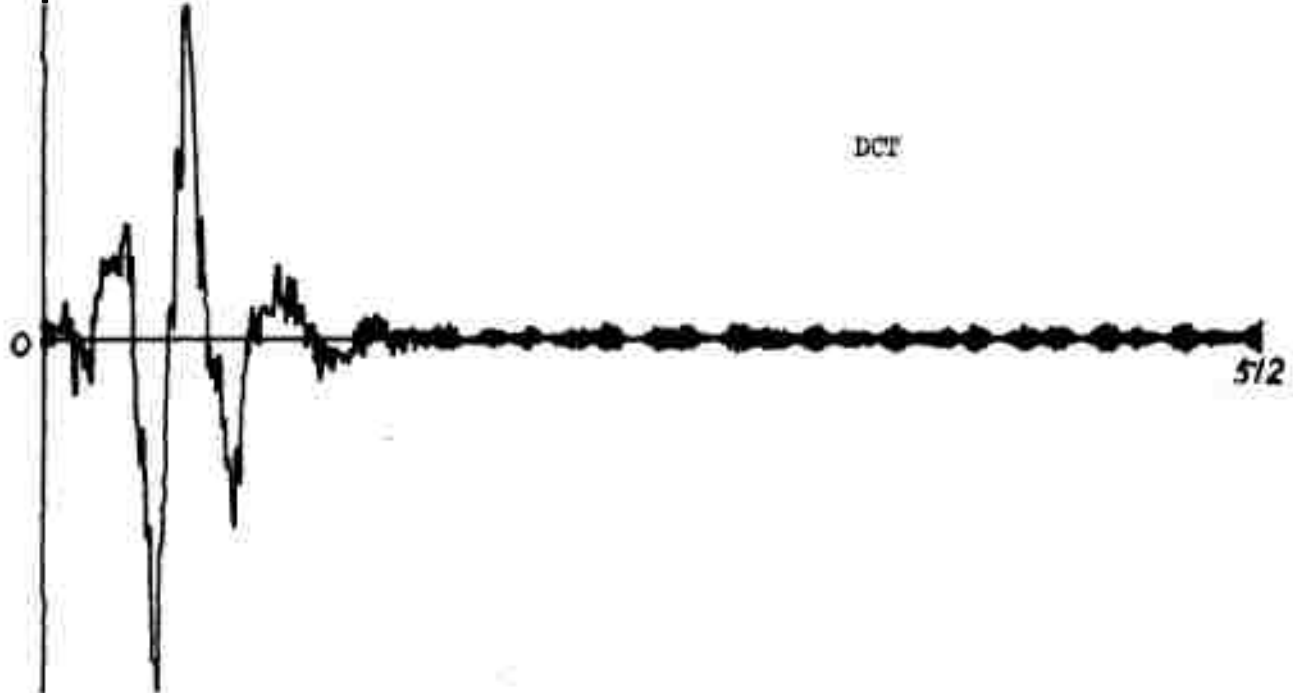
X052

EVENT NUMBER 1507
EXPLOSION



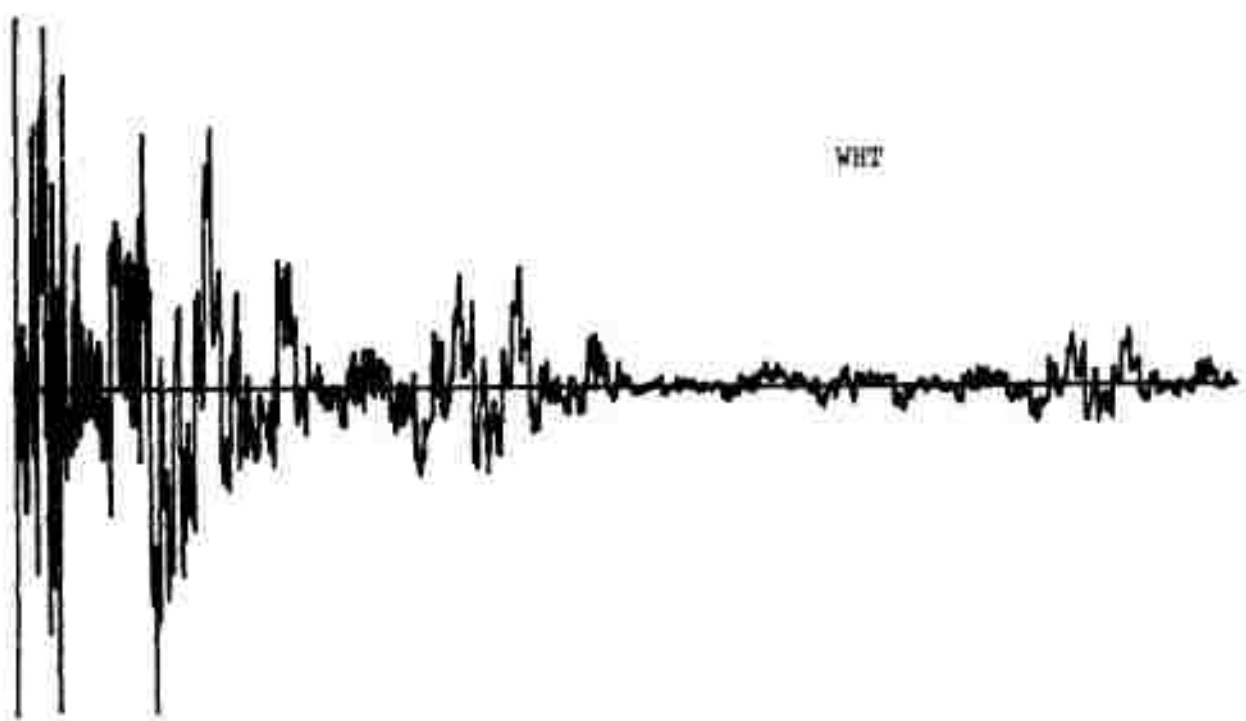
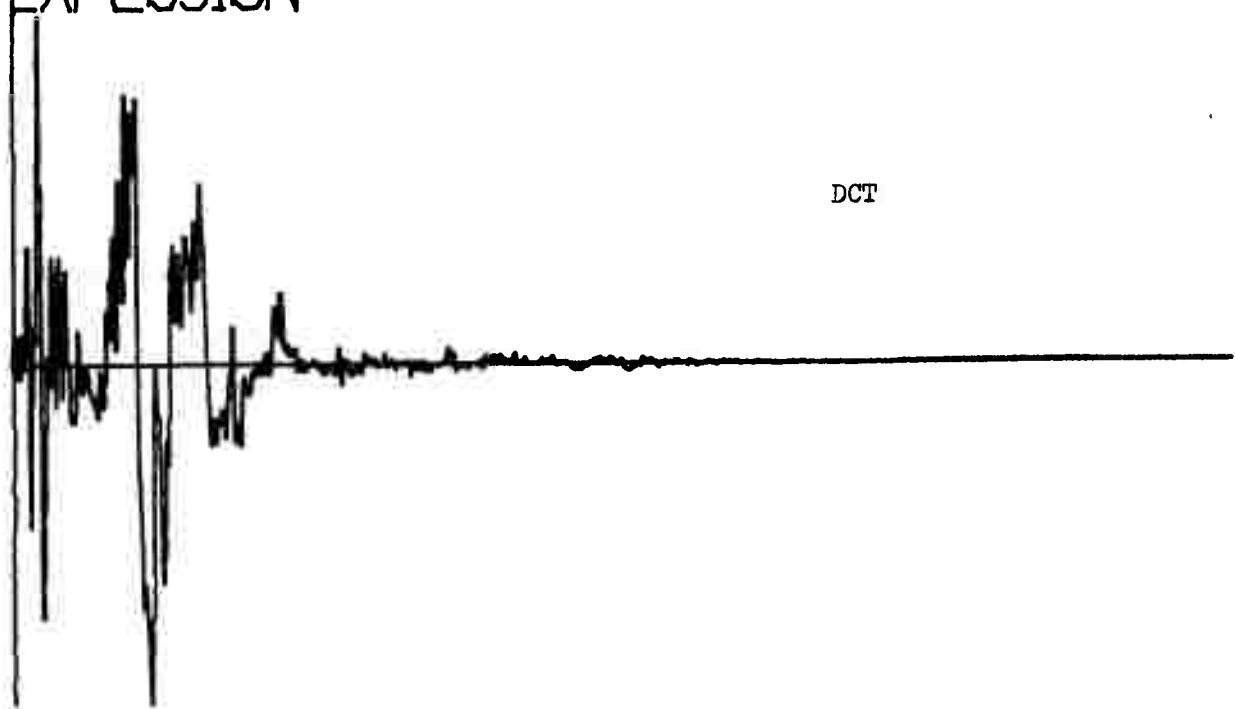
x054

EVENT NUMBER 1531
EXPLOSION



x056

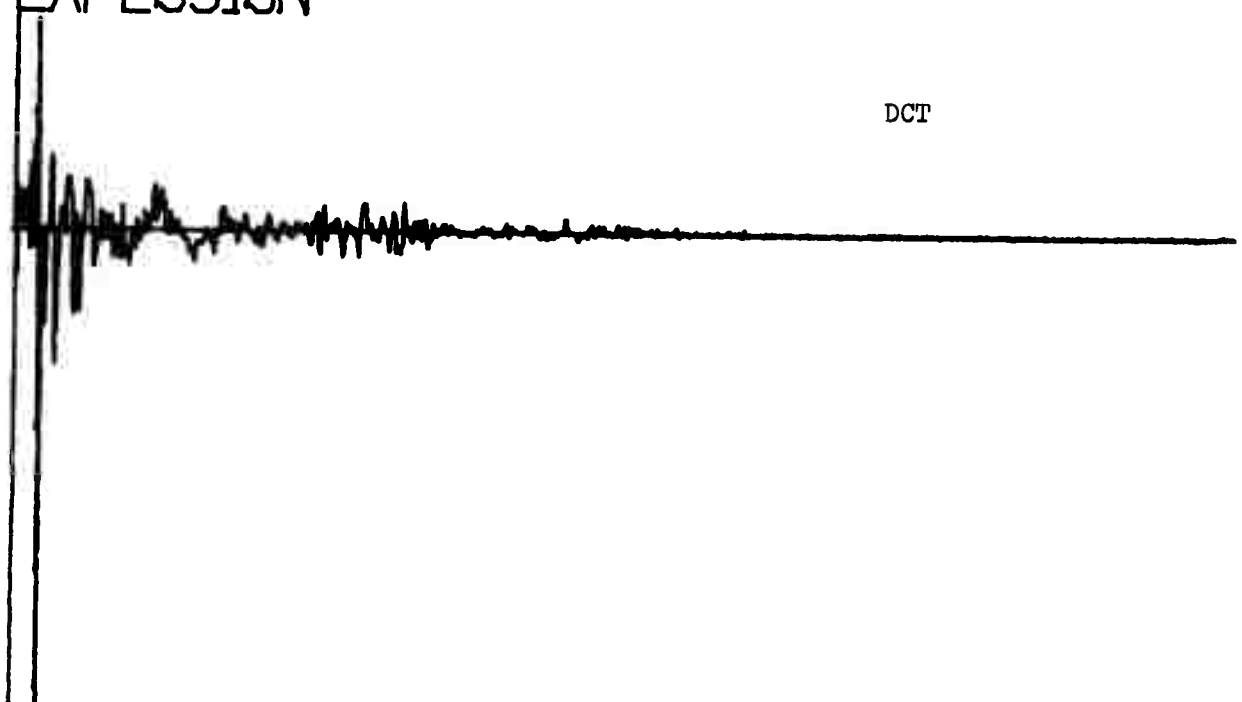
EVENT NUMBER 1512
EXPLOSION



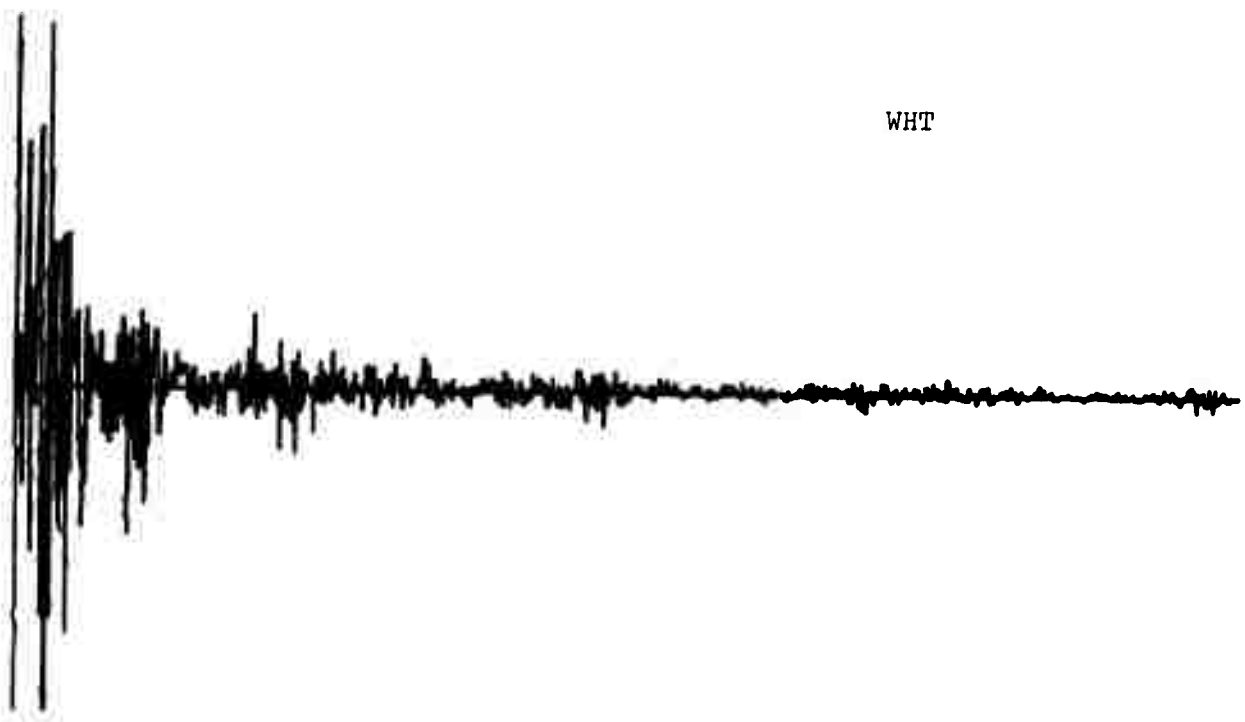
x058

EVENT NUMBER 1525
EXPLOSION

DCT



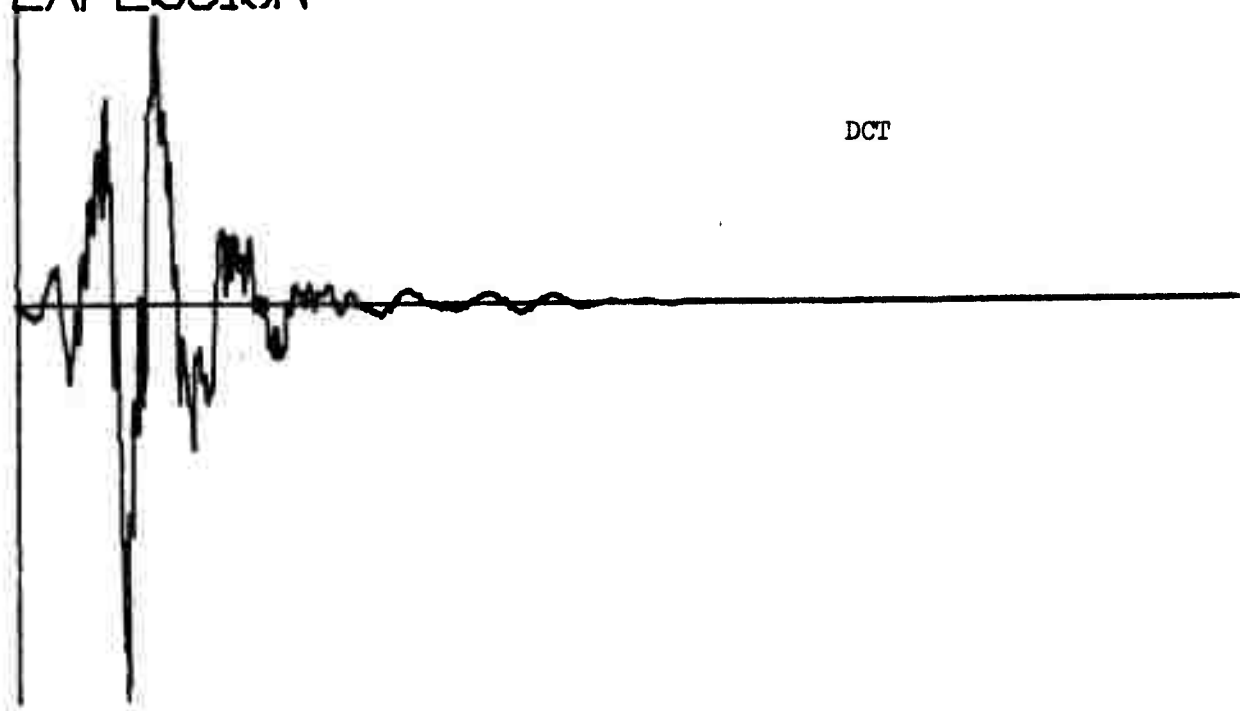
WHT



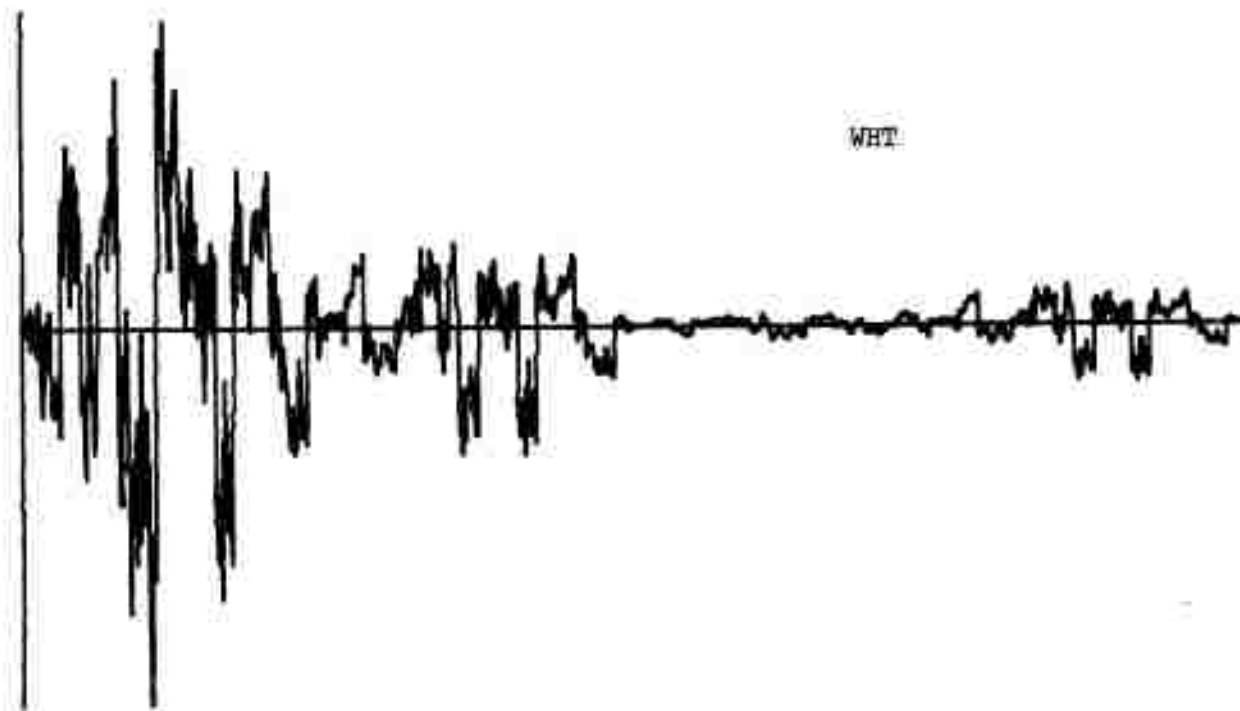
X060

EVENT NUMBER 1518
EXPLOSION

DCT

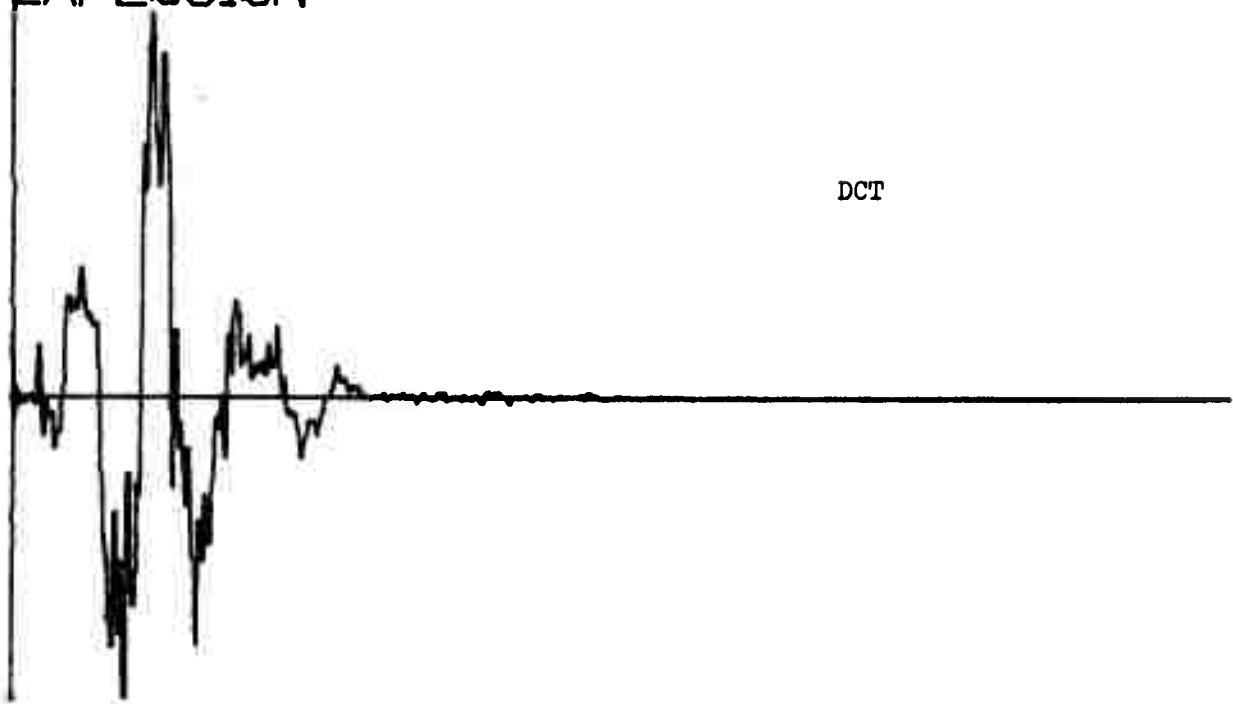


WHT

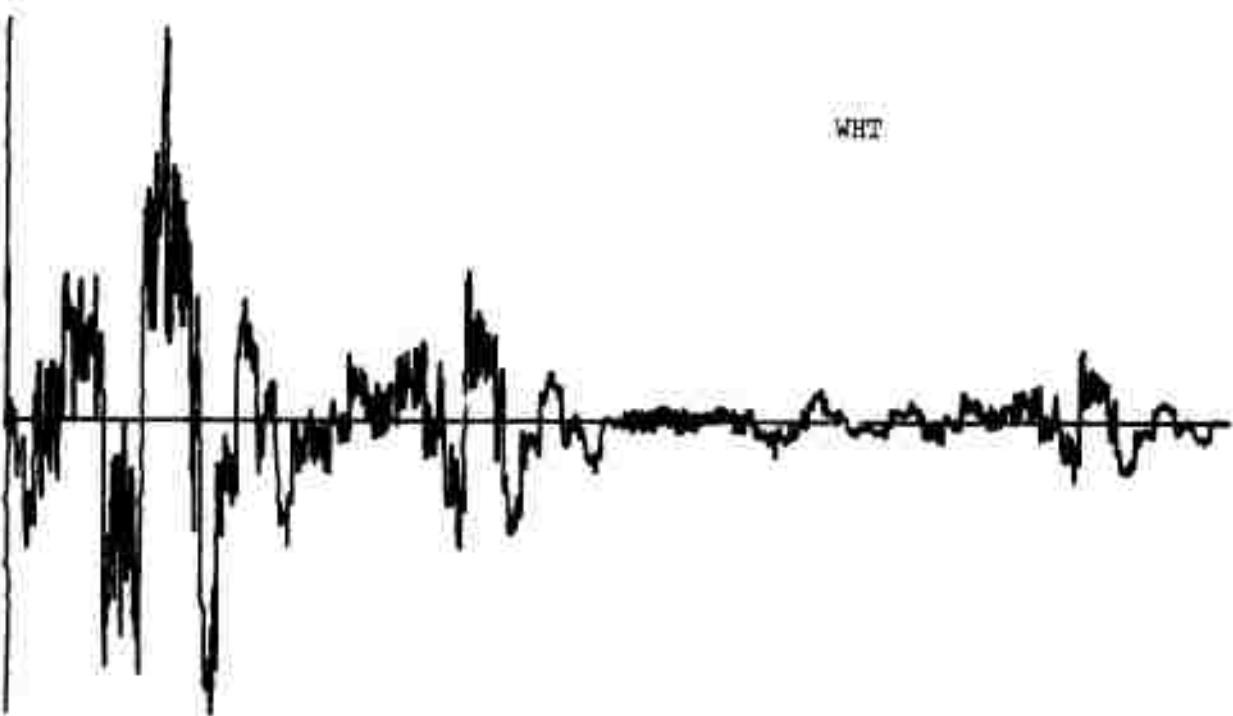


x062

EVENT NUMBER 1514
EXPLOSION



DCT

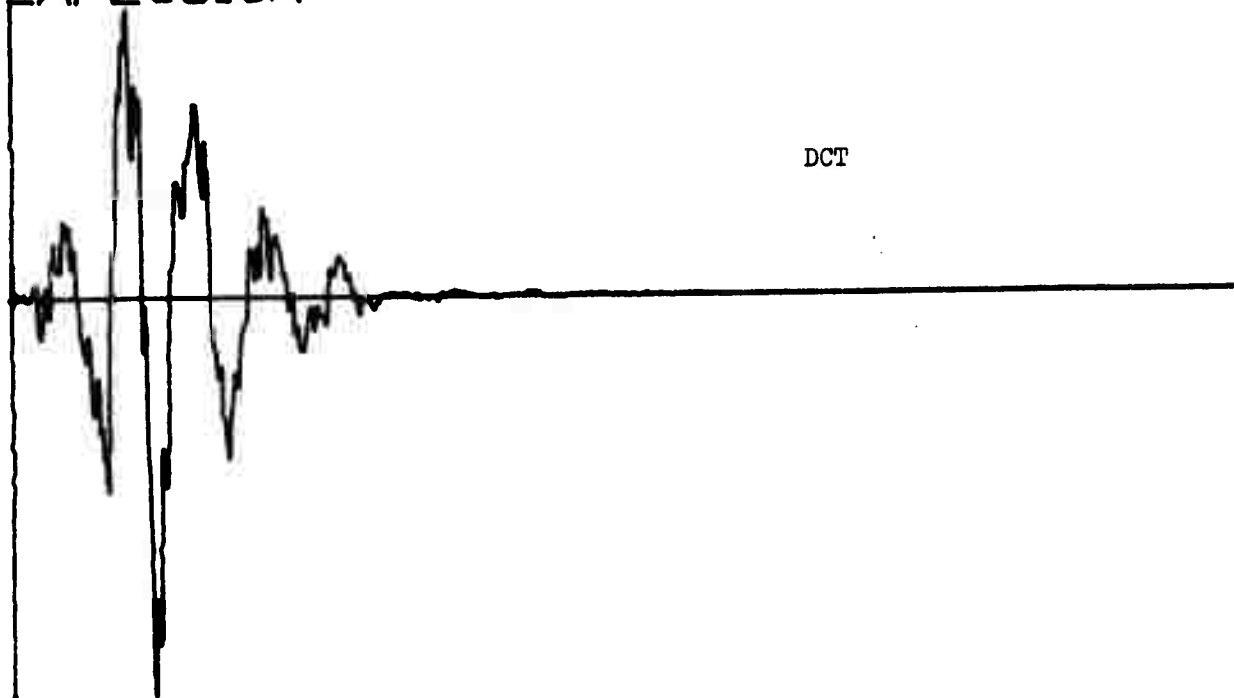


WHT

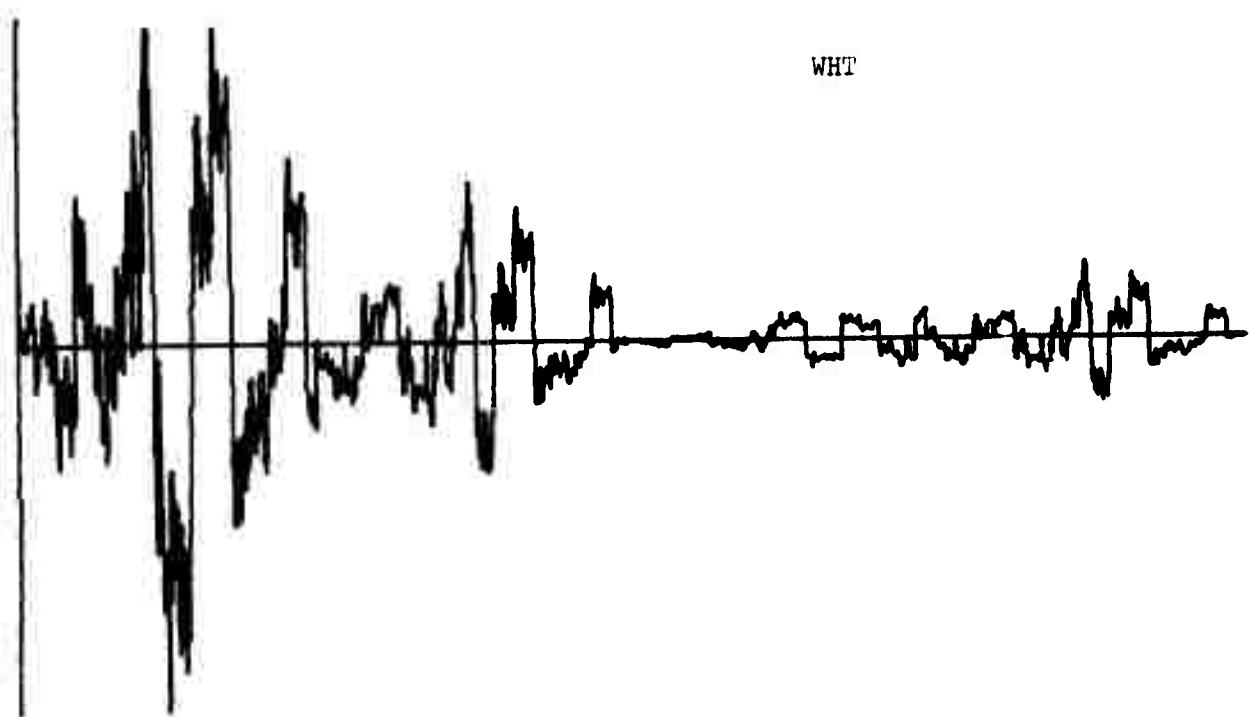
x064

EVENT NUMBER 1513

EXPLOSION



DCT

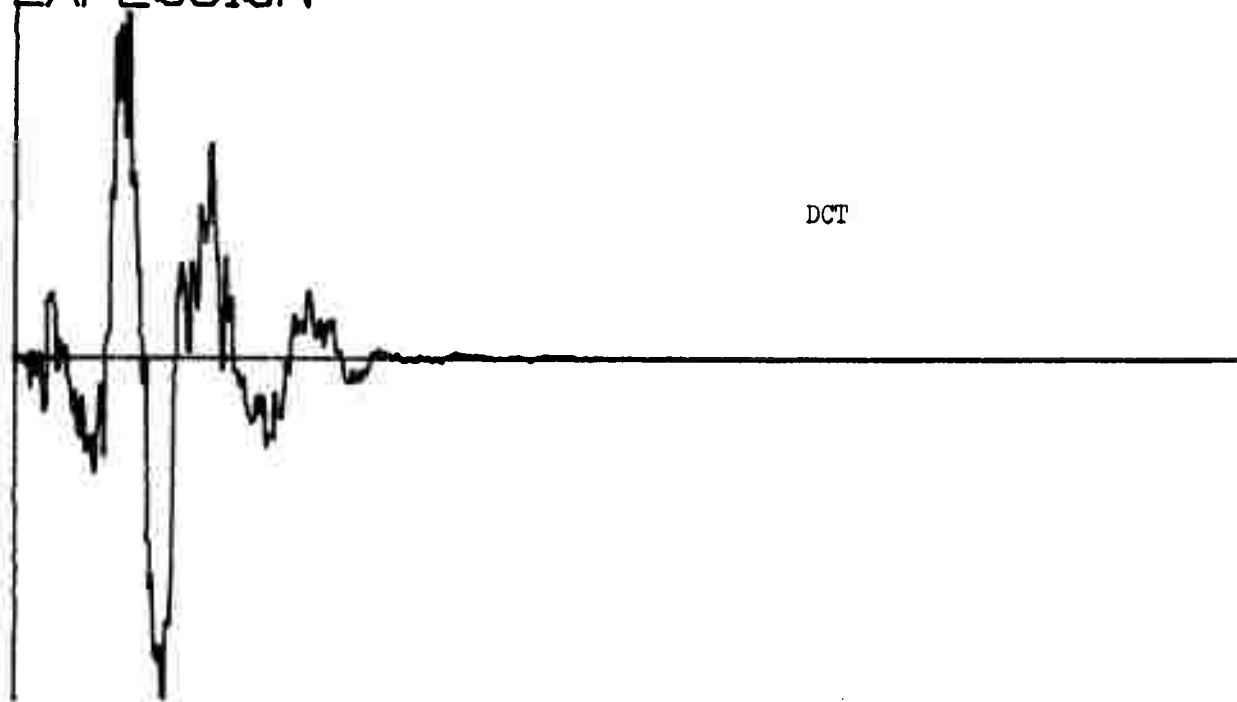


WHT

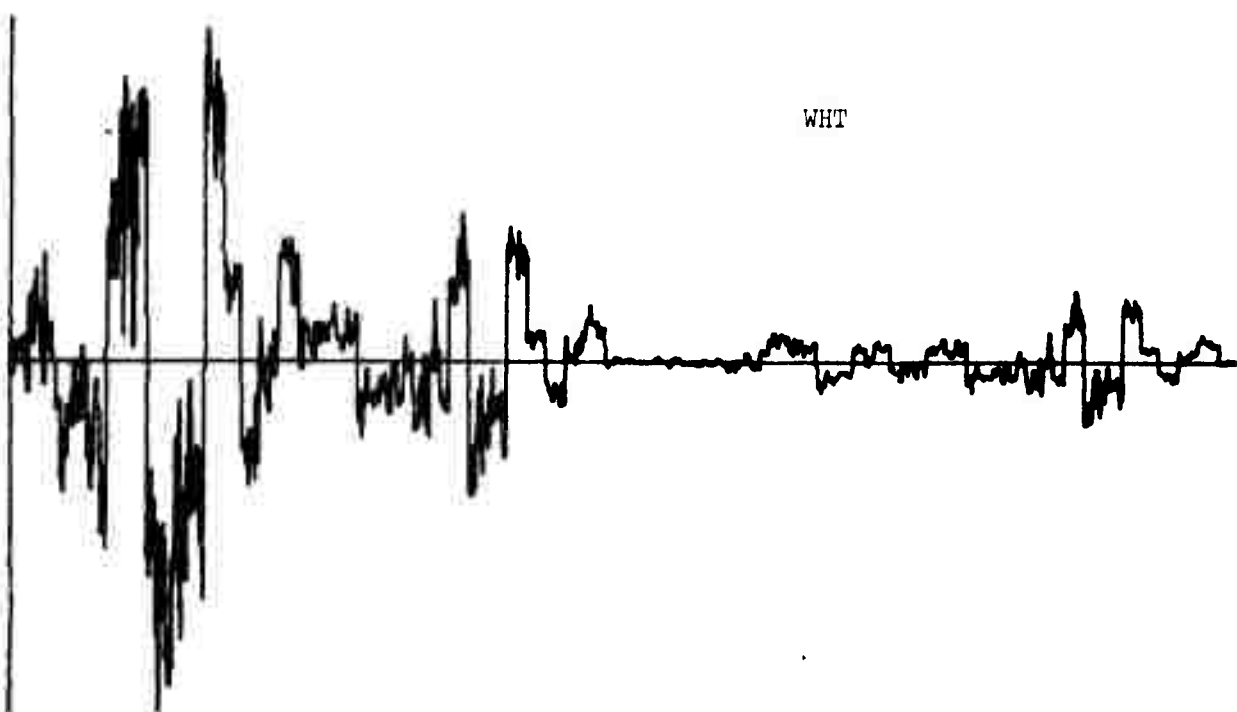
x066

EVENT NUMBER 1511

EXPLOSION



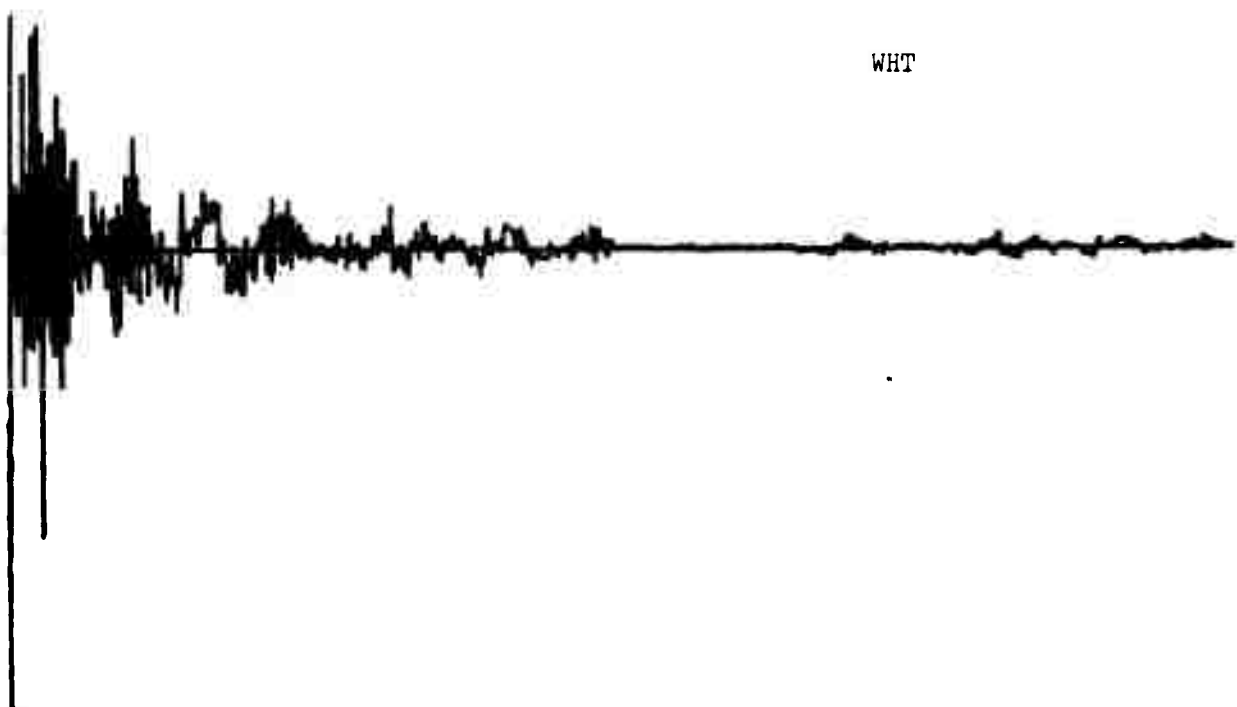
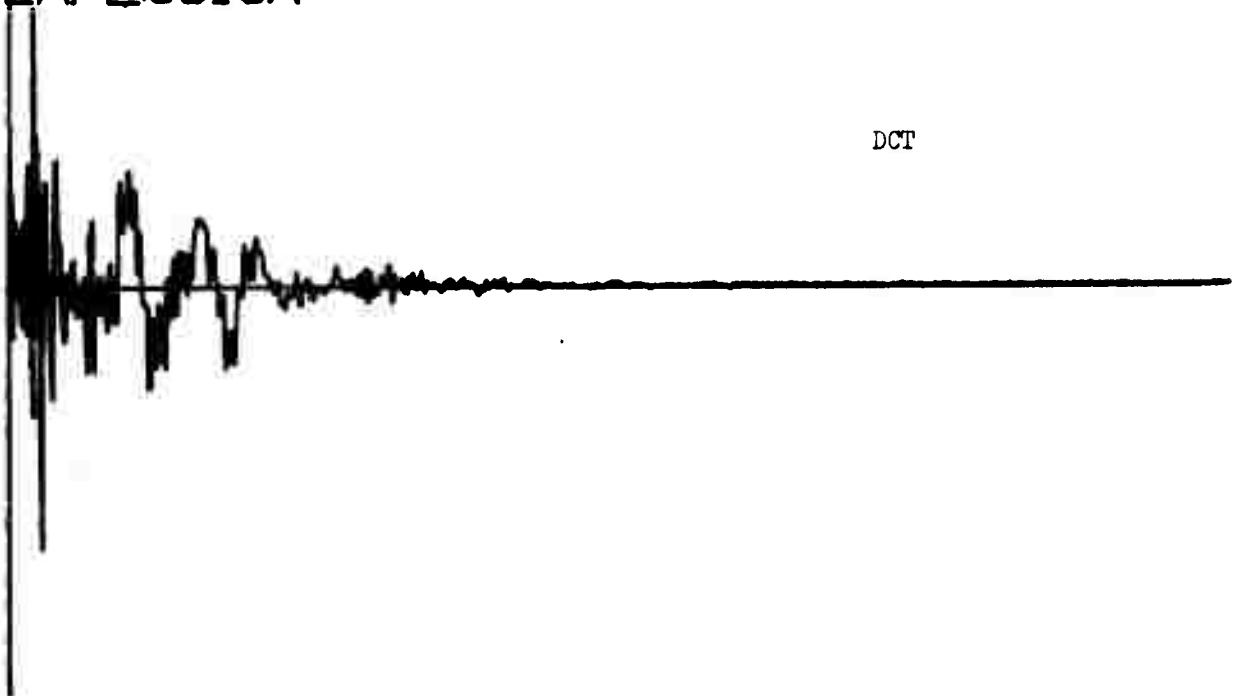
DCT



WHT

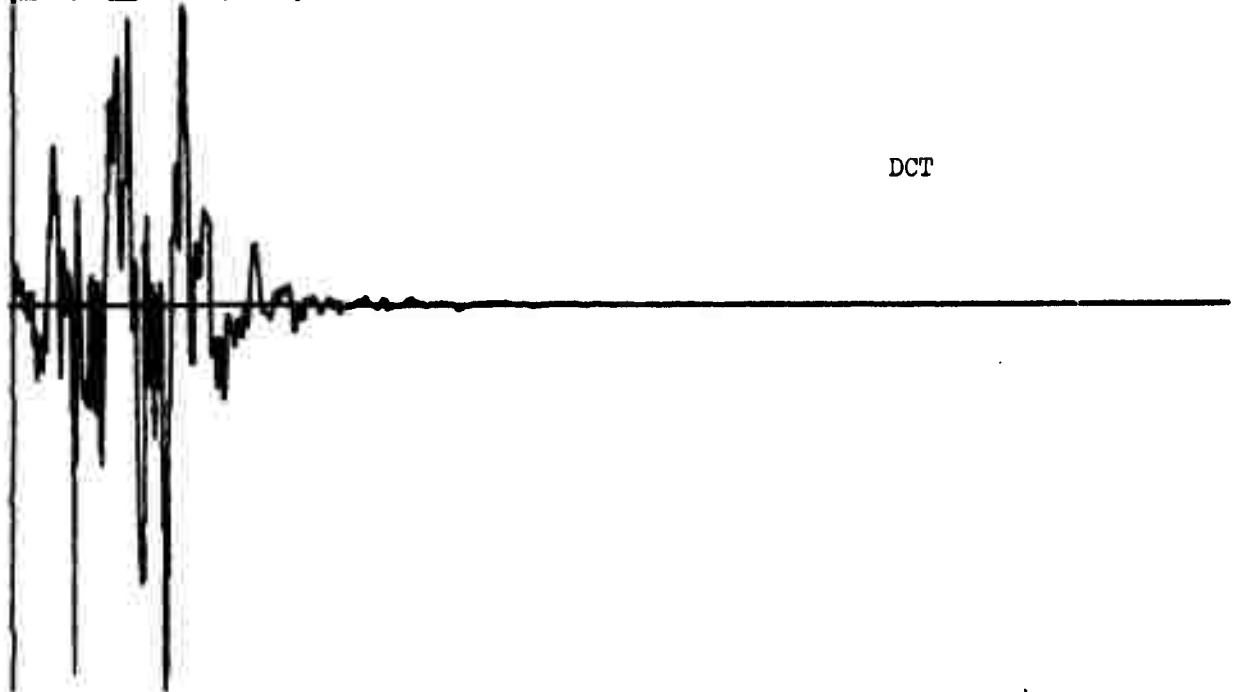
X068

EVENT NUMBER 1532
EXPLOSION

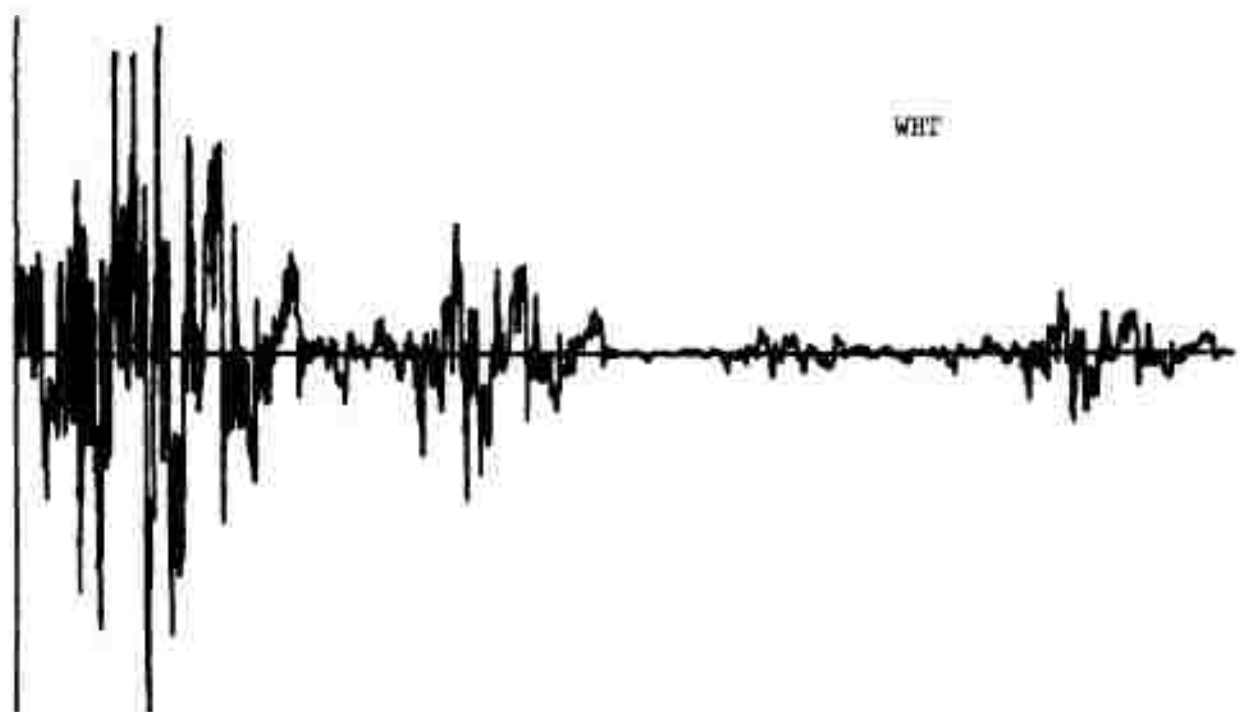


X070

EVENT NUMBER 1530
EXPLOSION



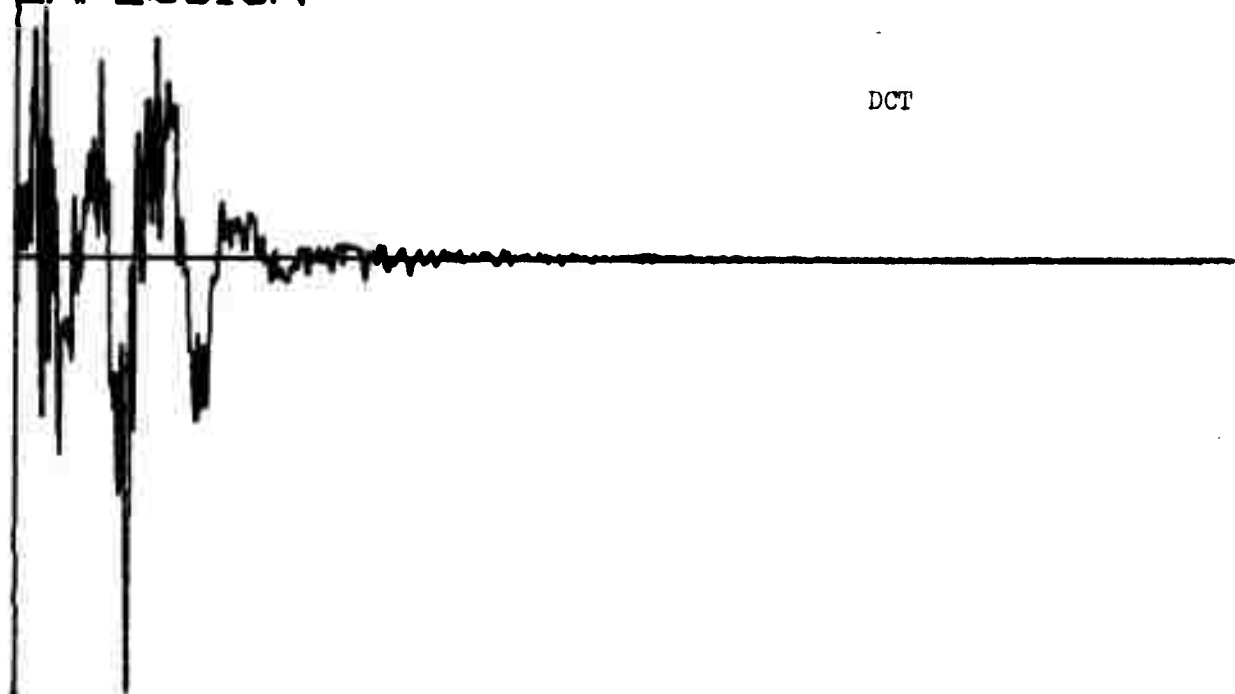
DCT



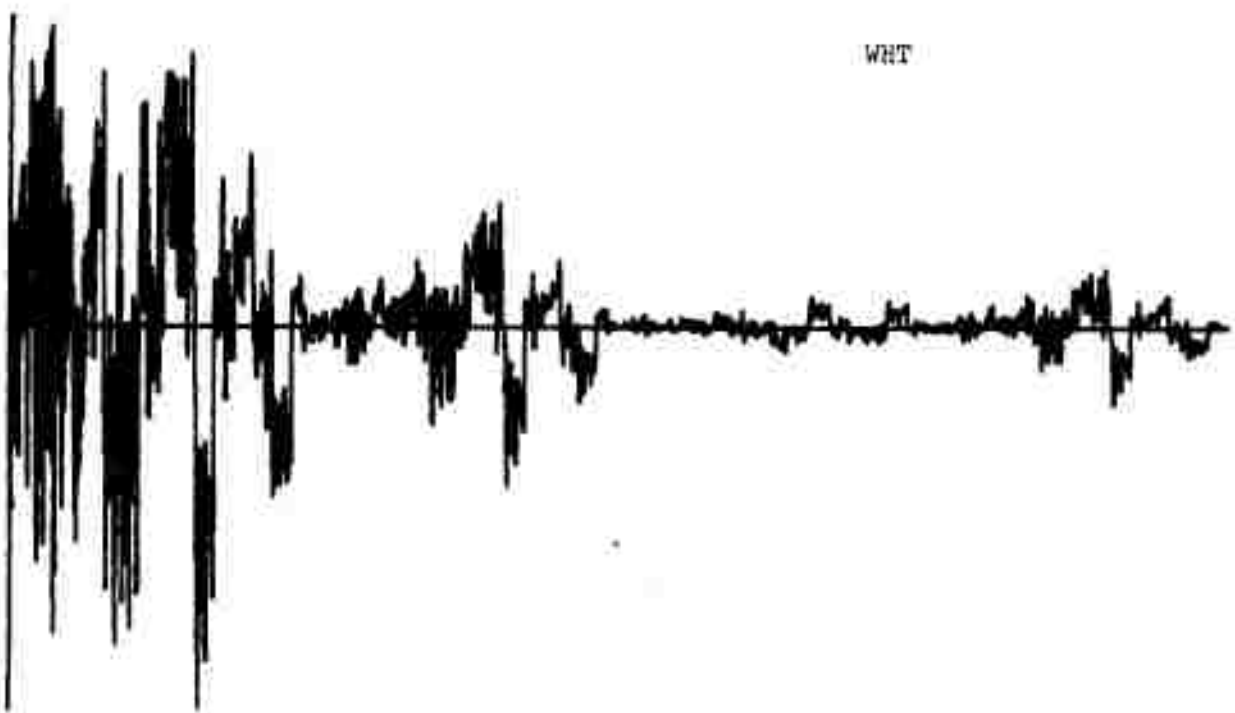
WHT

X072

EVENT NUMBER 1528
EXPLOSION



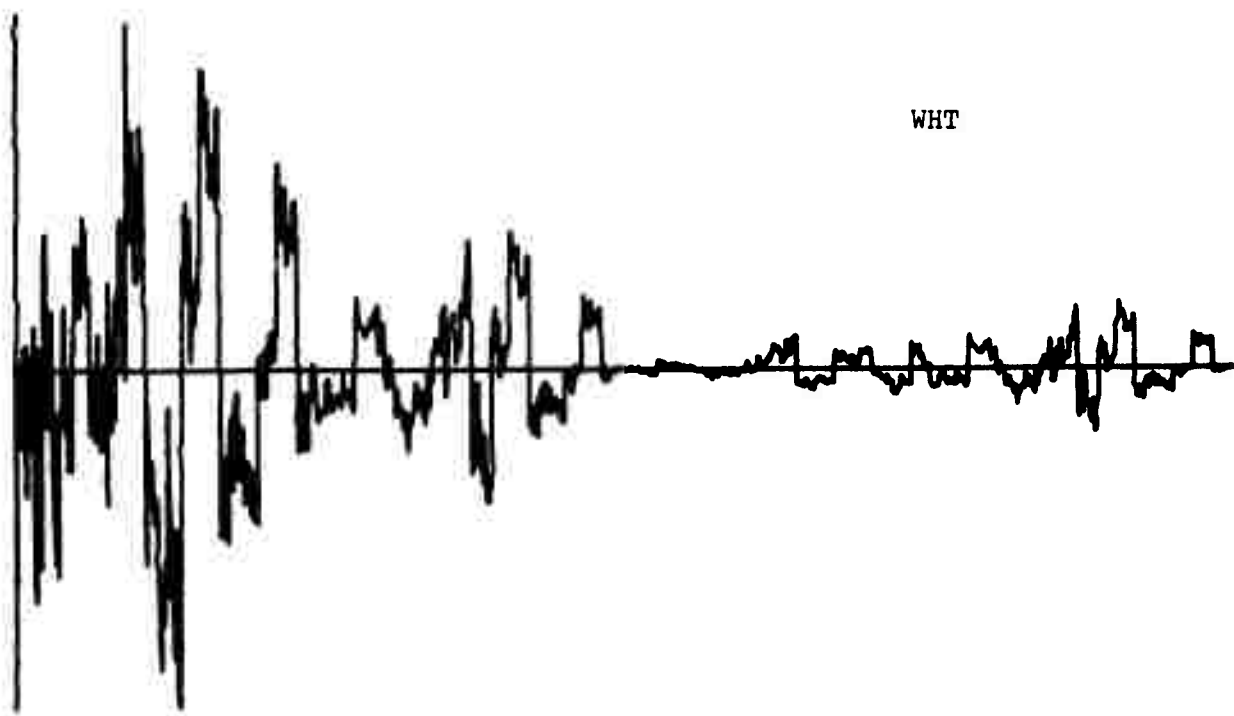
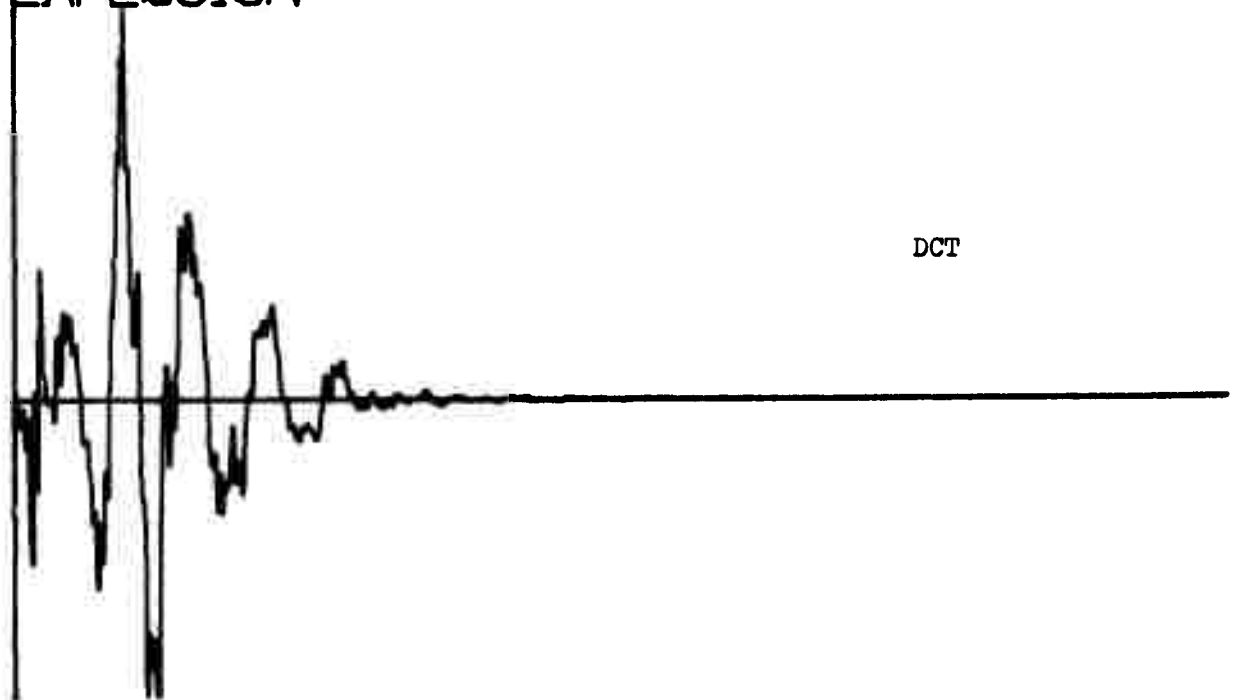
DCT



WHT

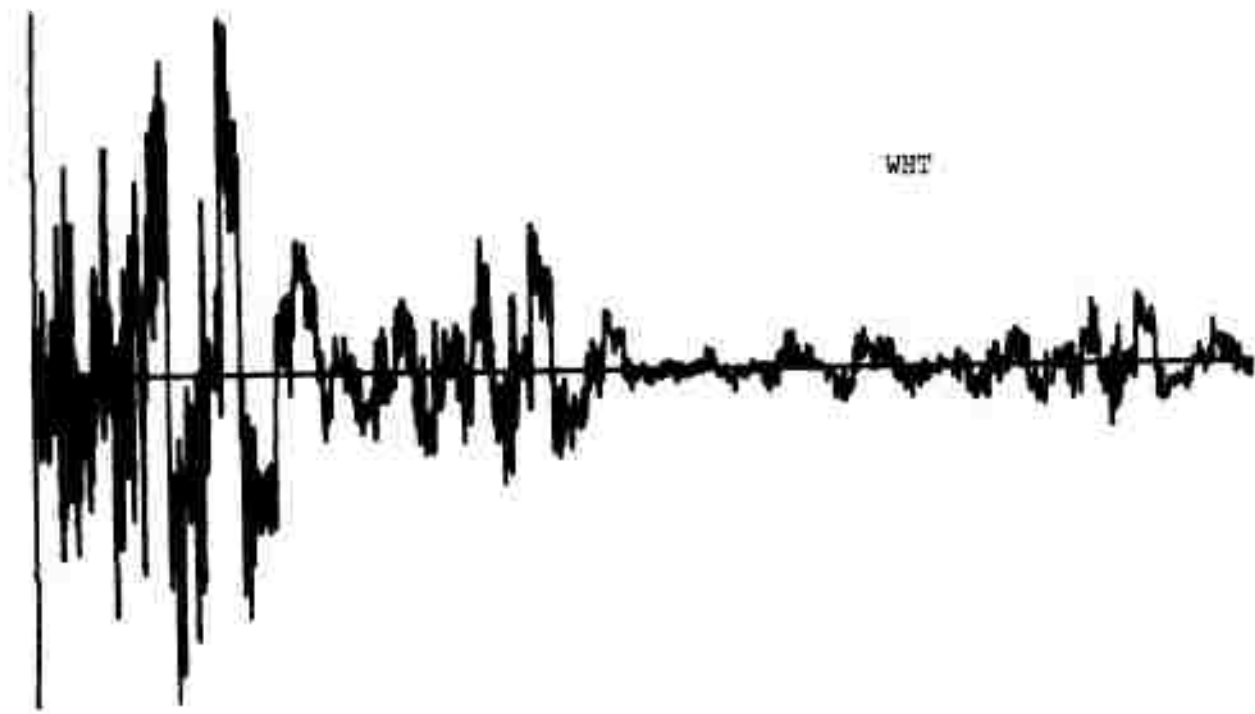
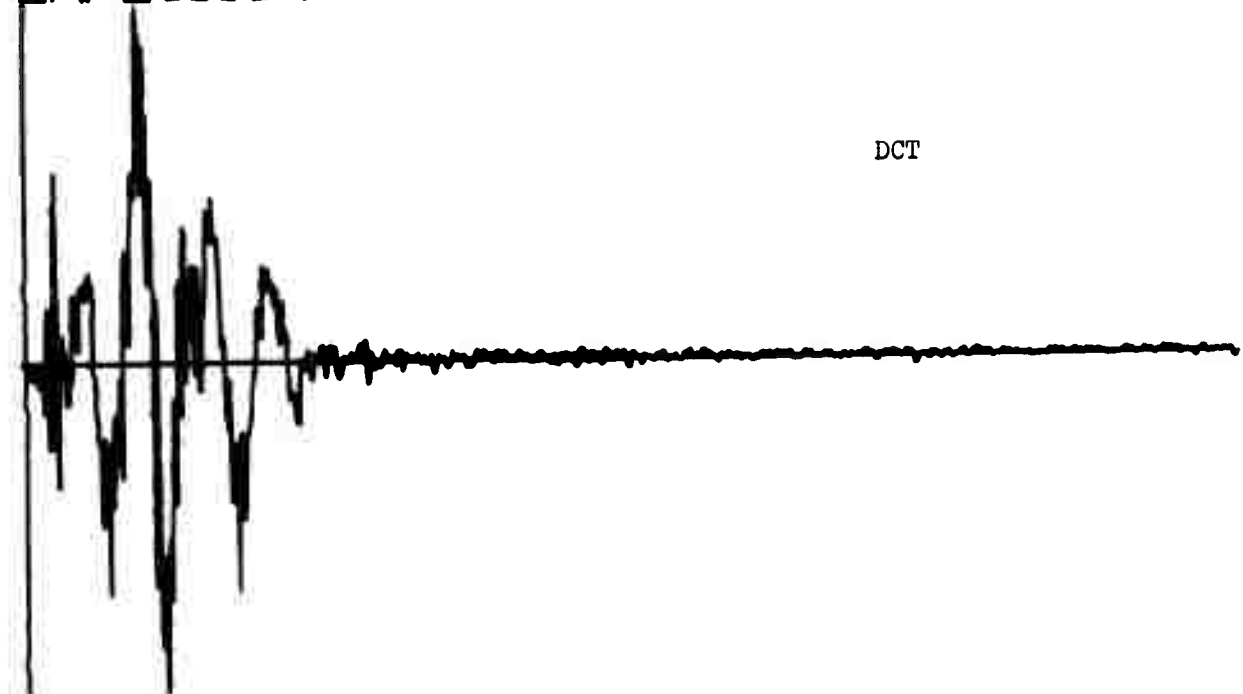
X074

EVENT NUMBER 1540
EXPLOSION



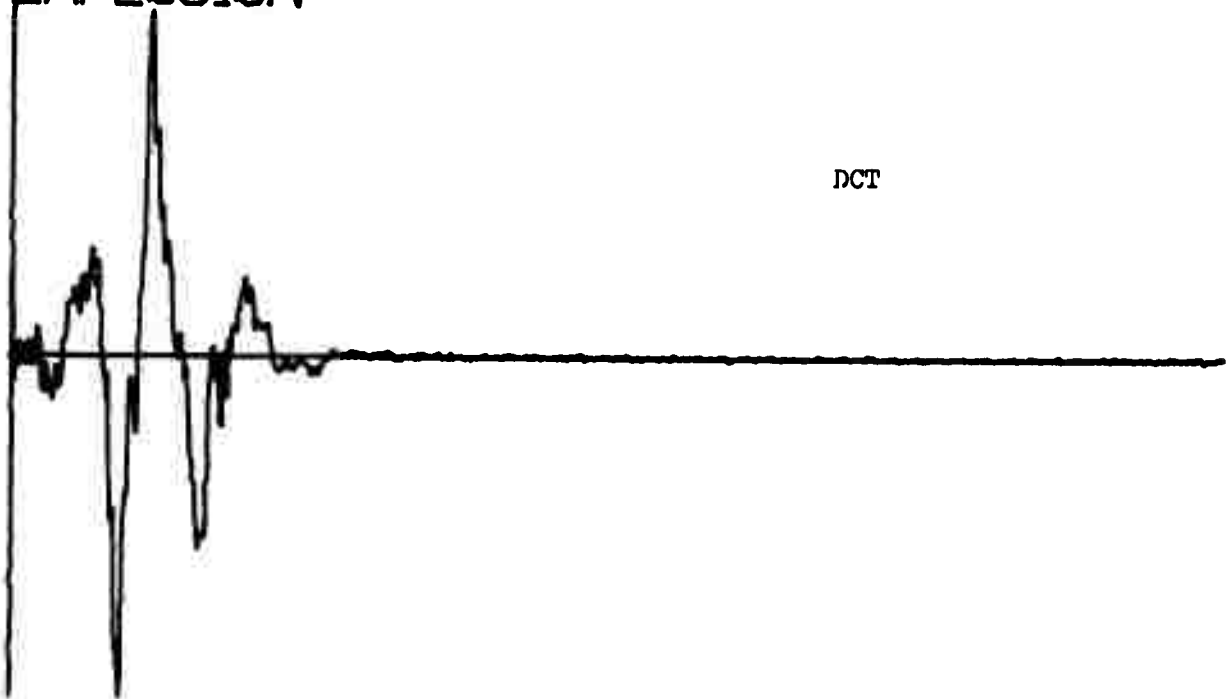
X076

EVENT NUMBER 1527
EXPLOSION

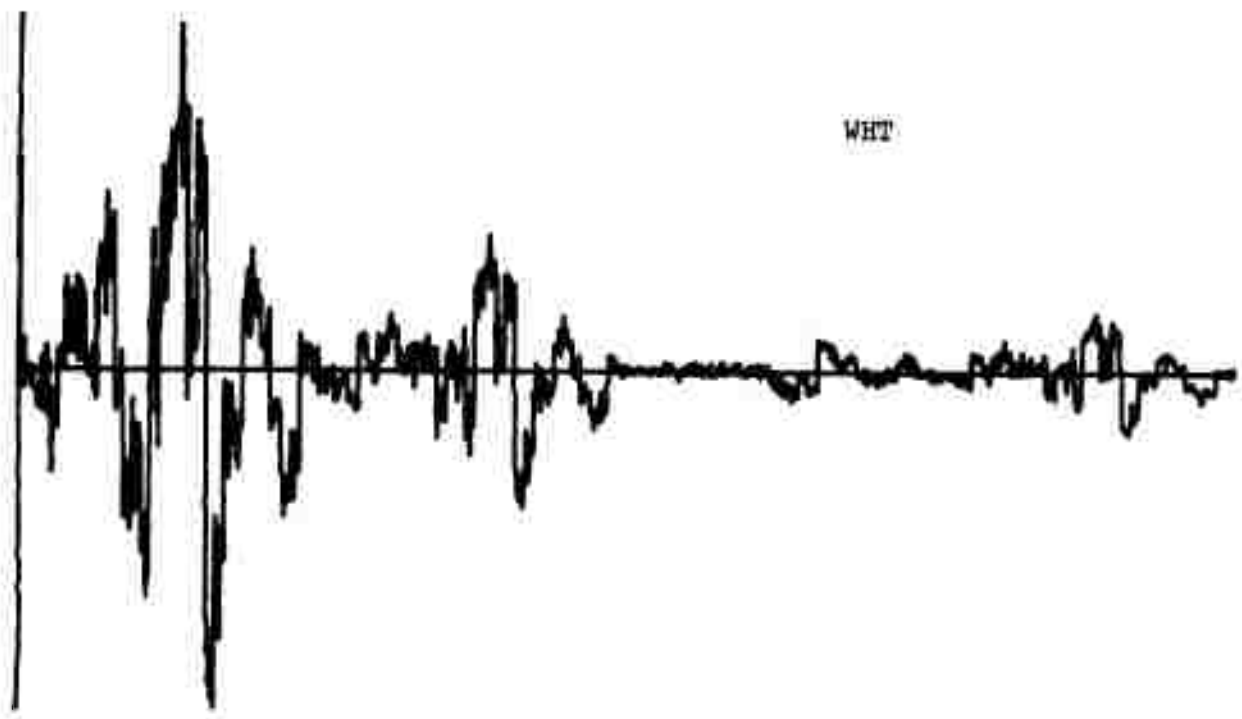


x078

EVENT NUMBER 1524
EXPLOSION



DCT

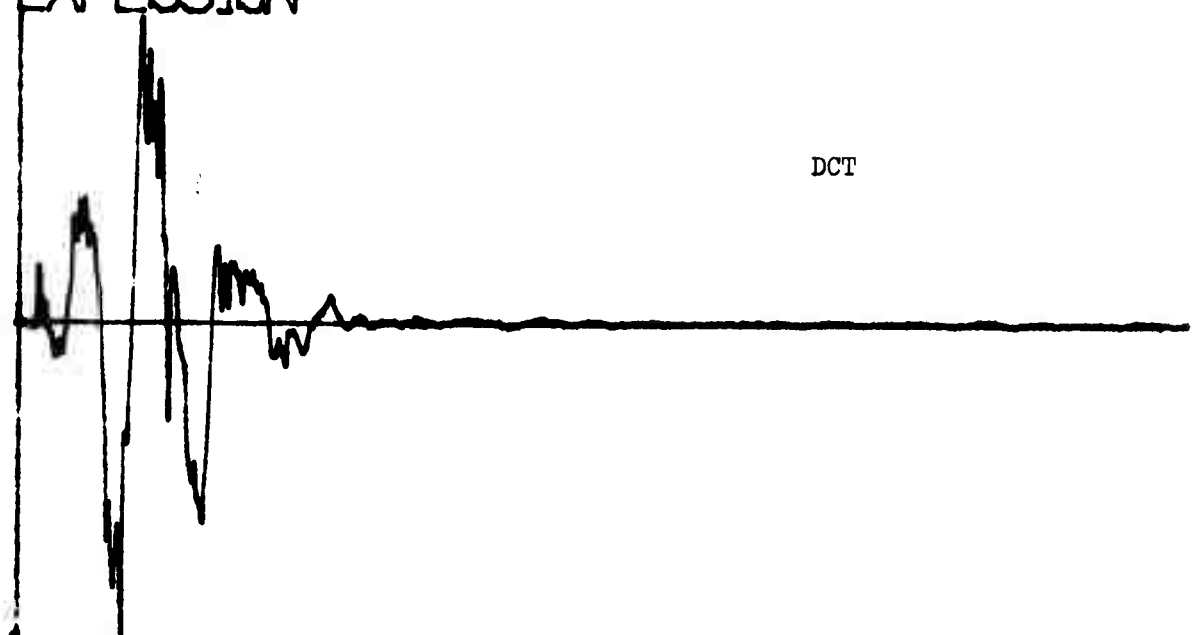


WHT

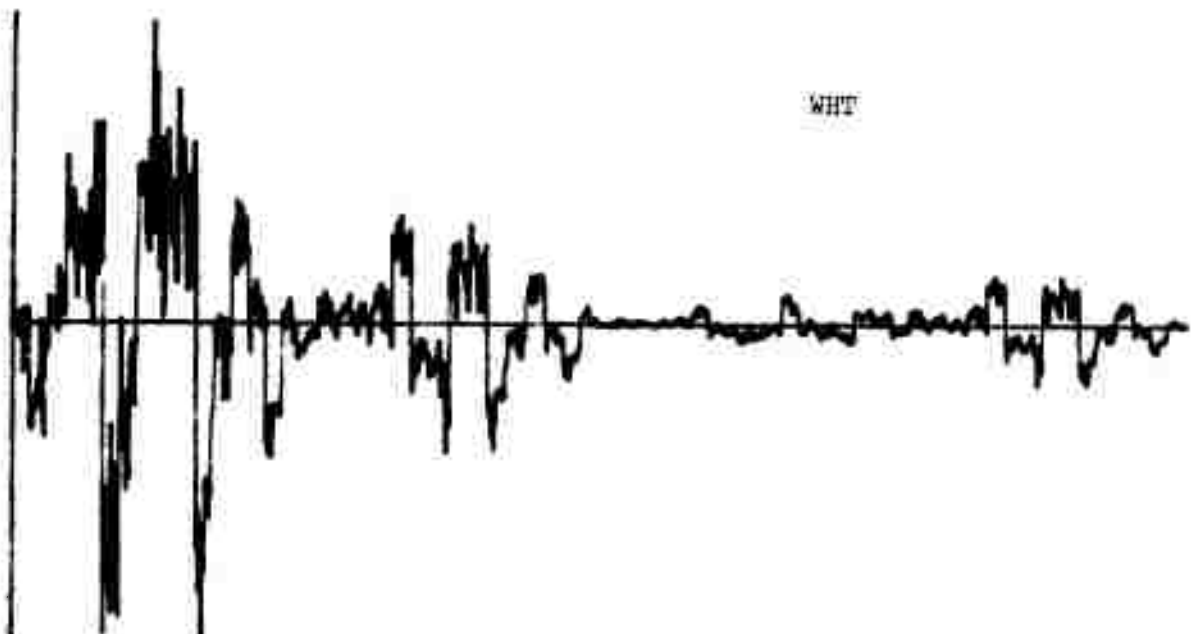
x080

EVENT NUMBER 1521
EXPLOSION

DCT



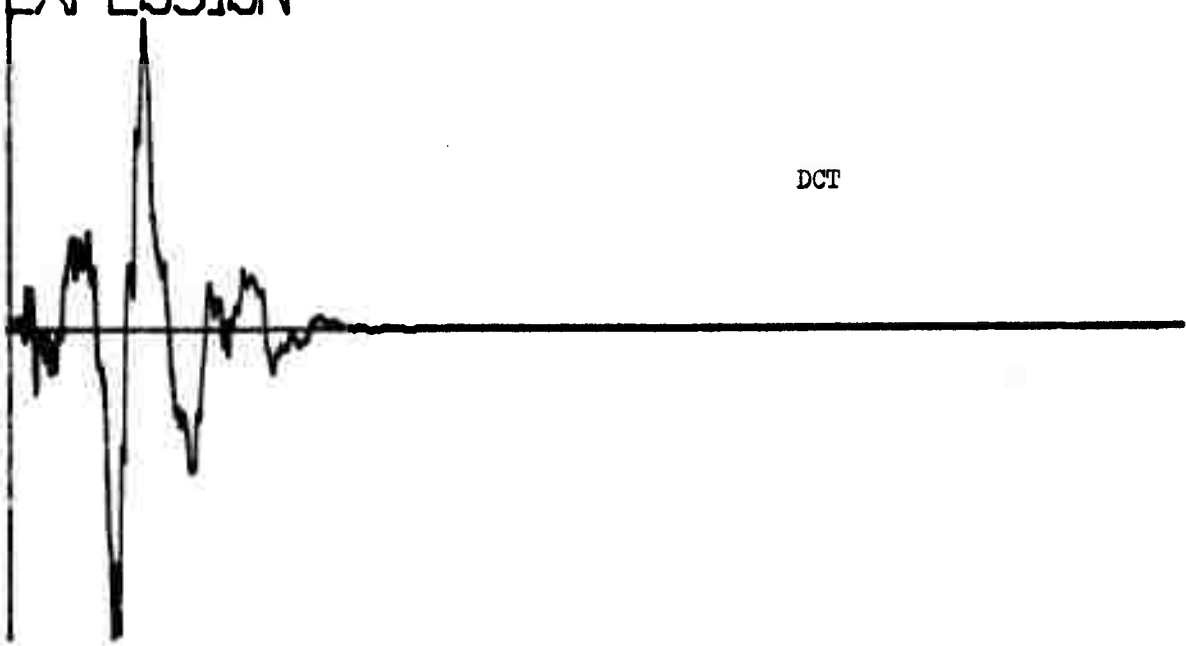
WHT



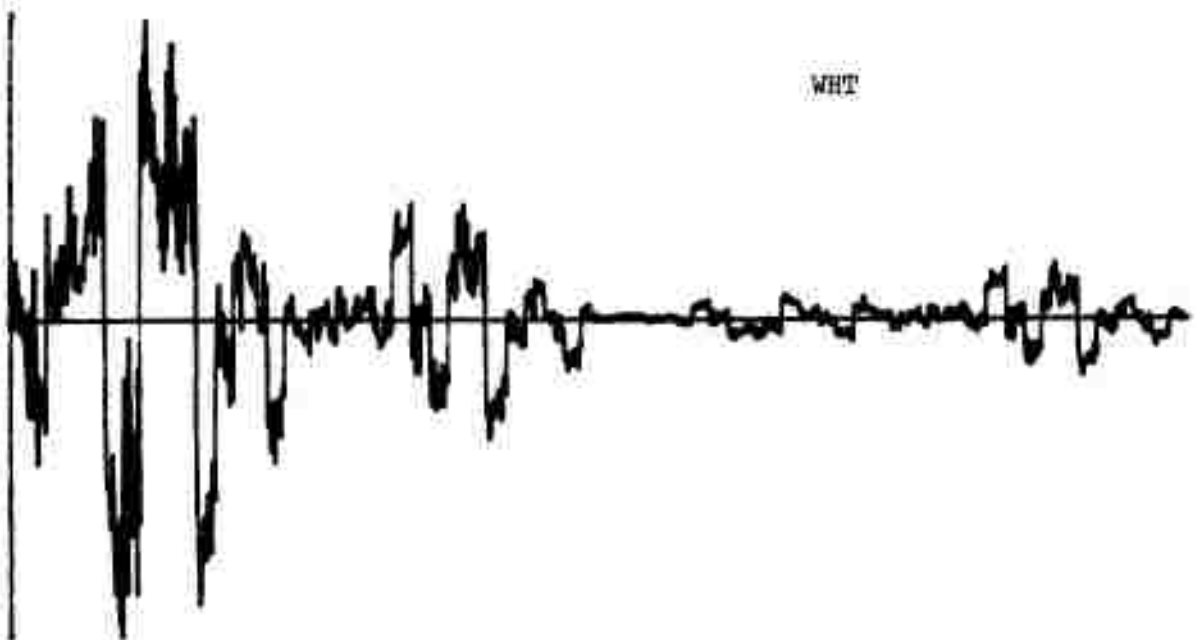
X082

EVENT NUMBER 1504
EXPLOSION

DCT



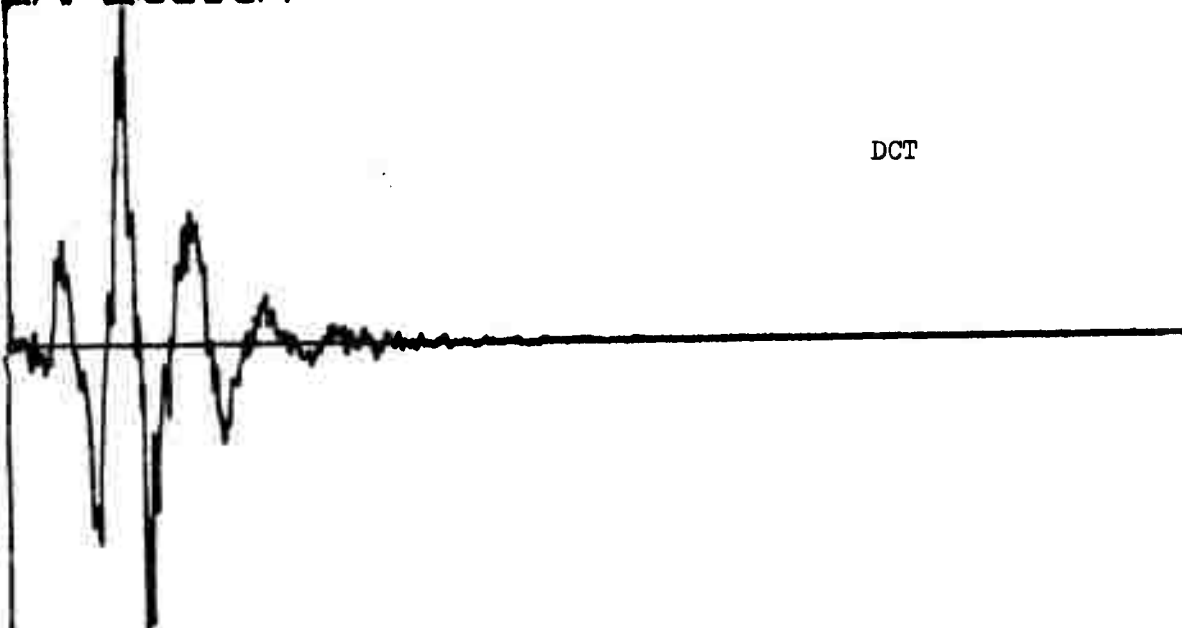
WHT



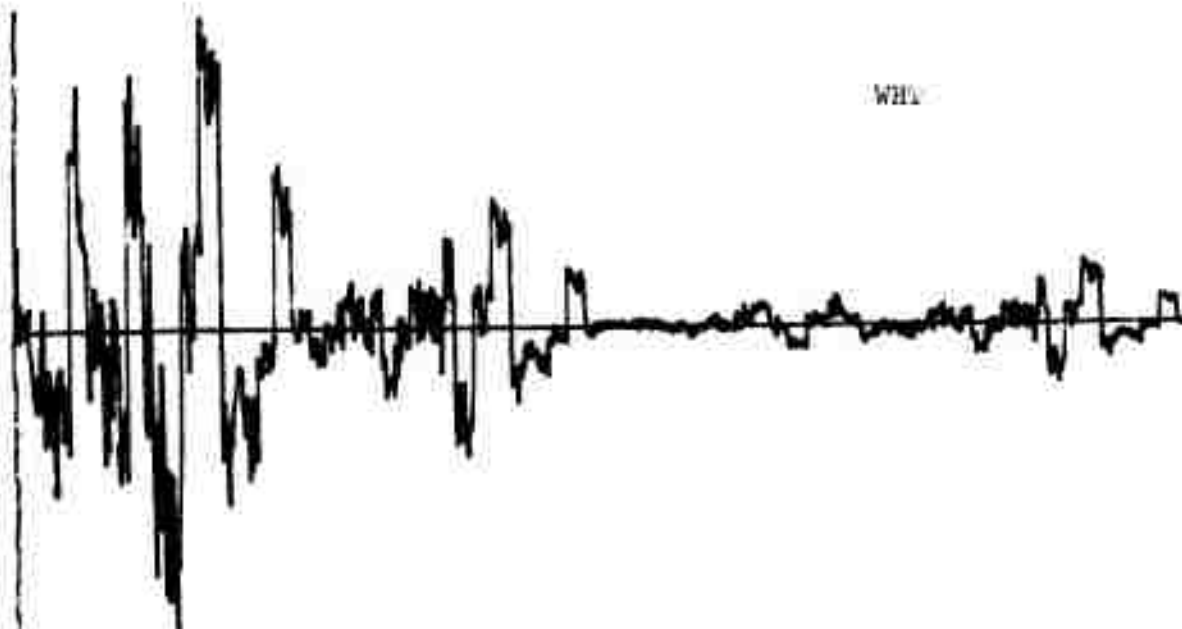
x084

EVENT NUMBER 1522
EXPLOSION

DCT



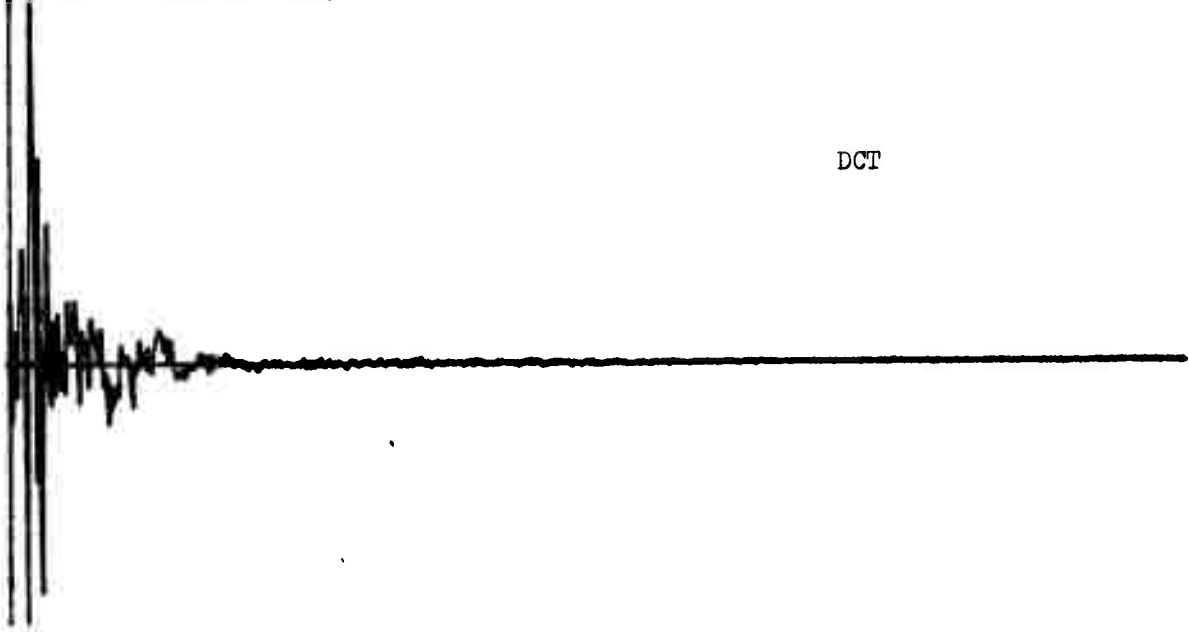
WHA



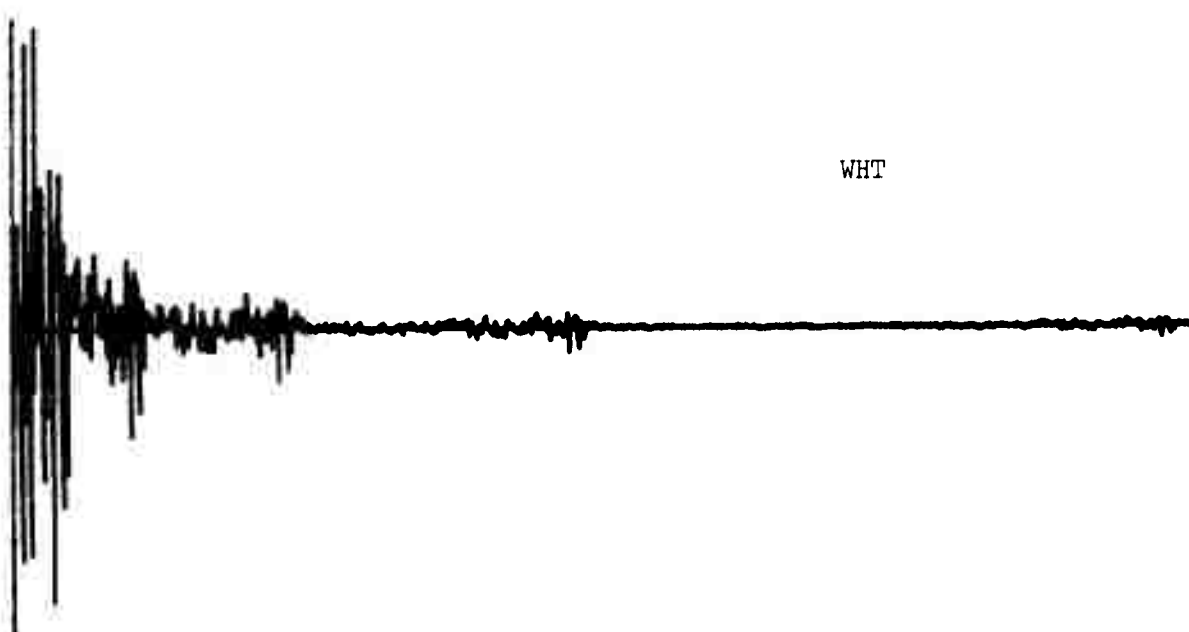
Q086

EVENT NUMBER 1208
EARTHQUAKE

DCT

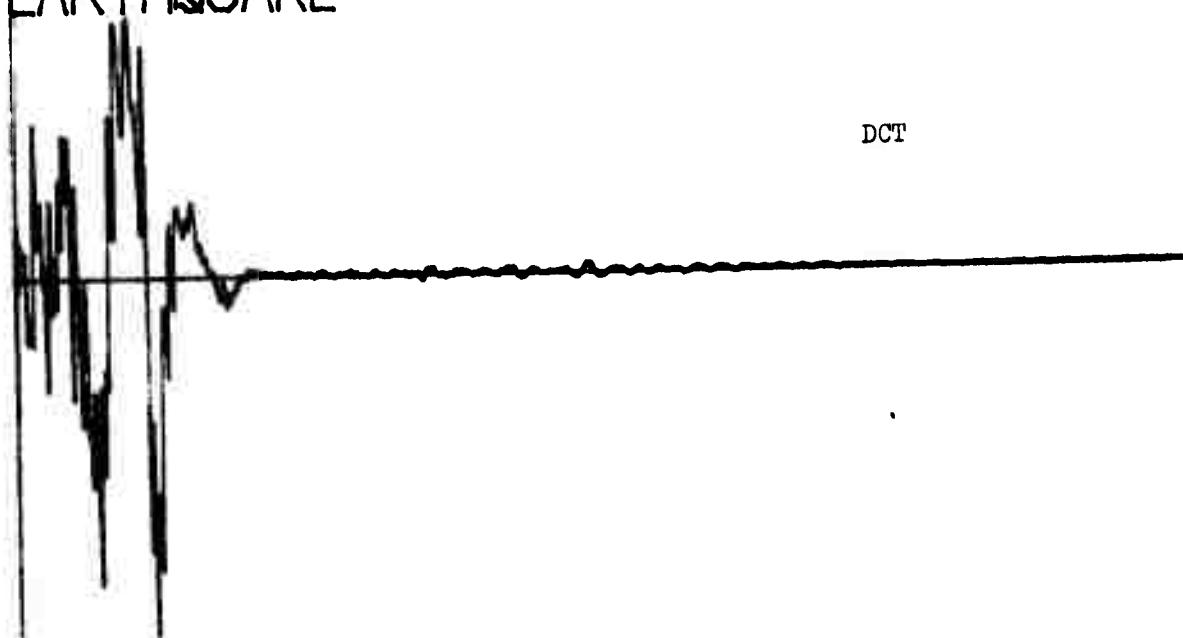


WHT

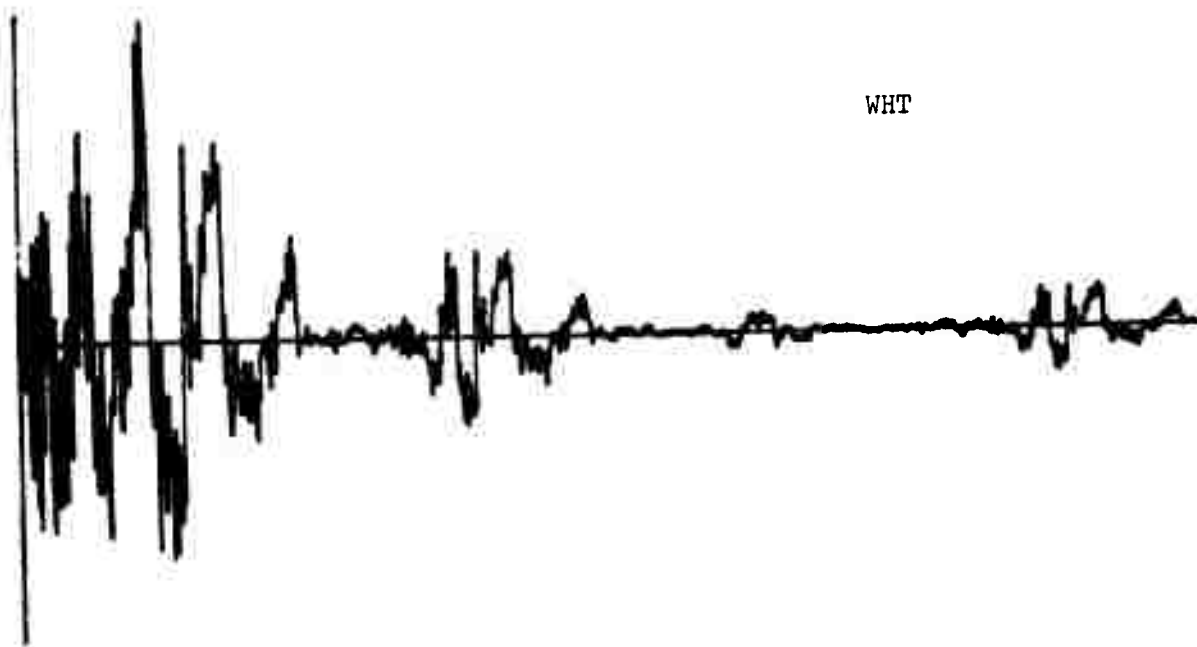


Q088

EVENT NUMBER 1009
EARTHQUAKE



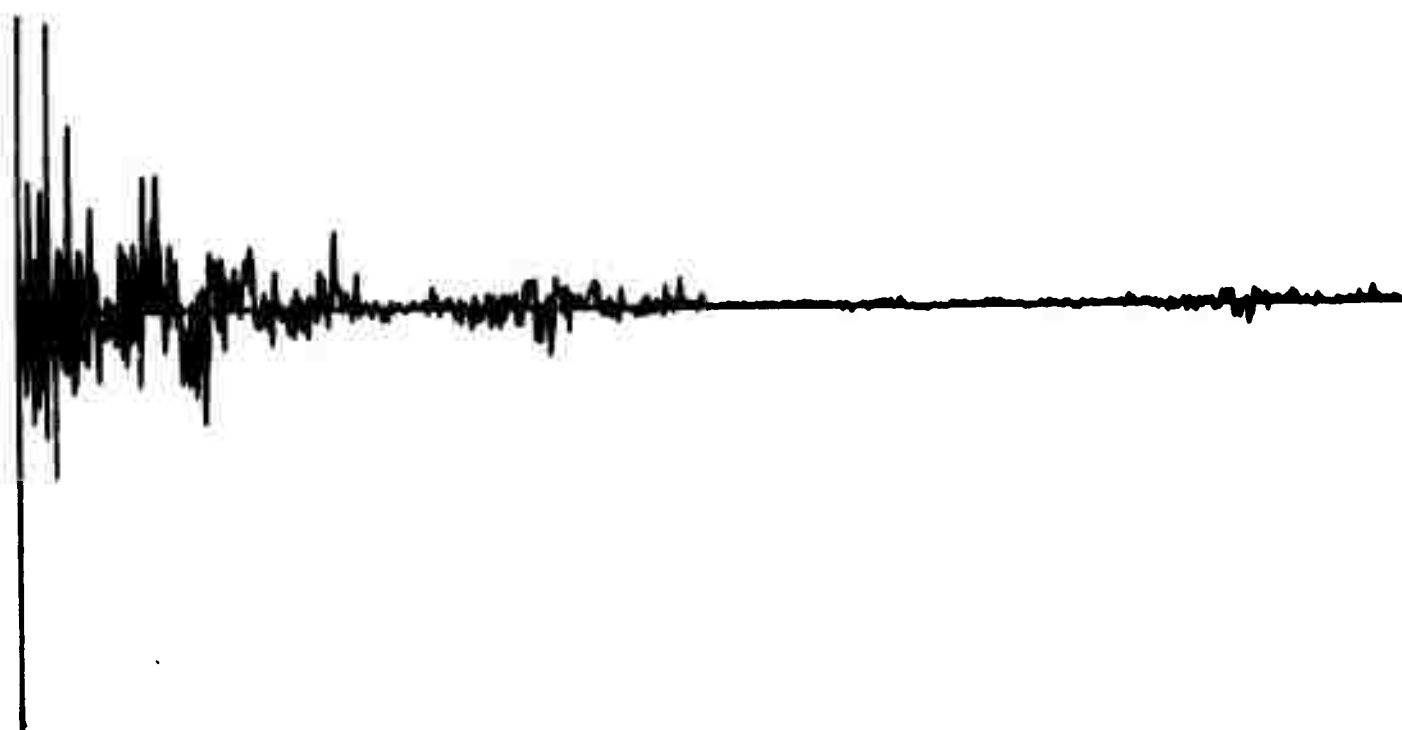
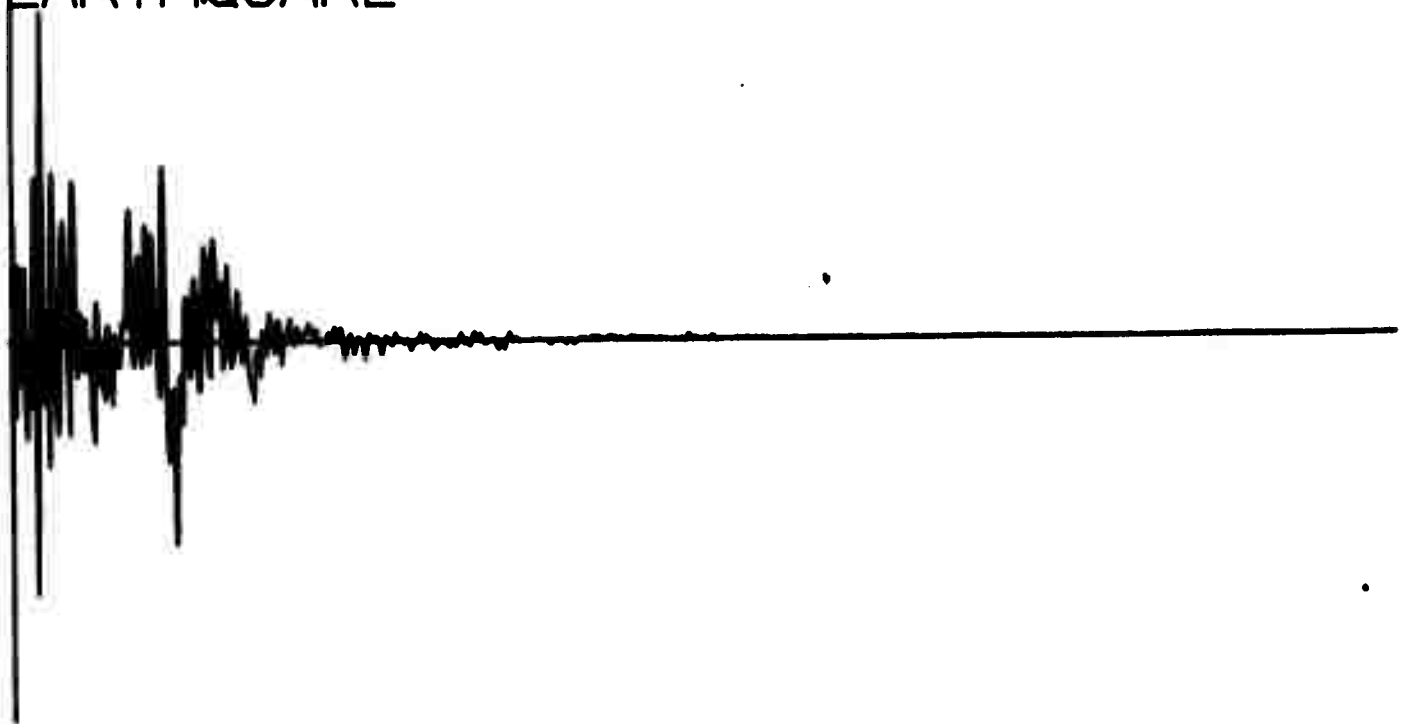
DCT



WHT

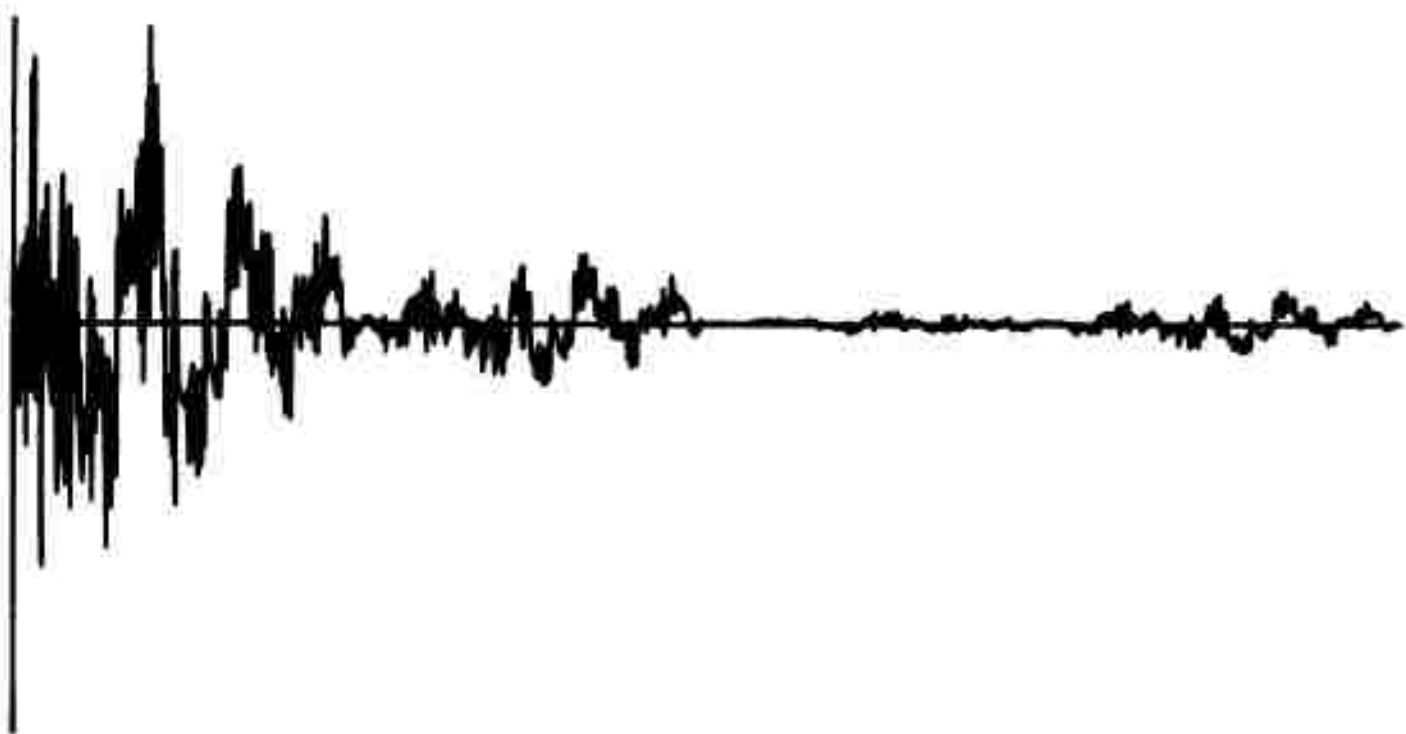
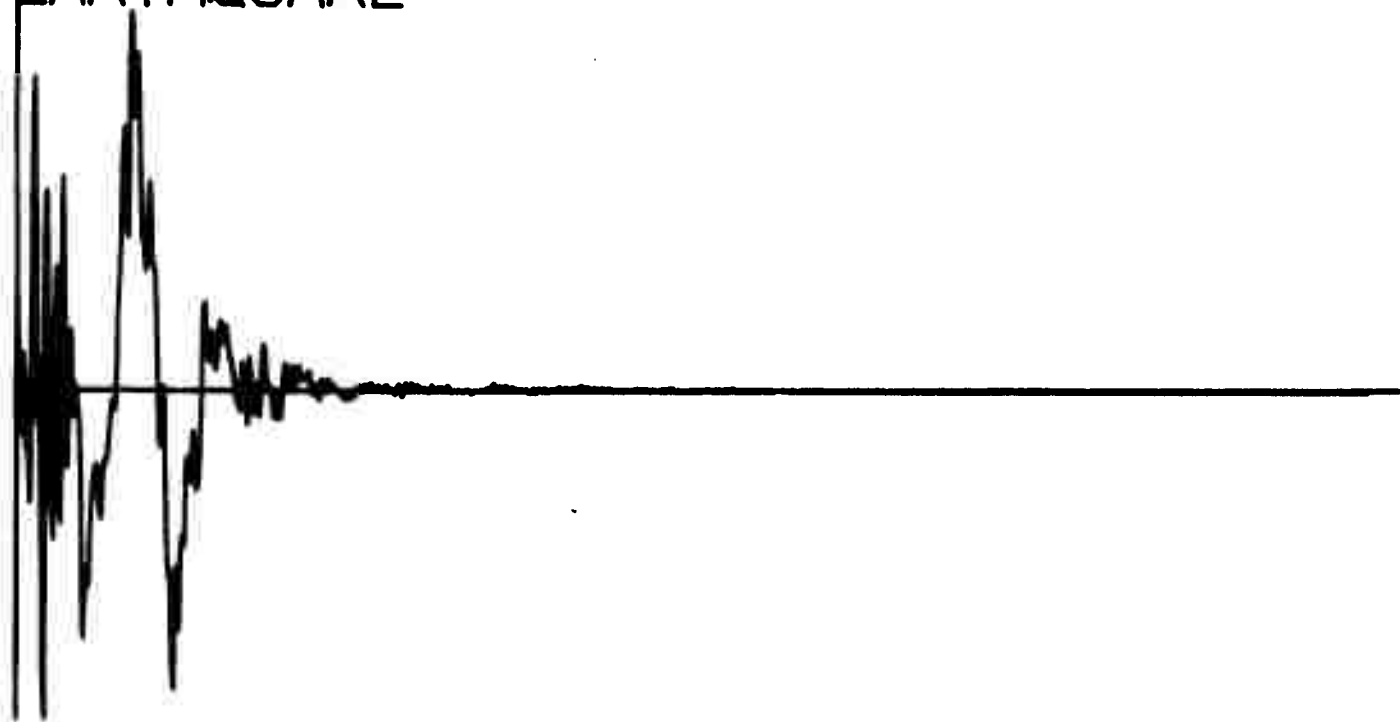
Q090

EVENT NUMBER 1011
EARTHQUAKE



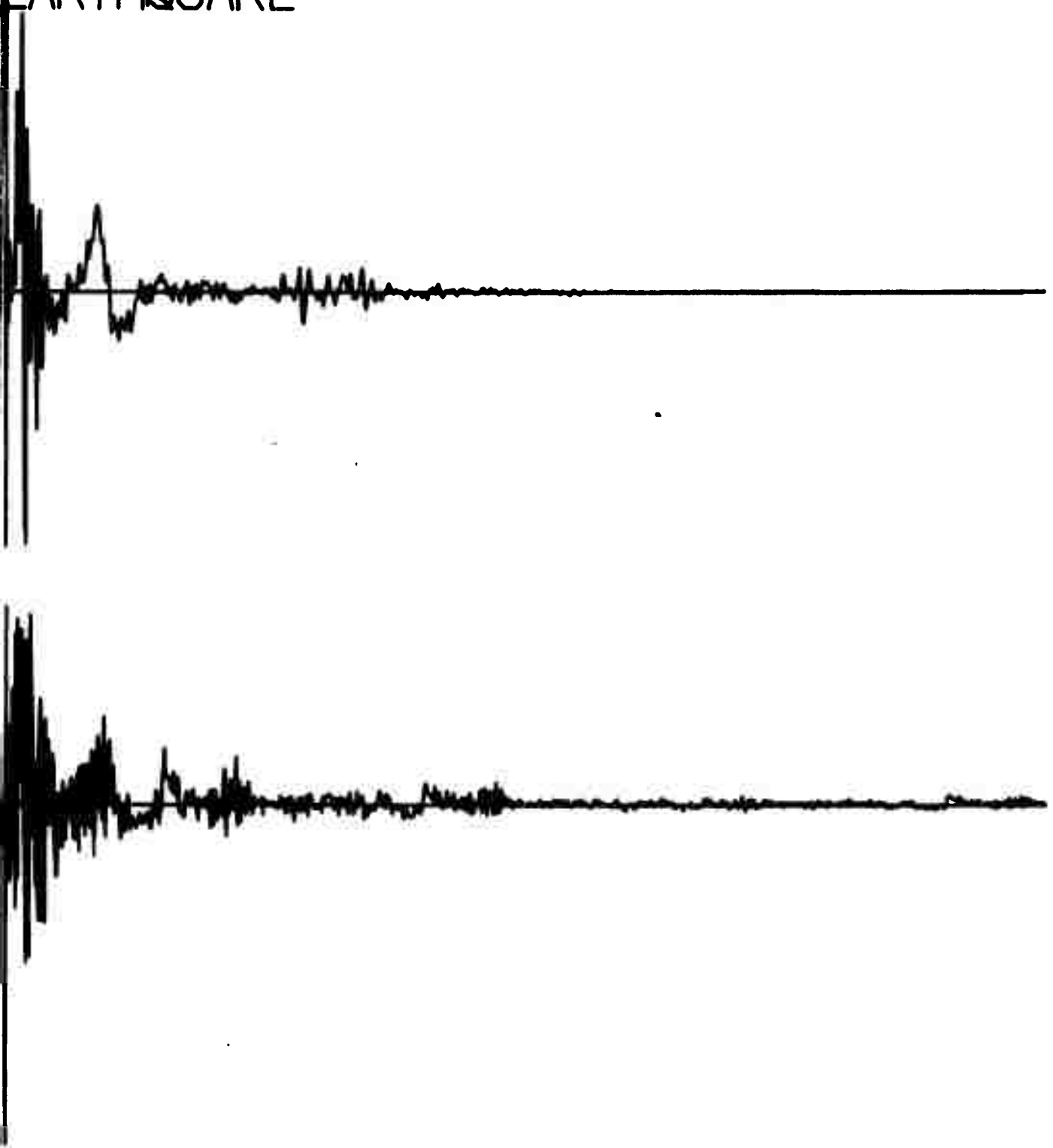
Q092

EVENT NUMBER 1023
EARTHQUAKE



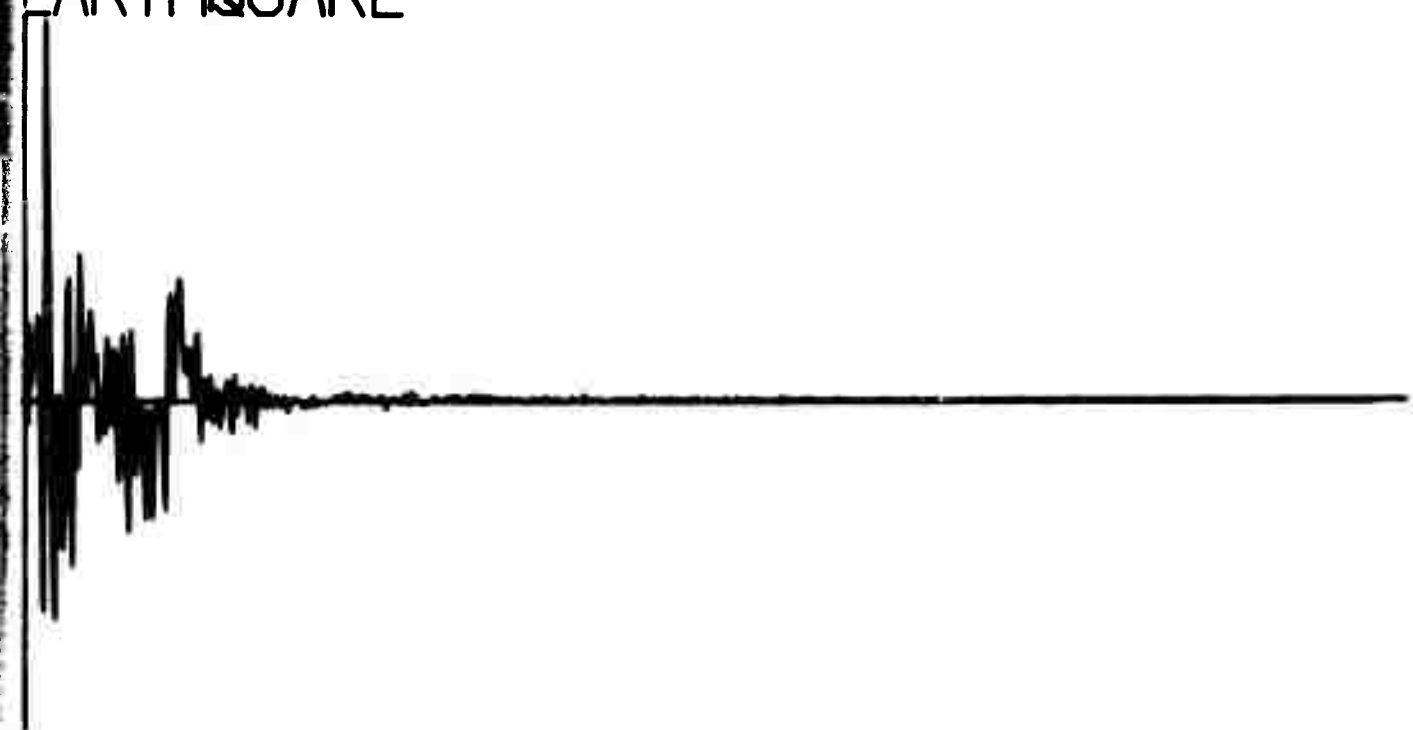
Q094

EVENT NUMBER 1020
EARTHQUAKE



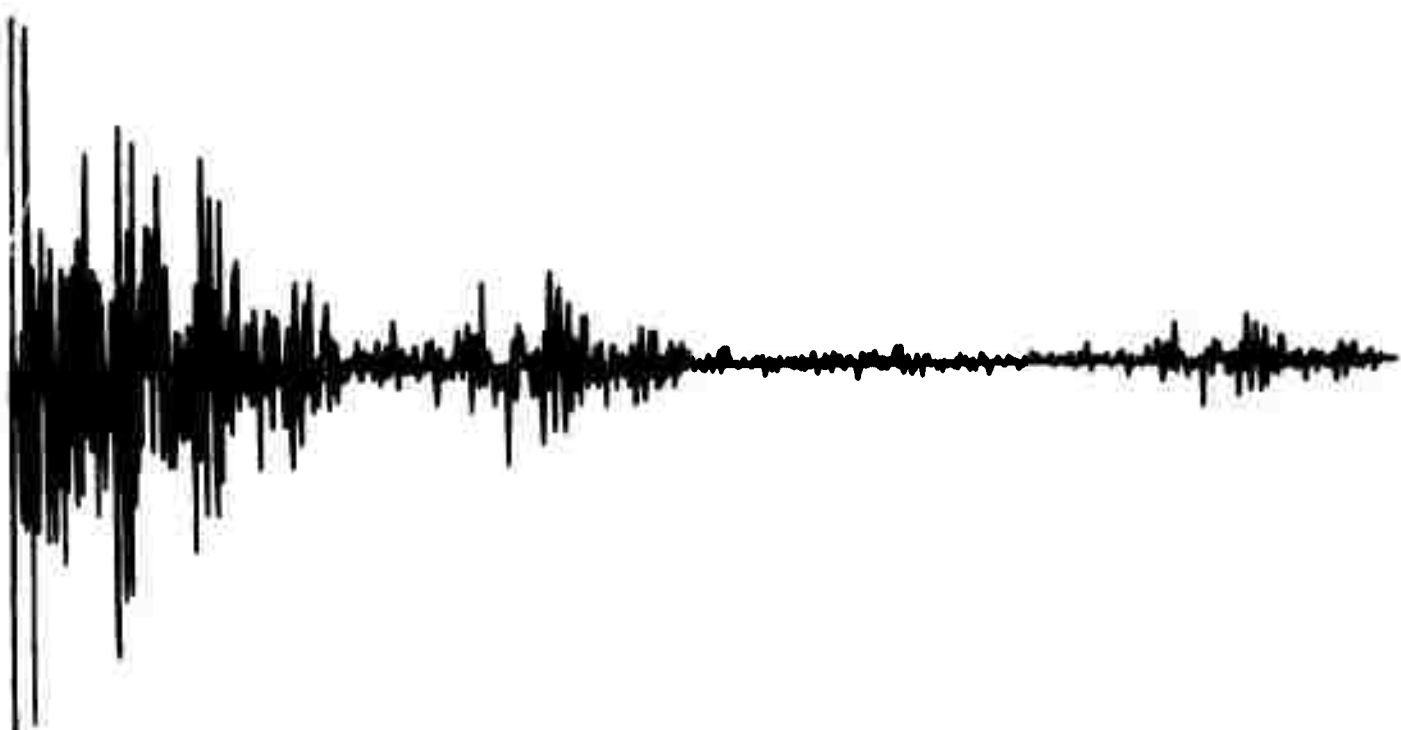
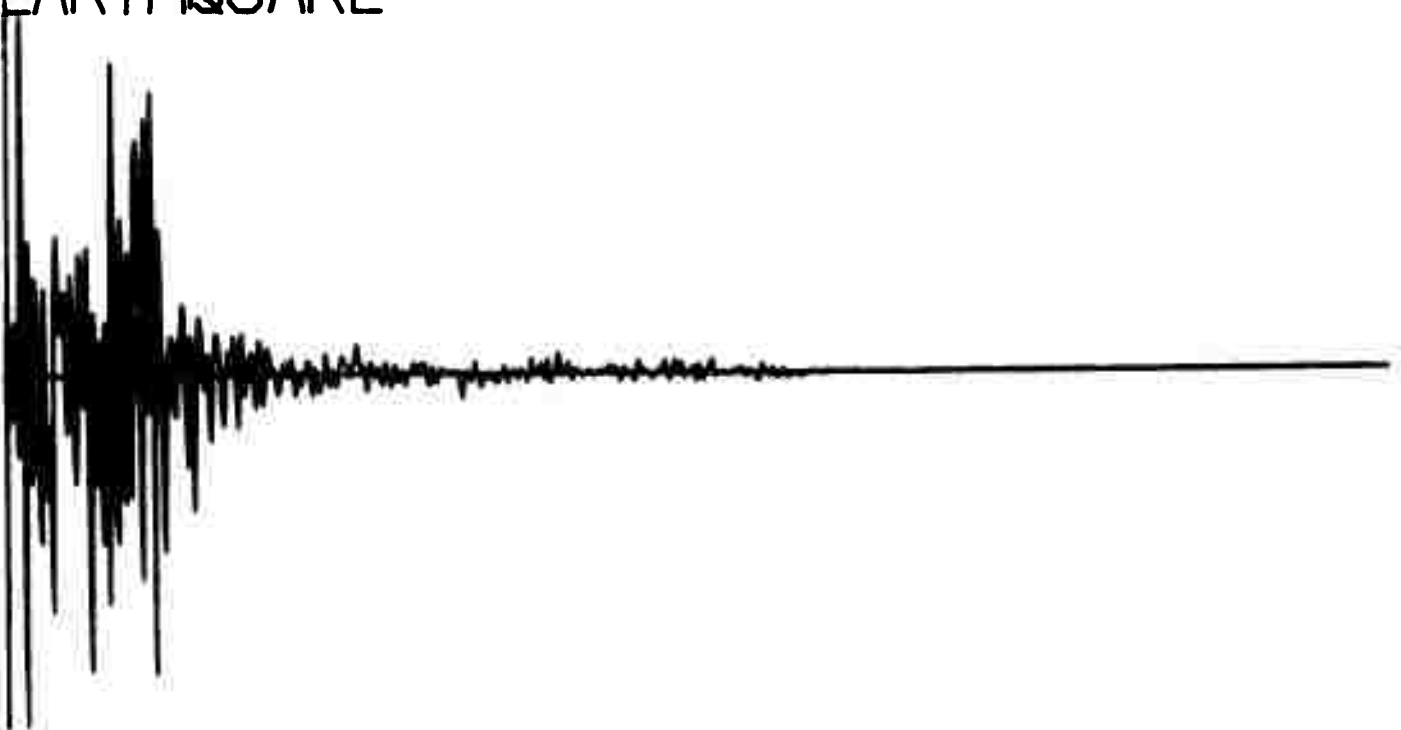
Q096

EVENT NUMBER 1029
EARTHQUAKE



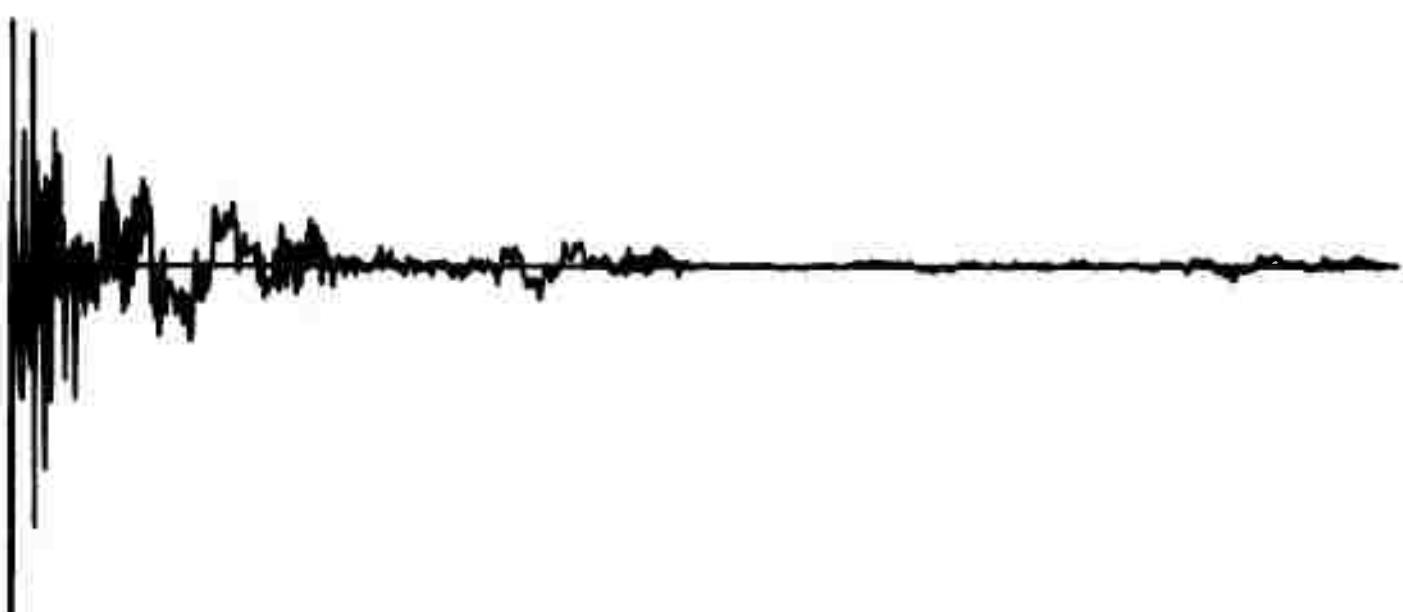
Q098

EVENT NUMBER 1030
EARTHQUAKE



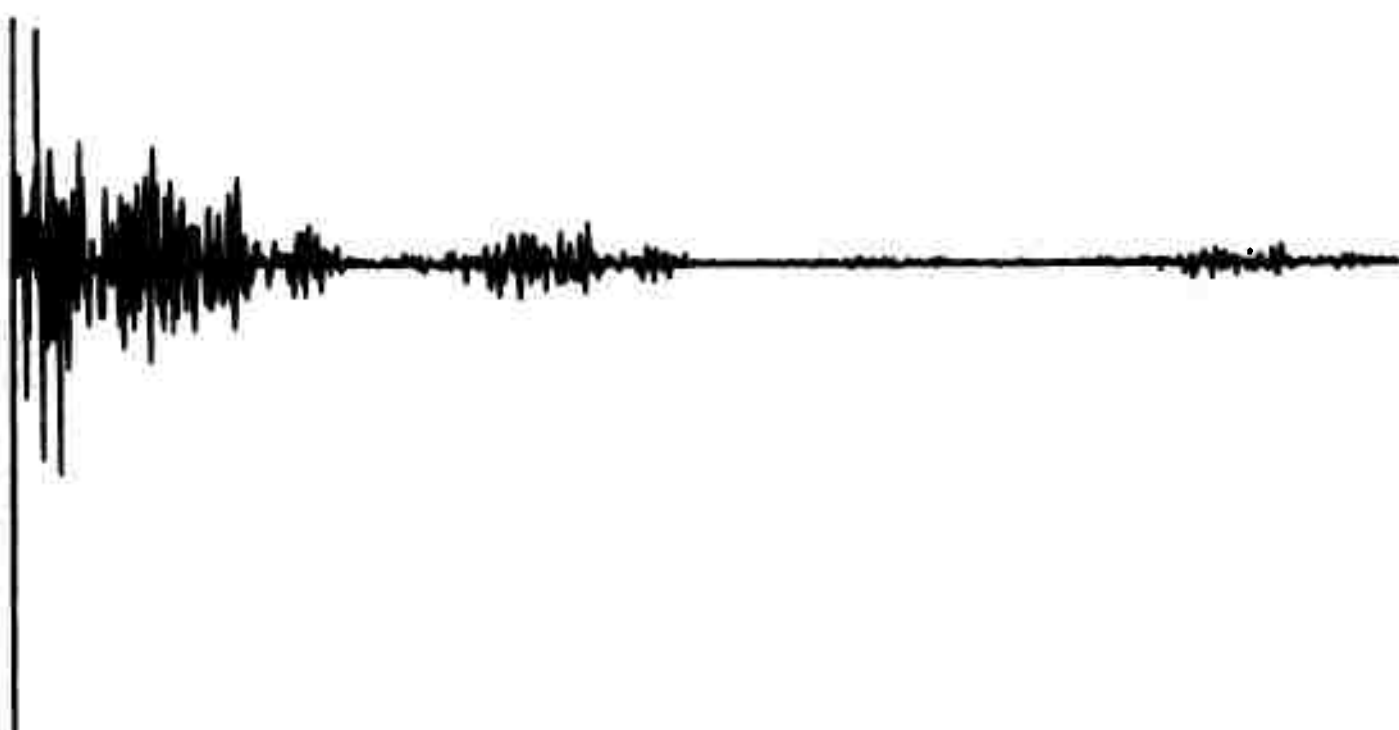
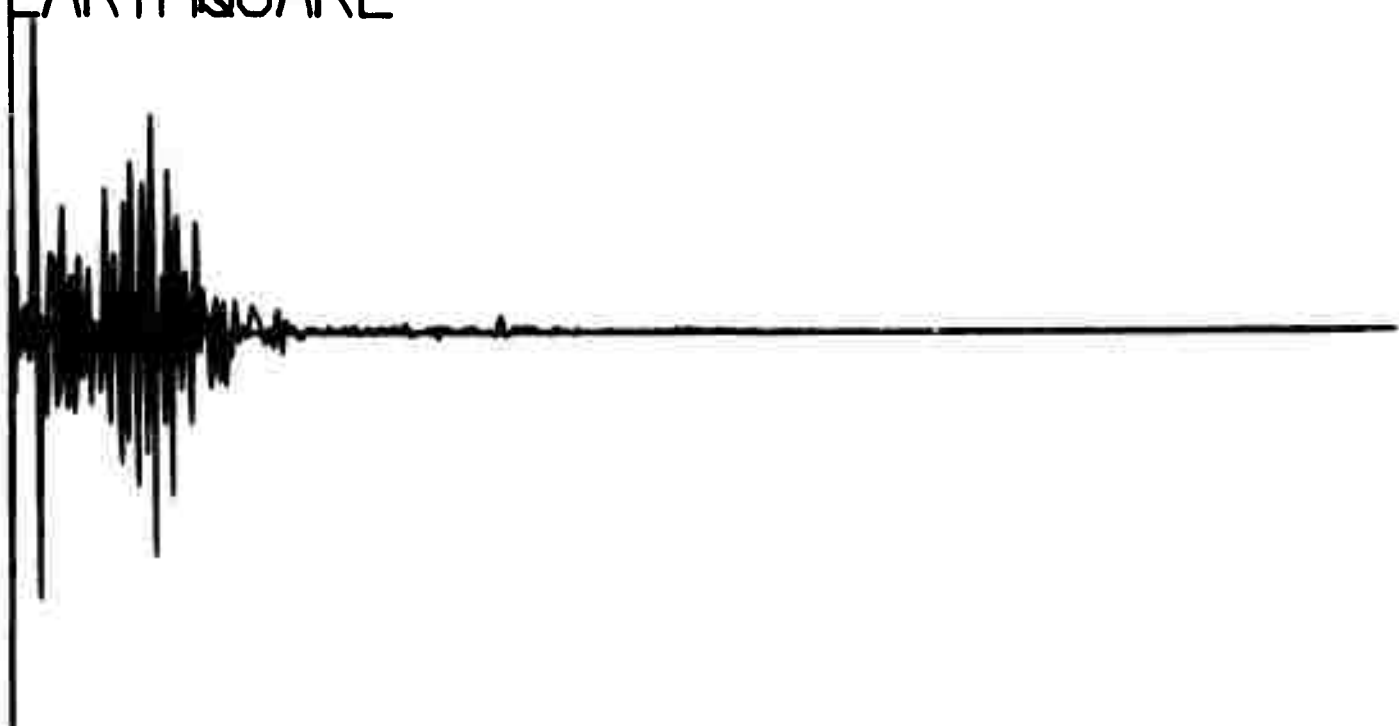
Q100

VENT NUMBER 1036
EARTHQUAKE



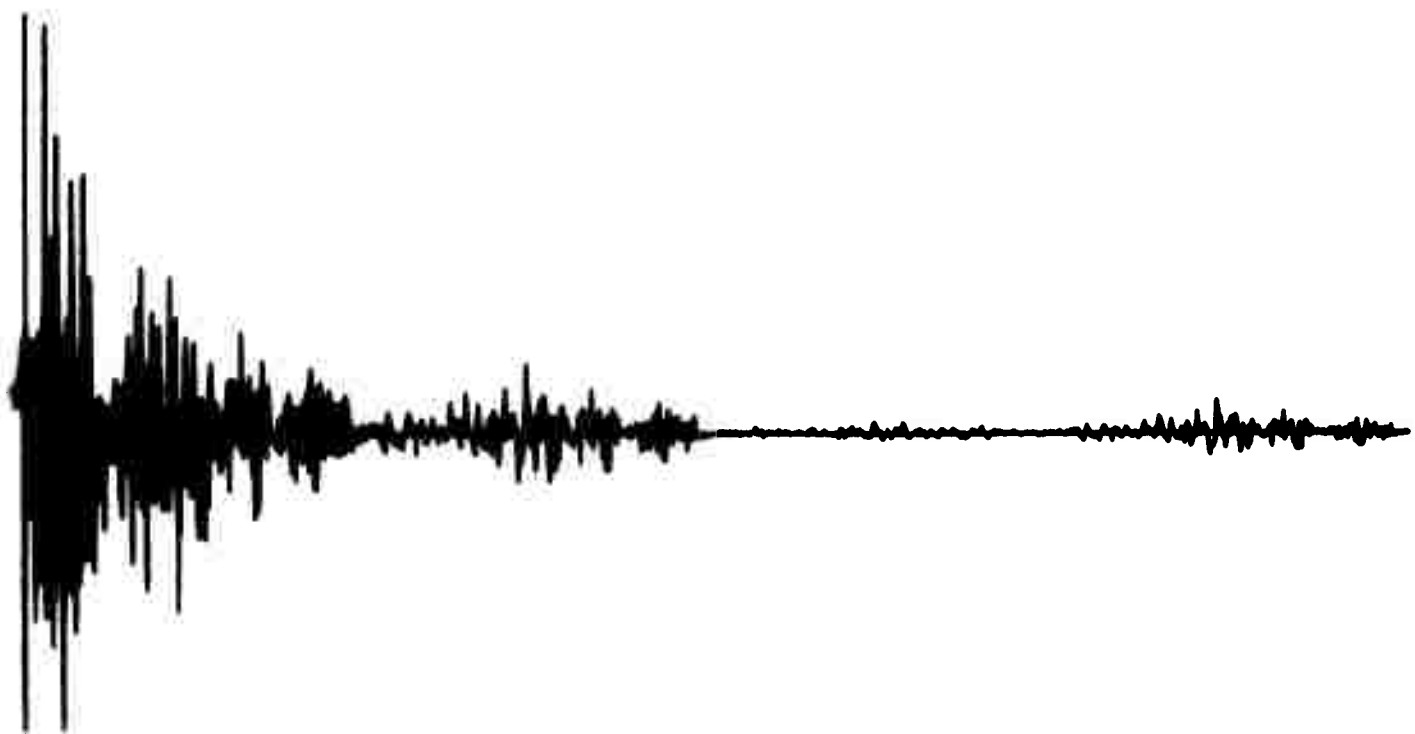
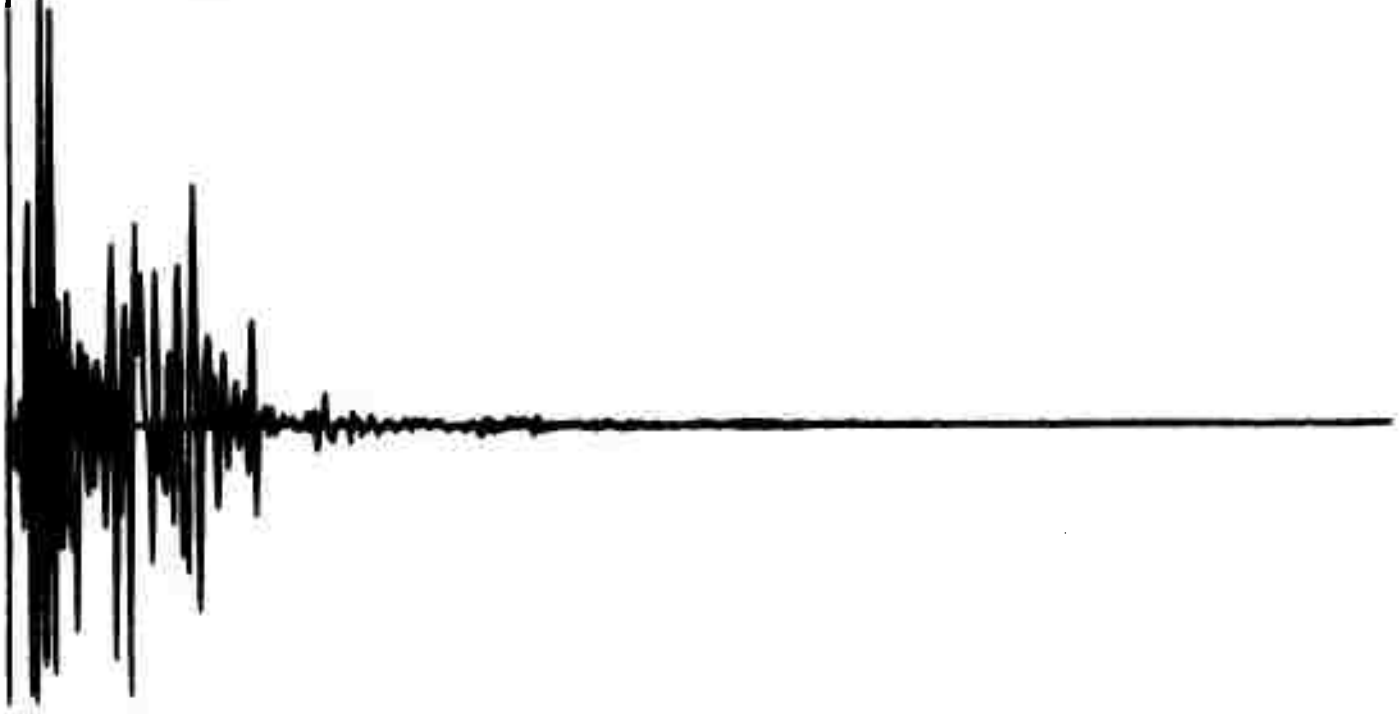
Q102

EVENT NUMBER 1040
EARTHQUAKE



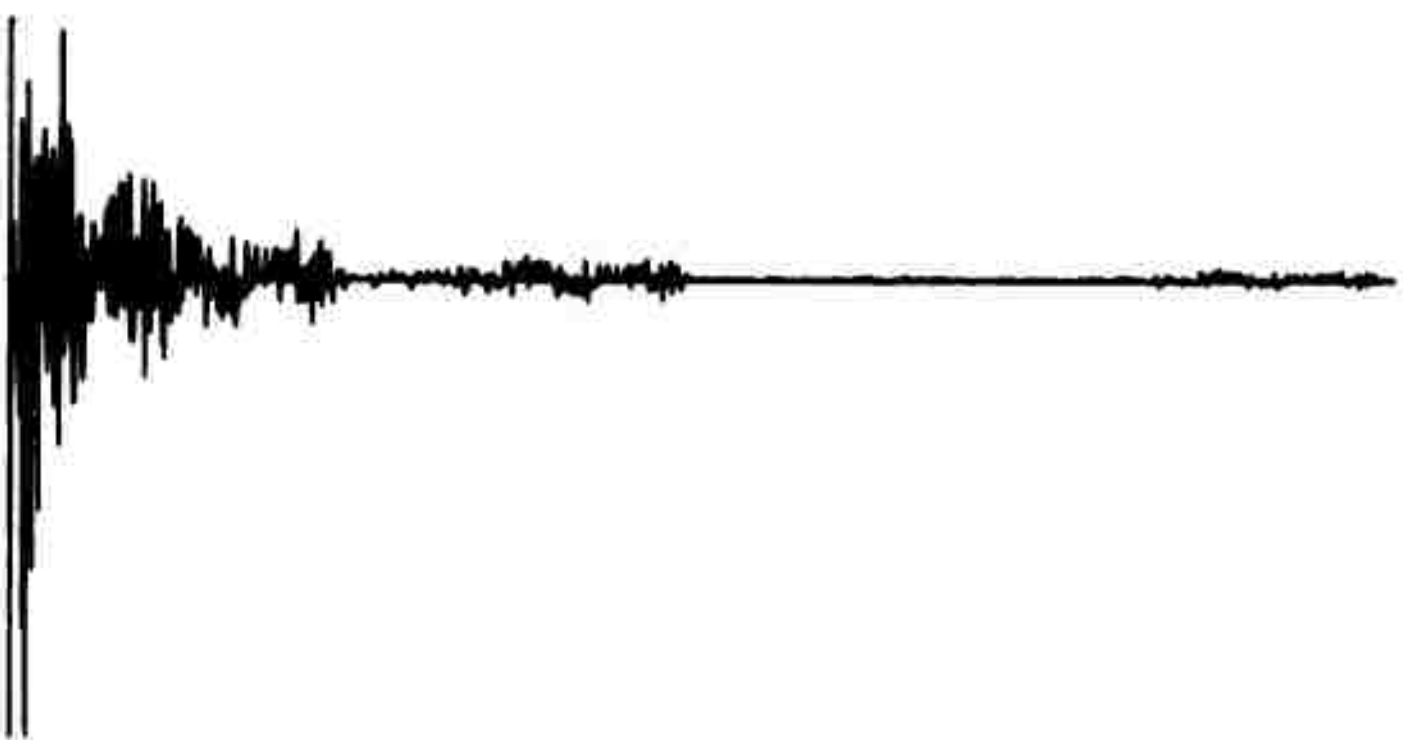
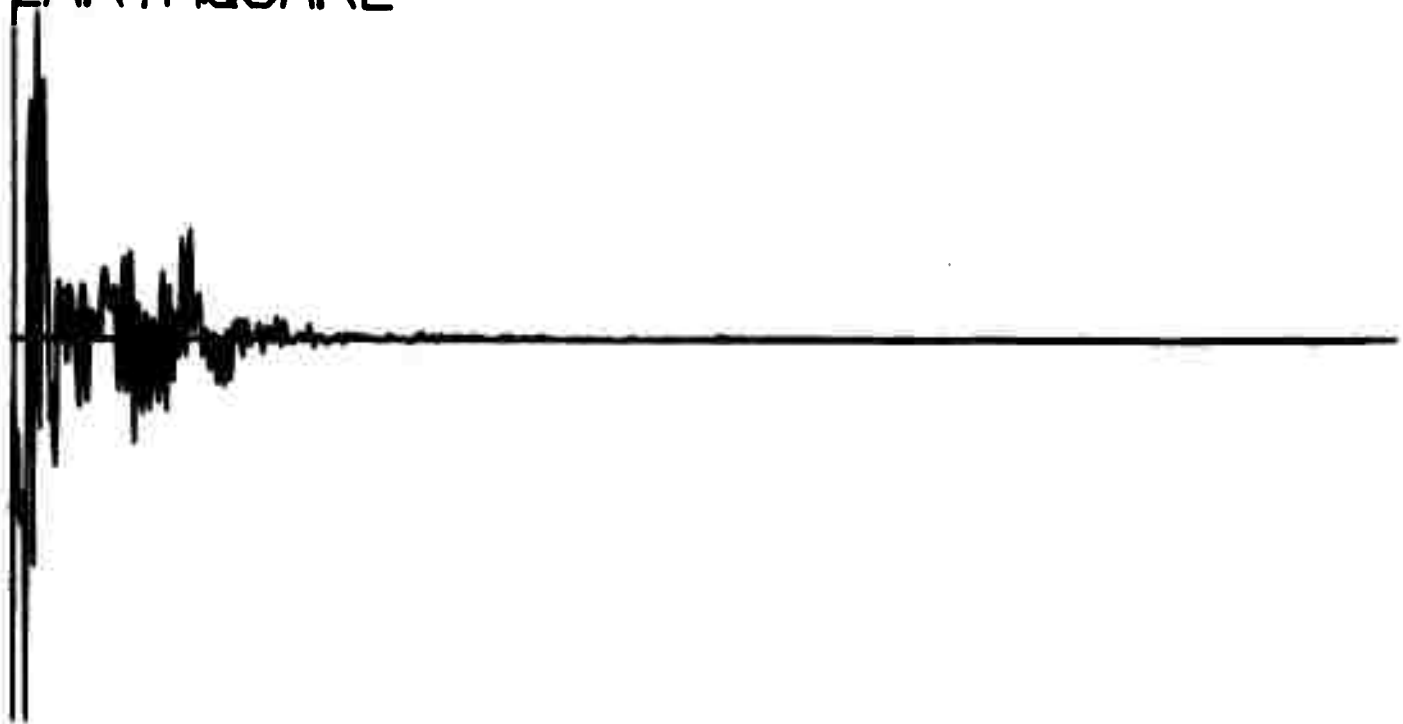
Q104

EVENT NUMBER 1059
EARTHQUAKE



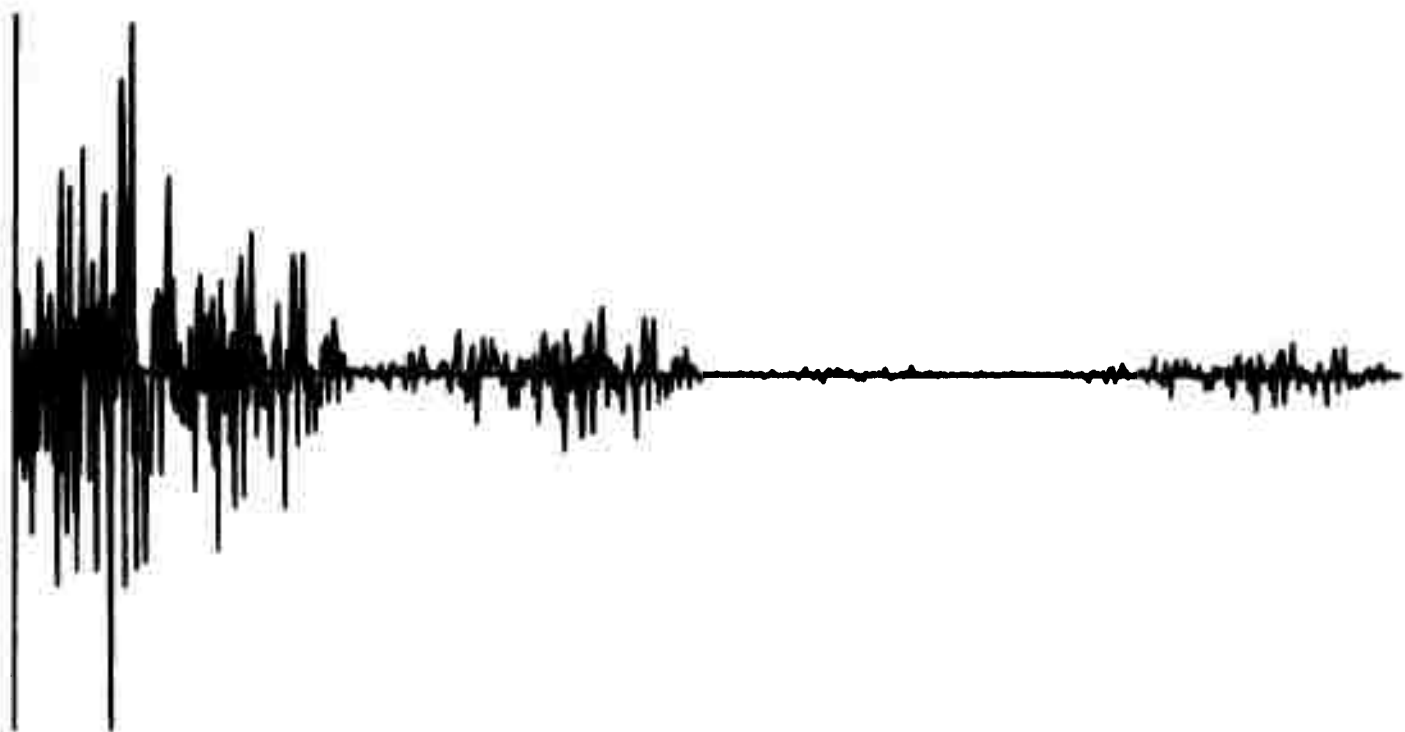
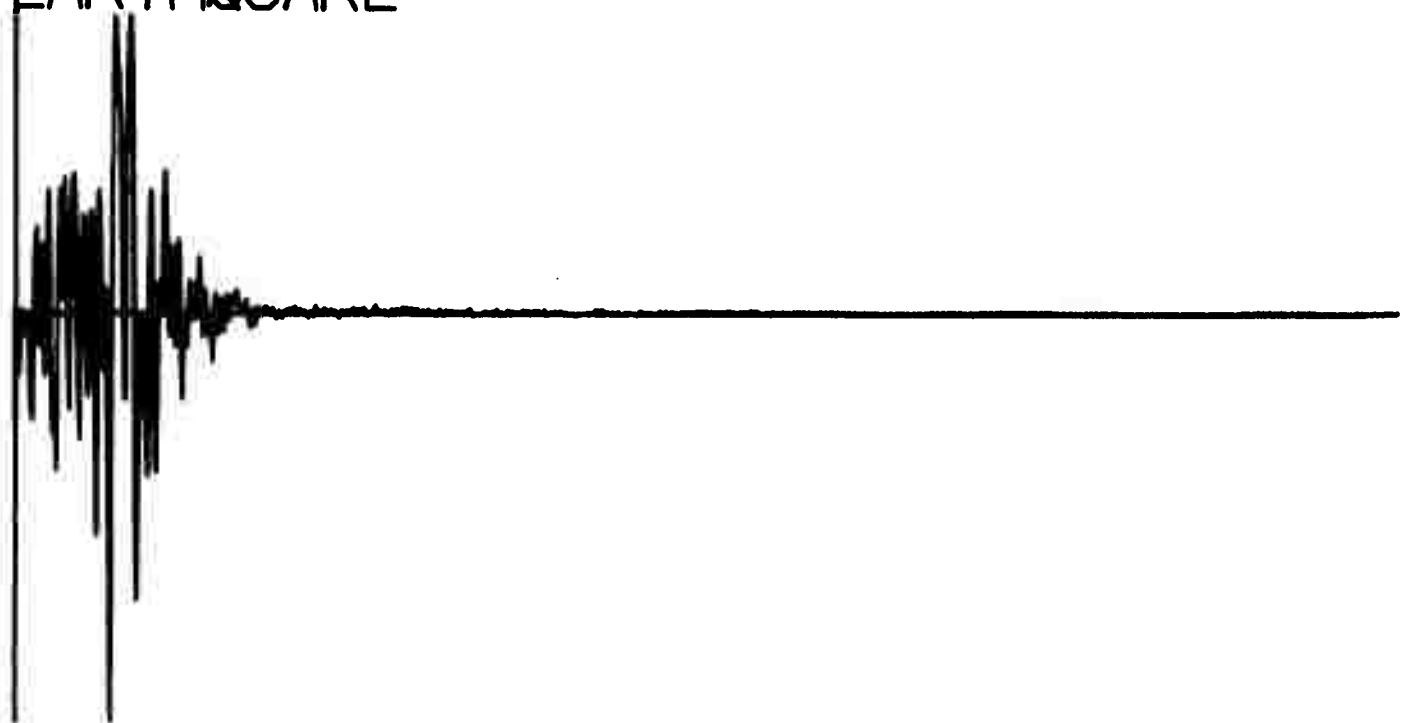
Q106

VENT NUMBER 1065
EARTHQUAKE



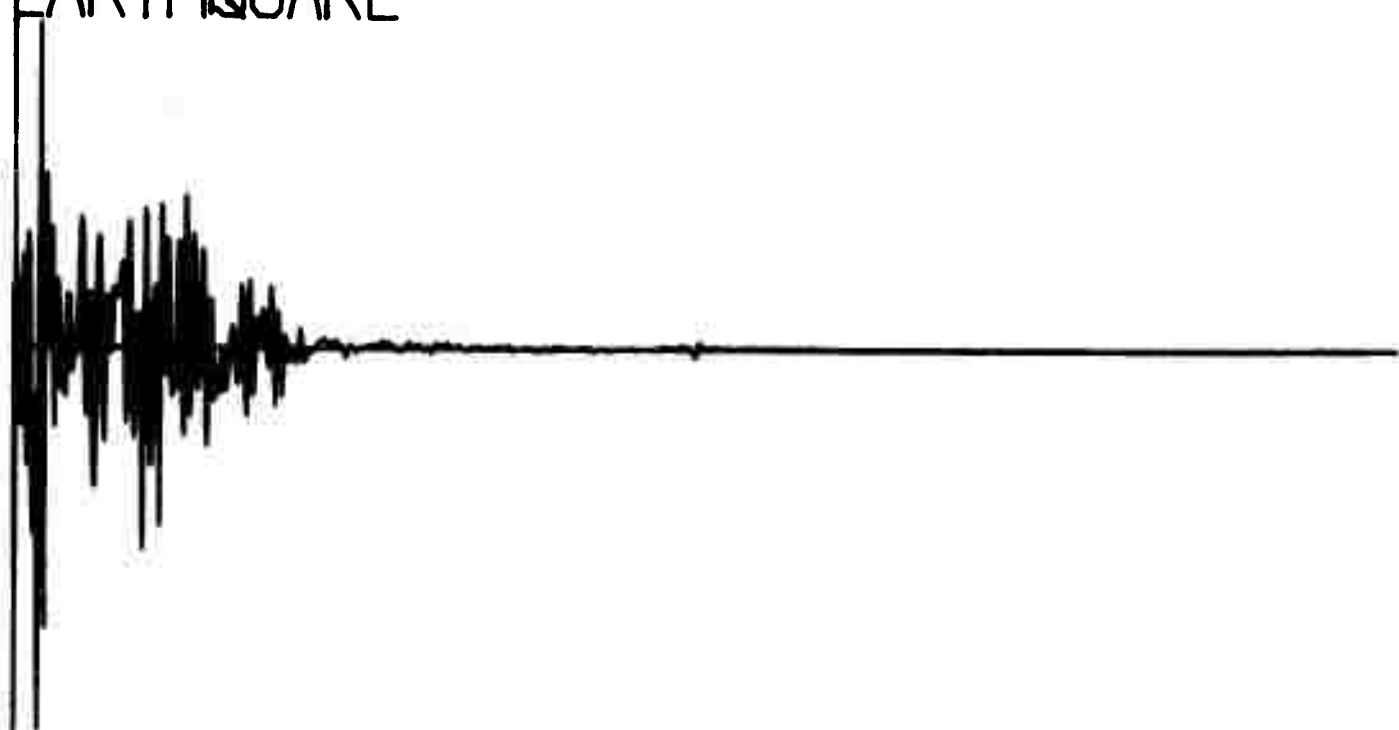
Q108

VENT NUMBER 1070
EARTHQUAKE



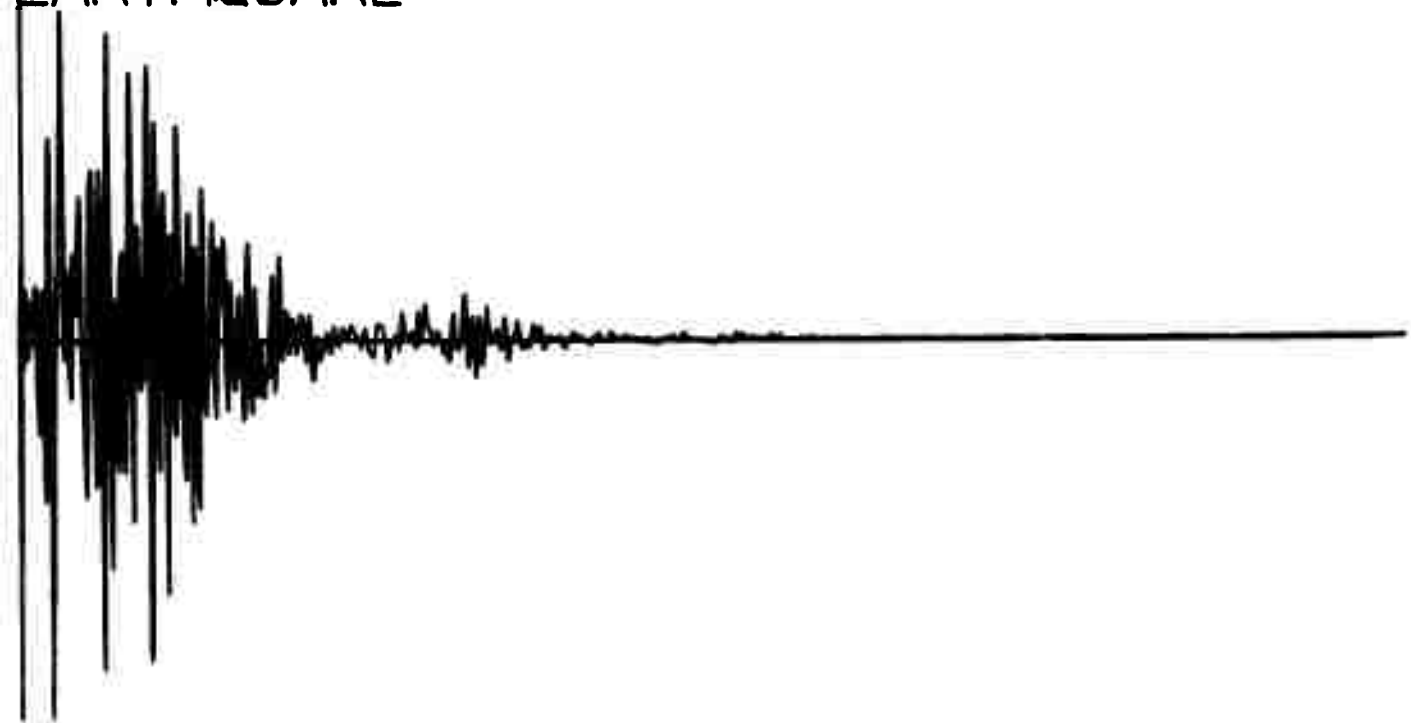
~~Q110~~

EVENT NUMBER 1066
EARTHQUAKE



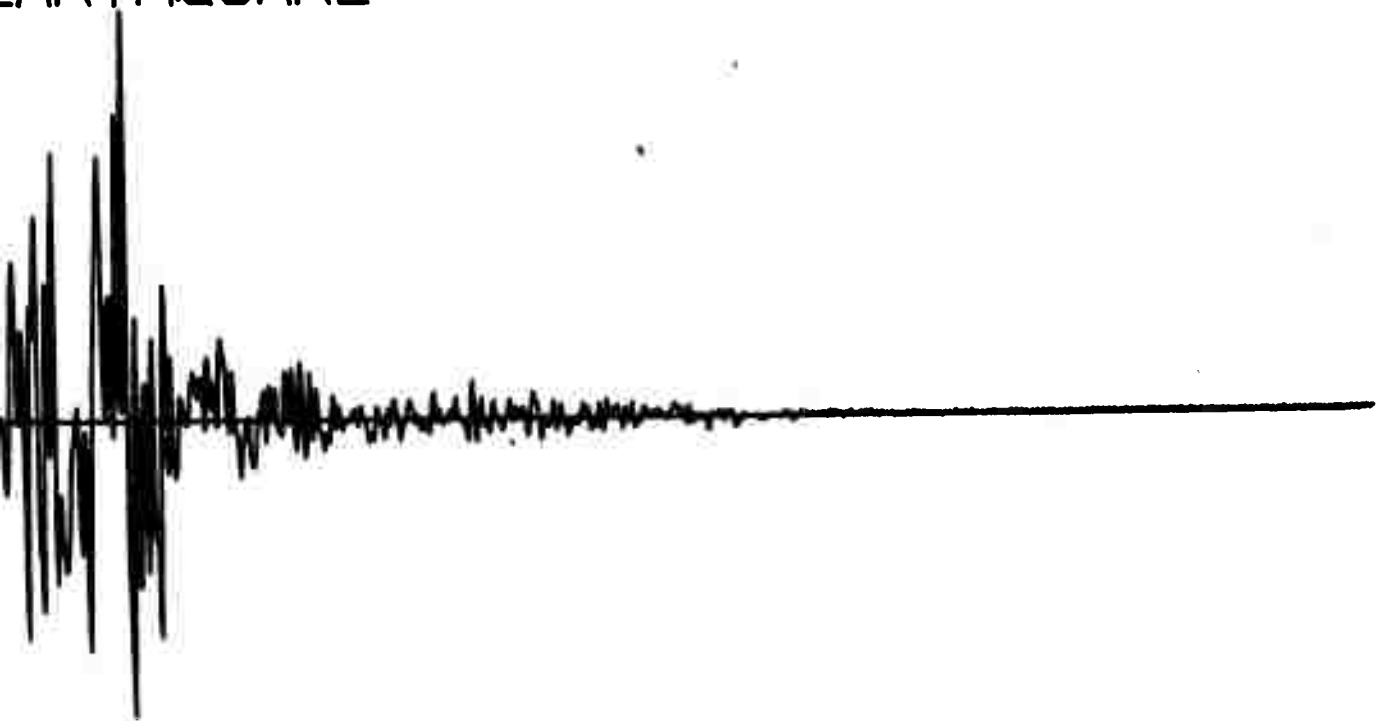
Q112

VENT NUMBER 1073
EARTHQUAKE



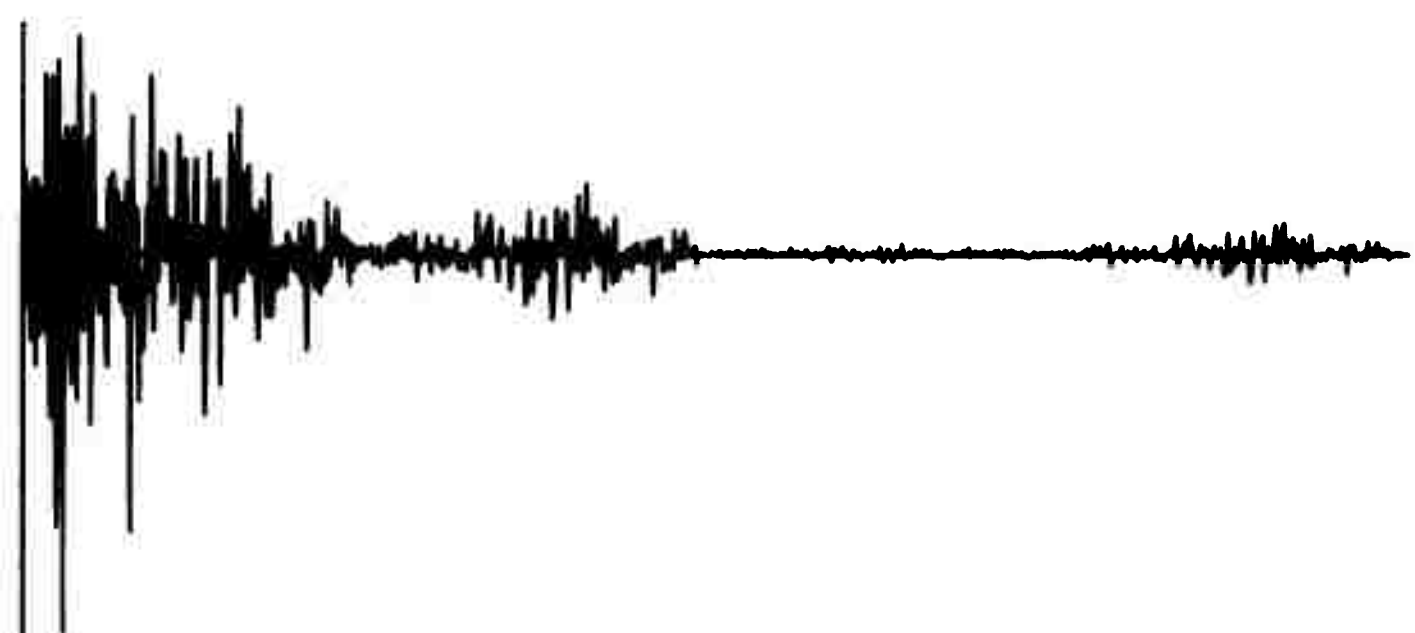
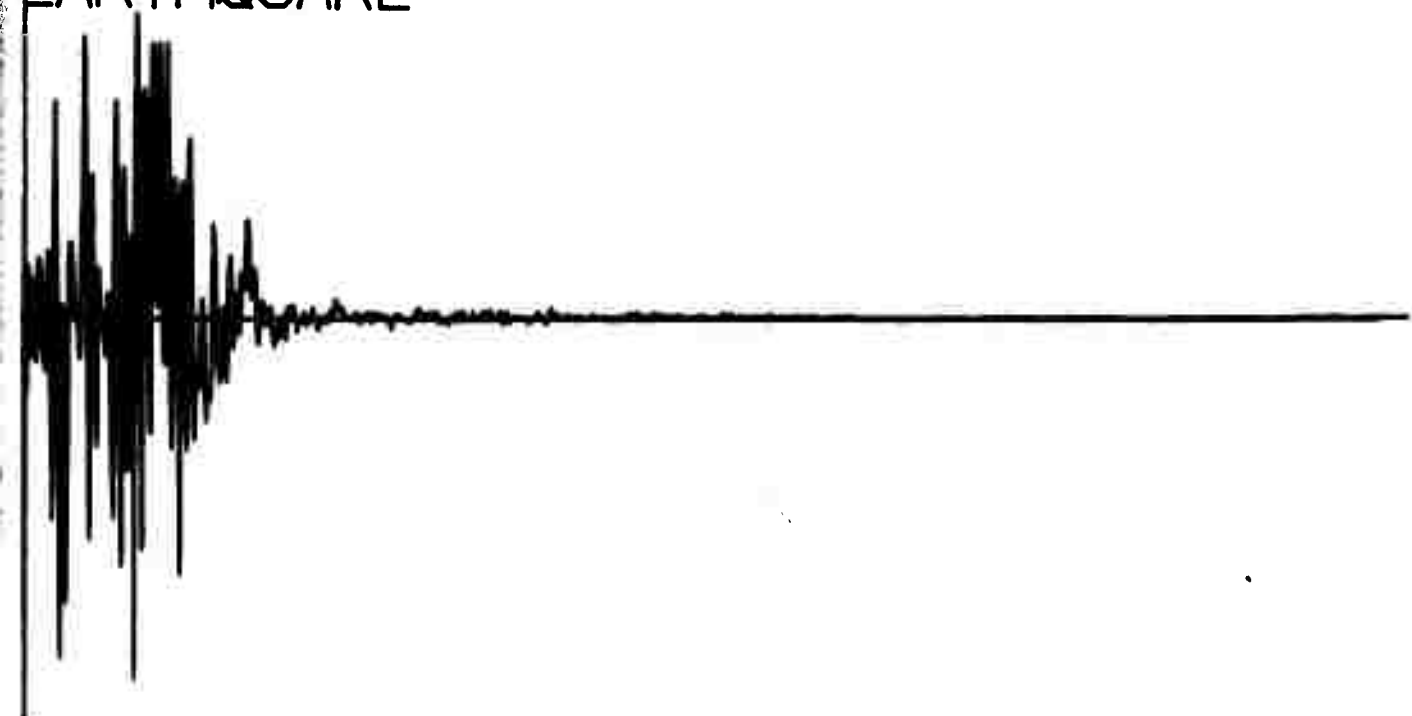
Q114

VENT NUMBER 1088
EARTHQUAKE



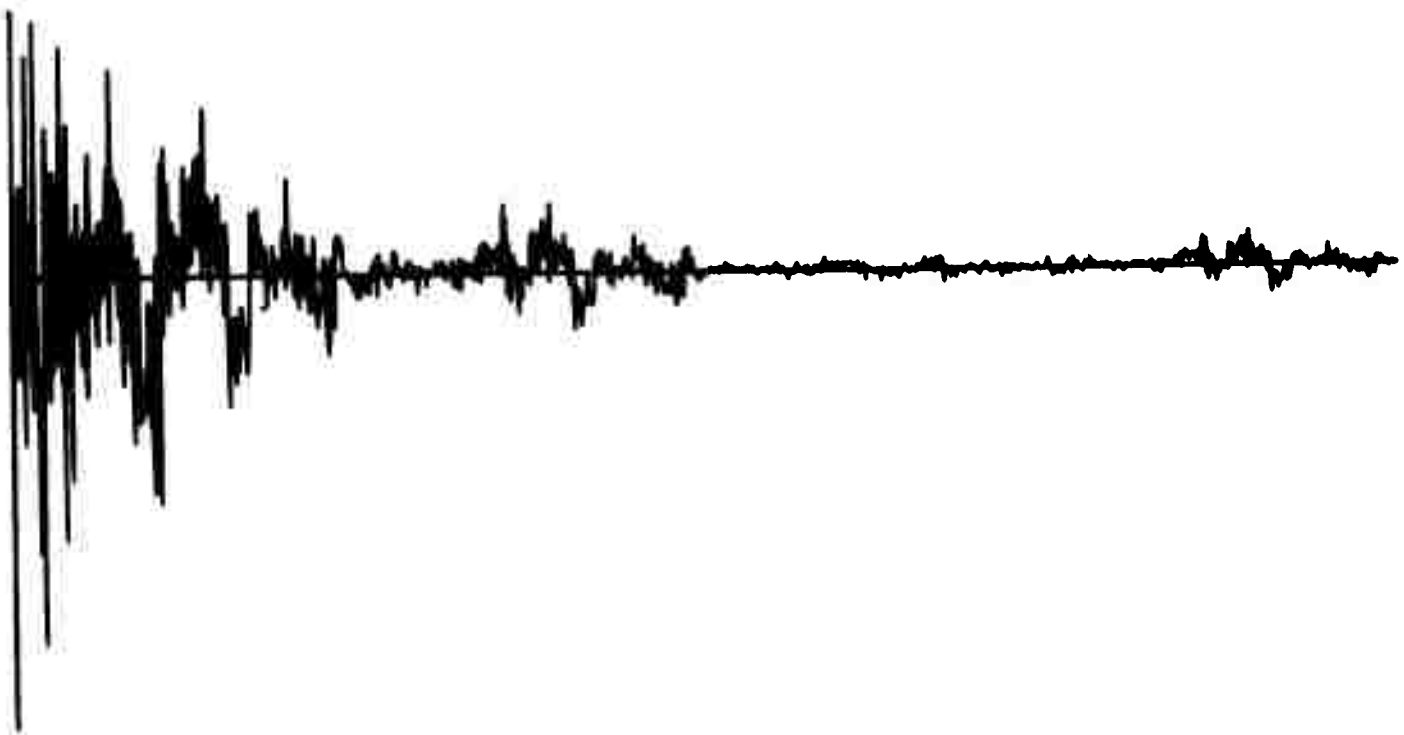
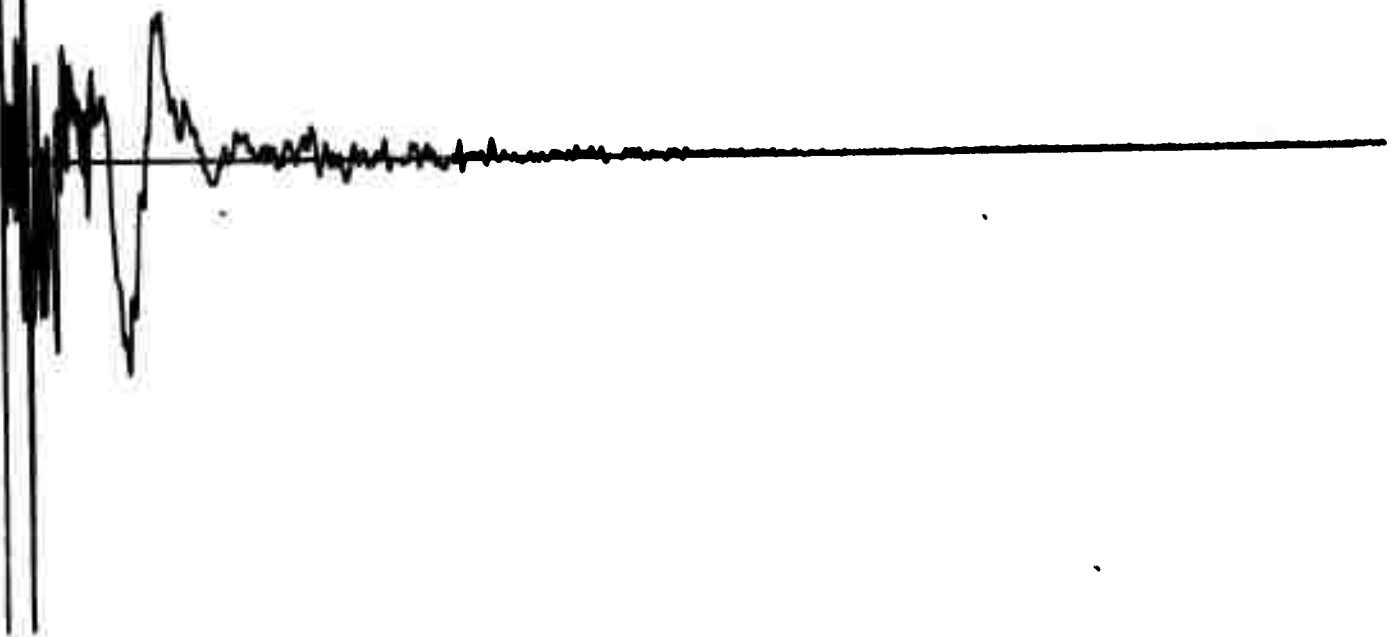
Q116

EVENT NUMBER 1084
EARTHQUAKE



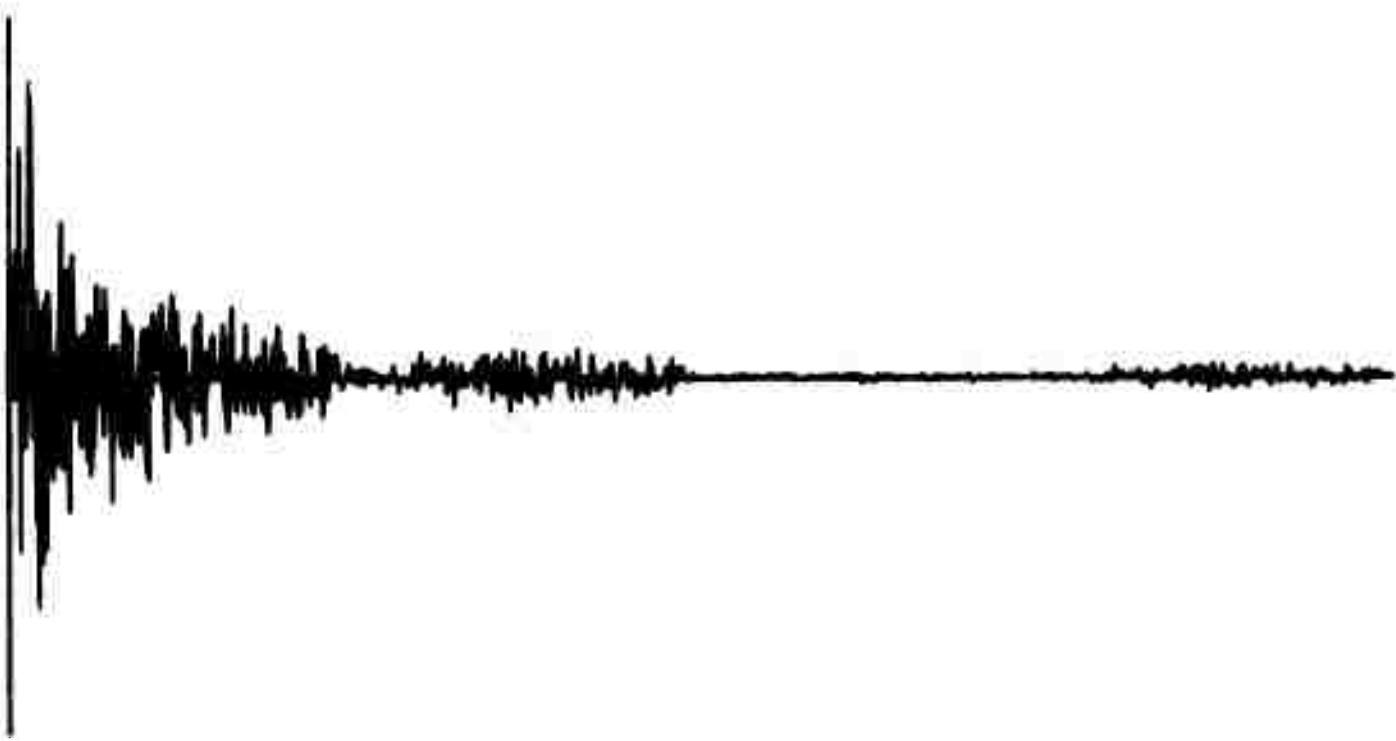
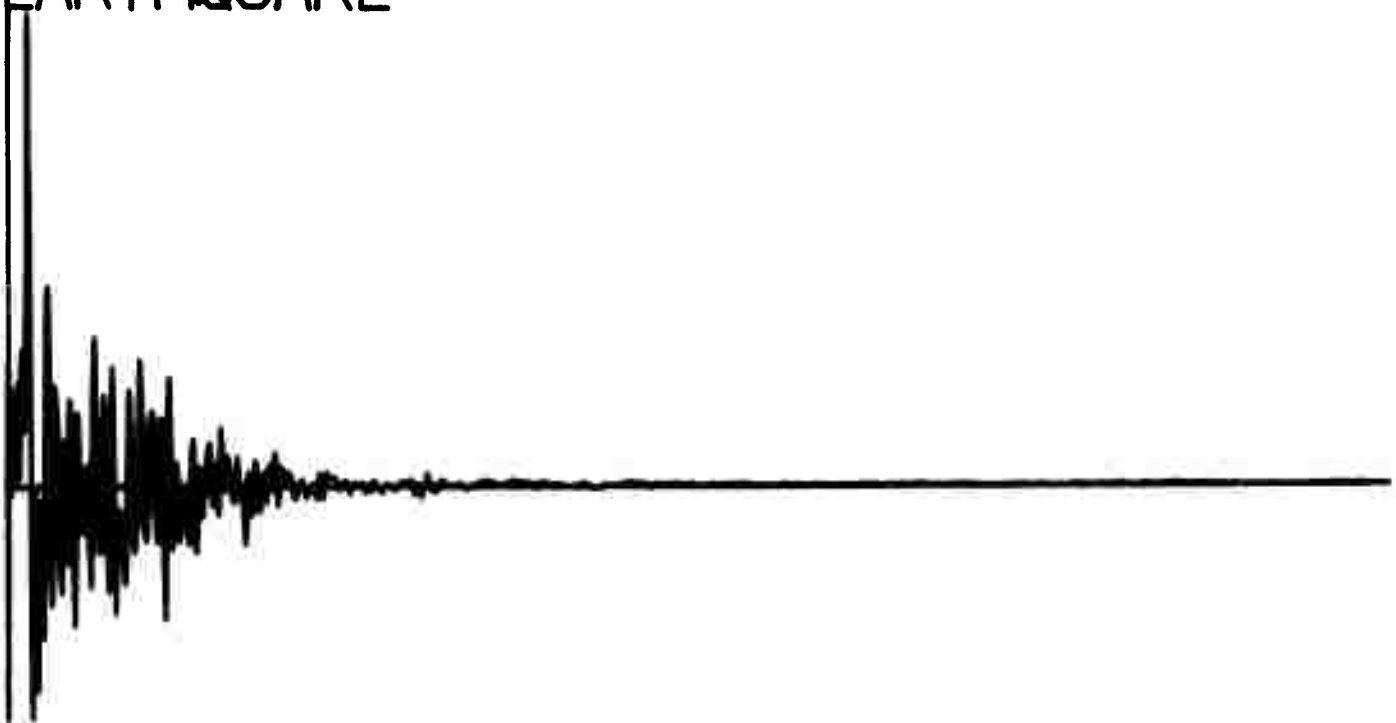
Q118

EVENT NUMBER 1083
EARTHQUAKE



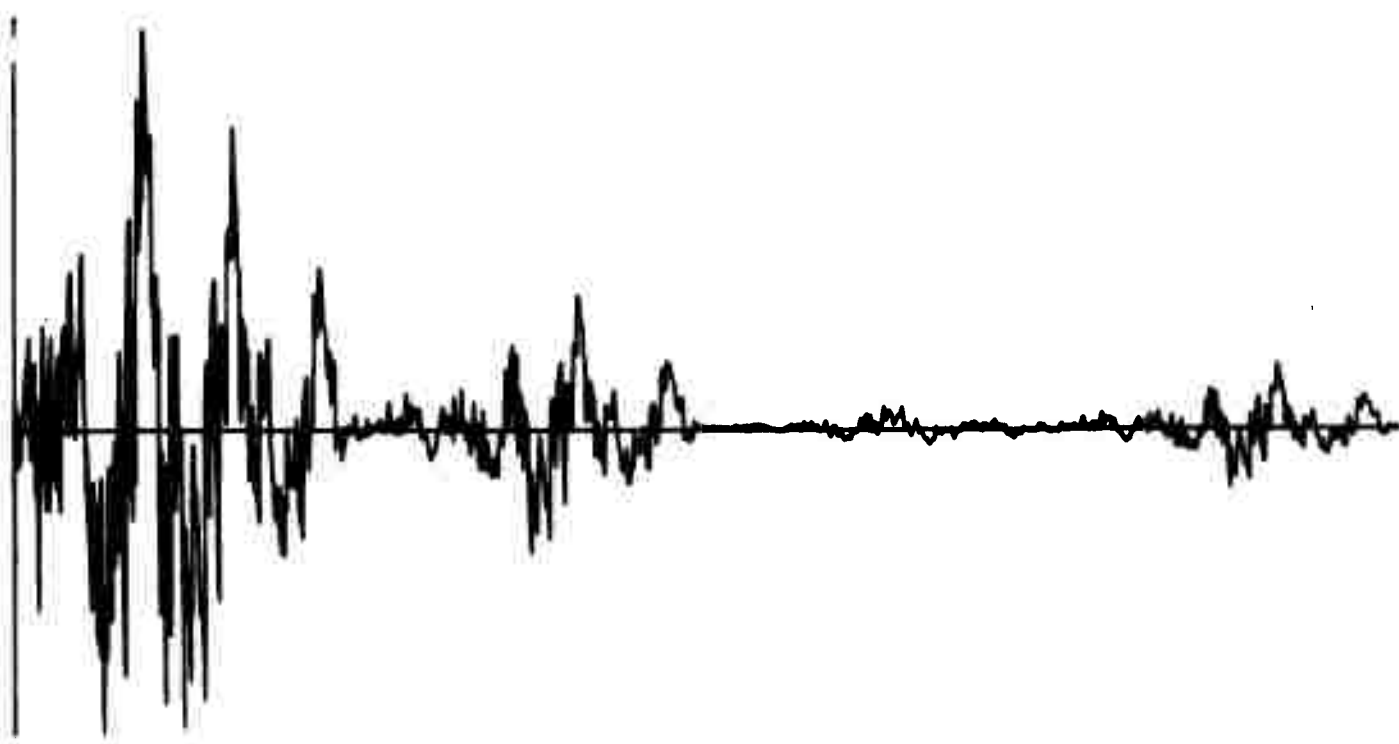
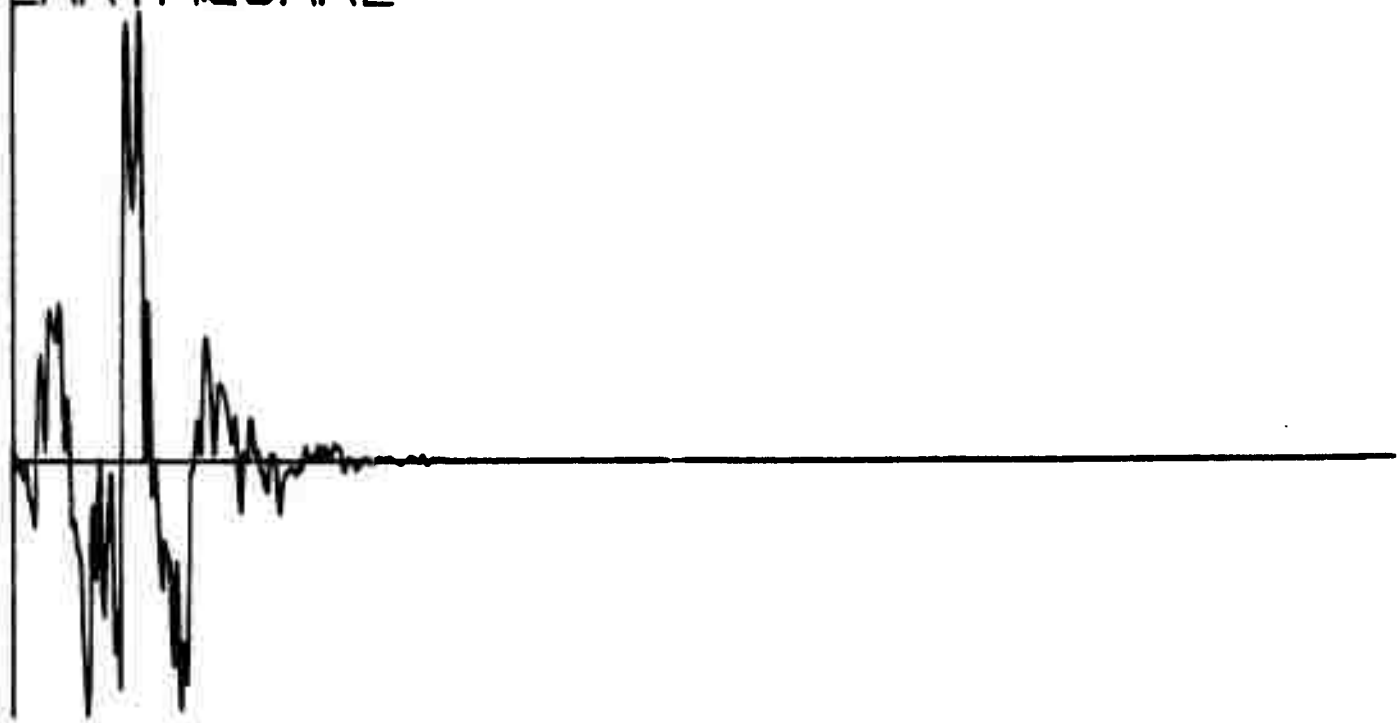
Q120

EVENT NUMBER 1089
EARTHQUAKE



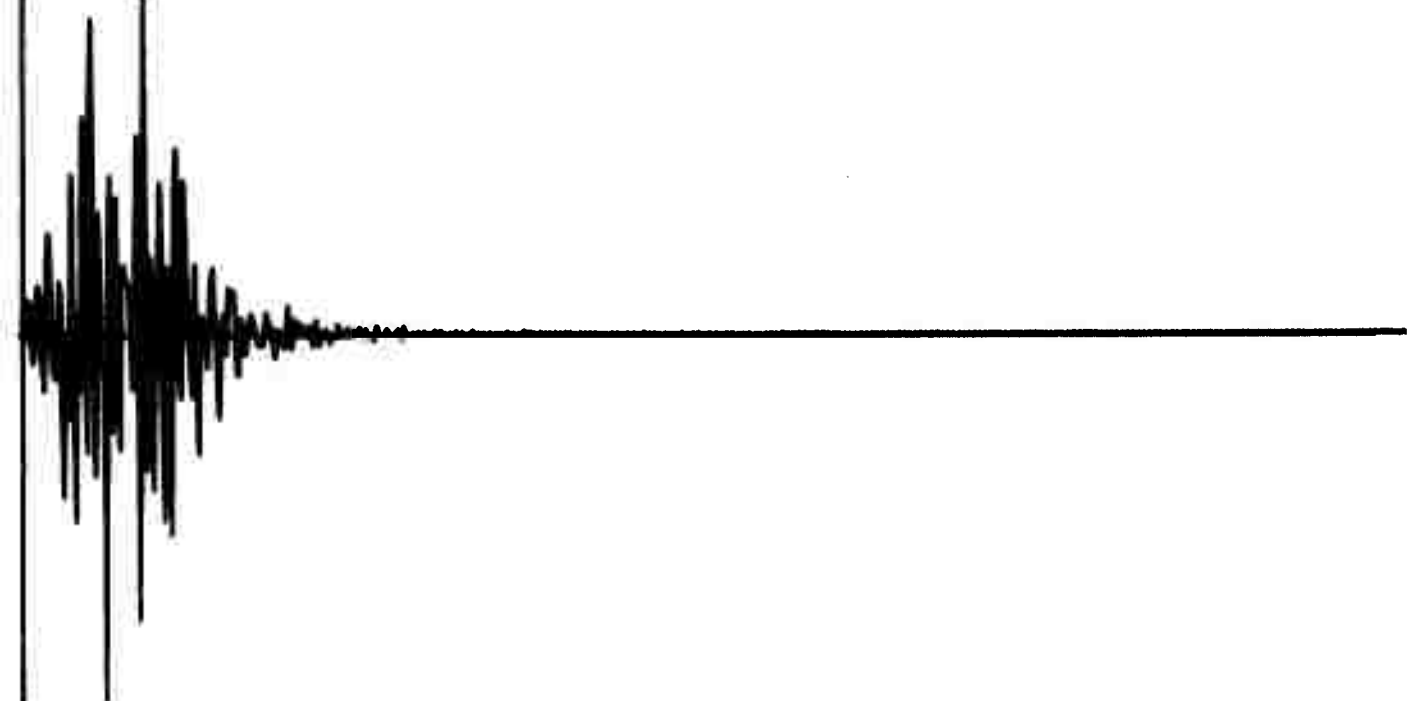
Q122

.VENT NUMBER 1111
EARTHQUAKE



Q124

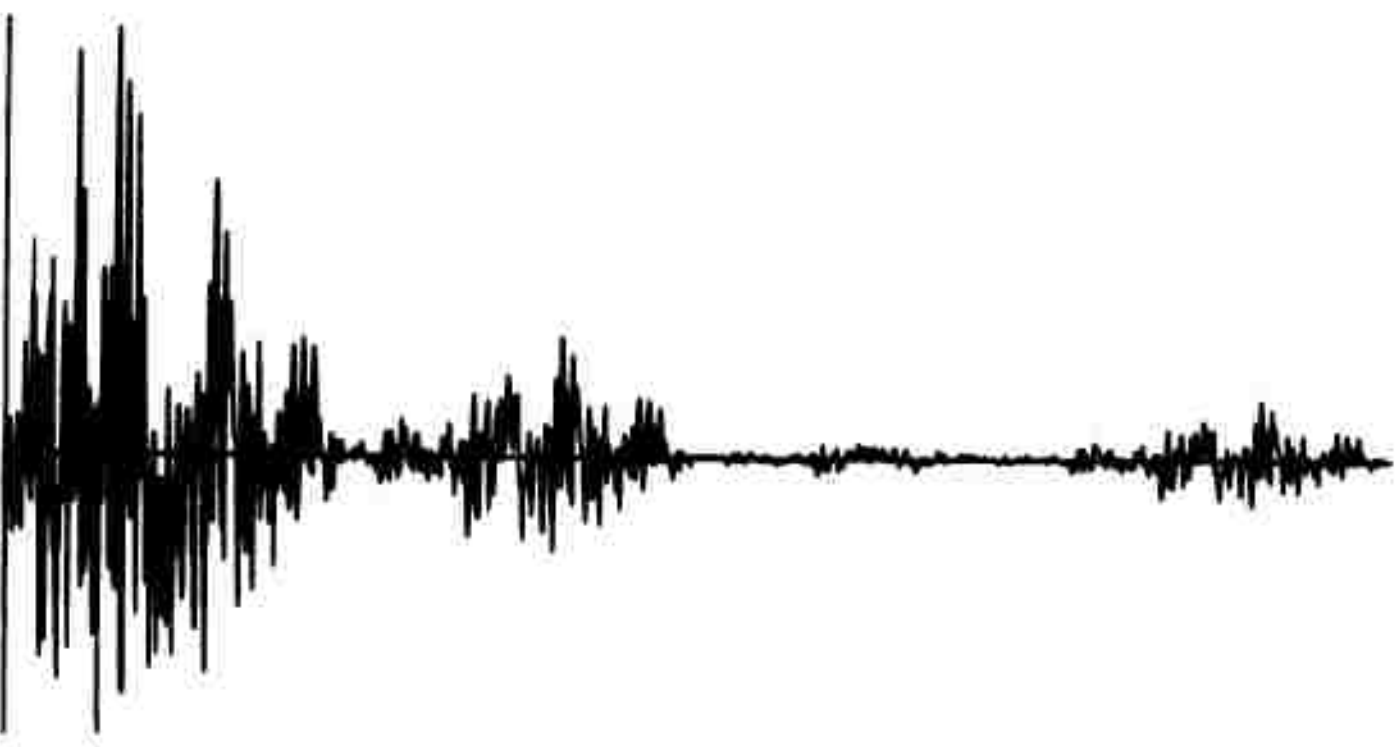
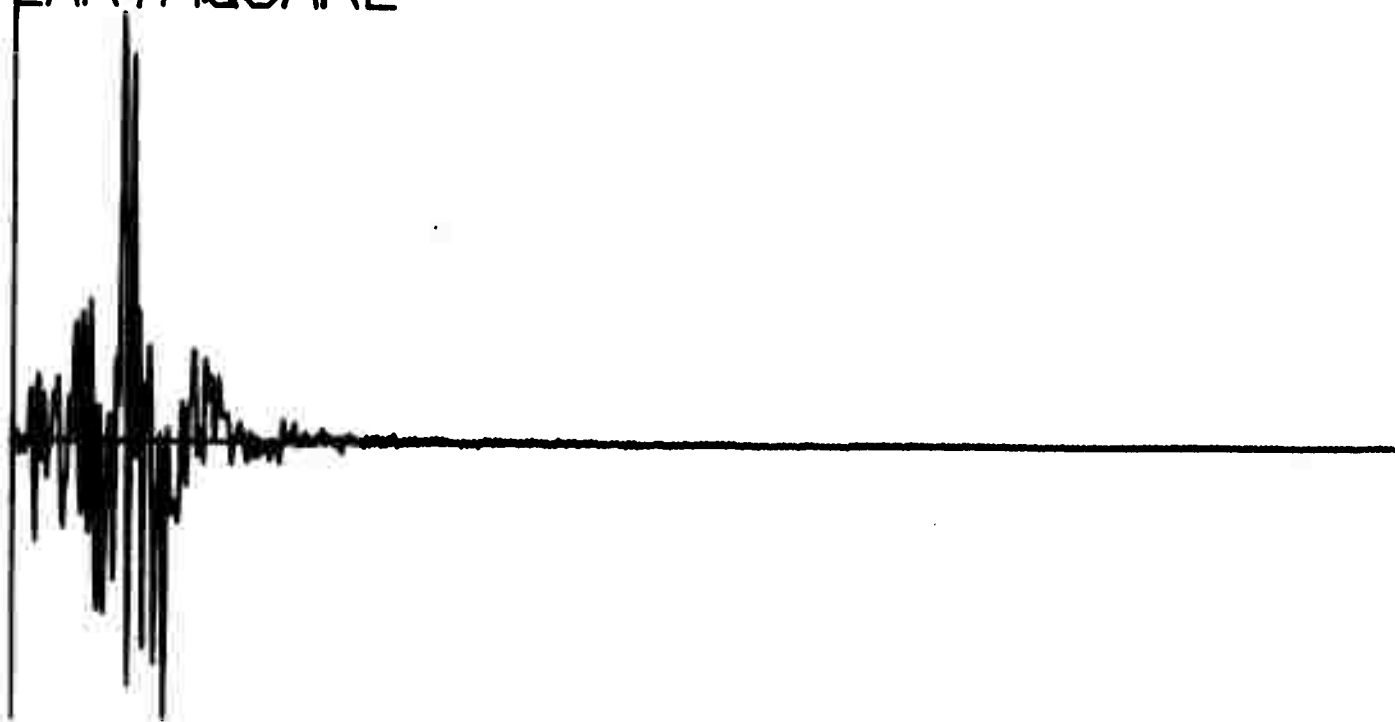
EVENT NUMBER 1113
EARTHQUAKE



Q126

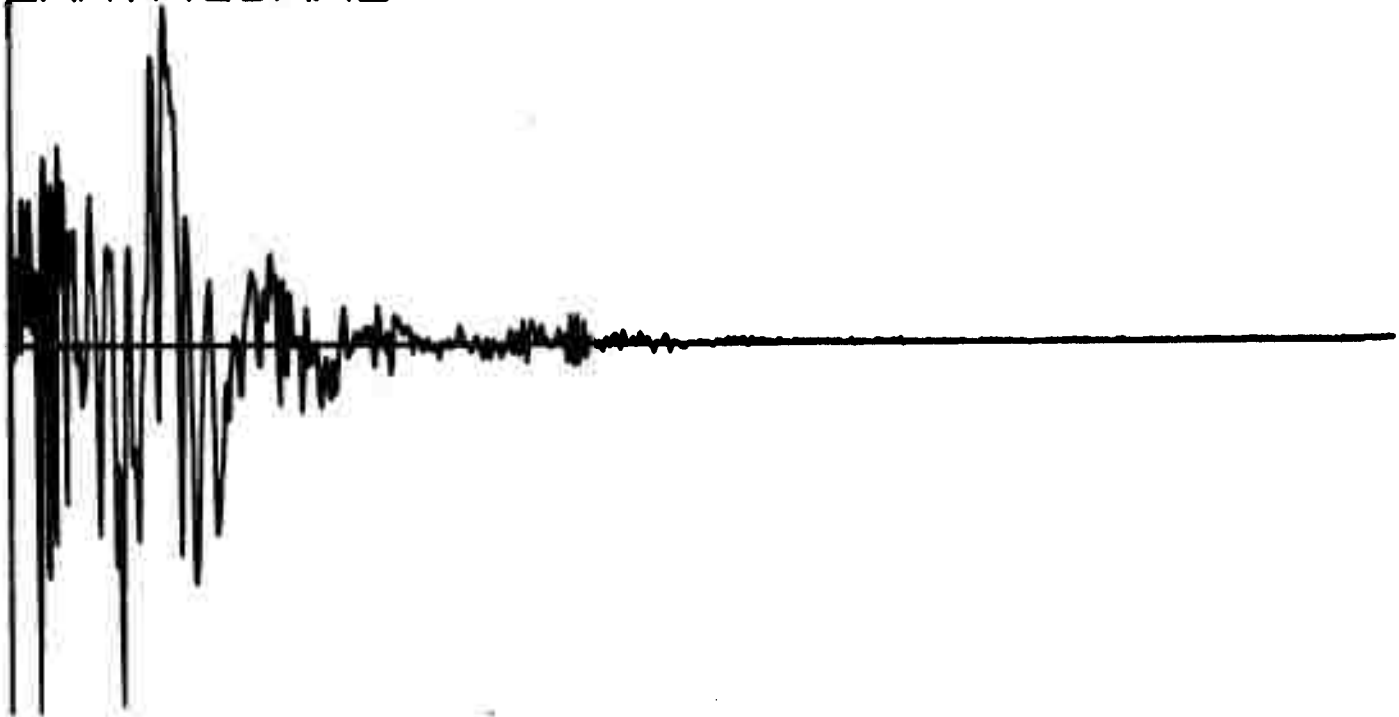
EVENT NUMBER 1201

EARTHQUAKE



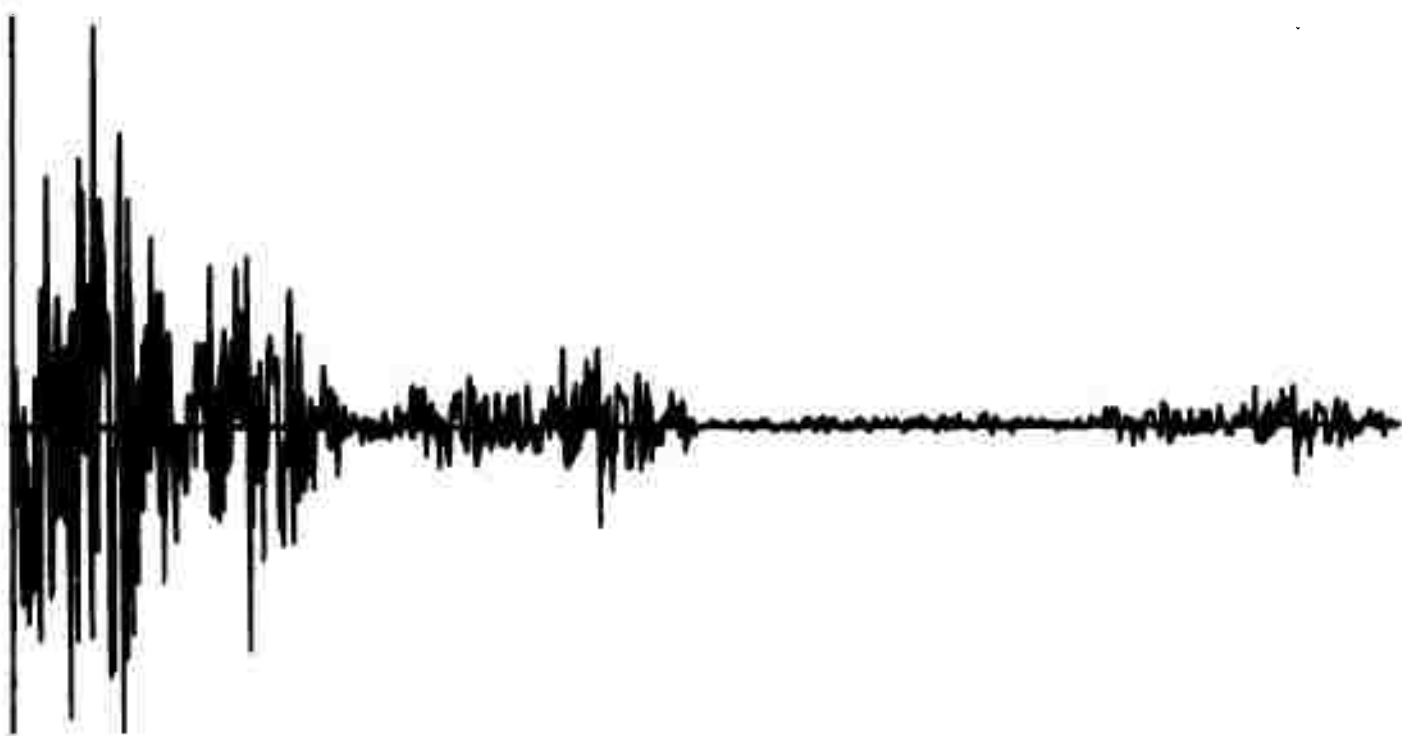
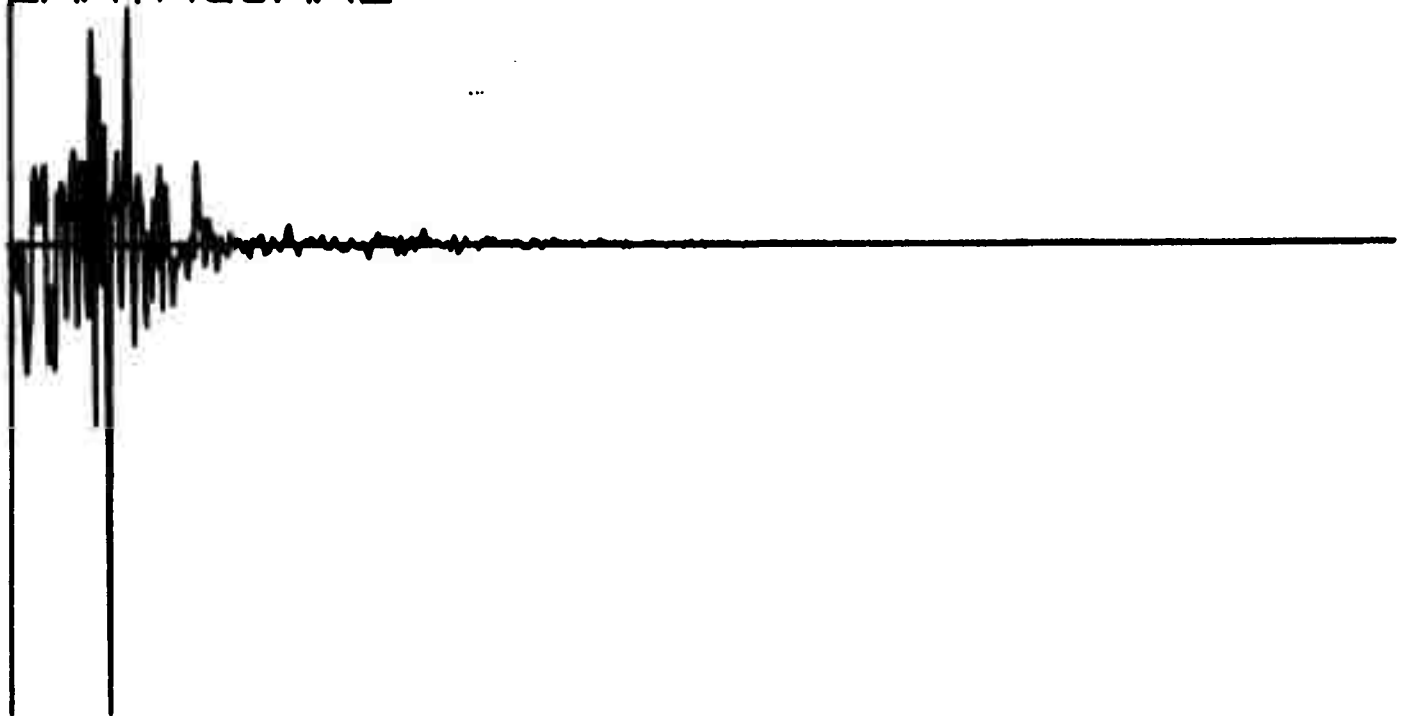
Q128

EVENT NUMBER 1104
EARTHQUAKE



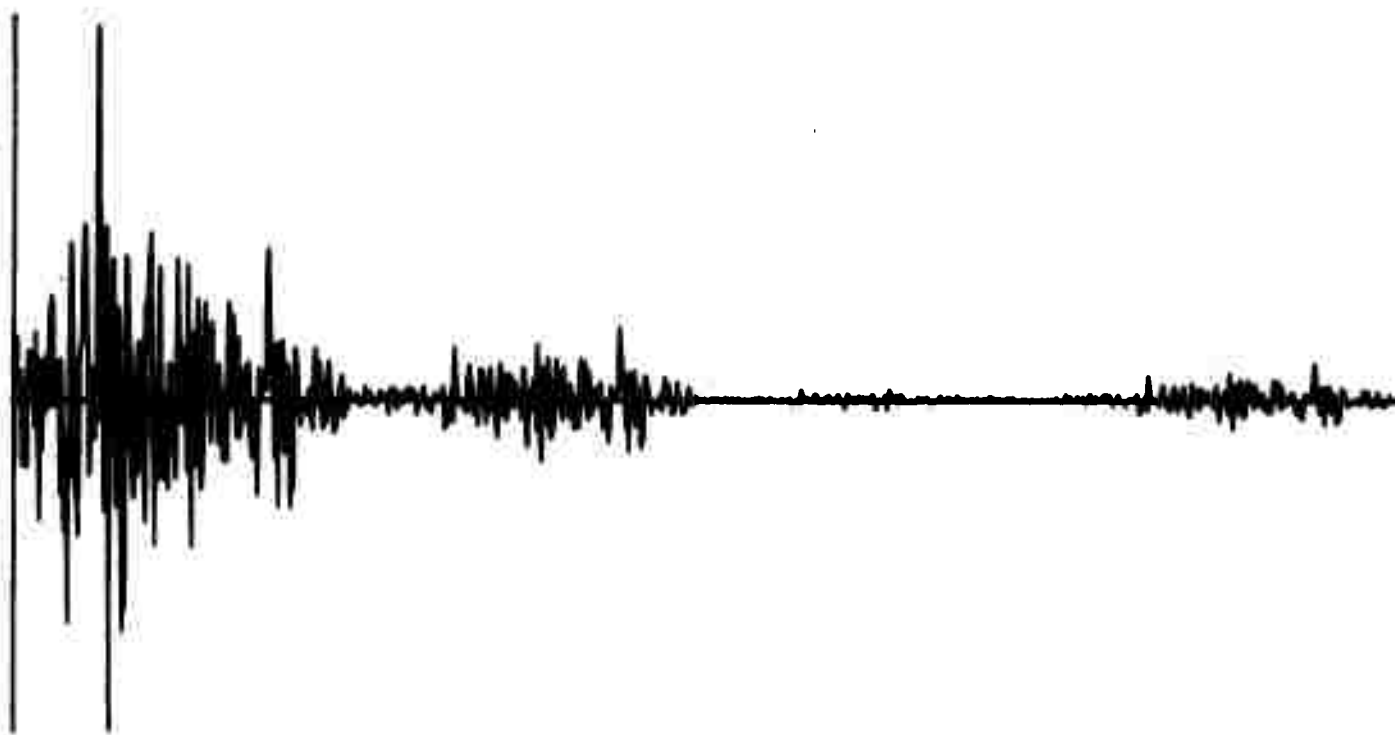
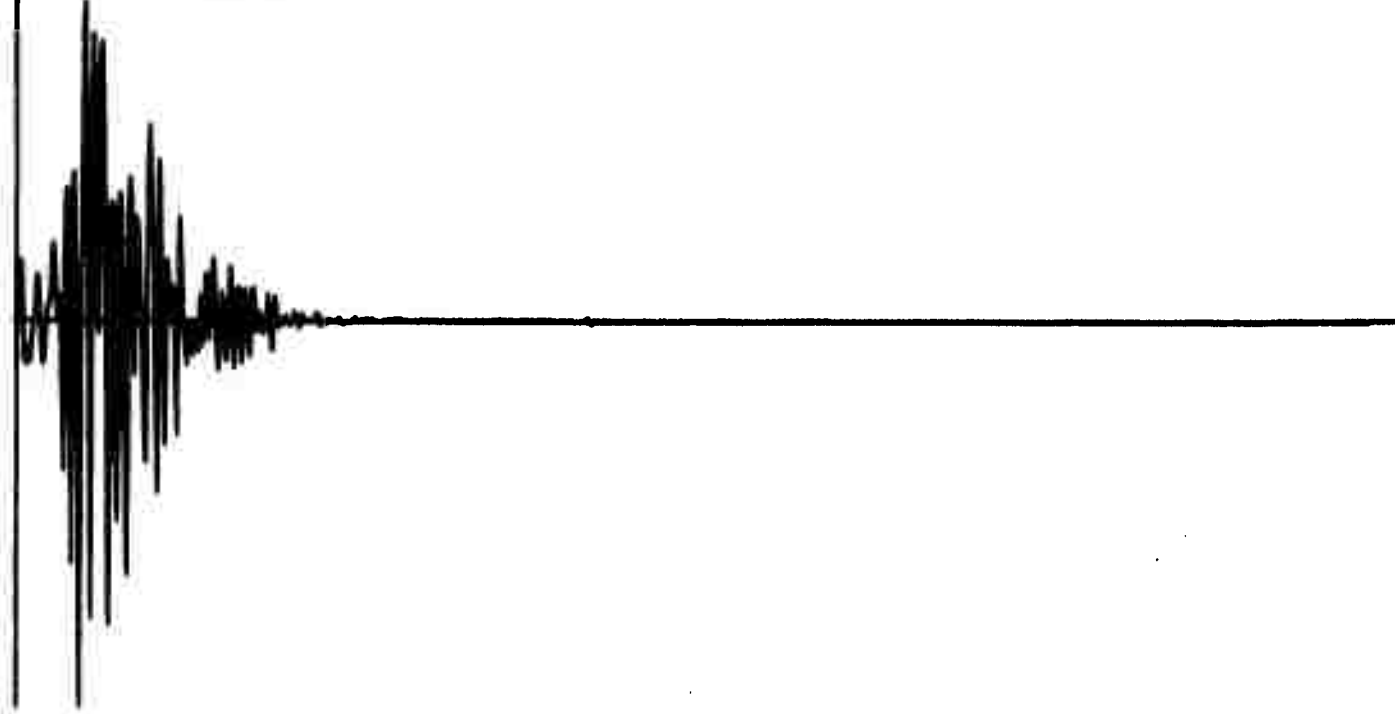
Q130

EVENT NUMBER 1068
EARTHQUAKE



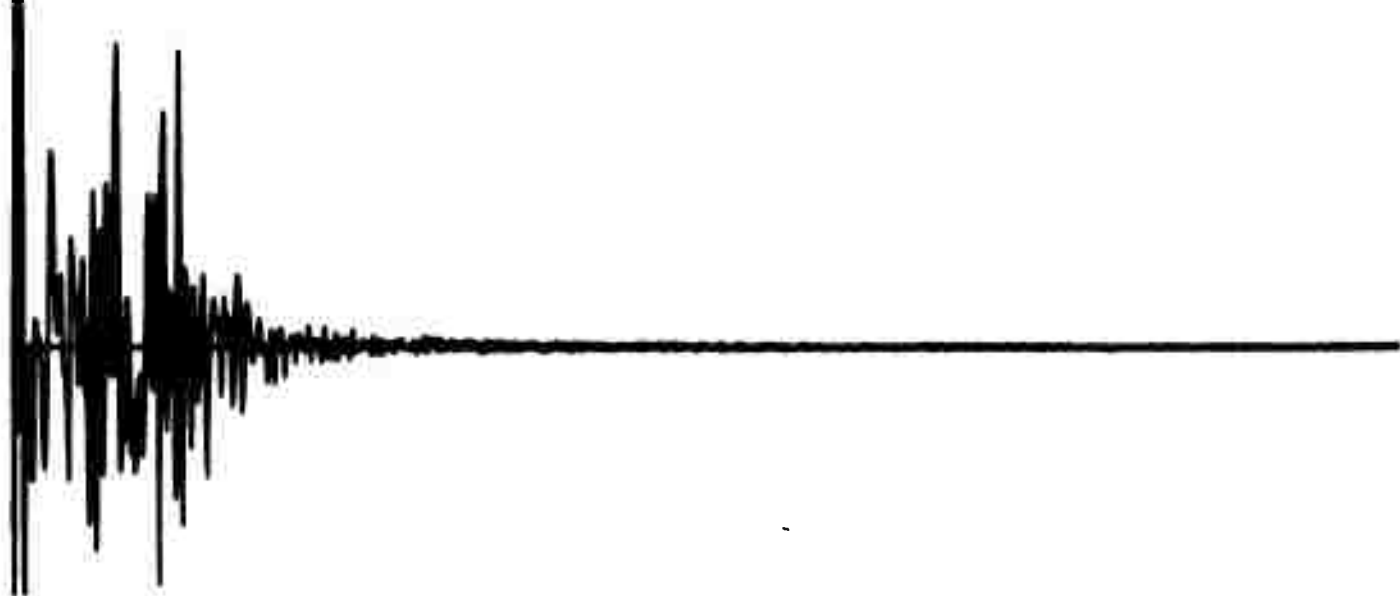
Q132

EVENT NUMBER 1114
EARTHQUAKE



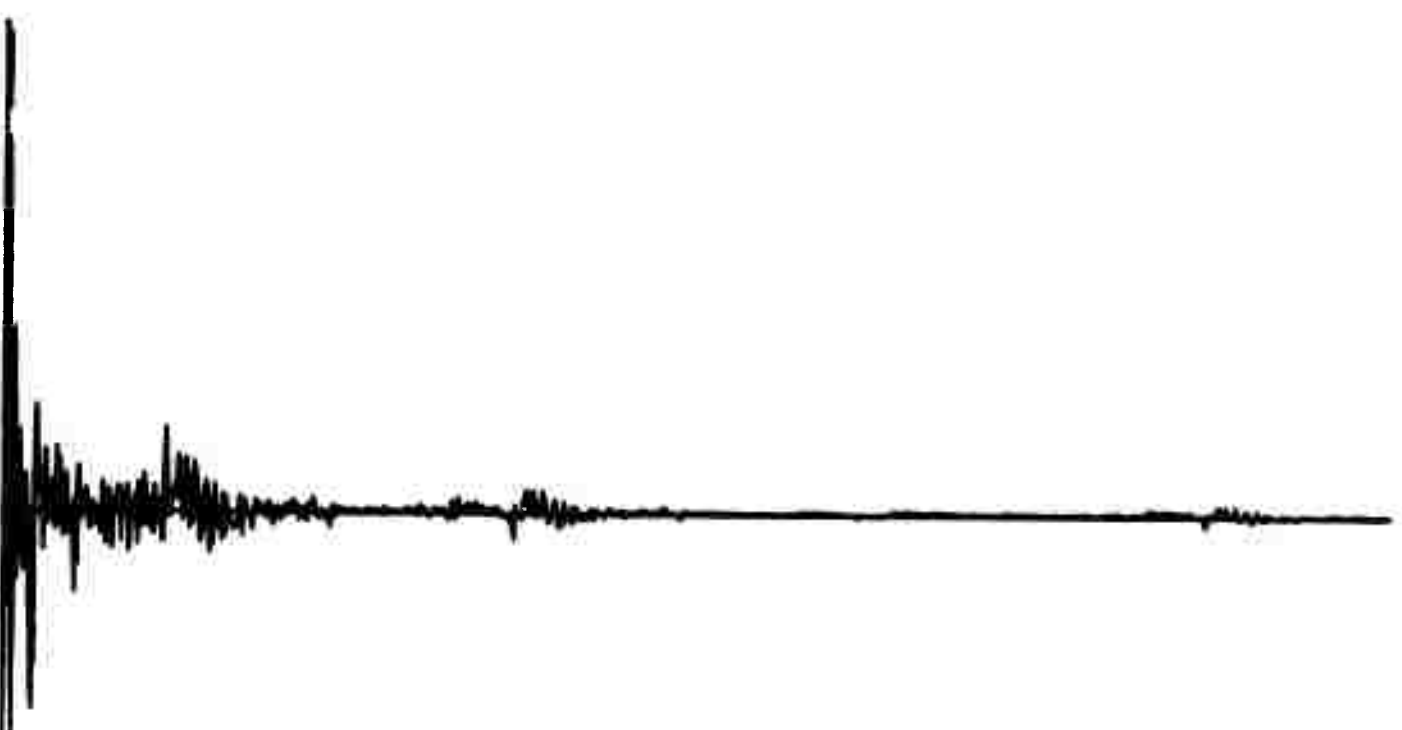
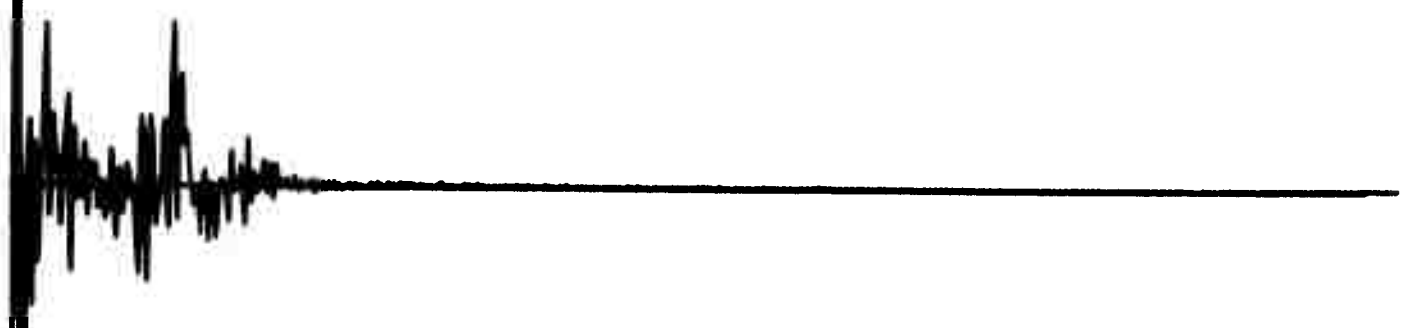
Q134

EVENT NUMBER 1115
EARTHQUAKE



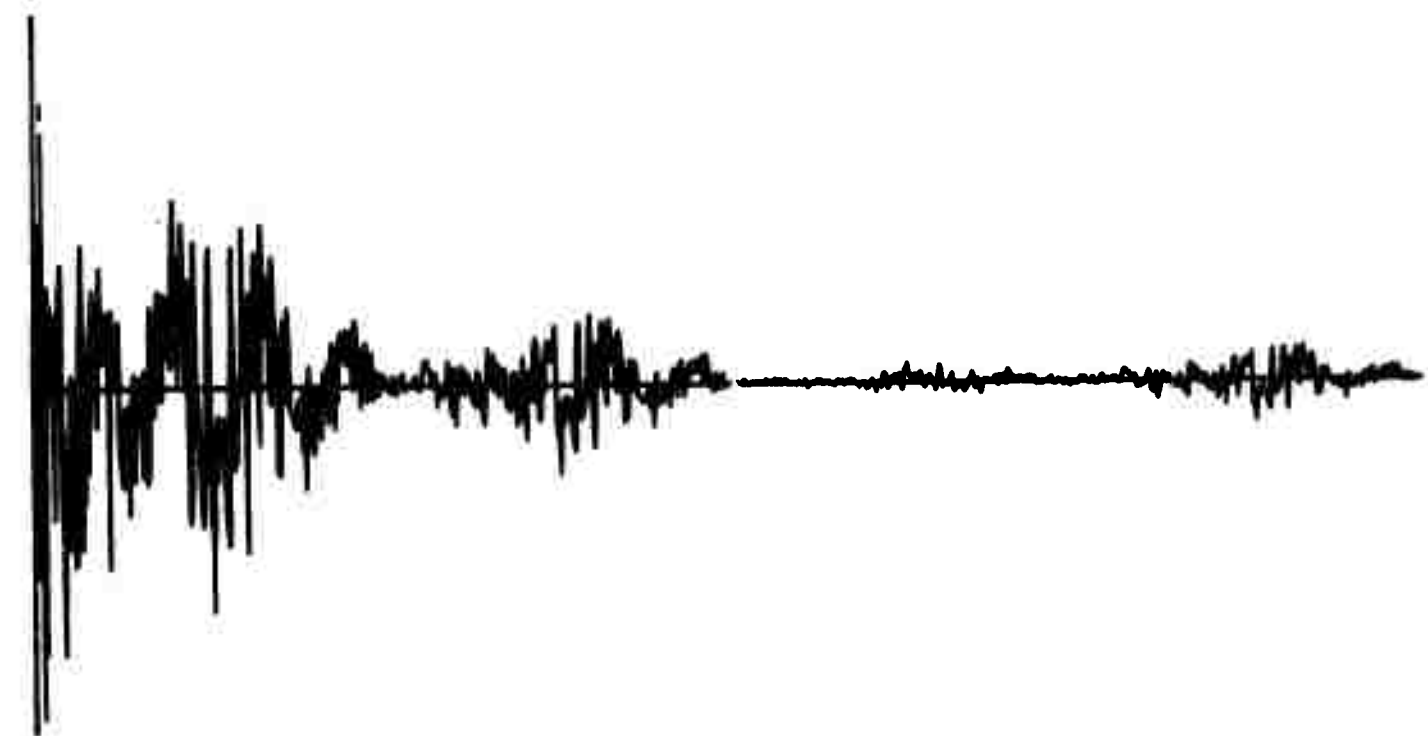
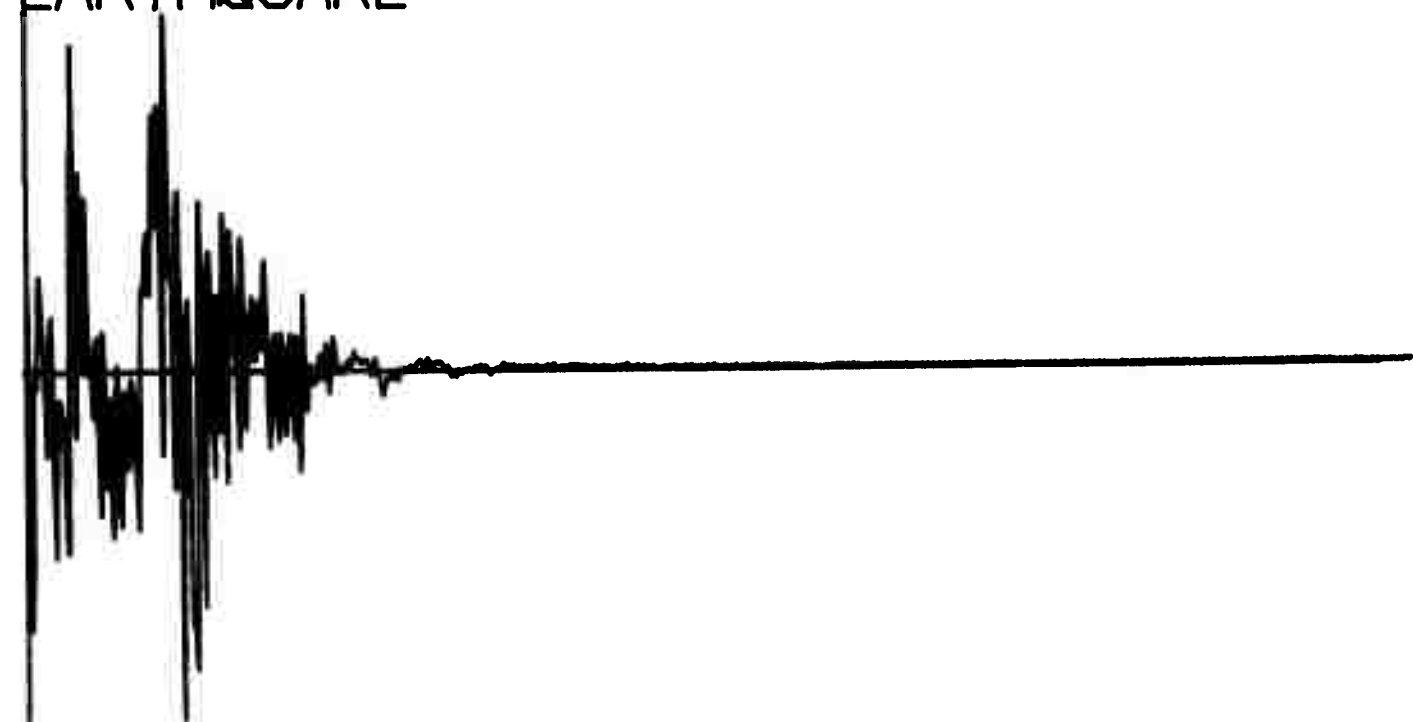
EVENT NUMBER 1116
EARTHQUAKE

Q136



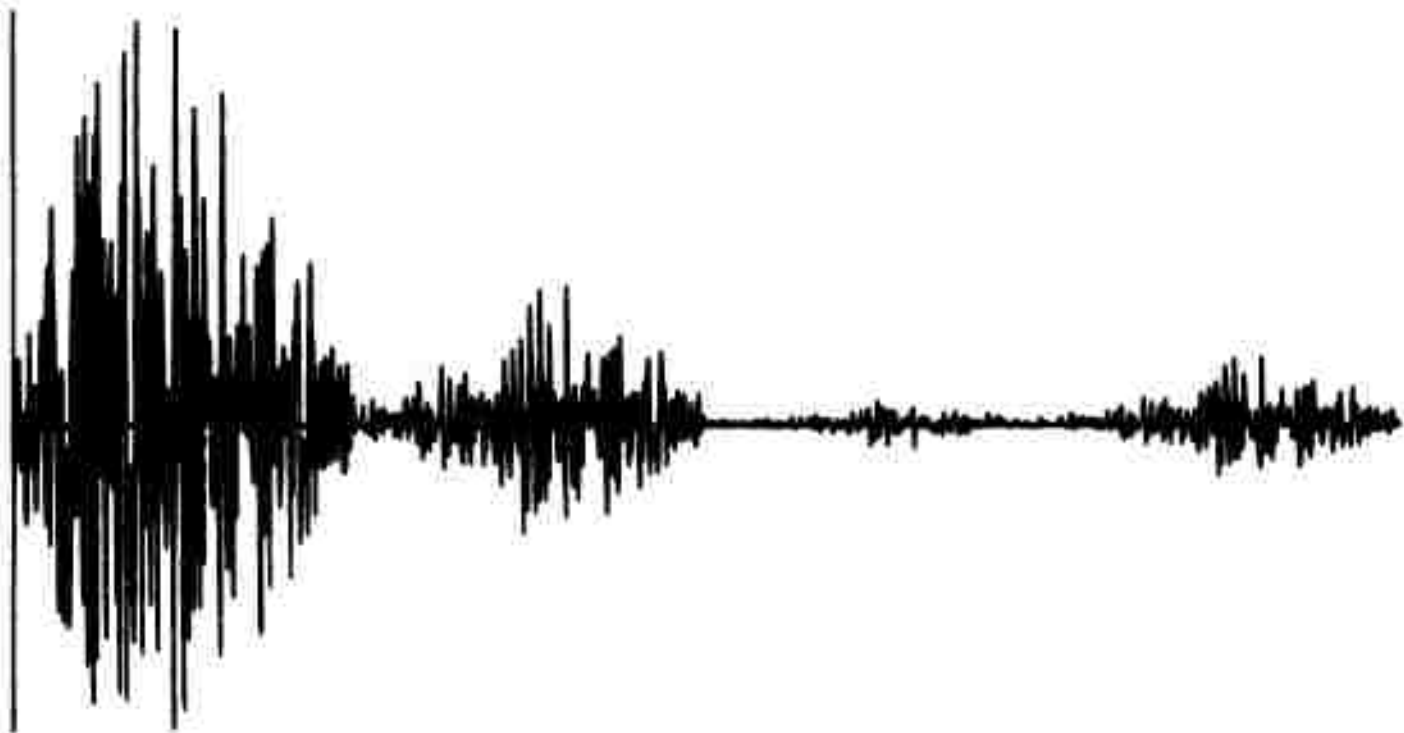
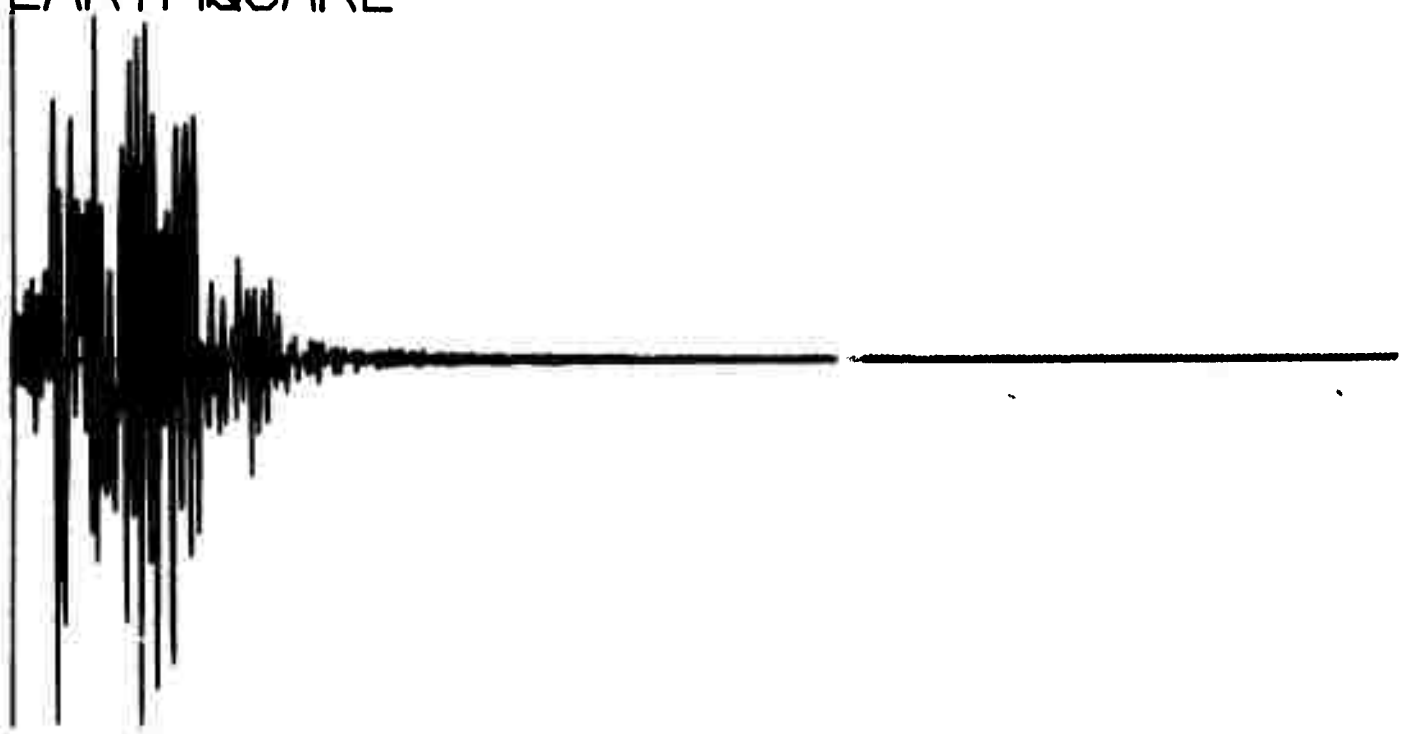
Q138

EVENT NUMBER 1117
EARTHQUAKE



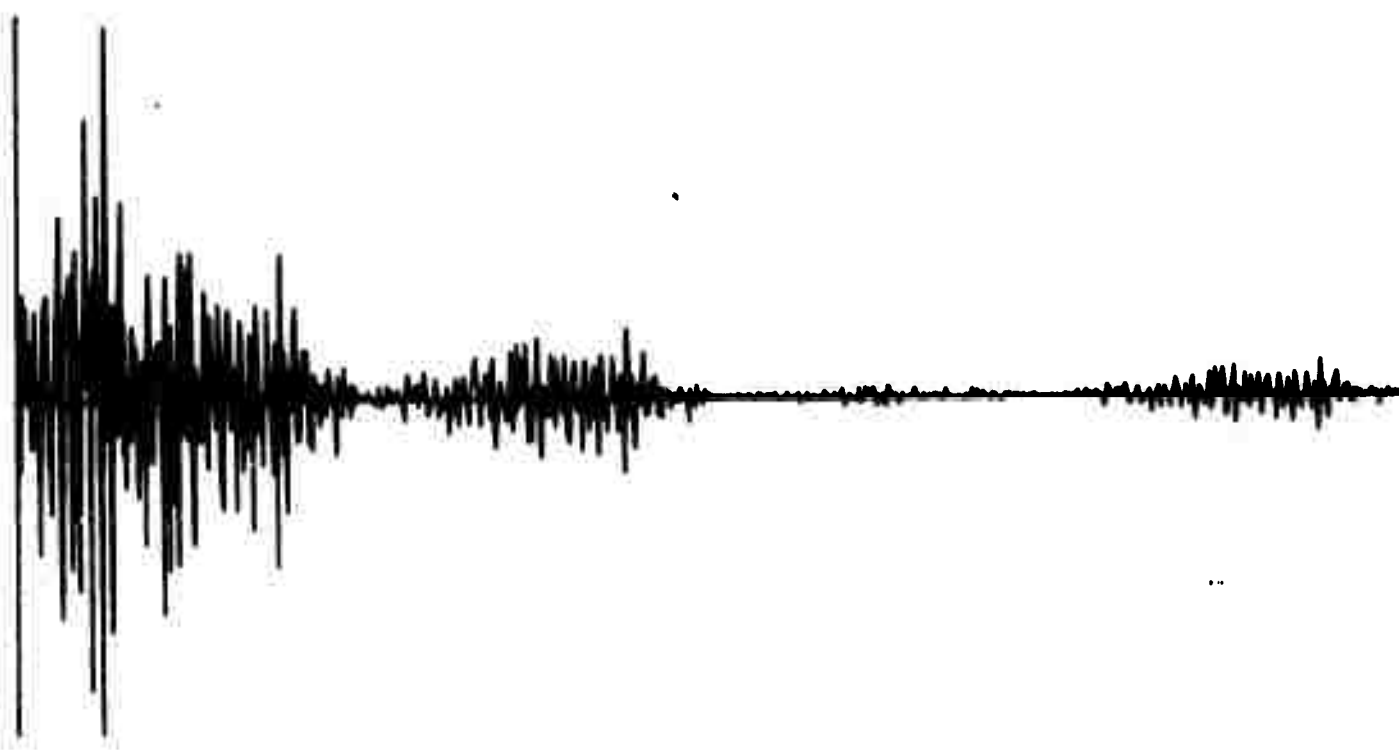
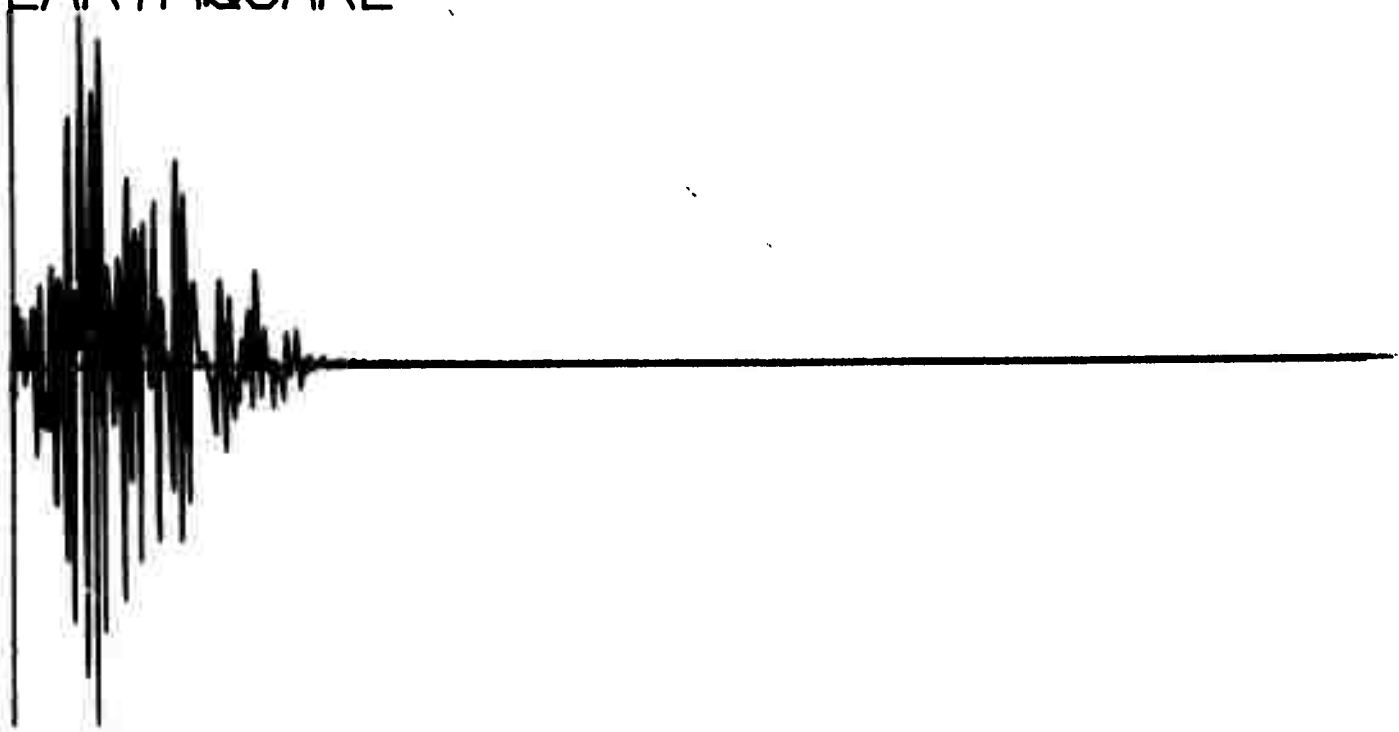
Q140

VENT NUMBER 1118
EARTHQUAKE



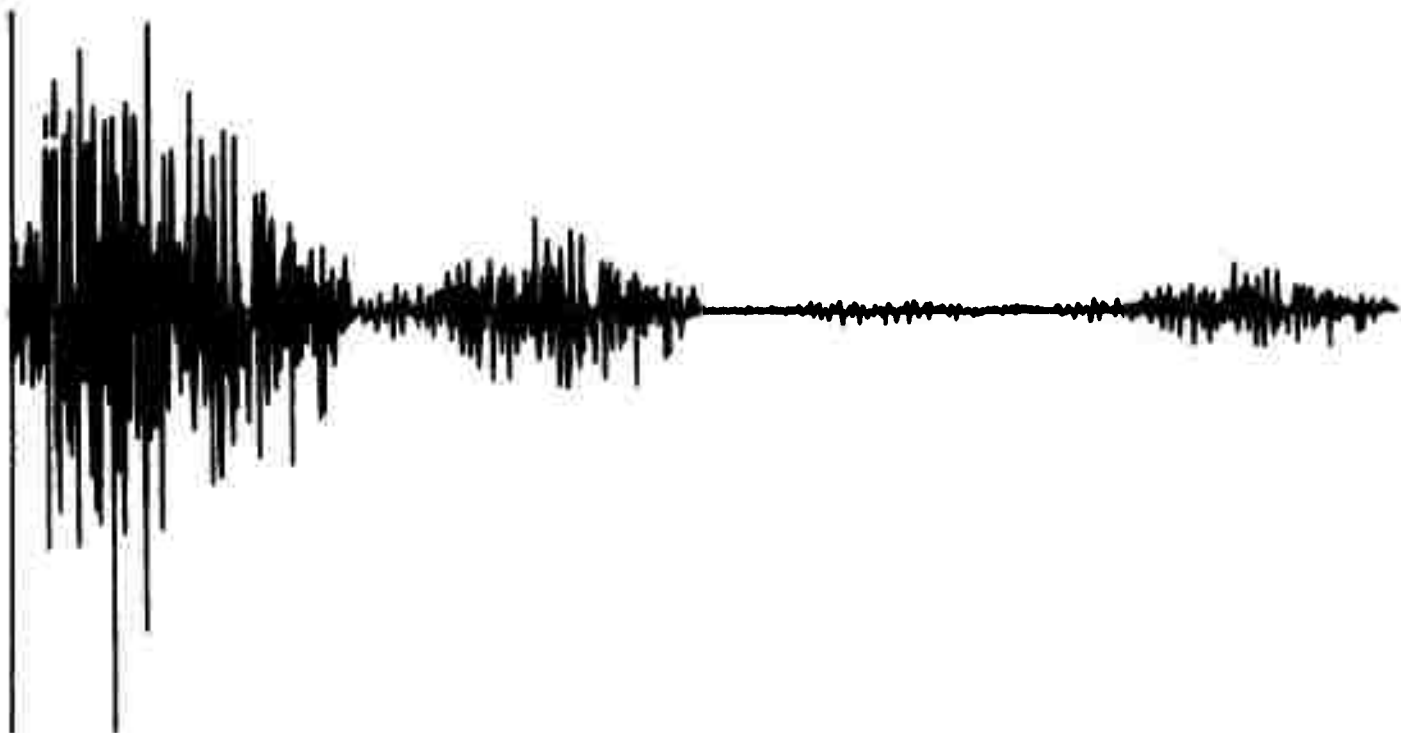
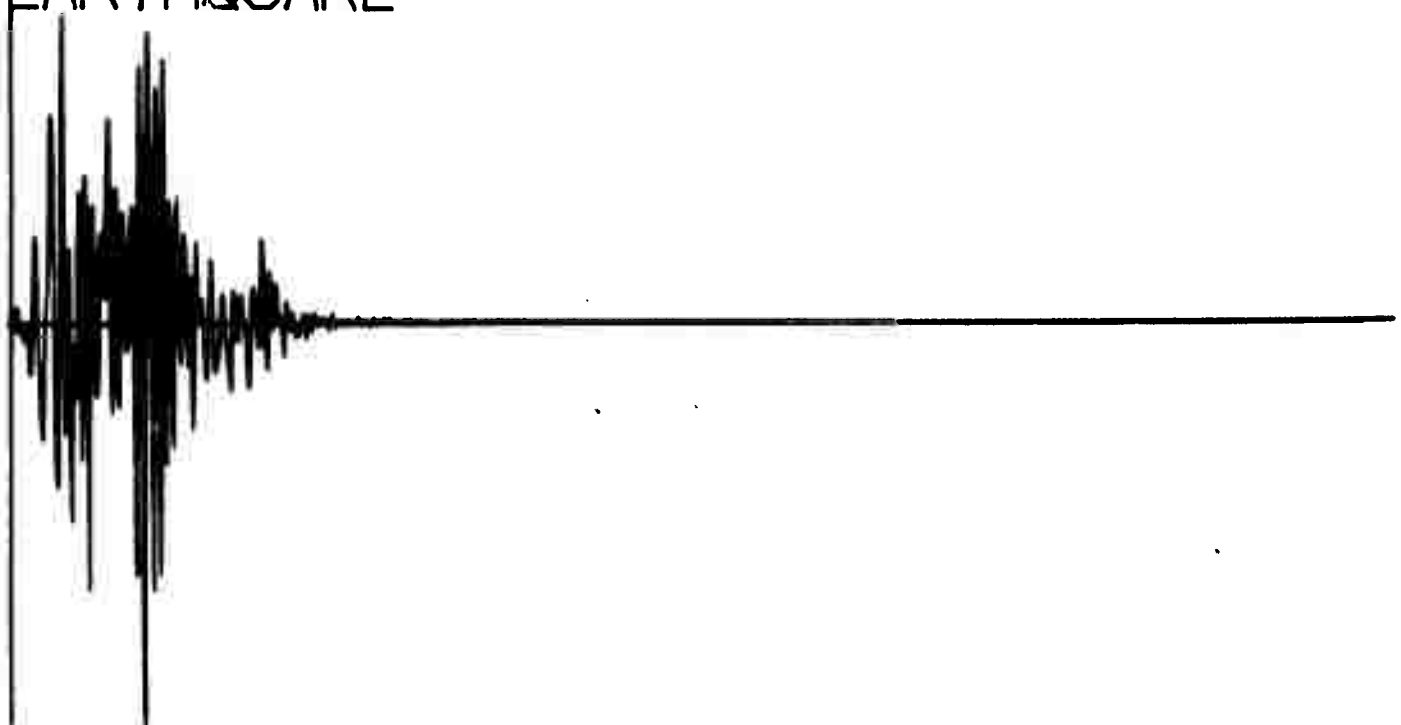
Q142

VENT NUMBER 1119
EARTHQUAKE



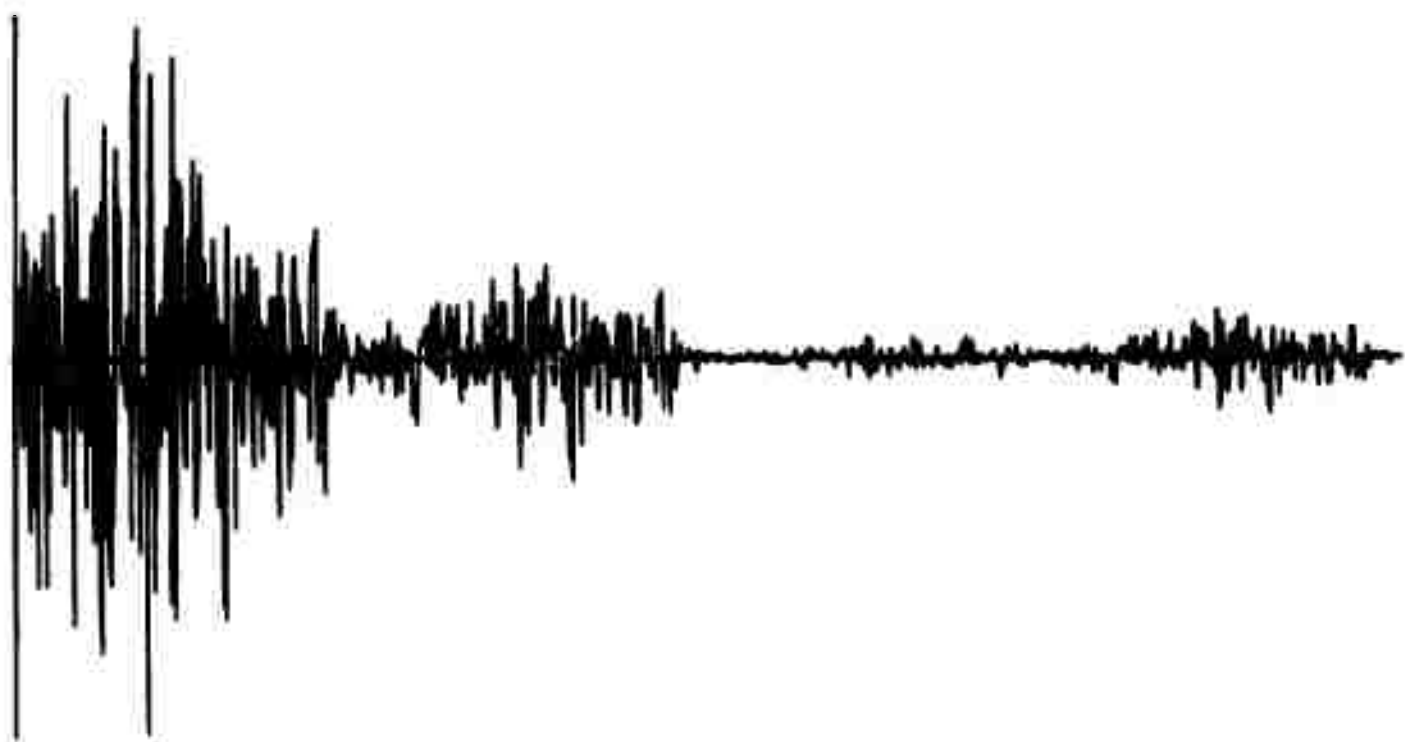
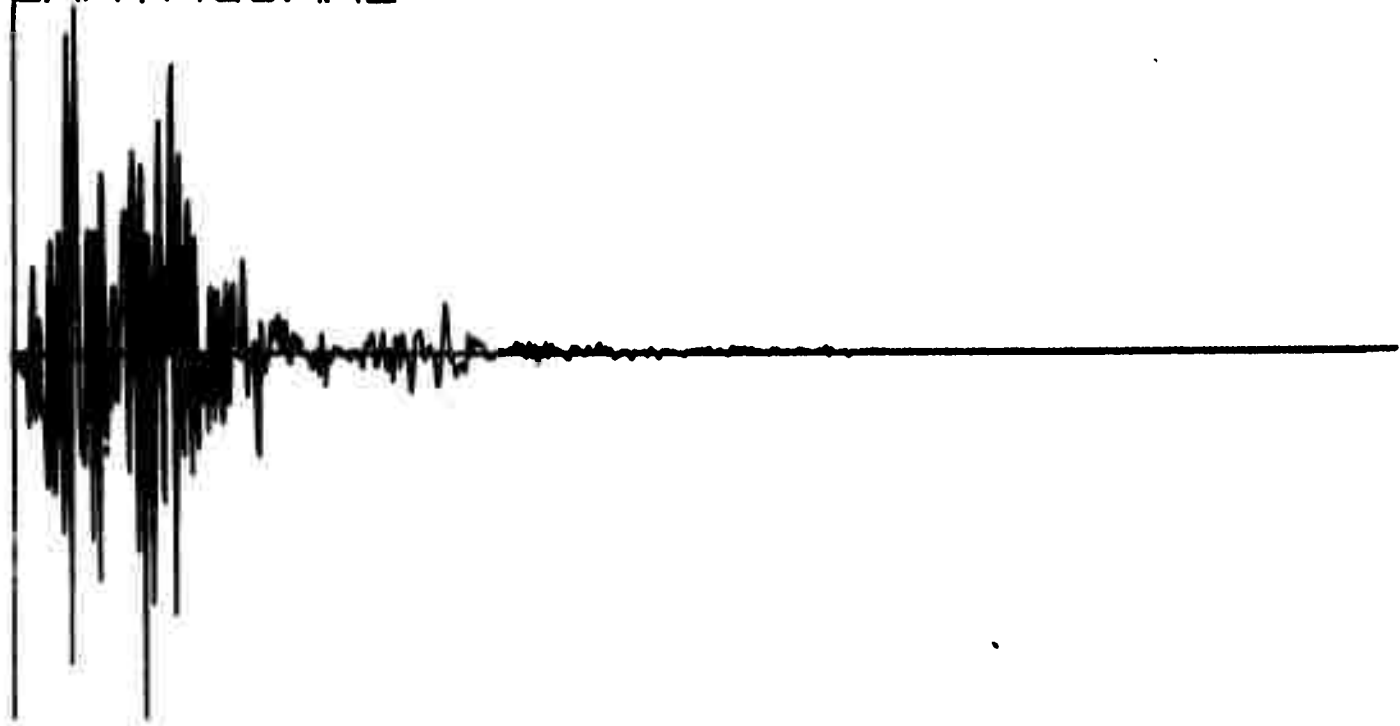
EVENT NUMBER 1142
EARTHQUAKE

Q144



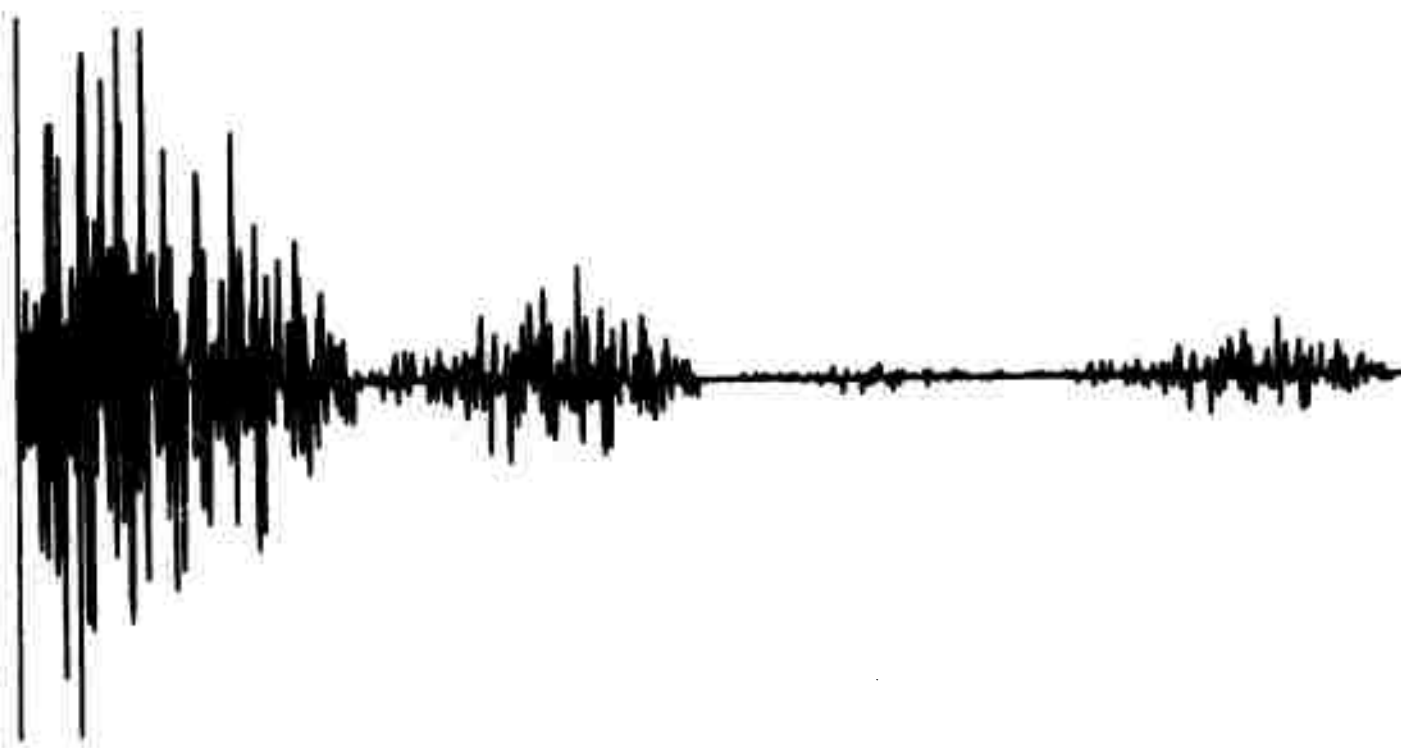
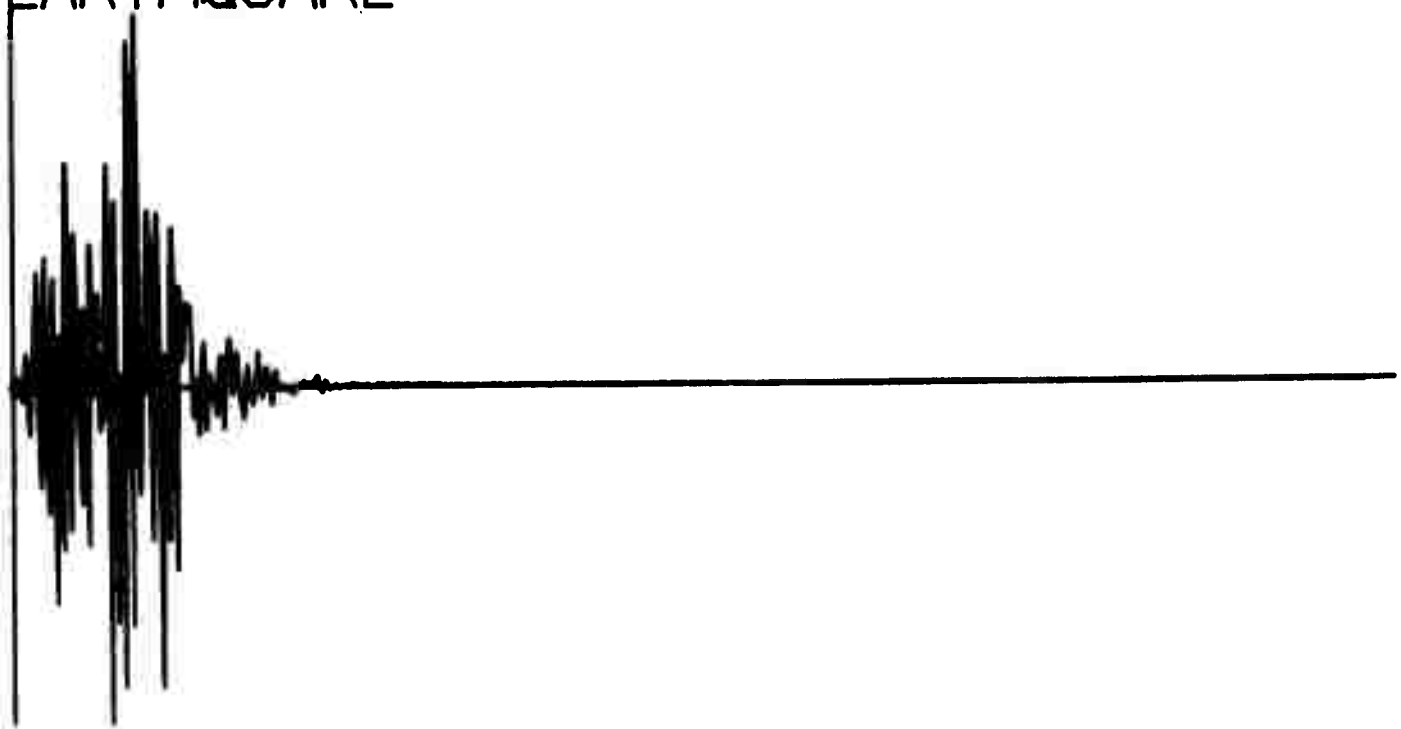
Q146

EVENT NUMBER 1132
EARTHQUAKE



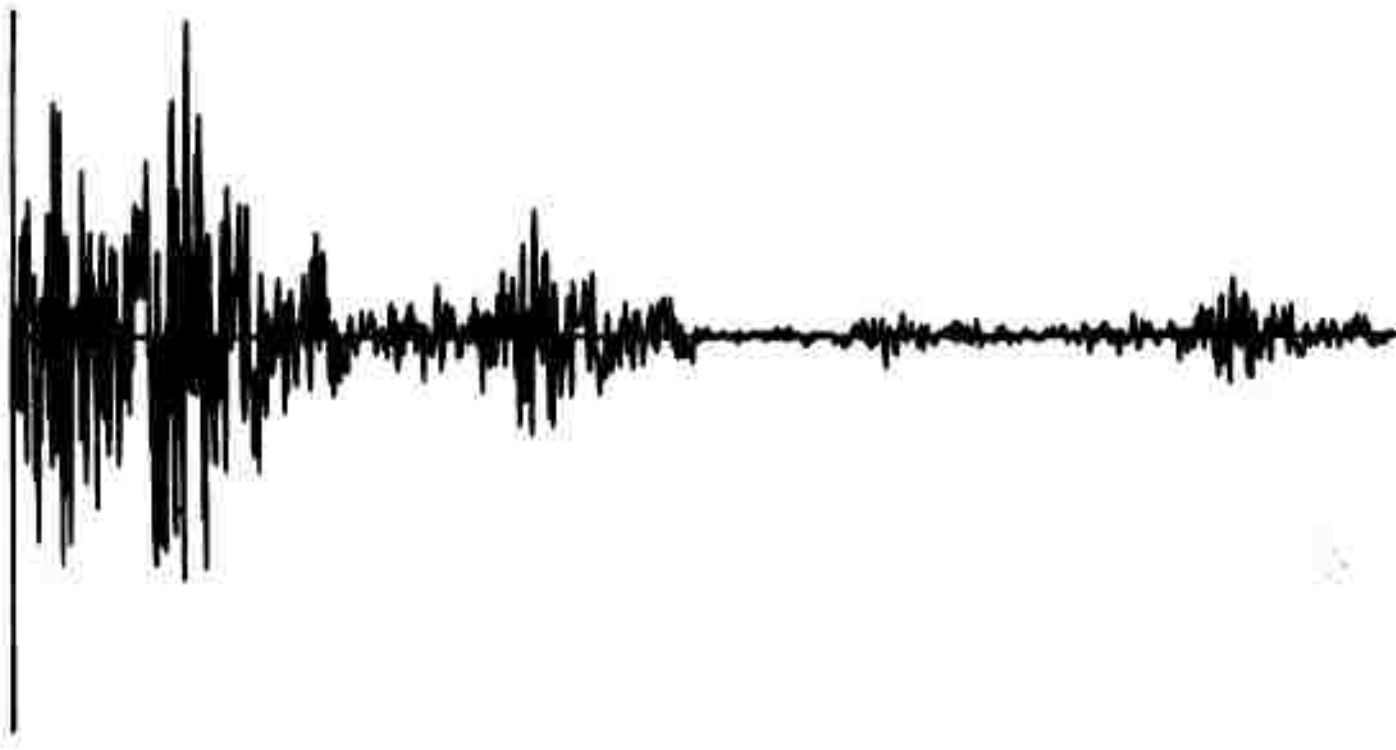
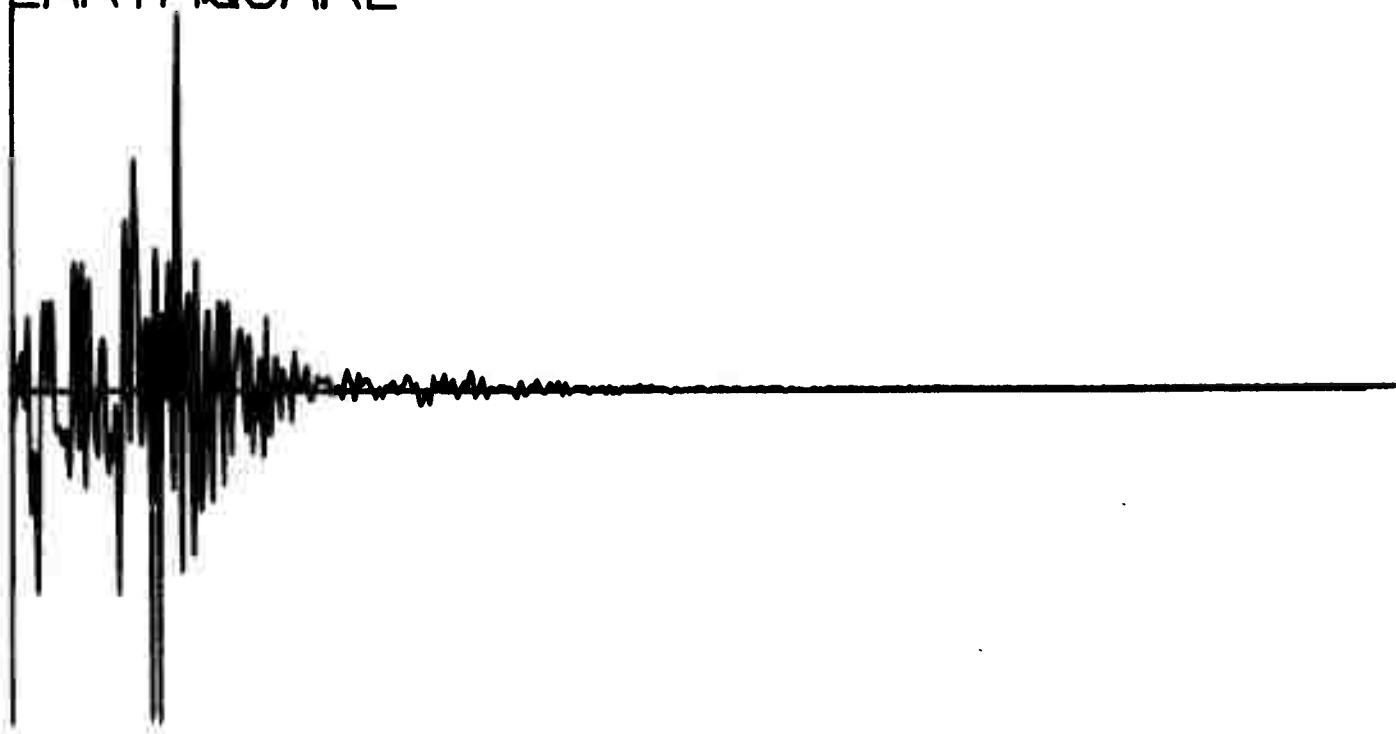
Q148

EVENT NUMBER 1131
EARTHQUAKE



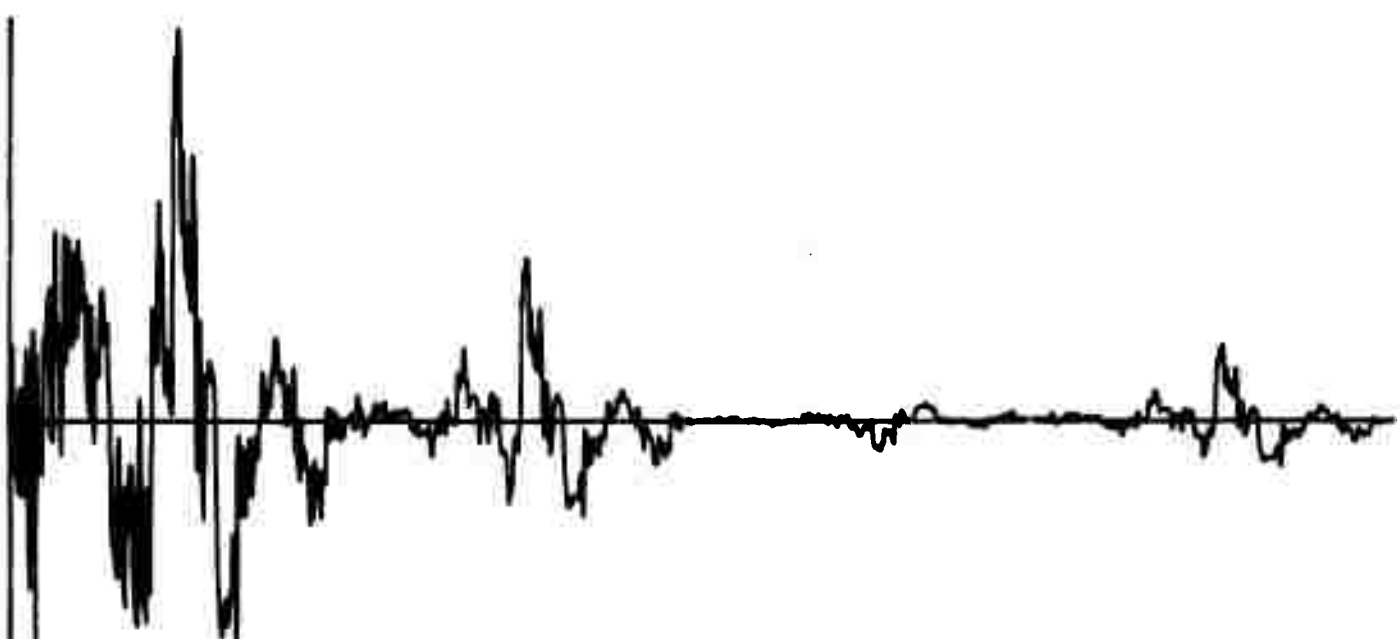
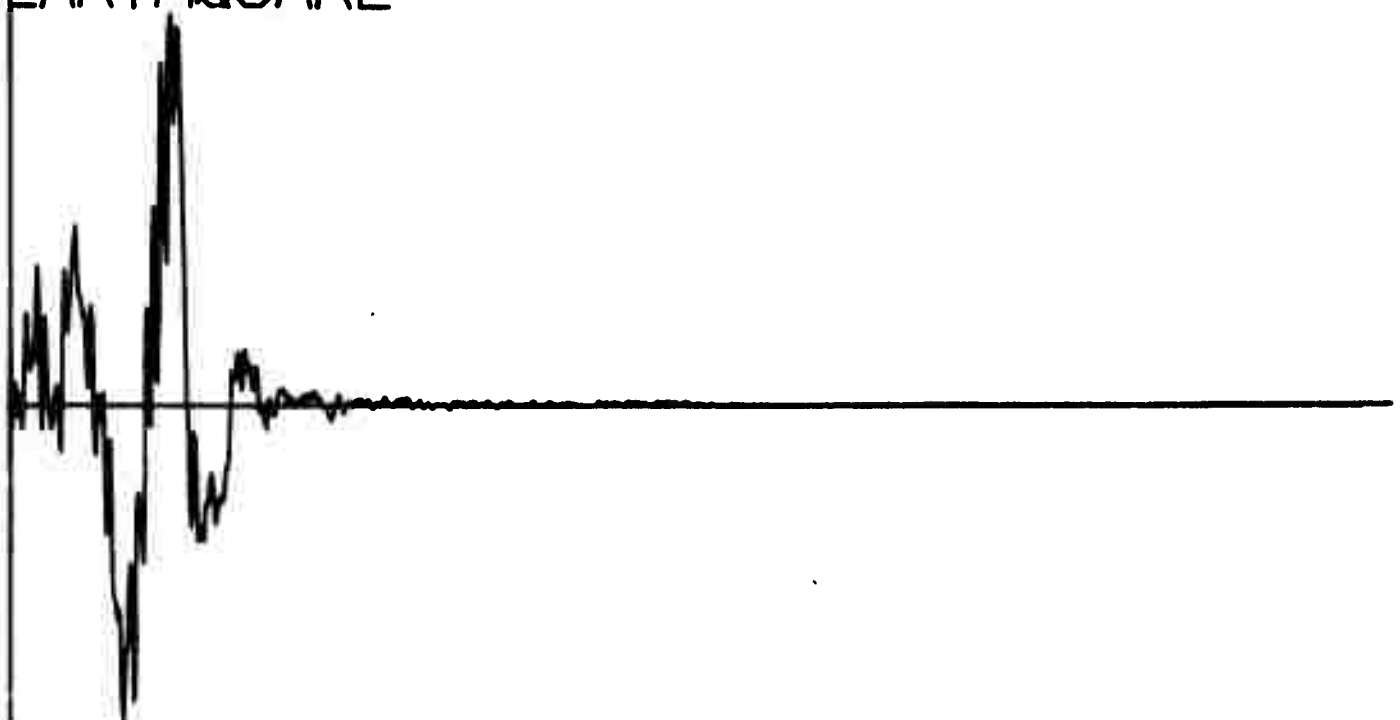
Q150

EVENT NUMBER 1130
EARTHQUAKE



Q152

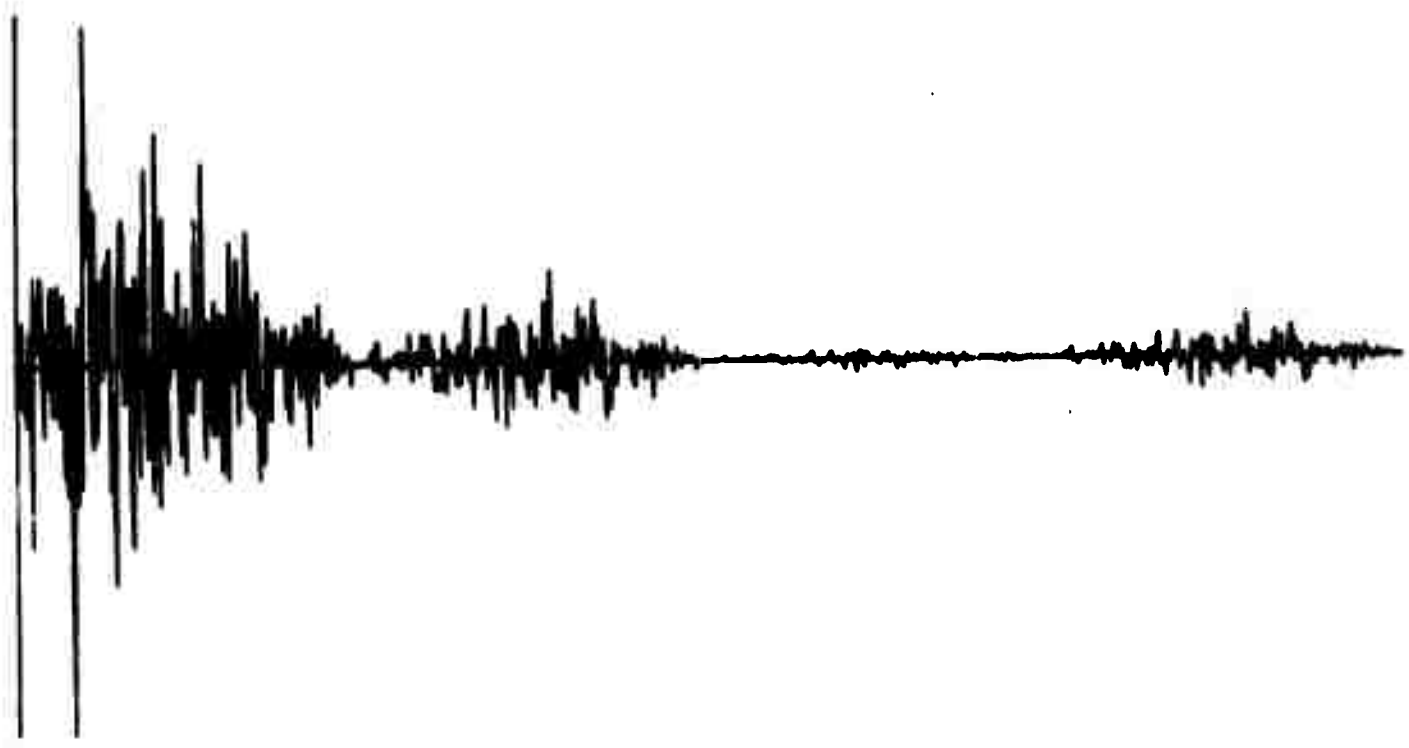
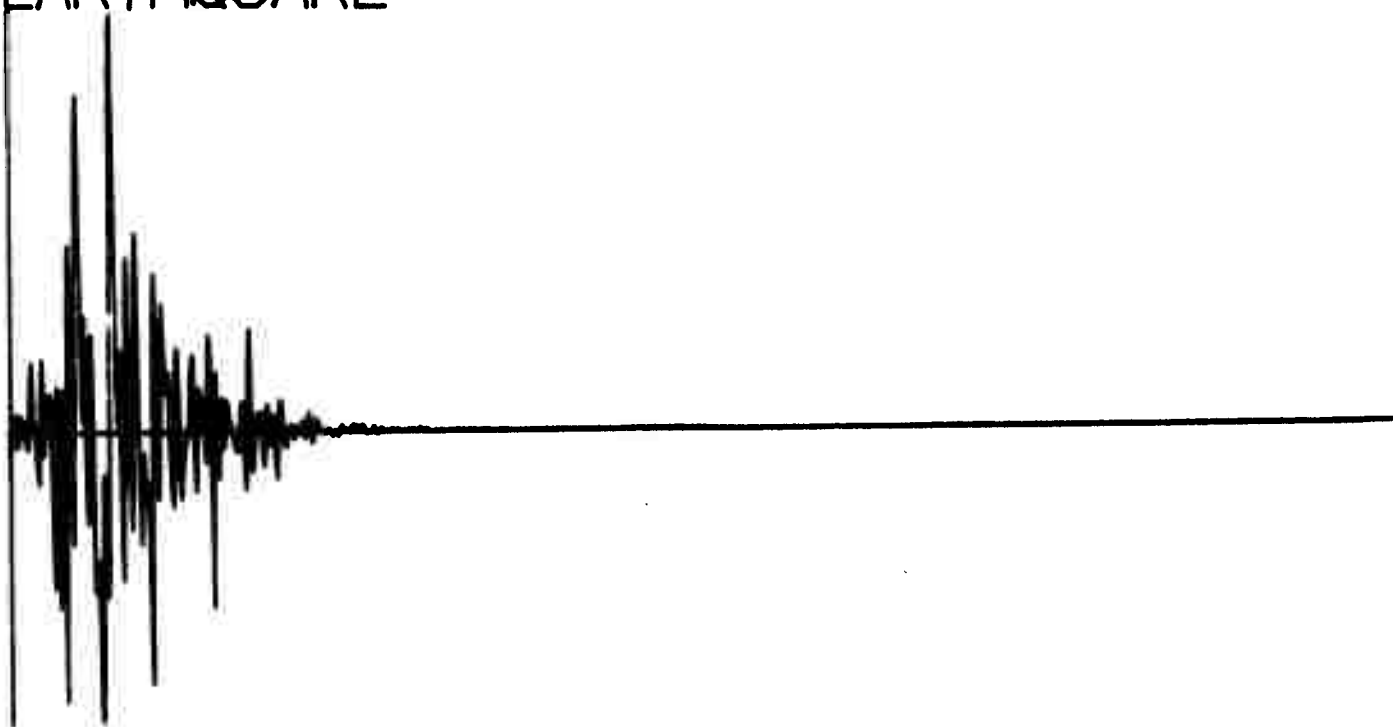
EVENT NUMBER 1159
EARTHQUAKE



Q154

EVENT NUMBER 1141

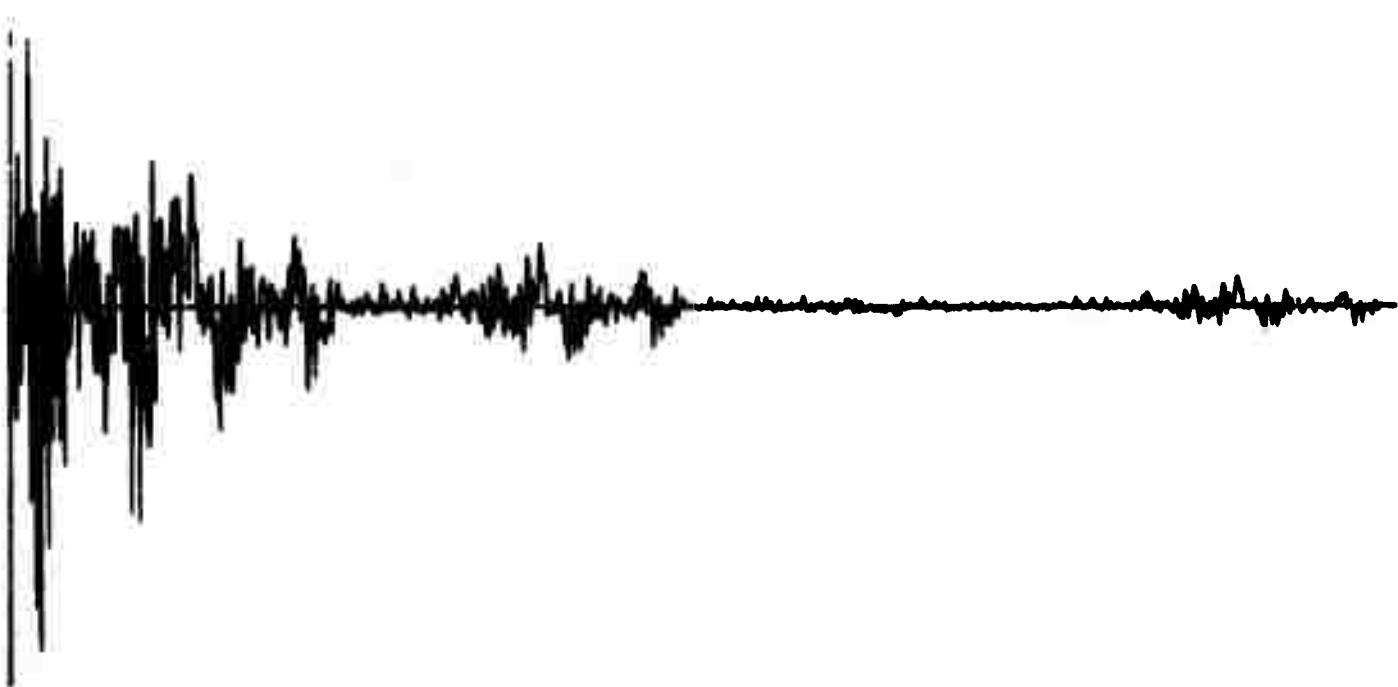
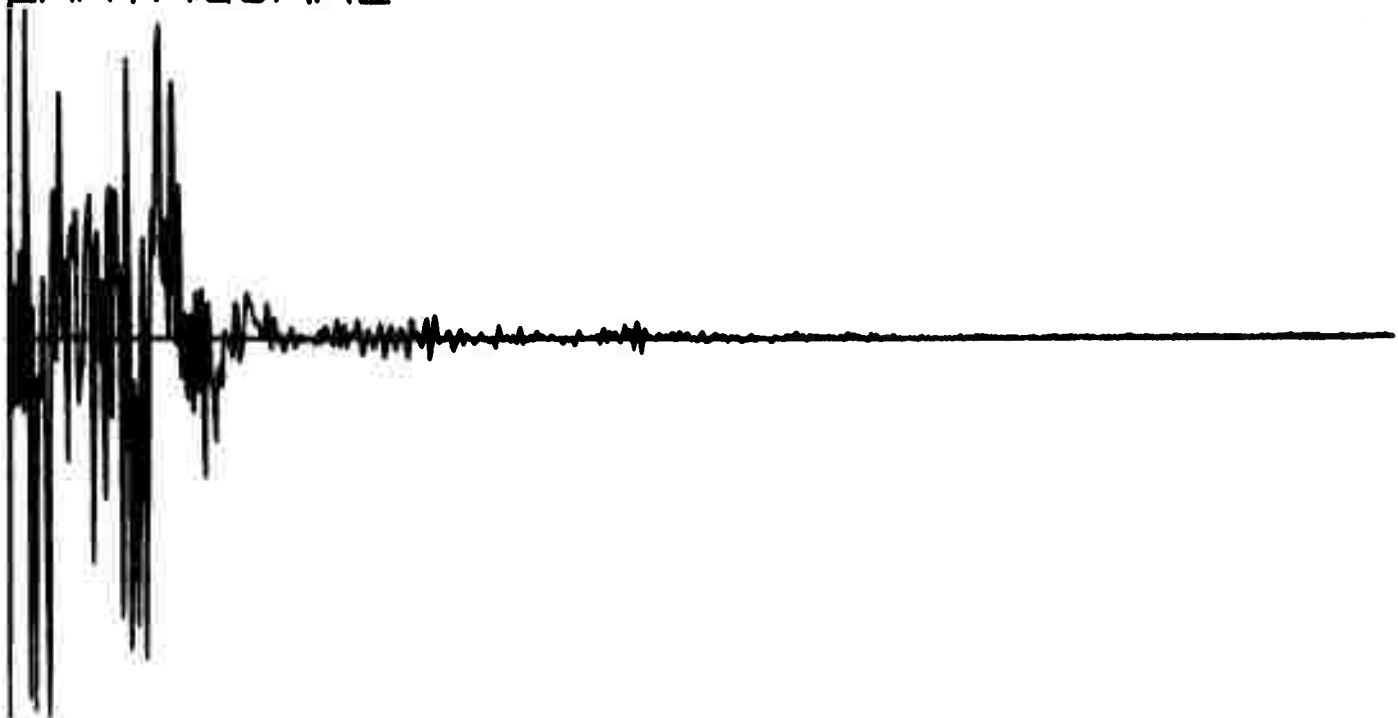
EARTHQUAKE



Q156

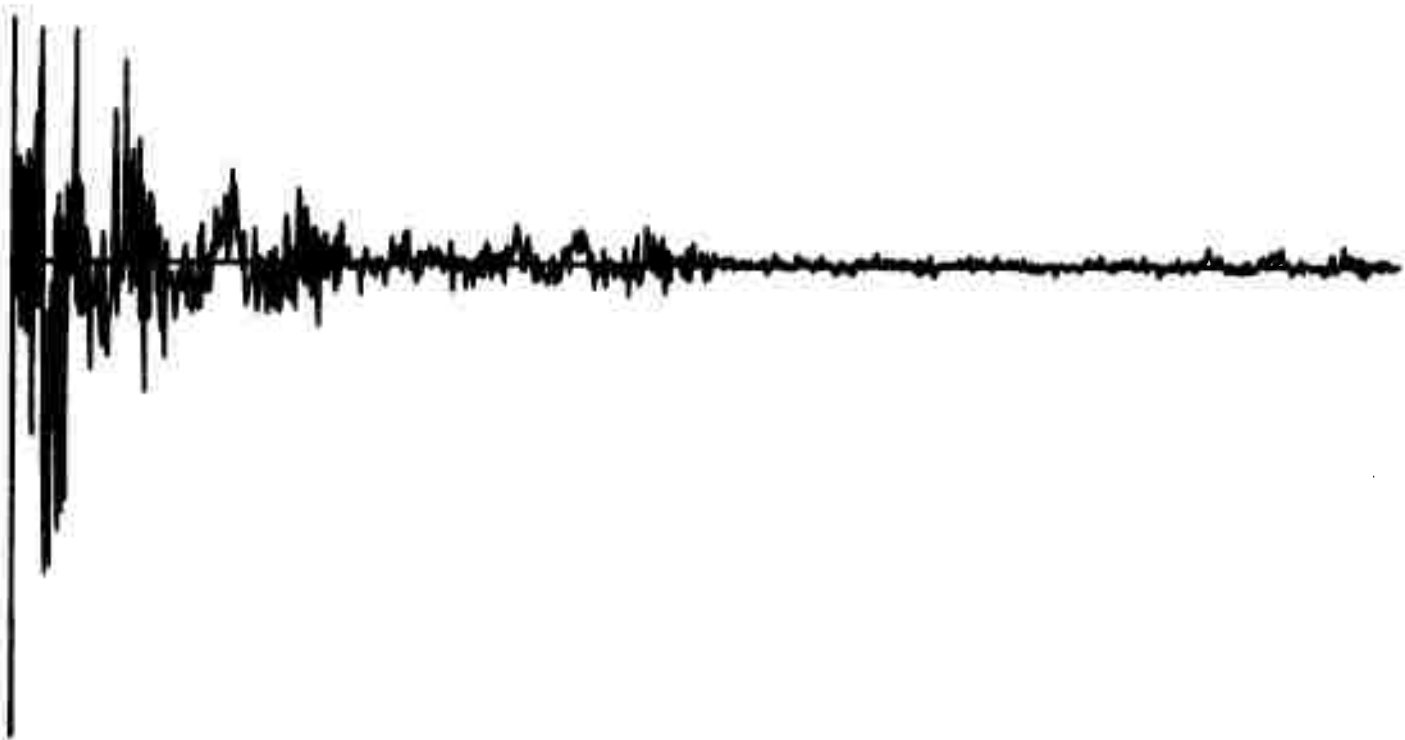
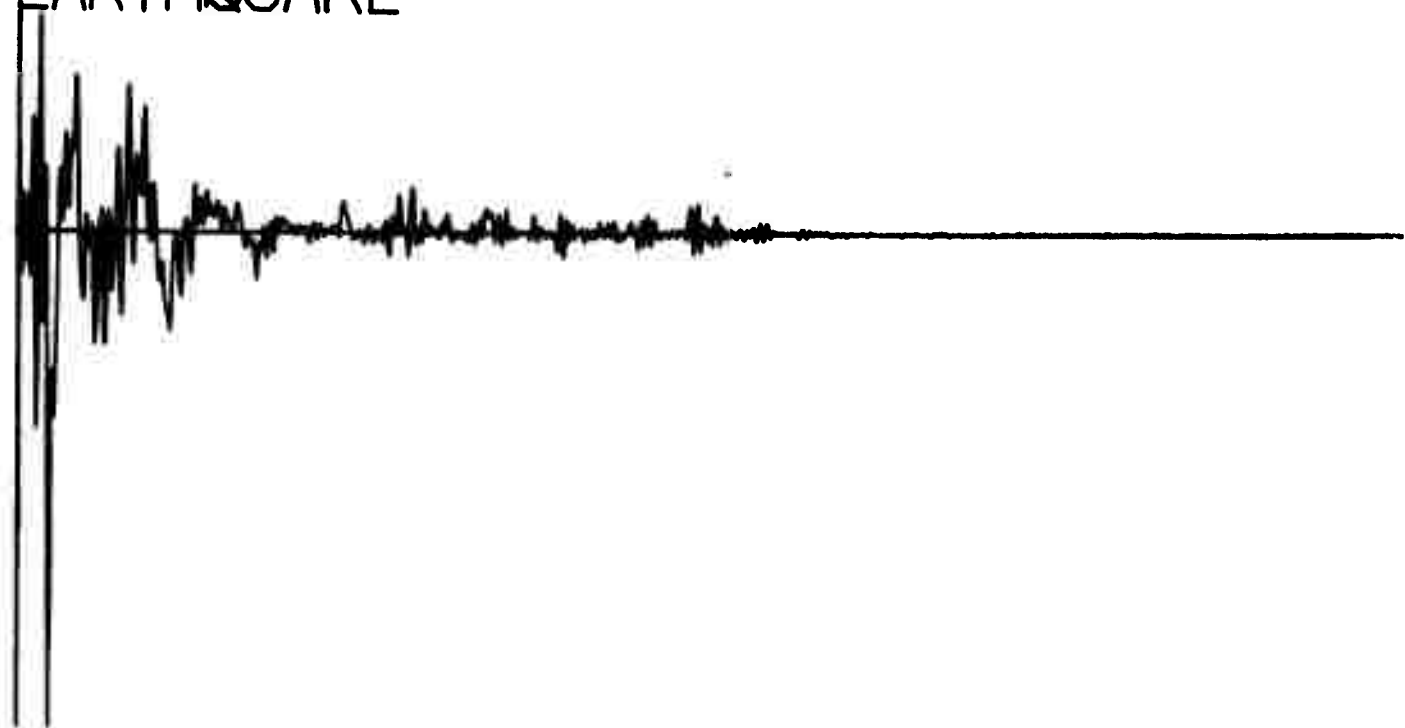
EVENT NUMBER 1205

EARTHQUAKE



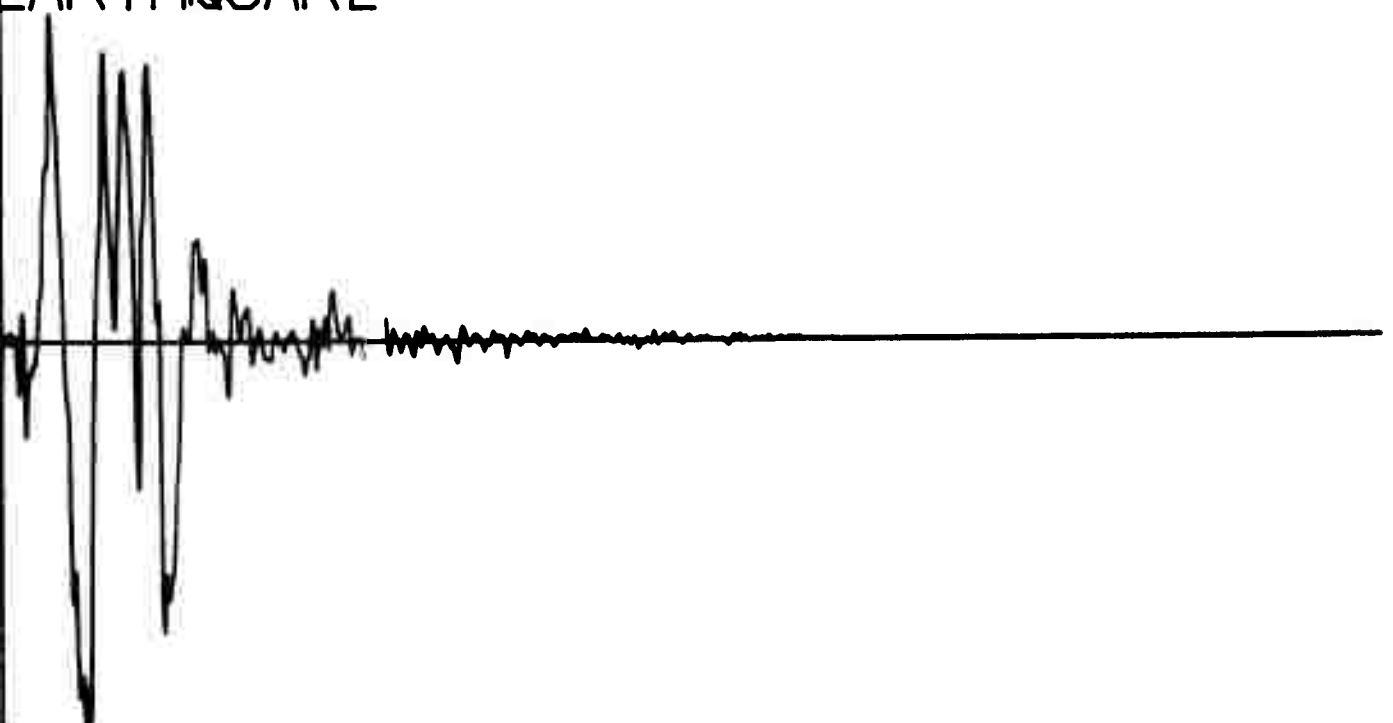
Q158

EVENT NUMBER 1207
EARTHQUAKE



Q160

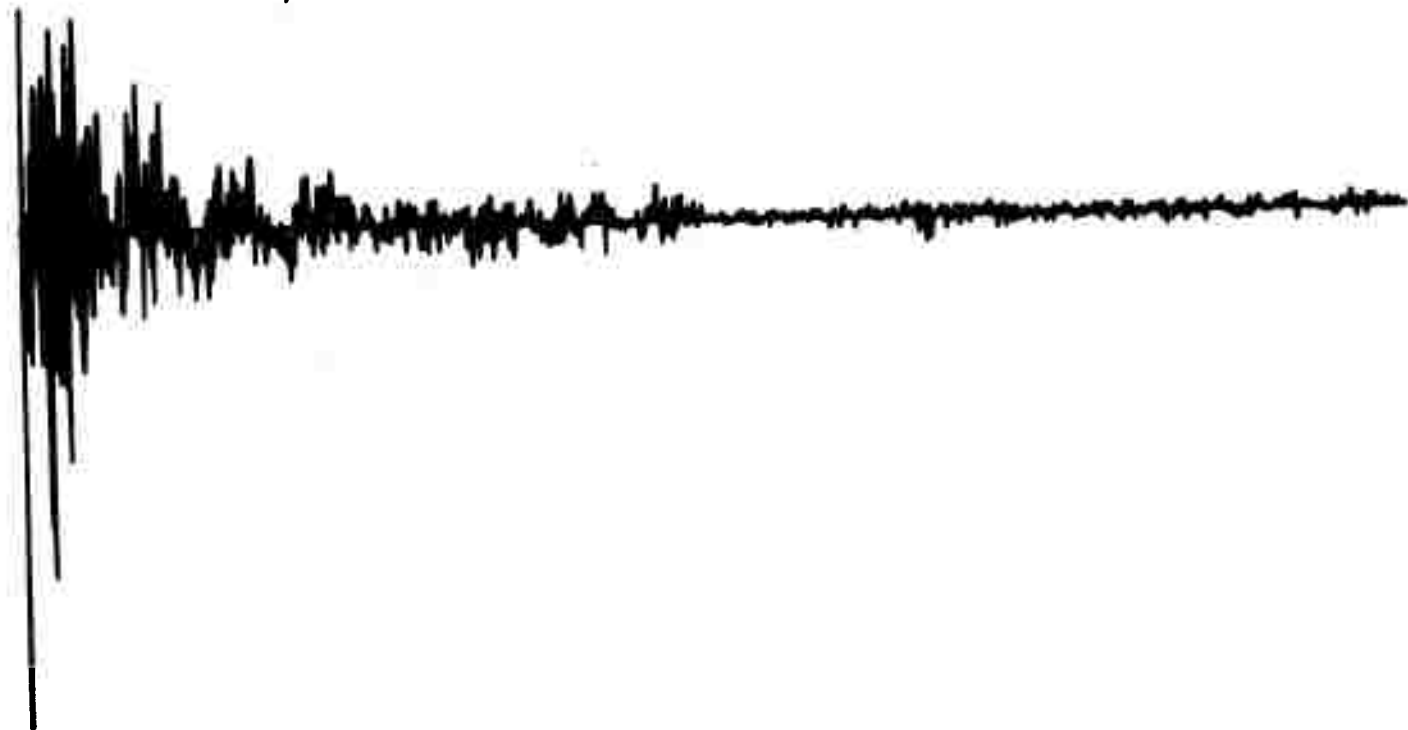
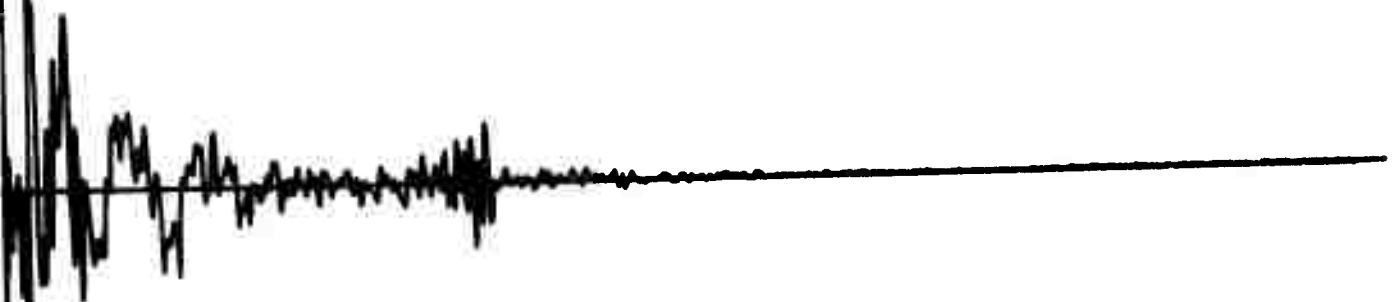
EVENT NUMBER 1209
EARTHQUAKE



Q162

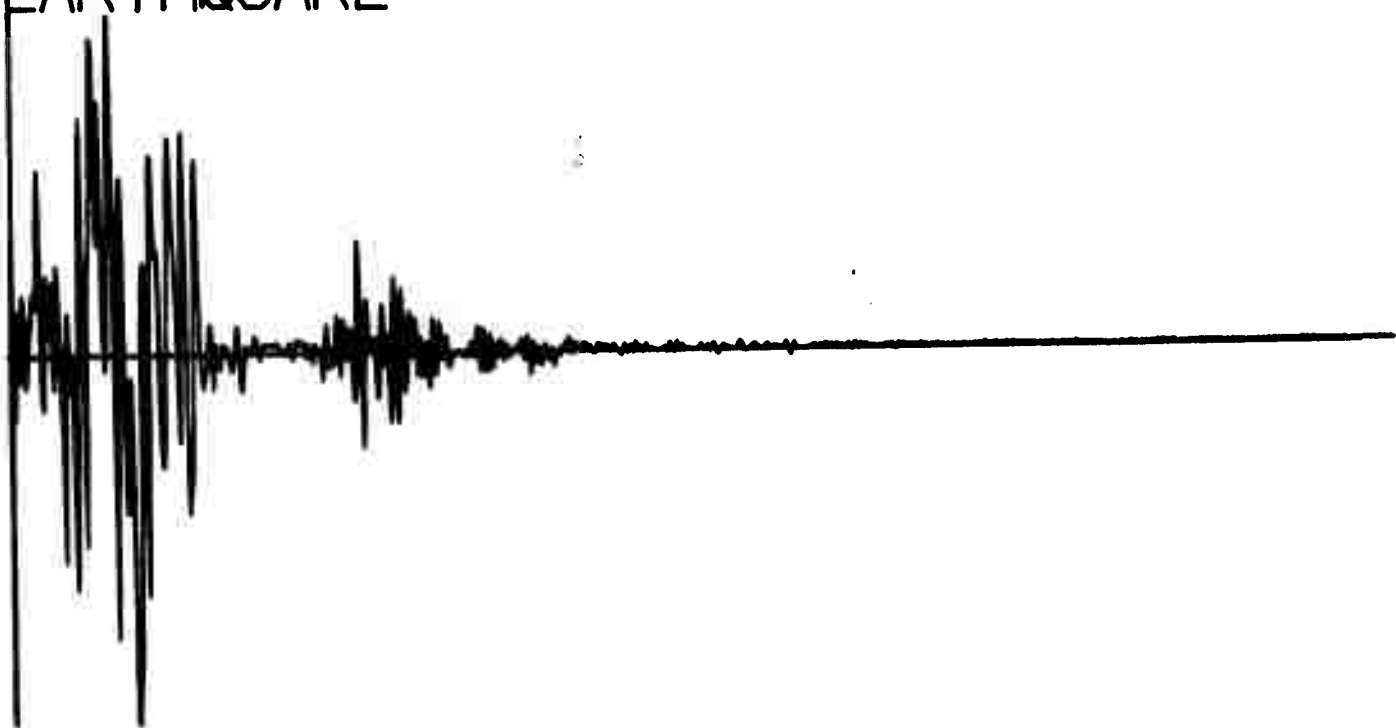
EVENT NUMBER 1214

EARTHQUAKE



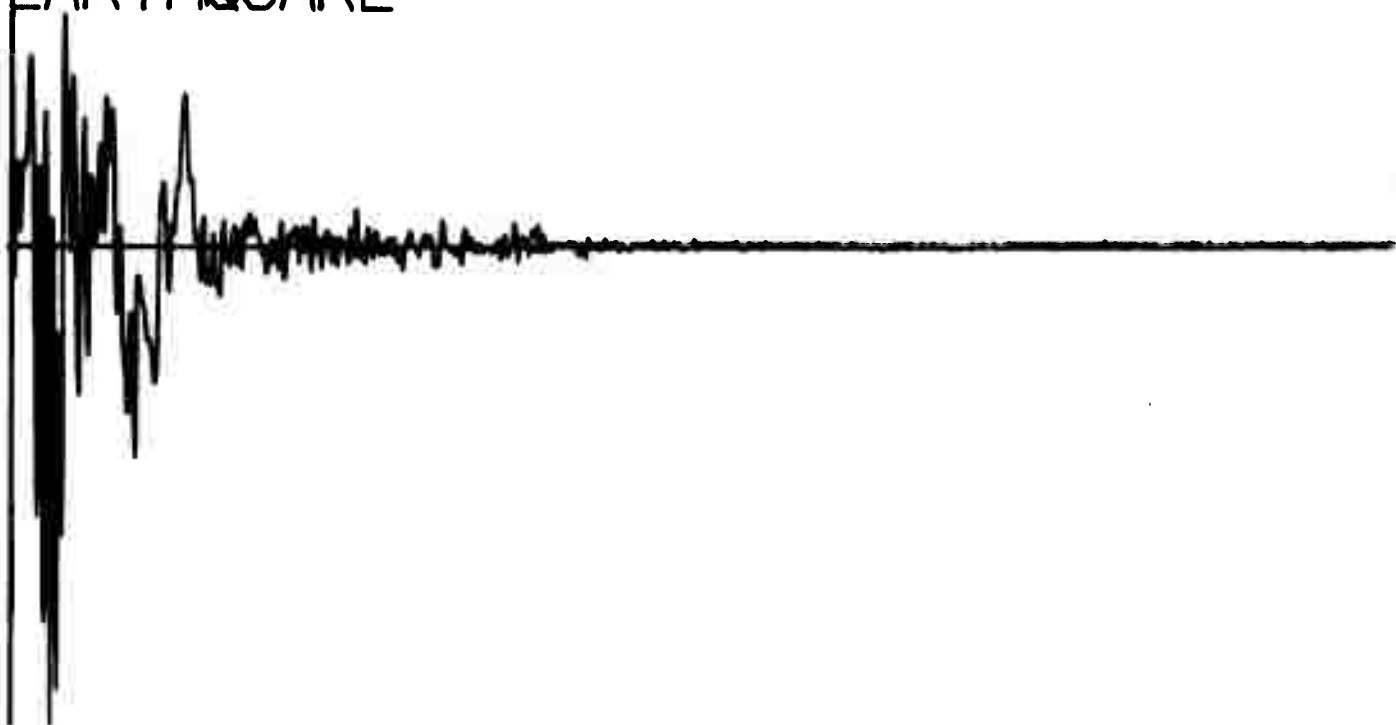
Q164

VENT NUMBER 1250
EARTHQUAKE



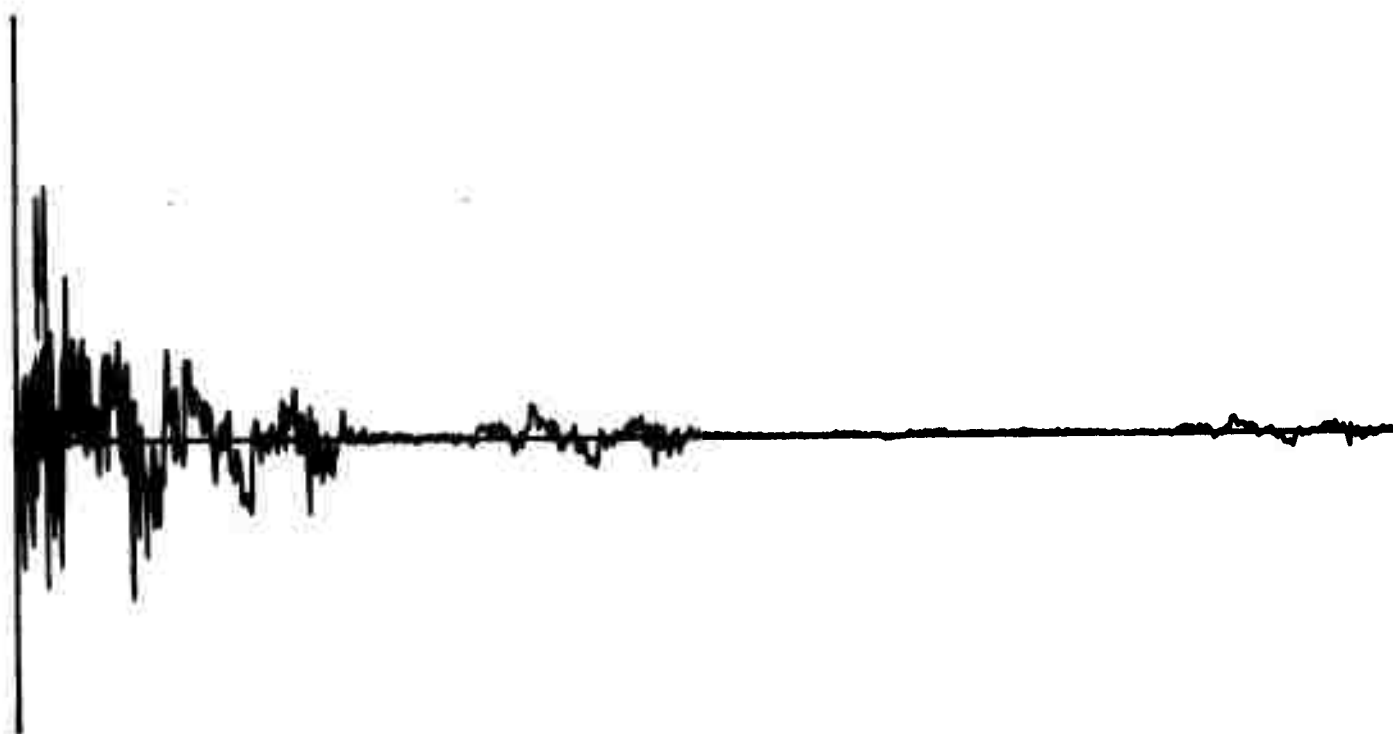
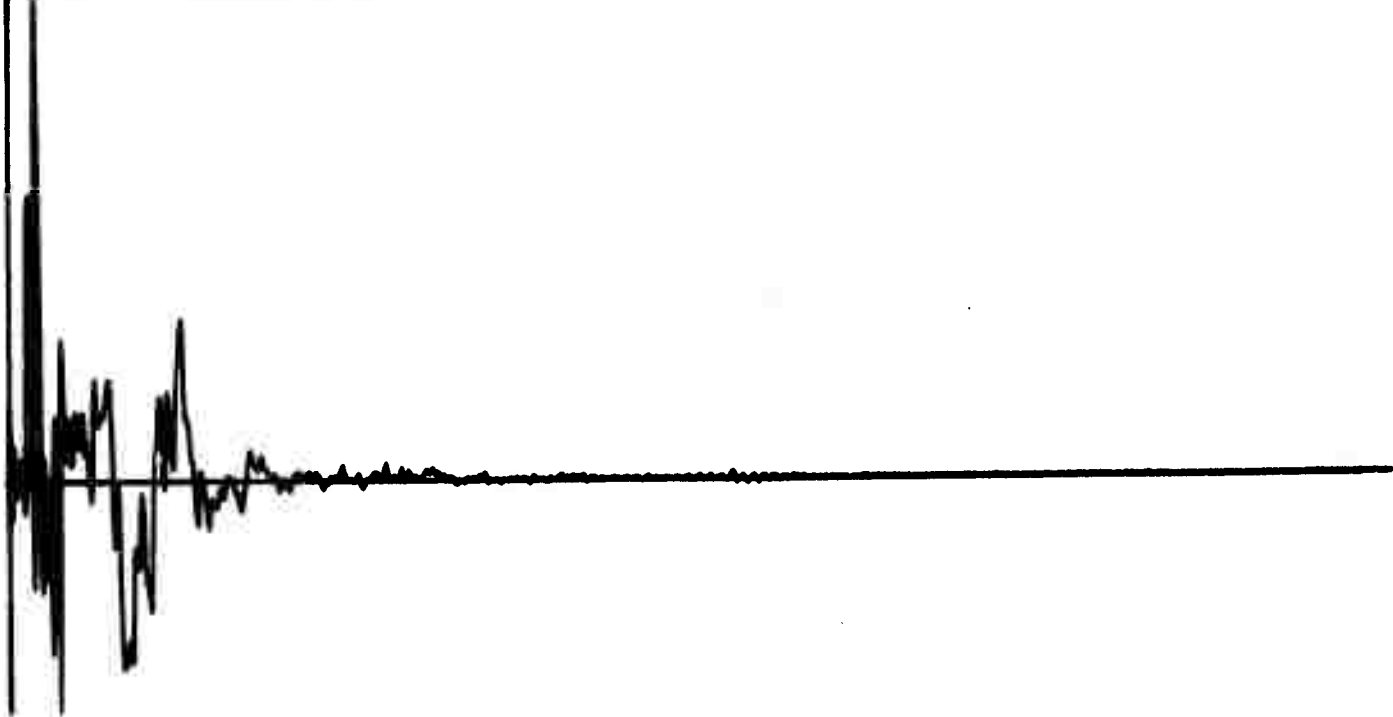
Q166

EVENT NUMBER 1224
EARTHQUAKE



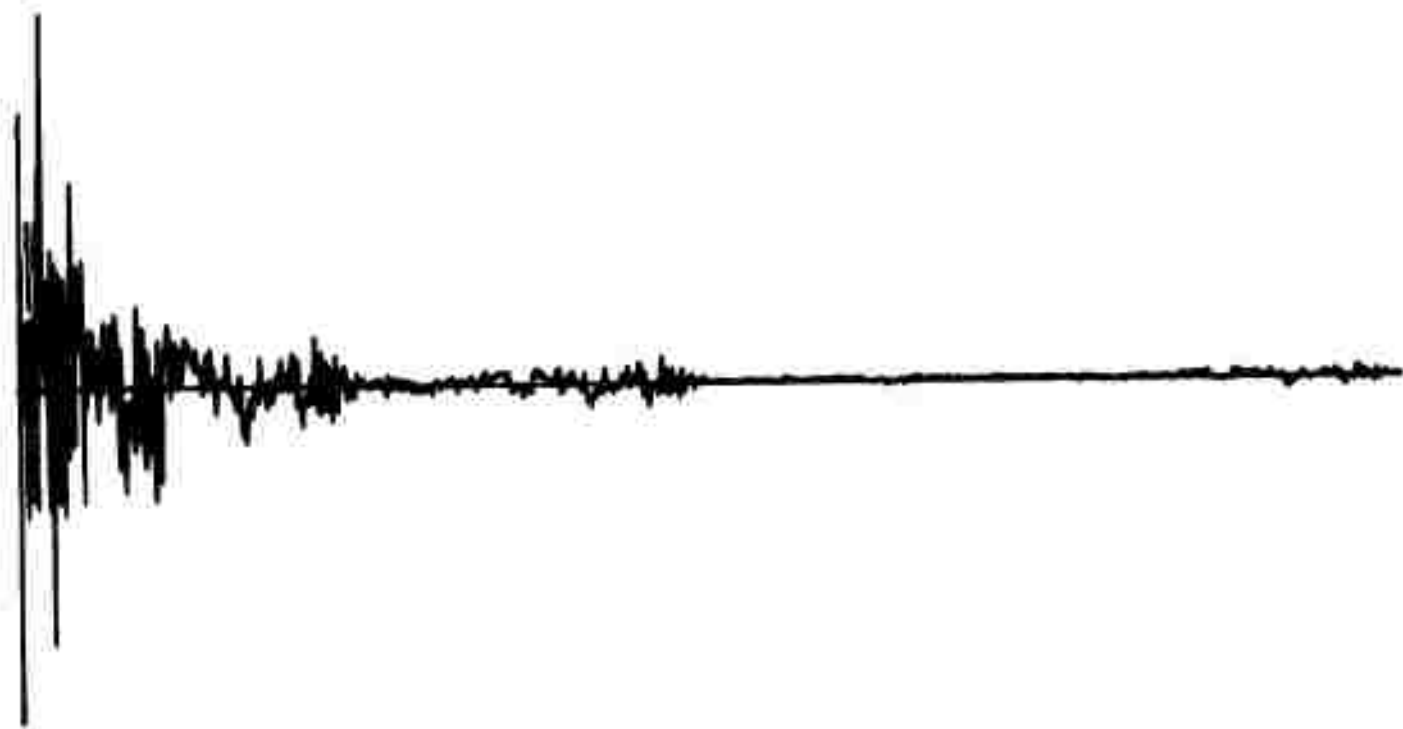
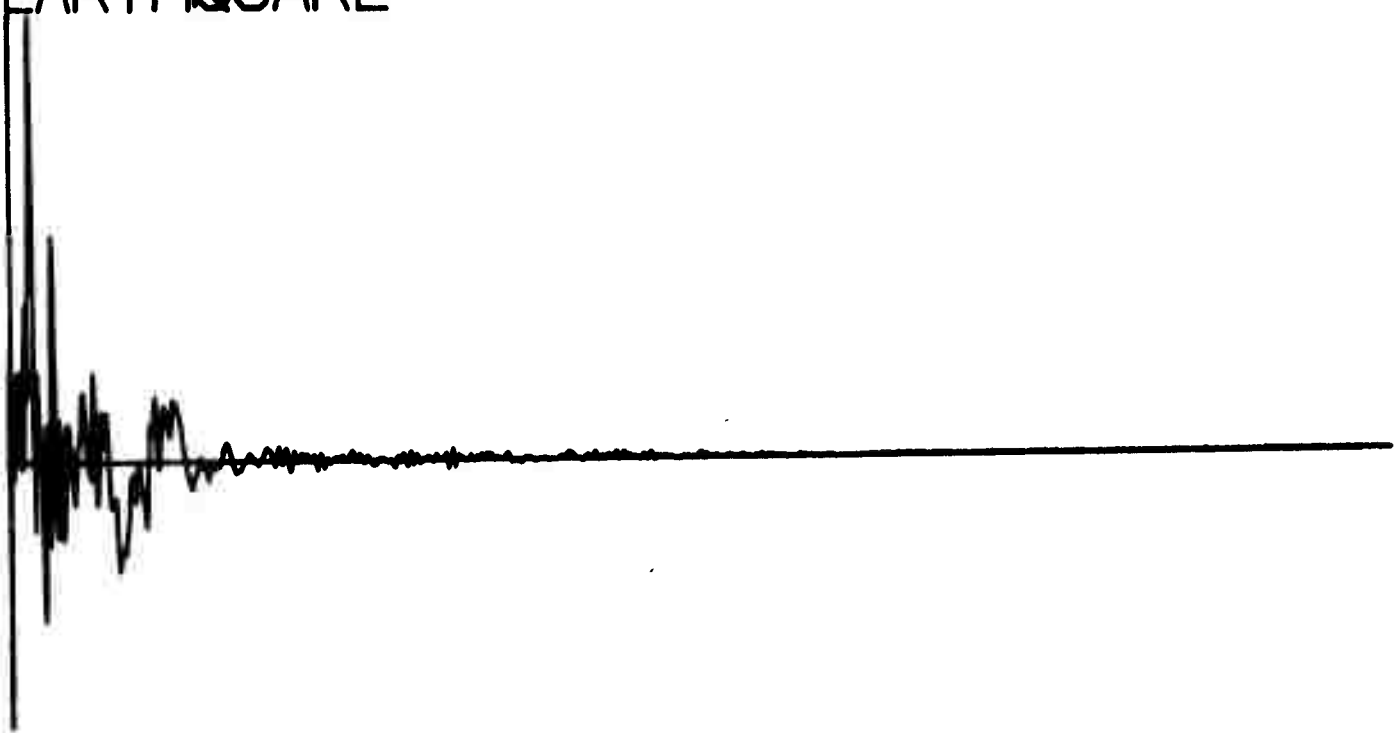
Q168

VENT NUMBER 1223
EARTHQUAKE



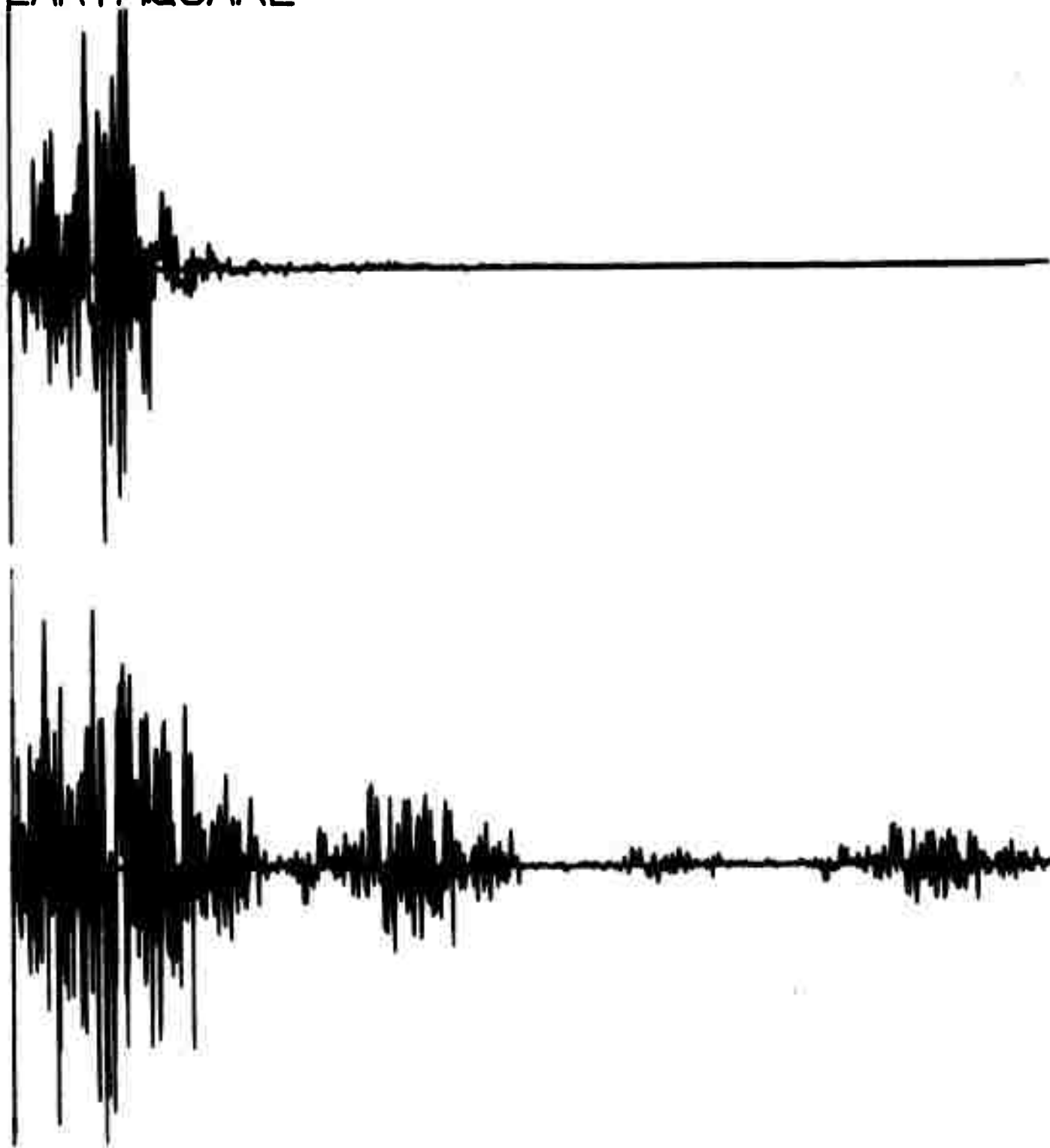
Q170

EVENT NUMBER 1222
EARTHQUAKE



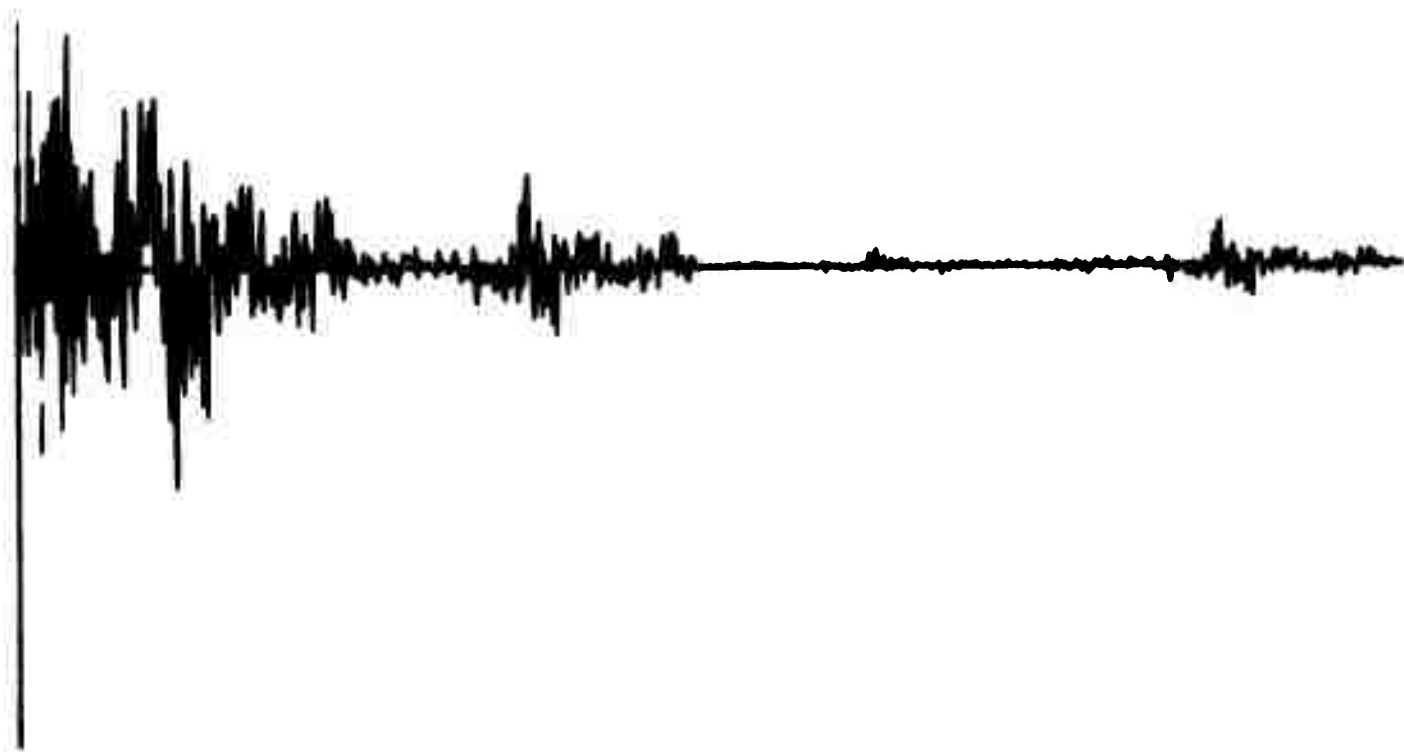
Q172

EVENT NUMBER 1035
EARTHQUAKE



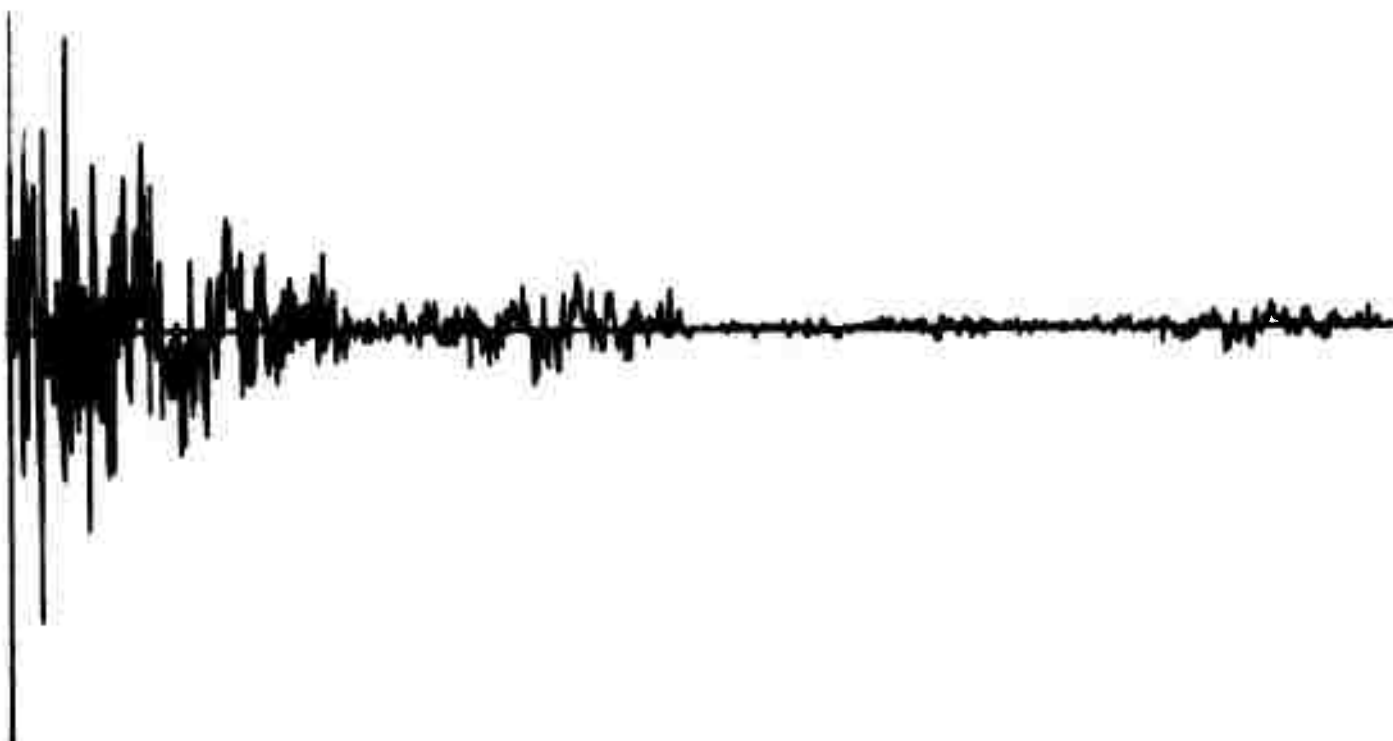
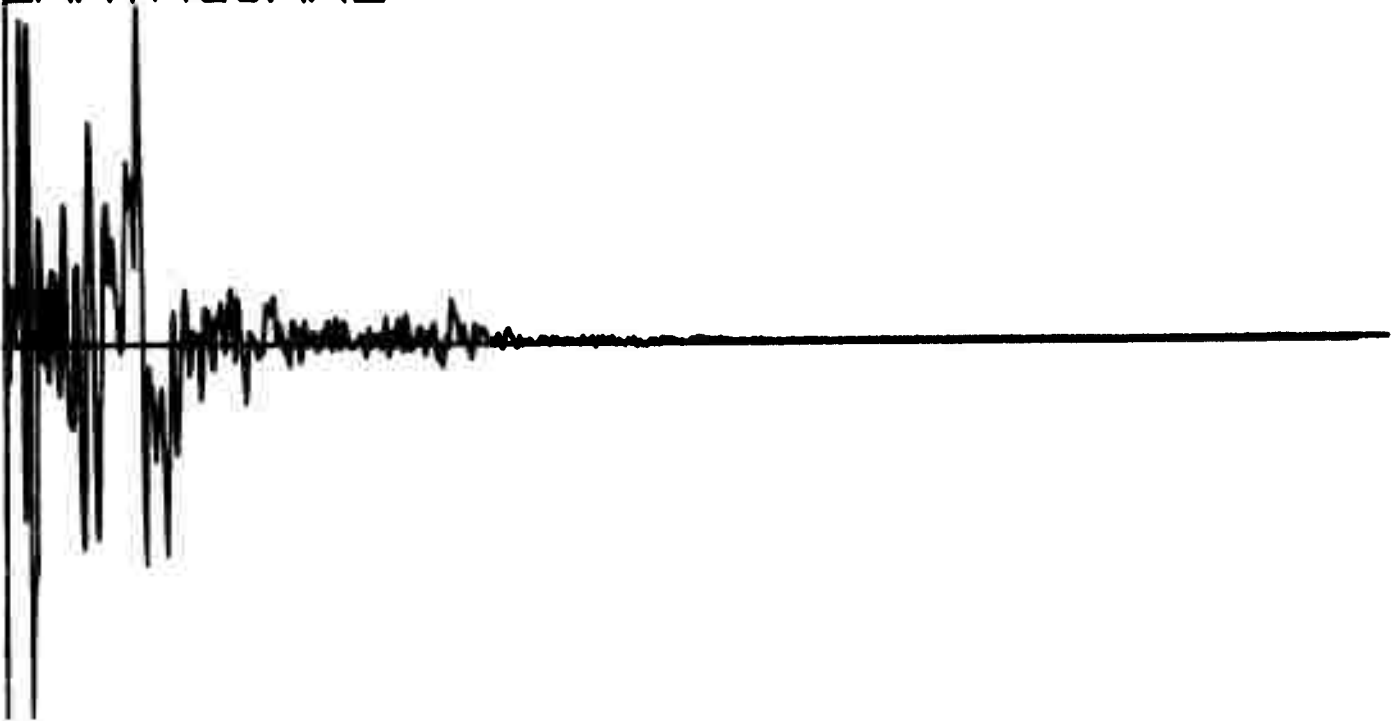
Q174

VENT NUMBER 1032
EARTHQUAKE



Q176

VENT NUMBER 1028
EARTHQUAKE



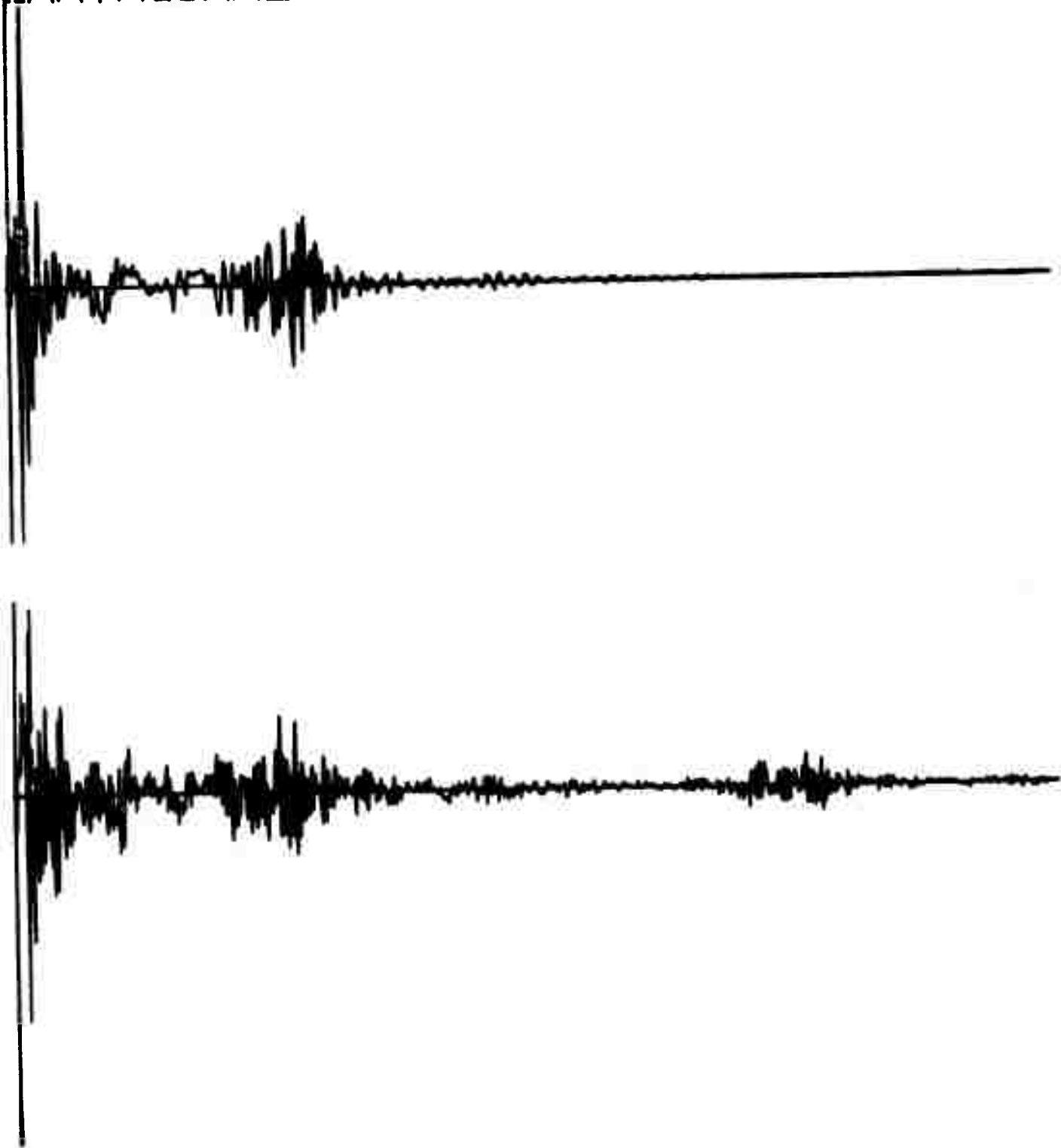
Q178

EVENT NUMBER 1027
EARTHQUAKE



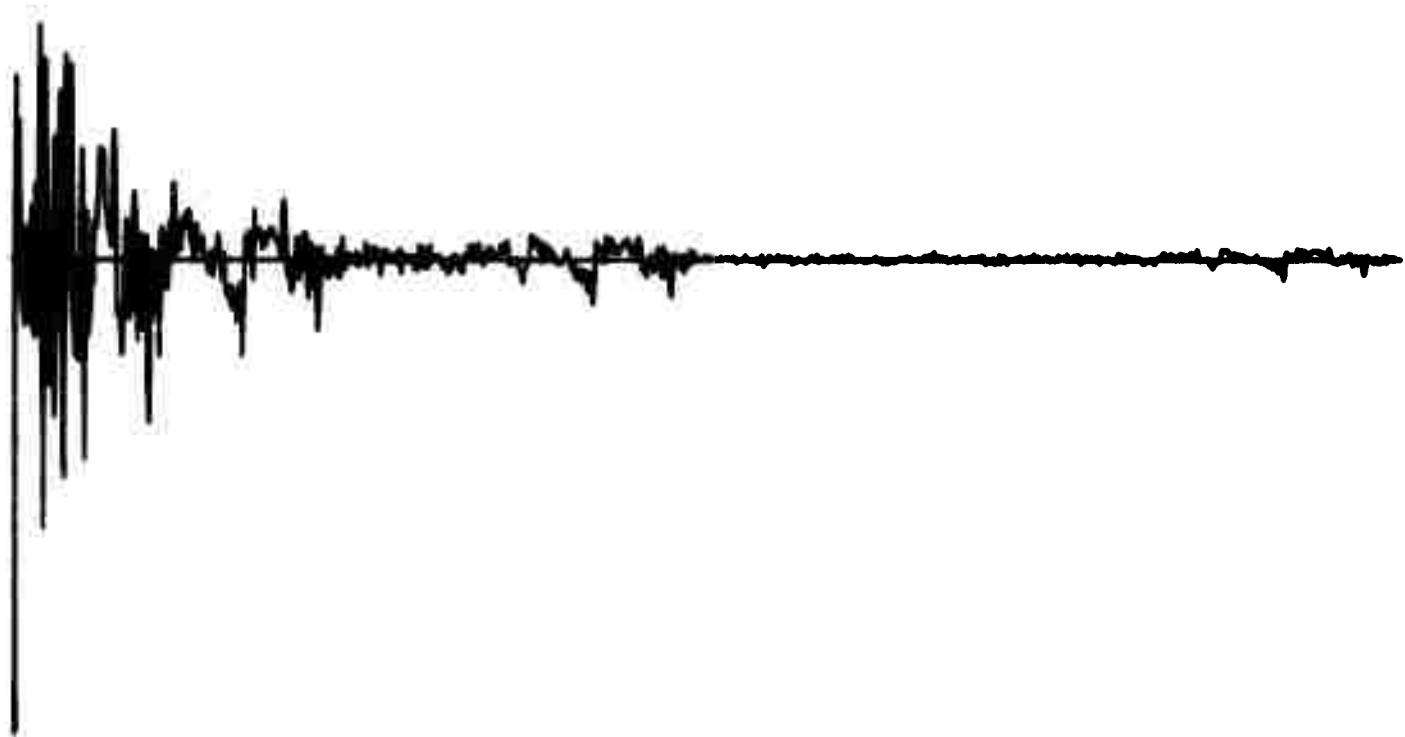
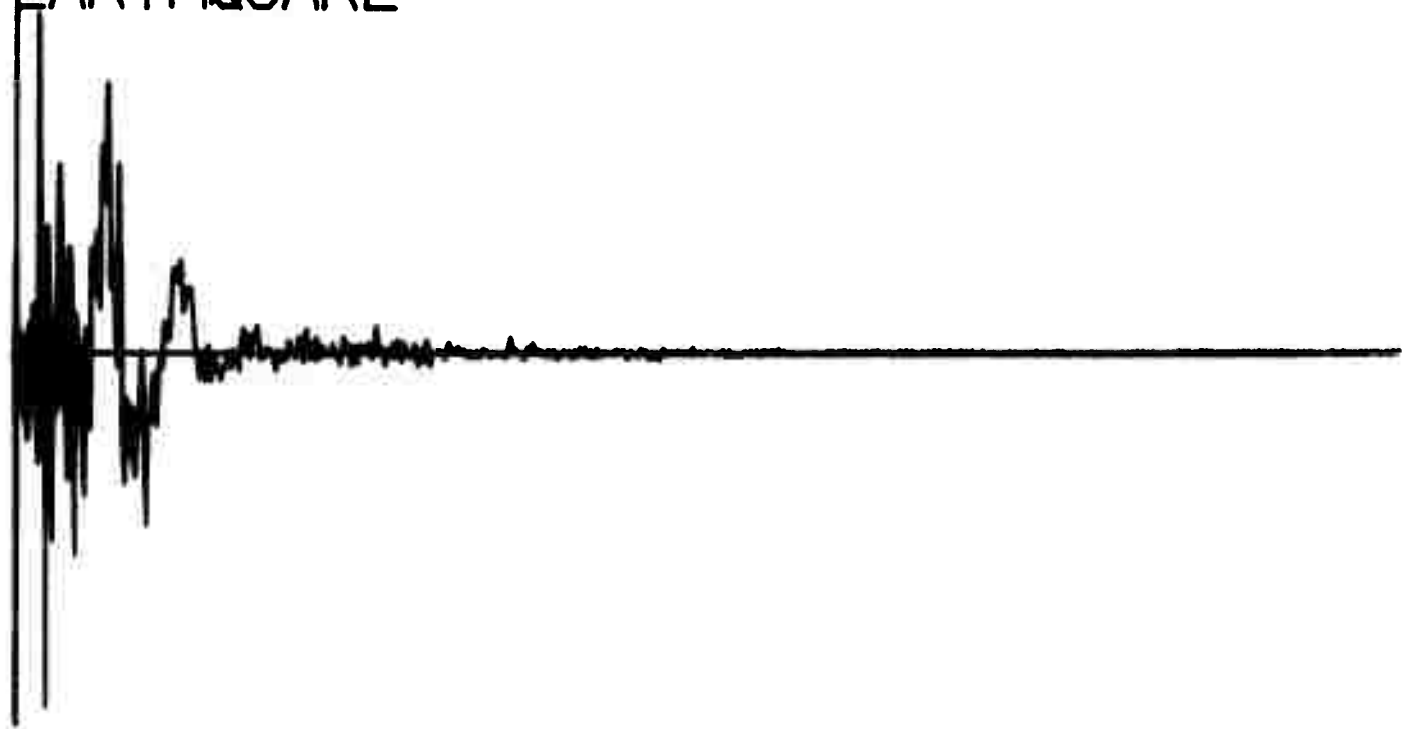
Q180

EVENT NUMBER 1025
EARTHQUAKE



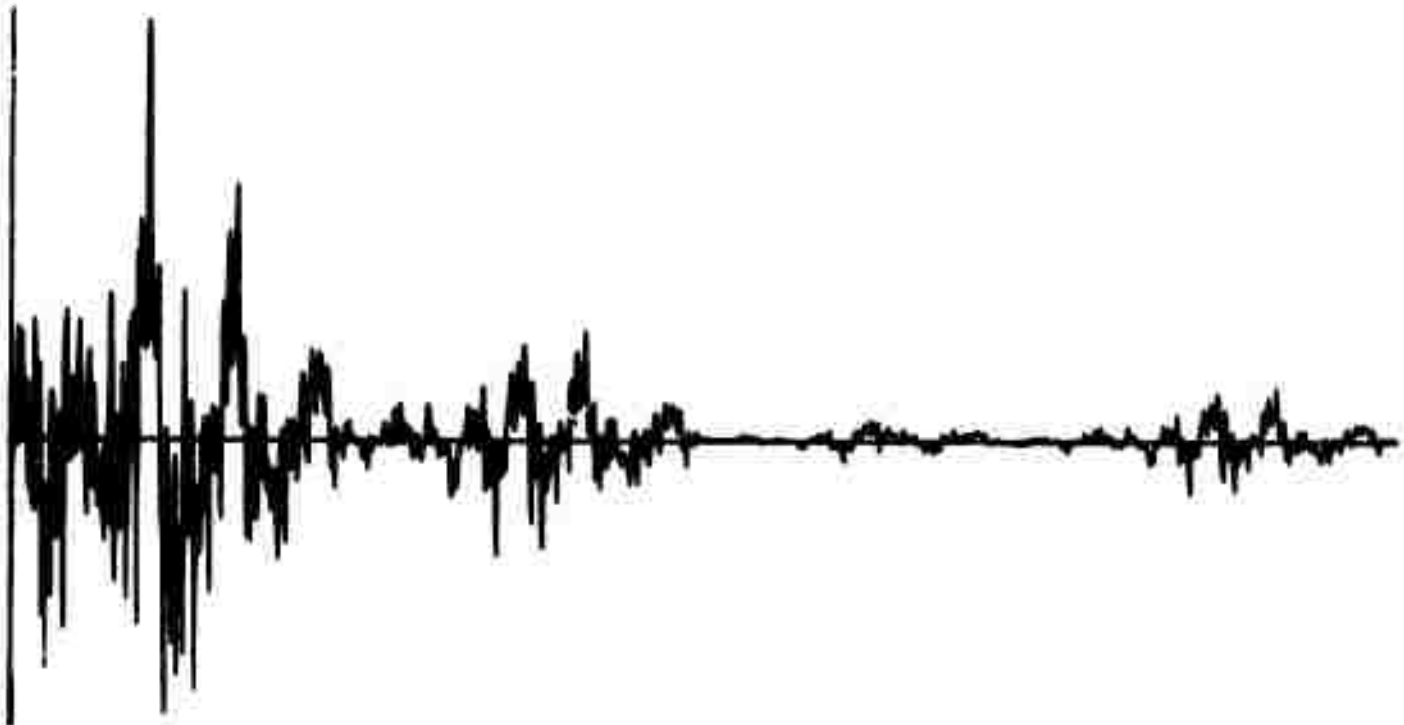
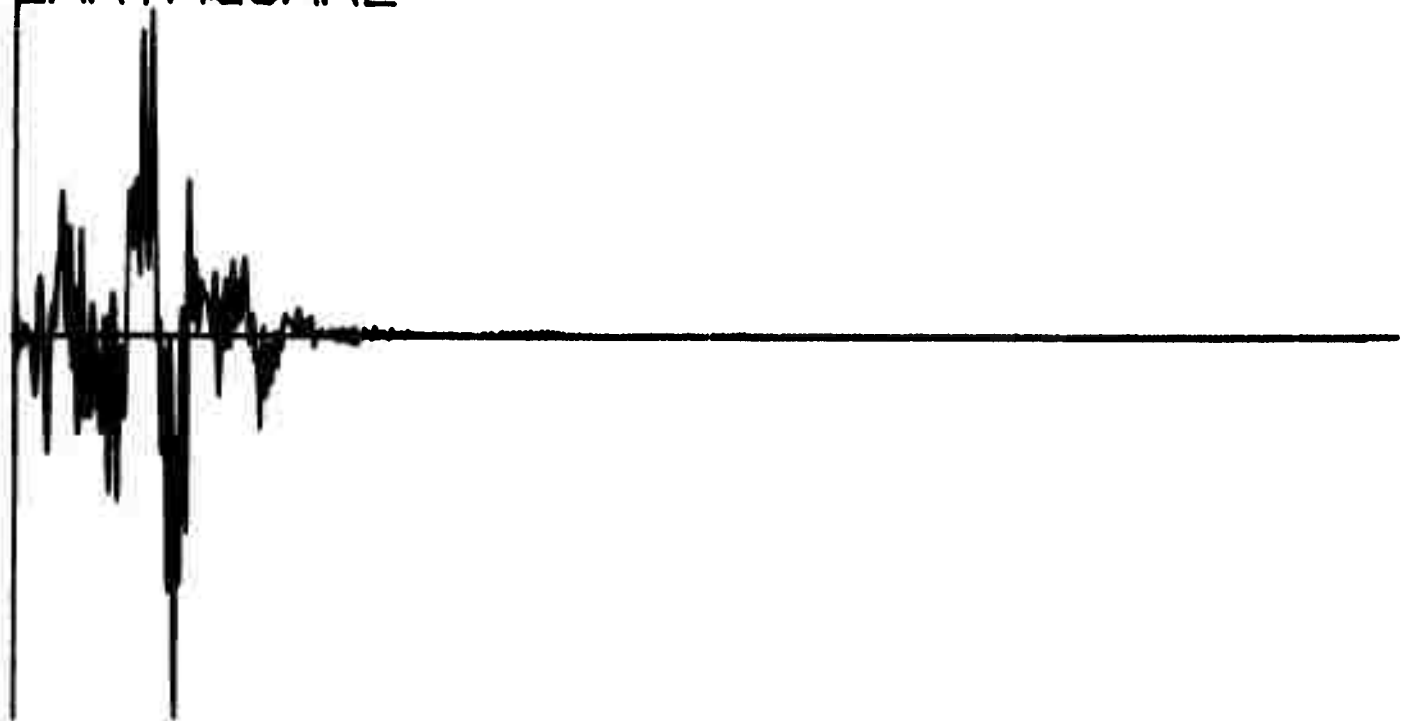
Q182

EVENT NUMBER 1019
EARTHQUAKE



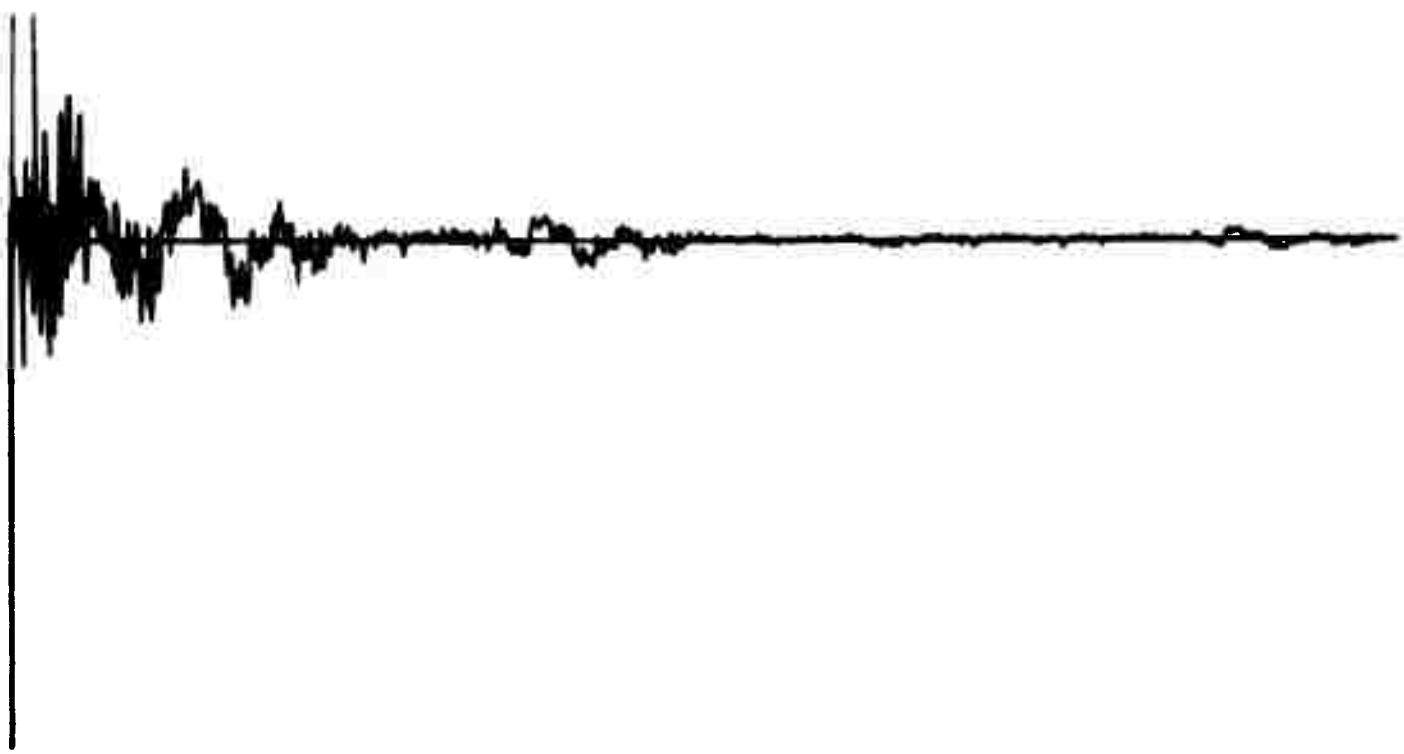
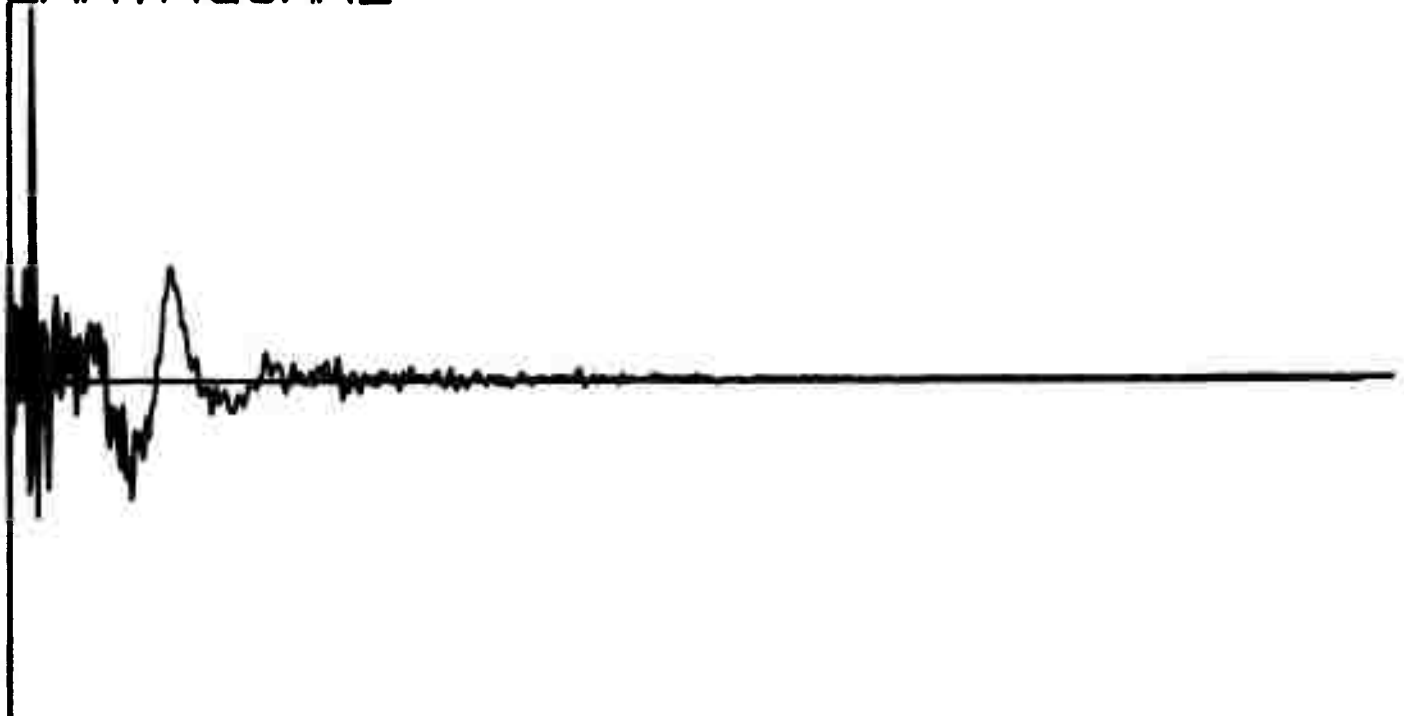
Q184

EVENT NUMBER 1003
EARTHQUAKE



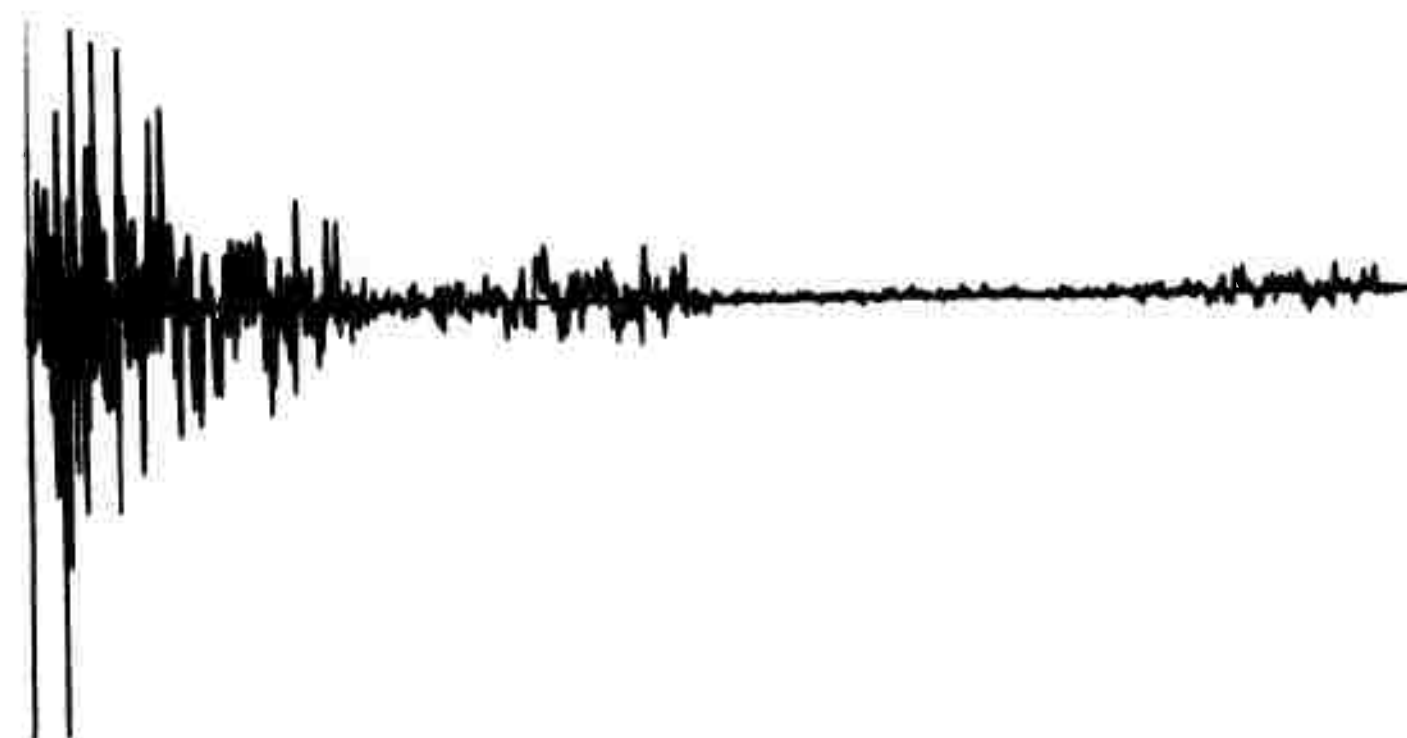
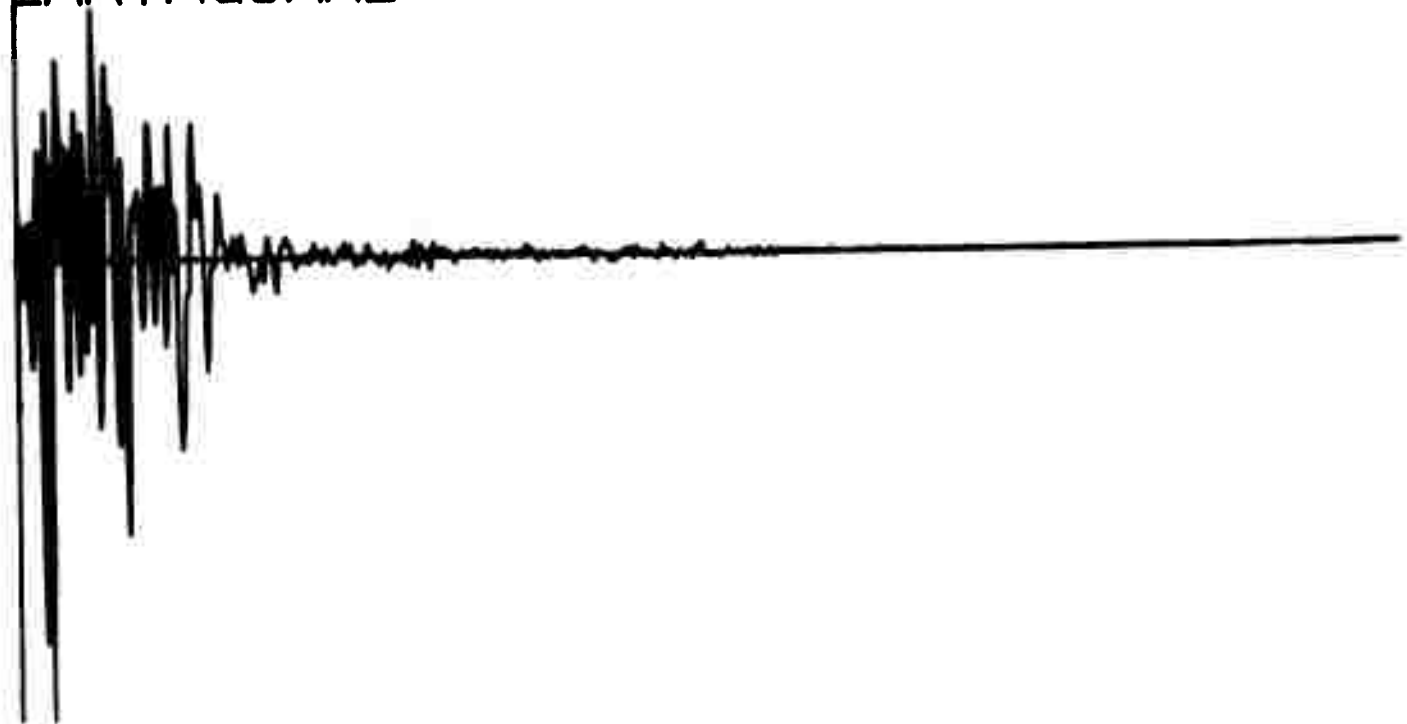
Q186

EVENT NUMBER 1002
EARTHQUAKE



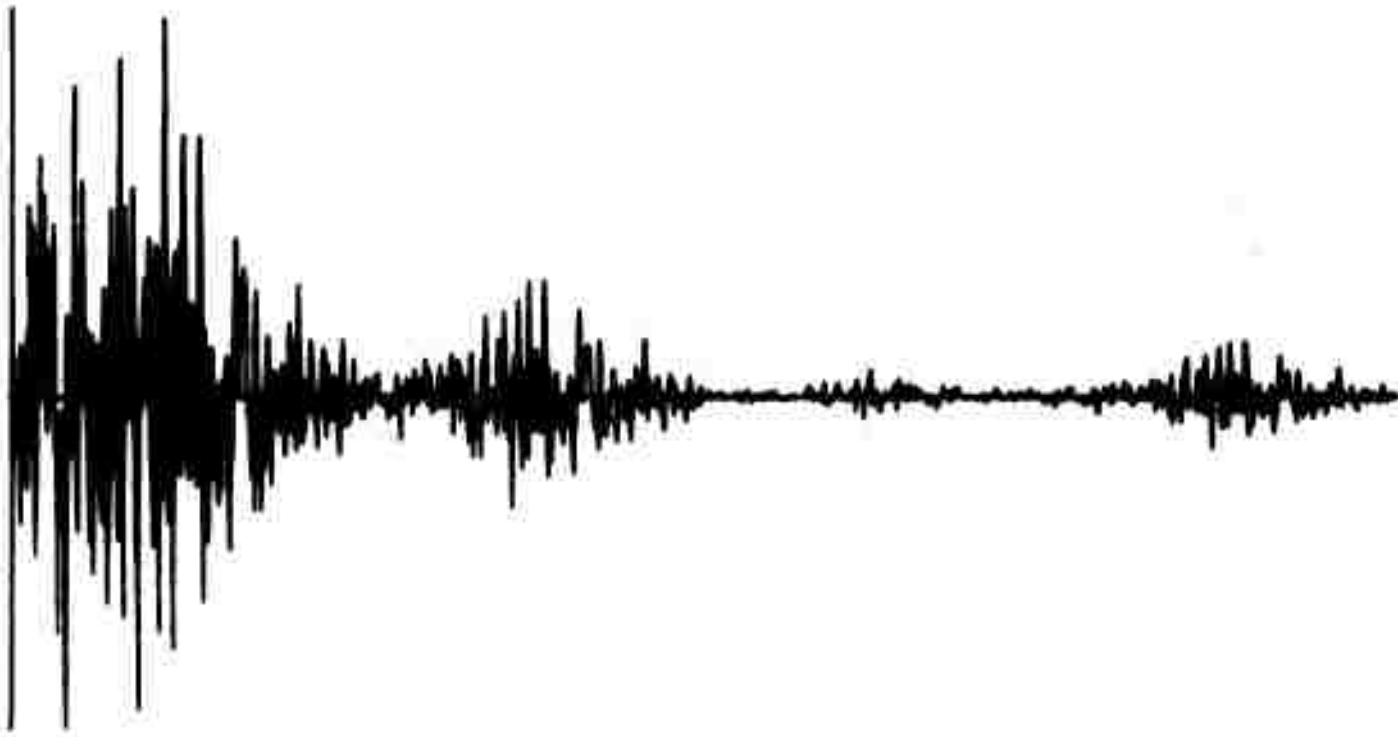
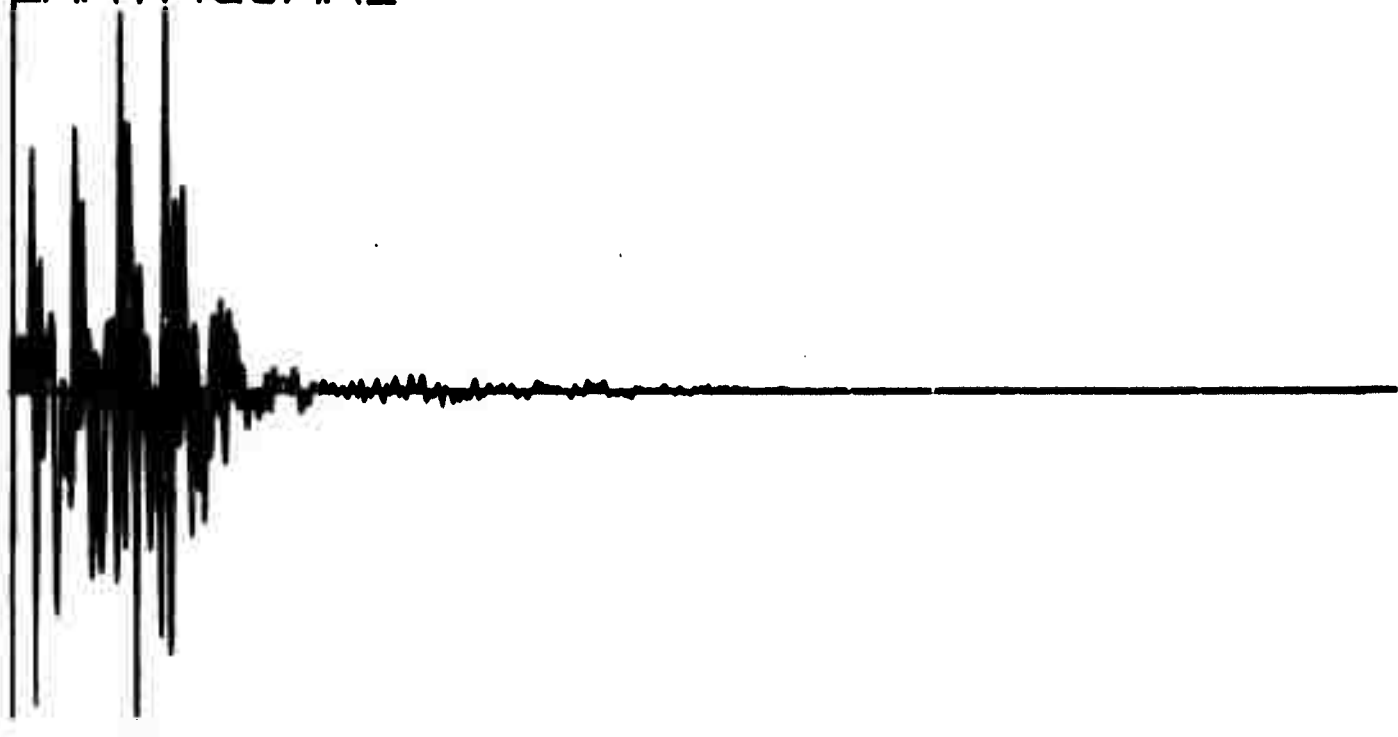
Q188

EVENT NUMBER 1096
EARTHQUAKE



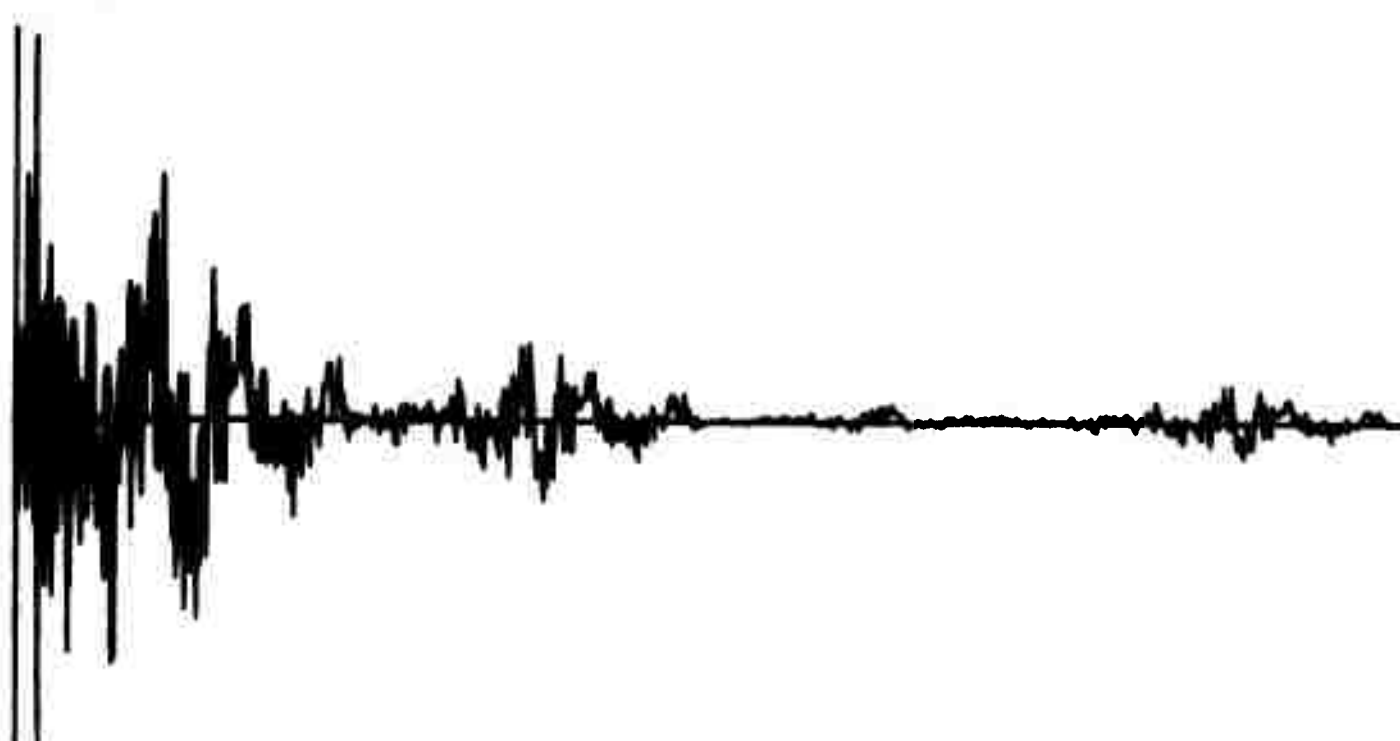
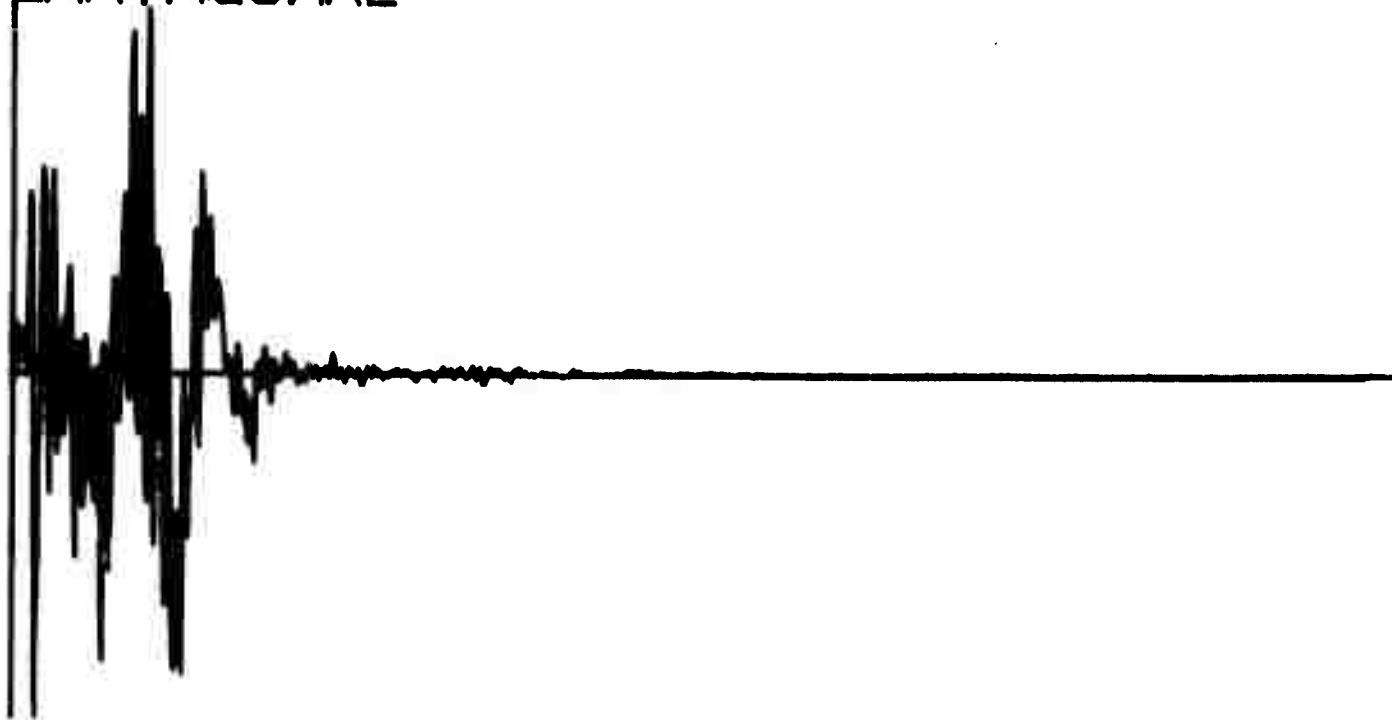
Q190

EVENT NUMBER 1093
EARTHQUAKE



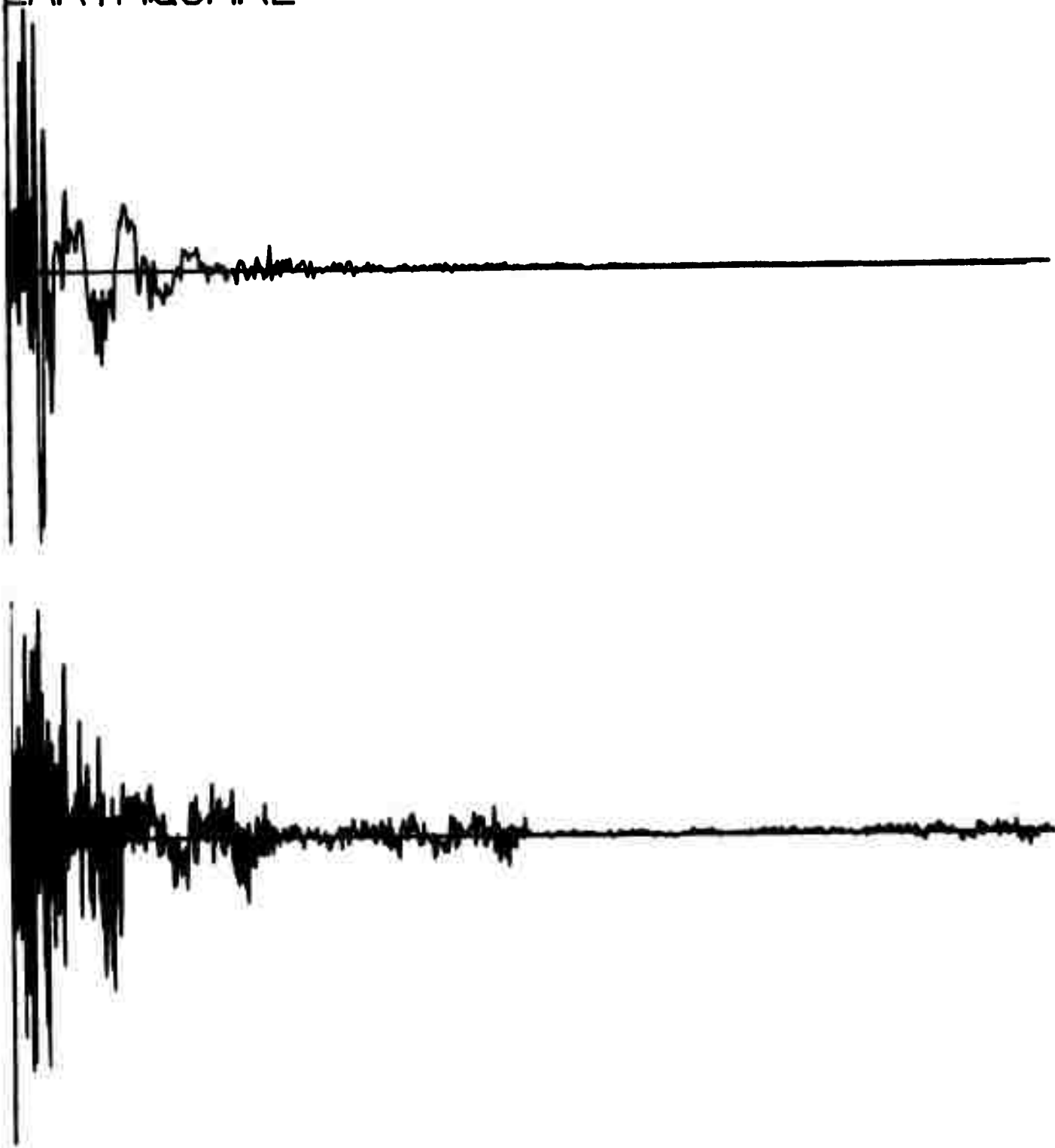
Q192

VENT NUMBER 1092
EARTHQUAKE



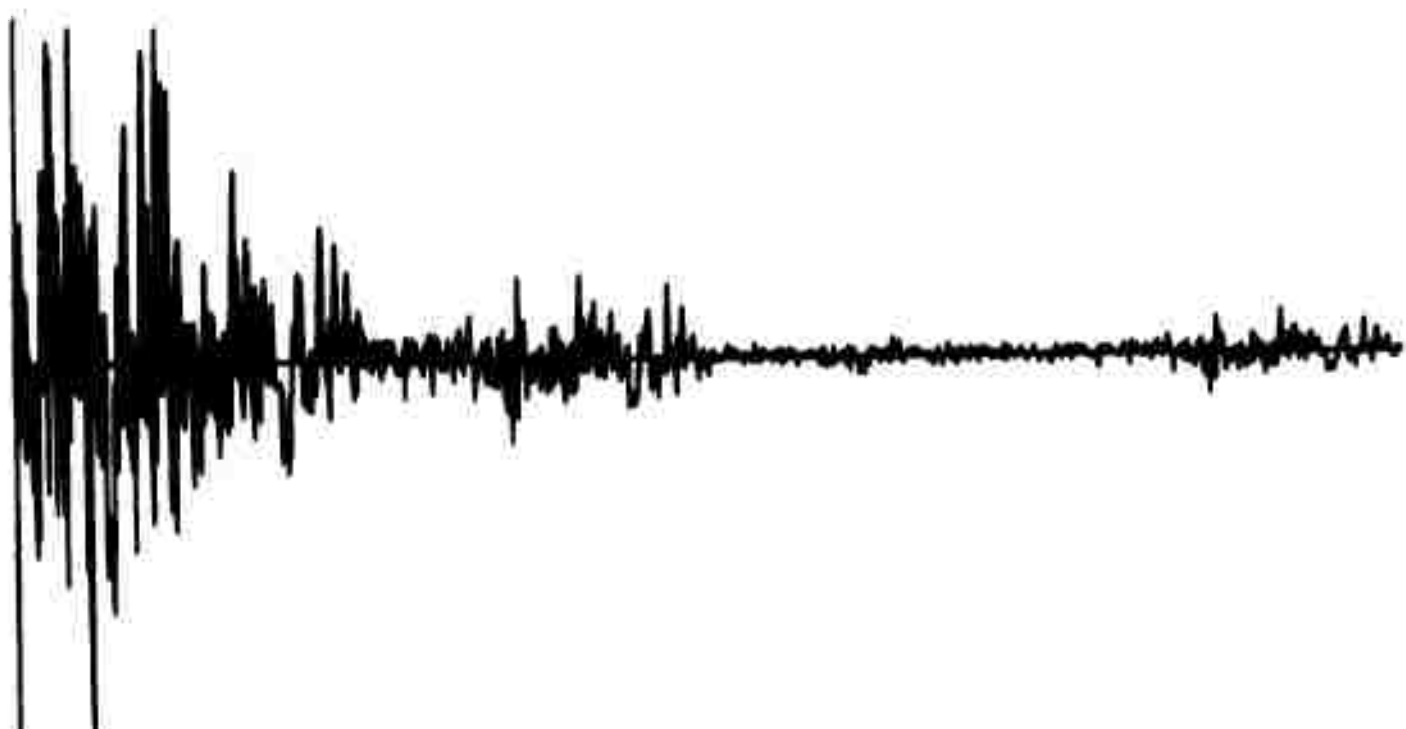
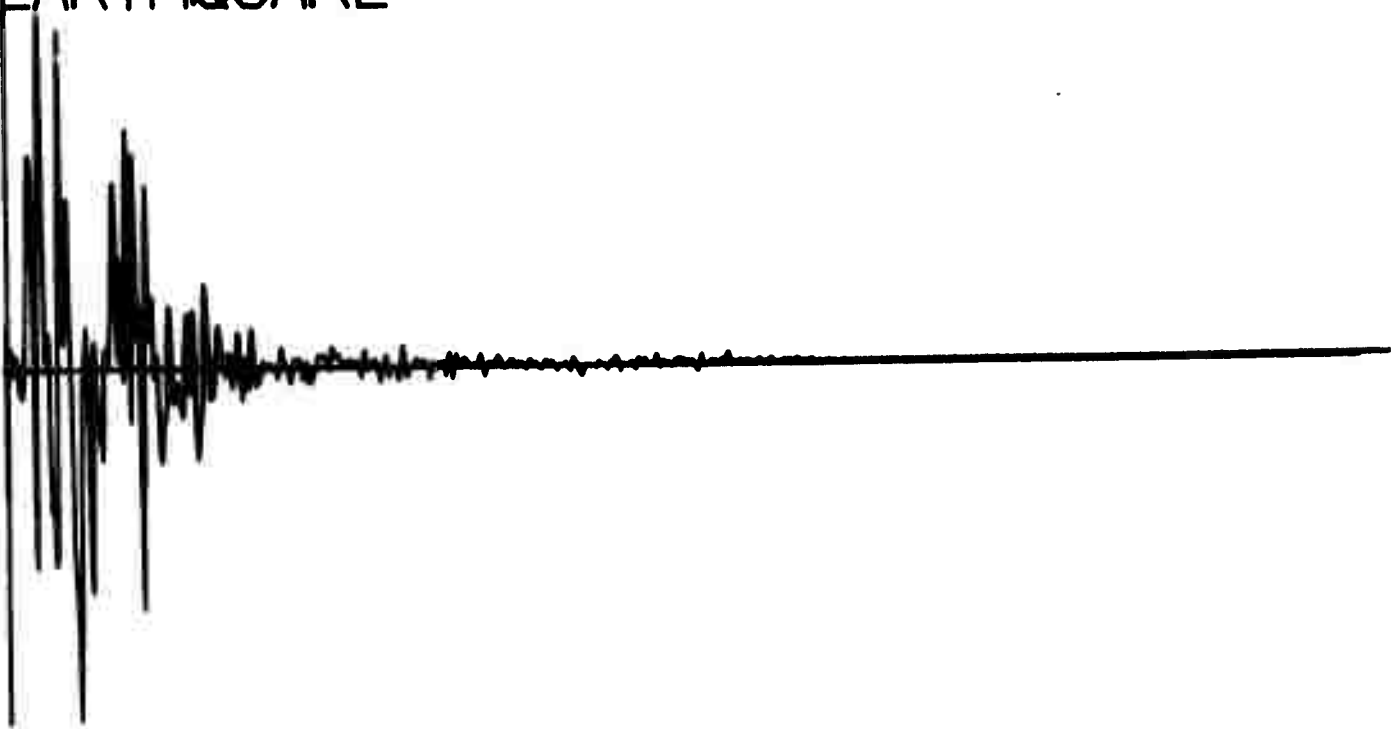
Q194

VENT NUMBER 1069
EARTHQUAKE



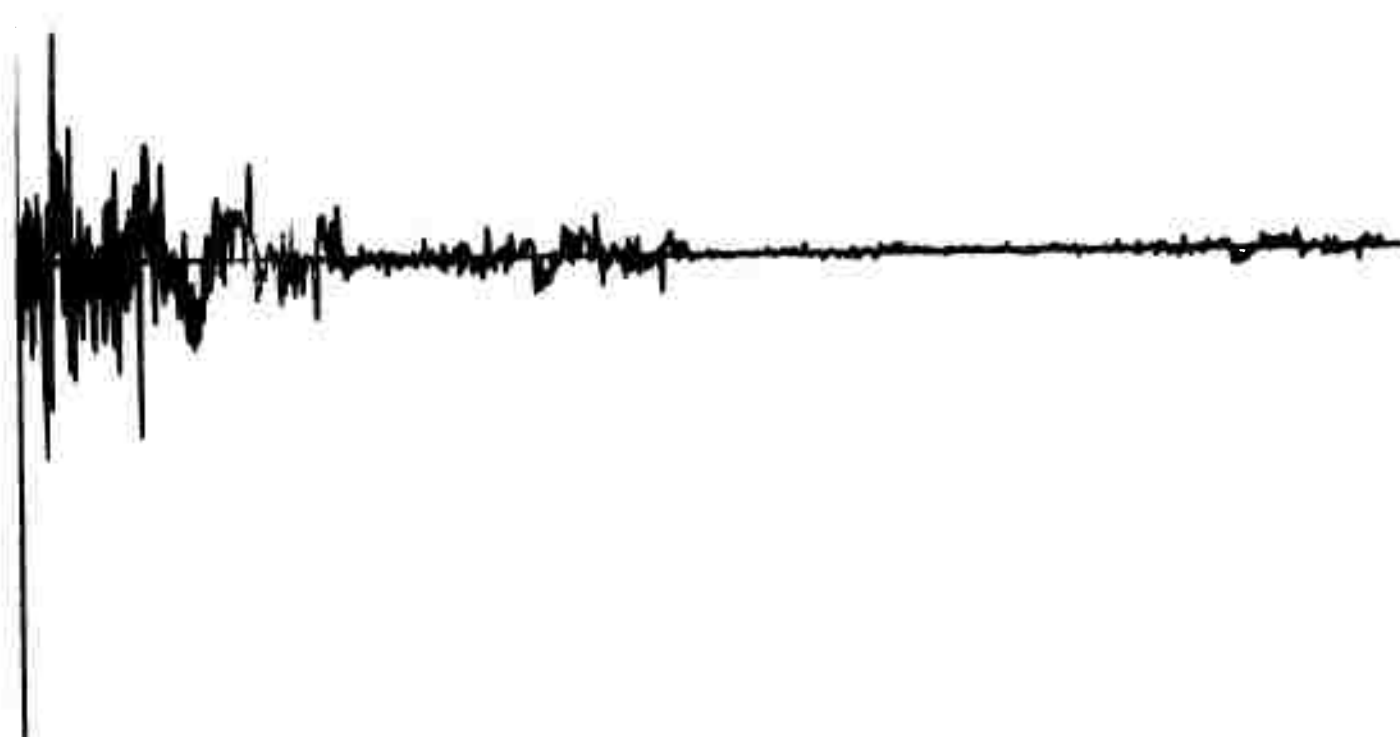
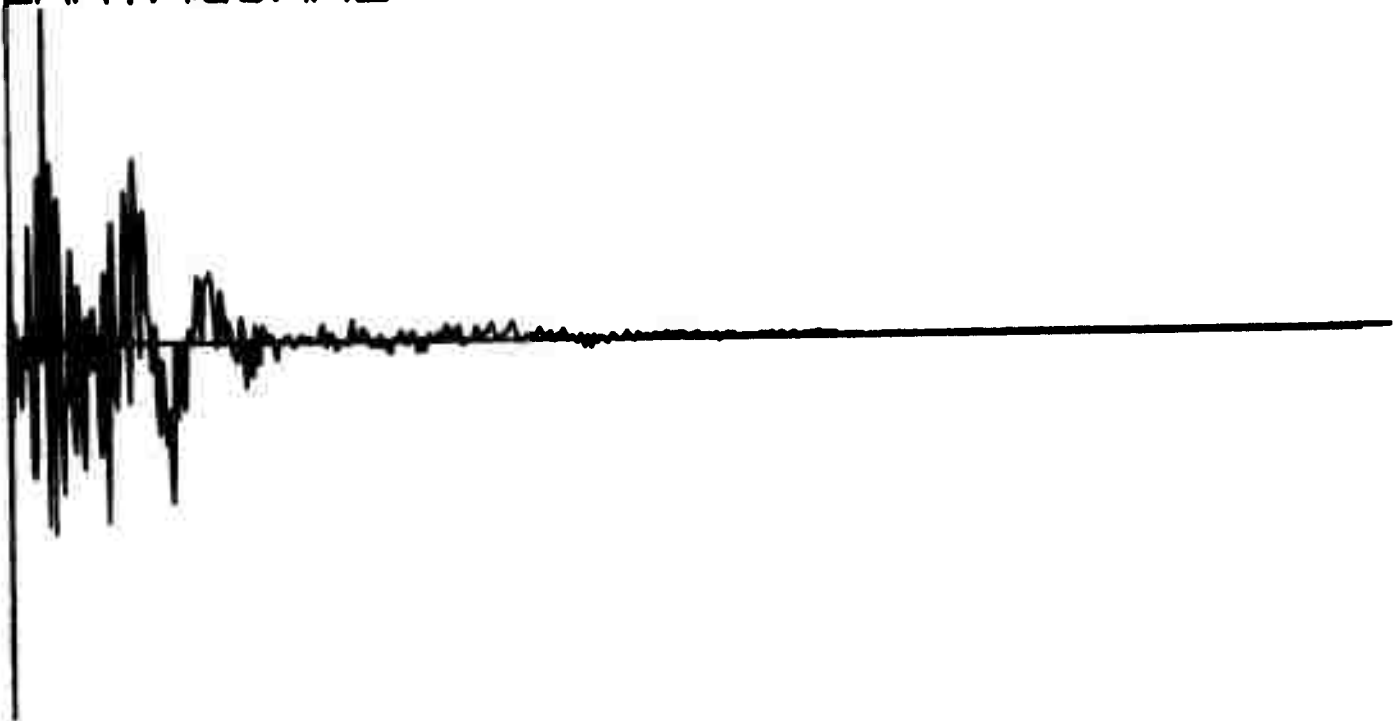
Q₁₉₆

VENT NUMBER 1051
EARTHQUAKE



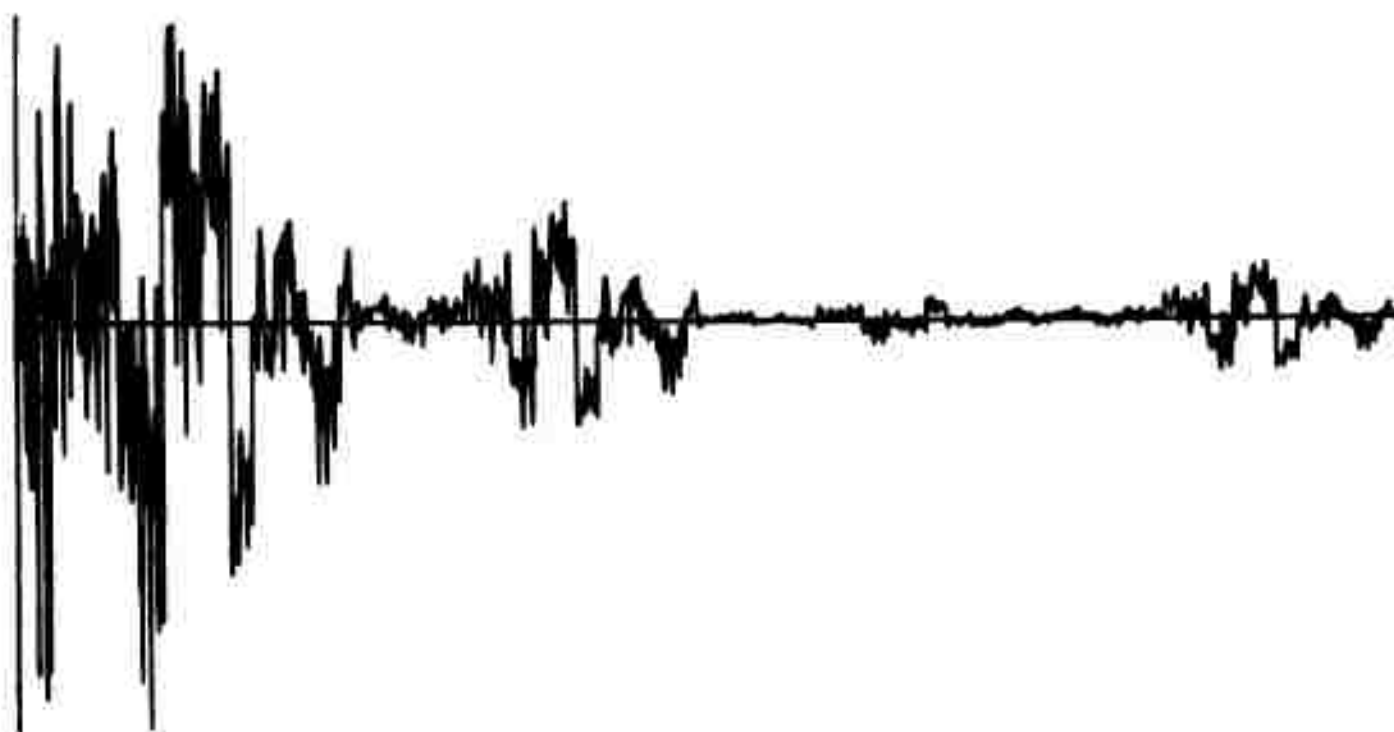
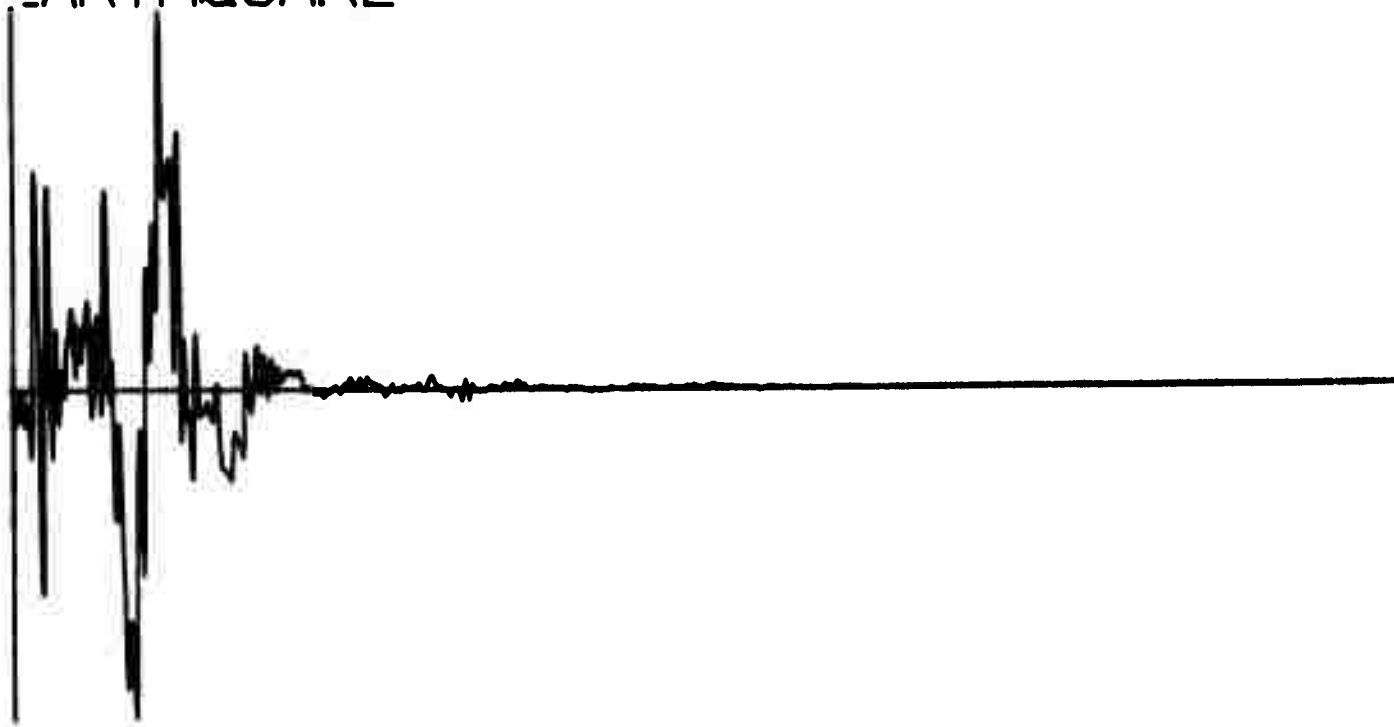
Q198

VENT NUMBER 1045
EARTHQUAKE



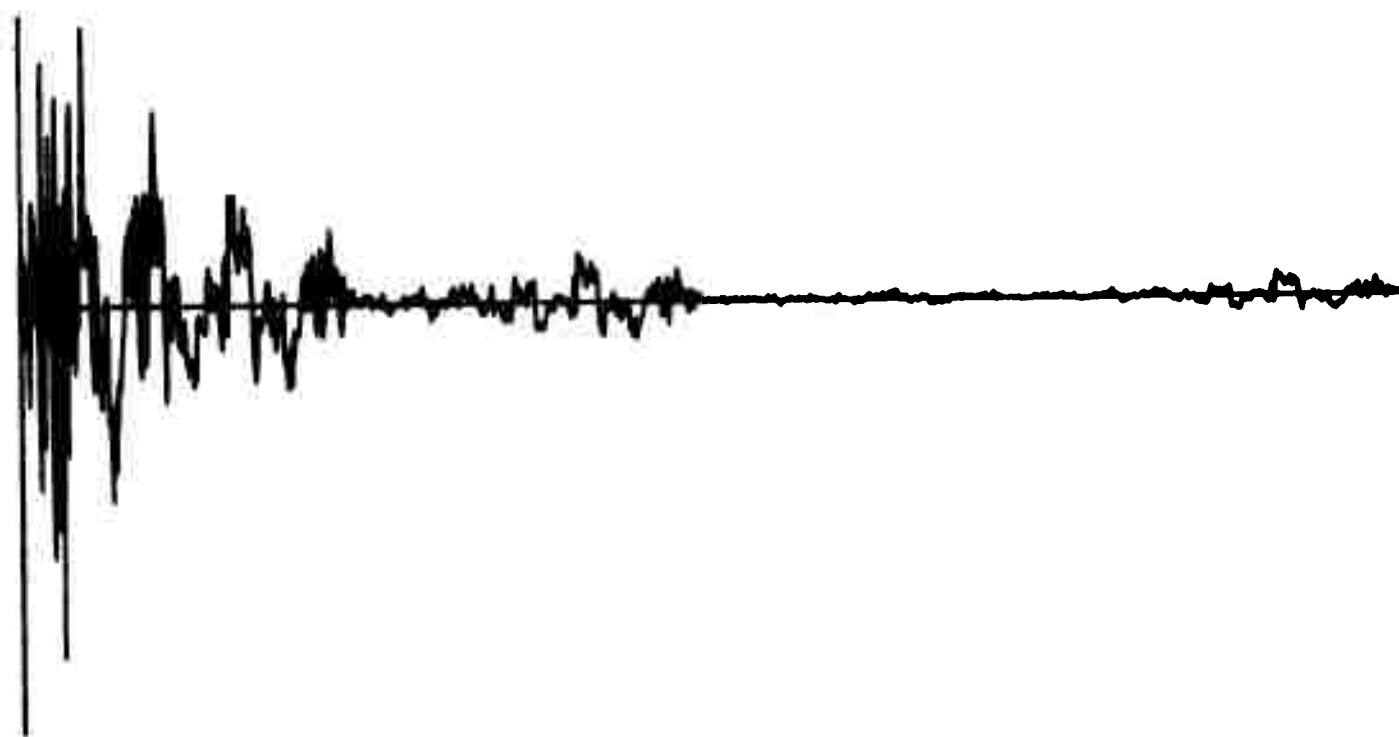
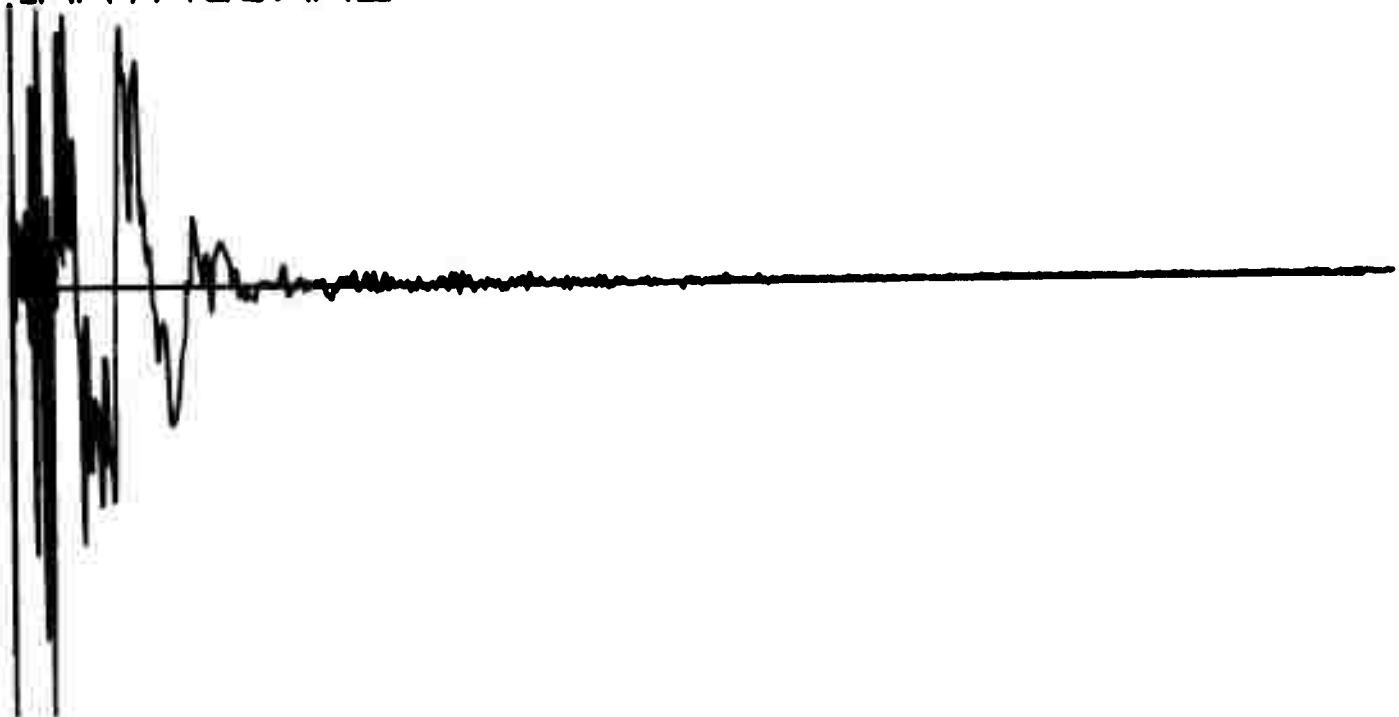
Q200

VENT NUMBER 1189
EARTHQUAKE



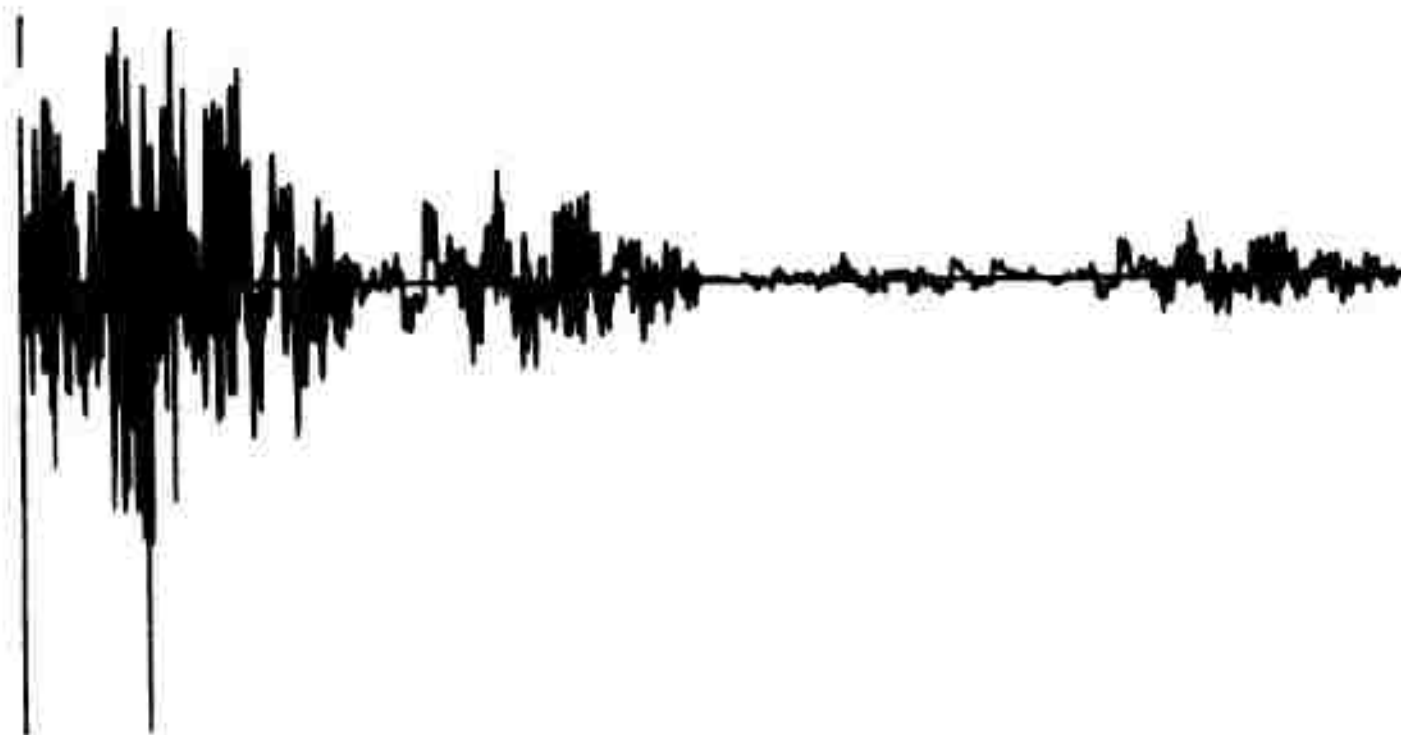
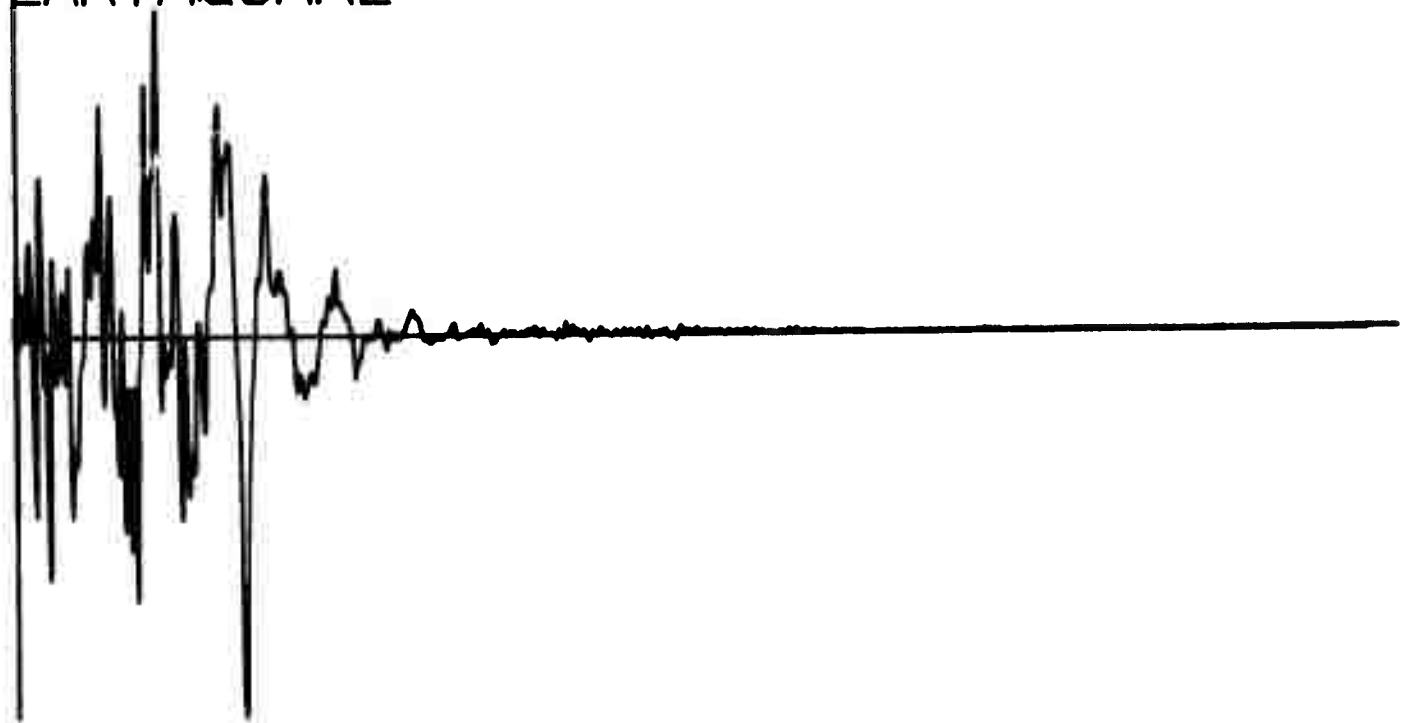
Q202

VENT NUMBER 1197
EARTHQUAKE



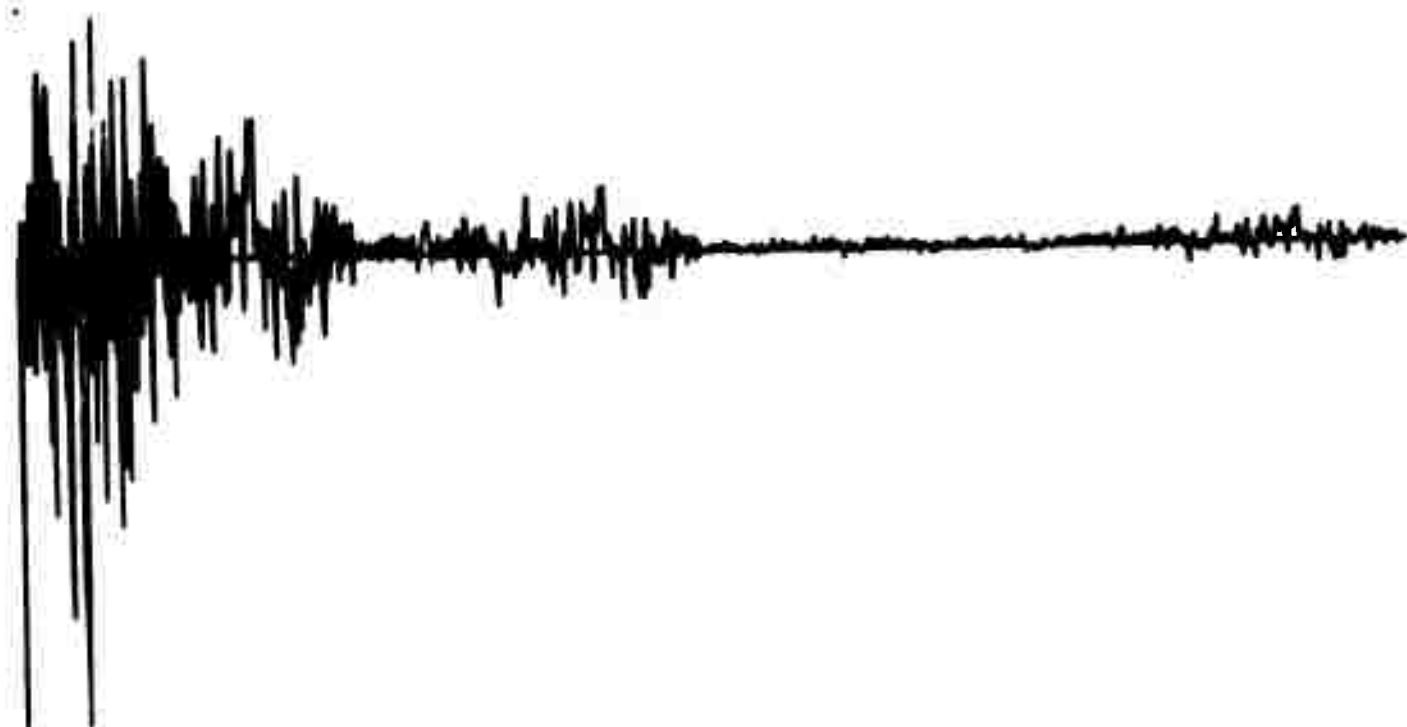
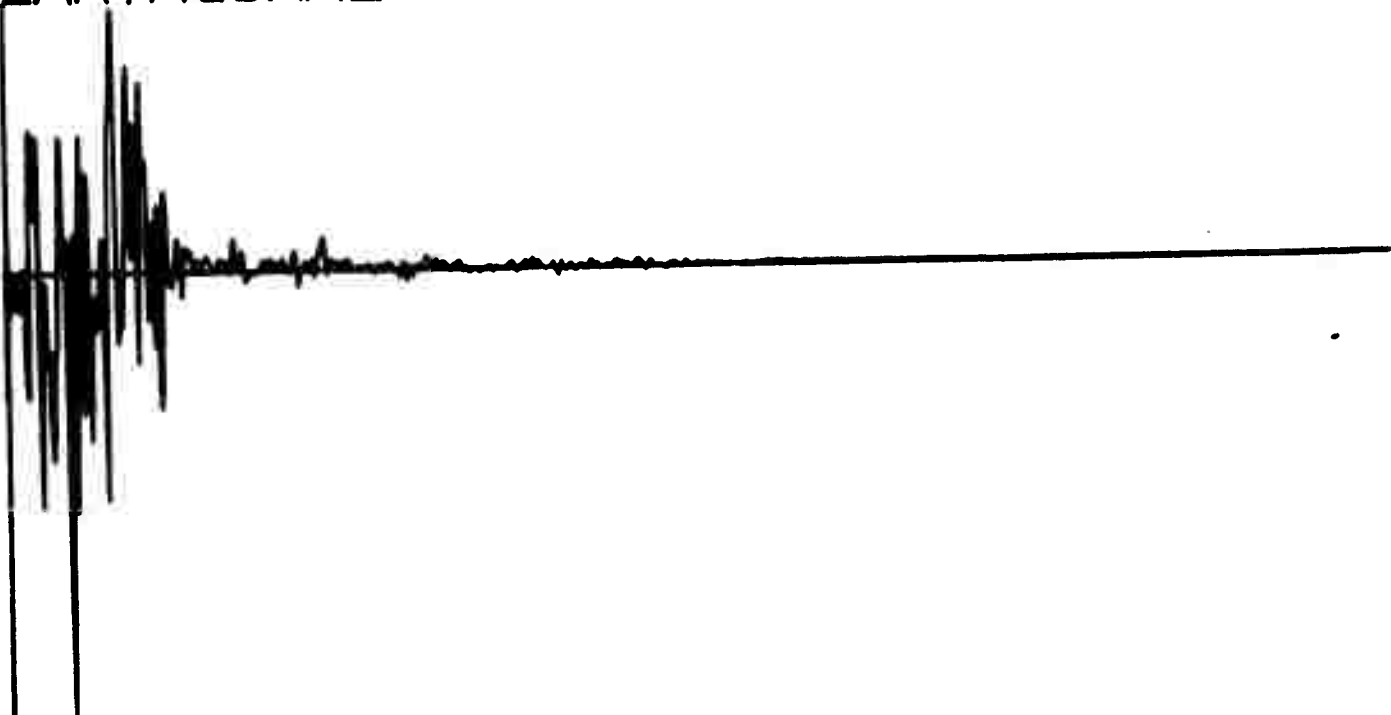
Q204

VENT NUMBER 1211
EARTHQUAKE



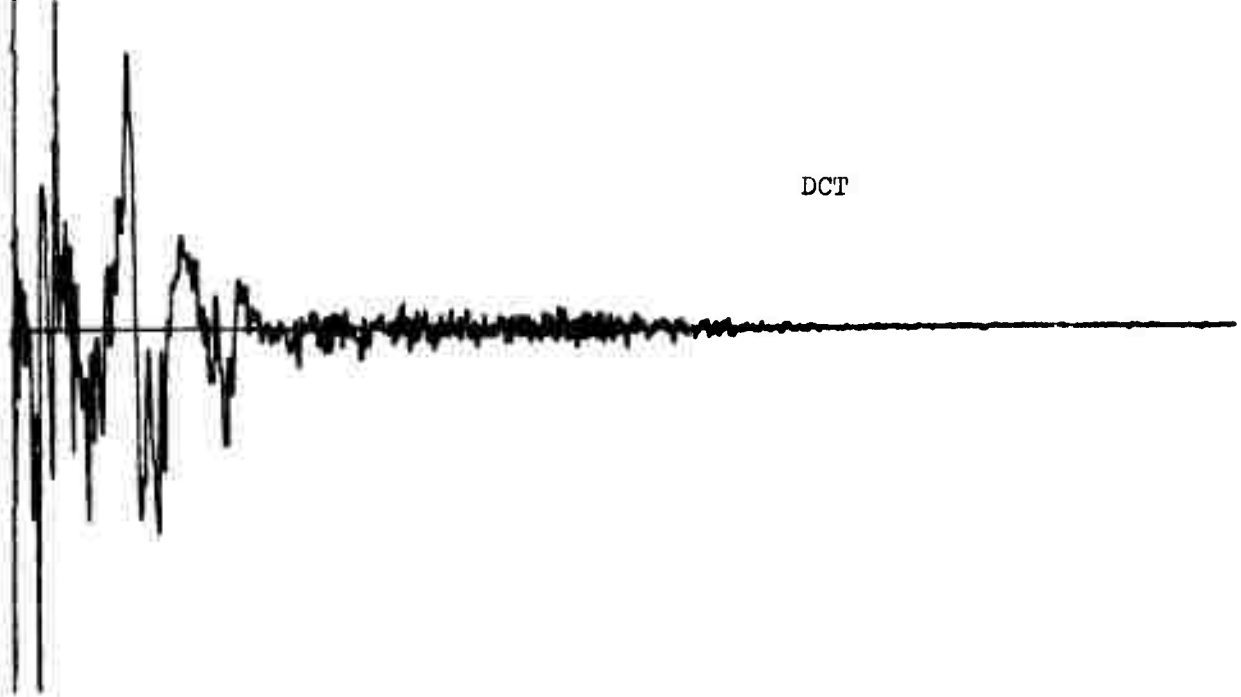
Q206

EVENT NUMBER 1212
EARTHQUAKE

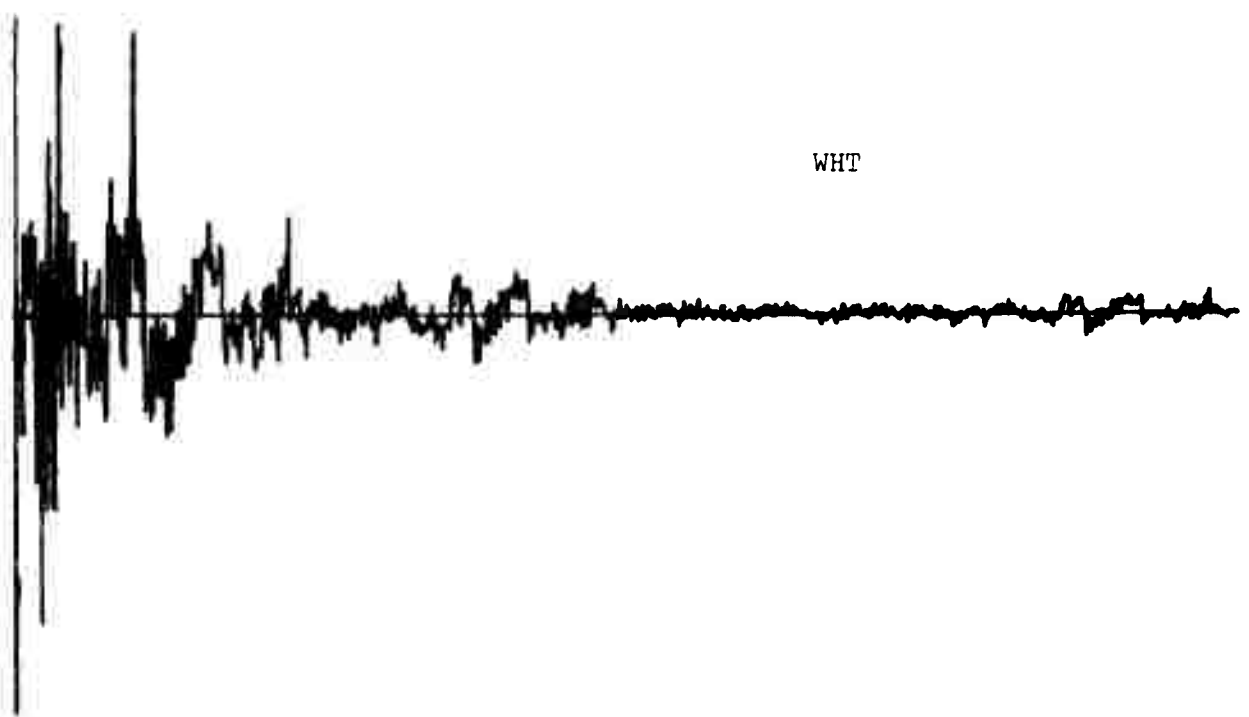


Q208

EVENT NUMBER 1213
EARTHQUAKE



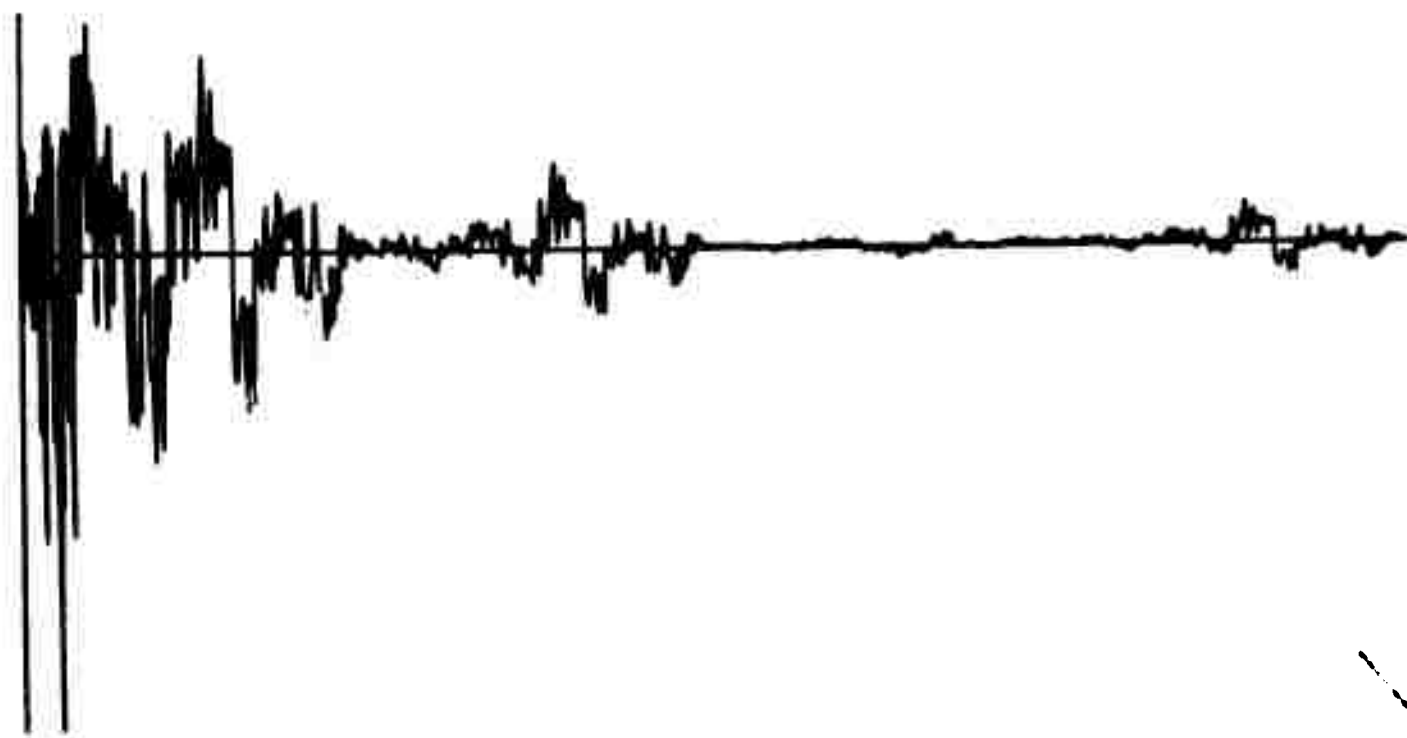
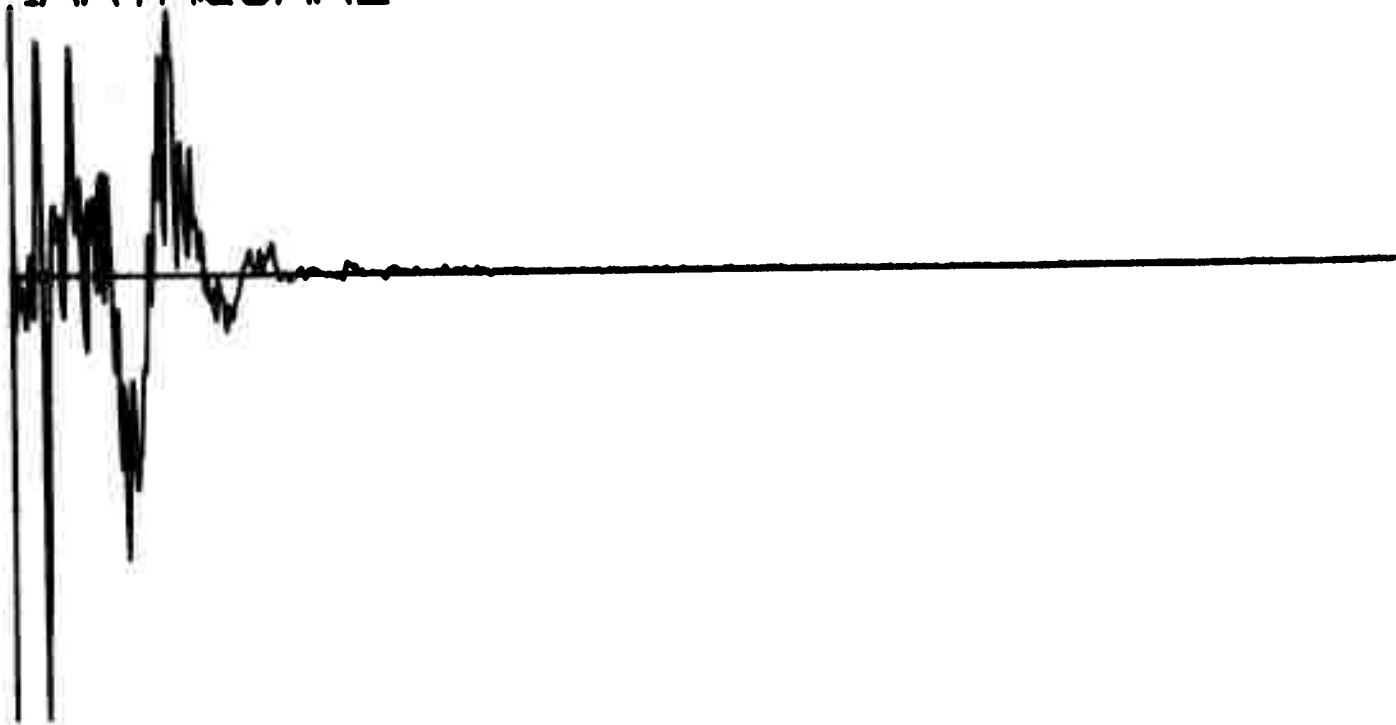
DCT



WHT

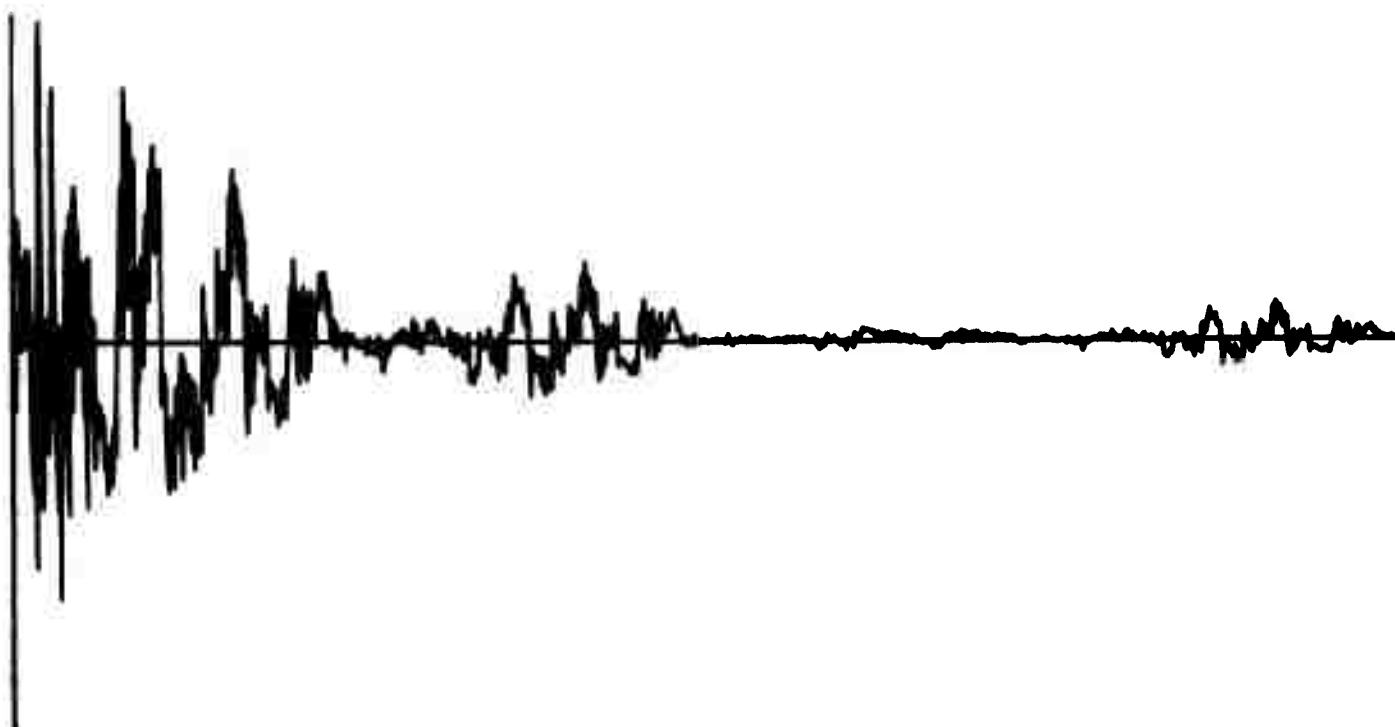
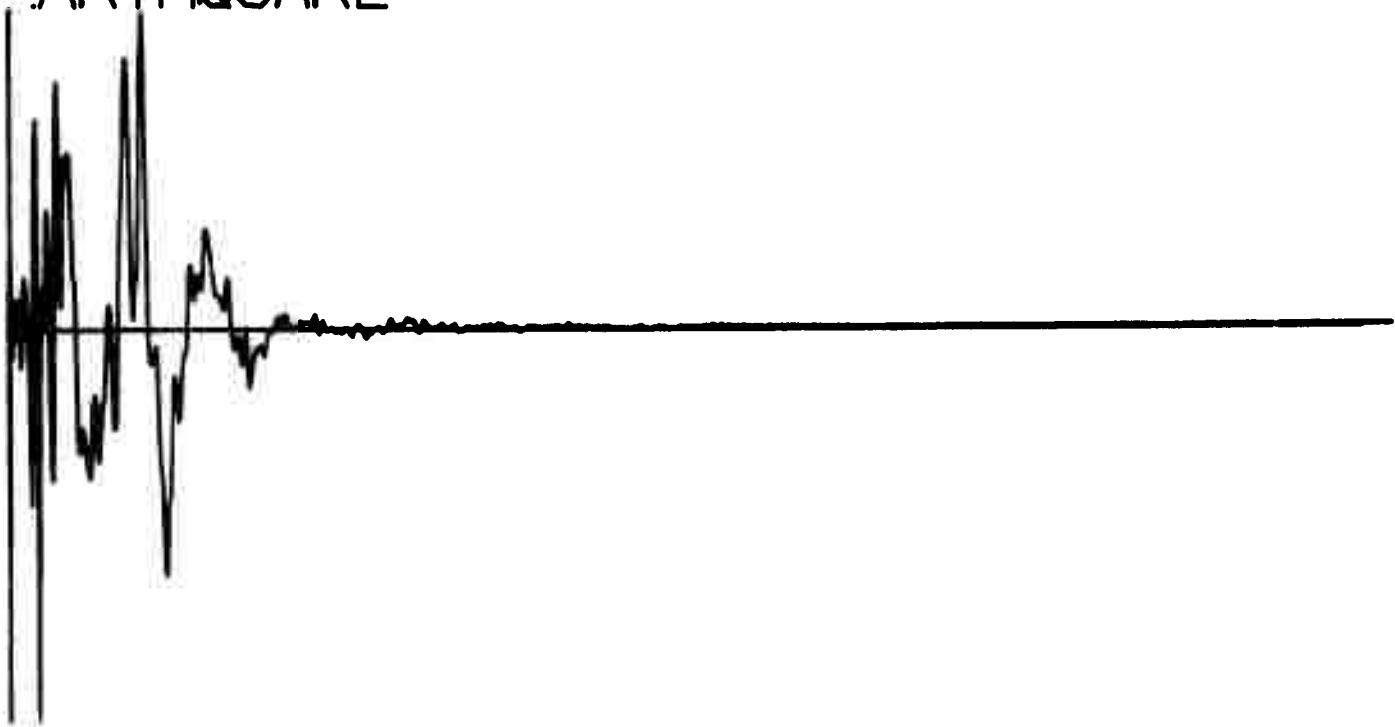
Q210

VENT NUMBER 1228
EARTHQUAKE



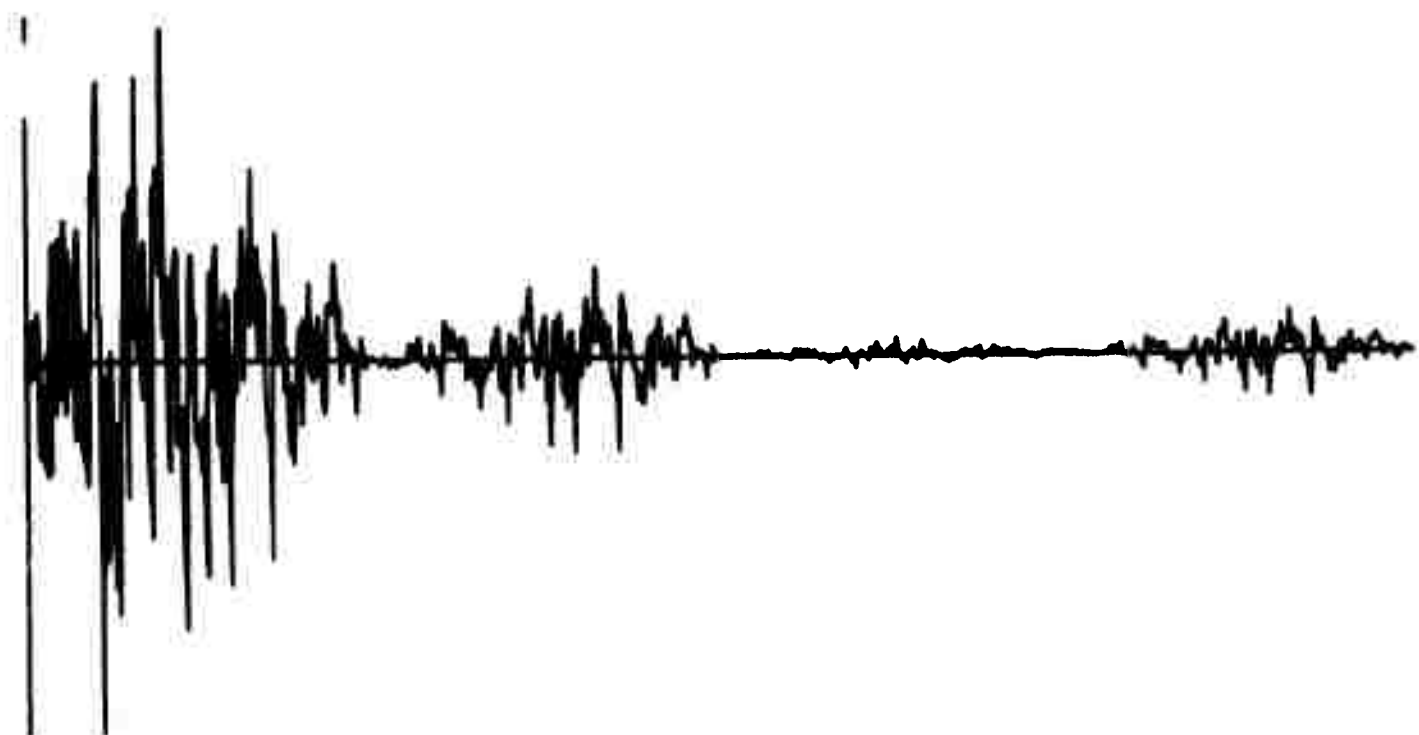
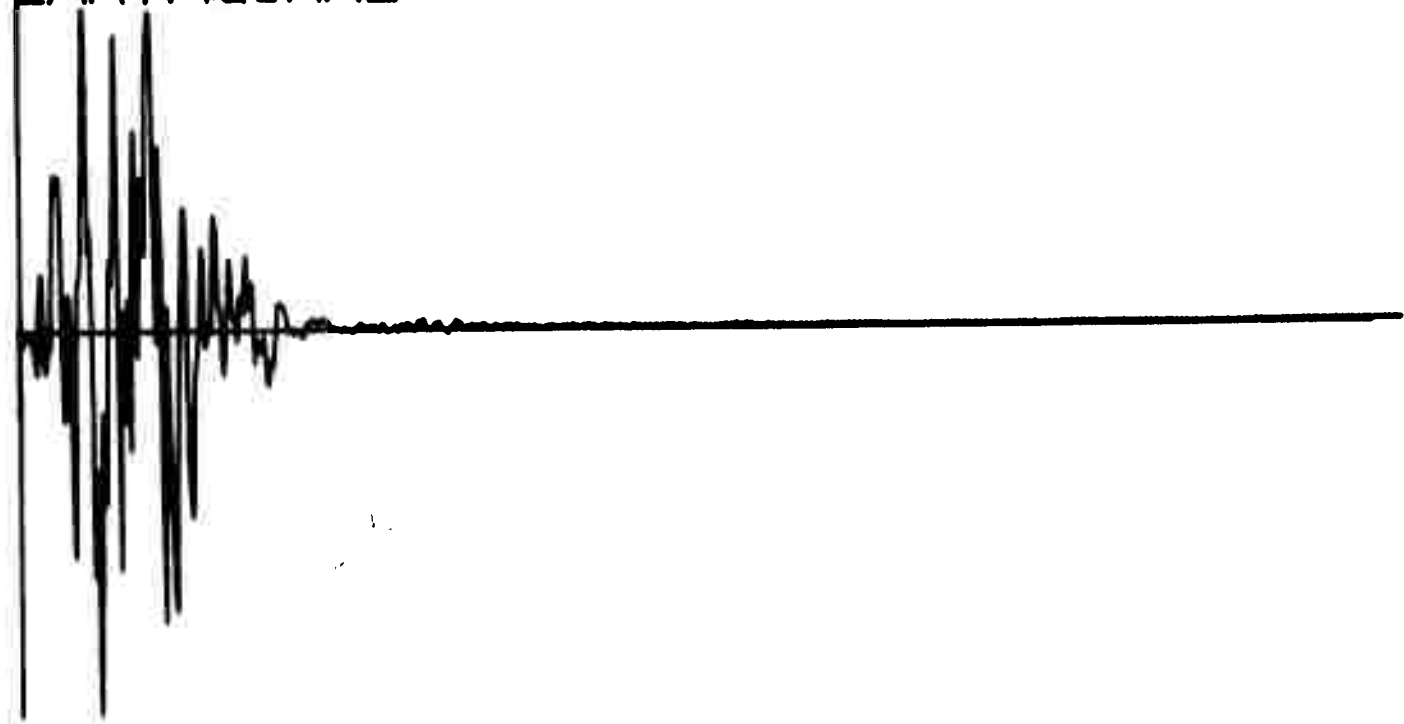
Q212

VENT NUMBER 1229
EARTHQUAKE



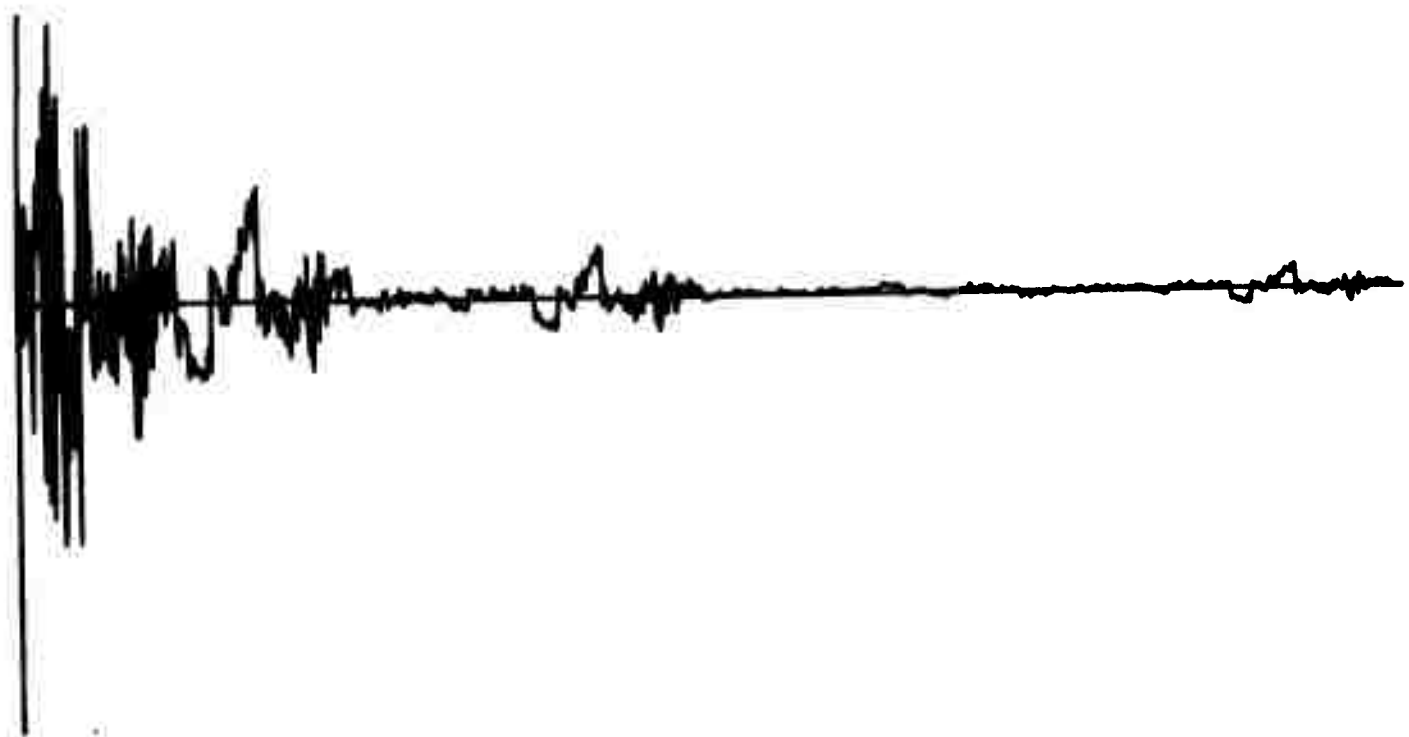
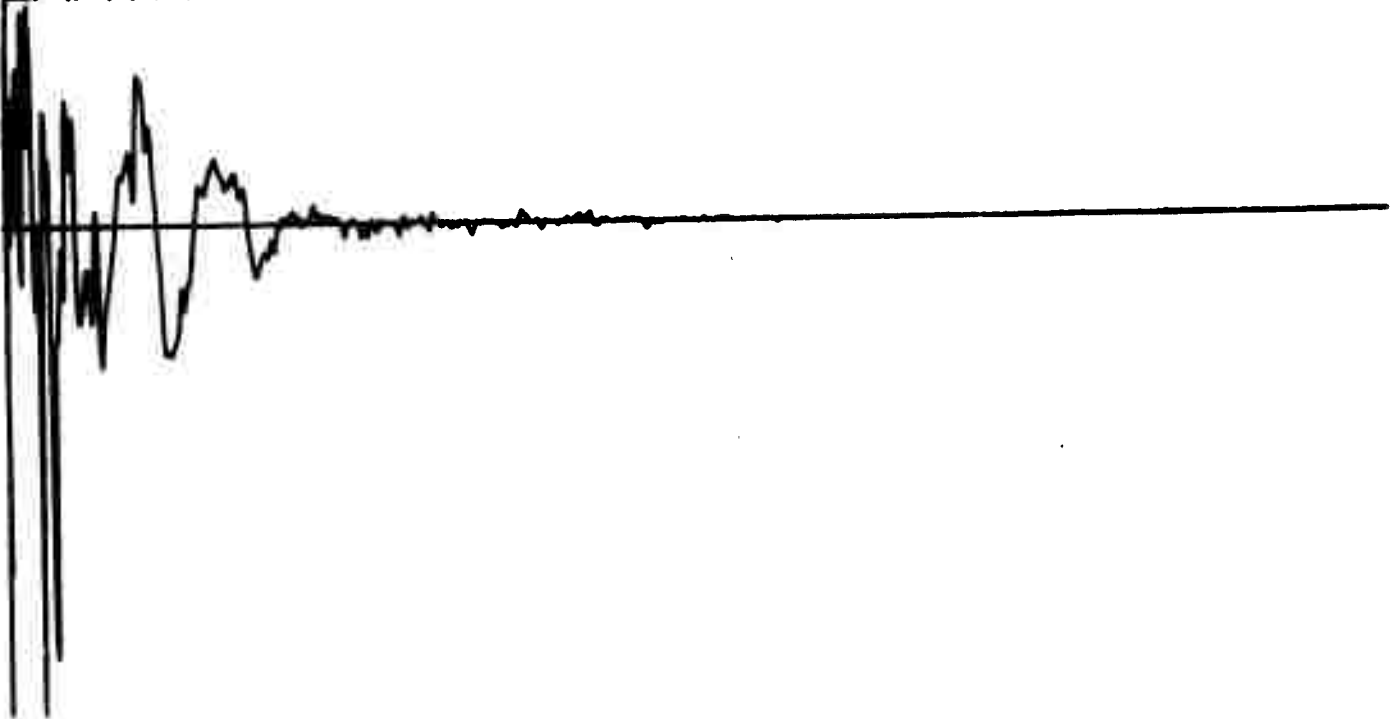
Q214

VENT NUMBER 1230
EARTHQUAKE



Q216

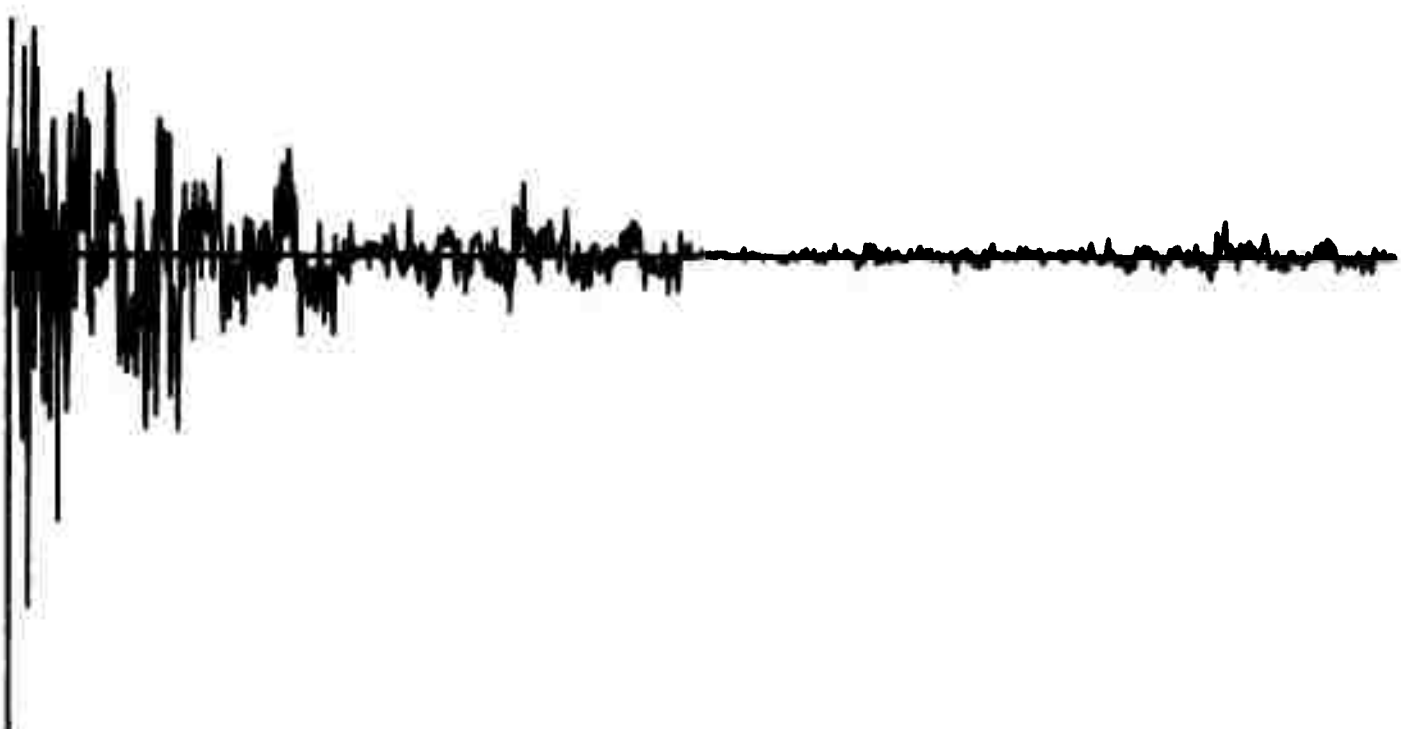
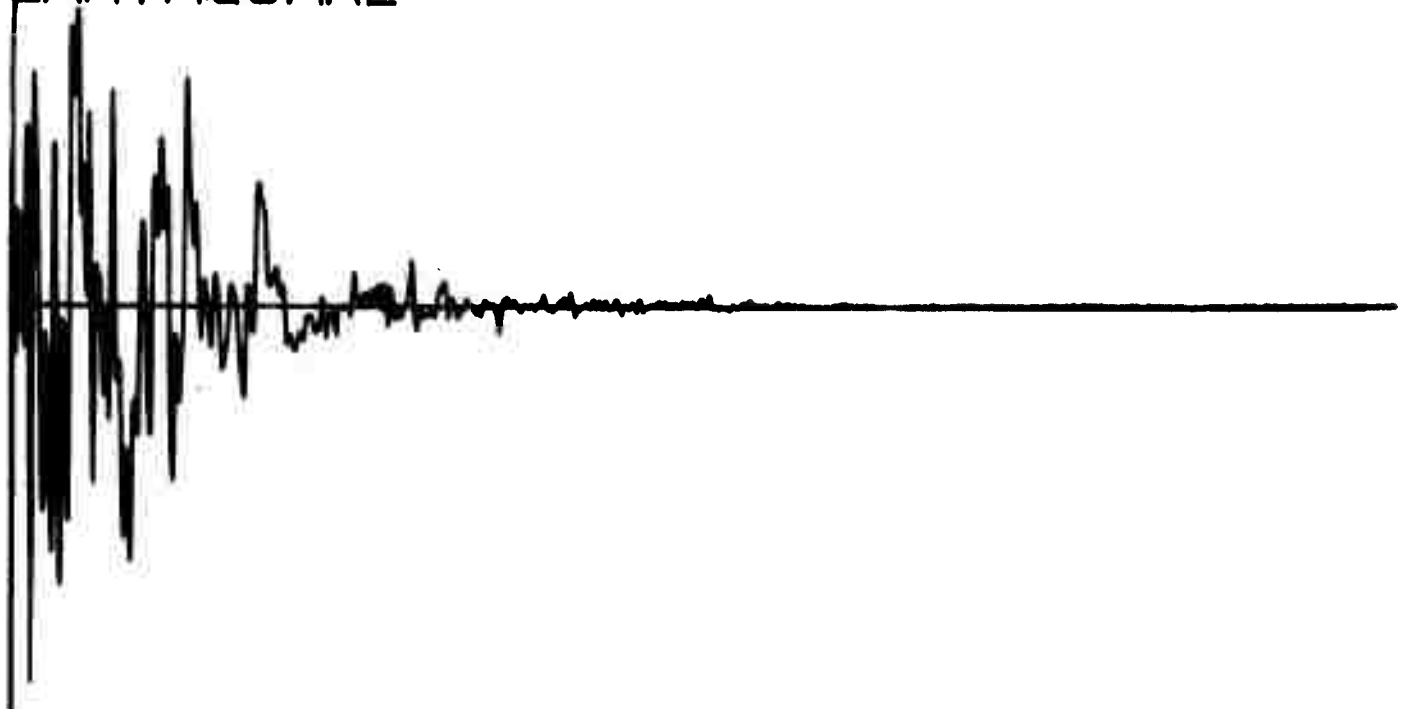
EVENT NUMBER 1231
EARTHQUAKE



Q218

EVENT NUMBER 1232

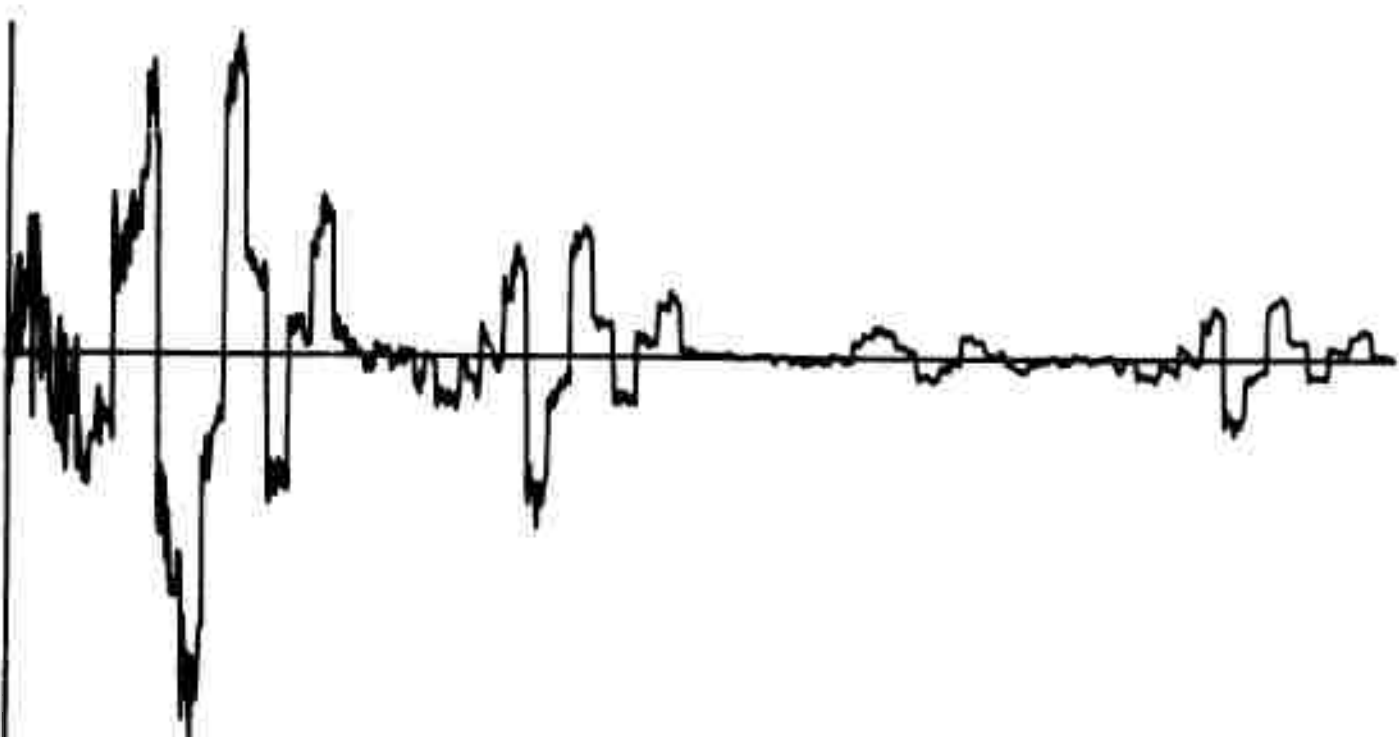
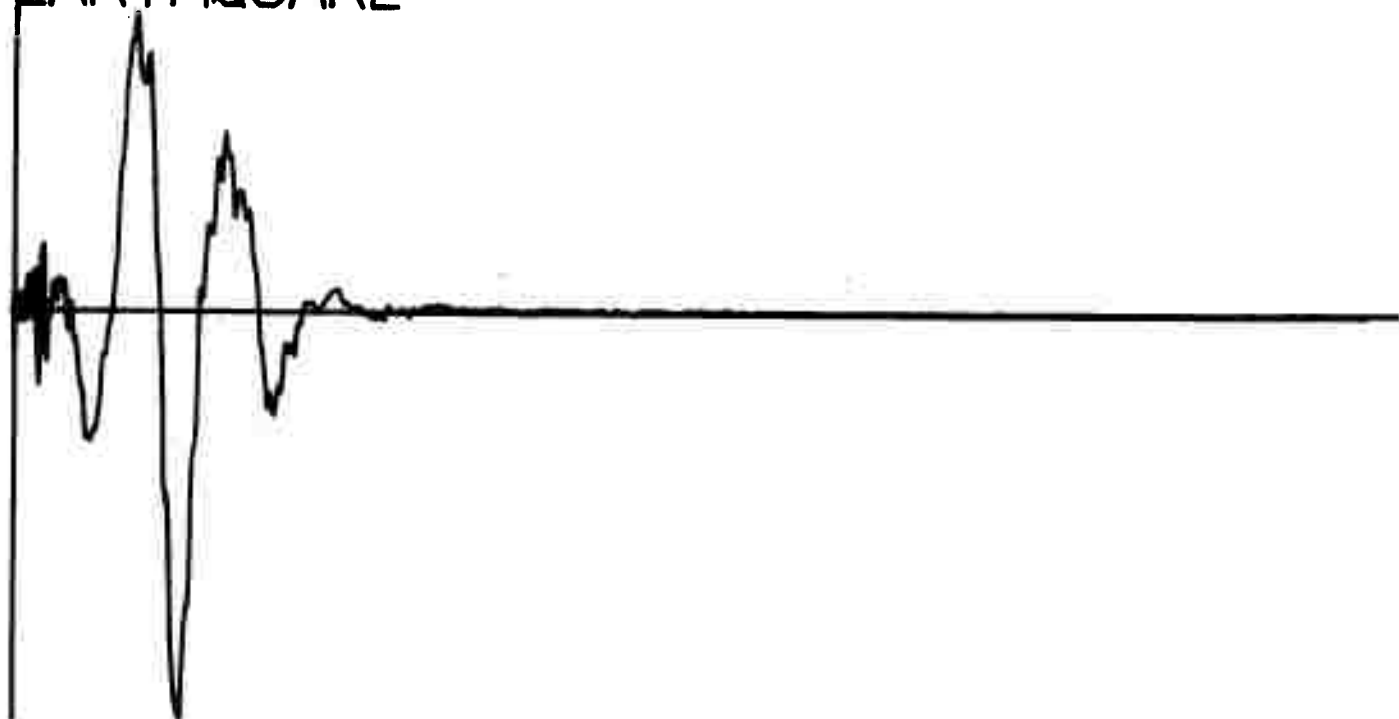
EARTHQUAKE



Q220

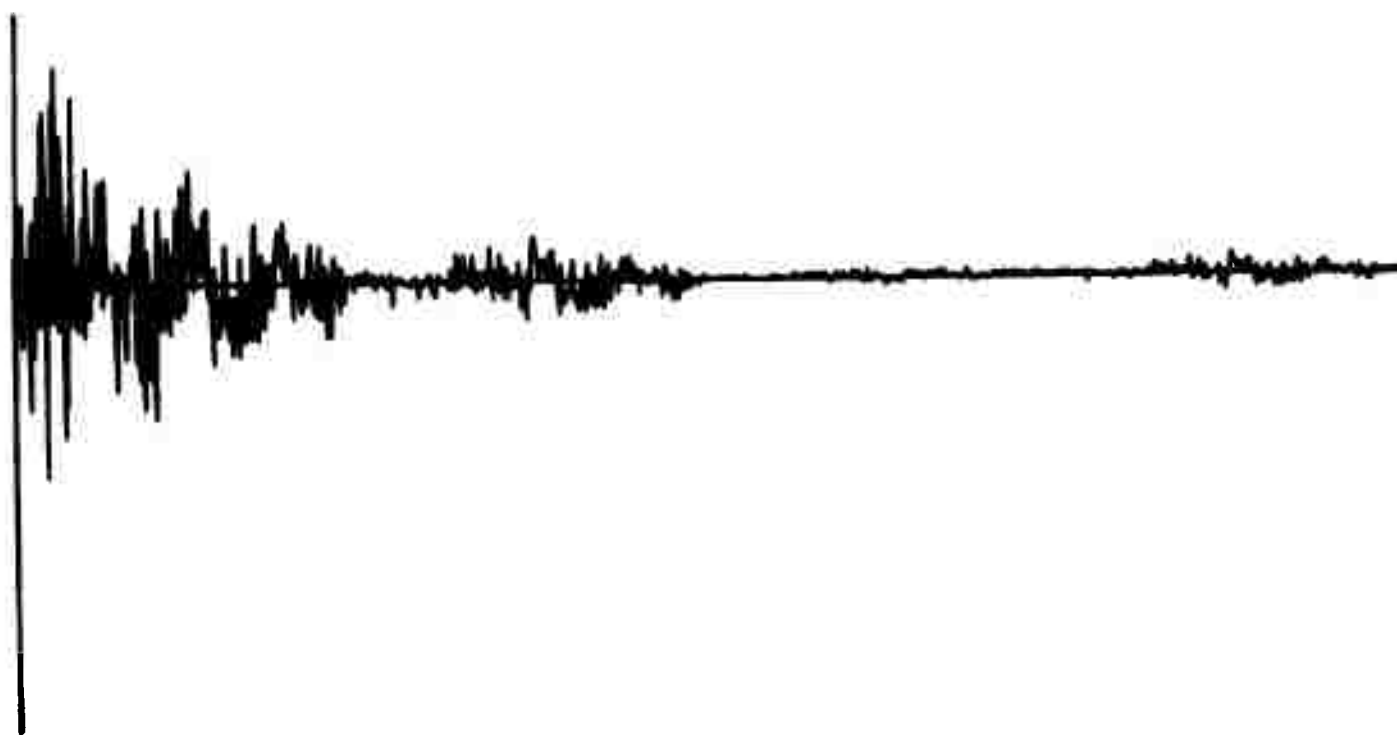
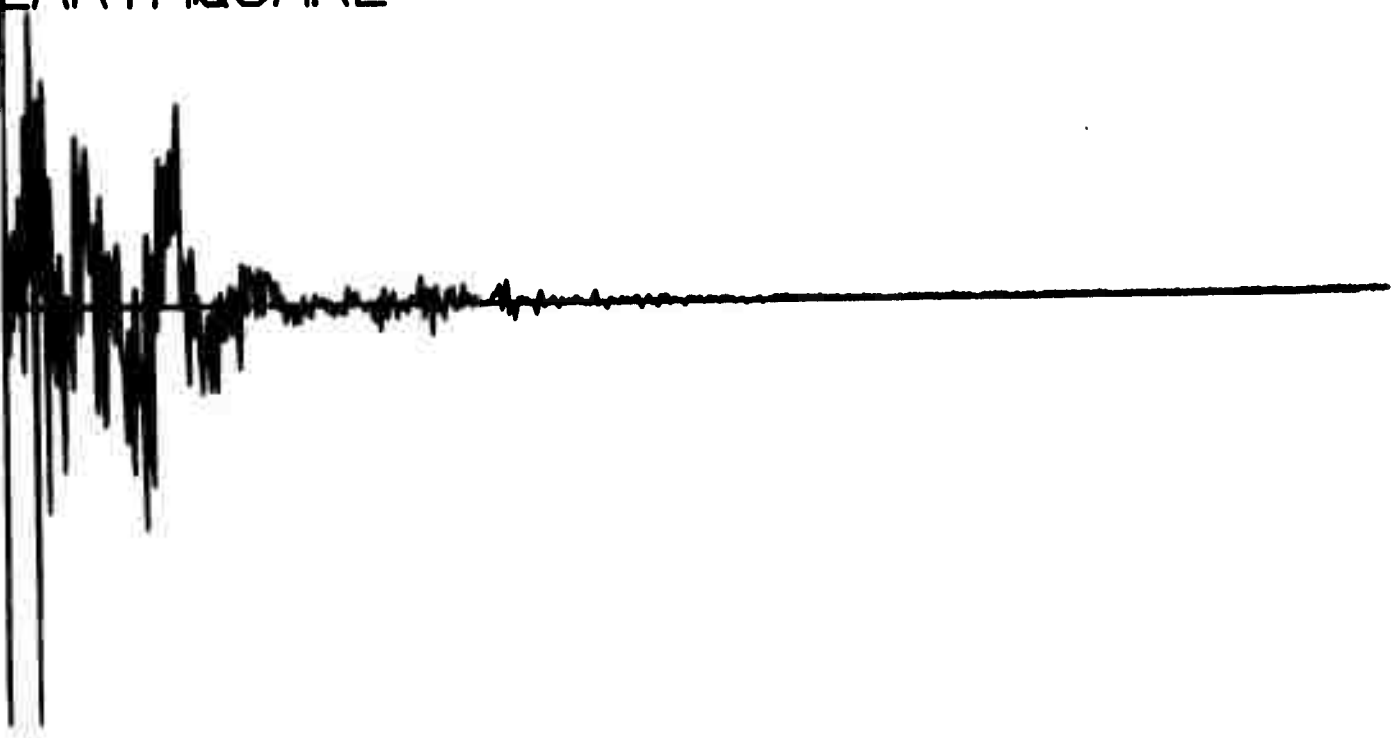
EVENT NUMBER 1238

EARTHQUAKE



Q222

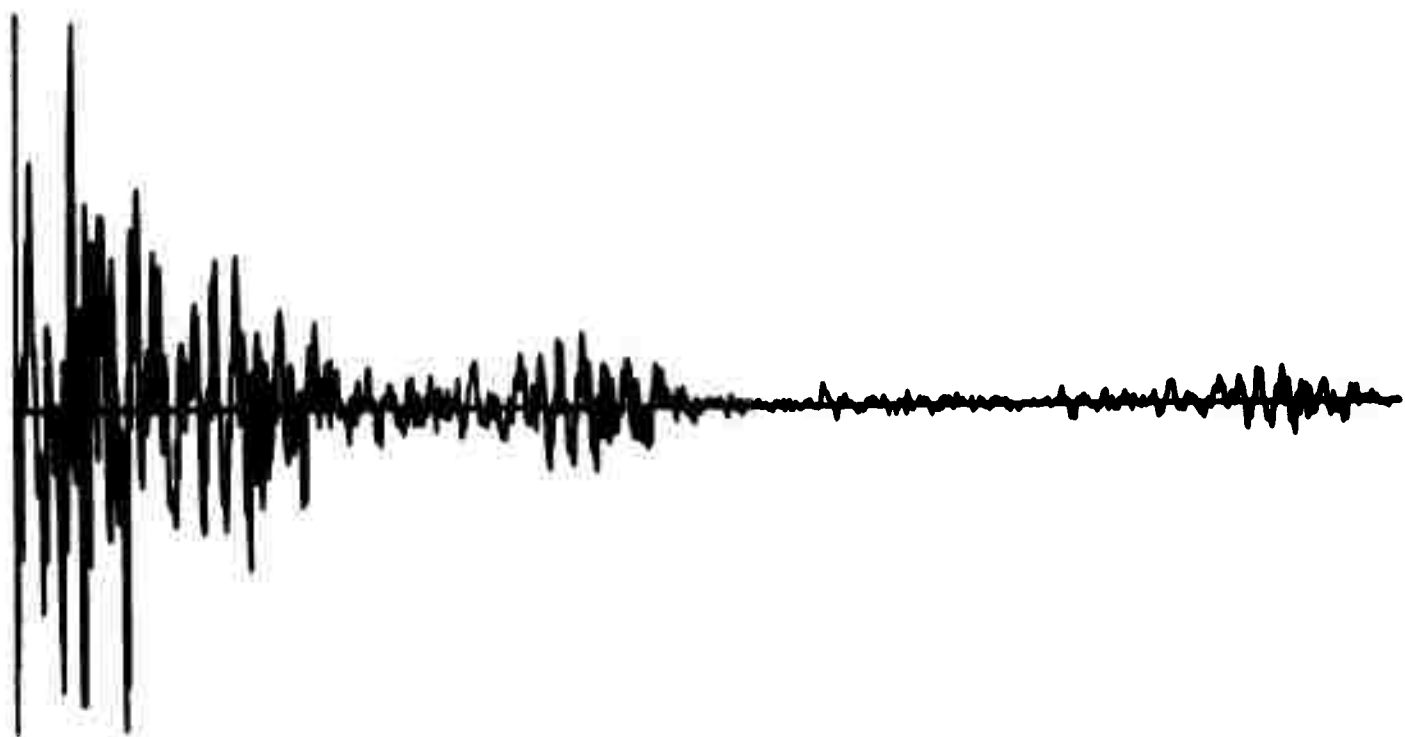
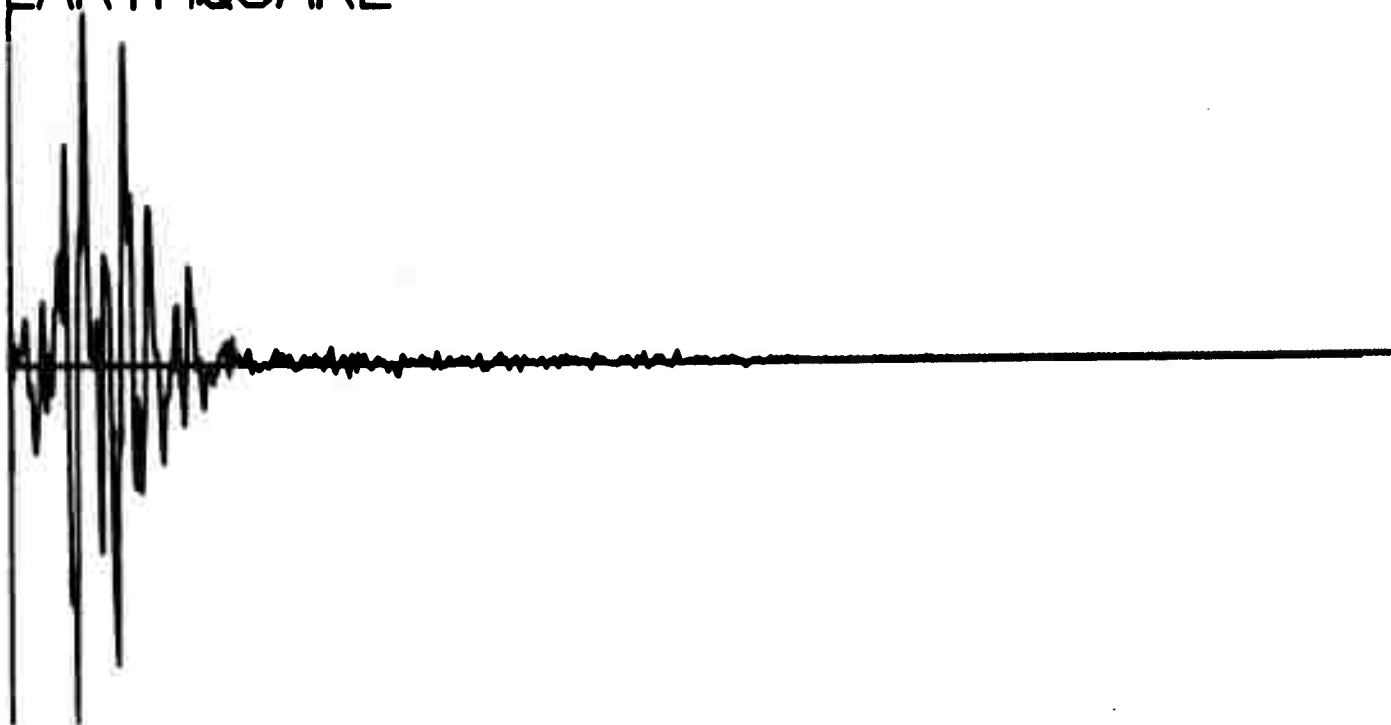
EVENT NUMBER 1239
EARTHQUAKE



Q224

EVENT NUMBER 1241

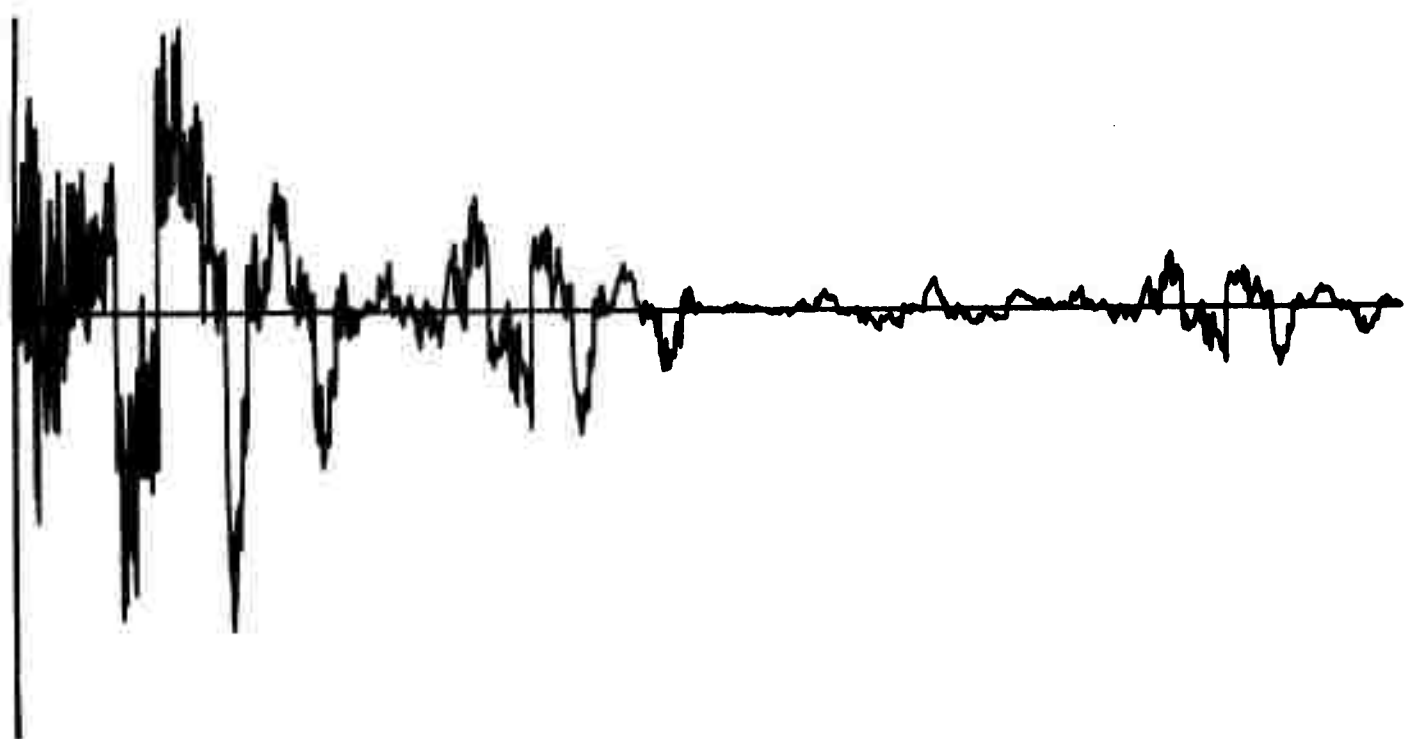
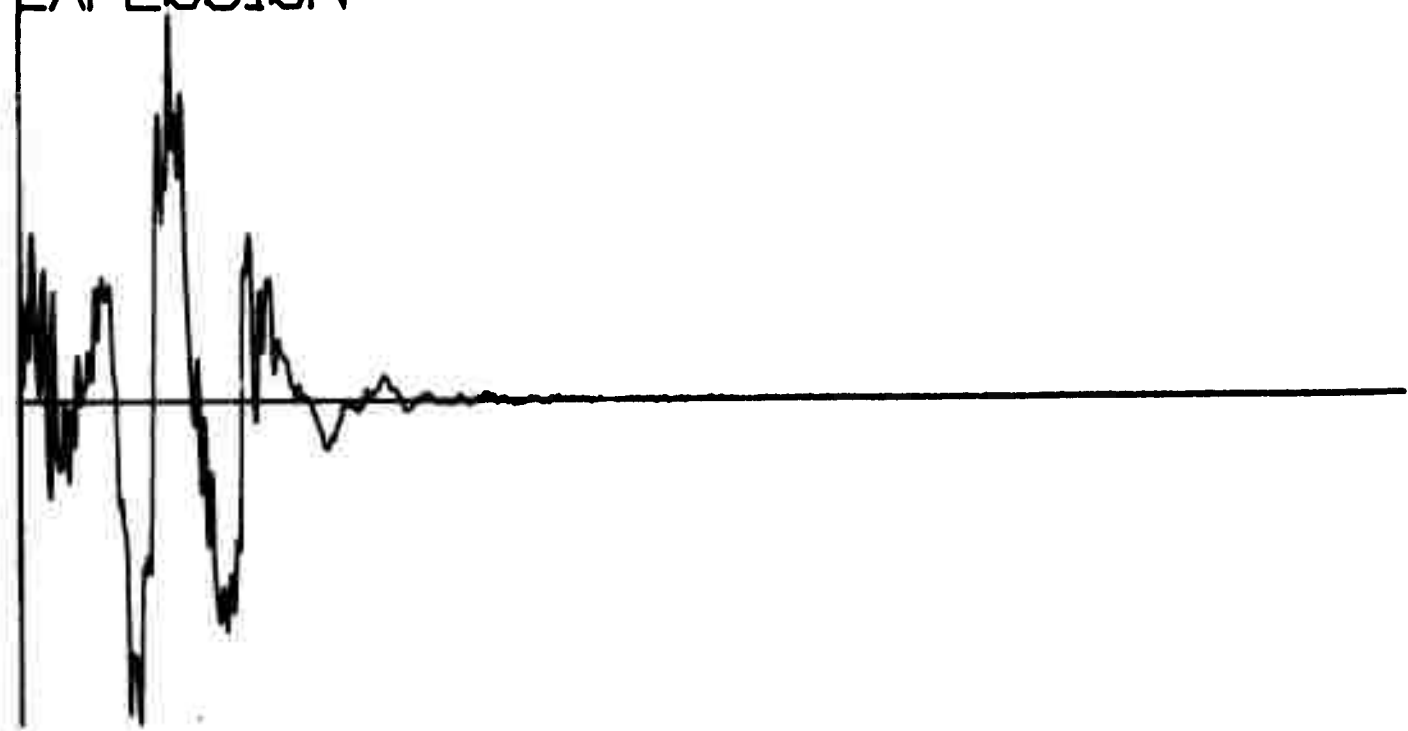
EARTHQUAKE



EVENT NUMBER 1533

EXPLOSION

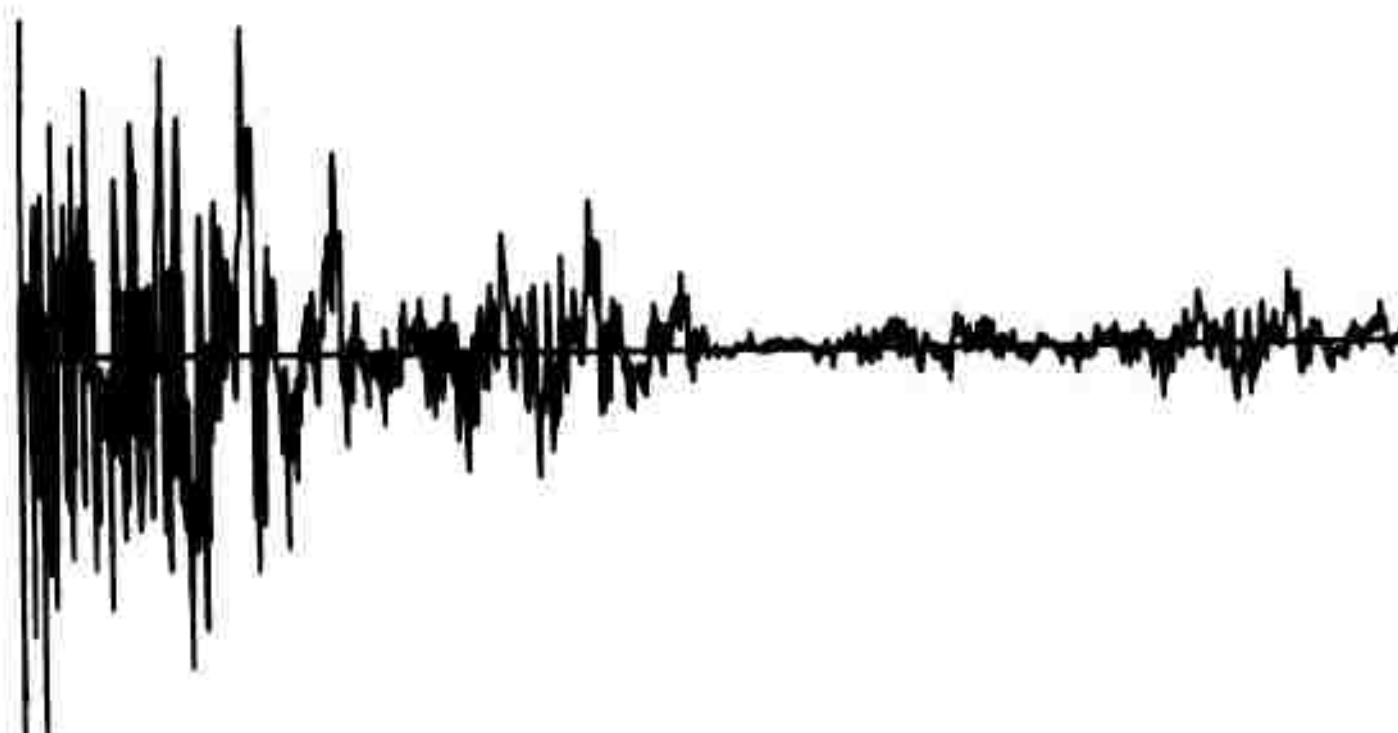
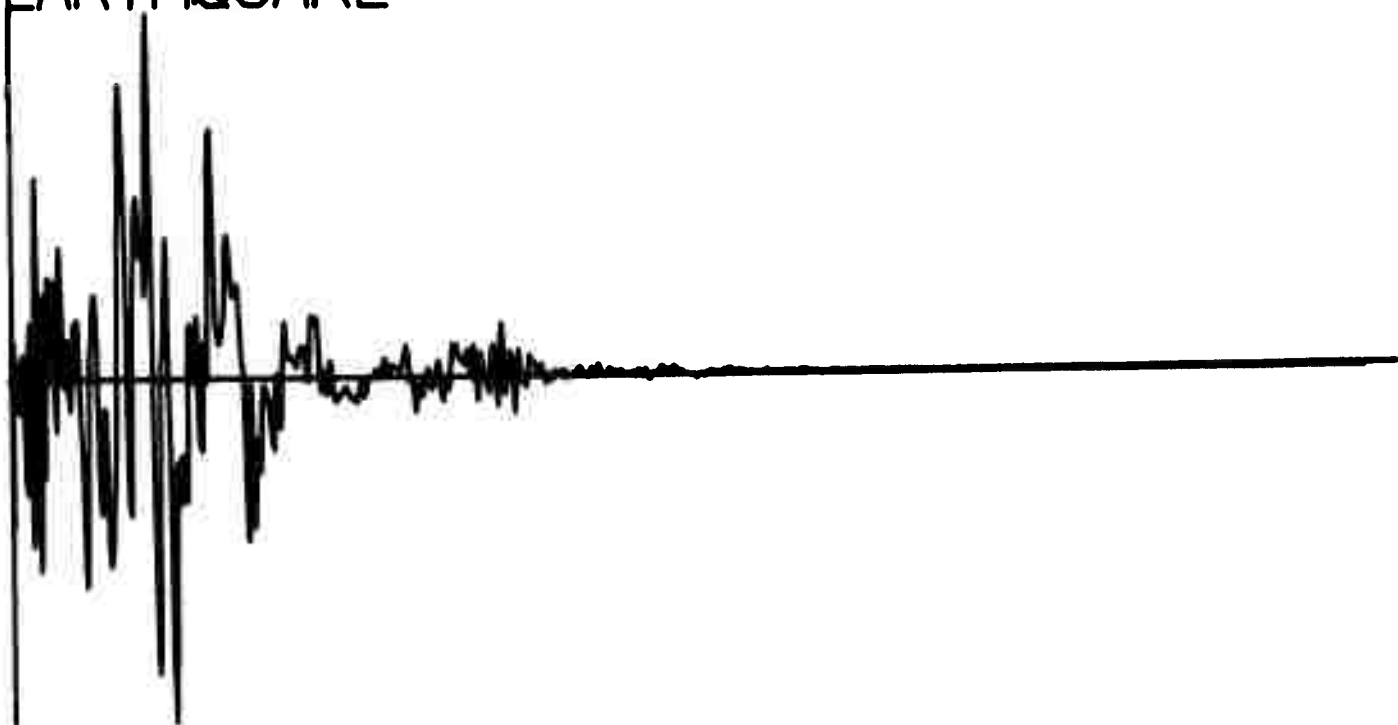
X226



Q228

EVENT NUMBER 1219

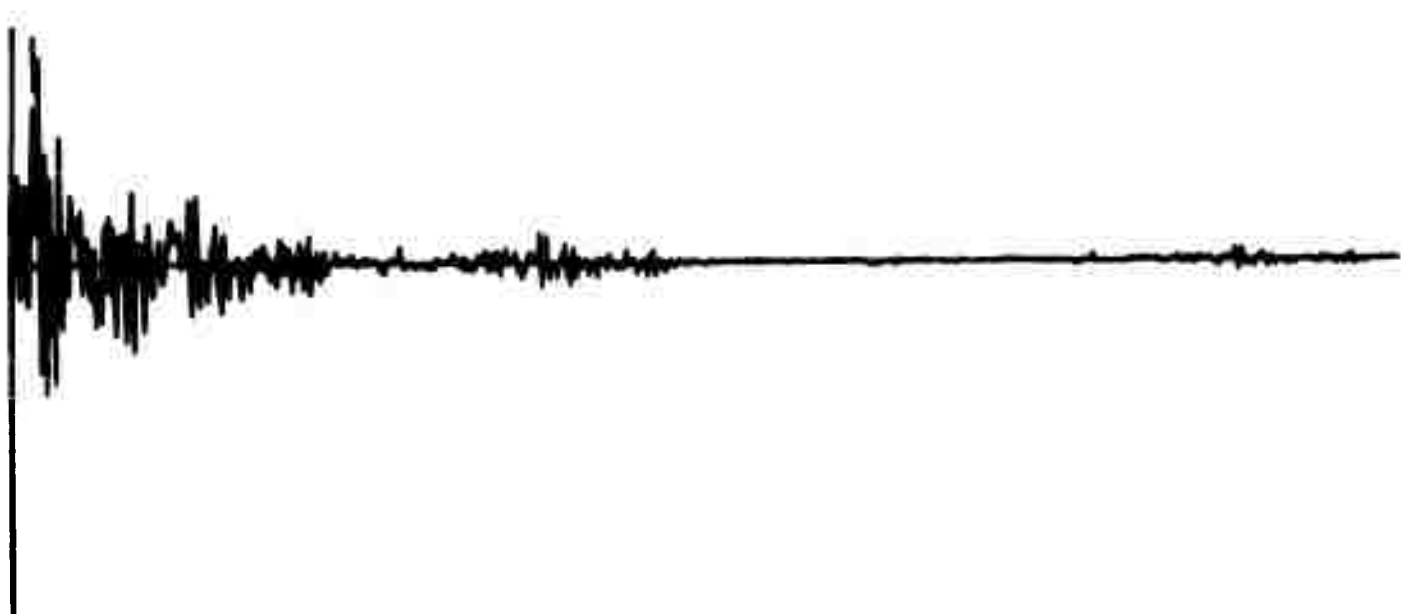
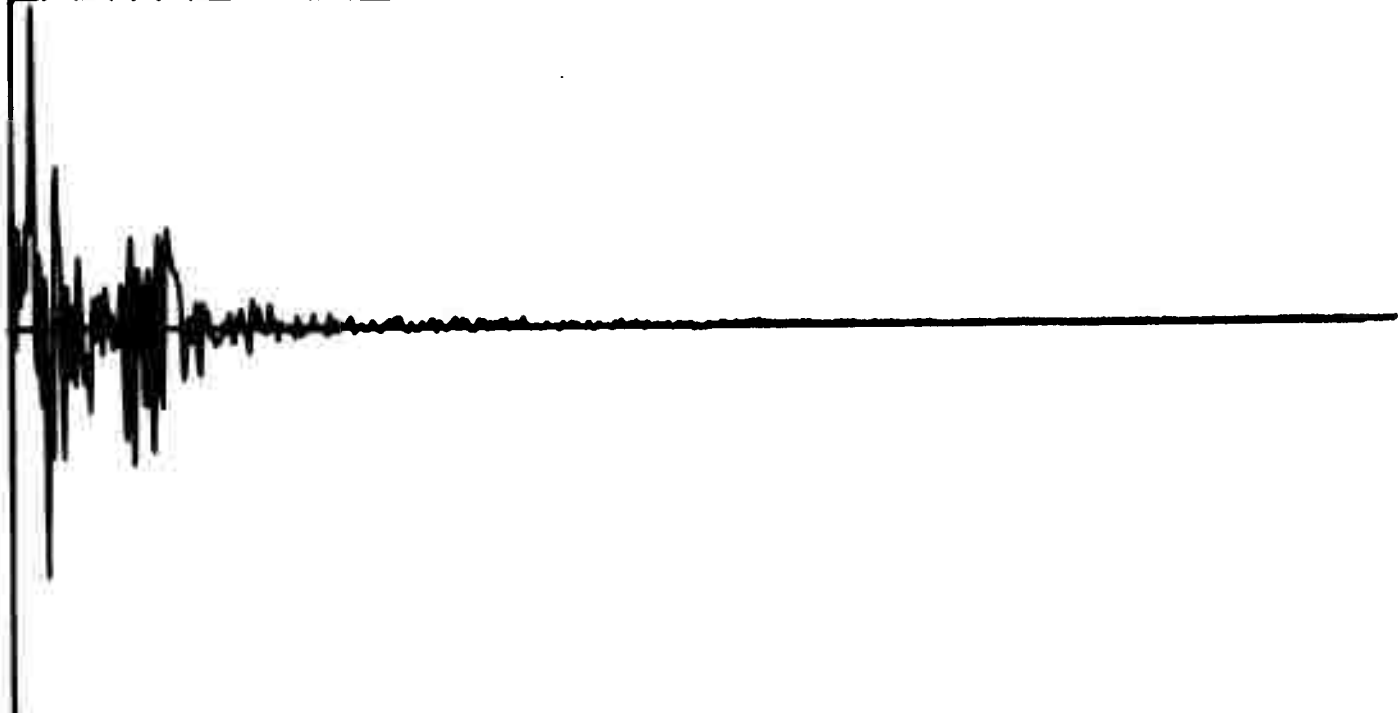
EARTHQUAKE



Q230

EVENT NUMBER 1245

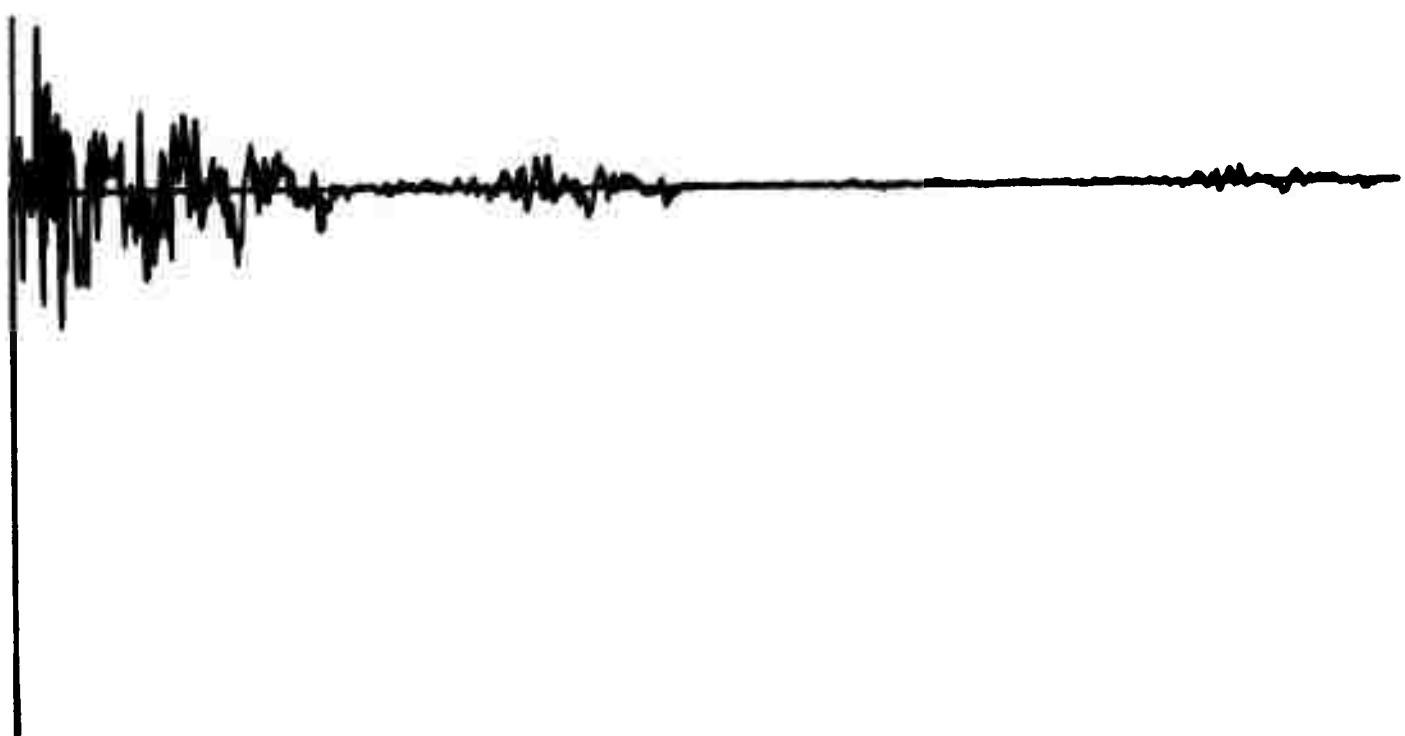
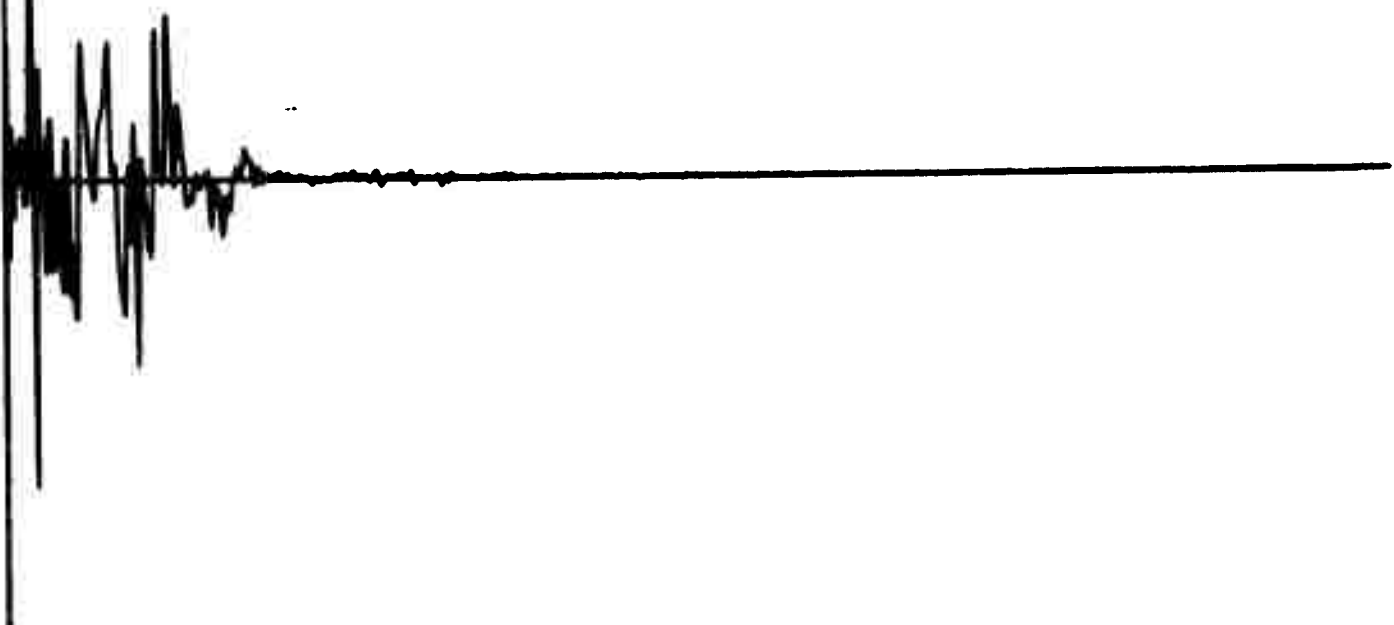
EARTHQUAKE



Q232

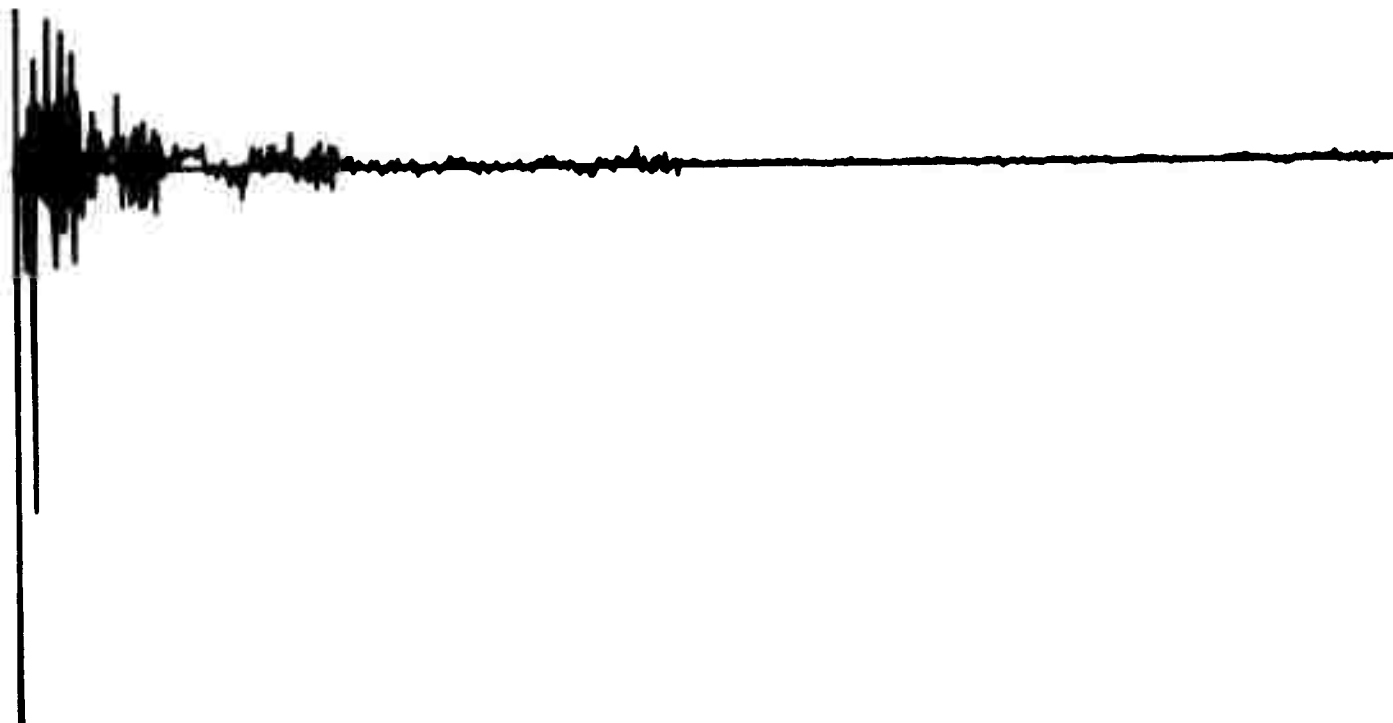
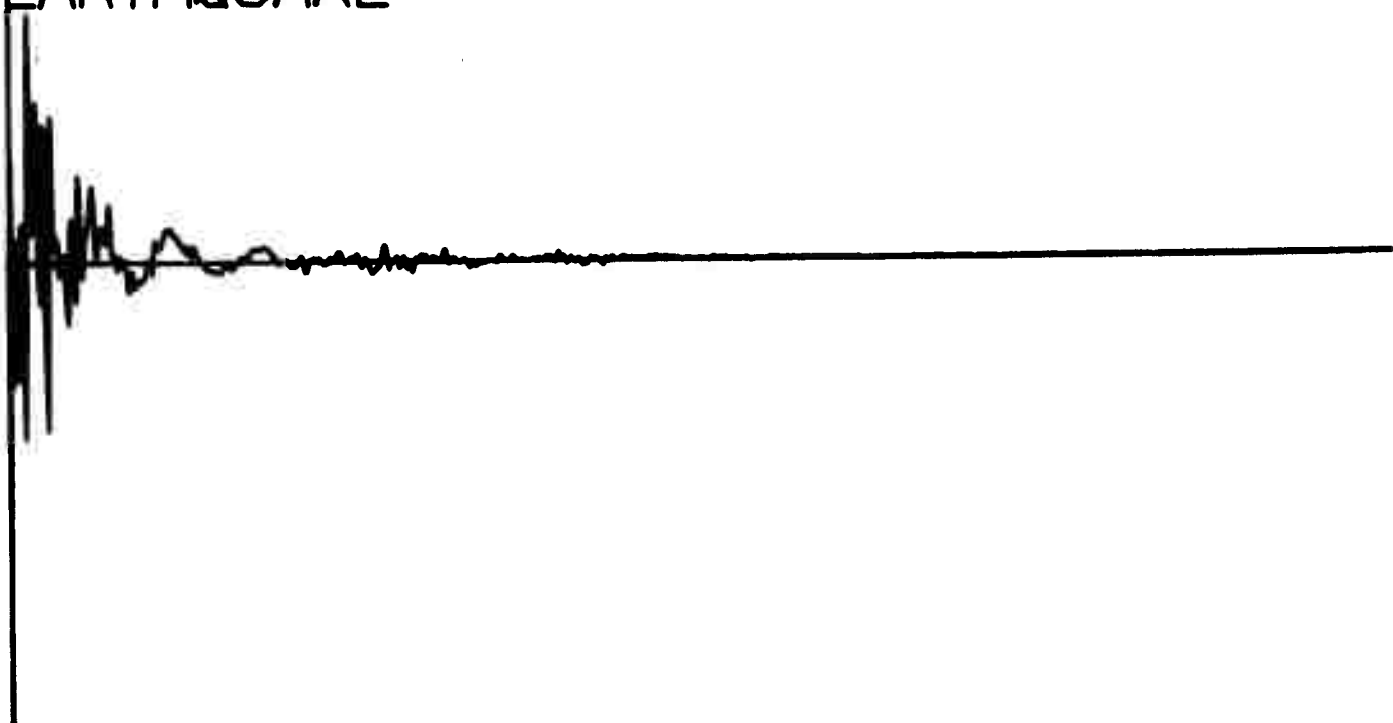
EVENT NUMBER 1247

EARTHQUAKE



Q234

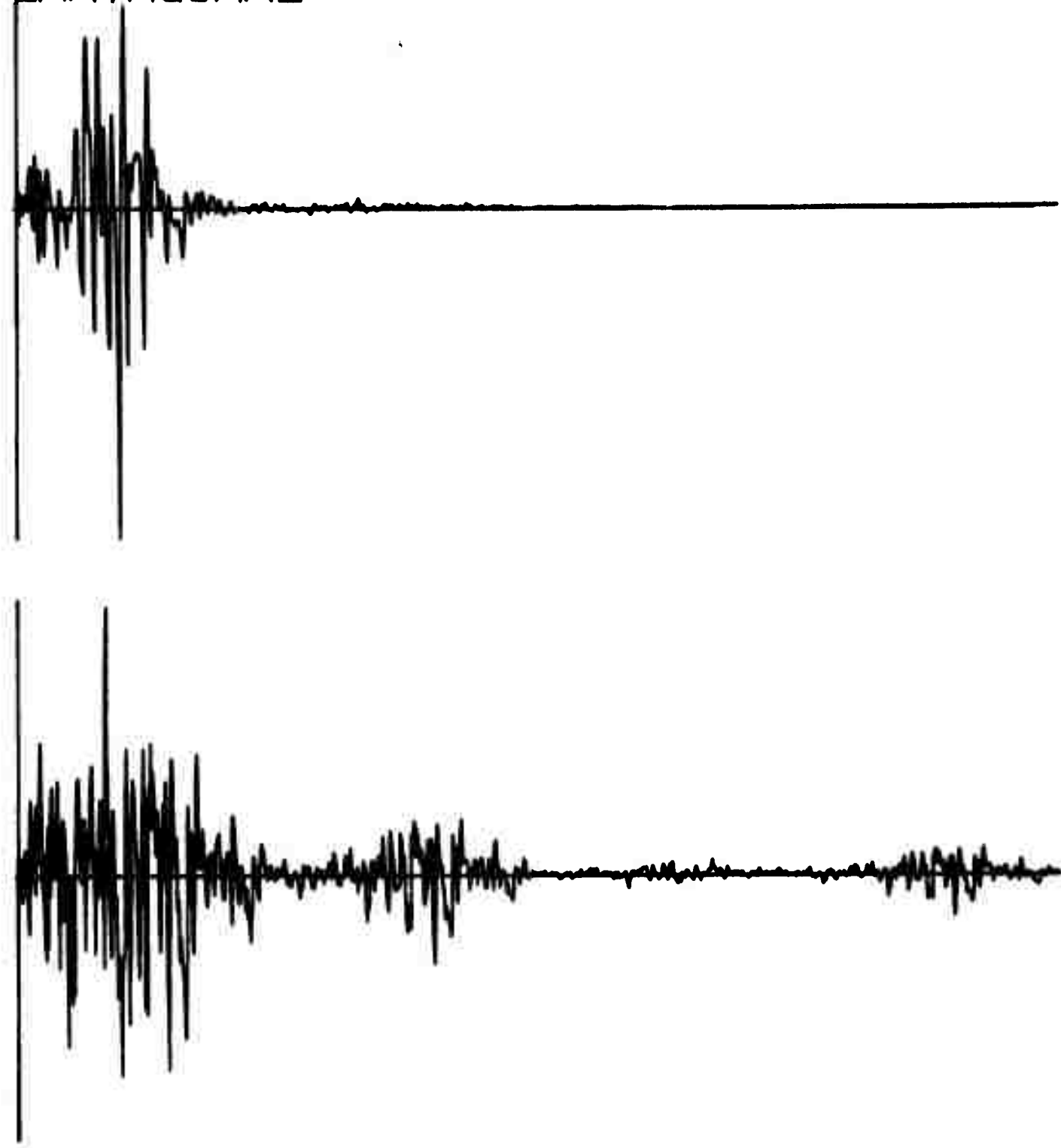
EVENT NUMBER 1248 EARTHQUAKE



Q236

EVENT NUMBER 1249

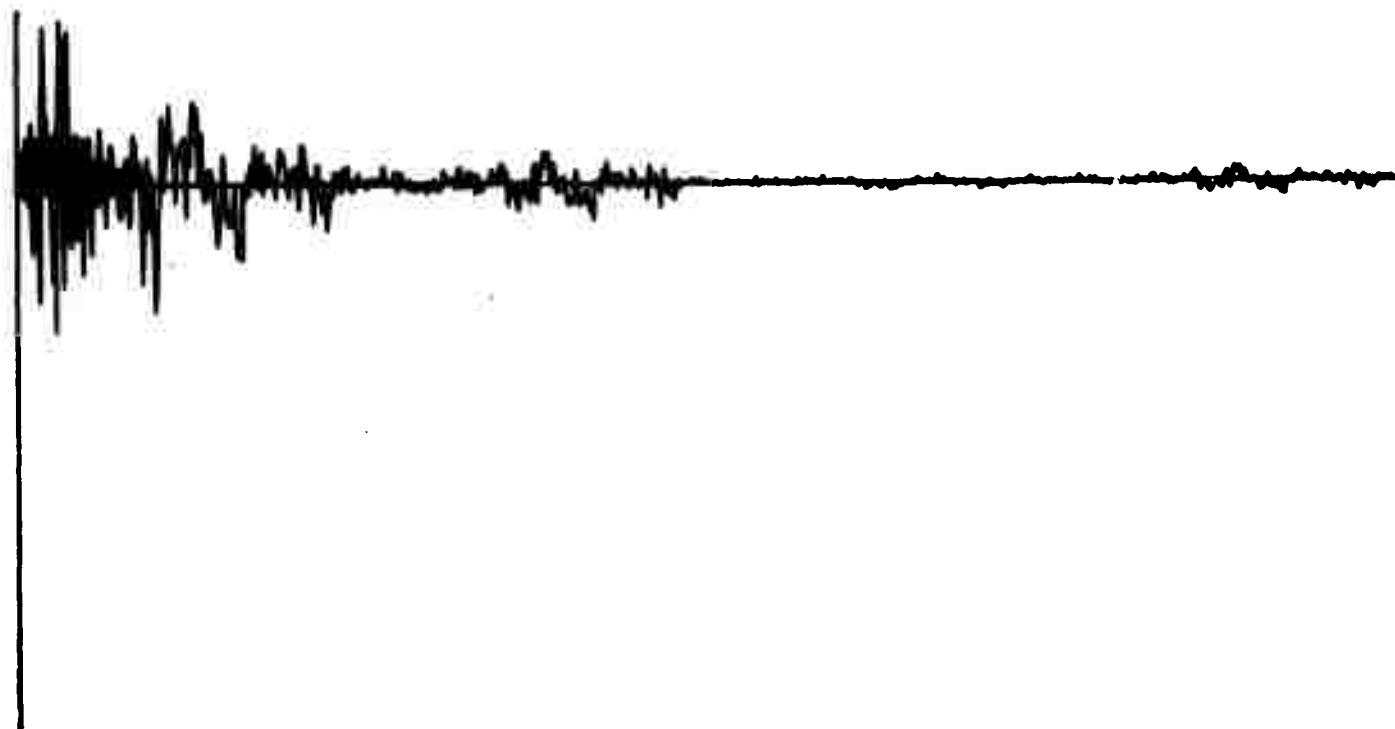
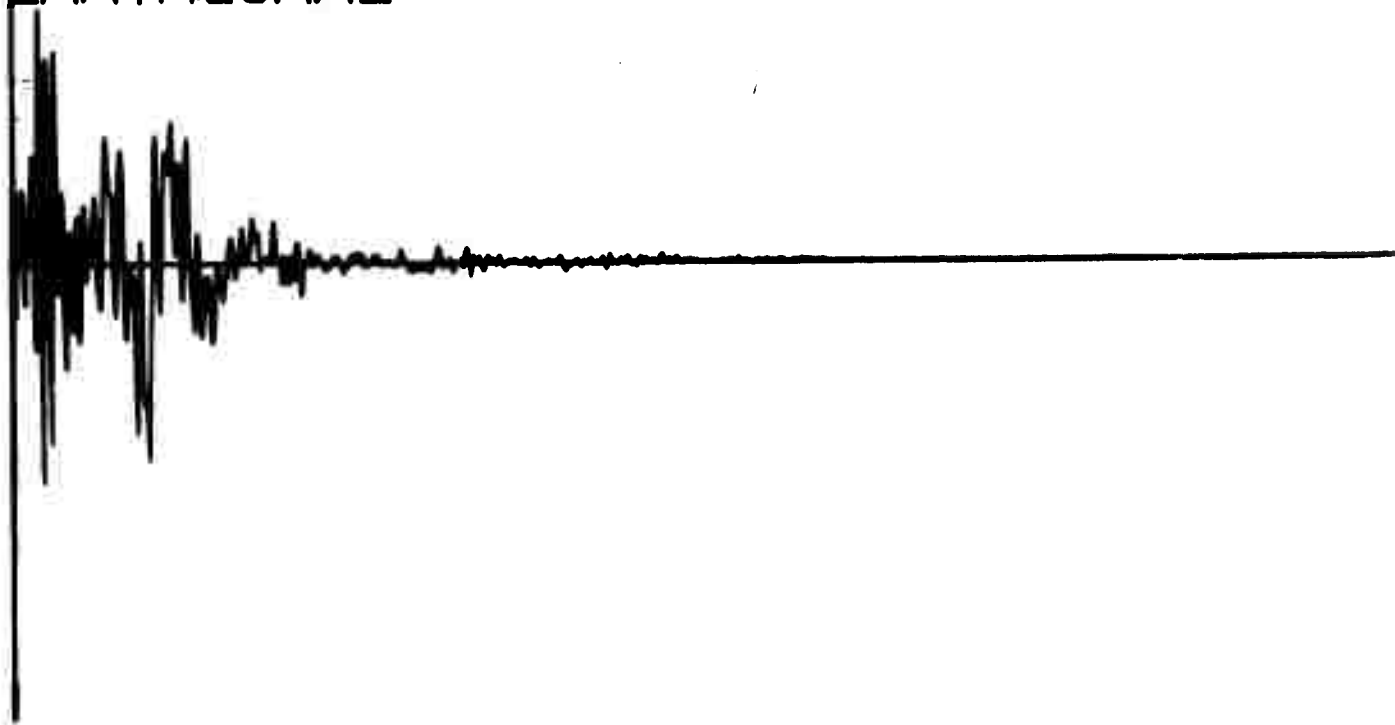
EARTHQUAKE



Q238

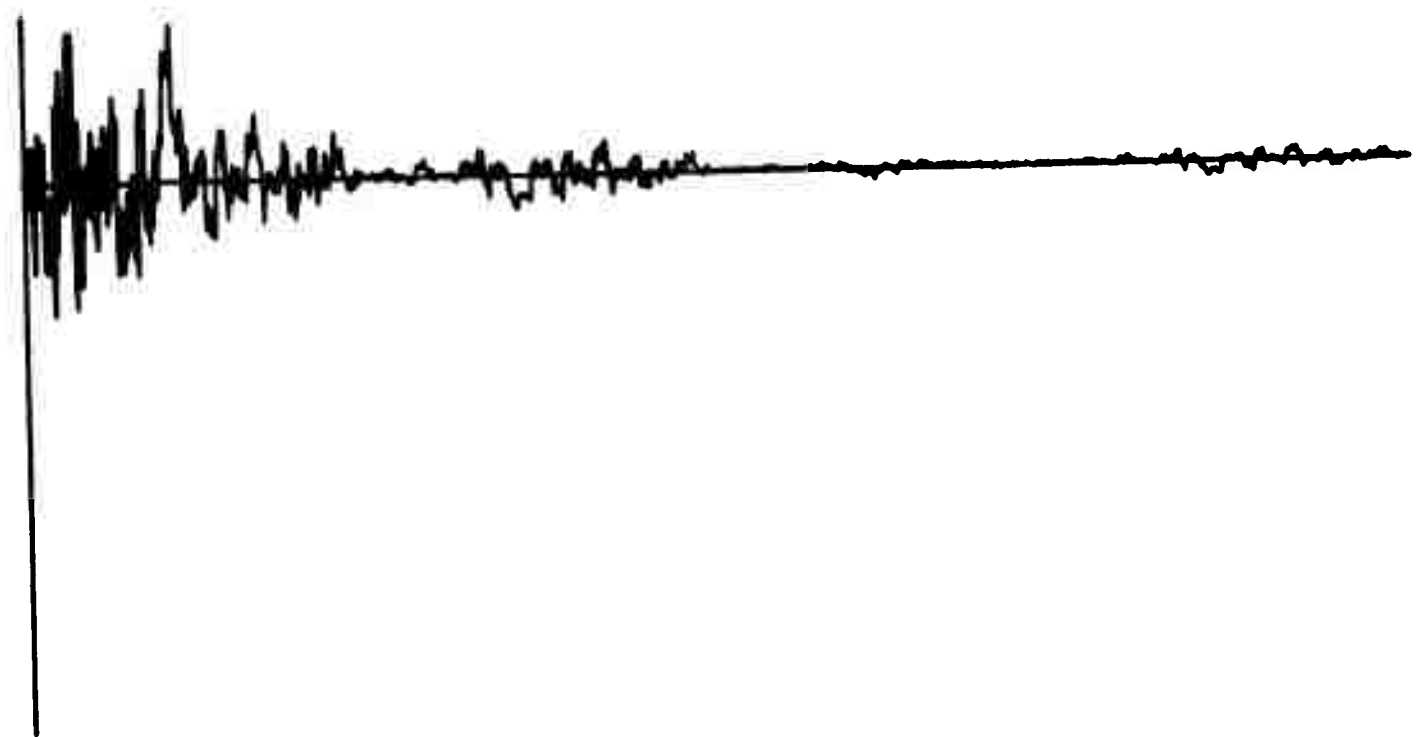
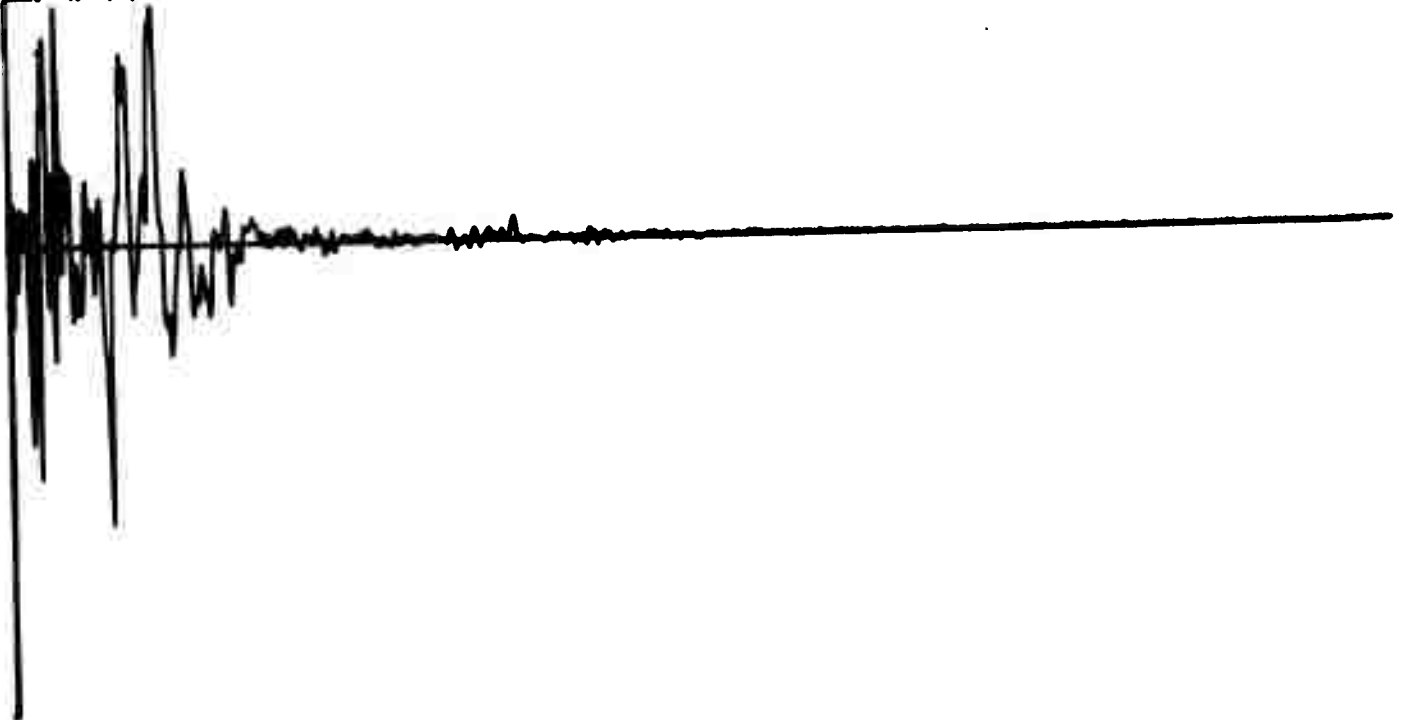
EVENT NUMBER 1251

EARTHQUAKE



Q240

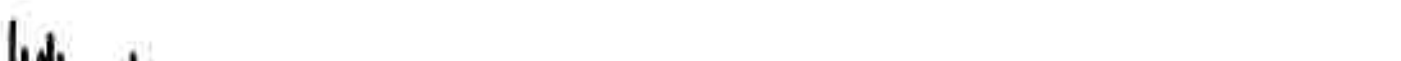
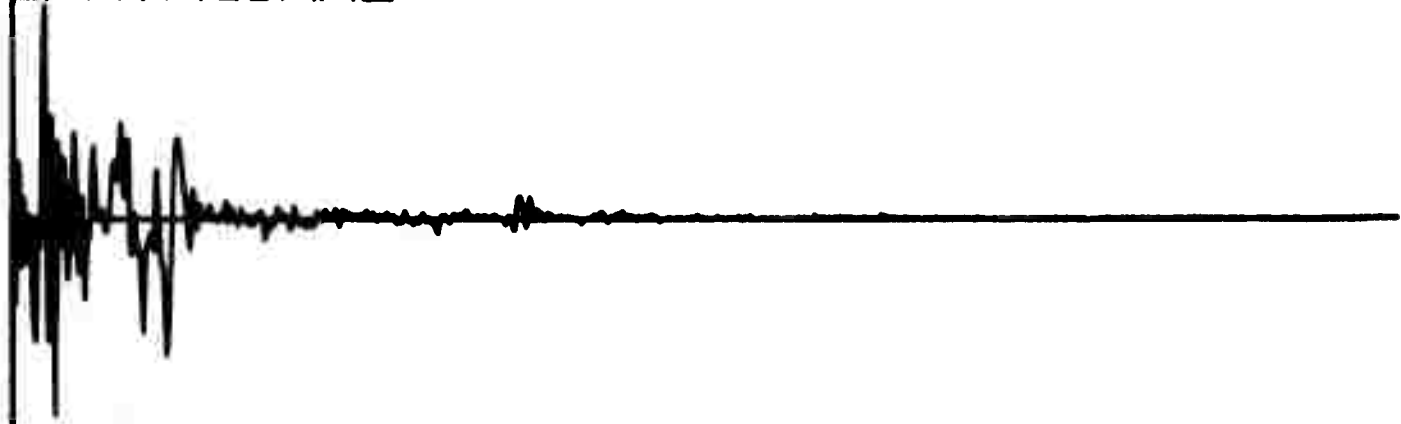
EVENT NUMBER 1253
EARTHQUAKE



Q242

EVENT NUMBER 1254

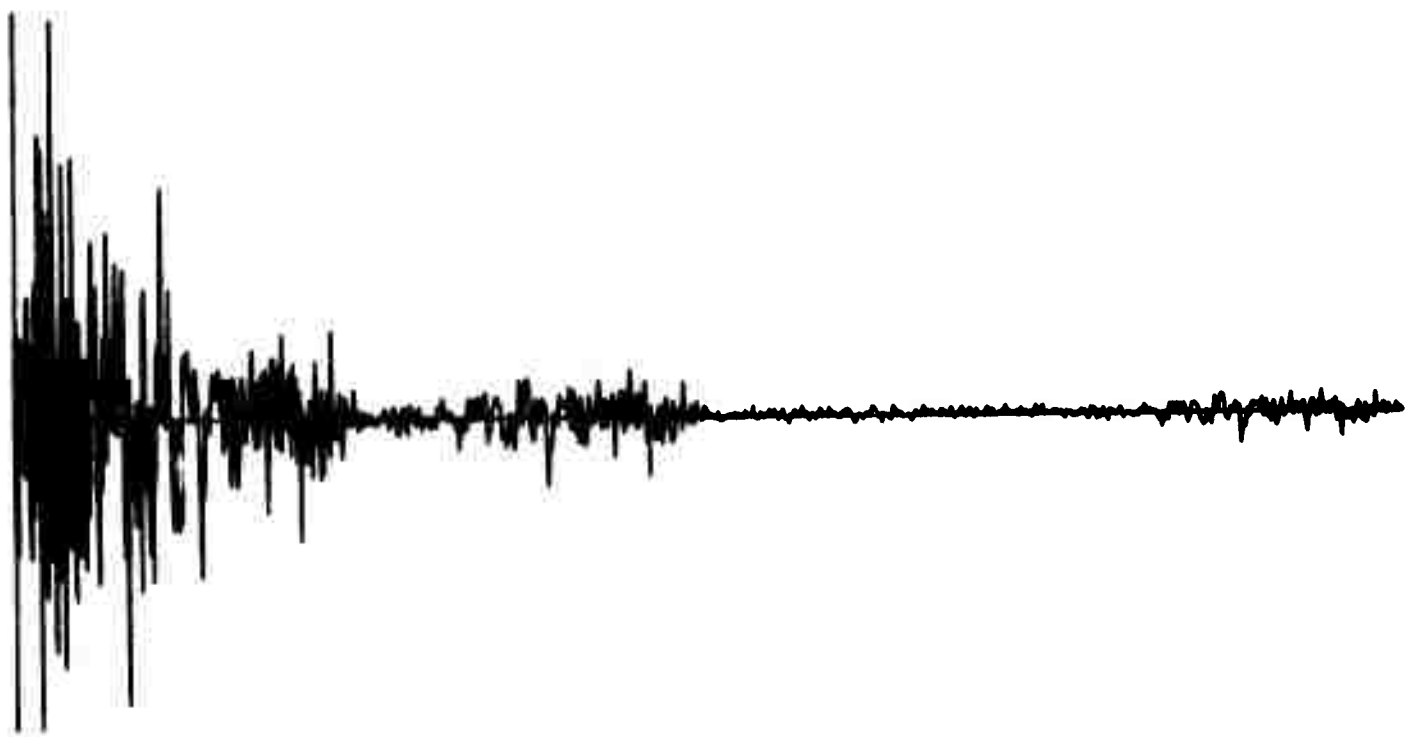
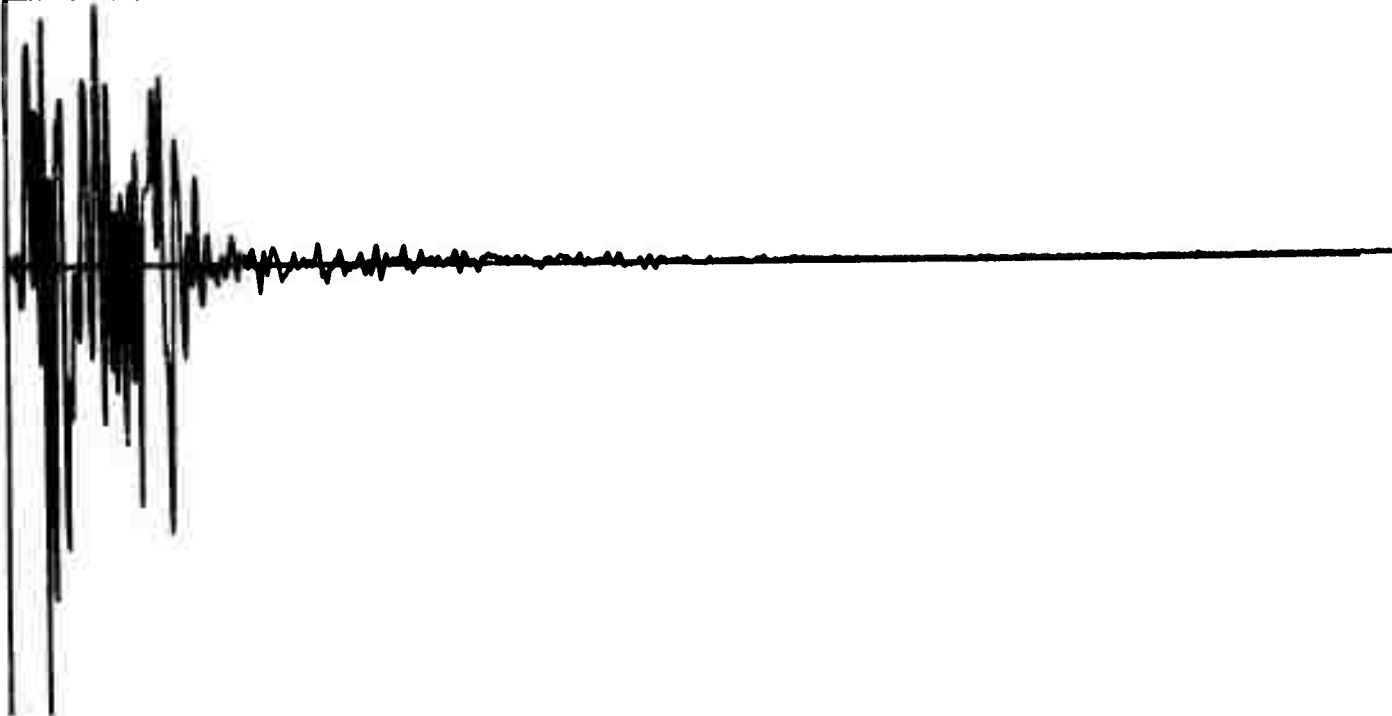
EARTHQUAKE



Q244

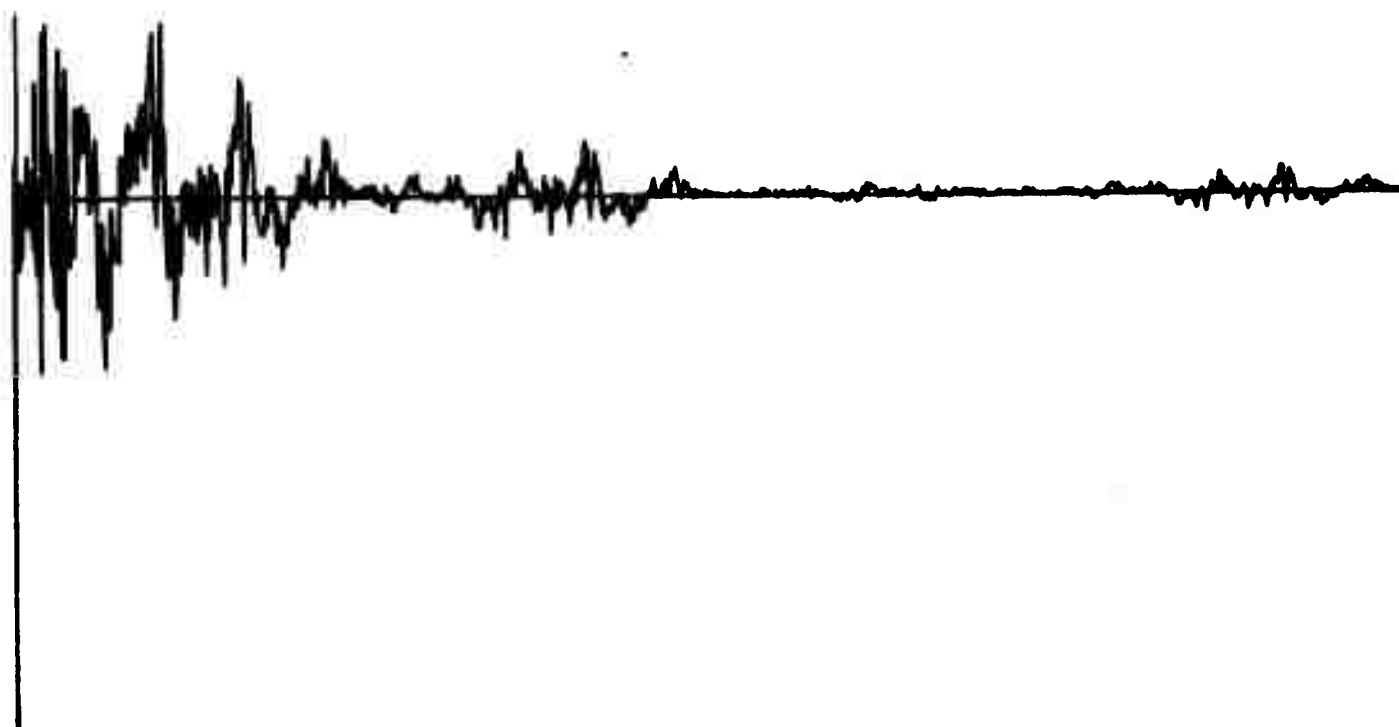
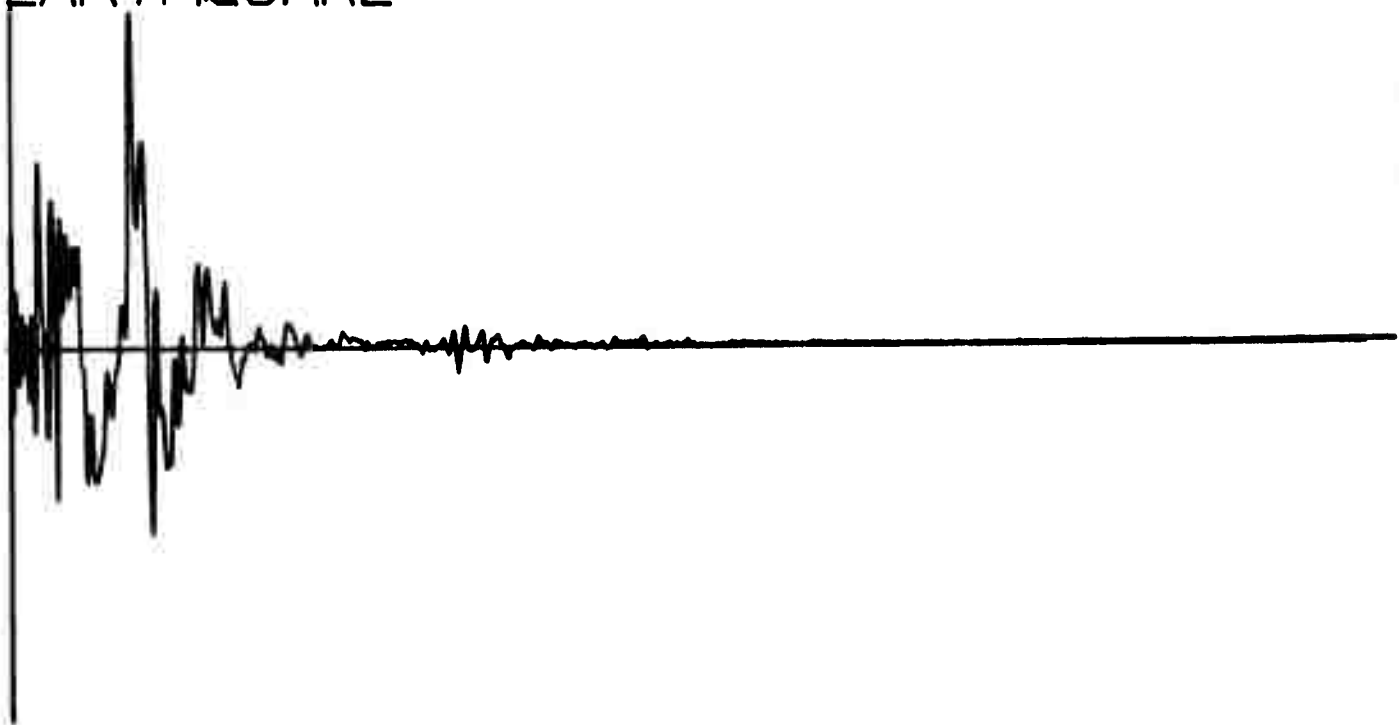
EVENT NUMBER 1256

EARTHQUAKE



Q246

EVENT NUMBER 1267
EARTHQUAKE



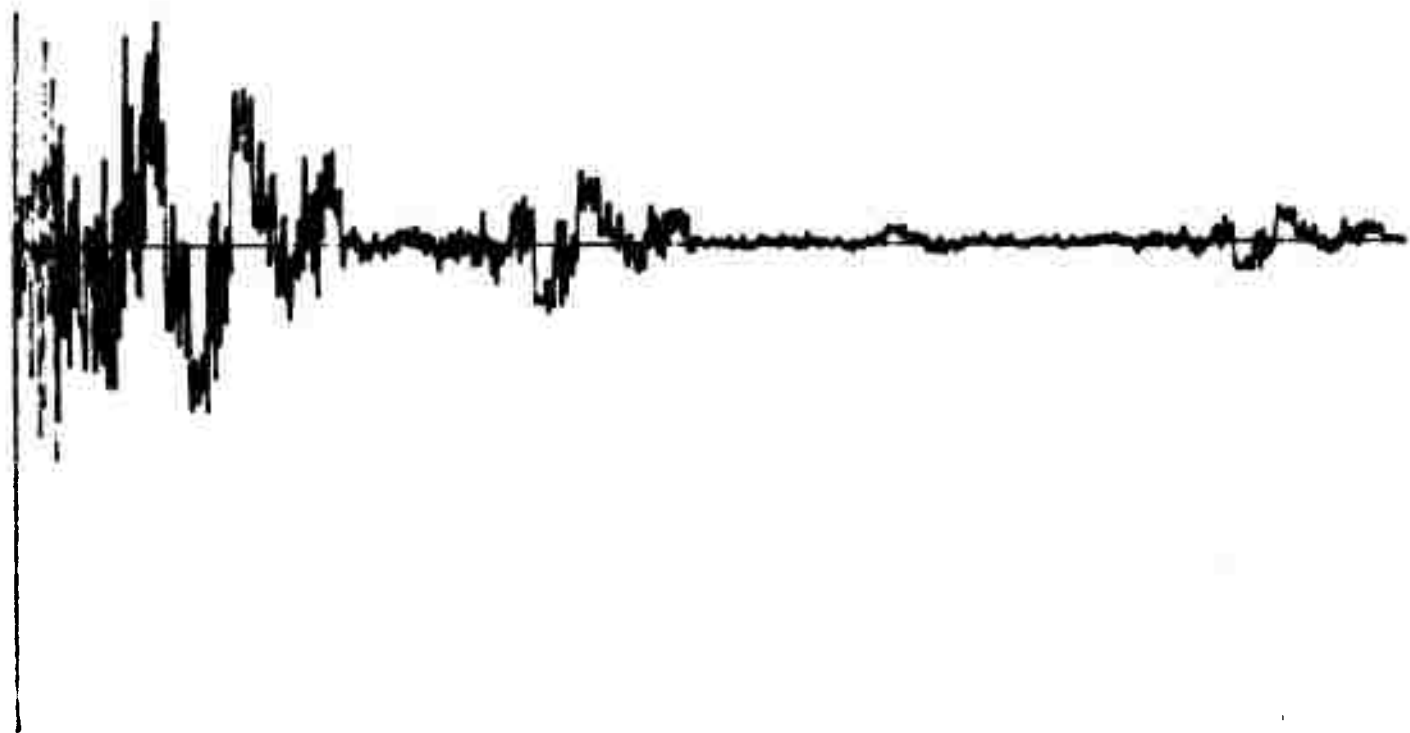
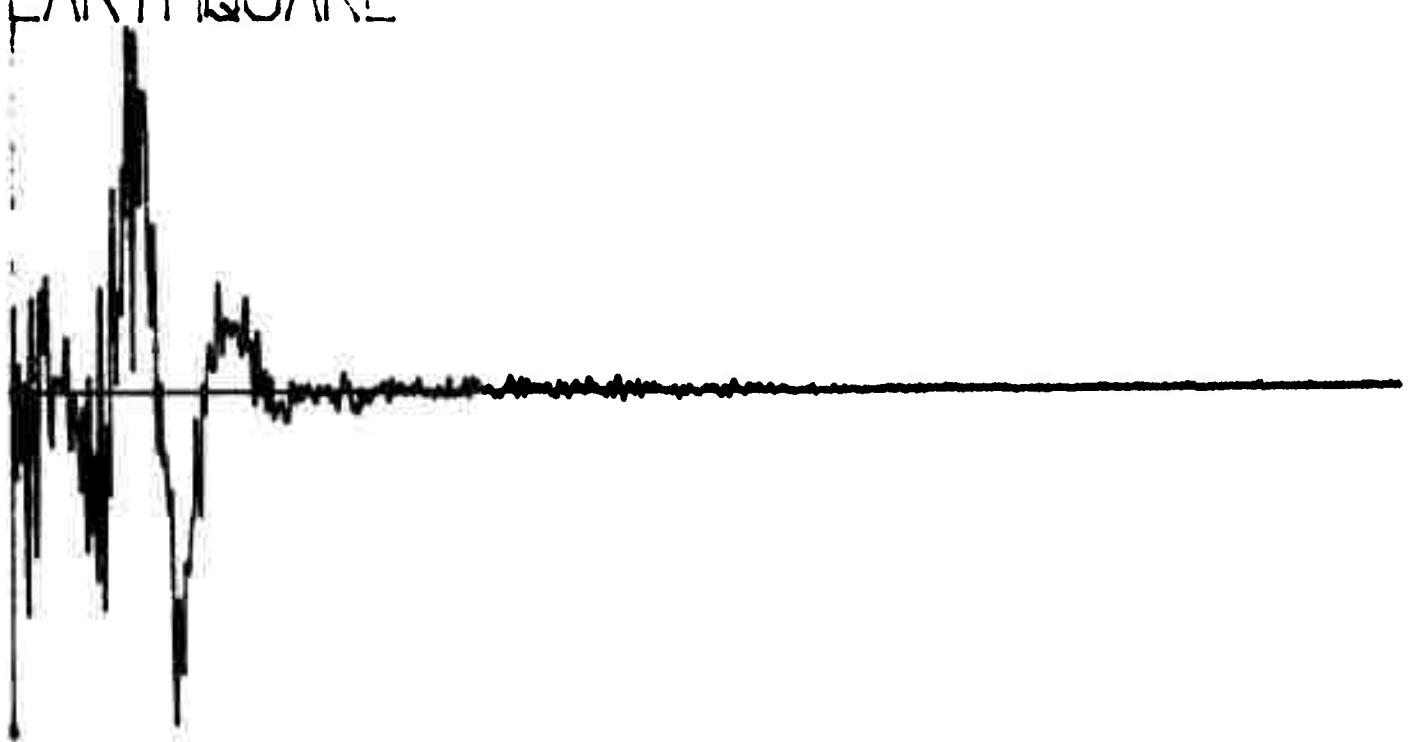
Q248

EVENT NUMBER 1258
EARTHQUAKE



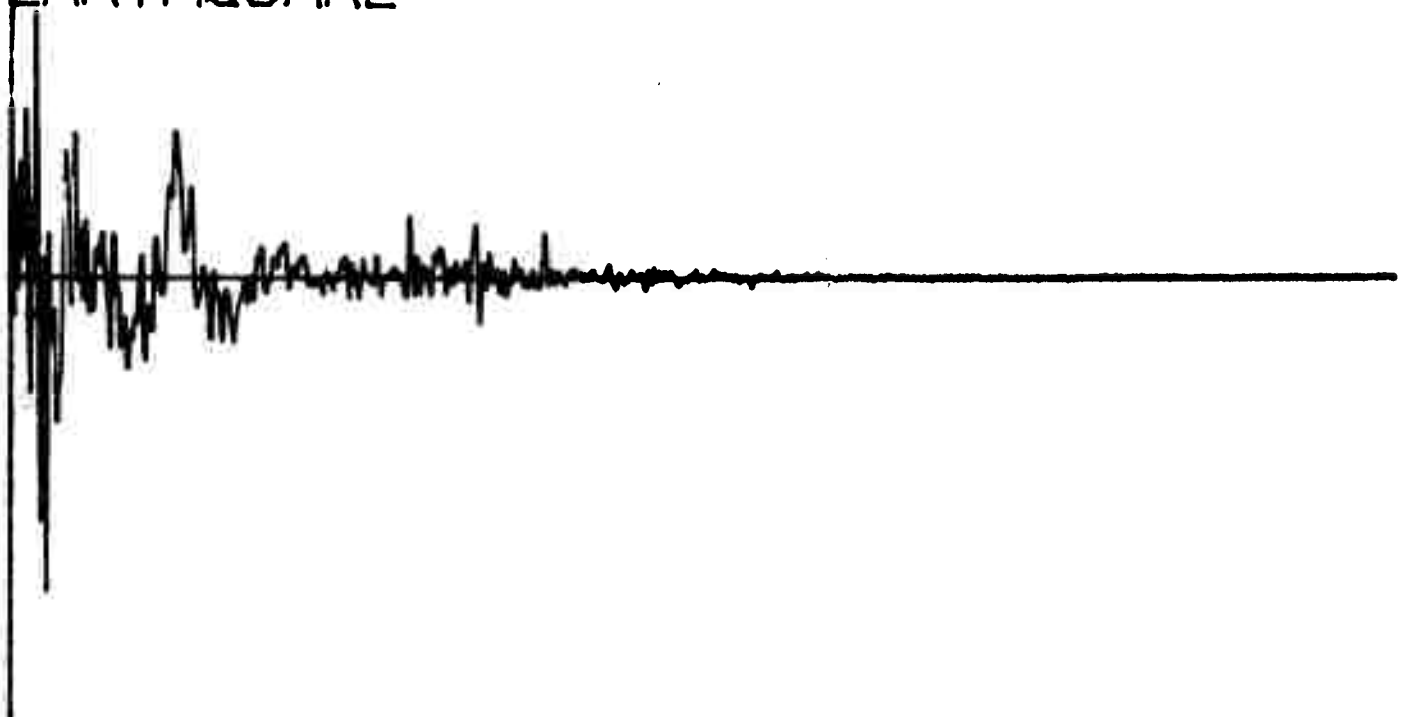
Q250

EVENT NUMBER 1259
EARTHQUAKE



Q252

EVENT NUMBER 1260
EARTHQUAKE



Q254

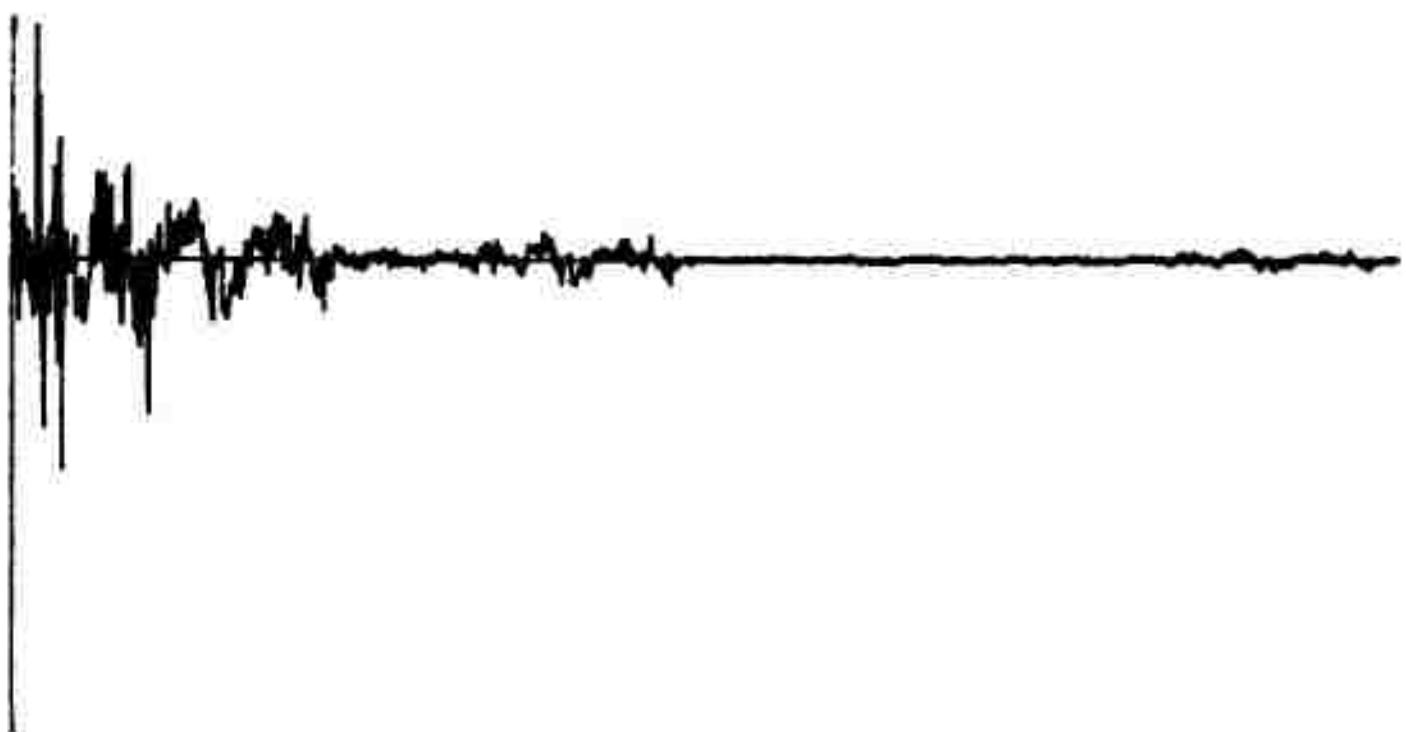
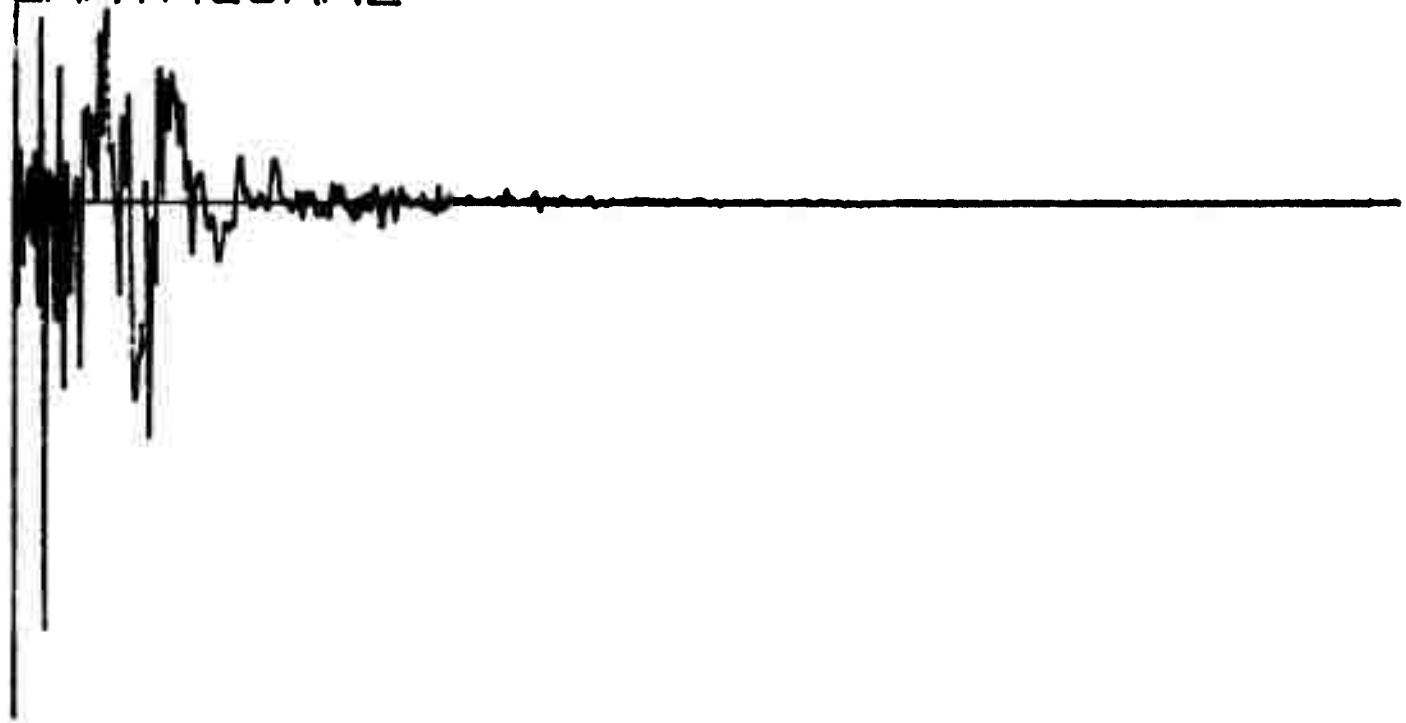
EVENT NUMBER 1261

EARTHQUAKE



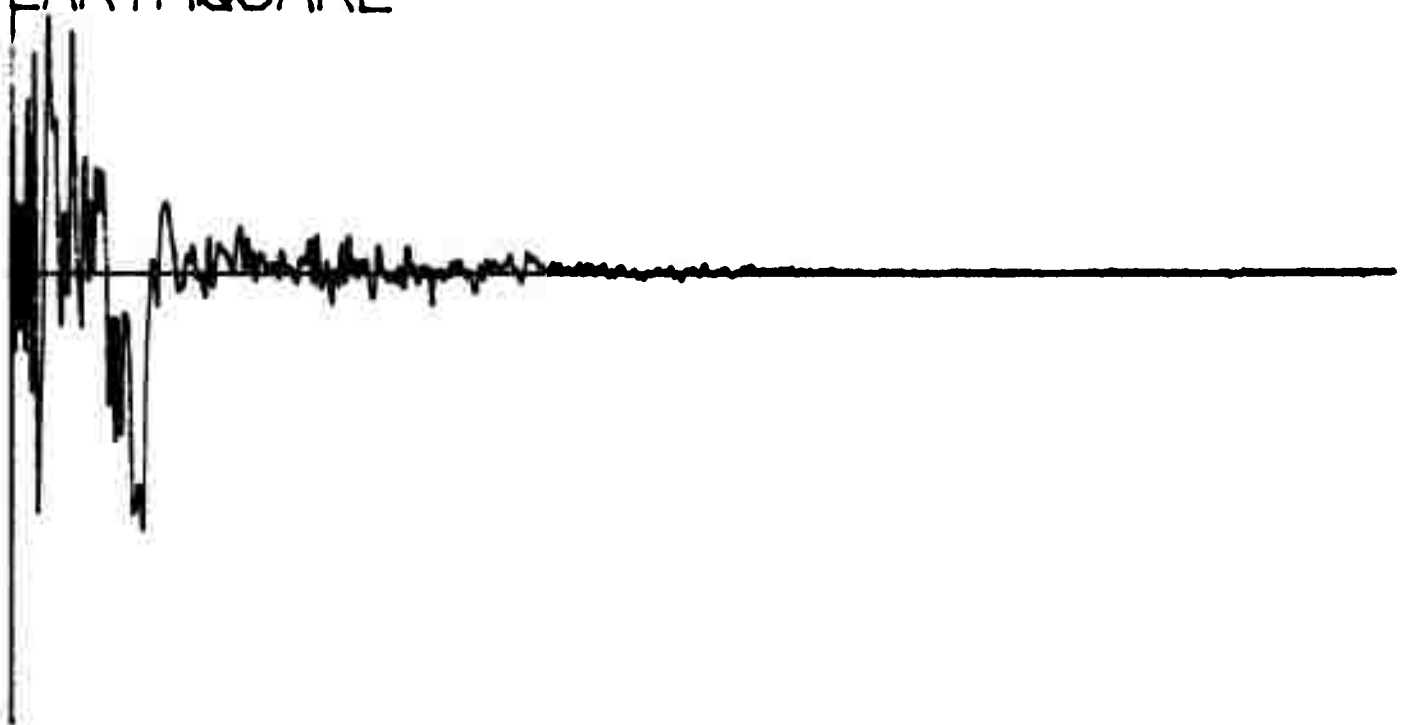
Q256

EVENT NUMBER 1262
EARTHQUAKE



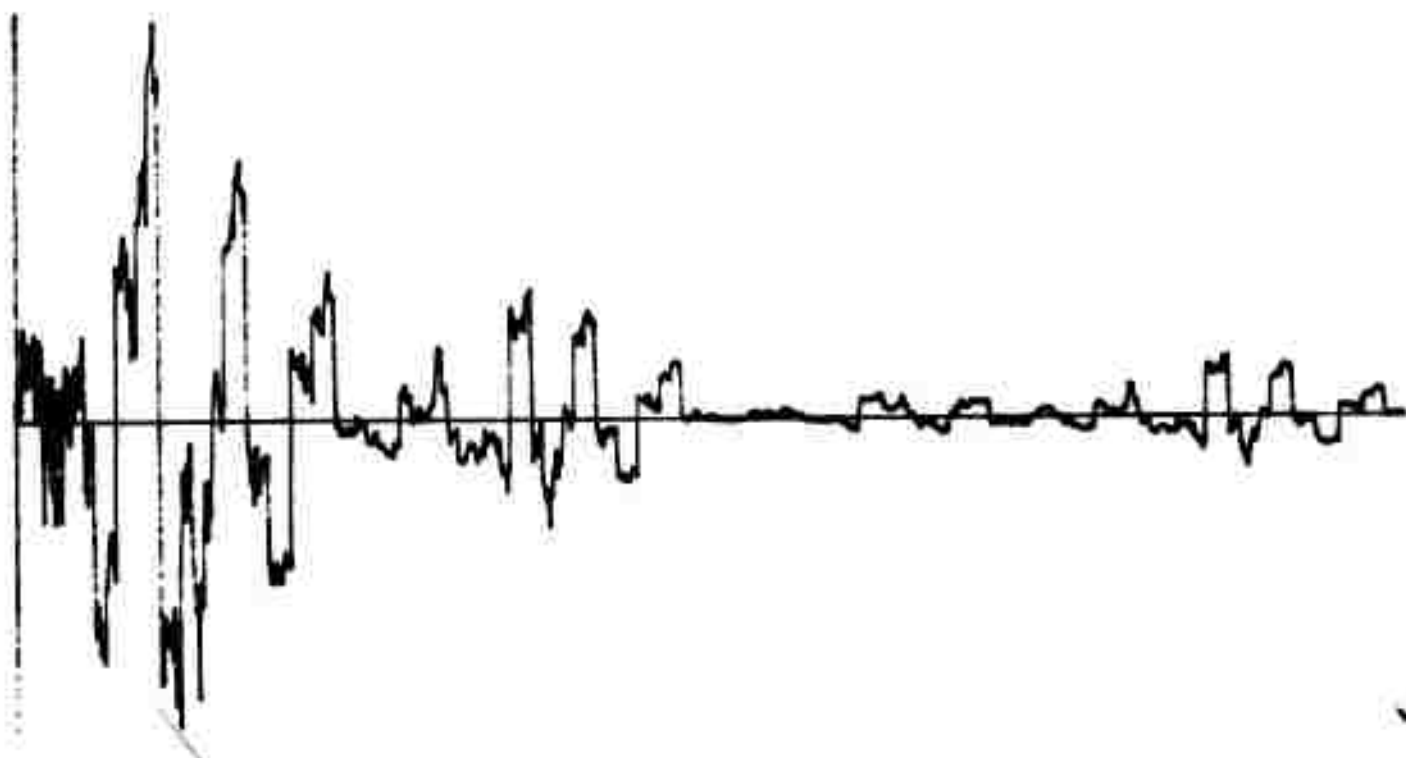
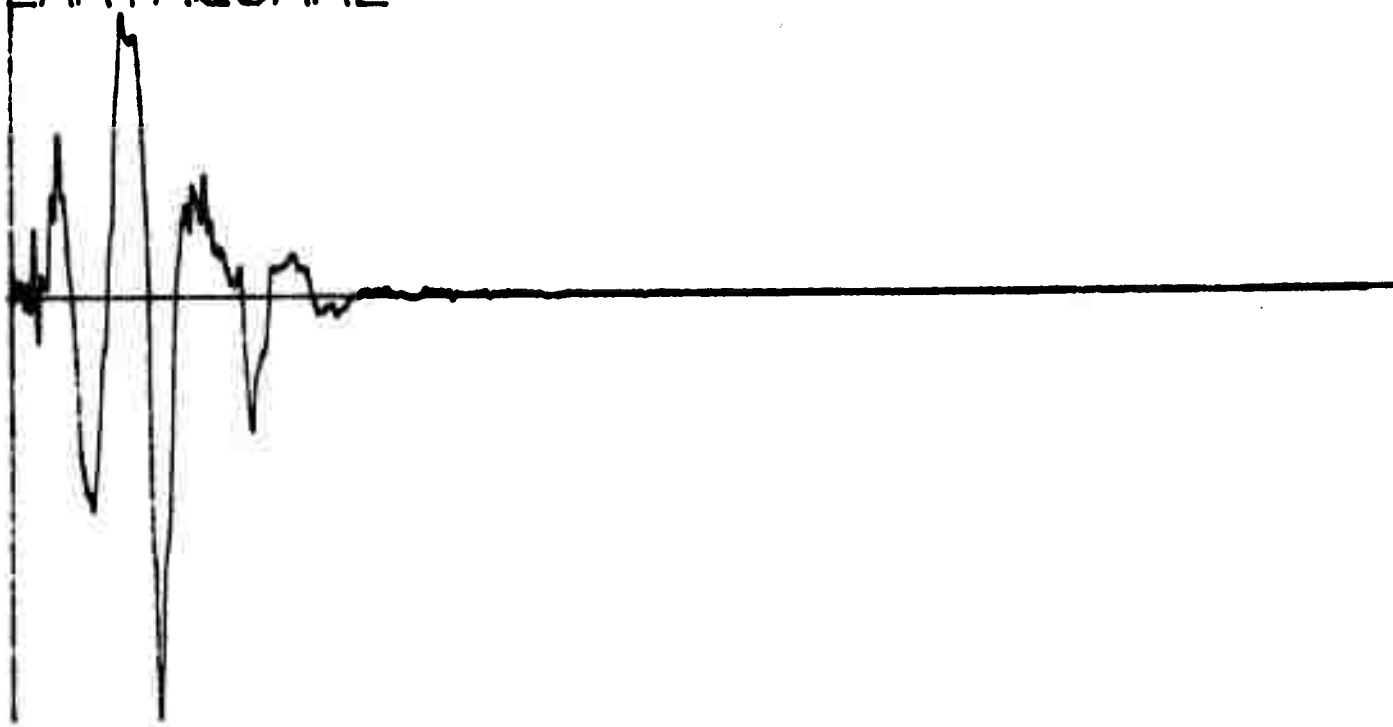
Q258

EVENT NUMBER 1264
EARTHQUAKE



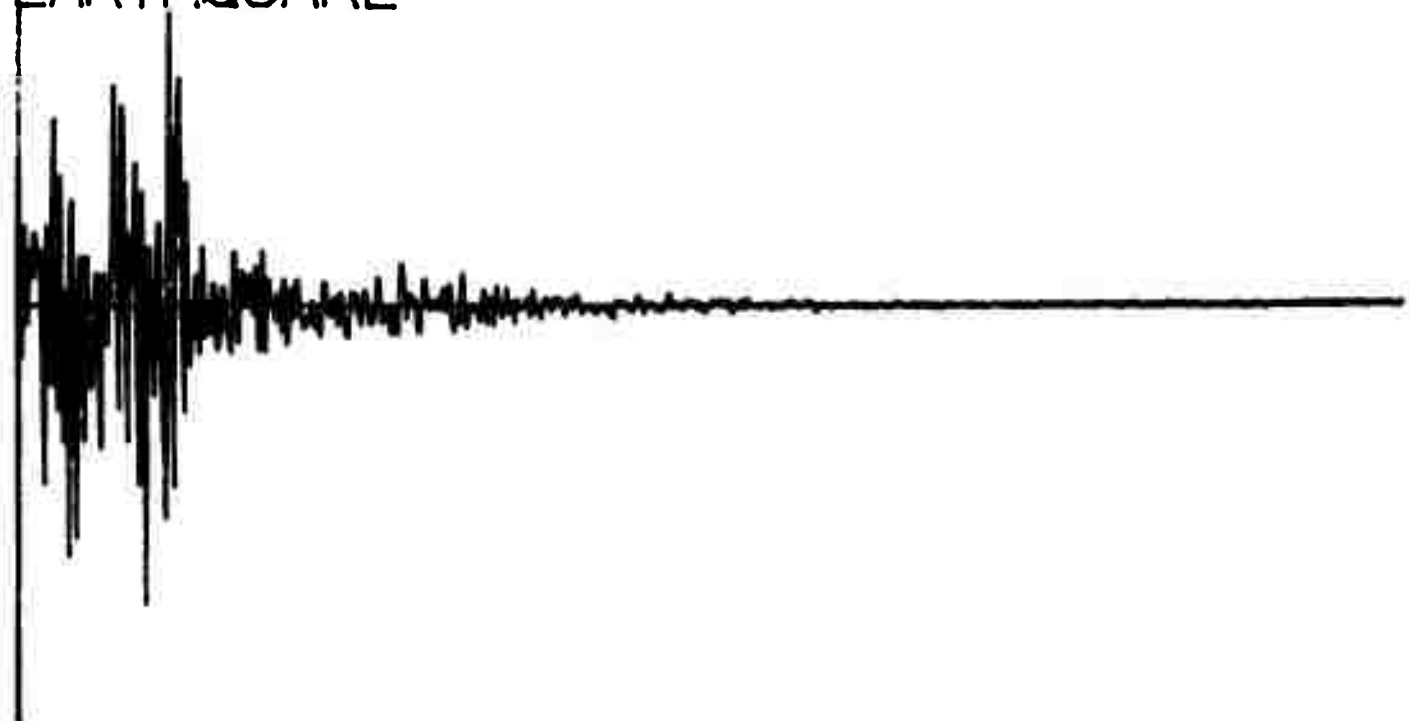
Q260

EVENT NUMBER 1263
EARTHQUAKE



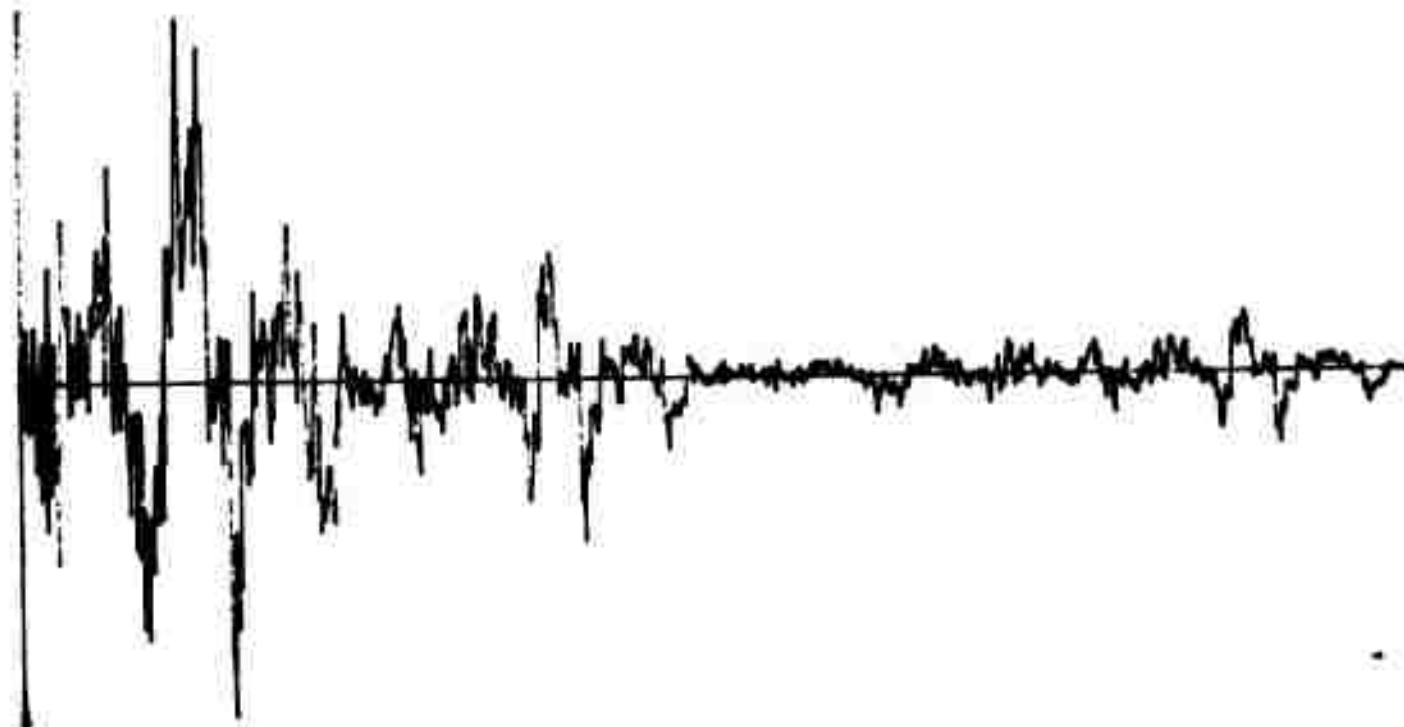
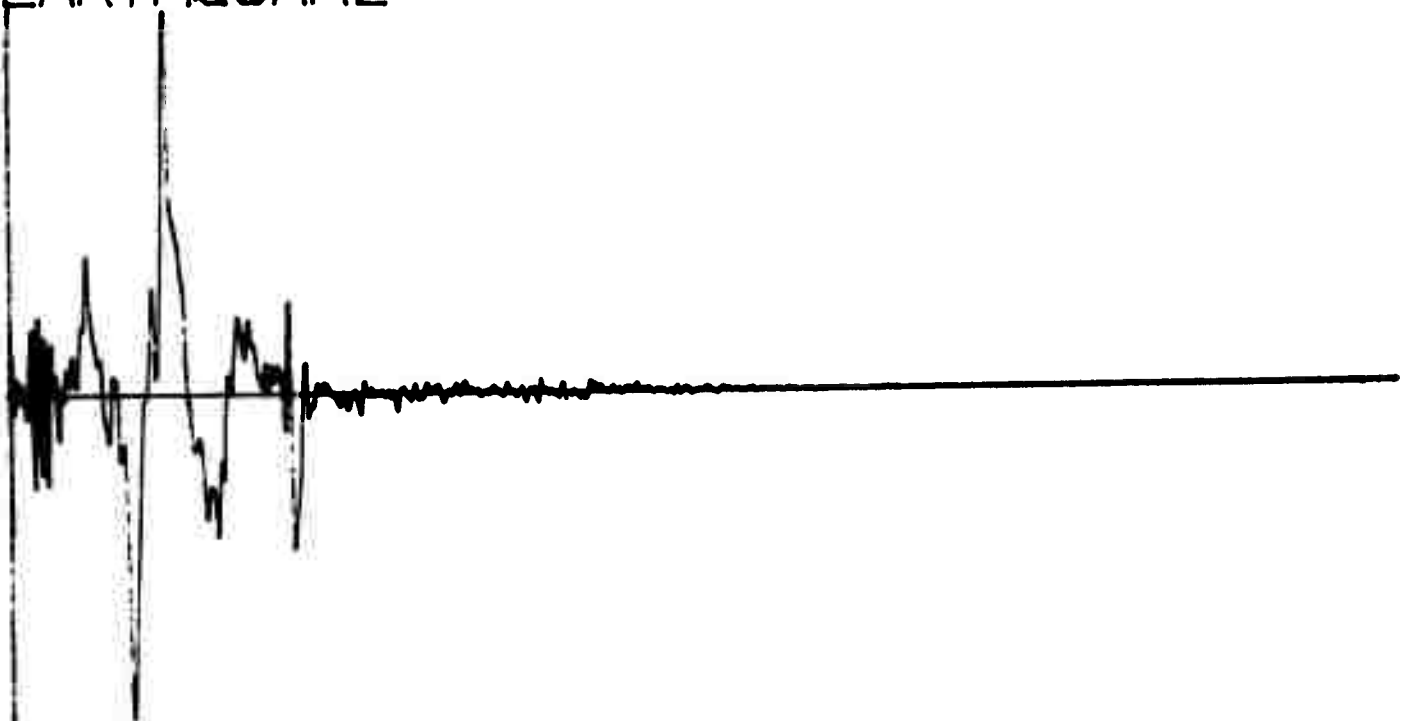
Q262

VENT NUMBER 1269
EARTHQUAKE



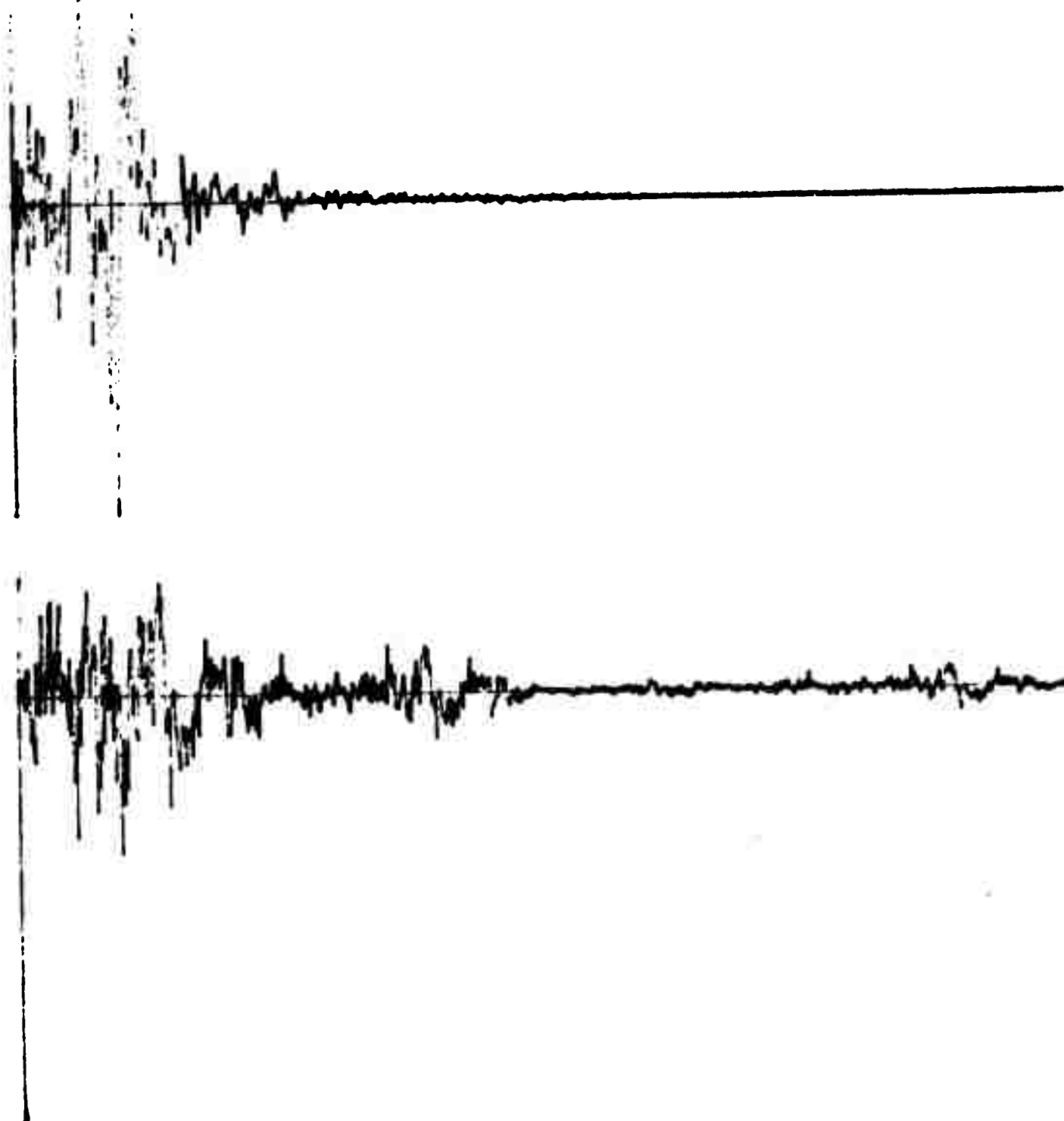
0264

EVENT NUMBER 1268
EARTHQUAKE



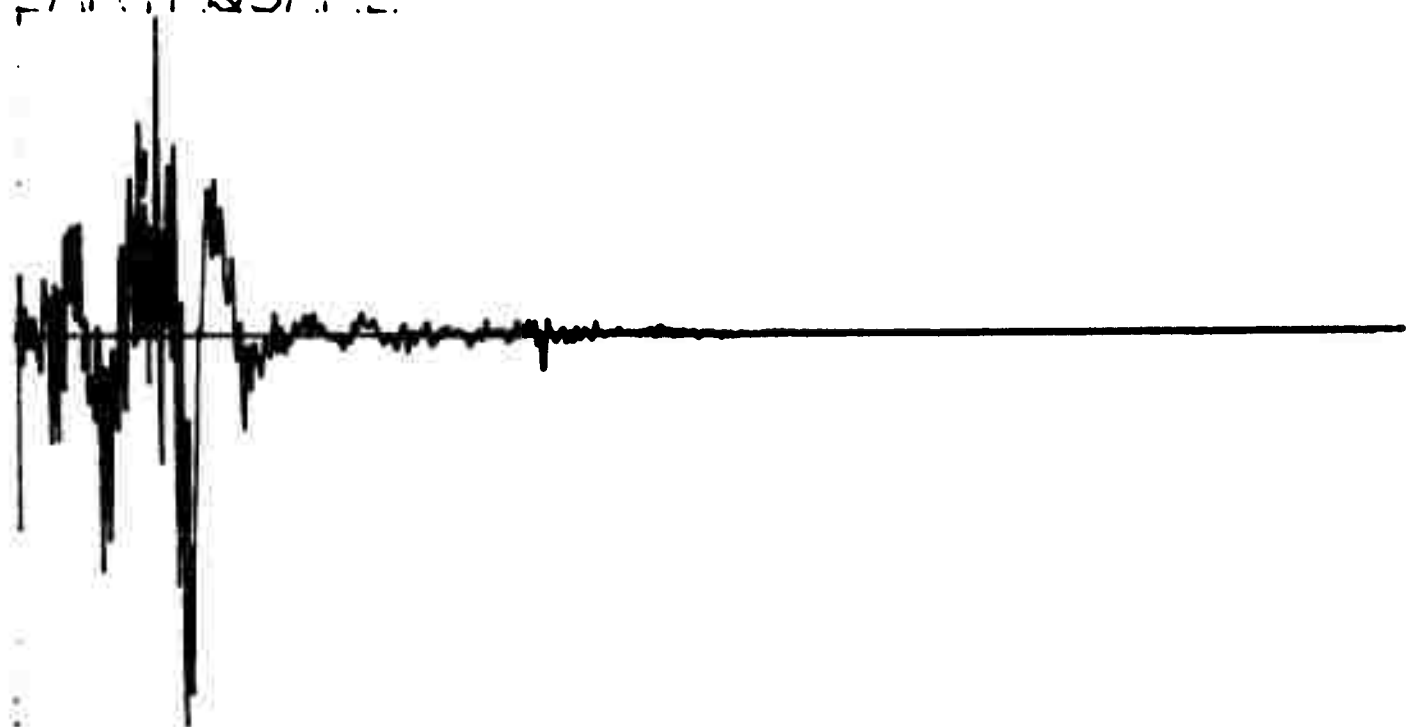
Q266

EVENT NUMBER 1270
EARTHQUAKE



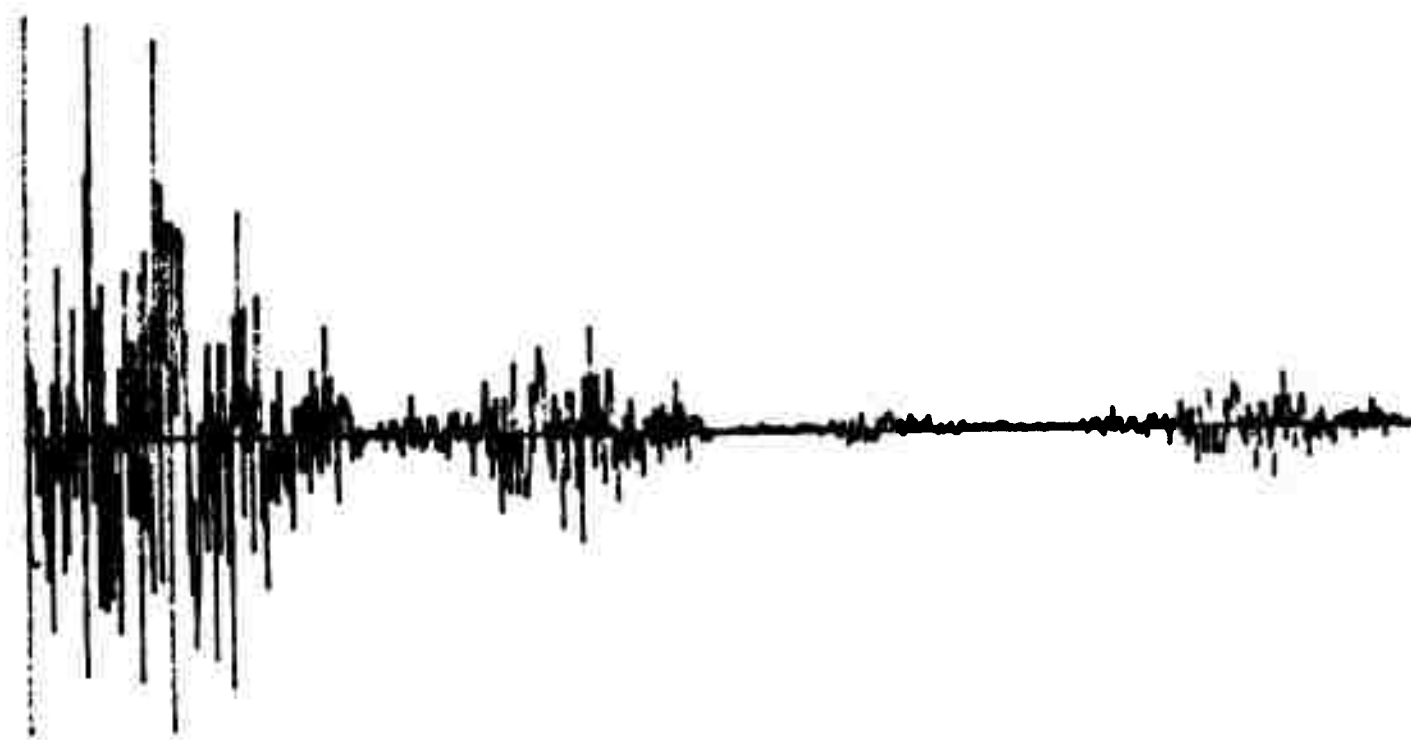
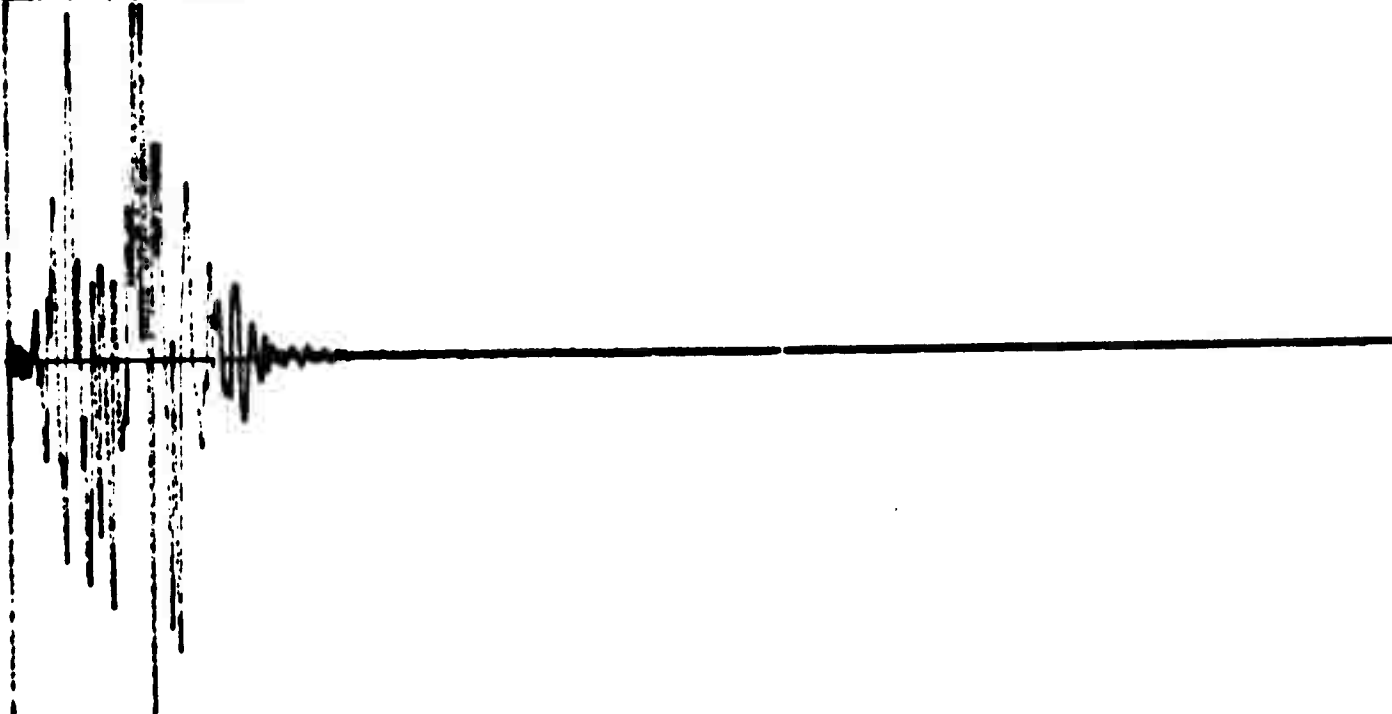
Q268

EVENT NUMBER 1271
EARTHQUAKE



Q270

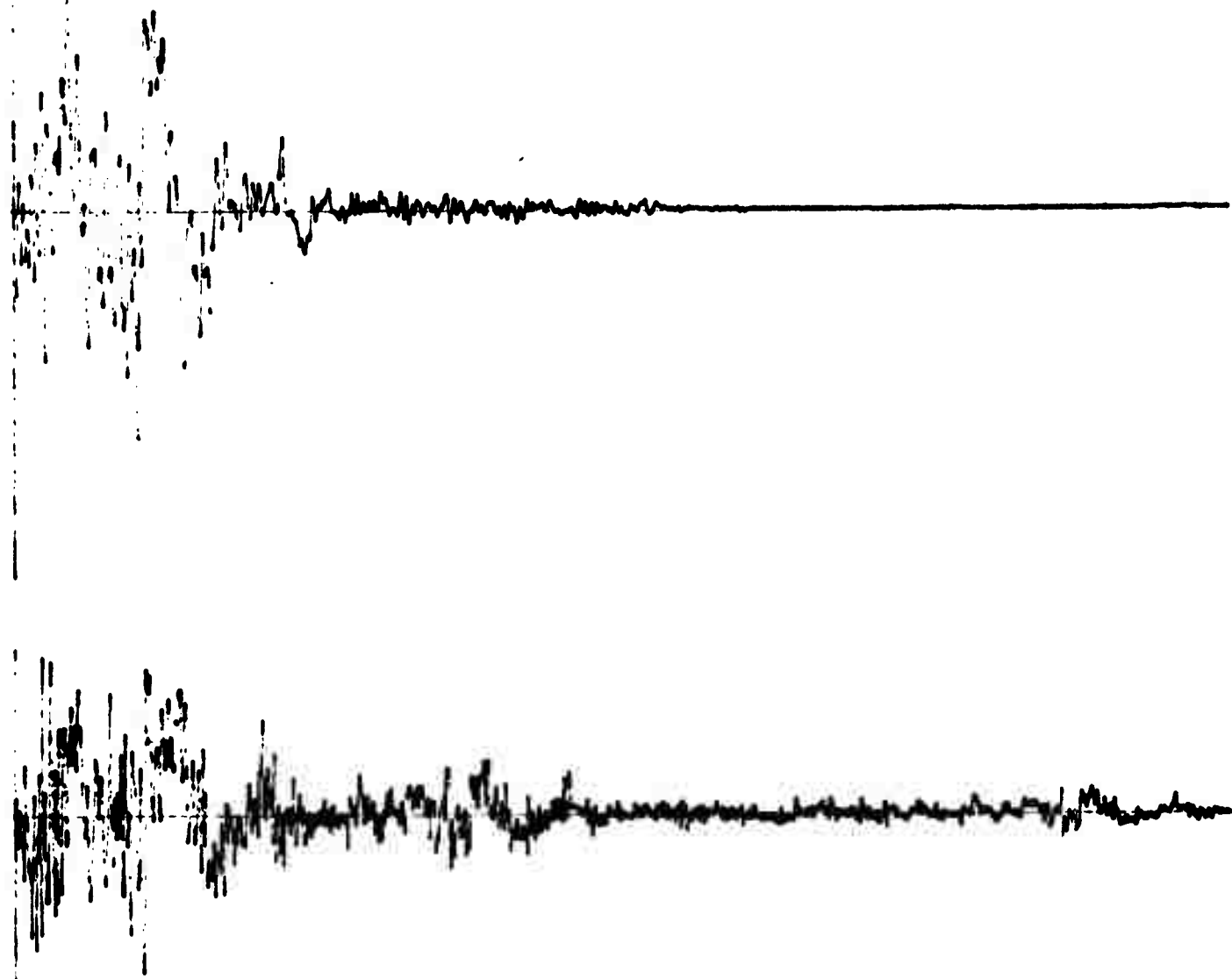
EVENT NUMBER 1266
EARTHQUAKE



Q212

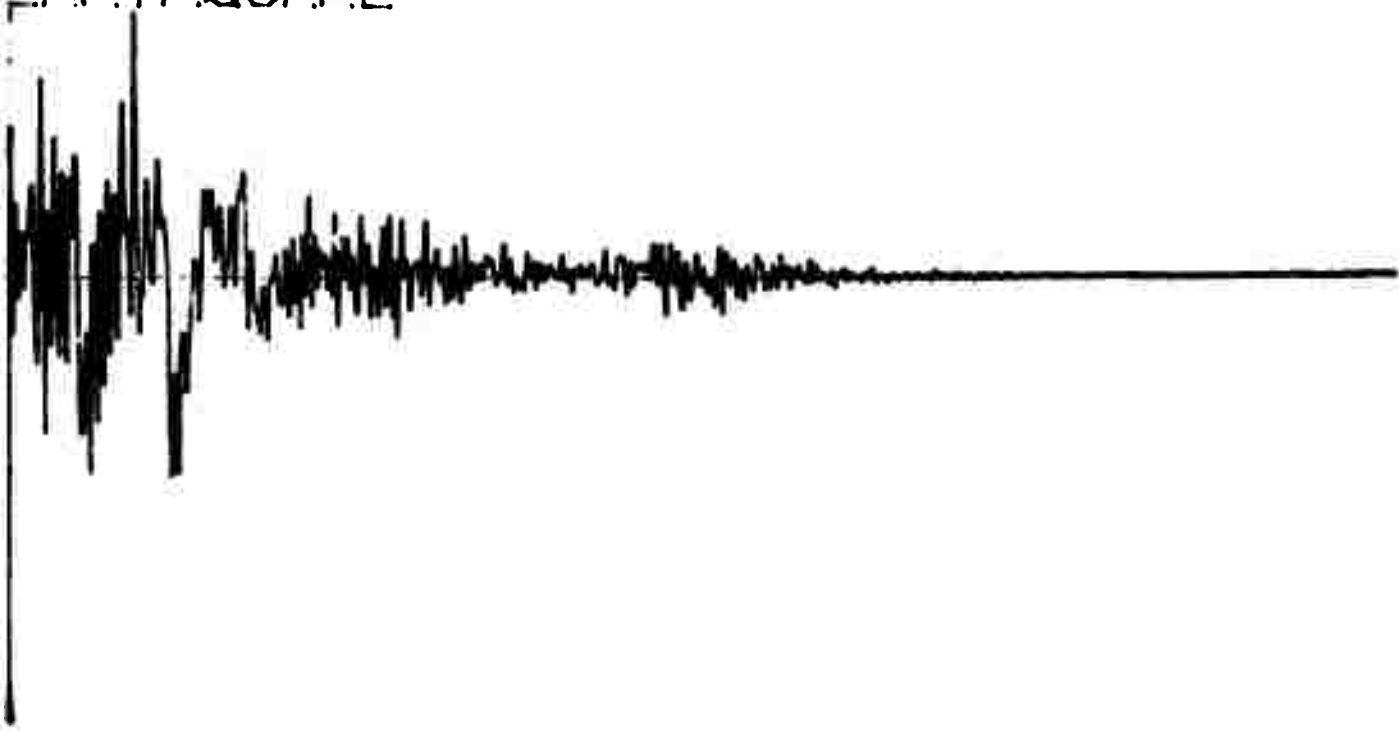
EVENT NUMBER 1272

EARTHQUAKE



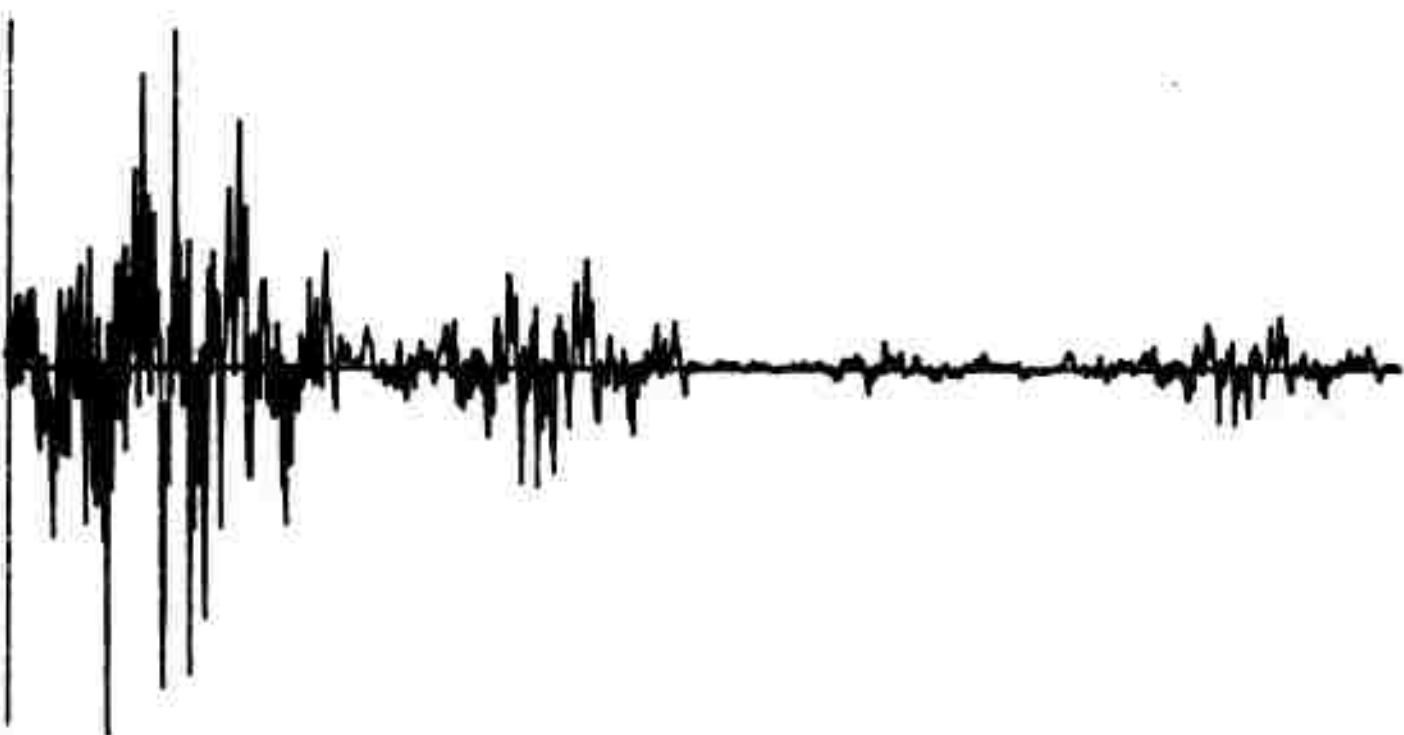
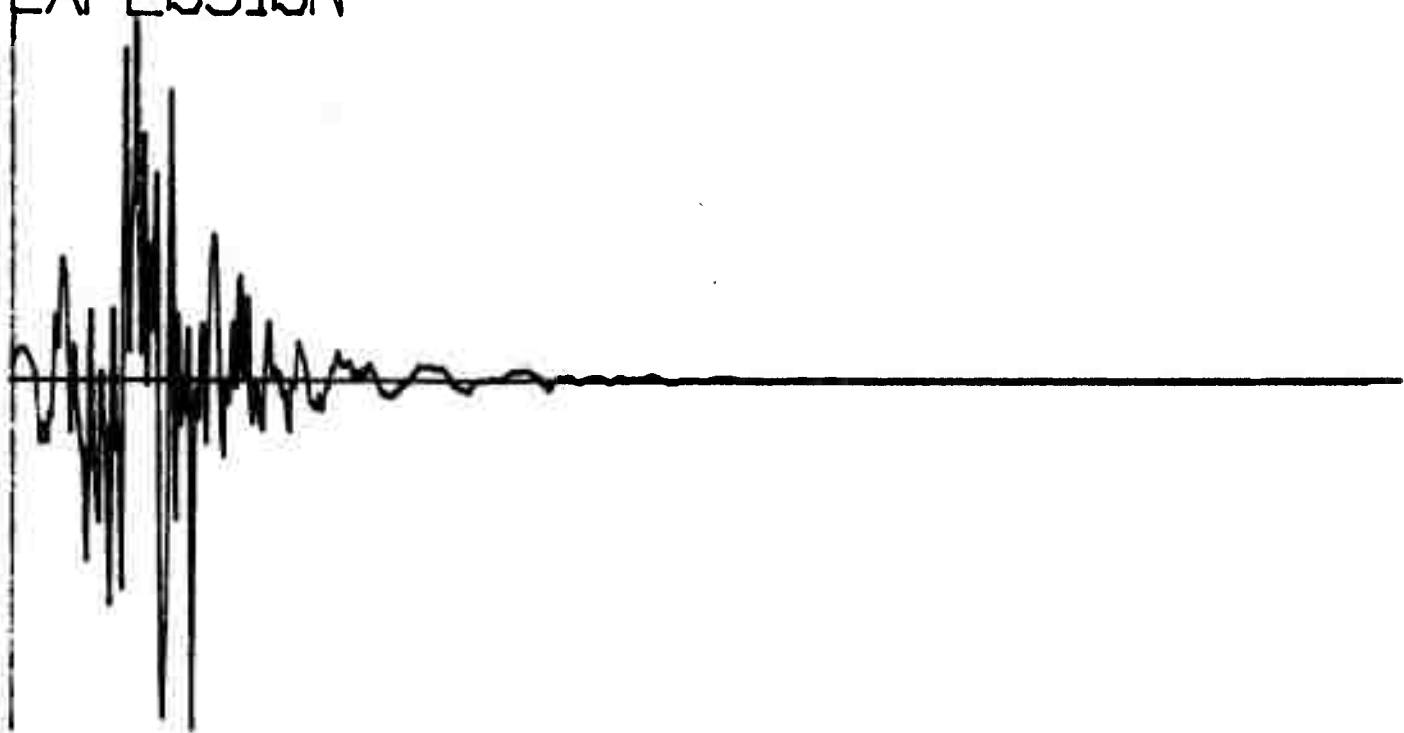
Q274

EVENT NUMBER 1273
EARTHQUAKE



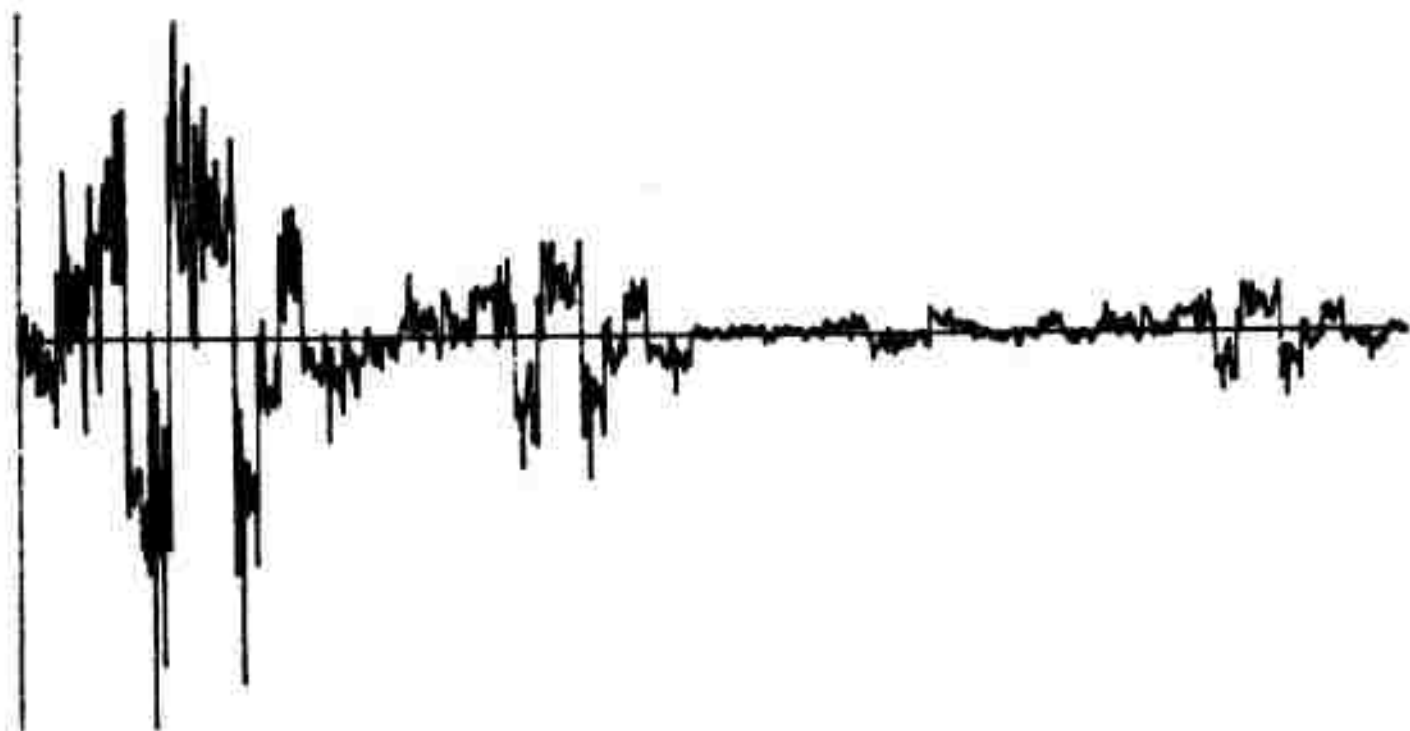
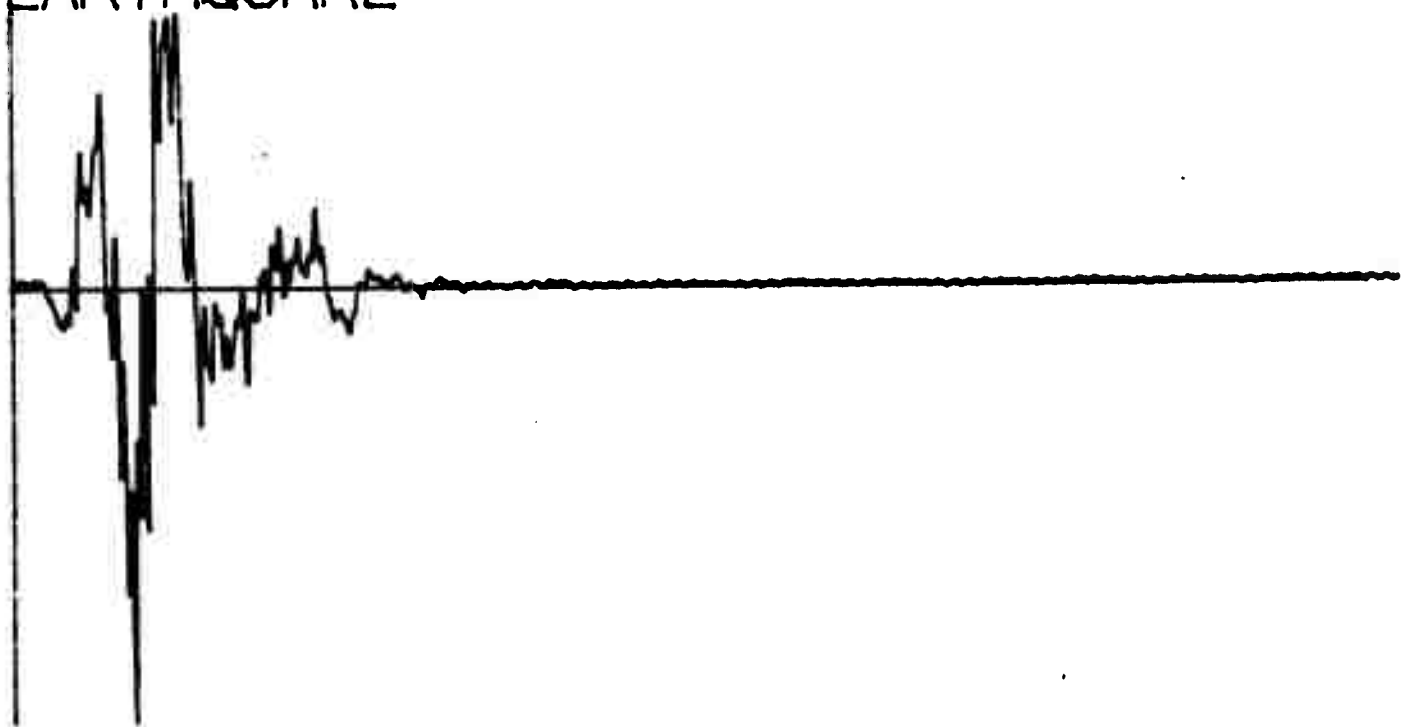
x276

EVENT NUMBER 1516
EXPLOSION



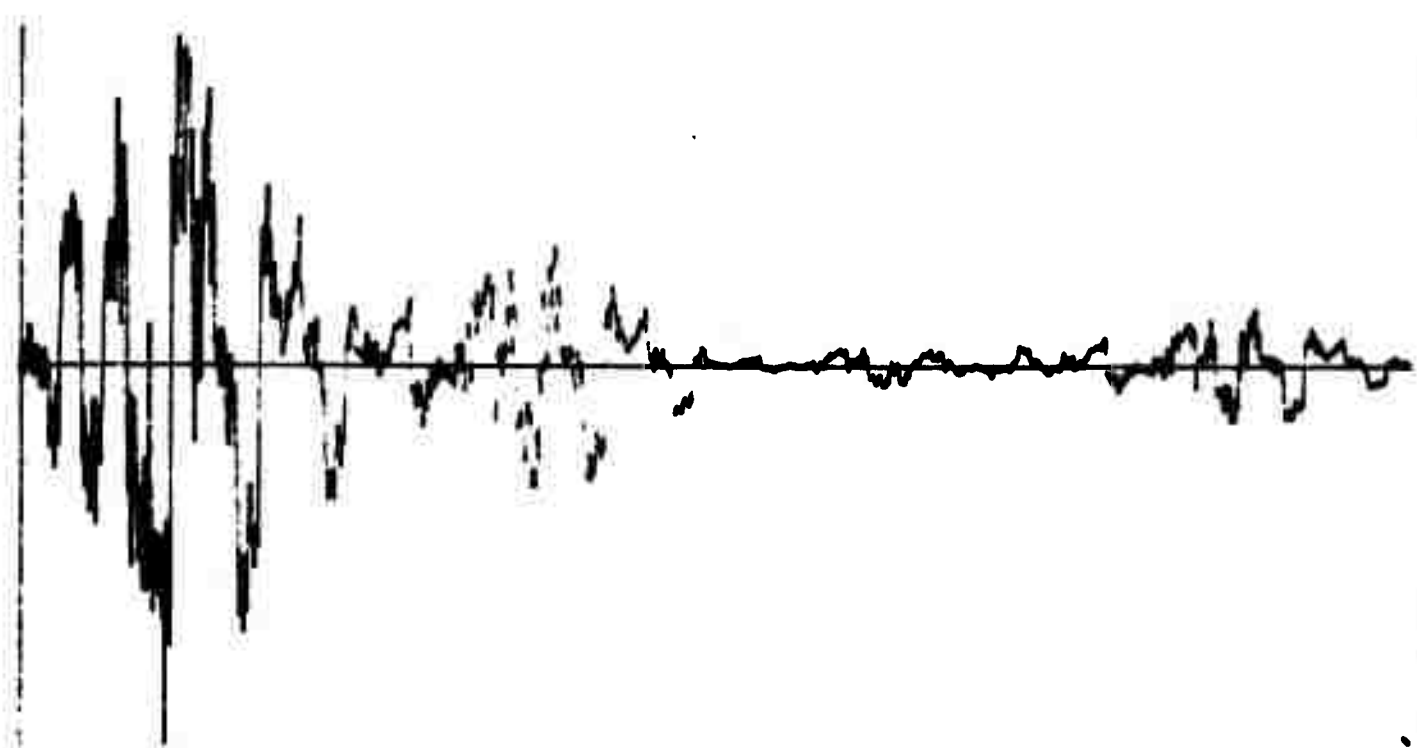
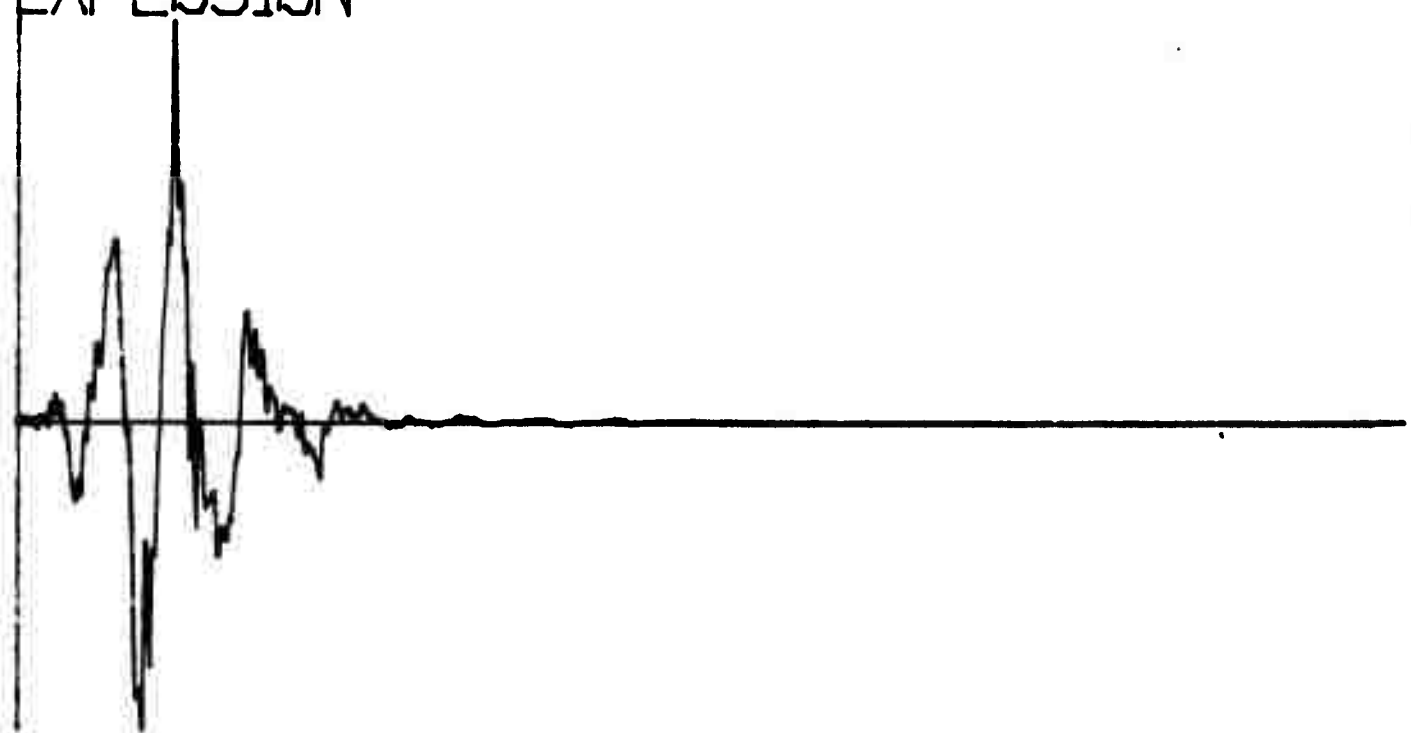
Q278

EVENT NUMBER 1543
EARTHQUAKE



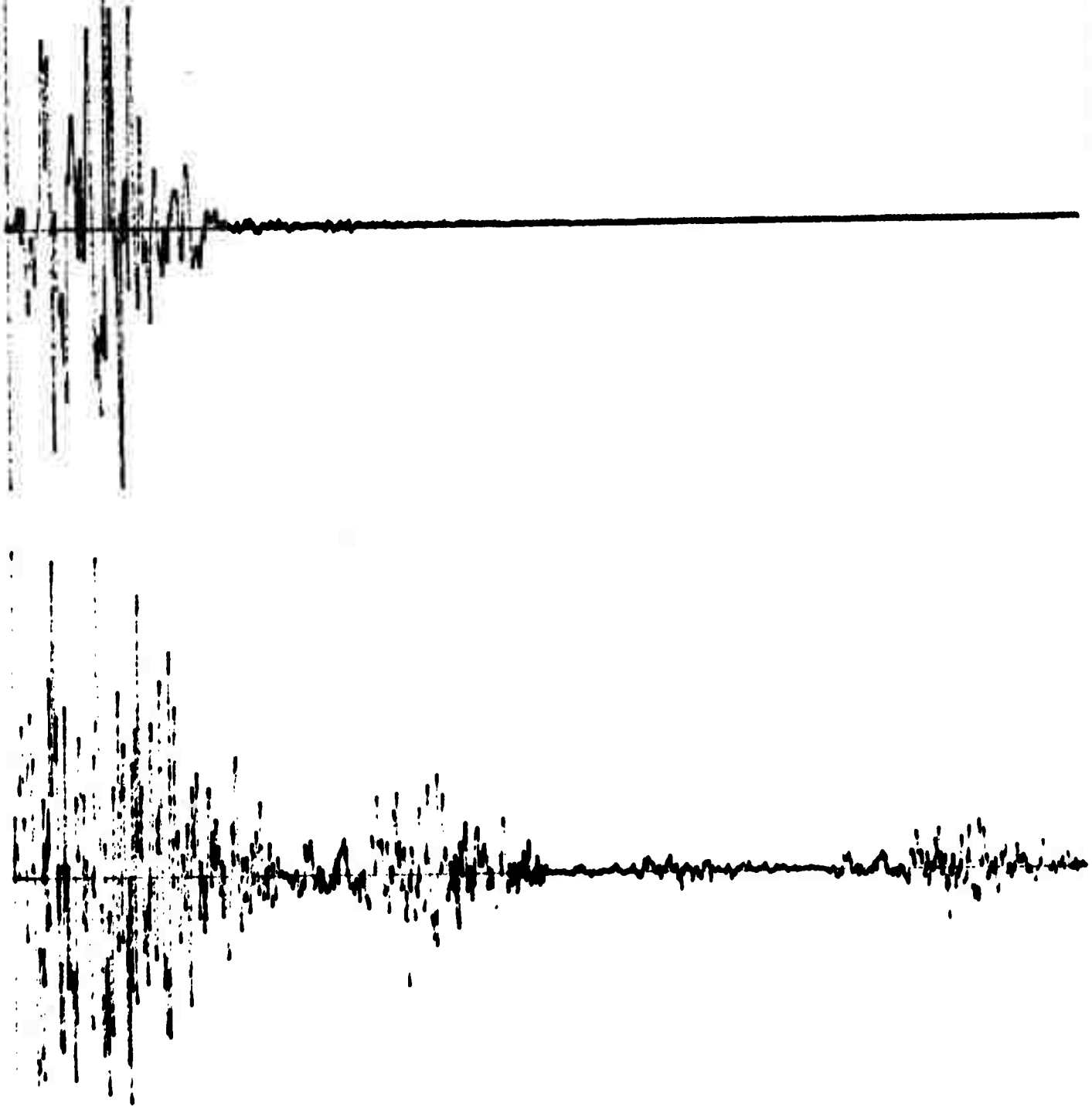
x280

EVENT NUMBER 1510
EXPLOSION



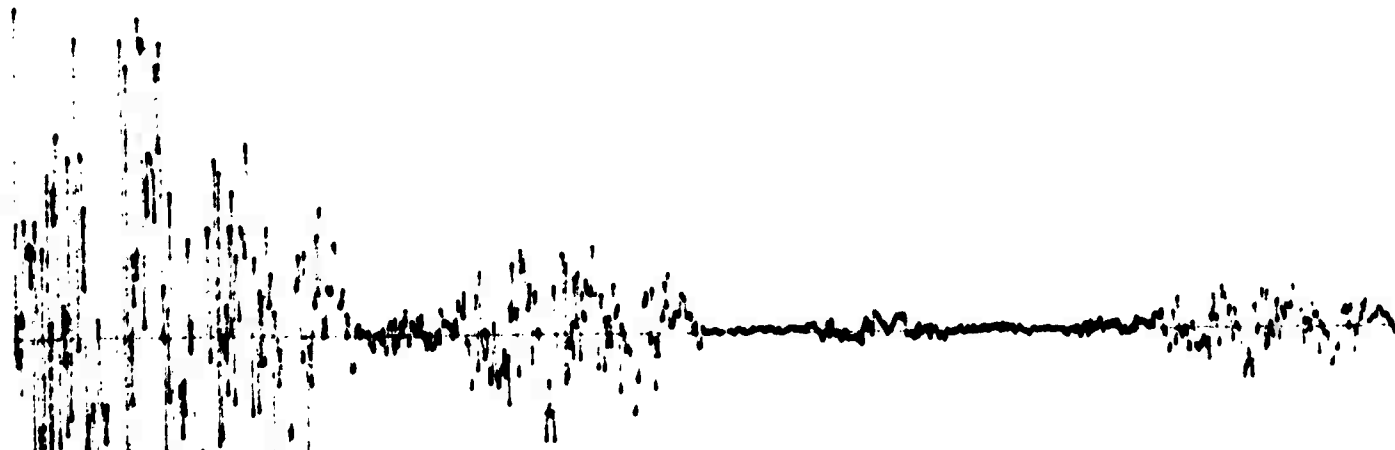
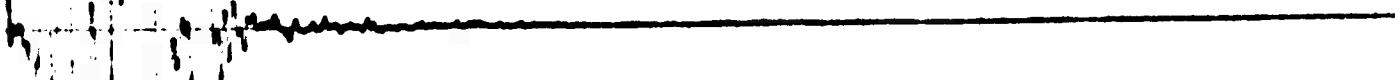
Q282

EVENT NUMBER 2021
EARTHQUAKE



Q284

EVENT NUMBER 2013
EARTHQUAKE



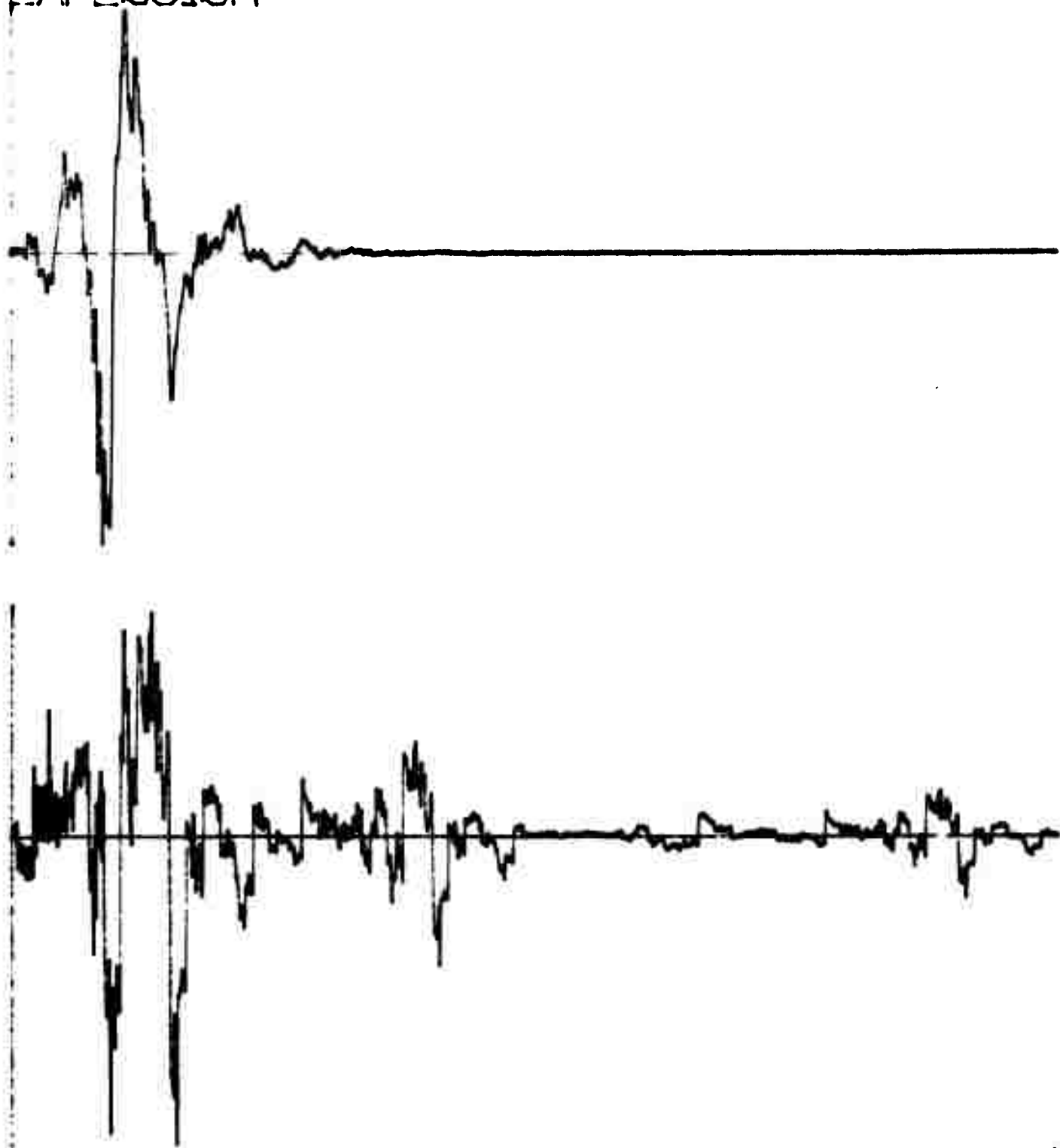
Q286

1ST MURDER 2000
2nd MURDER 2002.

EDTITUDE

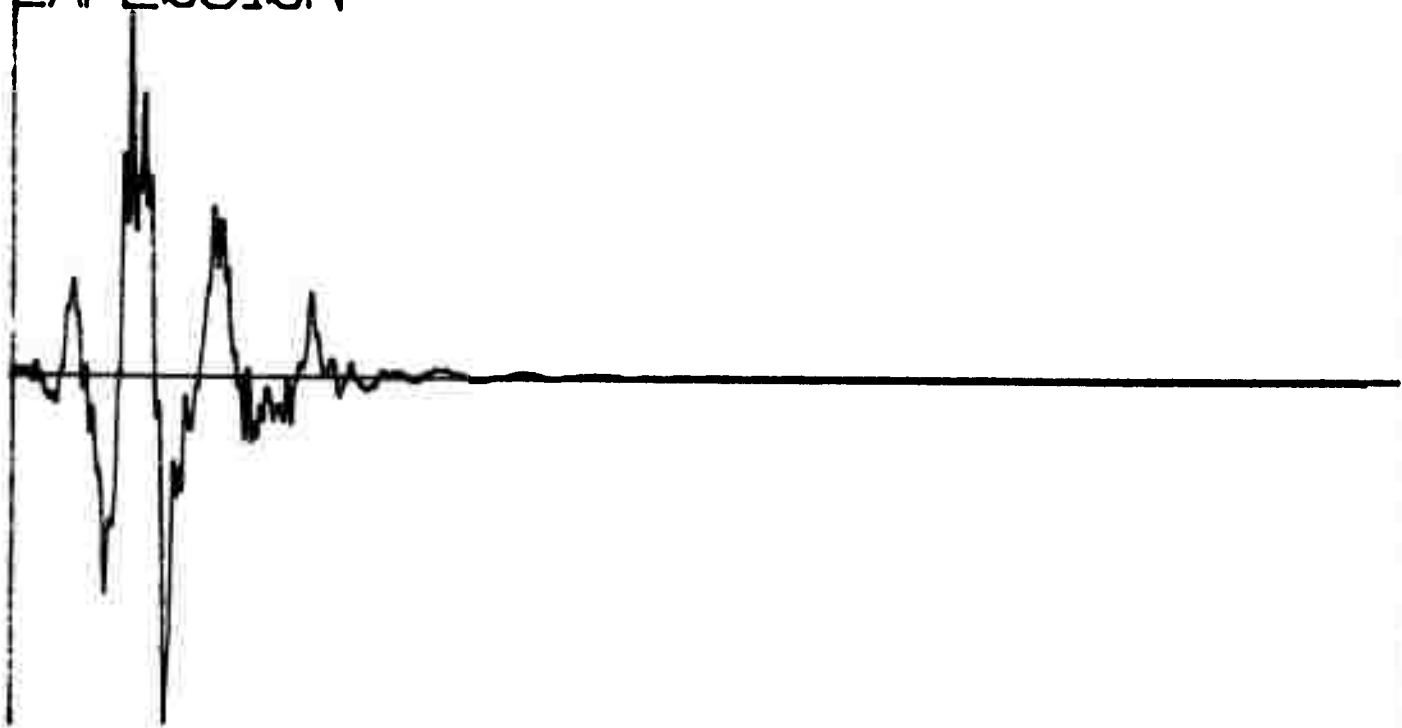
x288

EVENT NUMBER 1505
EXPLOSION



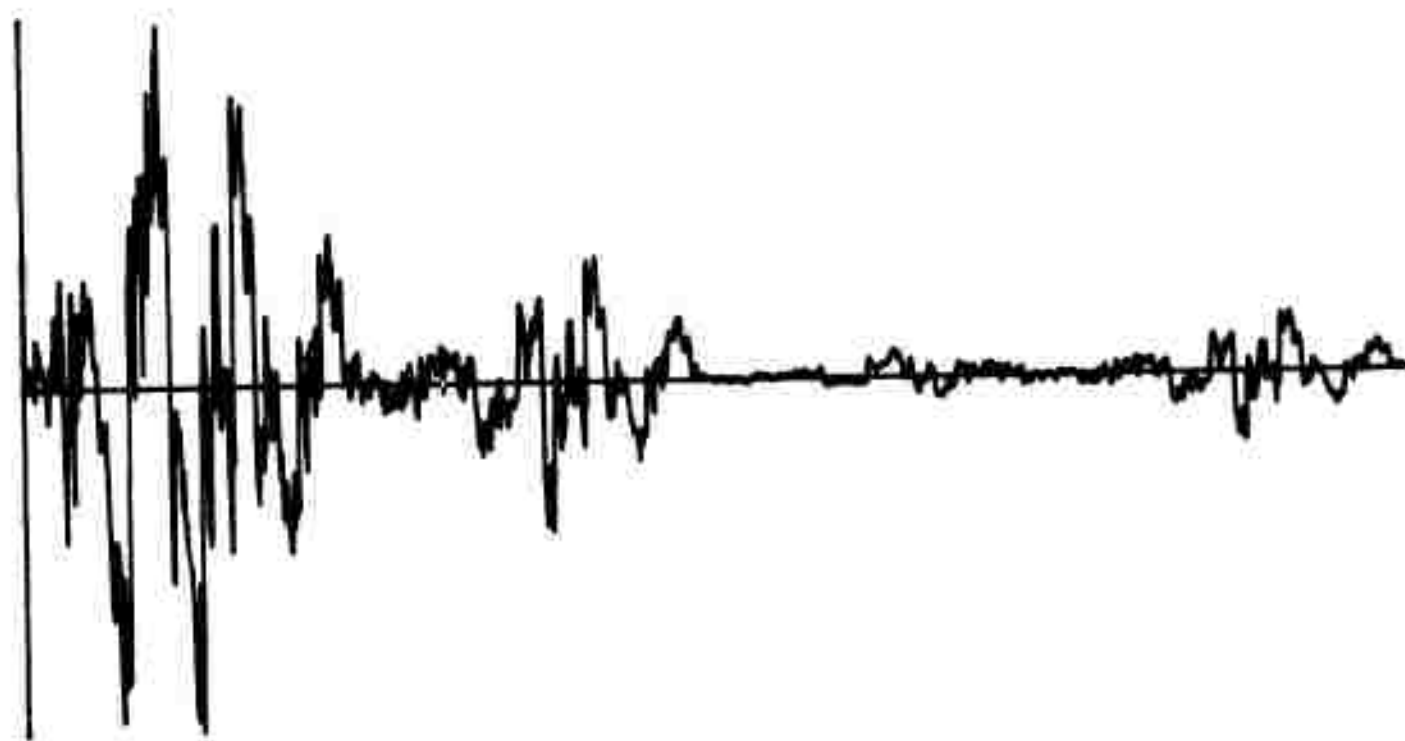
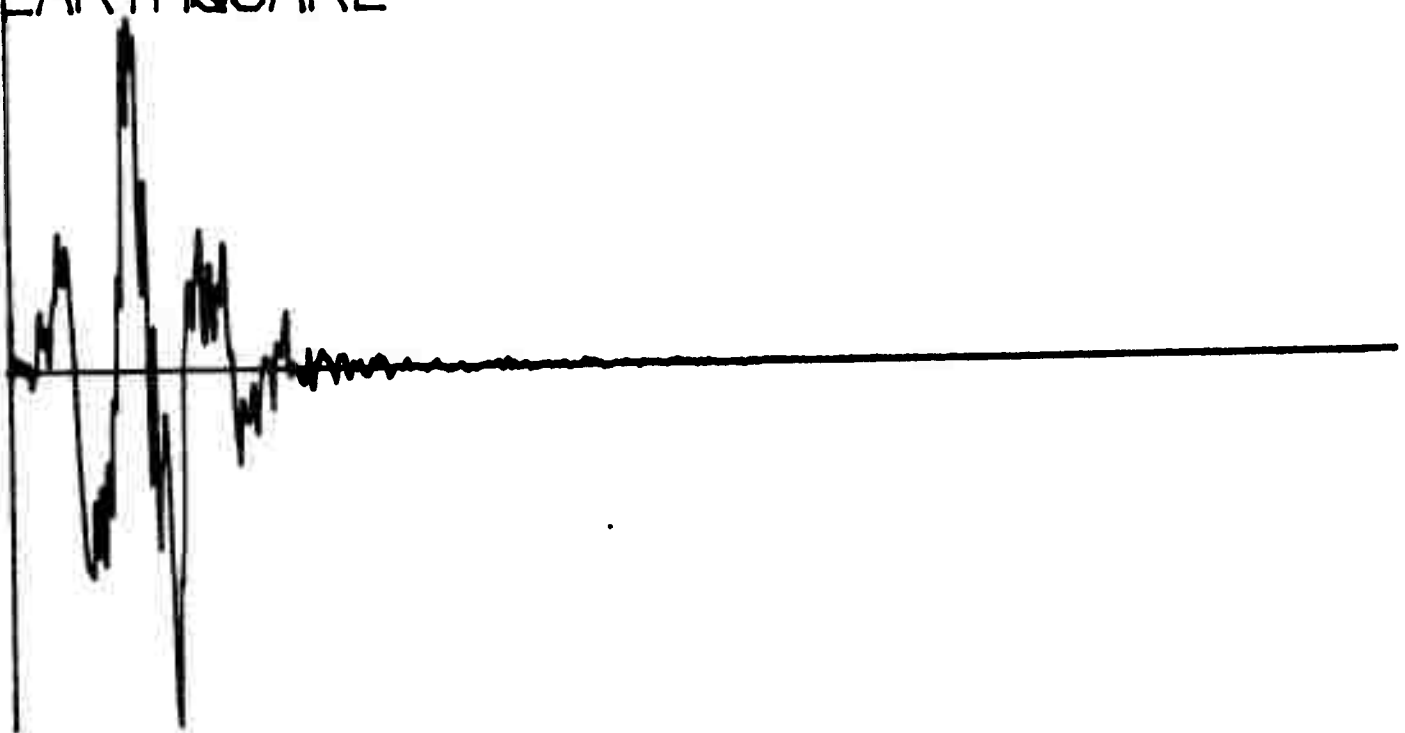
X290

EVENT NUMBER 1503
EXPLOSION



Q292

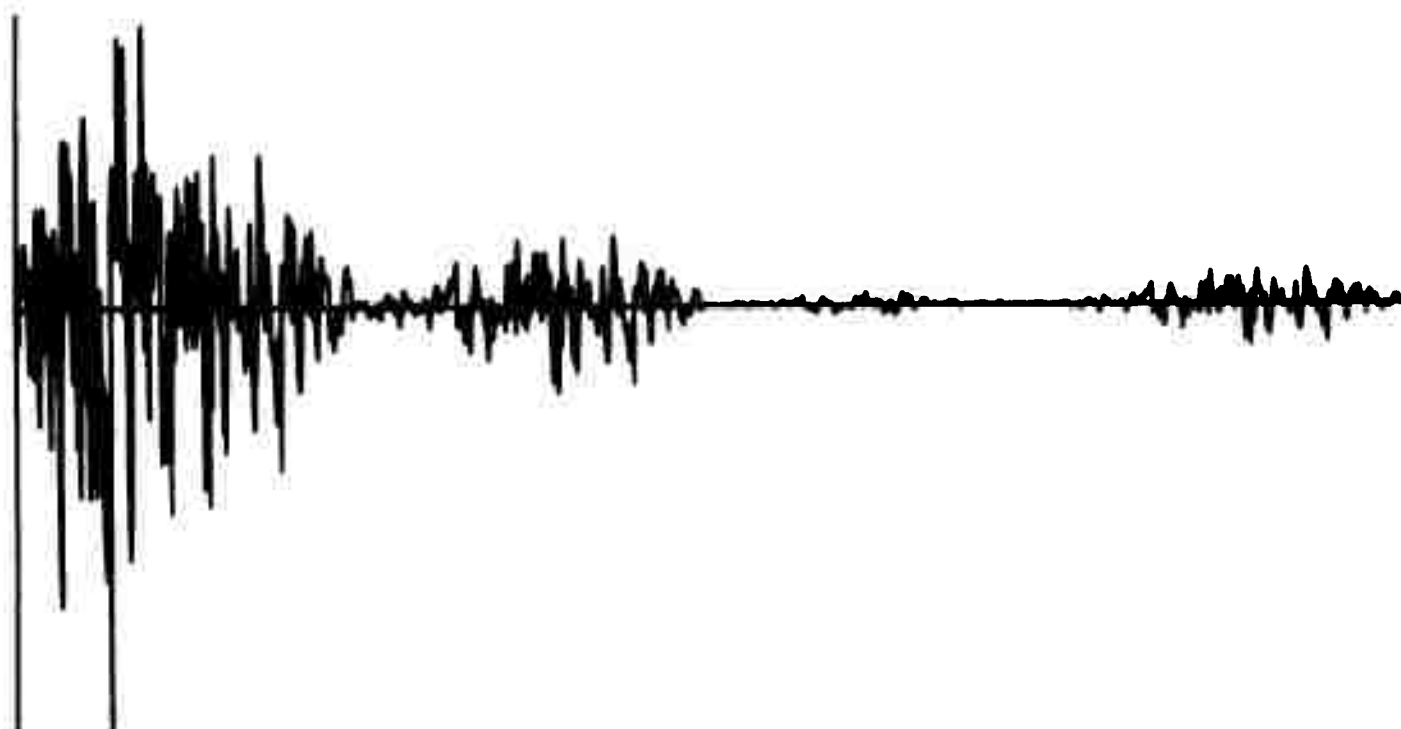
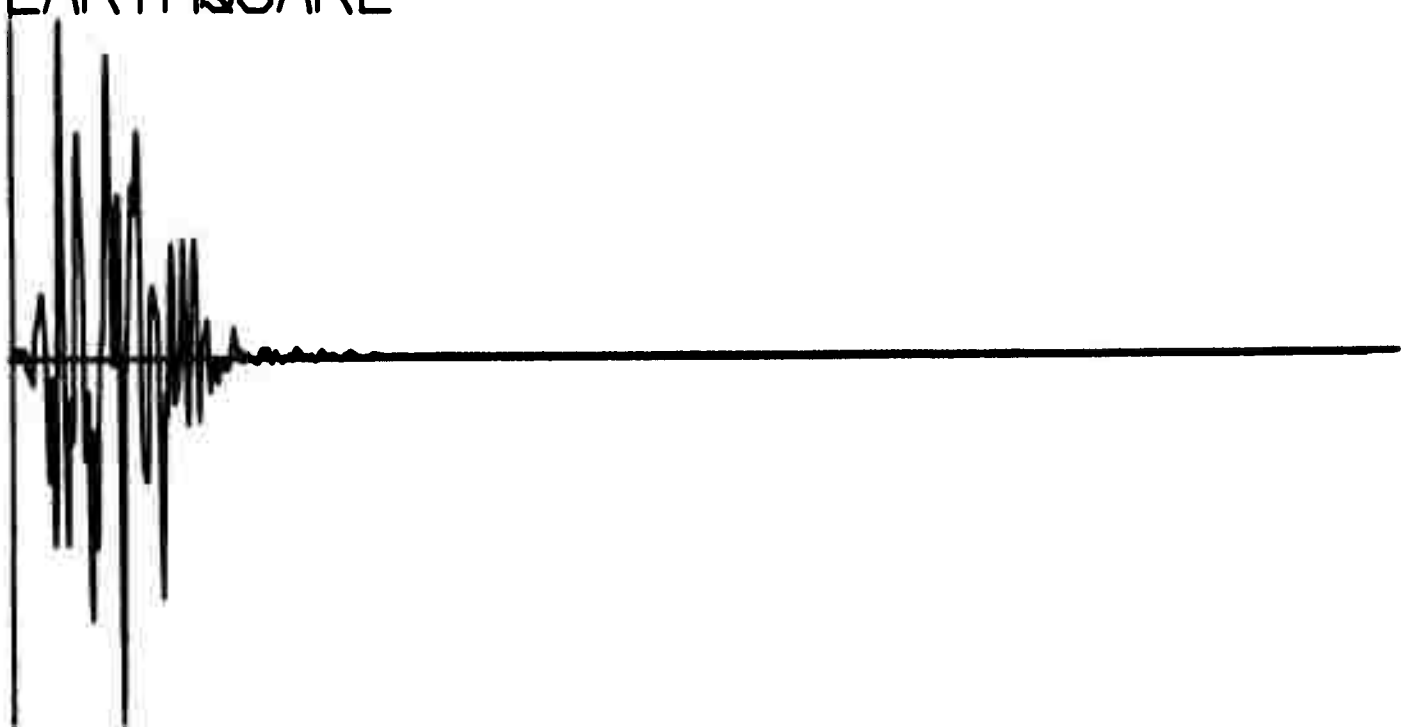
EVENT NUMBER 2004 EARTHQUAKE



Q294

EVENT NUMBER 2007

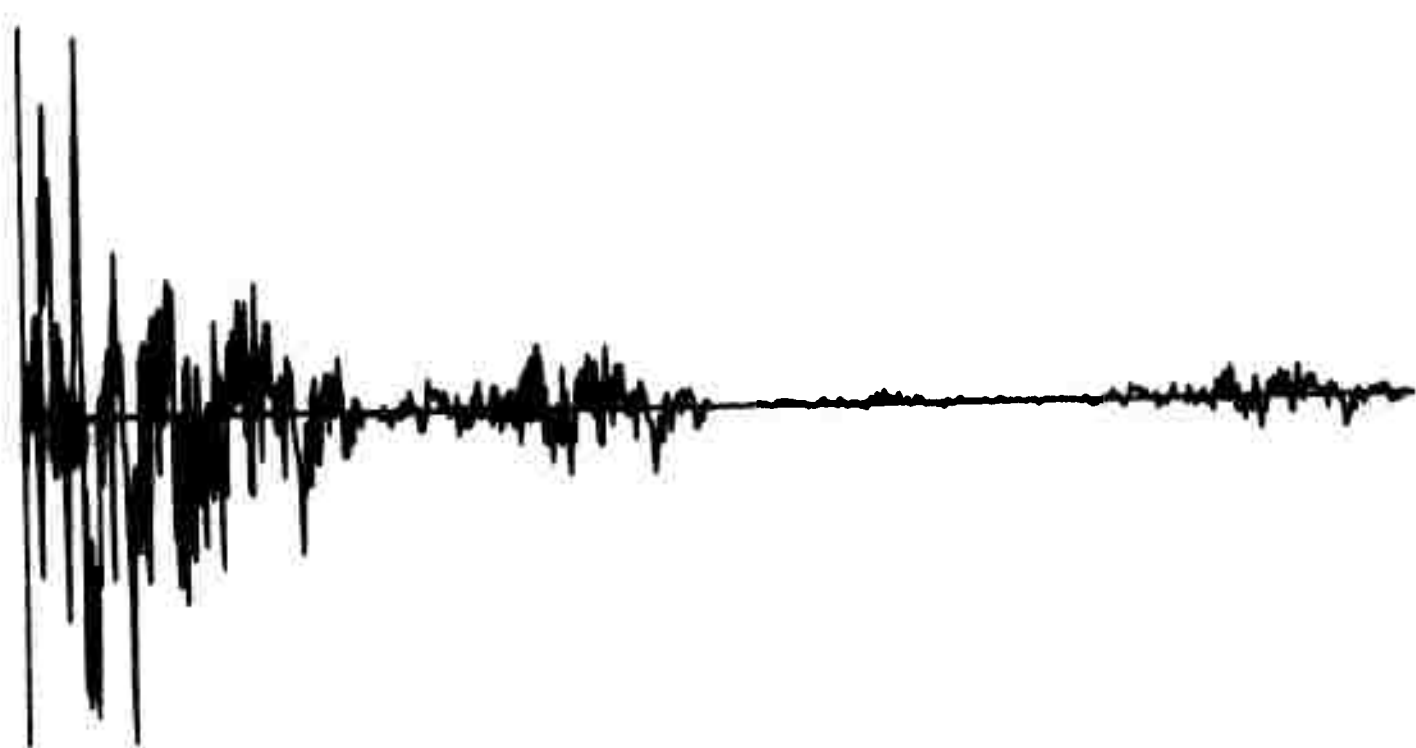
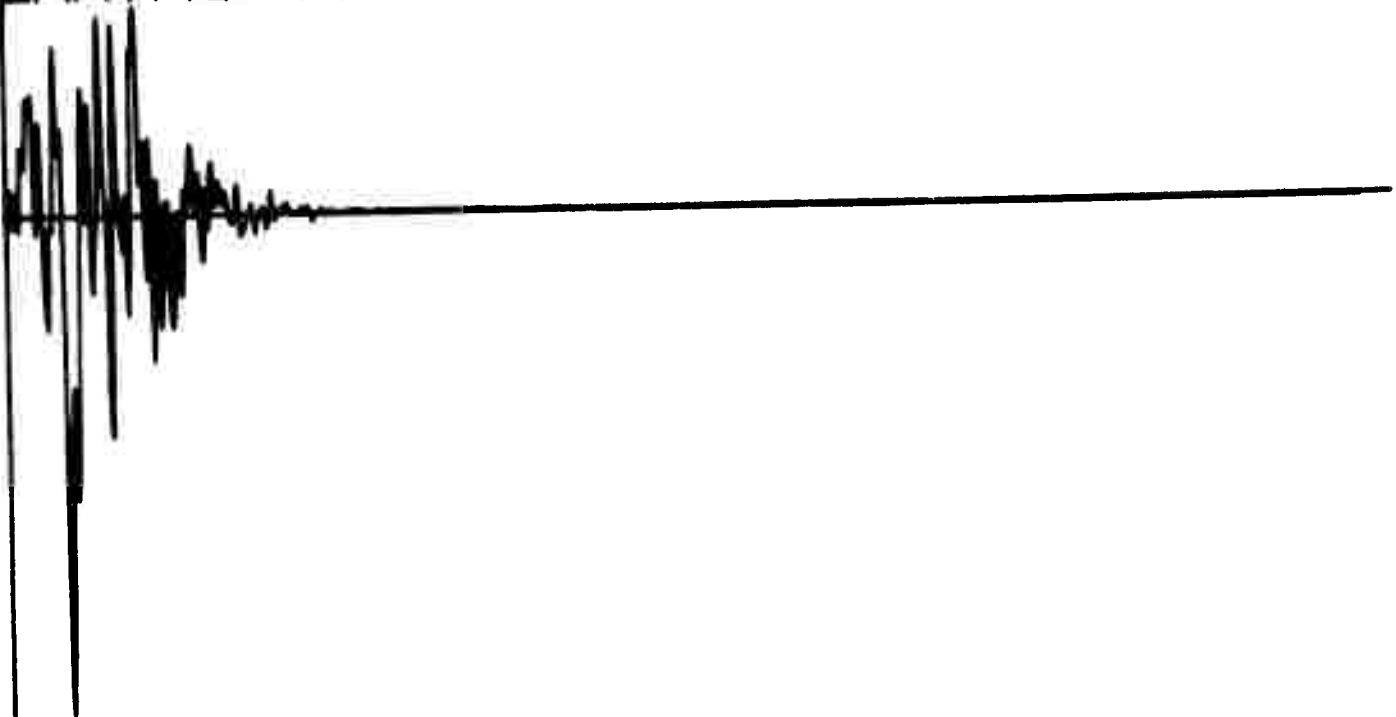
EARTHQUAKE



Q296

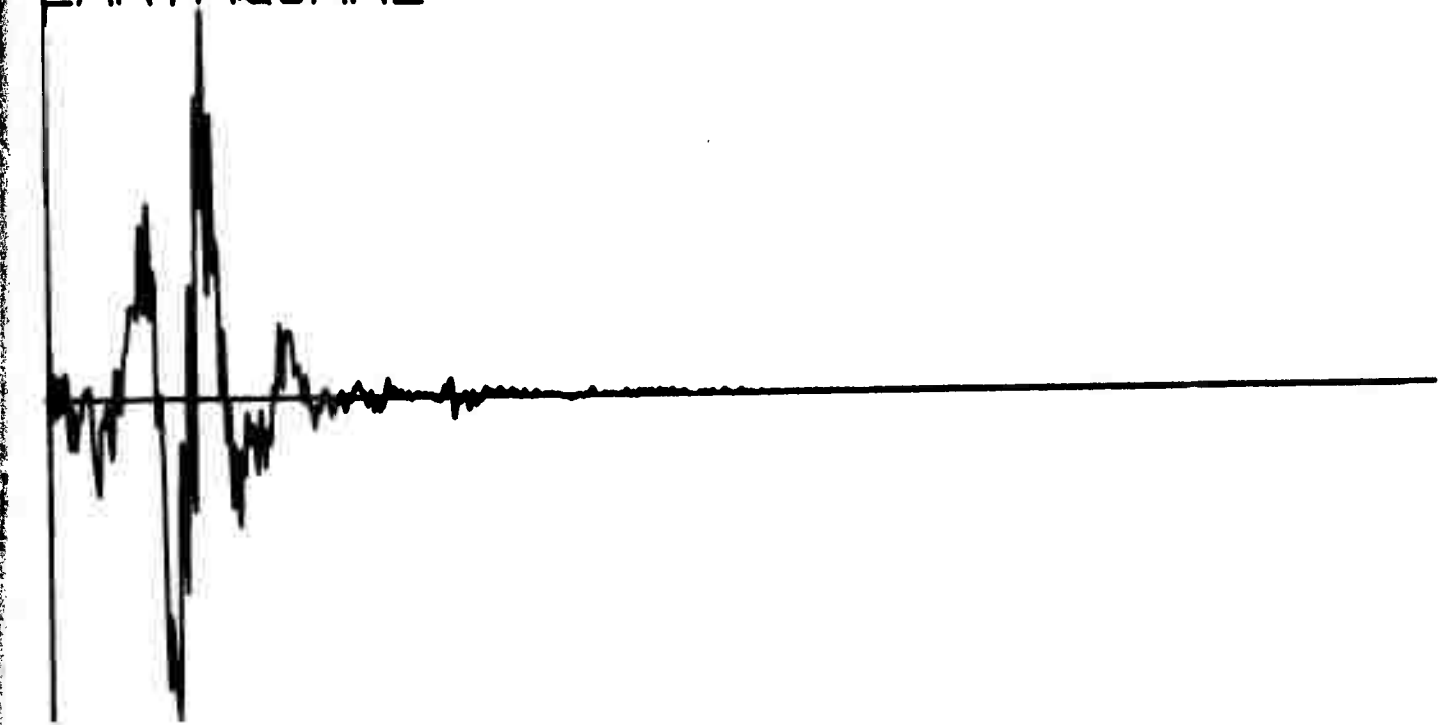
EVENT NUMBER 2015

EARTHQUAKE



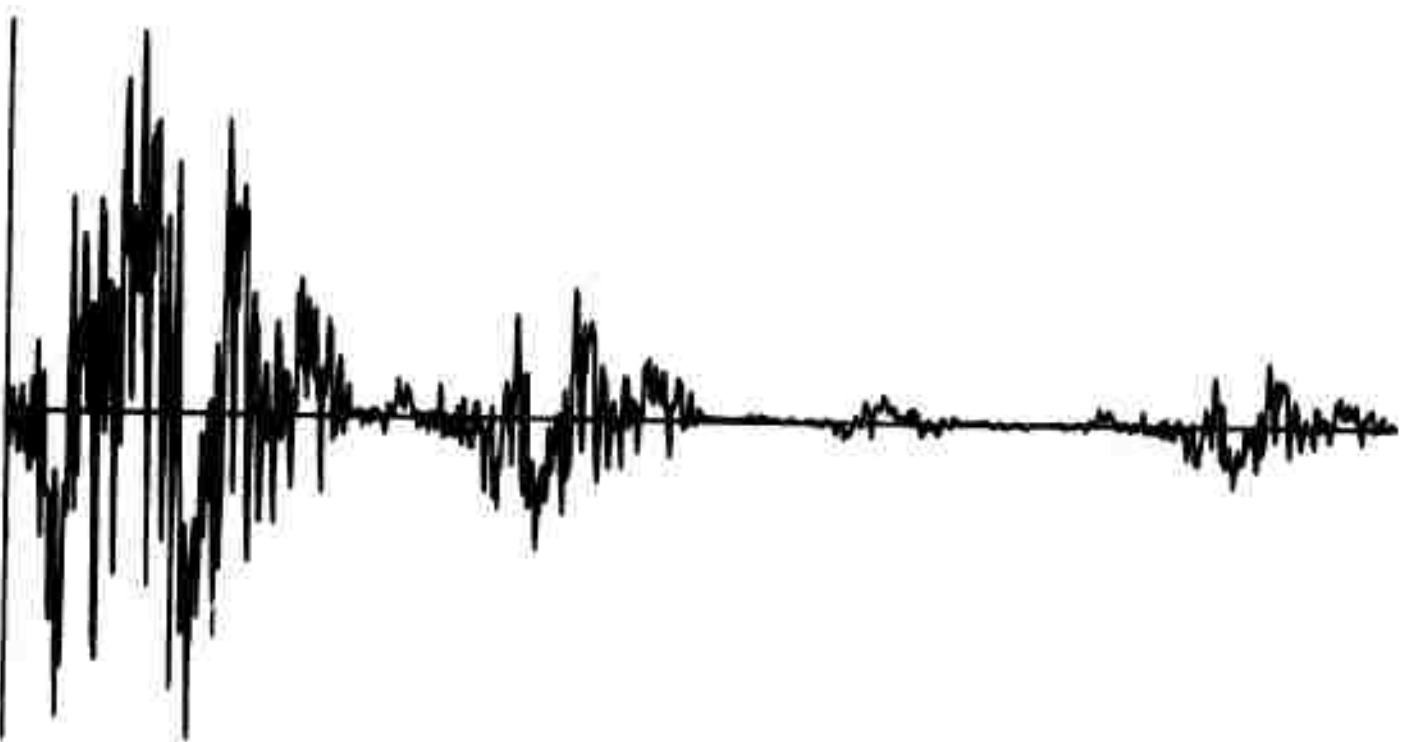
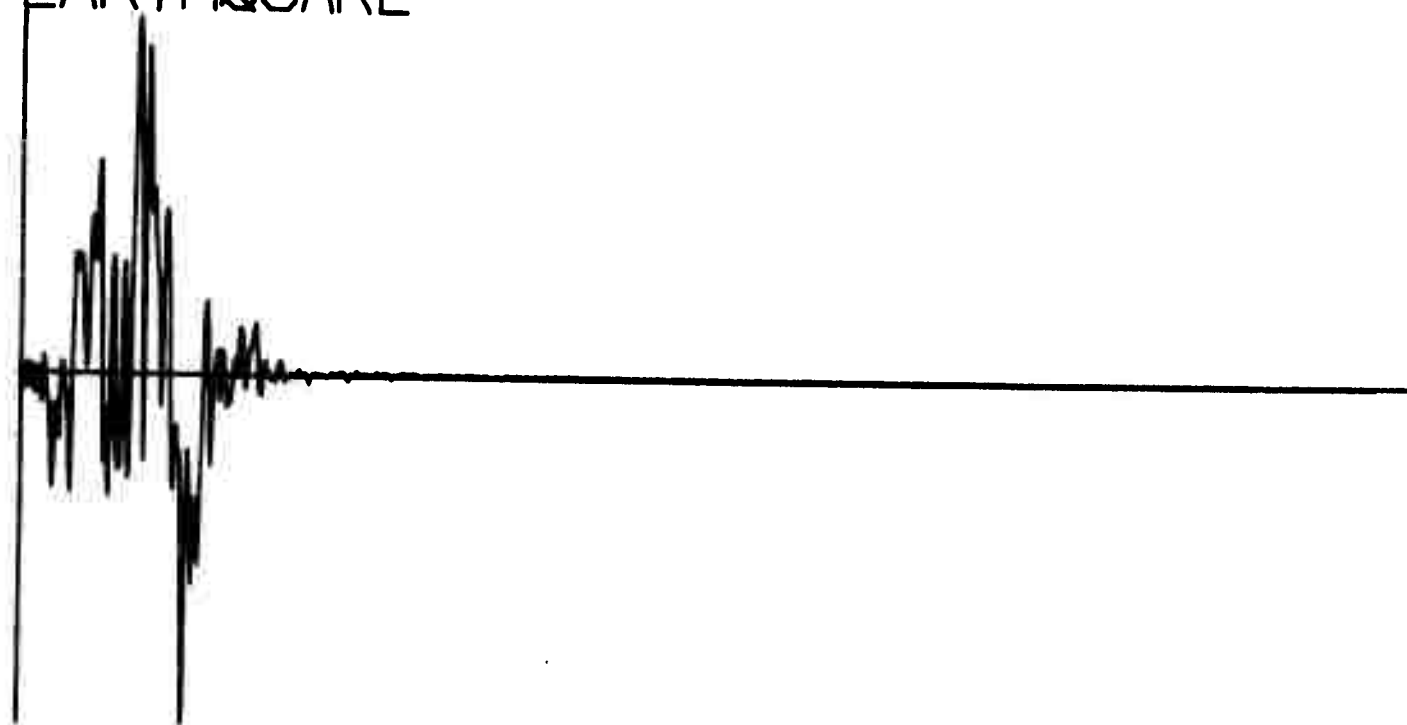
Q298

EVENT NUMBER 1300
EARTHQUAKE



EVENT NUMBER 1301
EARTHQUAKE

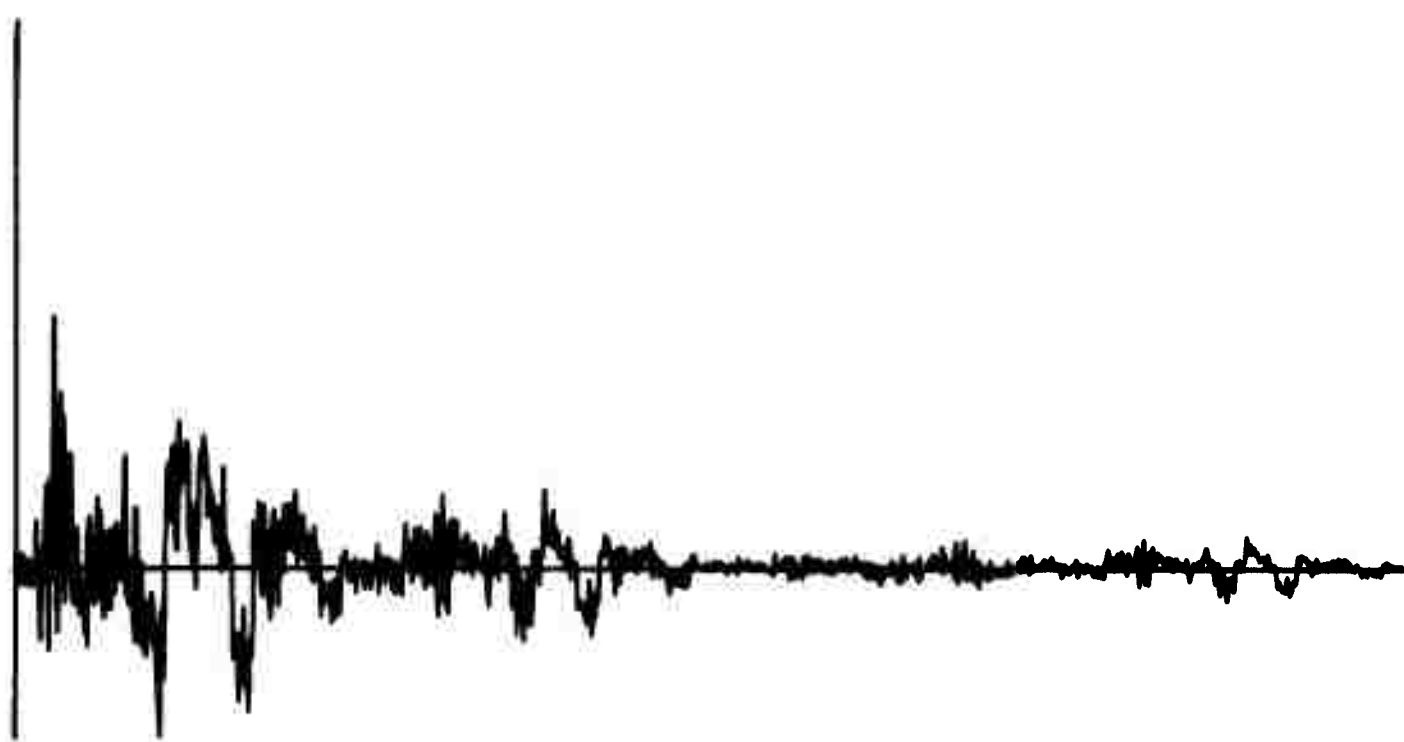
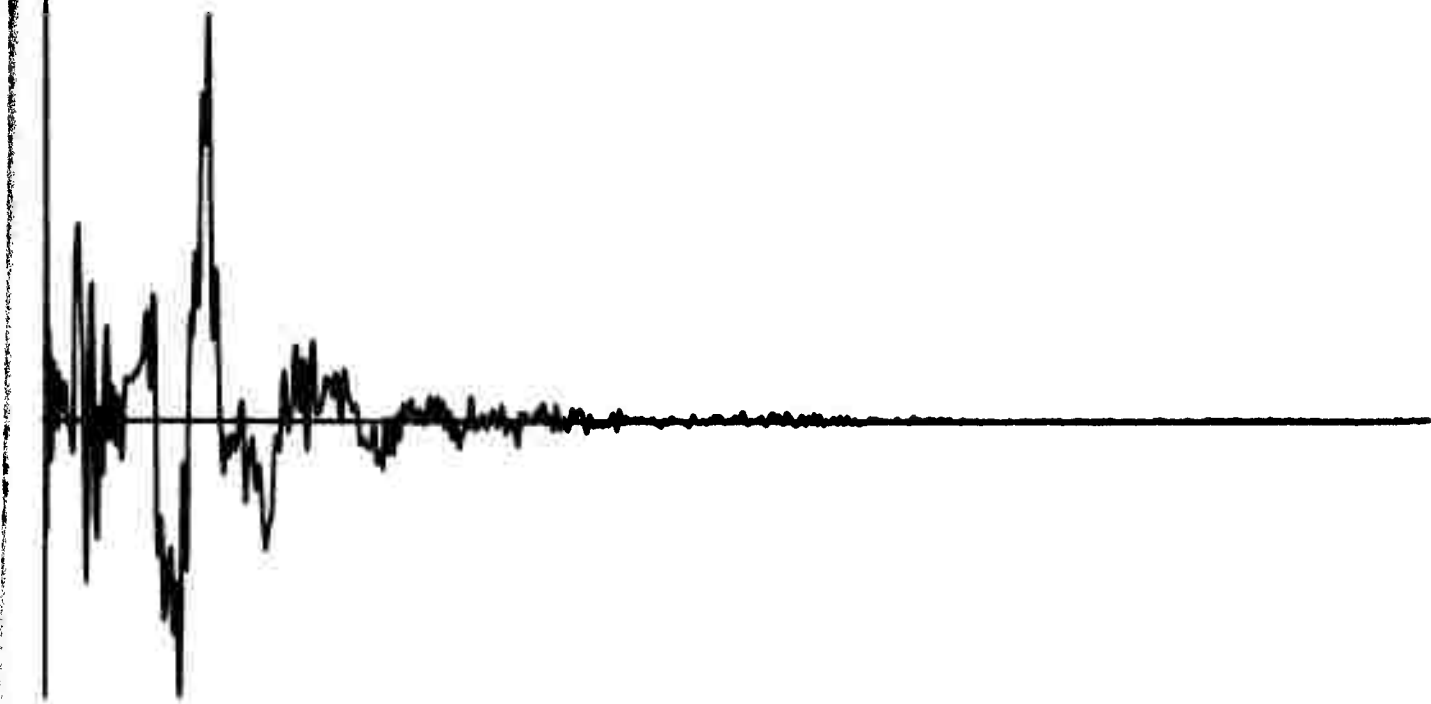
Q300



X302

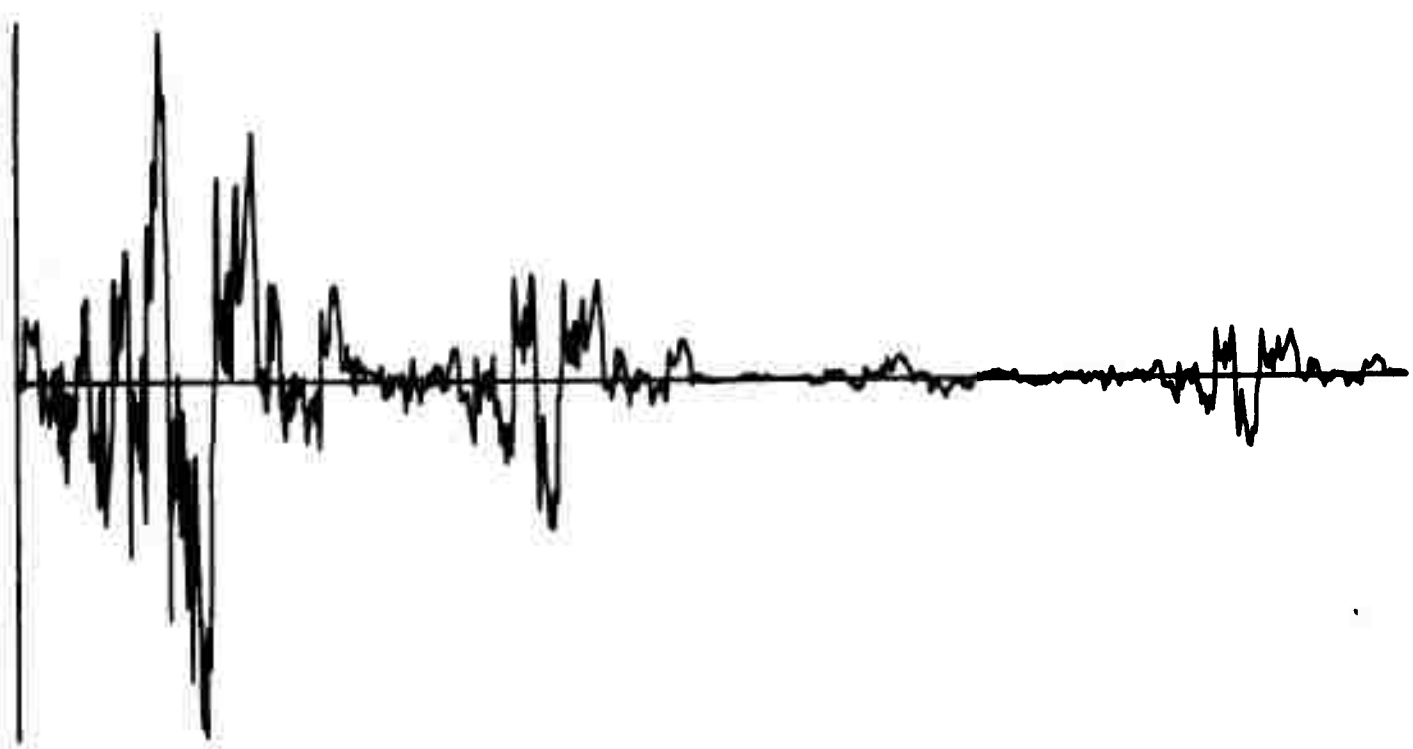
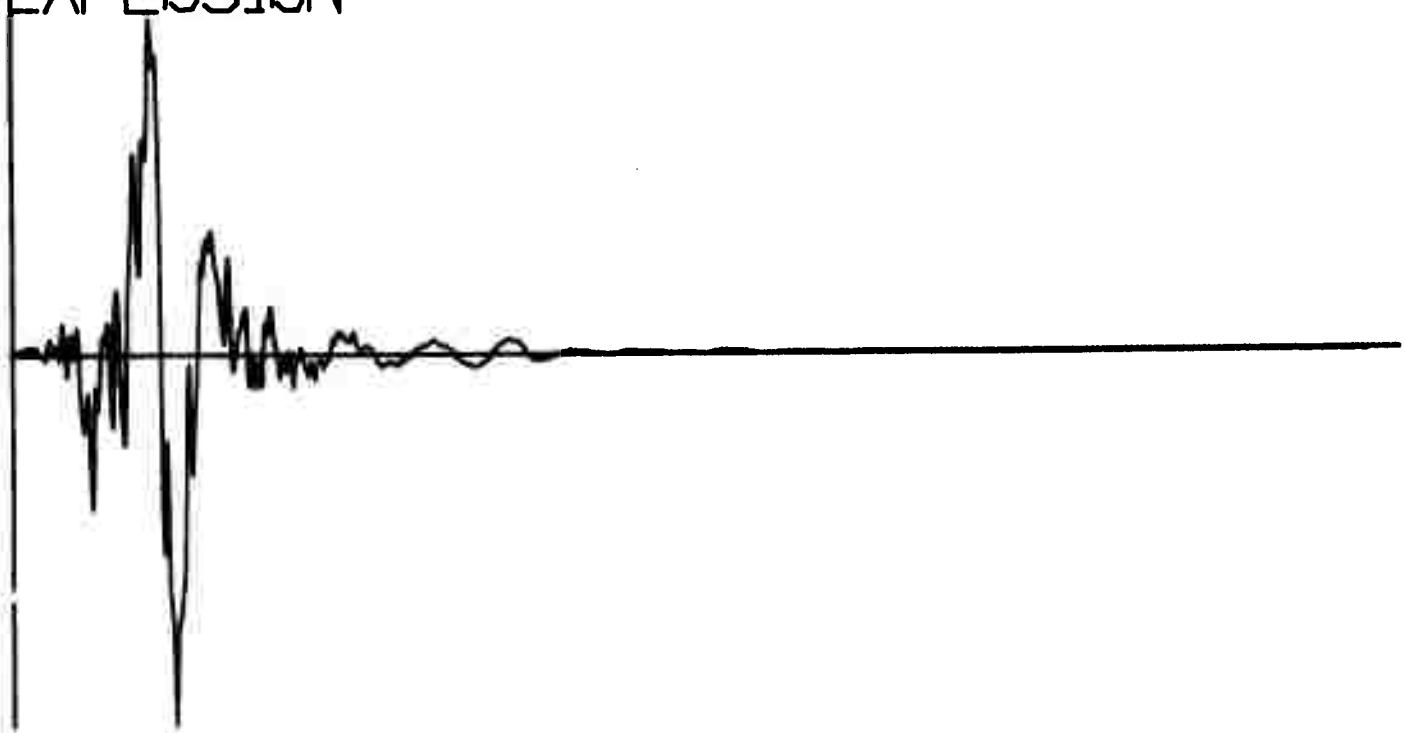
EVENT NUMBER 1535

EXPLOSION



X304

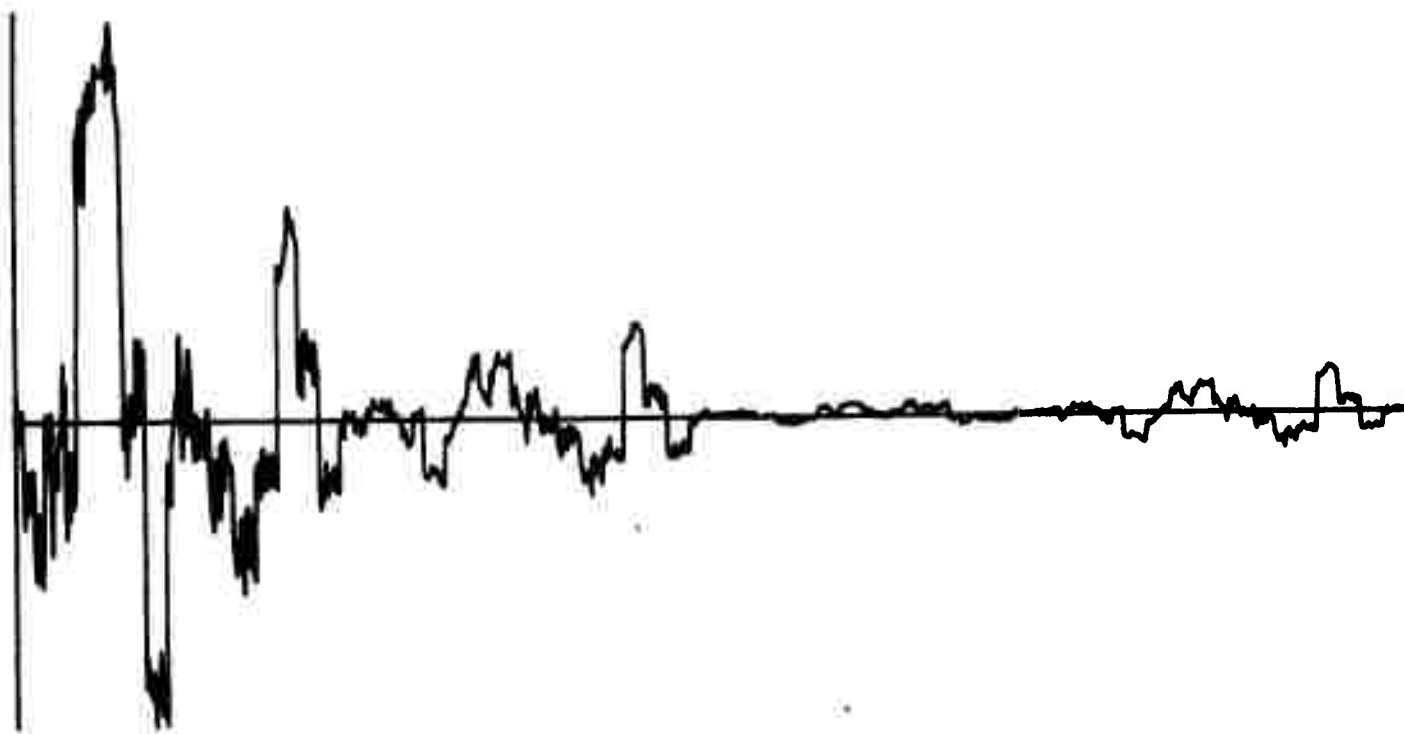
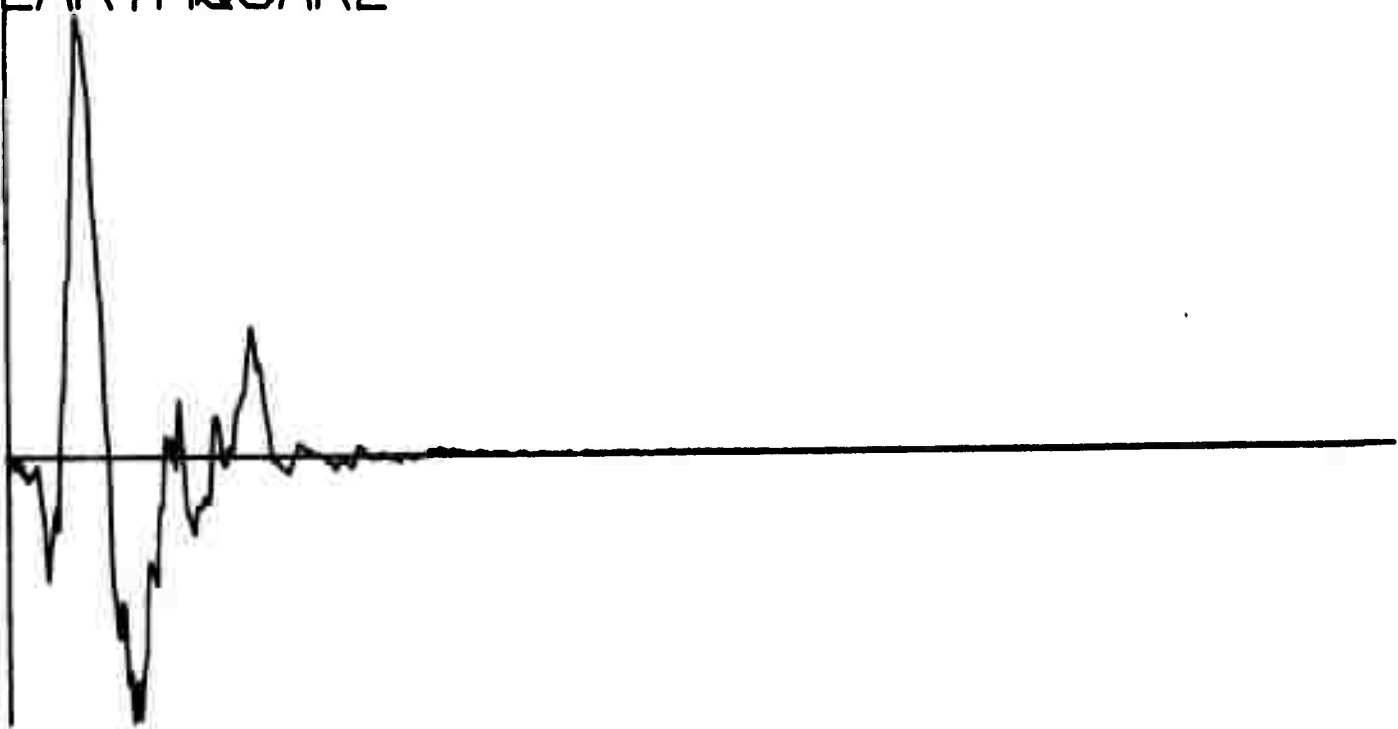
EVENT NUMBER 1506
EXPLOSION



Q306

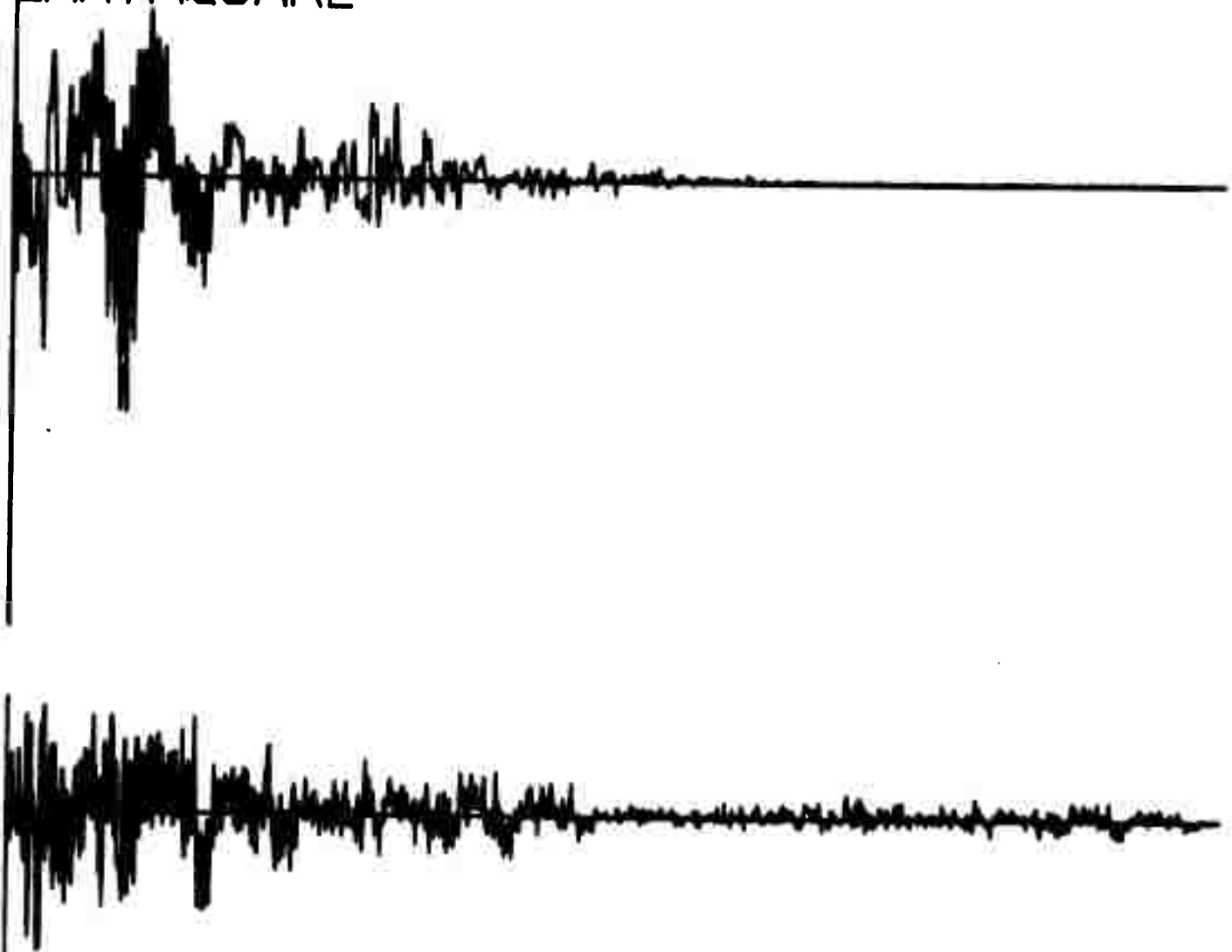
EVENT NUMBER 2022

EARTHQUAKE



EVENT NUMBER 1310
EARTHQUAKE

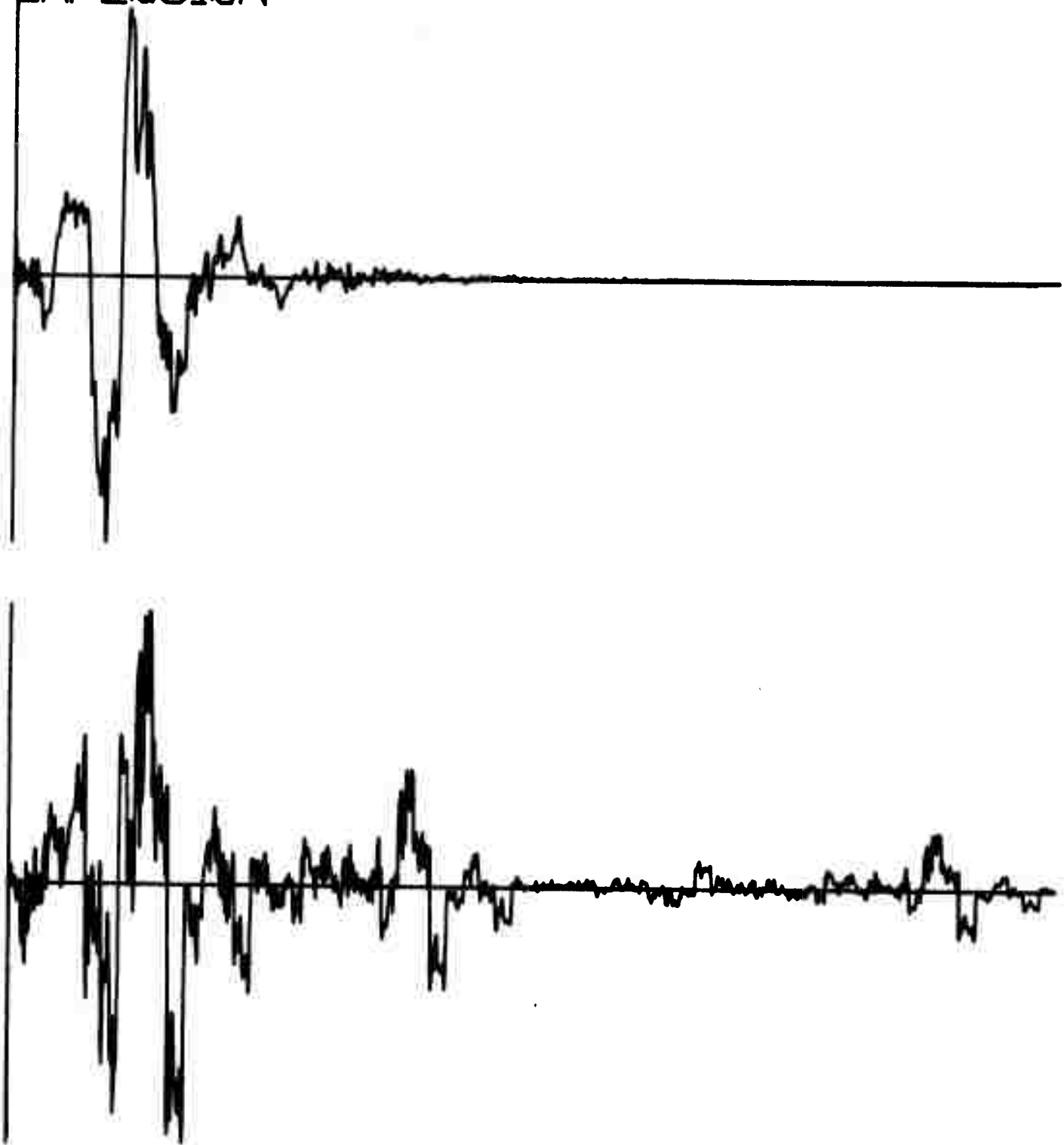
Q308



X310

EVENT NUMBER 1542

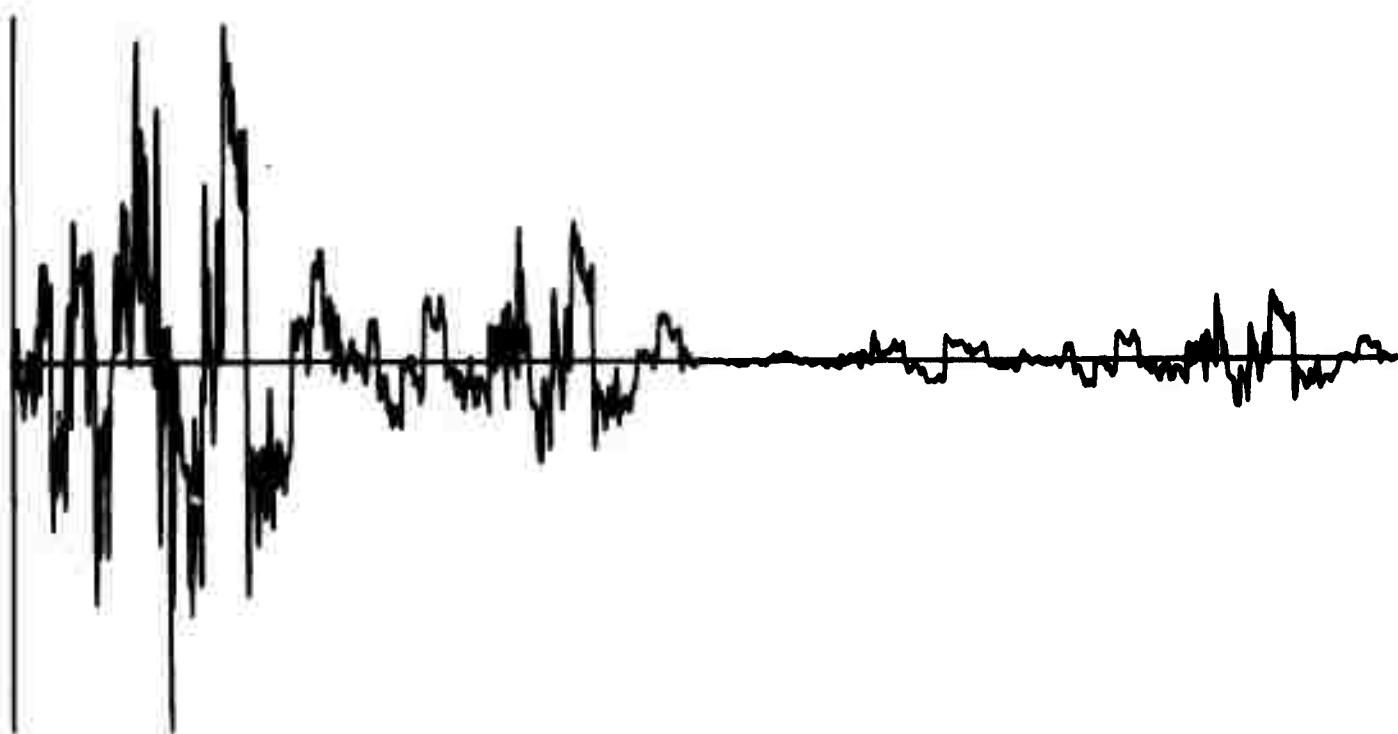
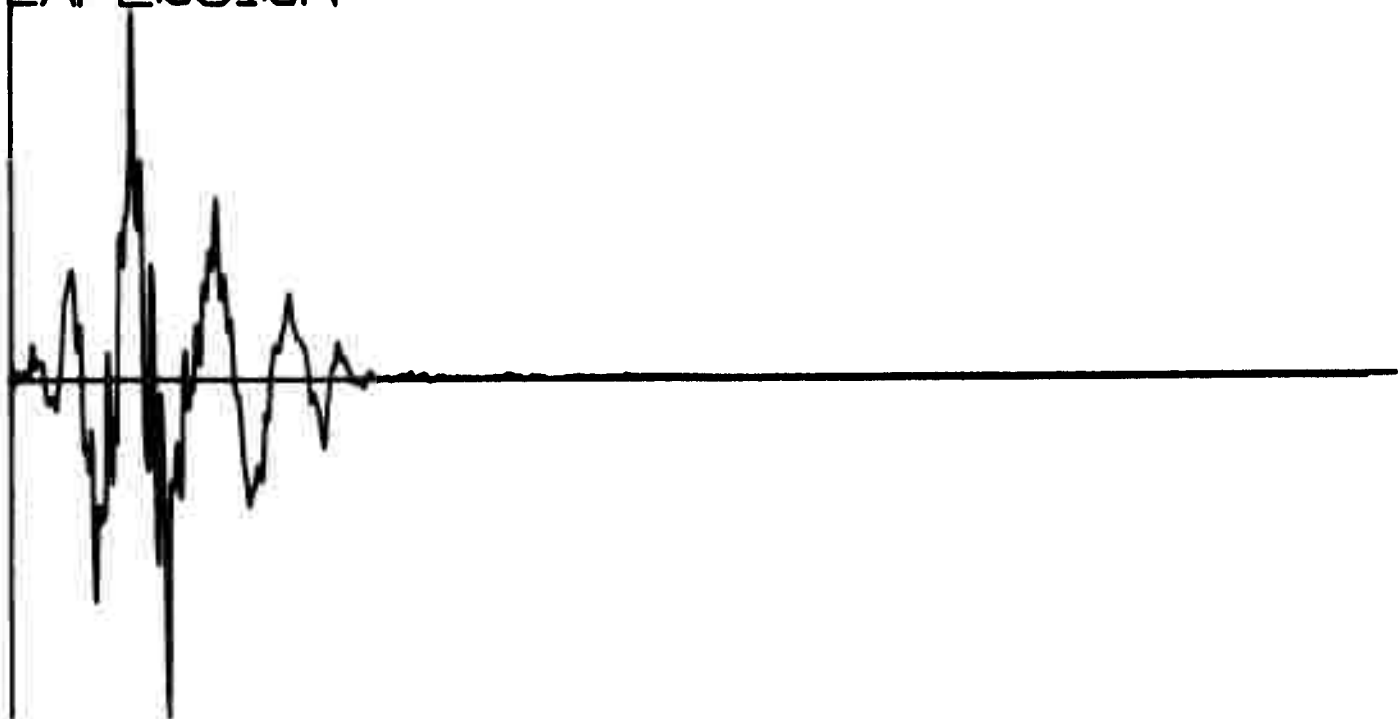
EXPLOSION



X312

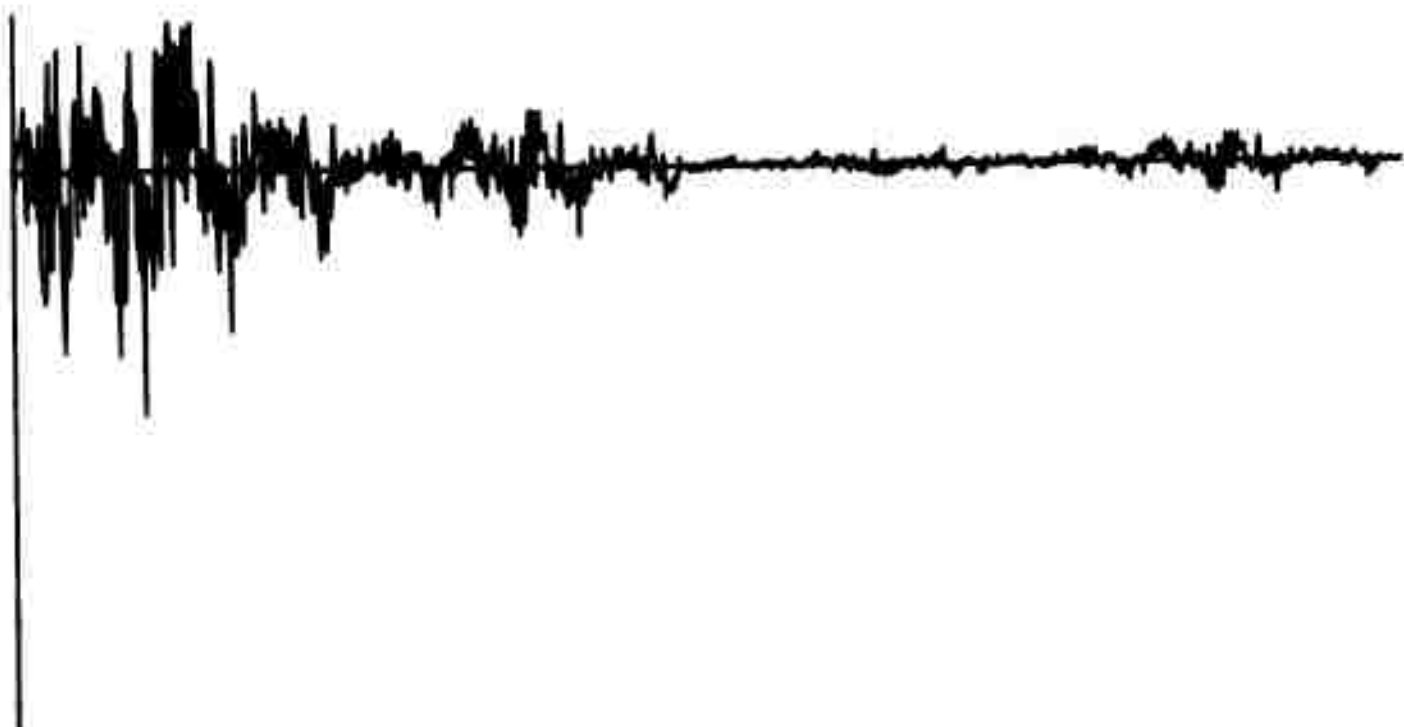
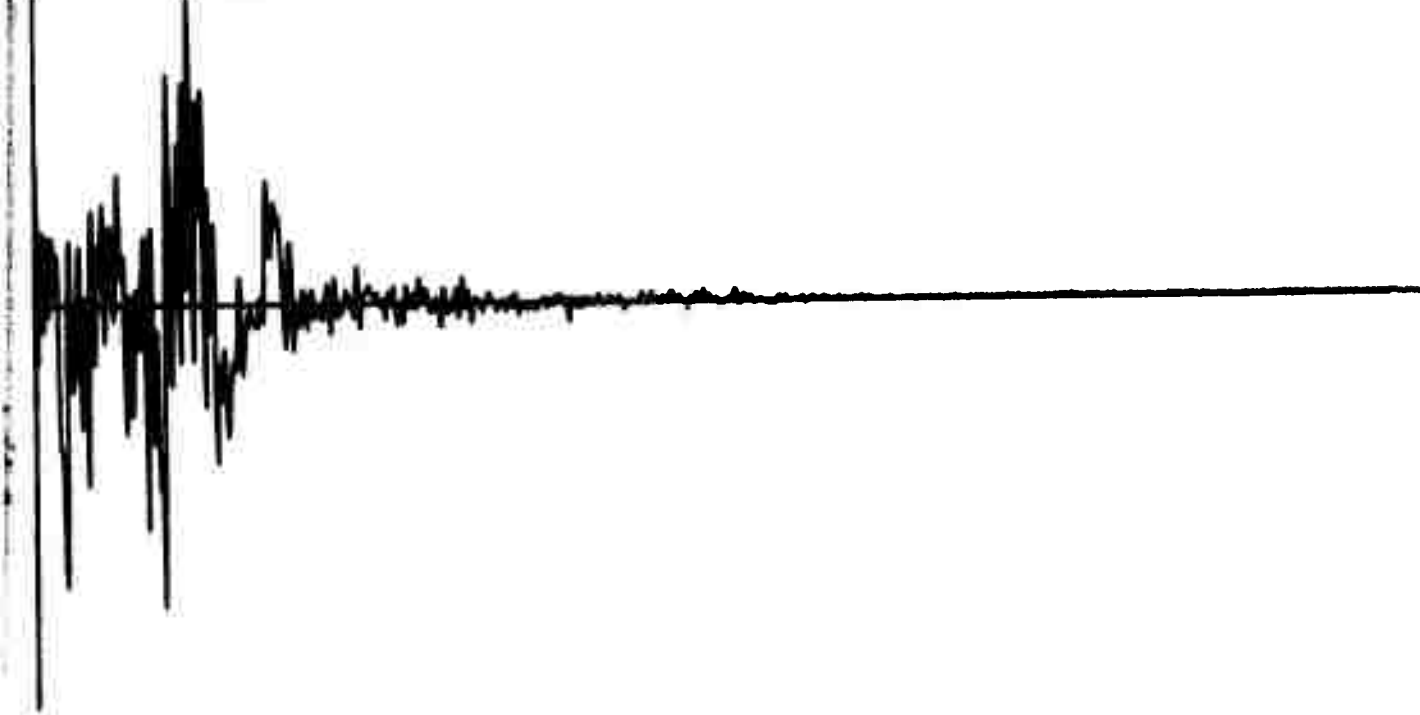
EVENT NUMBER 1541

EXPLOSION



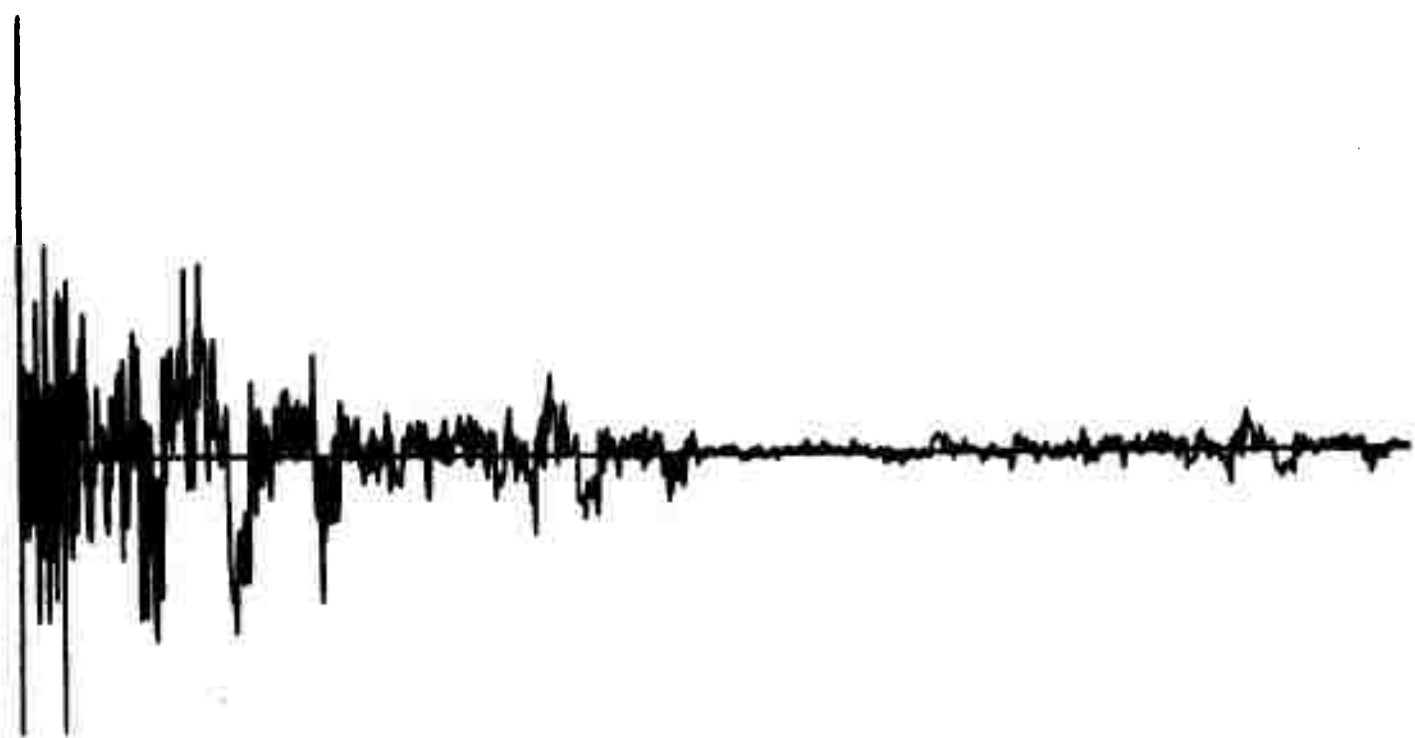
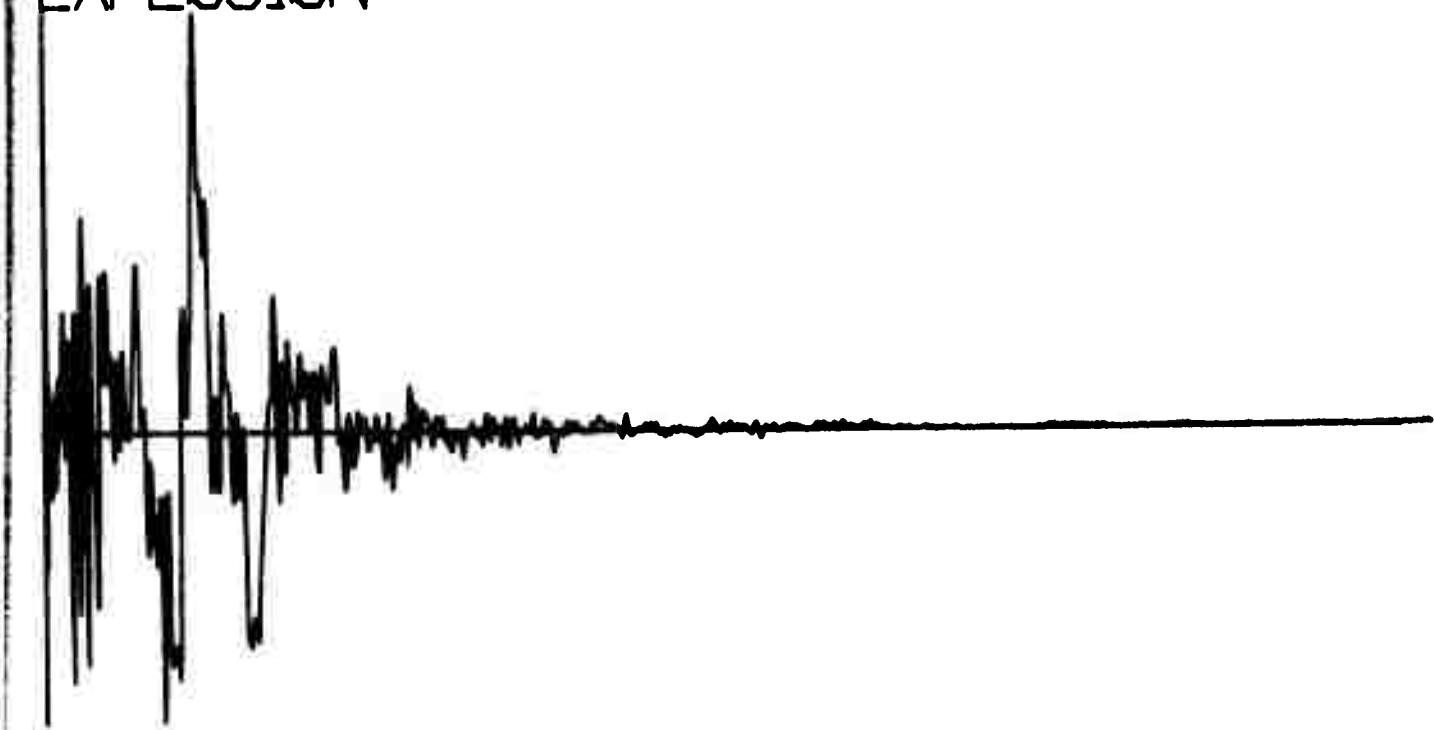
Q314

EVENT NUMBER 1304
EARTHQUAKE



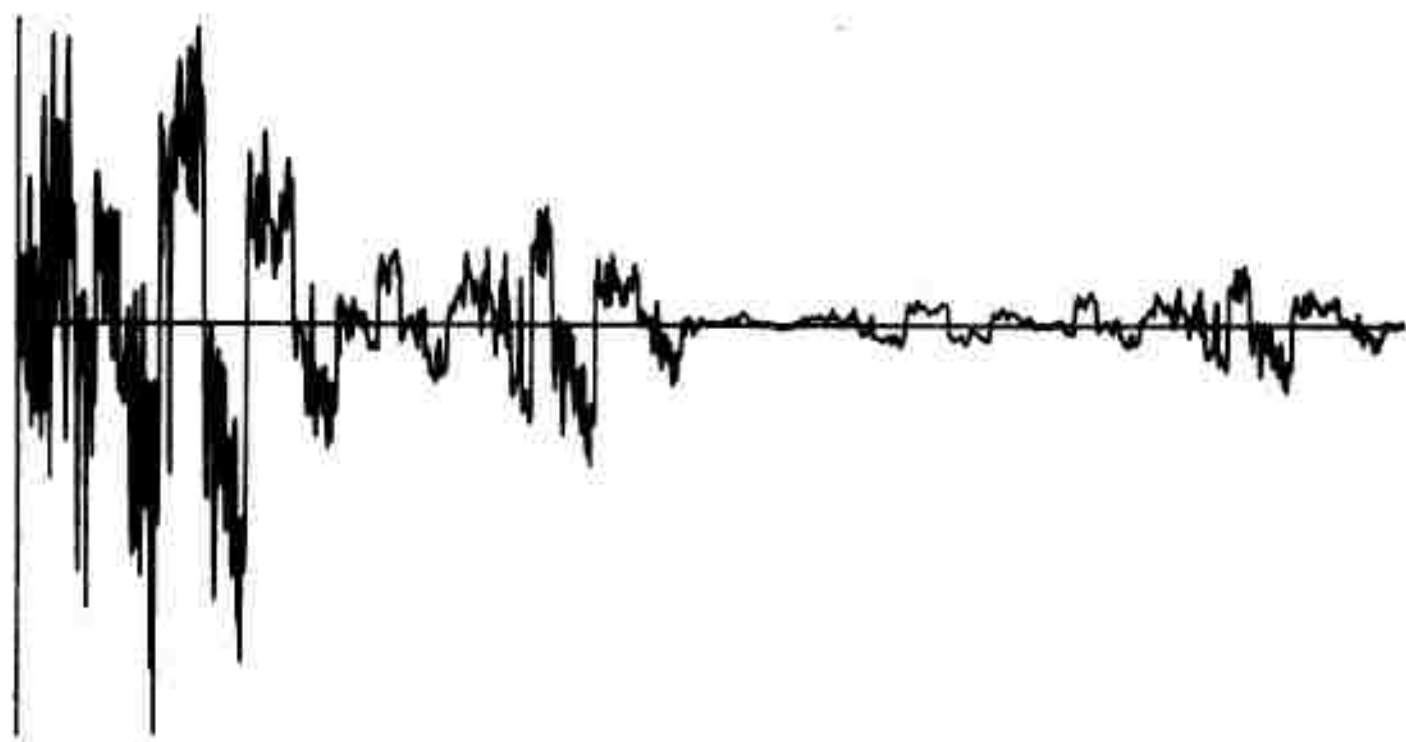
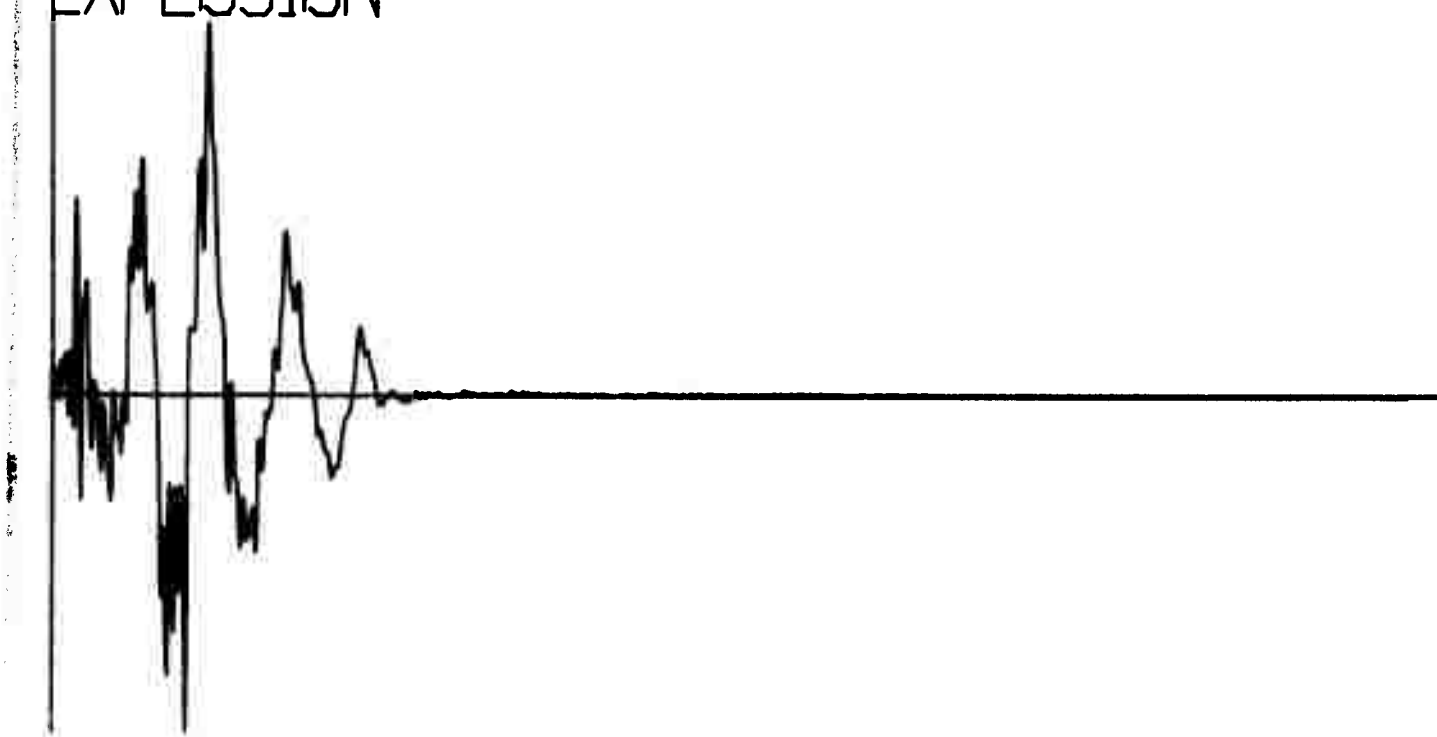
x316

EVENT NUMBER 1501
EXPLOSION



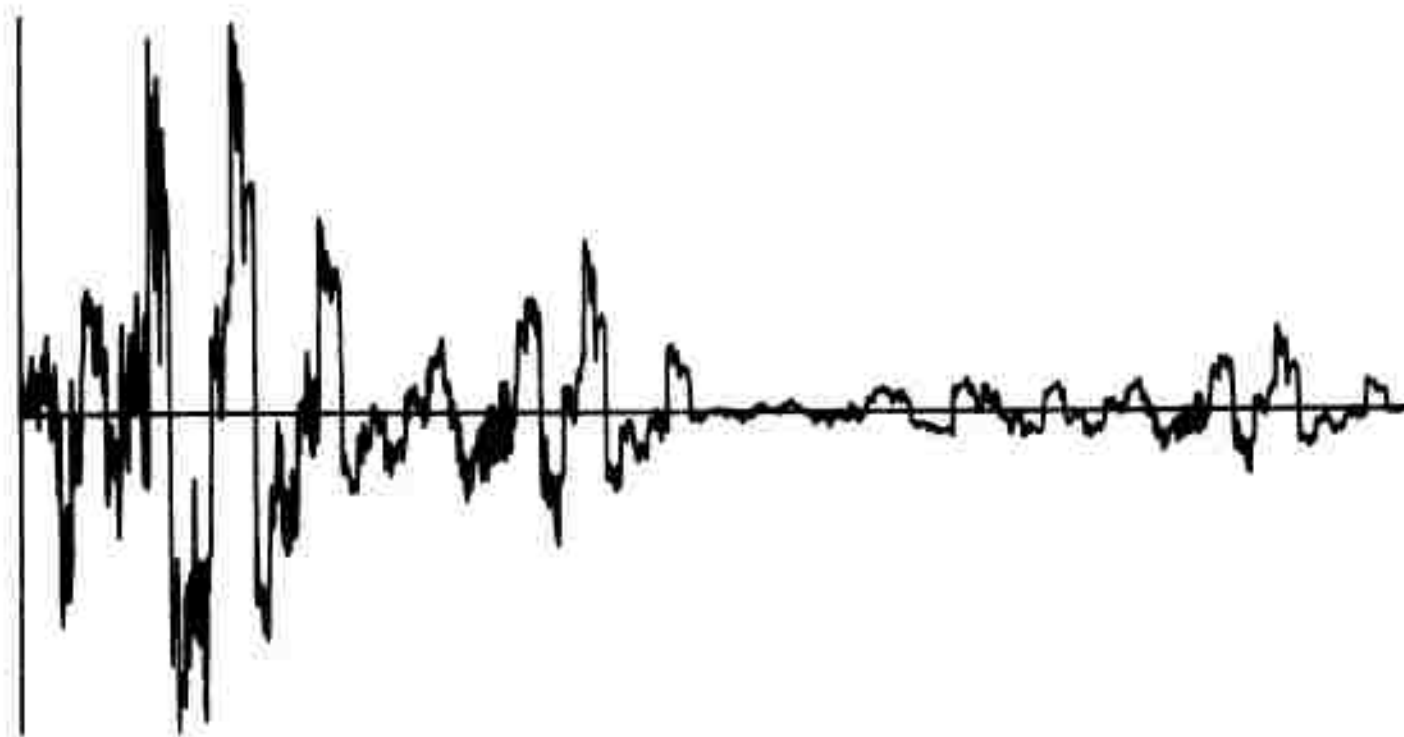
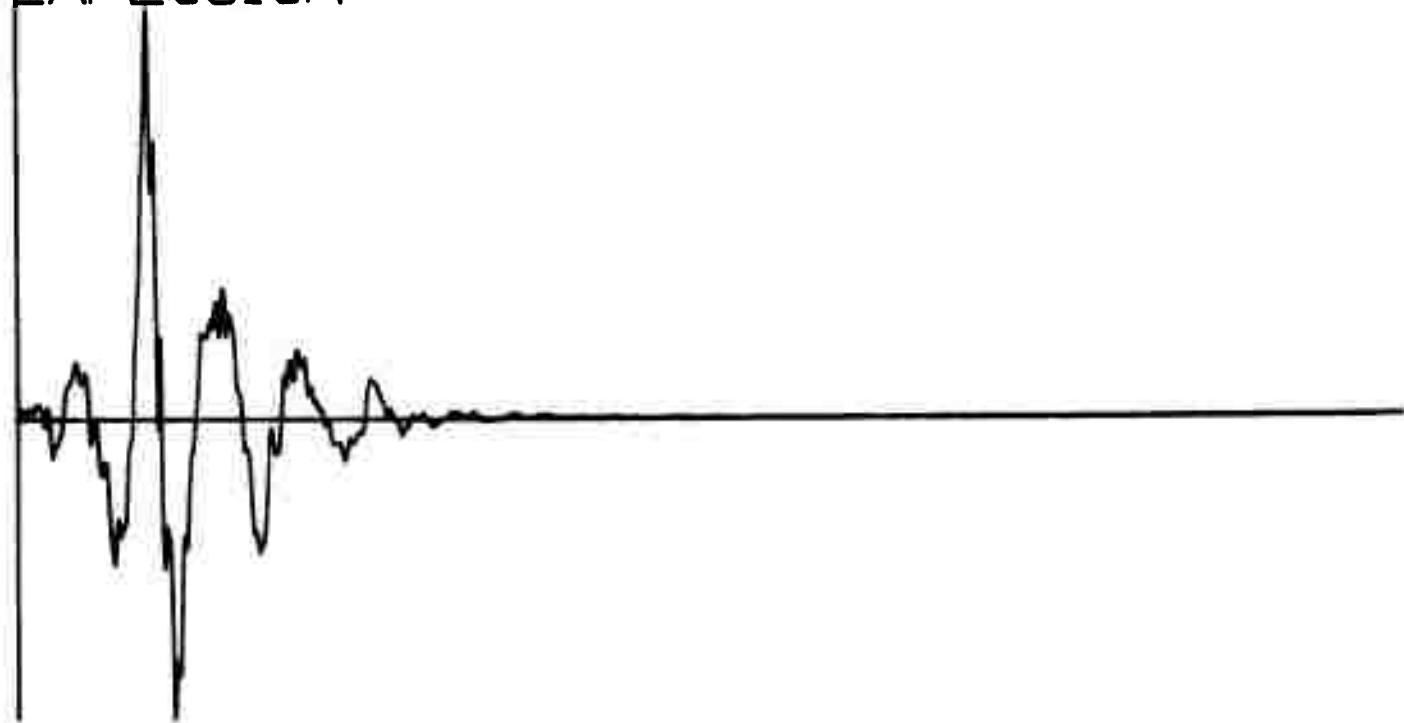
X318

EVENT NUMBER 1508
EXPLOSION



X320

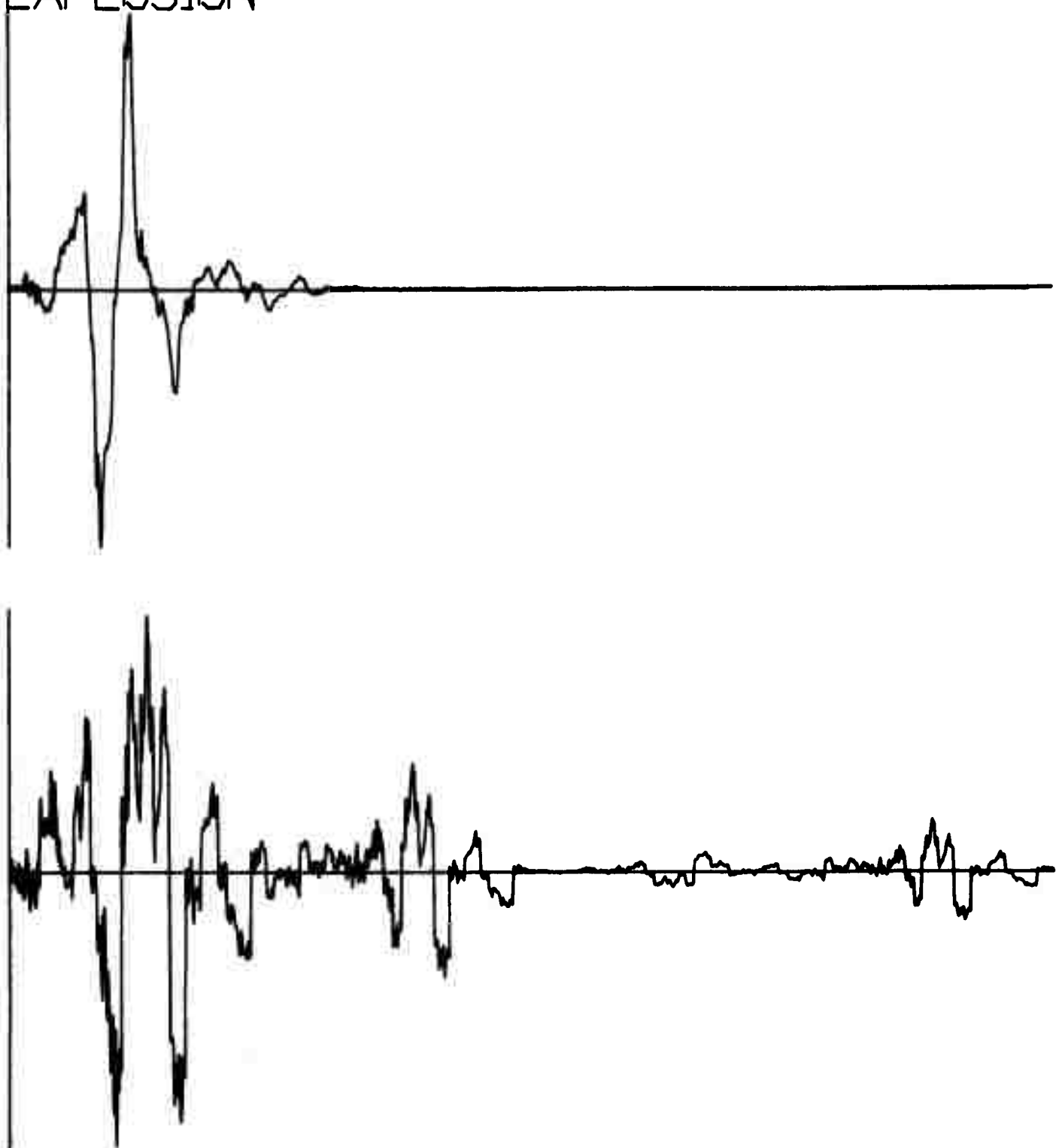
EVENT NUMBER 1523
EXPLOSION



X322

EVENT NUMBER 1529

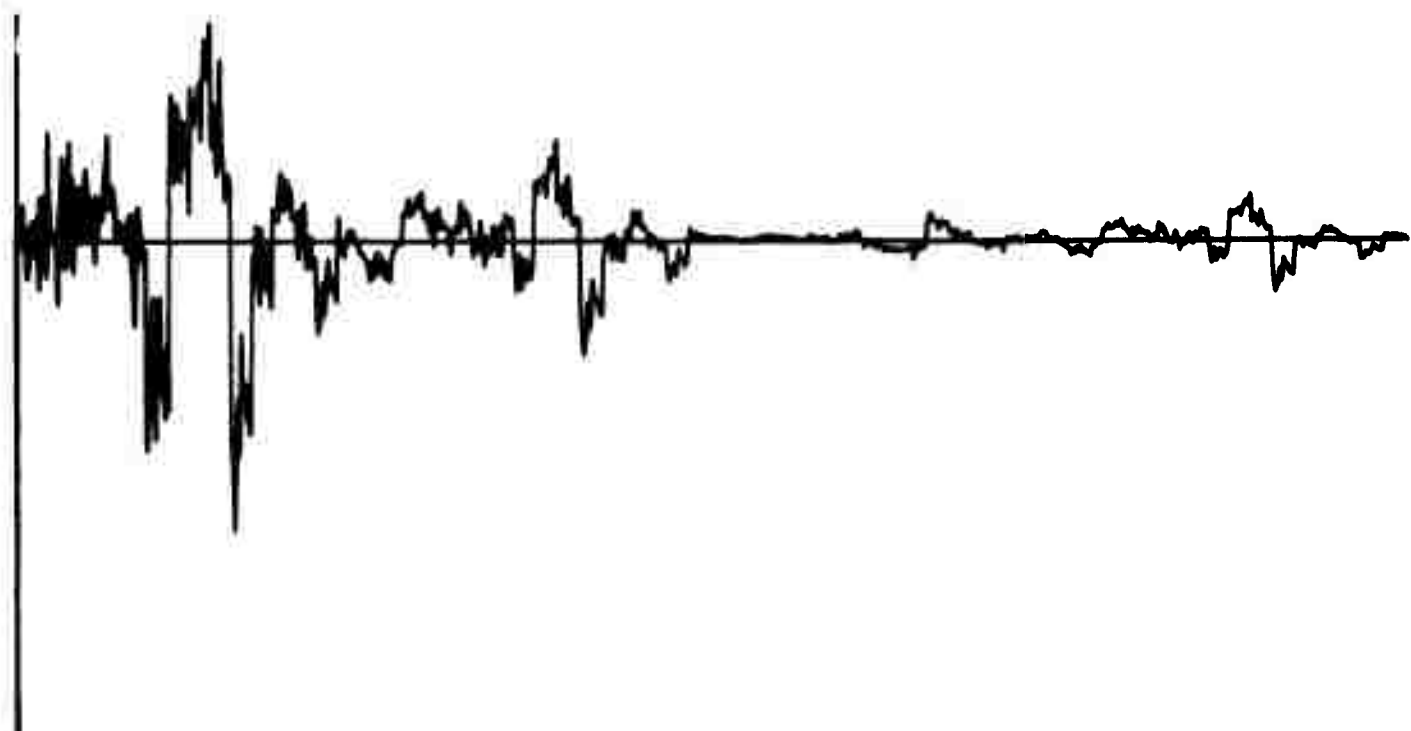
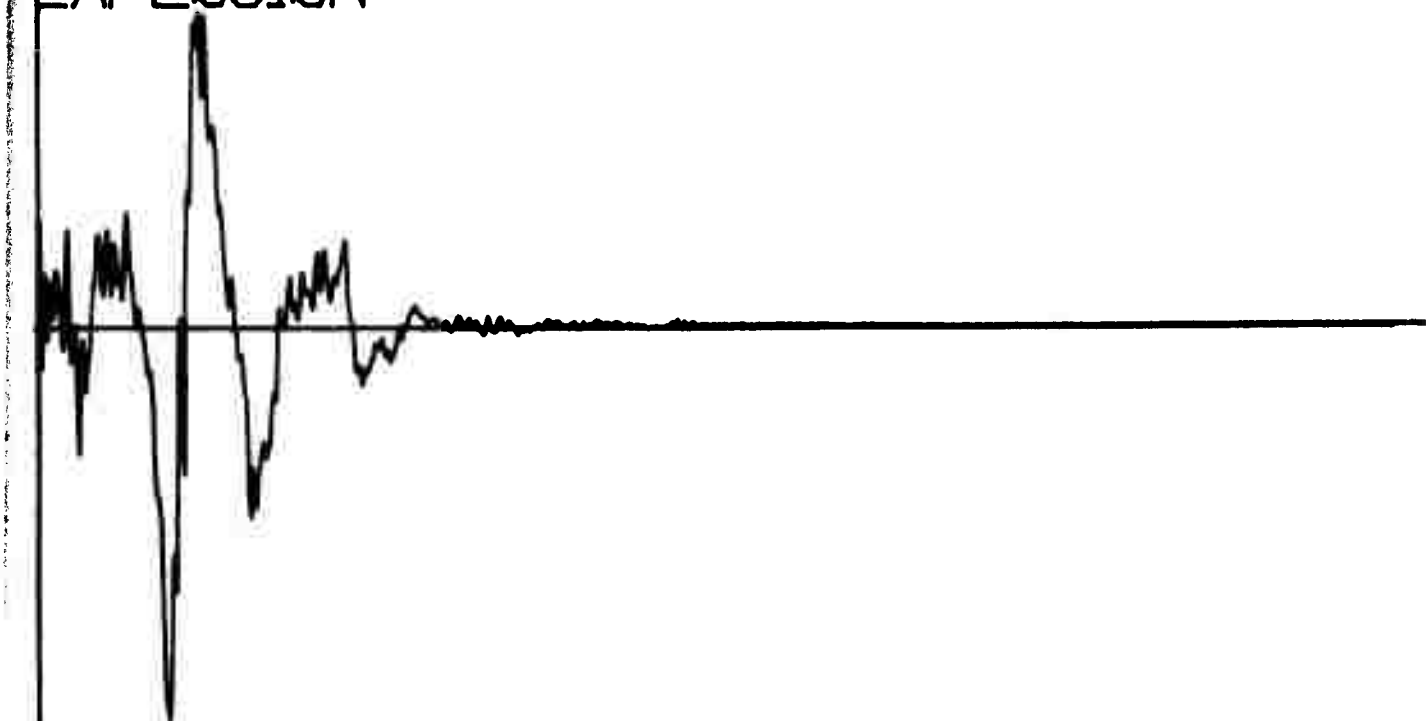
EXPLOSION



X324

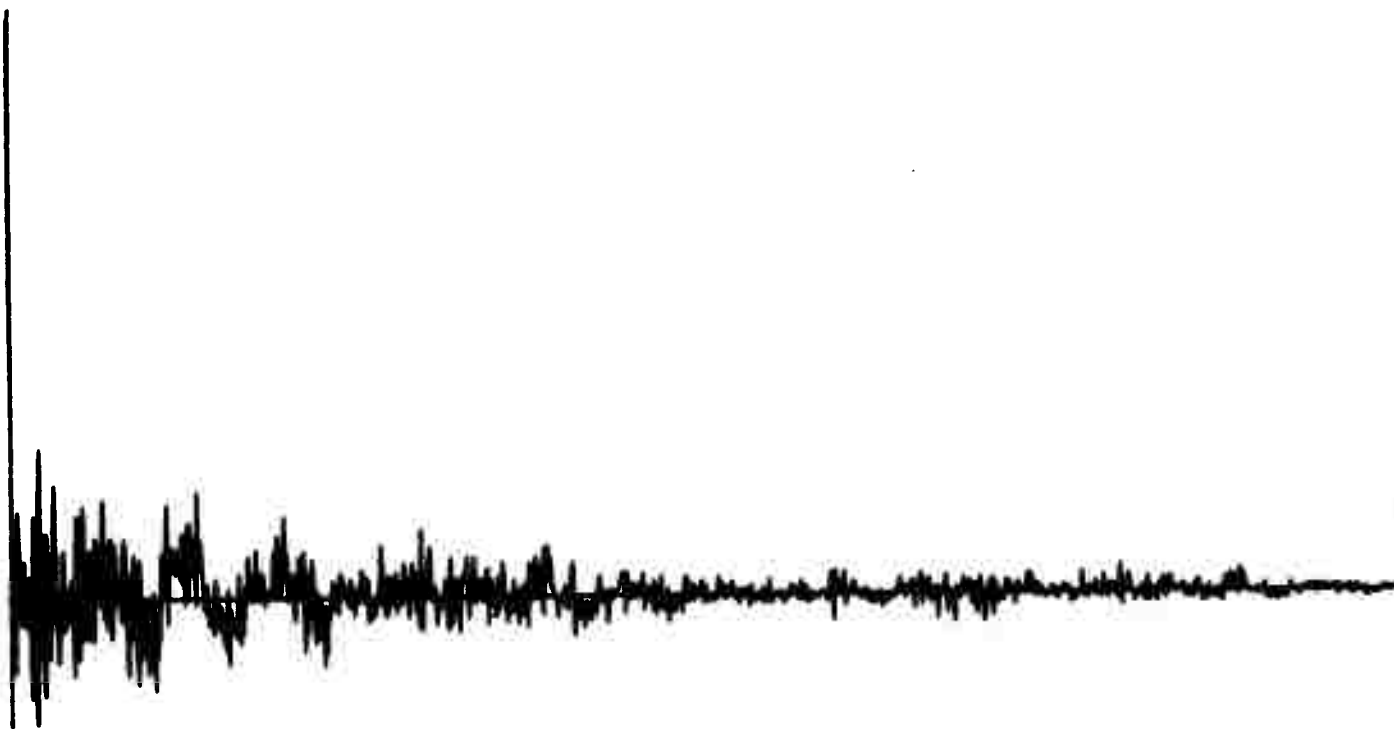
EVENT NUMBER 1534

EXPLOSION



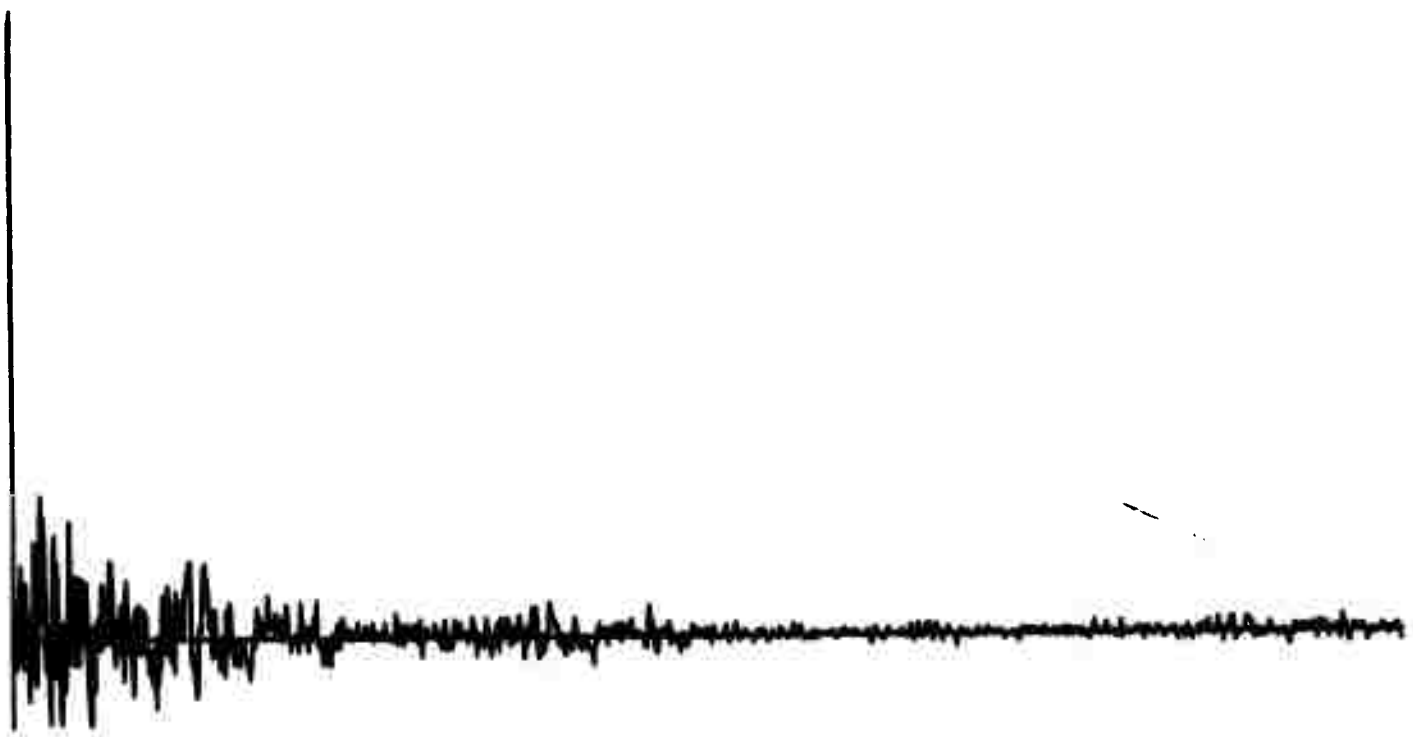
Q326

EVENT NUMBER 1313
EARTHQUAKE



Q328

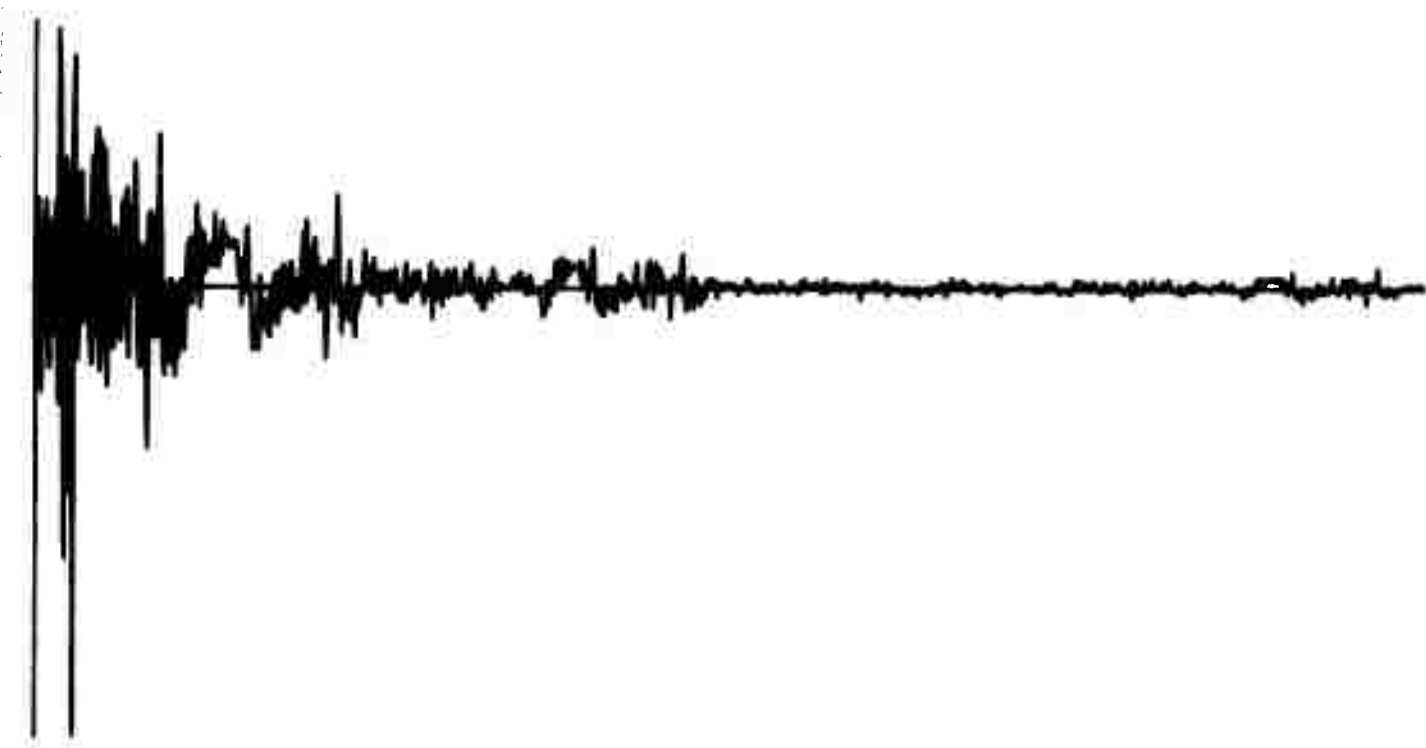
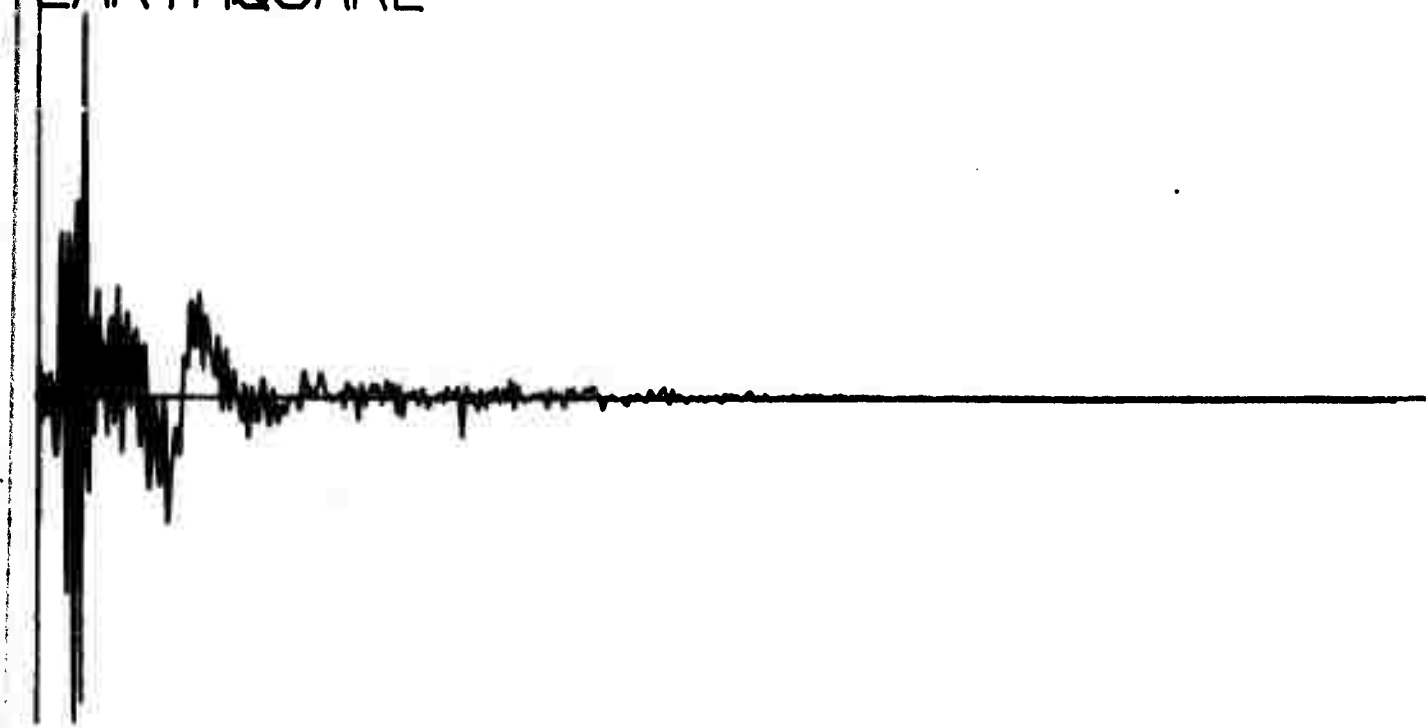
EVENT NUMBER 1314
EARTHQUAKE



Q330

EVENT NUMBER 1316

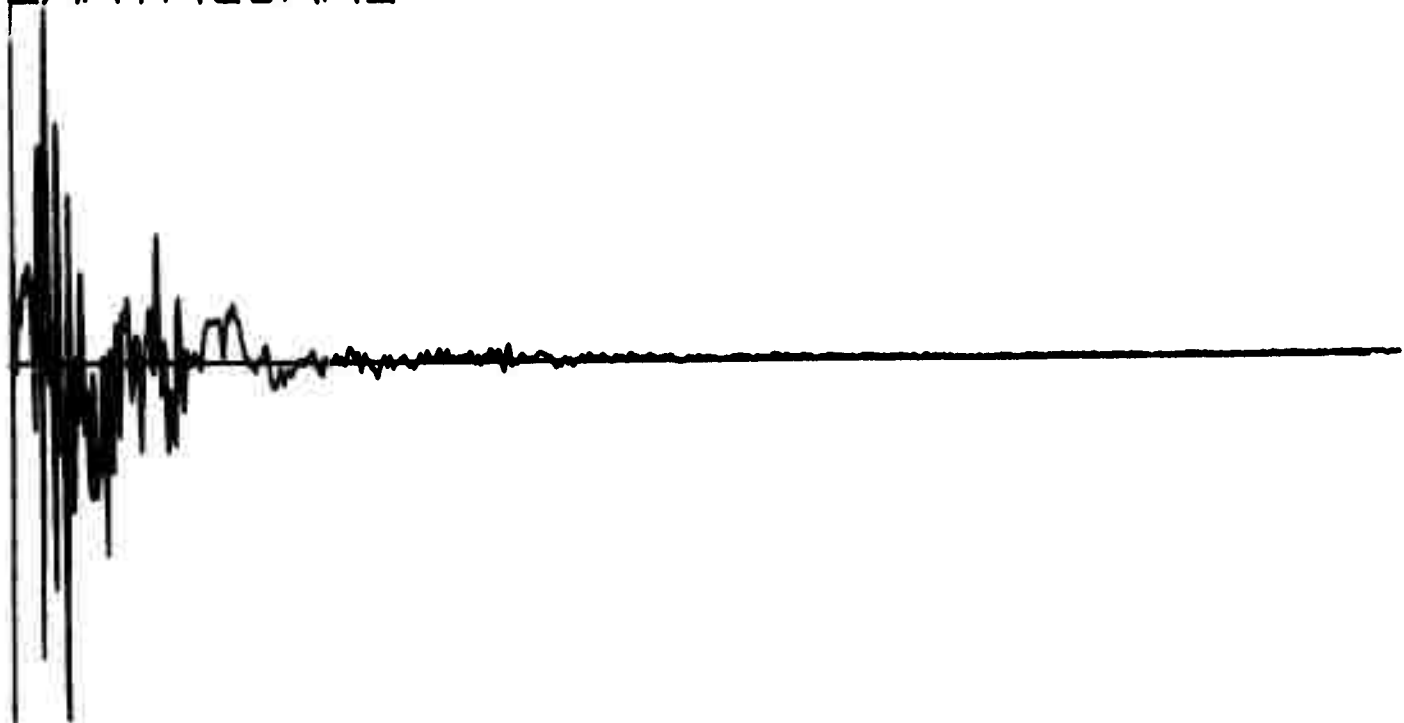
EARTHQUAKE



Q332

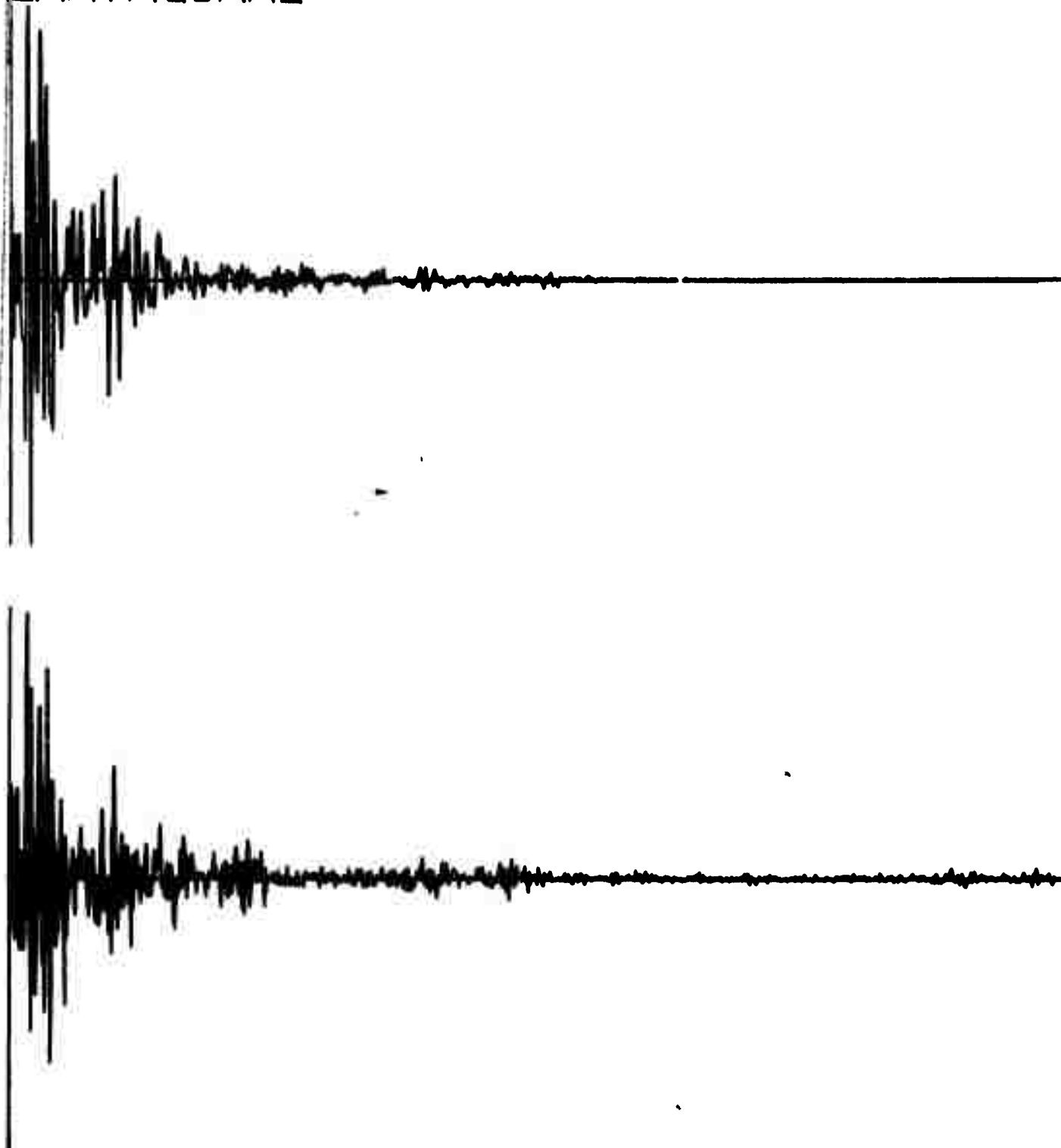
EVENT NUMBER 1318

EARTHQUAKE



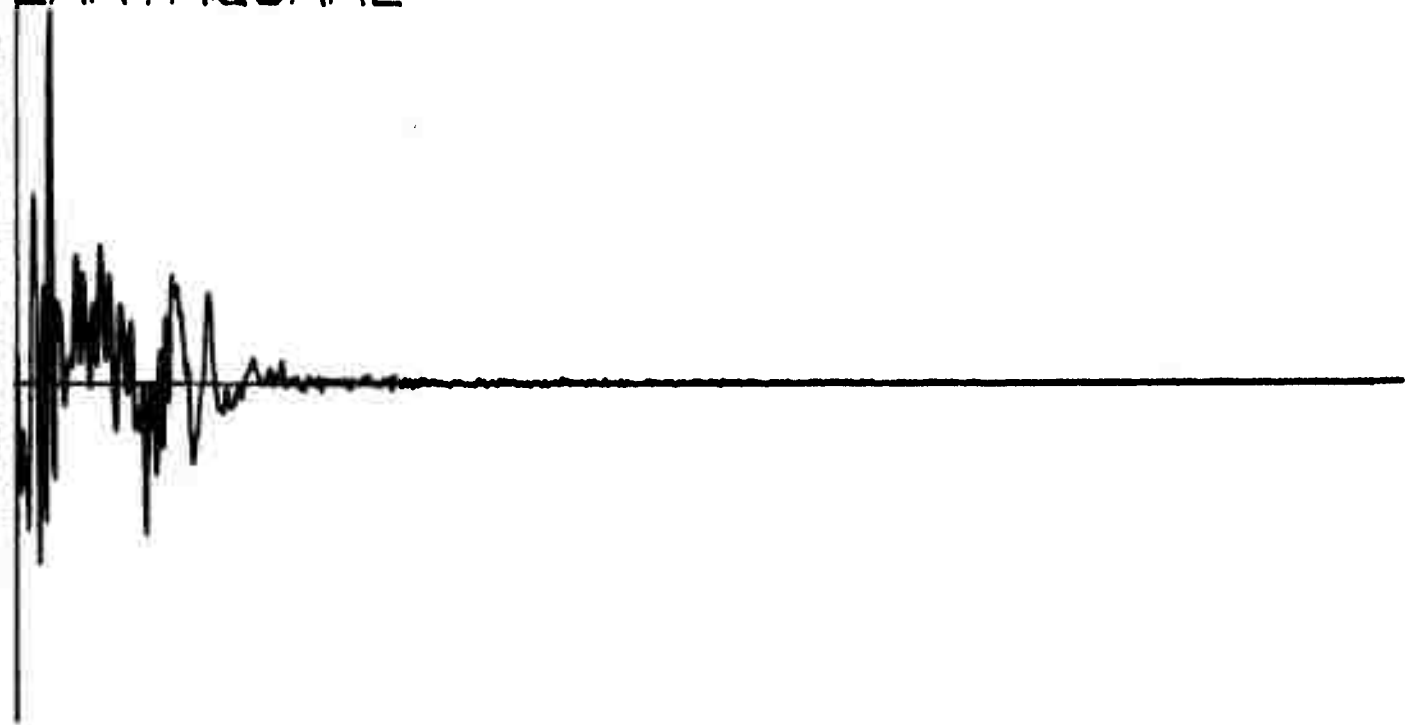
Q334

EVENT NUMBER 1319
EARTHQUAKE



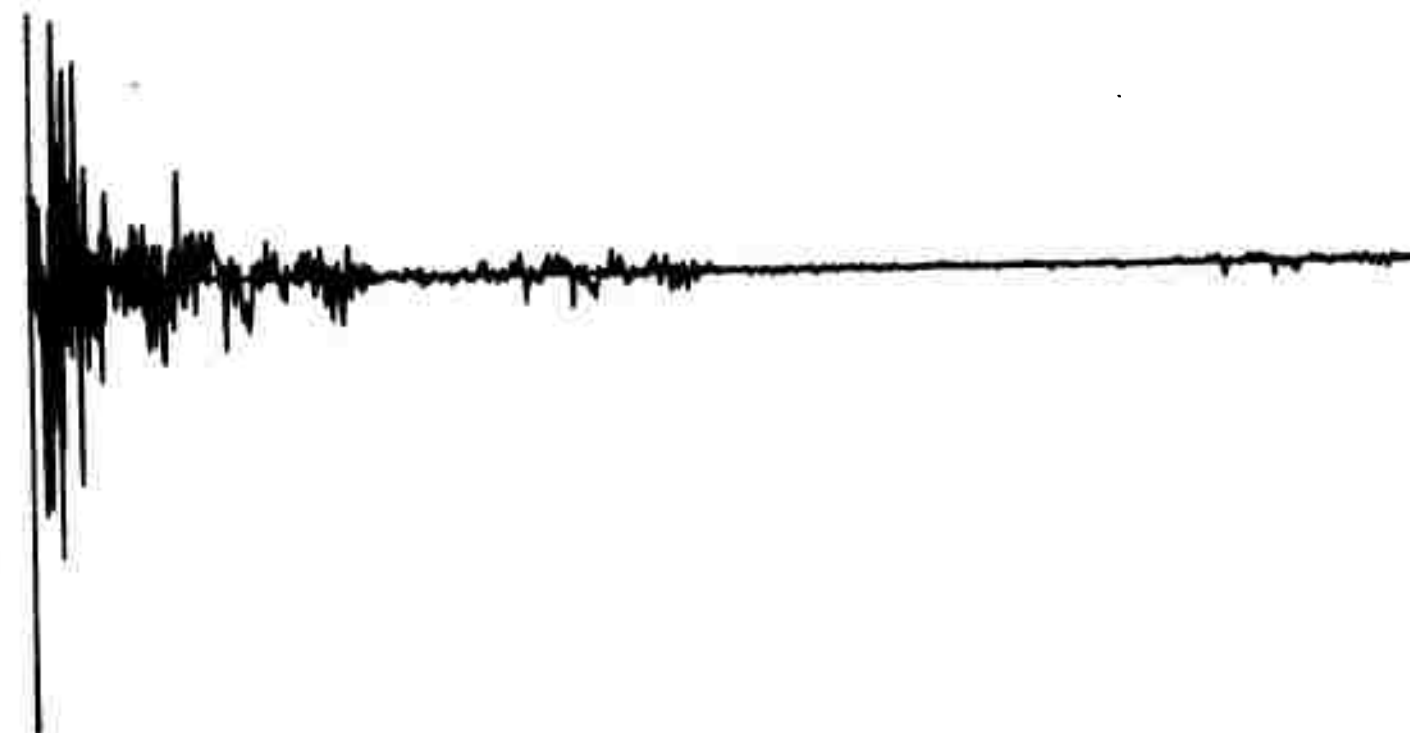
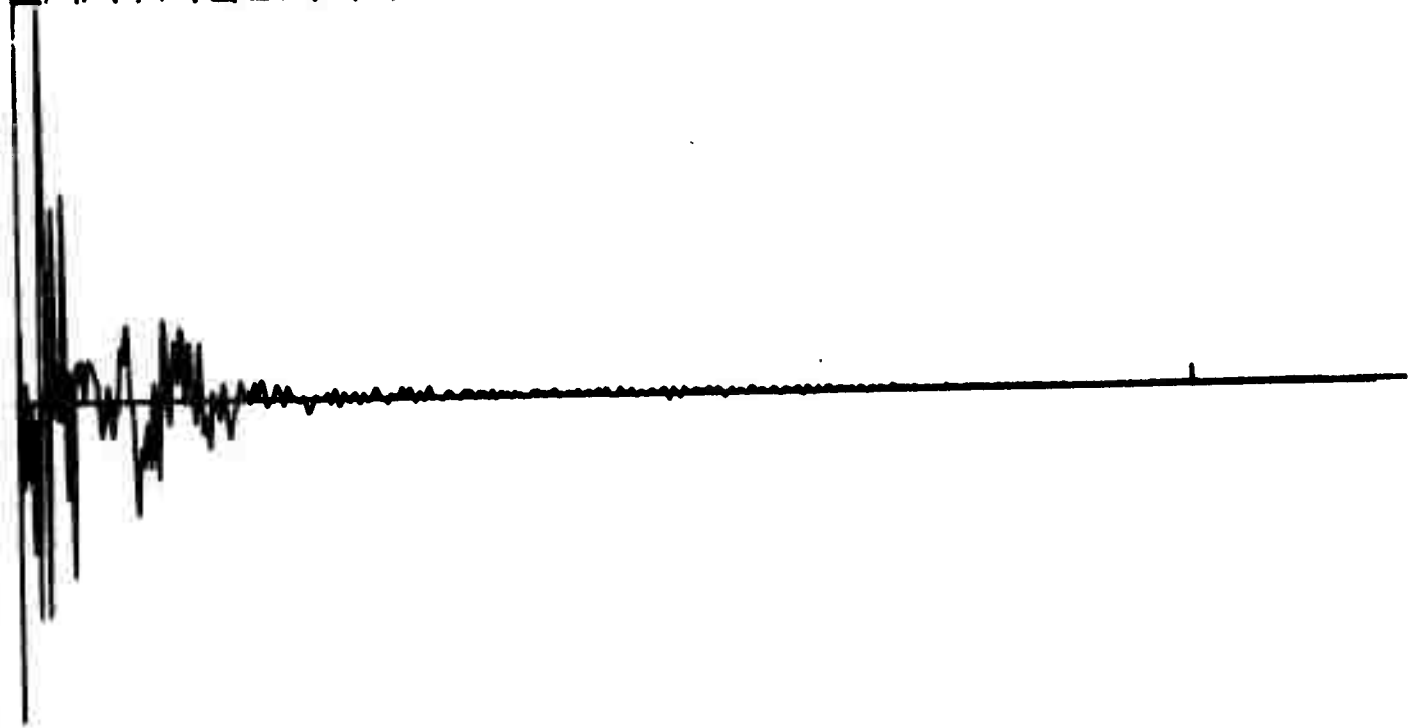
Q336

EVENT NUMBER 1320
EARTHQUAKE



Q338

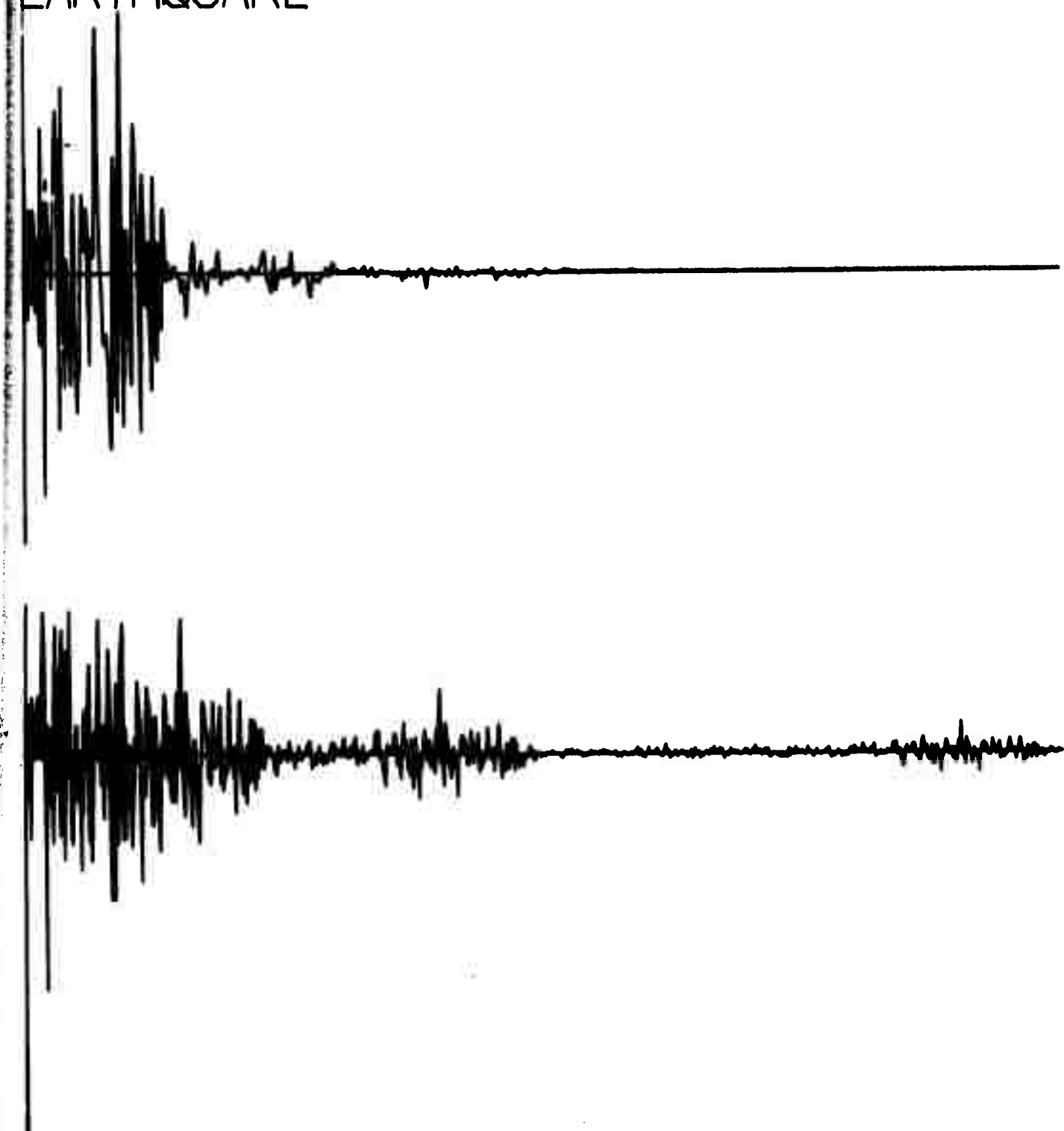
EVENT NUMBER 1321
EARTHQUAKE



Q340

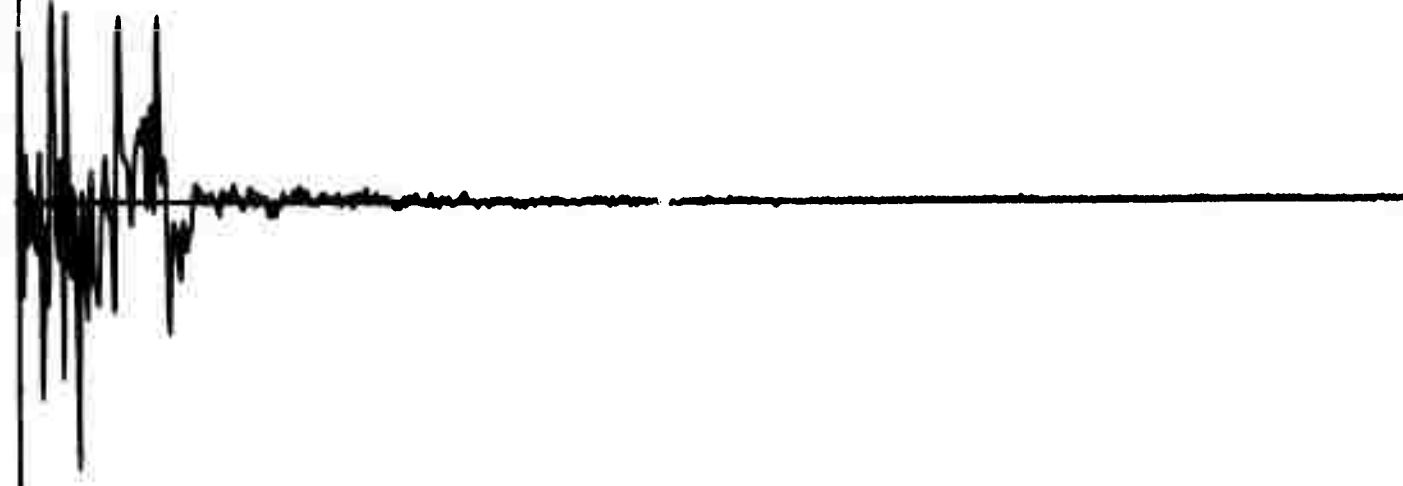
EVENT NUMBER 1322

EARTHQUAKE



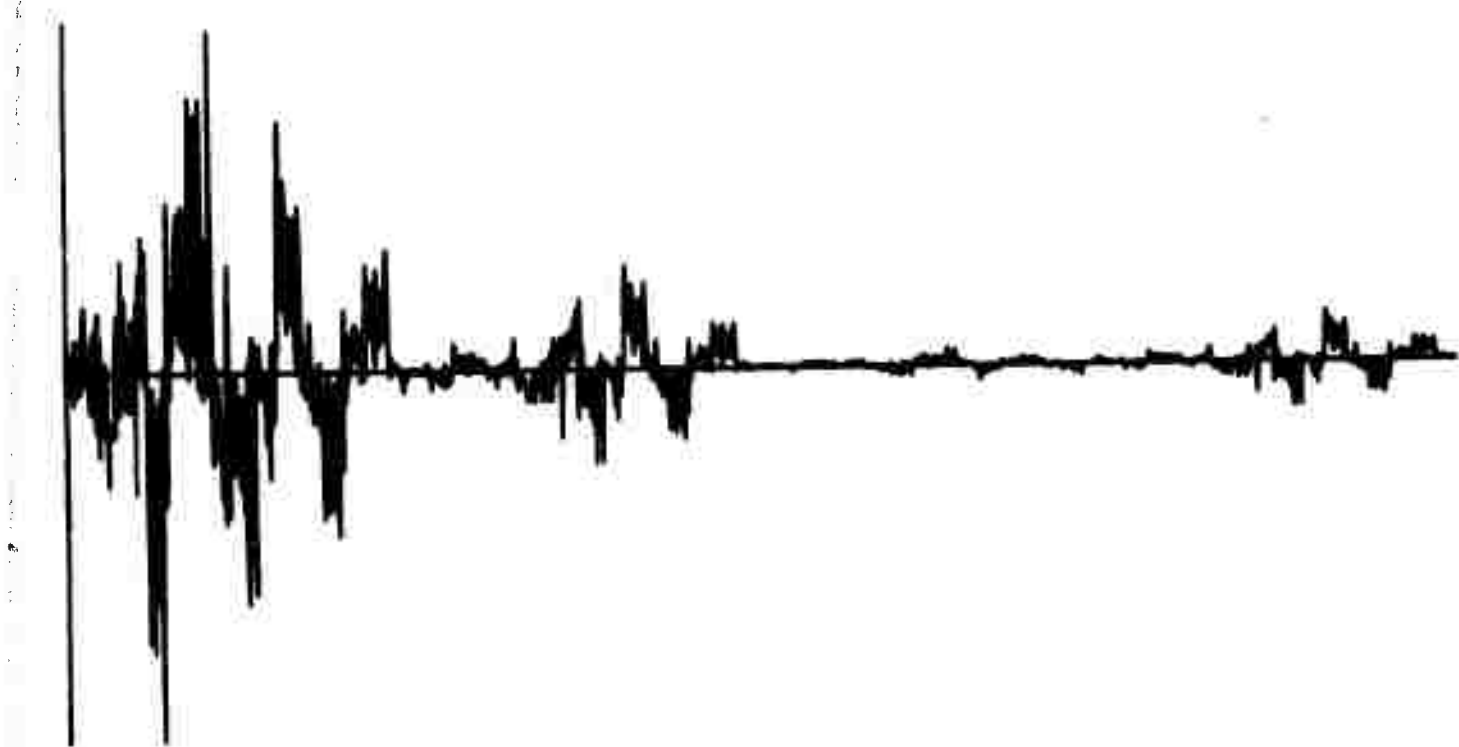
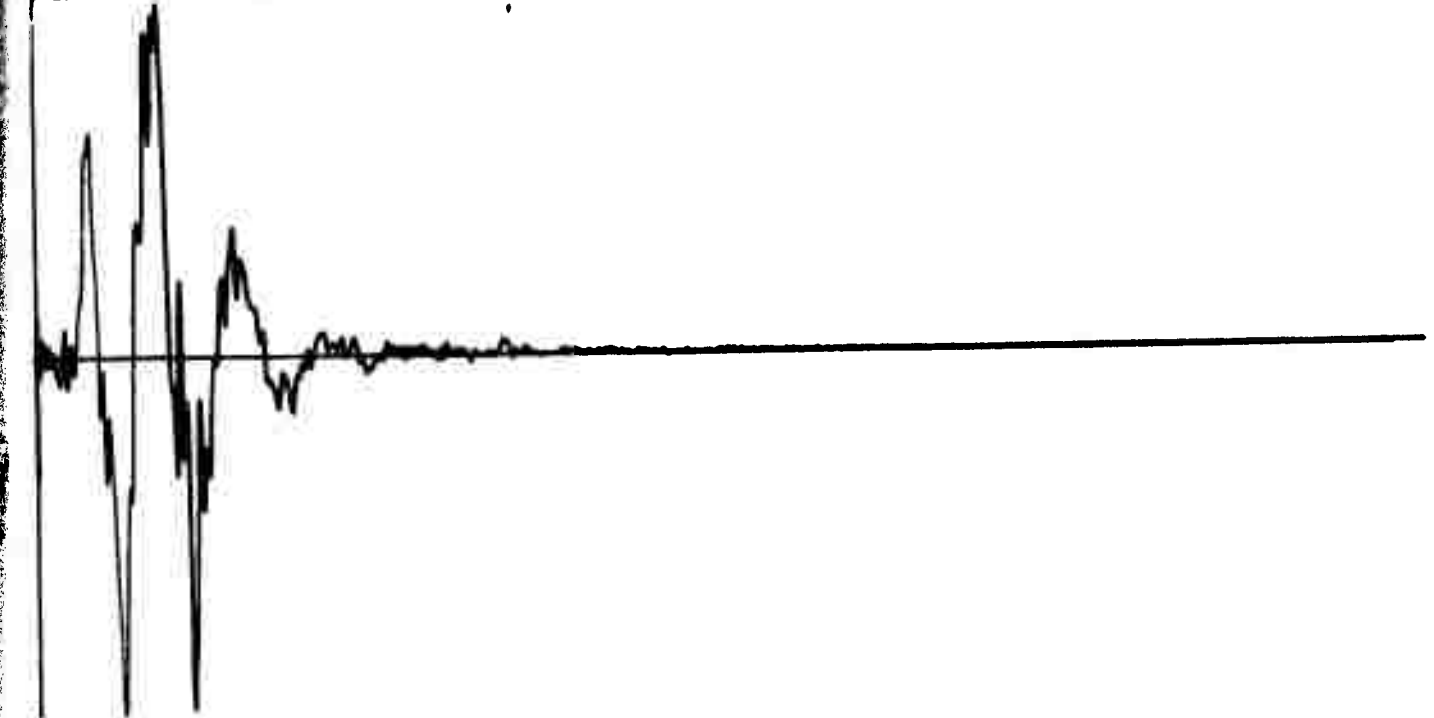
Q342

EVENT NUMBER 1275
EARTHQUAKE



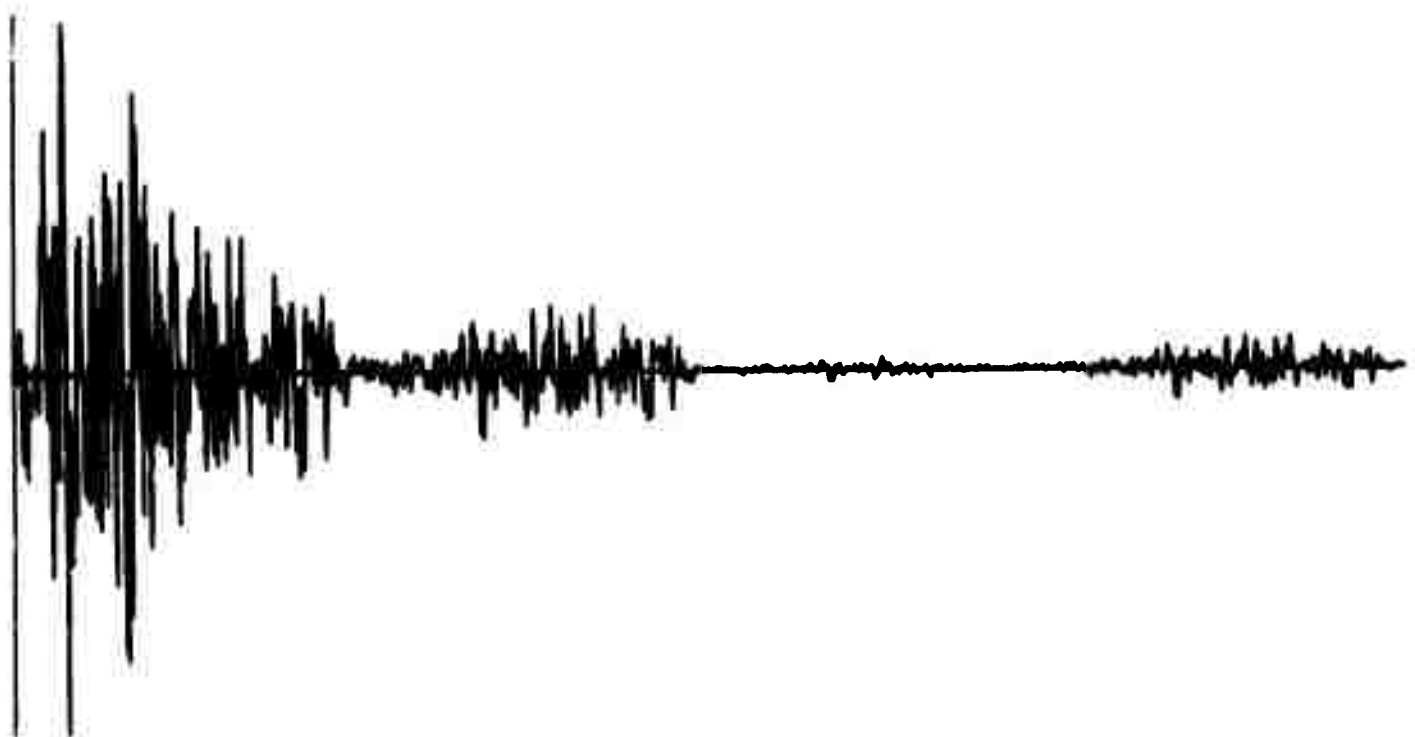
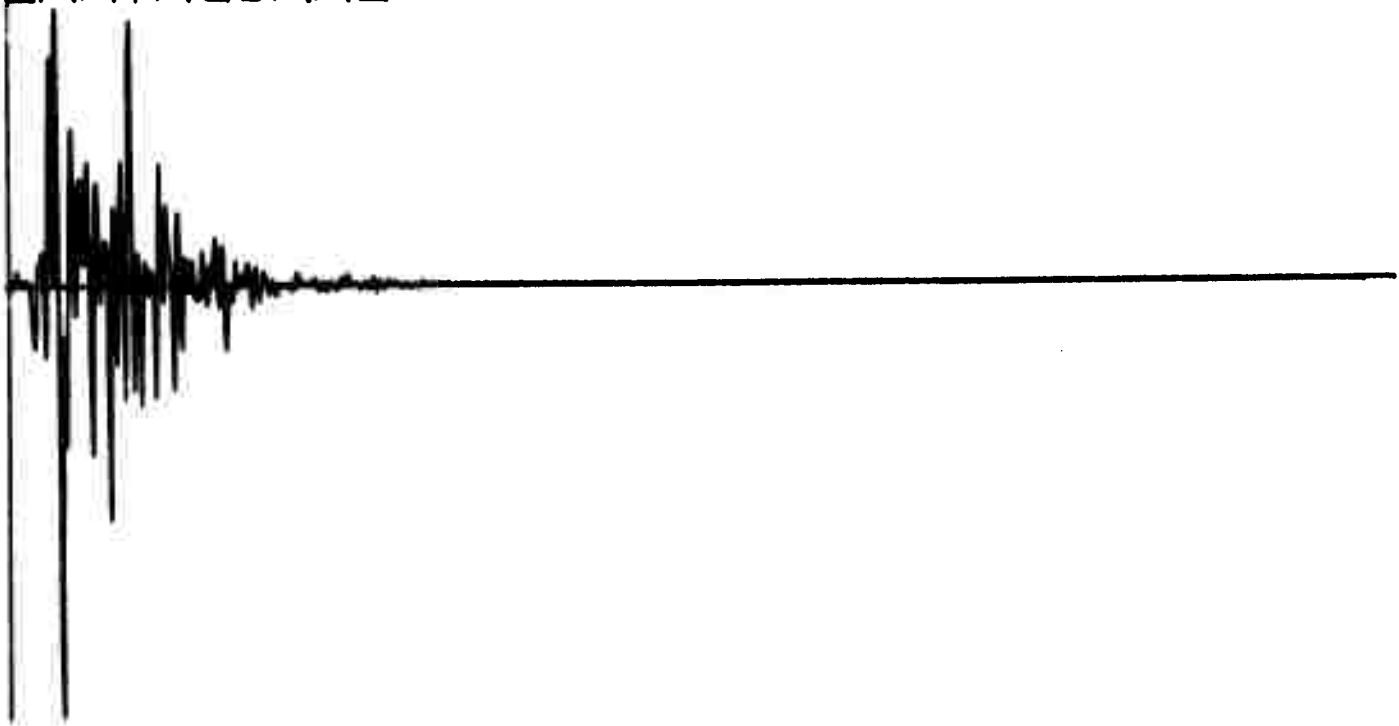
Q344

EVENT NUMBER 1278
EARTHQUAKE



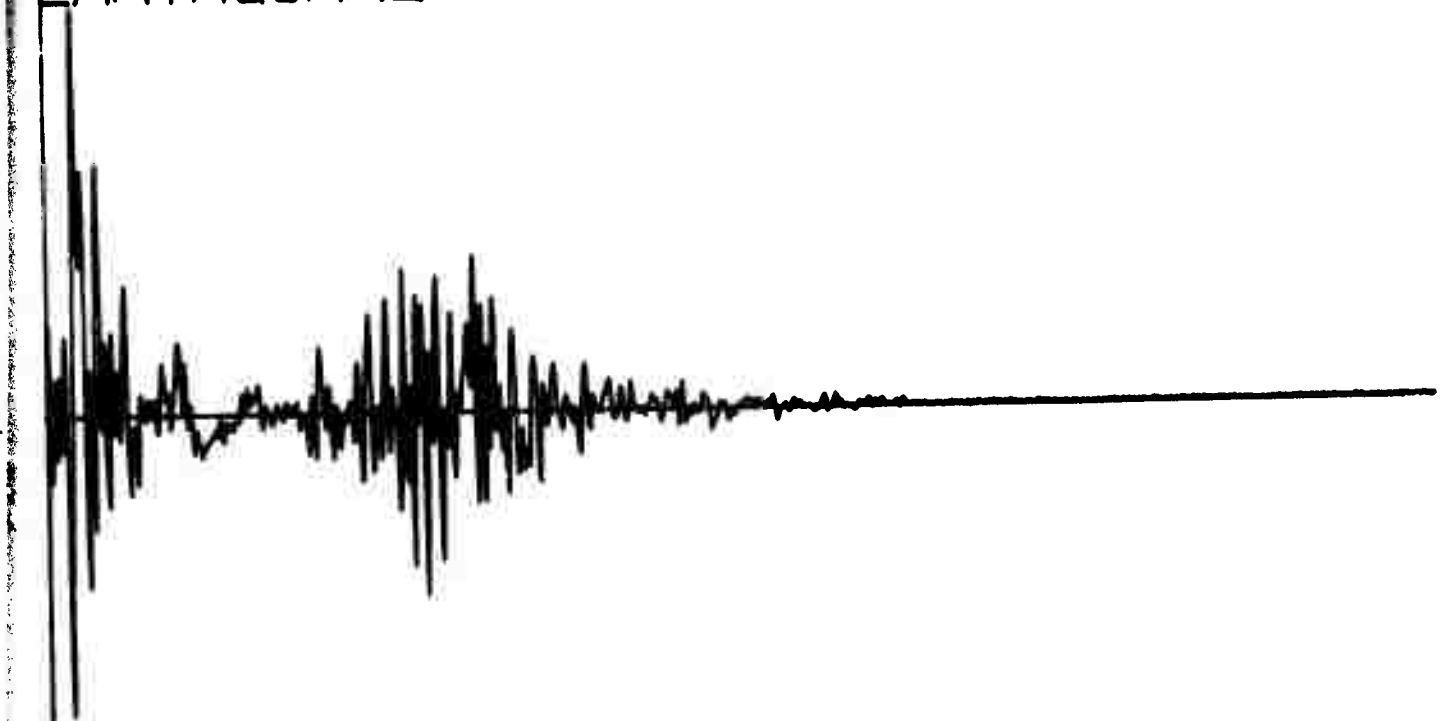
Q346

EVENT NUMBER 2000
EARTHQUAKE



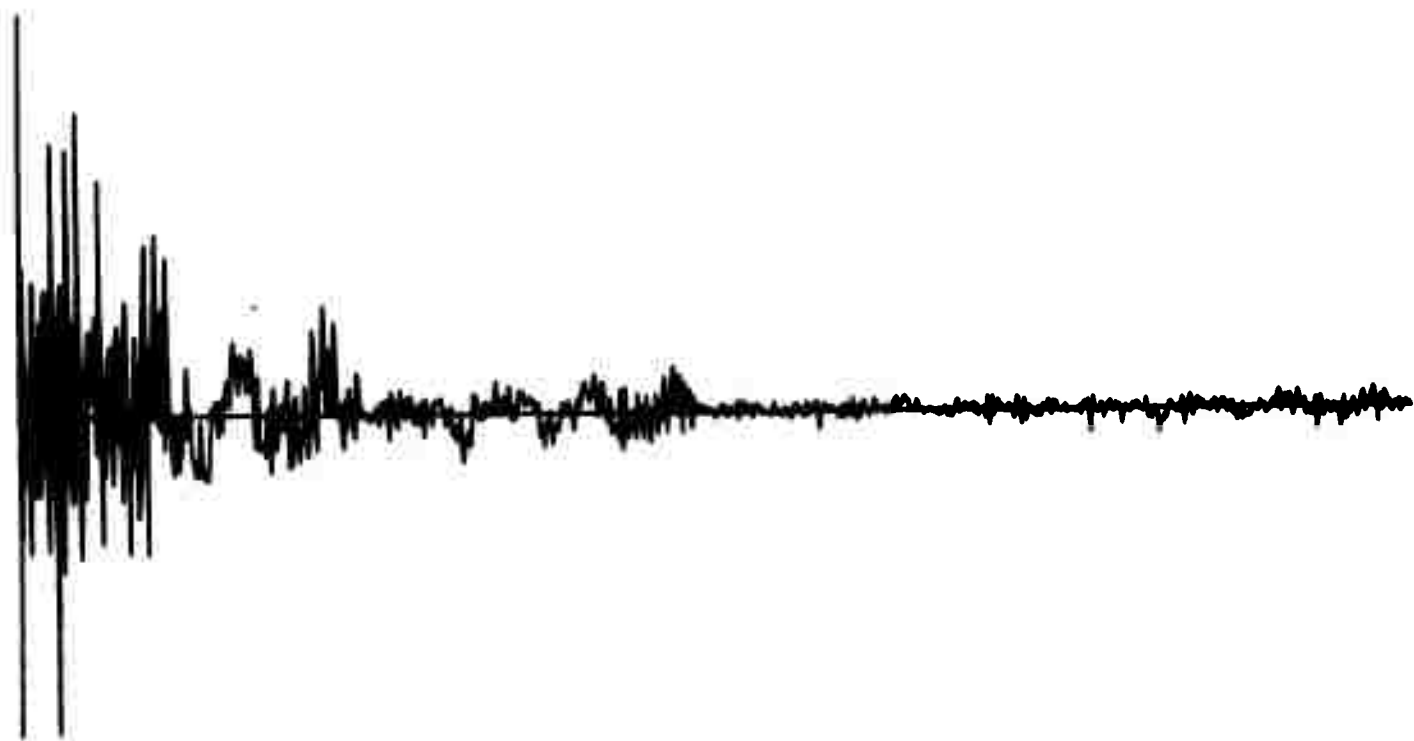
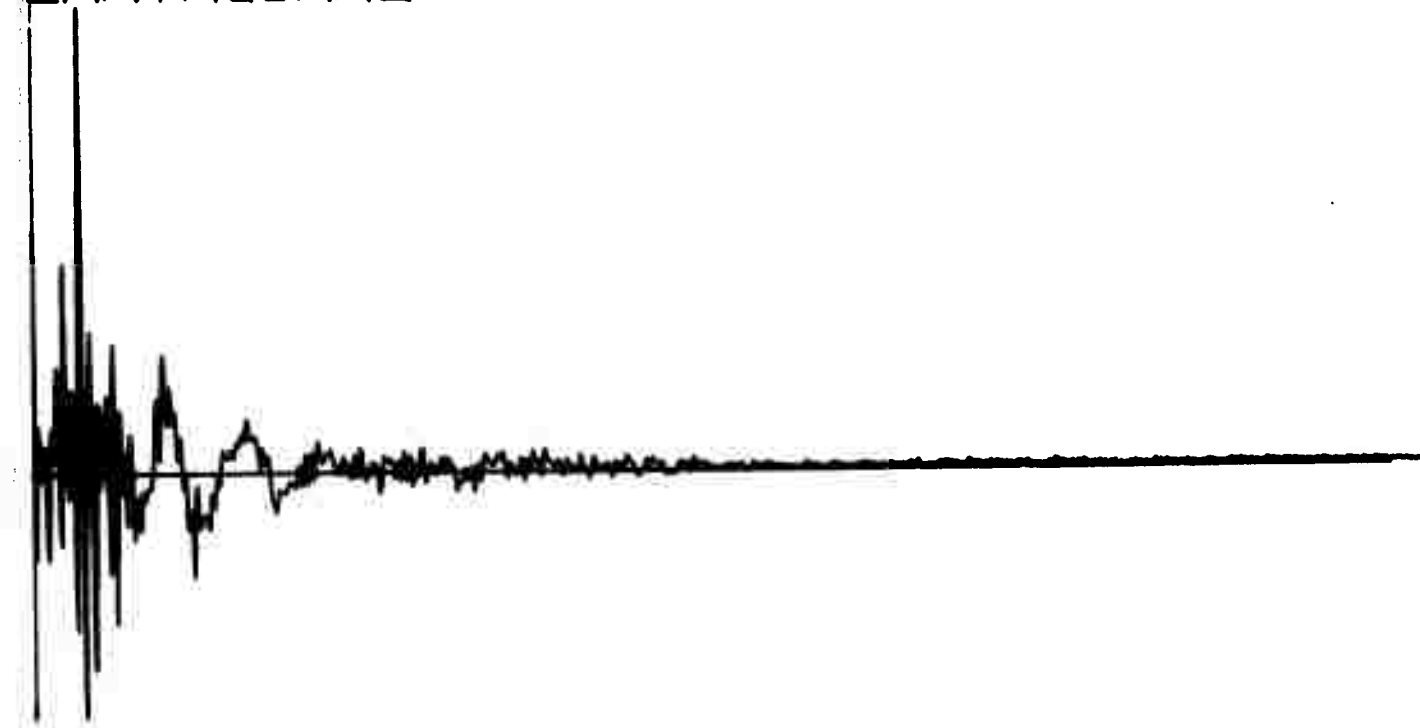
Q348

EVENT NUMBER 1058
EARTHQUAKE



Q350

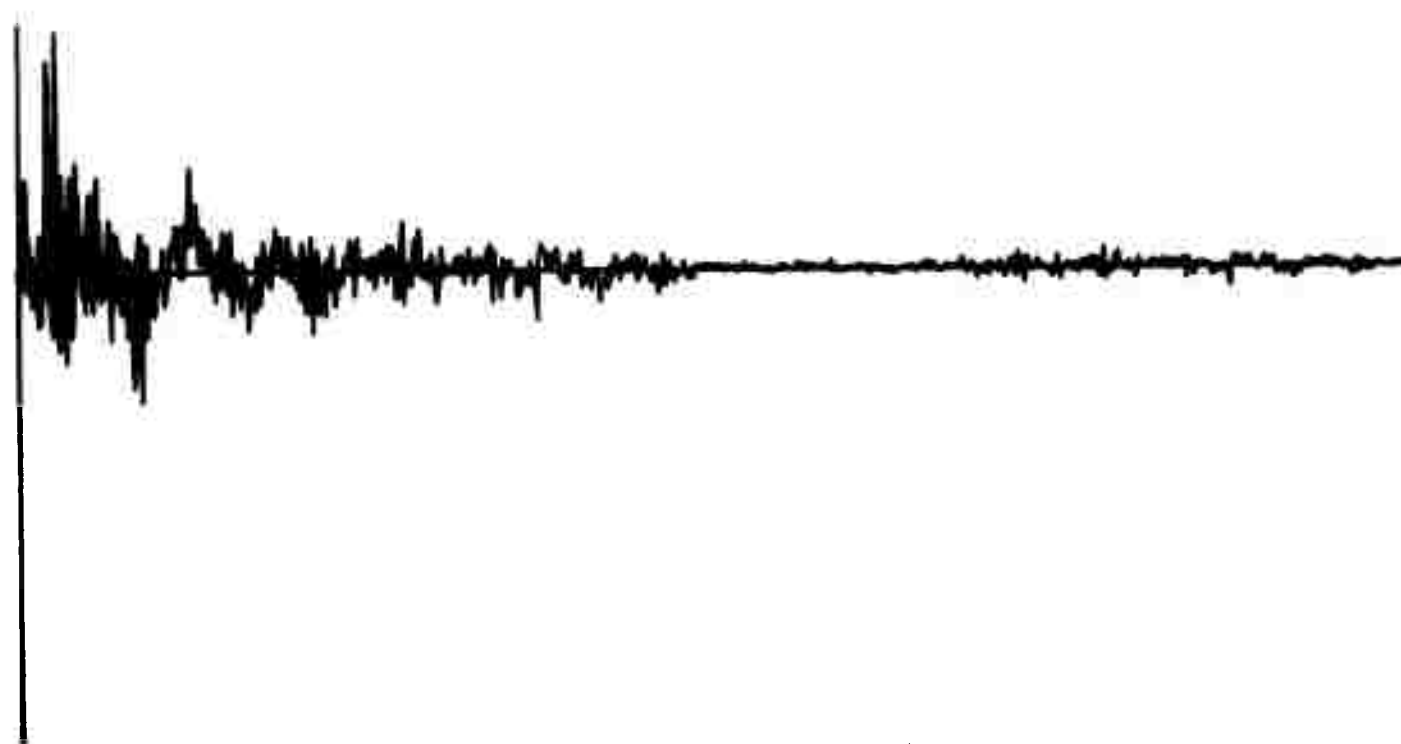
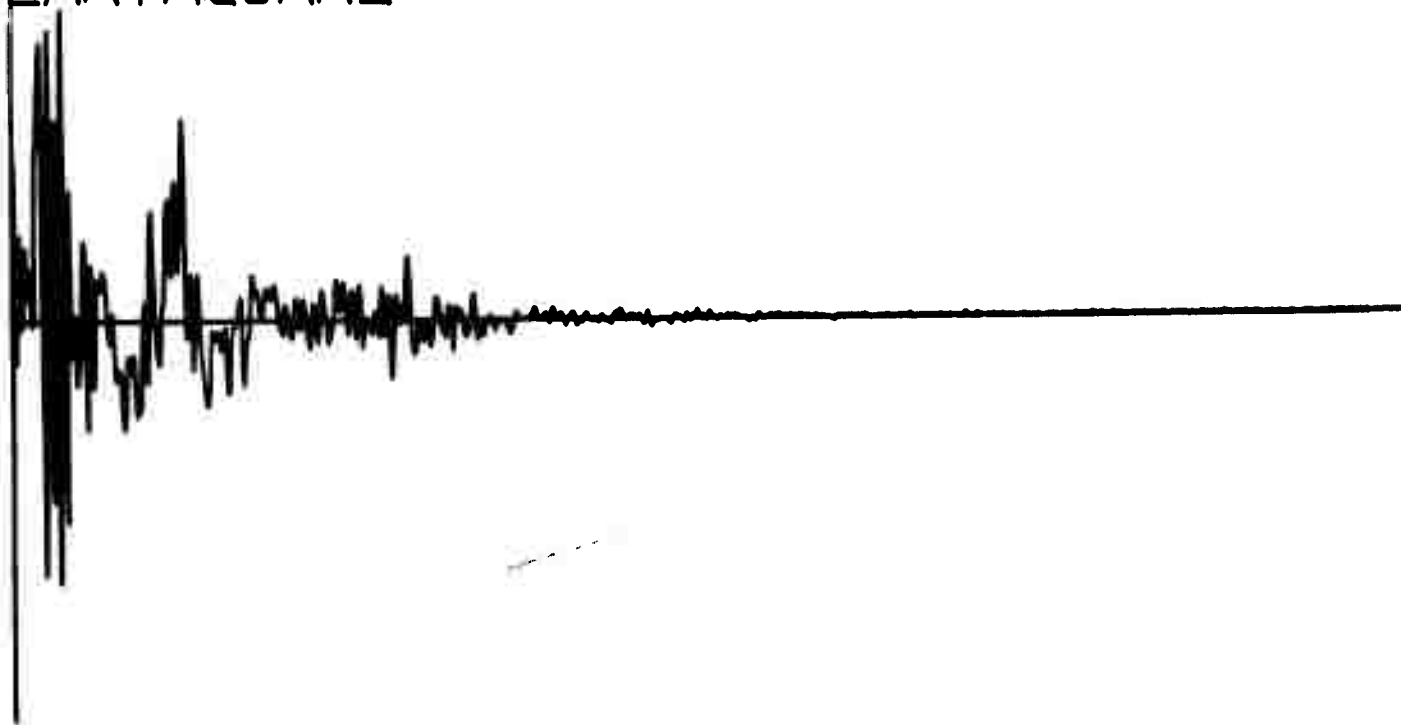
EVENT NUMBER 1311
EARTHQUAKE



Q352

EVENT NUMBER 1307

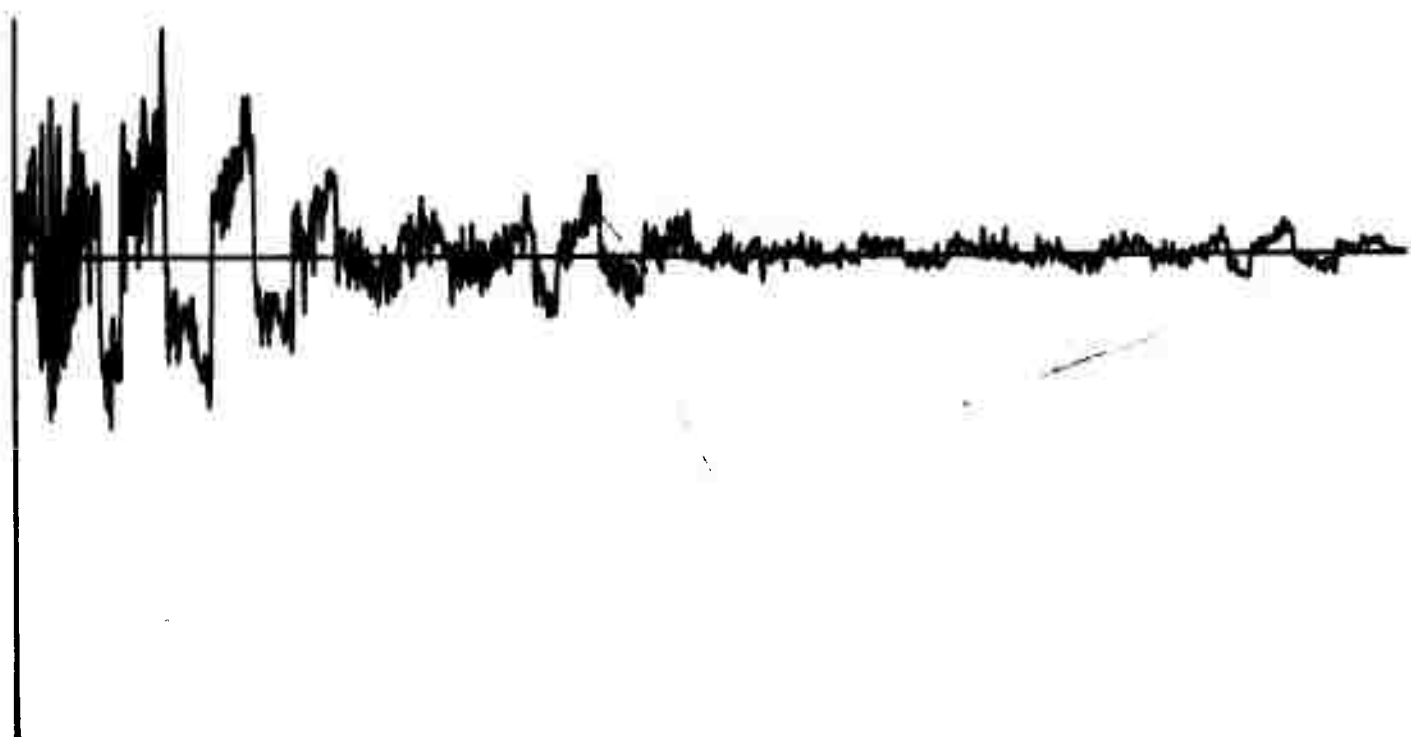
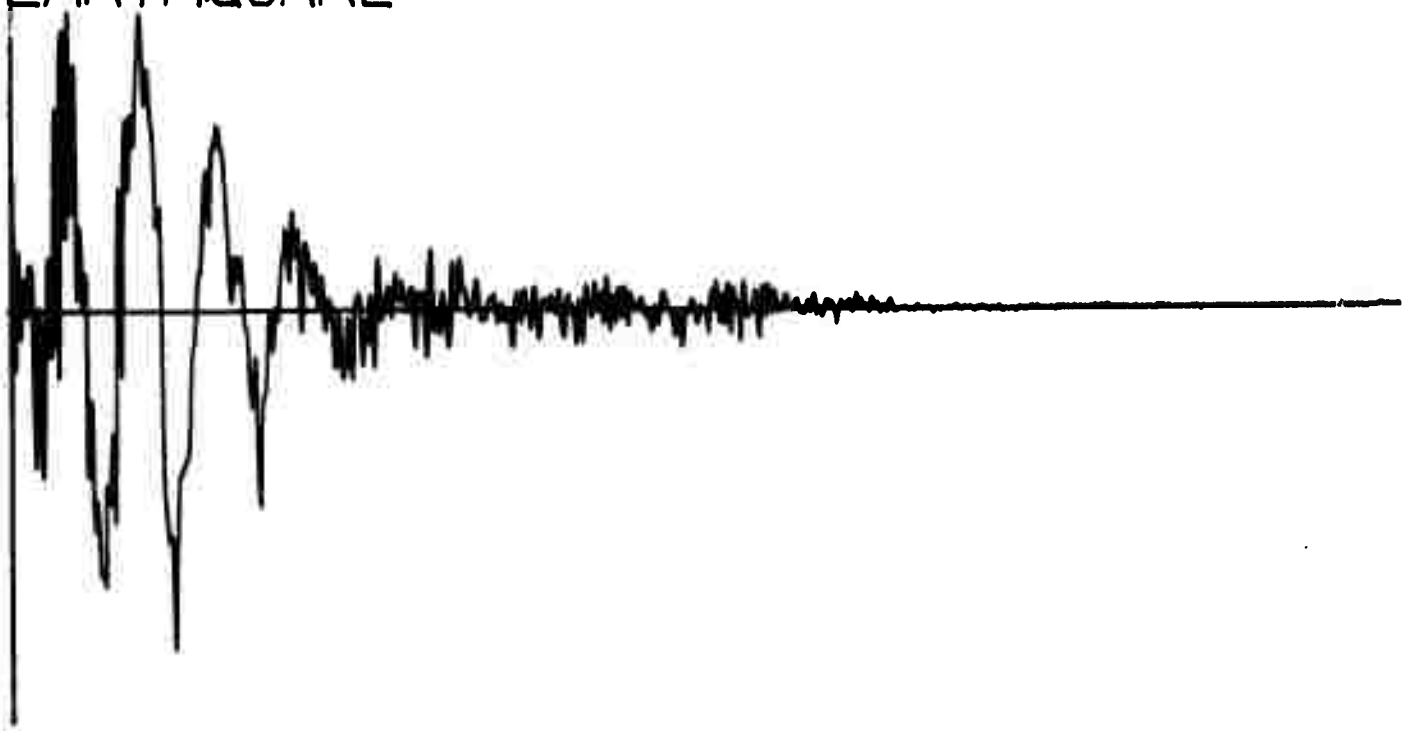
EARTHQUAKE



Q354

EVENT NUMBER 1306

EARTHQUAKE



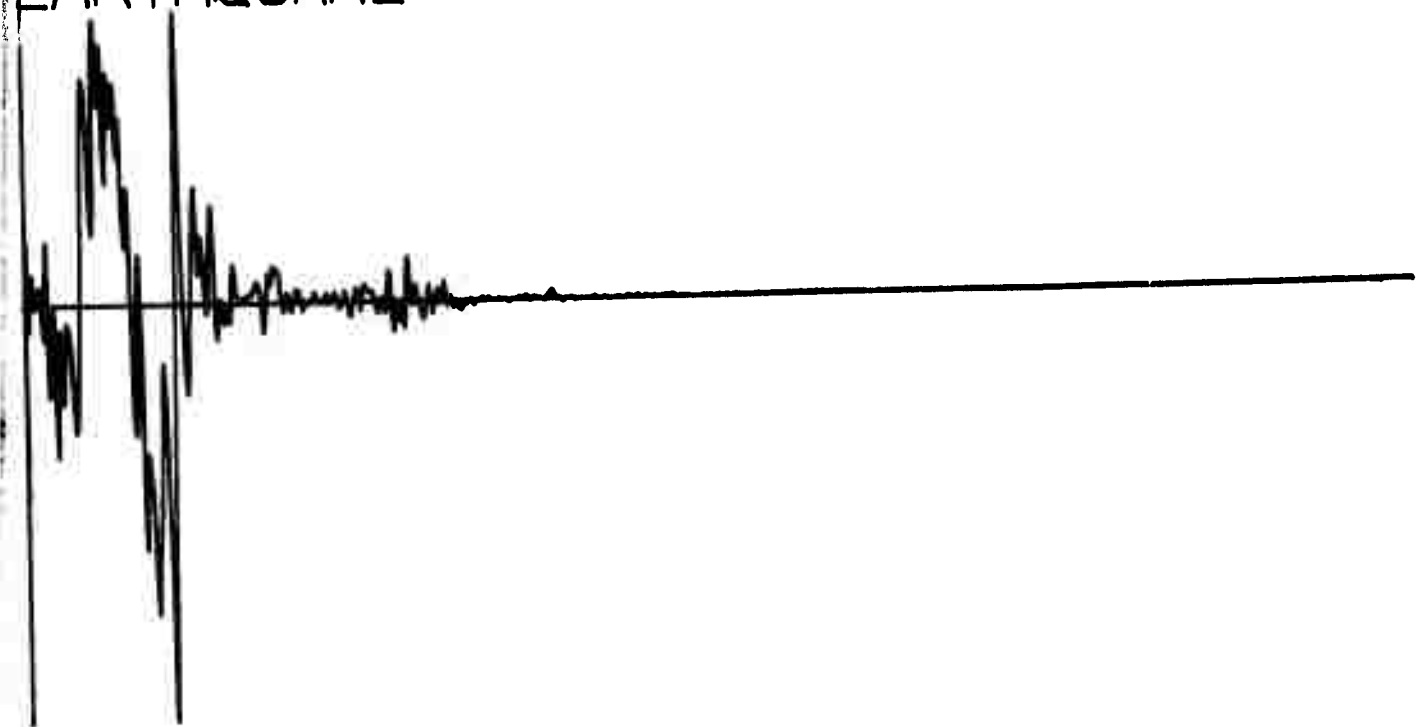
Q356

EVENT NUMBER 1276
EARTHQUAKE



Q358

EVENT NUMBER 1277
EARTHQUAKE



Q360

EVENT NUMBER 1324

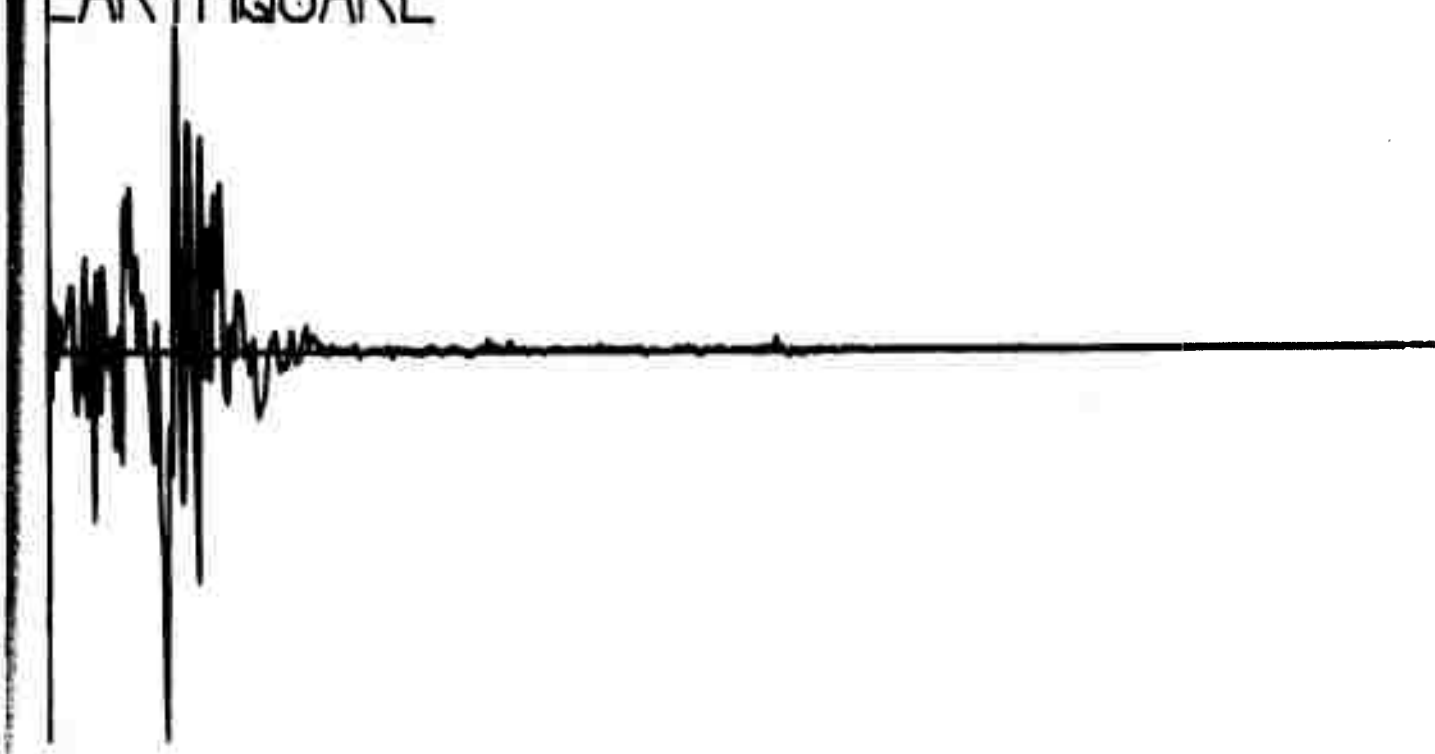
EARTHQUAKE



362
Q362

EVENT NUMBER 1325

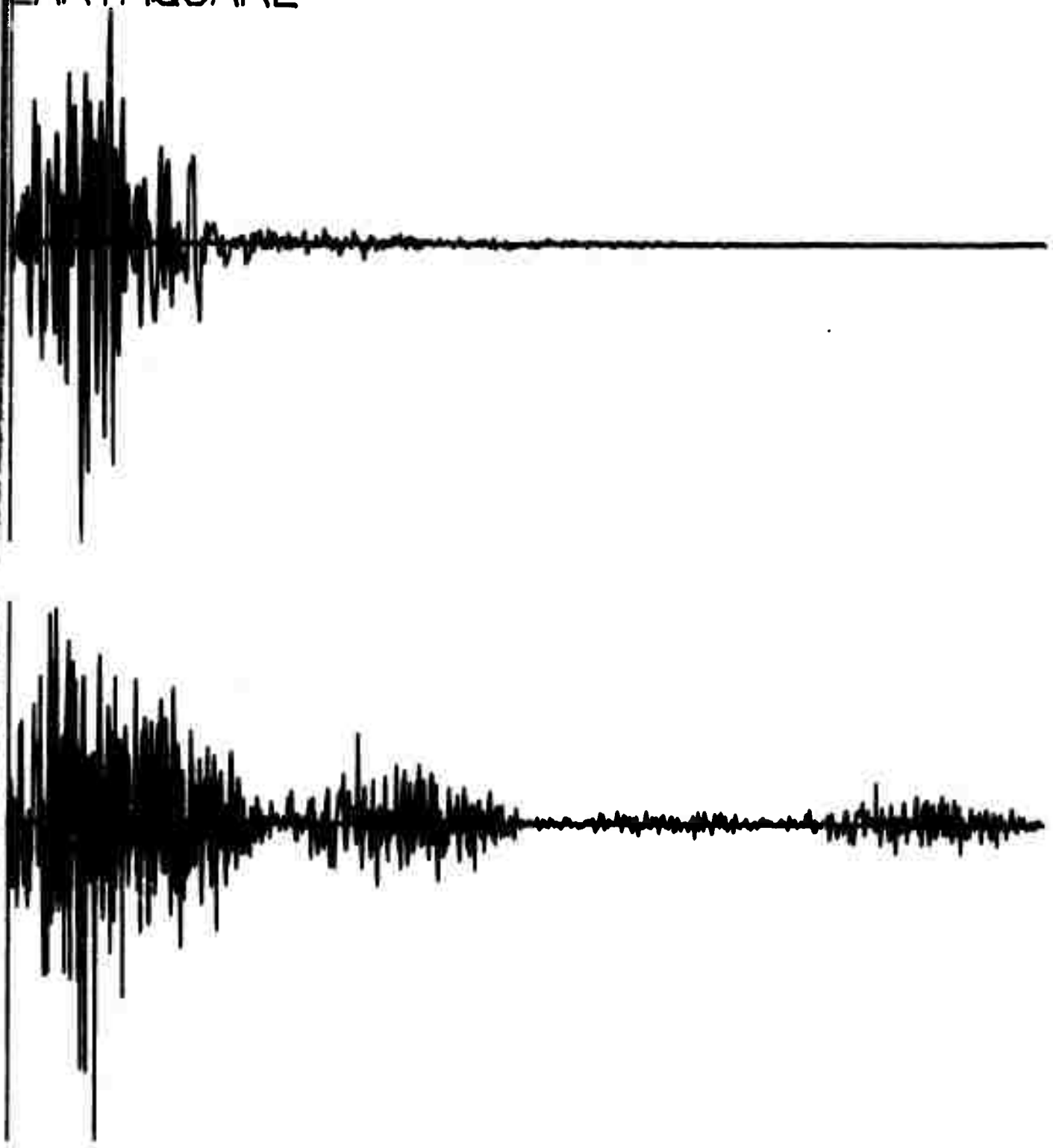
EARTHQUAKE



³⁶⁴
Q102

EVENT NUMBER 1326

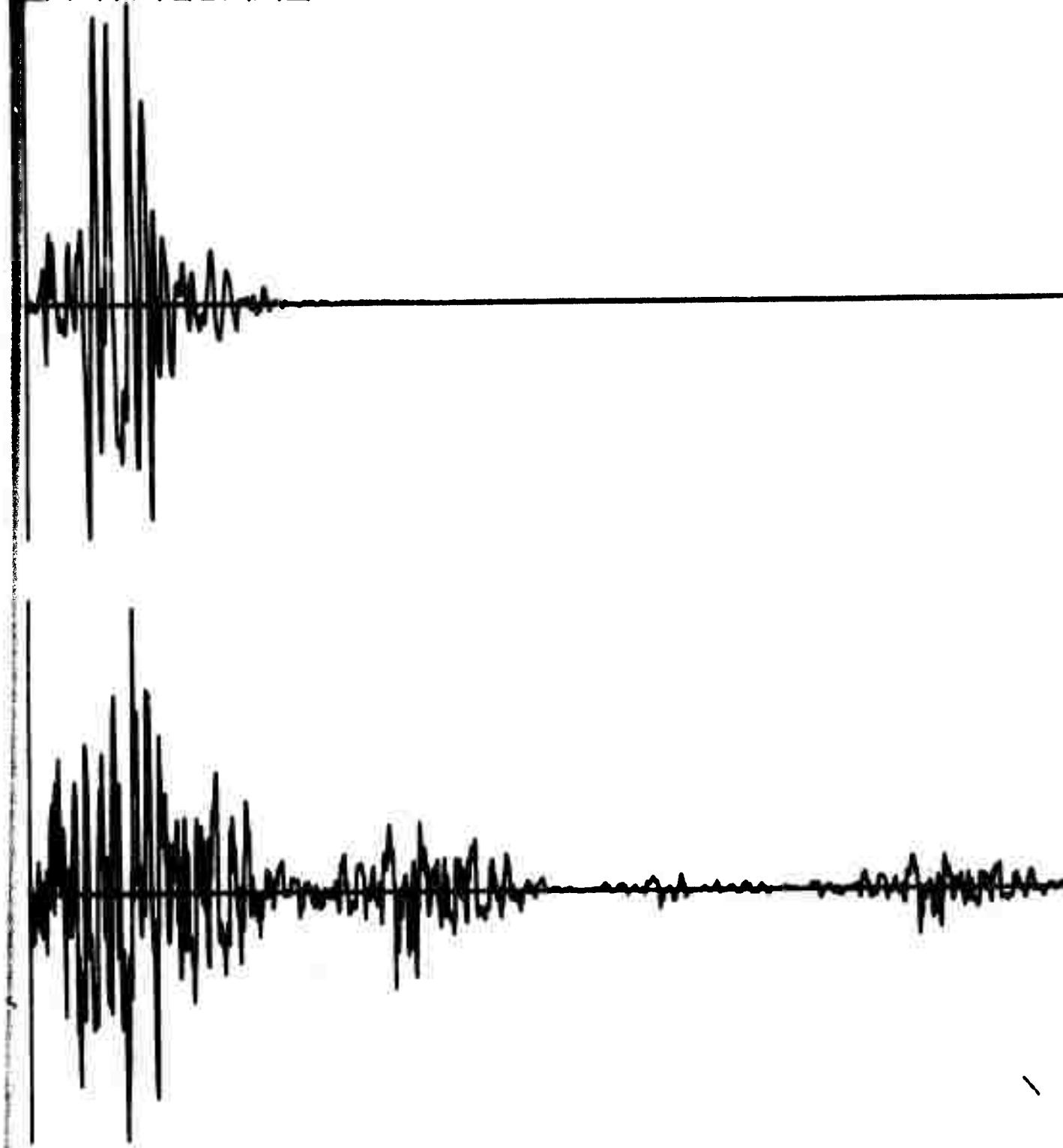
EARTHQUAKE



³⁶⁶
Q109

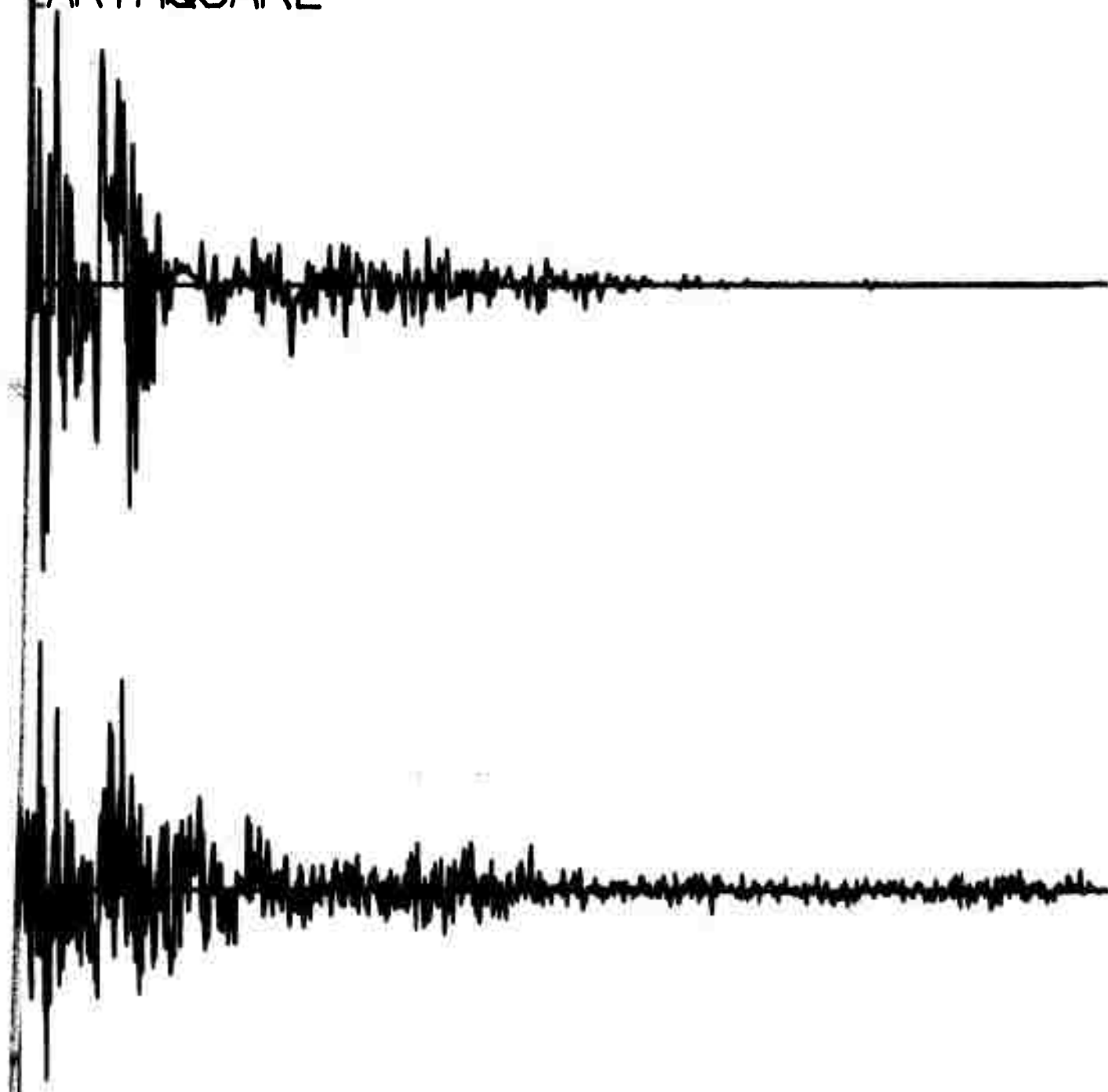
EVENT NUMBER 1328

EARTHQUAKE



³⁶⁸
Q184

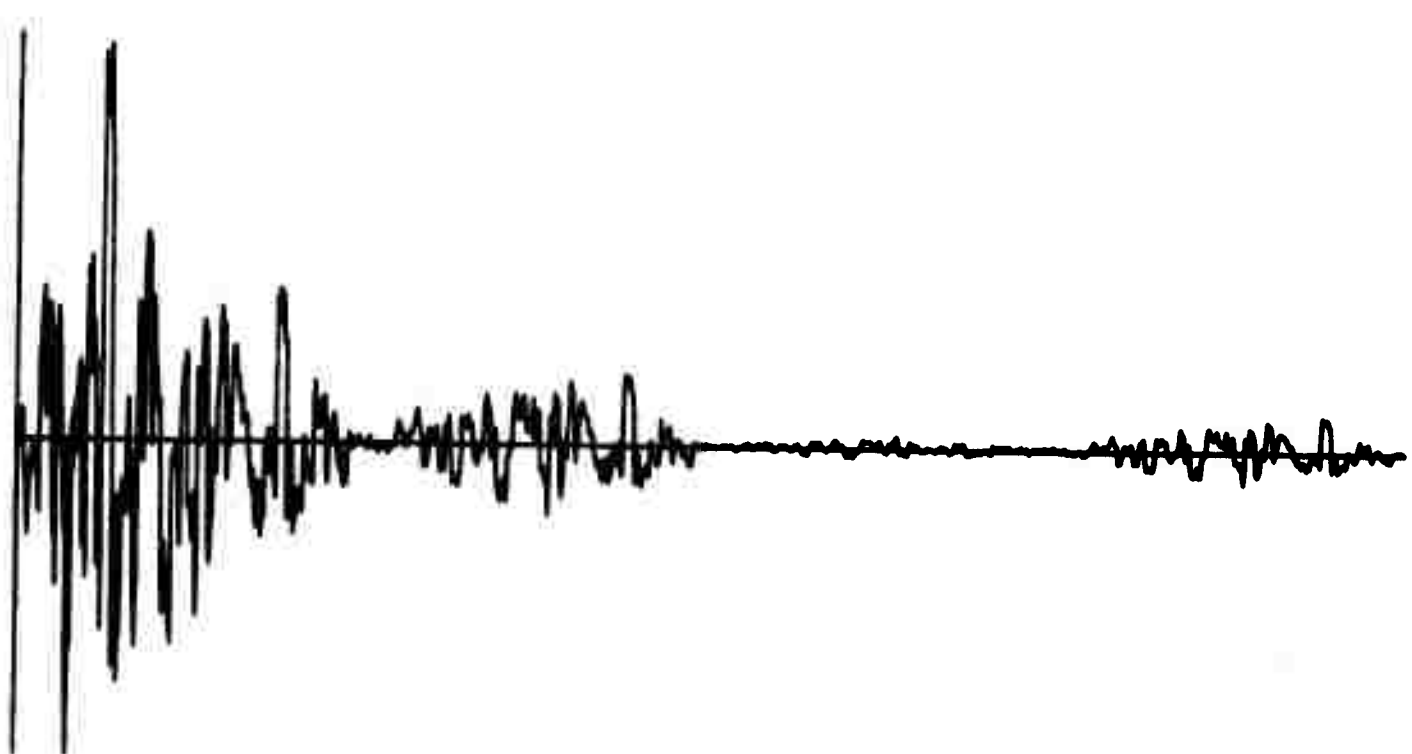
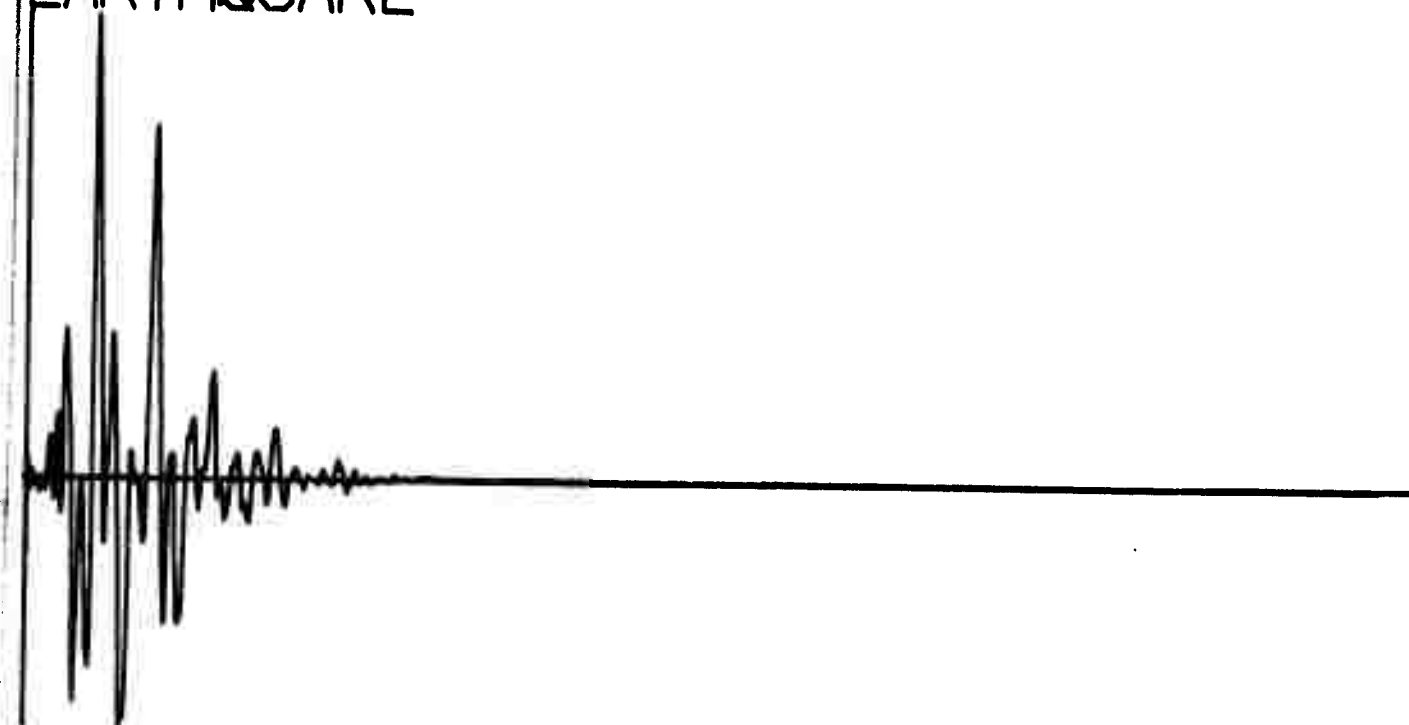
VENT NUMBER 1329
EARTHQUAKE



370
Q345

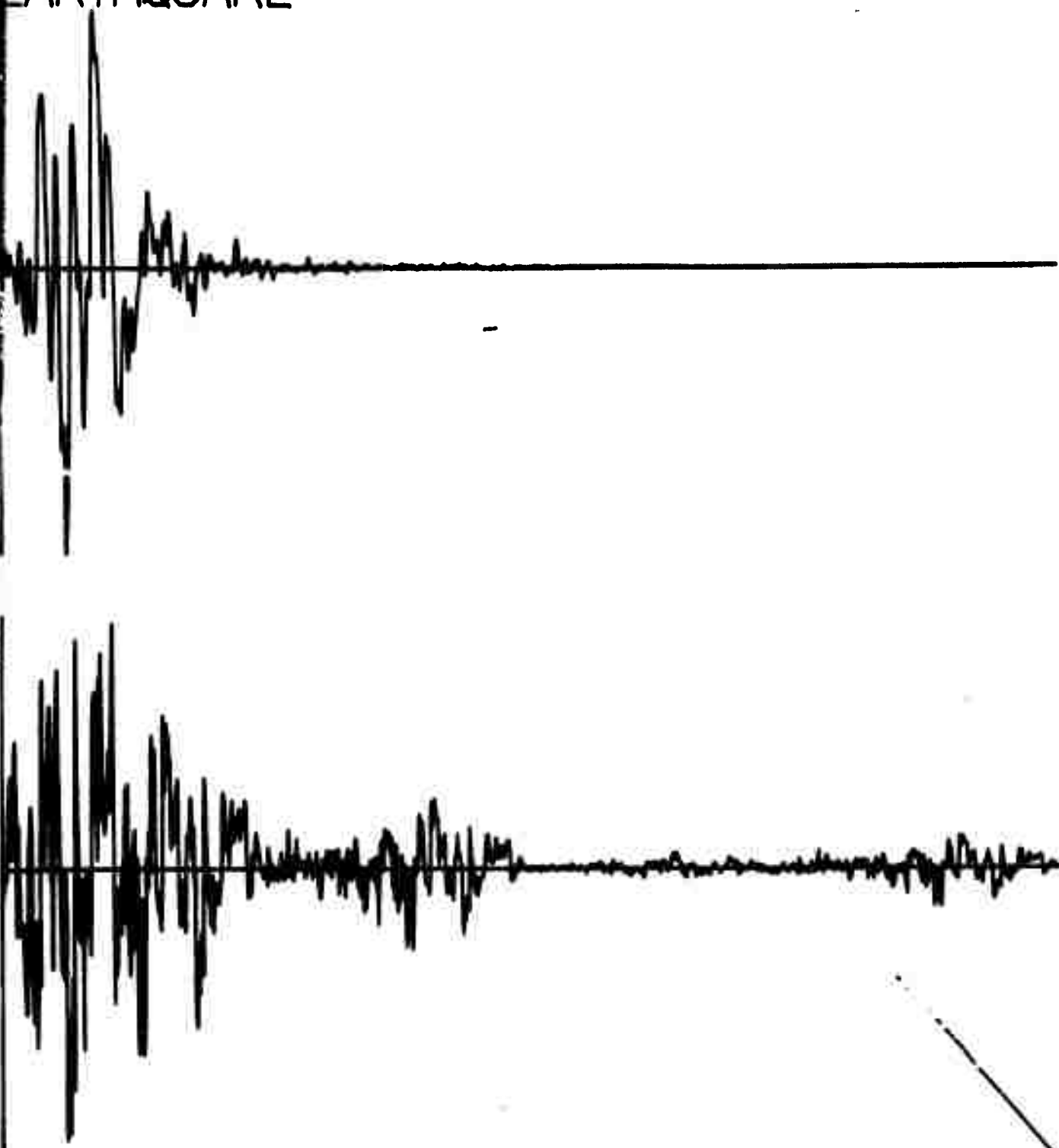
EVENT NUMBER 1330

EARTHQUAKE



372
Q106

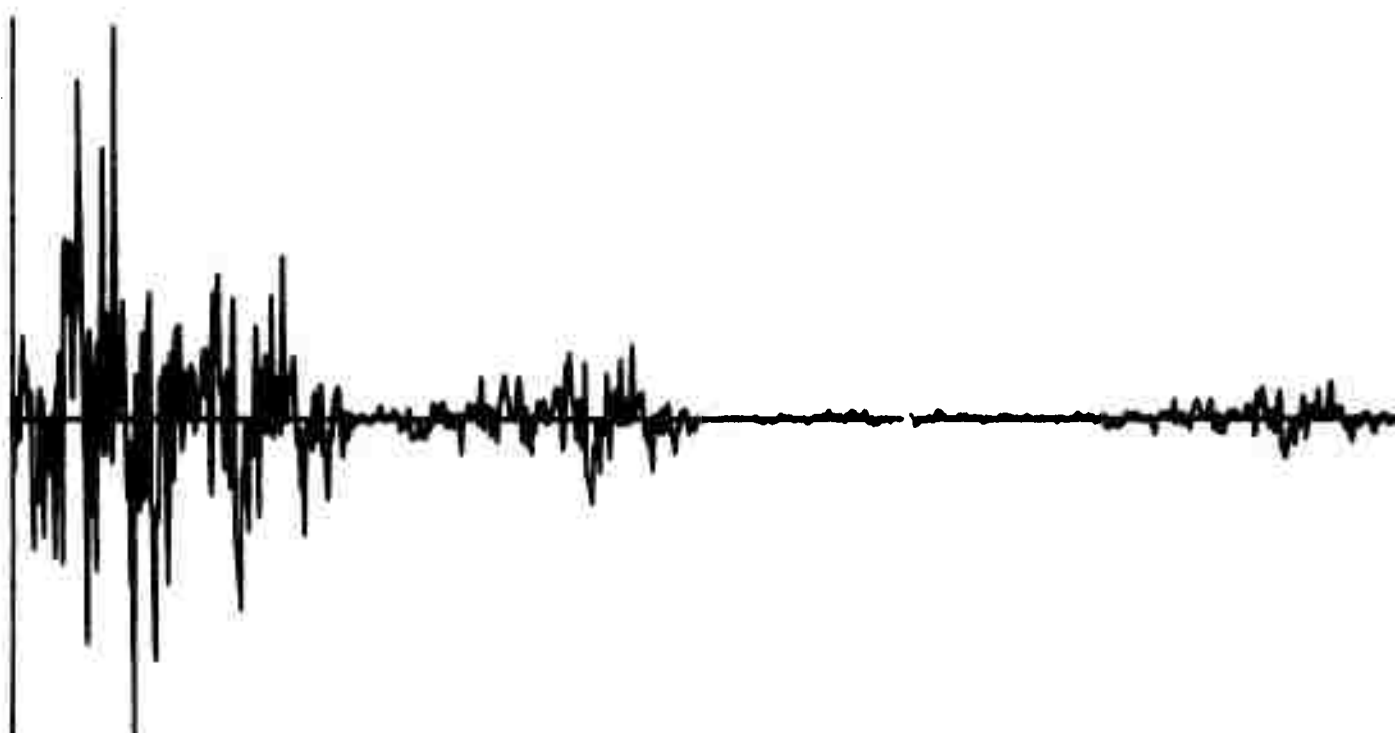
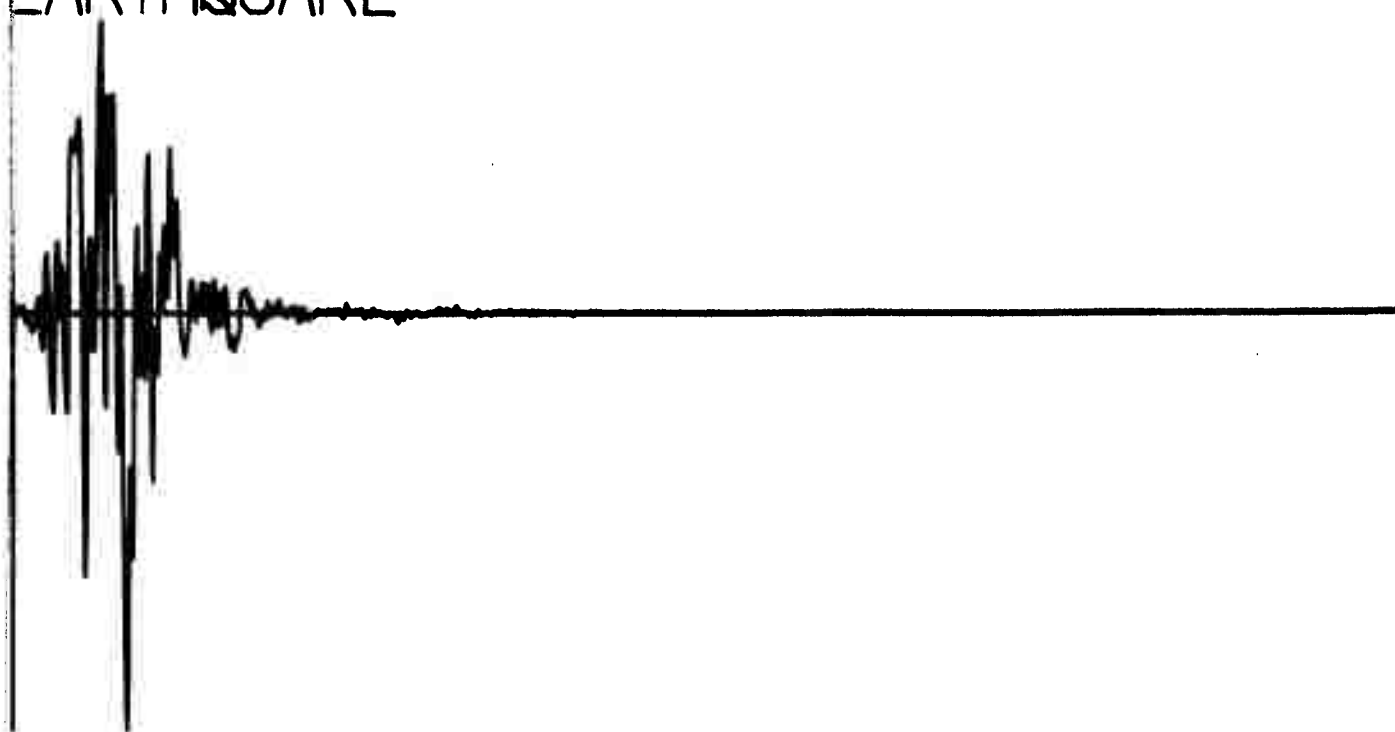
EVENT NUMBER 1331
EARTHQUAKE



374
Q187

EVENT NUMBER 1332

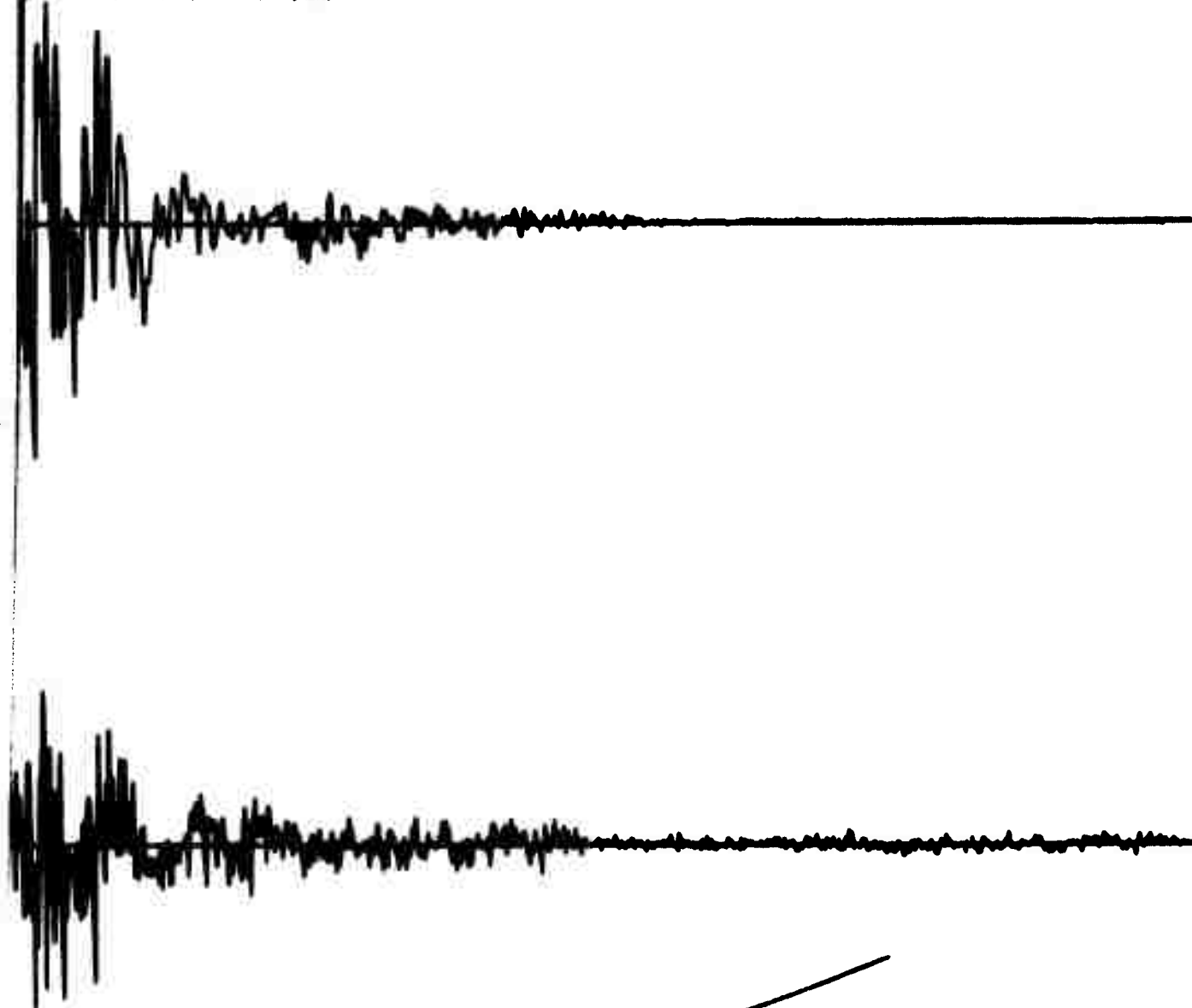
EARTHQUAKE



376
Q168

VENT NUMBER 1327

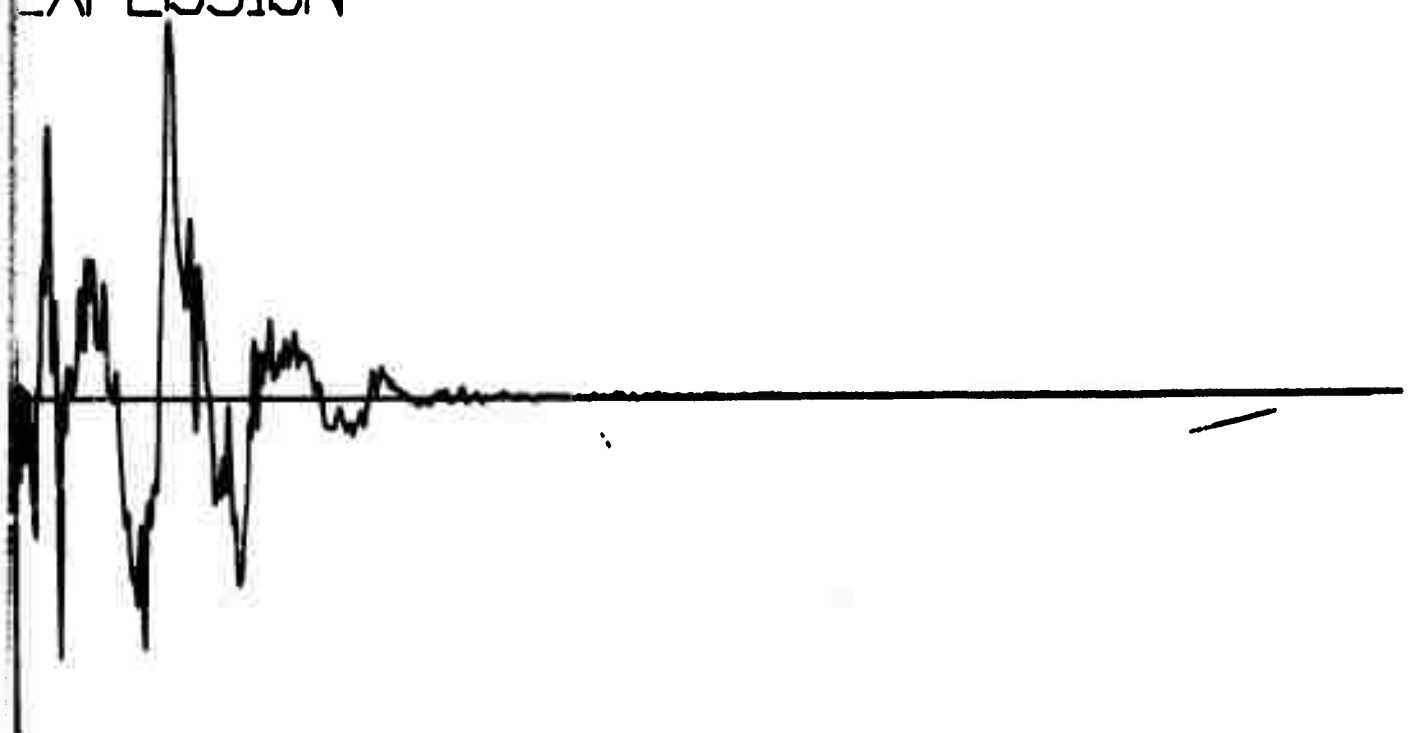
ARTHQUAKE



378
Q389

EVENT NUMBER 1552

EXPLOSION



380
x190

EVENT NUMBER 1550

EXPLOSION

